

# RADIO RECEIVER DESIGN

*By*

**K. R. STURLEY**

Ph.D., B.Sc., M.I.E.E., Sen. M.I.R.E.

*Head of Engineering Training Department,  
British Broadcasting Corporation*

*Late of Marconi School of Wireless Communication*

*Part II*

**AUDIO FREQUENCY AMPLIFIERS  
TELEVISION AND FREQUENCY MODULATED  
RECEIVER DESIGN**

*Second Impression*

NEW YORK  
**JOHN WILEY & SONS INC.**

440 FOURTH AVENUE

1948

*First Published* . . . 1945  
*Second Impression* . . . 1948

THIS BOOK IS PRODUCED IN COMPLETE  
CONFORMITY WITH THE AUTHORIZED  
ECONOMY STANDARDS

## AUTHOR'S PREFACE

STARTING with A.F. amplification, the procedure of analysing the remaining stages of a radio receiver is similar to that adopted in Part I. The principle of progressing from aerial to output is followed in the two chapters devoted to the special requirements of frequency modulated and television reception. To preserve continuity with Part I, the first chapter is numbered 9, and all sections, figures and expressions are prefixed by their chapter number. A glossary of the more important symbols and units, as well as a detailed table of contents, is included.

The author is again indebted to his wife for help in reading the proofs and to Marconi's Wireless Telegraph Company for permission to incorporate material originally used in lectures given at the Marconi School of Wireless Communication. In addition, he wishes to record his gratitude to Mr. M. Esterson, B.Sc., for useful criticism of the script and checking of the calculations.

*May* 1944.

## ACKNOWLEDGMENTS

REFERENCES to sources of information will be found in the Bibliographies and footnotes, but the author particularly wishes to acknowledge his indebtedness to the following for permission to use diagrams from their publications.

<i>Name of Journal or Manufacturer</i>	<i>Figure Numbers</i>
<i>Electronic Engineering</i> . . . . .	15.3 to 15.10
<i>Journal of the Institution of Electrical Engineers</i> . . . . .	16.1
<i>Marconi Review</i> . . . . .	13.19
<i>Proceedings of the Institute of Radio Engineers</i> . . . . .	9.15 10.15, 10.25 13.4, 13.11 14.1a, 14.1b
Radio Manufacturers Association (England) . . . . .	14.6a, 14.6b
<i>R.C.A. Journal</i> . . . . .	15.1 16.9a, 16.11, 16.13, 16.14, 16.16
<i>Wireless Engineer</i> . . . . .	10.4, 10.6, 10.20, 10.21 11.16, 11.17 12.9a, b and c 15.18a to 15.21
<i>Wireless World</i> . . . . .	9.18 to 9.21 11.15a, 11.19, 11.20 12.20 13.3 16.22, 16.27 Table 11.1
Messrs. Cosmos Manufacturing Company . . . . .	16.26
Messrs. Electrical Musical Industries . . . . .	13.14
Messrs. Pye Radio . . . . .	16.20, 16.24, 16.31
Messrs. Radio Corporation of America . . . . .	12.19 13.9a, 13.9b 15.11, 15.22 to 15.24, 15.26, 15.27

# PART II

## CONTENTS

CHAPTER	PAGE
9. AUDIO FREQUENCY AMPLIFIERS . . . . .	1
9.1. Introduction . . . . .	1
9.2. The Characteristics required of an A.F. Amplifier . . . . .	1
9.3. Resistance-Capacitance Coupling Circuits . . . . .	6
1. Frequency Response and Amplification . . . . .	6
2. A Comparison between the Triode and Tetrode as an A.F. Amplifier . . . . .	14
3. The Grid Leak and its Effect on the Anode Load . . . . .	18
4. Self-Bias for a RC Coupled Amplifier . . . . .	19
5. The Effect of the Screen Decoupling Circuit on the Frequency Response of a Tetrode Amplifier . . . . .	22
6. The Effect of the Anode Decoupling Circuit on the Frequency Response of an A.F. Amplifier . . . . .	25
9.4. The Transformer Coupled Amplifier . . . . .	28
9.5. The RC Coupled Transformer Amplifier . . . . .	38
9.6. Tone Control Circuits . . . . .	41
1. Introduction . . . . .	41
2. Types of Tone Control Circuits . . . . .	42
3. High Frequency Attenuation . . . . .	43
4. High Frequency Intensification . . . . .	44
5. Low Frequency Attenuation . . . . .	47
6. Low Frequency Intensification . . . . .	48
7. Response confined to a Band of Audio Frequencies . . . . .	50
8. Elimination of a Narrow Band of Frequencies . . . . .	52
9. Combined Volume and Tone Control . . . . .	54
<i>Bibliography</i> . . . . .	55
10. THE POWER OUTPUT STAGE . . . . .	56
10.1. Introduction . . . . .	56
10.2. Conditions for Maximum Power Output . . . . .	56
10.3. The Characteristics required of an Output Valve . . . . .	65
10.4. The Calculation of Power Output and Harmonic Distortion . . . . .	66
10.5. Audio Frequency Distortion with a Complex Anode Load Impedance . . . . .	73
10.6. Measurement of Power Output and Distortion . . . . .	76
1. Measurement with a Mains Frequency Voltage Source . . . . .	76
2. Measurement with a 400-c.p.s. Voltage Source . . . . .	77
10.7. Non-Linear Harmonic and Intermodulation Distortion in Power Output Valves . . . . .	79
10.8. Push-Pull Operation . . . . .	84
1. Introduction . . . . .	84
2. Methods of Producing the Push-Pull Grid Voltage . . . . .	86
3. Types of Push-Pull Stages . . . . .	89
4. Class A Push-Pull . . . . .	89
5. Class B Push-Pull . . . . .	92

CHAPTER	PAGE
10. THE POWER OUTPUT STAGE— <i>continued</i>	
10.8. Push-Pull Operation— <i>continued</i>	
6. The Driver Stage for Class B Positive Drive . . . . .	95
7. Class AB Positive Drive . . . . .	97
10.9. The Output Transformer . . . . .	97
1. The Design of an Output Transformer . . . . .	97
2. Output Transformer Attenuation (Frequency) Dis-	
tortion . . . . .	102
3. Output Transformer Amplitude (Harmonic) Dis-	
tortion . . . . .	104
10.10. Negative Feedback . . . . .	111
1. Introduction . . . . .	111
2. Types of Negative Feedback . . . . .	114
3. Voltage Feedback . . . . .	114
4. Current Feedback . . . . .	116
5. Bridge Feedback . . . . .	117
6. Negative Feedback with a Cathode Follower Valve	118
7. Balanced Feedback . . . . .	120
8. Instability in Feedback Amplifiers . . . . .	122
9. The Application of Negative Feedback to the	
Output Stage . . . . .	124
10. Two-Stage Feedback Circuits . . . . .	128
<i>Bibliography</i> . . . . .	131
11. POWER SUPPLIES . . . . .	133
11.1. Introduction . . . . .	133
11.2. A.C. Receiver Power Supply . . . . .	133
1. Introduction . . . . .	133
2. The Mains Transformer . . . . .	134
3. The H.T. Rectifier . . . . .	142
4. The H.T. Rectifier with Resistance Load . . . . .	145
5. The H.T. Rectifier with Capacitive Load . . . . .	146
6. The H.T. Rectifier with Inductive Load . . . . .	154
7. Voltage Multiplier Rectifier Circuits . . . . .	159
8. The Rectifier Ripple Filter . . . . .	160
9. The Filter Inductance with an Air Gap . . . . .	164
10. Grid Bias Supplies . . . . .	172
11.3. The Power Supply for the A.C./D.C. Receiver . . . . .	172
11.4. Vibrator H.T. Supply . . . . .	174
<i>Bibliography</i> . . . . .	178
12. AUTOMATIC GAIN CONTROL . . . . .	180
12.1. Introduction . . . . .	180
12.2. Principle of Operation . . . . .	180
12.3. Methods of obtaining the A.G.C. Bias Voltage . . . . .	181
12.4. Non-Amplified A.G.C. . . . .	182
1. Unbiased Diode A.G.C. . . . .	182
2. Biased or Delayed Diode A.G.C. . . . .	186
3. Distortion due to Biased Diode A.G.C. . . . .	189
4. Biased A.G.C. using the Audio Frequency Detector	191
12.5. Amplified A.G.C. Systems . . . . .	192
1. Introduction . . . . .	192
2. R.F. Amplified A.G.C. . . . .	193
3. A.G.C. using a combined R.F. and A.F. Amplifier . . . . .	193
4. D.C. Amplified A.G.C. . . . .	195
5. Anode-Bend Amplified A.G.C. . . . .	198

CHAPTER	PAGE
12. AUTOMATIC GAIN CONTROL— <i>continued</i>	
12.6. The Filter between A.G.C. Detector and the Controlled Stages . . . . .	198
12.7. Dual A.G.C. . . . .	202
12.8. Interchannel Noise Suppression or Quiet A.G.C. . . . .	202
1. Introduction . . . . .	202
2. Biased Detector, Quiet A.G.C. . . . .	203
3. Interchannel Noise Suppression by a Variable Capacitance across the A.F. Detector Load Resistance . . . . .	204
4. Noise Suppression by means of a Biased A.F. Amplifier . . . . .	205
12.9. Noise Limiters . . . . .	206
12.10. Audio Frequency A.G.C. . . . .	207
1. Introduction . . . . .	207
2. A.G.C. with Decreasing Amplification for Increasing A.F. Input . . . . .	208
3. A.G.C. providing Contrast Expansion . . . . .	209
<i>Bibliography</i> . . . . .	212
13. PUSH-BUTTON, REMOTE AND AUTOMATIC TUNING CONTROL . . . . .	214
13.1. Introduction . . . . .	214
13.2. Push-button Tuning . . . . .	214
1. Introduction . . . . .	214
2. Mechanical Rotation of the Tuning Capacitor . . . . .	215
3. Electrical Rotation of the Tuning Capacitor . . . . .	215
4. Preset Tuned Circuits . . . . .	217
13.3. Remote Control . . . . .	219
1. Introduction . . . . .	219
2. Rotation of the Tuning Capacitor . . . . .	219
3. Pulse Control using Mains Supply Wiring . . . . .	219
4. R.F. Pulses from a Portable Oscillator . . . . .	222
5. Transfer of R.F. and Frequency Changer Stages to the Remote Point . . . . .	222
6. Magnetic Remote Tuning . . . . .	222
7. Tuned Lines . . . . .	223
13.4. Automatic Frequency Correction . . . . .	224
1. Introduction . . . . .	224
The Discriminator . . . . .	224
3. The Variable Reactance Control Unit . . . . .	245
4. Estimation of A.F.C. Overall Performance . . . . .	260
<i>Bibliography</i> . . . . .	262
14. MEASUREMENT OF RECEIVER OVERALL PERFORMANCE . . . . .	264
14.1. Introduction . . . . .	264
14.2. Definitions . . . . .	264
1. Standard Input Voltage . . . . .	264
2. Standard Output Power . . . . .	265
3. Sensitivity . . . . .	265
4. Selectivity . . . . .	265
5. Fidelity or Frequency Response . . . . .	265
6. Harmonic Distortion . . . . .	266
7. Noise . . . . .	266
8. Hum . . . . .	266
9. Automatic Gain Control . . . . .	266
10. Standard Aerial . . . . .	266

CHAPTER	PAGE
14. MEASUREMENT OF RECEIVER OVERALL PERFORMANCE— <i>continued</i>	
14.3. The Apparatus required for the Overall Electrical Measurements . . . . .	266
1. Standard Signal Generator . . . . .	266
2. Standard Dummy Aerial . . . . .	267
3. The Shielded Pick-up Coil for Frame Aerial Receivers . . . . .	267
4. Output Meter . . . . .	268
5. Beat Frequency Oscillator . . . . .	269
6. Distortion Factor Meter . . . . .	269
7. Harmonic Analyser . . . . .	269
14.4. Receiver Adjustments . . . . .	269
14.5. Test Specifications . . . . .	269
1. Sensitivity . . . . .	269
2. Selectivity . . . . .	272
3. Electrical Frequency Response . . . . .	278
4. Harmonic Distortion . . . . .	279
5. Noise . . . . .	280
6. Hum . . . . .	281
7. Automatic Gain Control . . . . .	282
8. Frequency Changer Interference Effects . . . . .	283
9. Oscillator Frequency Drift . . . . .	284
10. Automatic Frequency Correction . . . . .	285
14.6. Acoustical Tests . . . . .	285
14.7. Definitions . . . . .	285
1. Frequency Response . . . . .	285
2. Intensity Level . . . . .	285
3. Loudness Level . . . . .	285
4. Overall Acoustic Sensitivity . . . . .	286
5. Distortion Factor . . . . .	286
6. Total Harmonic Content . . . . .	286
7. Free Space Conditions and their Approximation . . . . .	286
8. Hum . . . . .	286
14.8. Additional Apparatus . . . . .	286
14.9. Acoustical Measurements . . . . .	289
1. Frequency Response . . . . .	289
2. Acoustic Sensitivity . . . . .	290
3. Hum . . . . .	291
4. Acoustic Output and Distortion Factor . . . . .	292
<i>Bibliography</i> . . . . .	293
15. FREQUENCY MODULATED RECEPTION . . . . .	294
15.1. Introduction . . . . .	294
15.2. The Advantages and Disadvantages of Frequency Modulation . . . . .	296
15.3. The Frequency Modulation Receiver . . . . .	301
15.4. The Aerial Input . . . . .	303
15.5. The R.F. Amplifier Stage . . . . .	303
15.6. The Frequency Changer and Oscillator Stages . . . . .	315
15.7. The Intermediate Frequency Amplifier . . . . .	320
15.8. The Amplitude Limiter . . . . .	328
1. Introduction . . . . .	328
2. The Saturated Amplifier Limiter . . . . .	329
3. The Negative Feedback A.G.C. Limiter . . . . .	332
4. The A.F. Neutralizing Limiter . . . . .	333



CHAPTER	PAGE
15. FREQUENCY MODULATED RECEPTION— <i>continued</i>	
15.9. The Frequency-Amplitude Converter . . . . .	334
1. Introduction . . . . .	334
2. The Amplitude Discriminator Converter . . . . .	335
3. The Phase Discriminator Converter . . . . .	340
4. The Integrating Converter . . . . .	349
5. The Counter Type of F.M. Detector . . . . .	352
6. The Hexode Frequency-to-Amplitude Converter . . . . .	353
15.10. Methods of Frequency Modulation Compression in the Receiver . . . . .	353
1. Introduction . . . . .	353
2. Compression by Frequency Modulation of the Local Oscillator . . . . .	354
3. The Frequency Divider Compressor . . . . .	355
4. Frequency Compression by Submultiple Locked Oscillator . . . . .	357
<i>Bibliography</i> . . . . .	358
16. TELEVISION RECEPTION . . . . .	360
16.1. Introduction . . . . .	360
16.2. The Essential Features of a Television Receiver . . . . .	364
16.3. The Aerial Circuit . . . . .	368
16.4. The R.F. Amplifier . . . . .	371
16.5. The Fixed Tuned R.F. Television Receiver . . . . .	377
16.6. The Superheterodyne Television Receiver . . . . .	381
1. Introduction . . . . .	381
2. The Frequency Changer Stage . . . . .	384
3. The Oscillator . . . . .	390
4. The I.F. Amplifier . . . . .	391
5. Audio Signal I.F. Filter Circuits . . . . .	399
16.7. The Detector Stage . . . . .	410
16.8. Vision Frequency Amplification . . . . .	419
1. Introduction . . . . .	419
2. High Frequency Performance . . . . .	421
3. Low Frequency Performance . . . . .	431
4. Restoration of the D.C. Component . . . . .	436
16.9. Synchronising Pulse Separation . . . . .	438
1. Introduction . . . . .	438
2. Amplitude Separation of the Vision and Synchronising Components . . . . .	439
3. Frequency Separation of the Frame and Line Pulses . . . . .	441
16.10. The Scanning Generator . . . . .	446
1. Introduction . . . . .	446
2. The Gas-filled Relay Valve Scanning Generator . . . . .	447
3. The Multivibrator Scanning Generator . . . . .	449
4. The Blocking Oscillator Scanning Generator . . . . .	451
16.11. The Deflecting Circuits and Amplifiers . . . . .	454
1. Introduction . . . . .	454
2. Electrostatic Deflection . . . . .	456
3. Electromagnetic Deflection . . . . .	458
16.12. Power Supplies and Focusing of the C.R. Tube . . . . .	461
1. Introduction . . . . .	461
2. Electrostatic Focusing and the C.R. Tube Power Supply . . . . .	462

CHAPTER	PAGE
16. TELEVISION RECEPTION— <i>continued</i>	
16.12. Power Supplies and Focusing of the c.r. Tube— <i>continued</i>	
3. Magnetic Focusing and the c.r. Tube Power Supply . . . . .	463
<i>Bibliography</i> . . . . .	465
APPENDIX 3A. THÉVENIN'S THEOREM . . . . .	467
INDEX . . . . .	469

# GLOSSARY

## OF THE MORE IMPORTANT SYMBOLS USED IN THE TEXT

### *Symbols*

<i>R</i> . . . .	resistance.
<i>L</i> . . . .	inductance.
<i>M</i> . . . .	mutual inductance, also modulation ratio.
<i>C</i> . . . .	capacitance.
<i>I</i> . . . .	current (R.M.S. or D.C. value), $\hat{I}$ peak value of A.C. current.
<i>E</i> . . . .	voltage (R.M.S. or D.C. value), $\hat{E}$ peak value of A.C. voltage.
<i>P</i> . . . .	power.
<i>X</i> . . . .	reactance of an inductance ( $2\pi fL$ ), or of a capacitance $\left(\frac{1}{2\pi fC}\right)$
<i>Z</i> . . . .	impedance of a resistance and reactance.
<i>G</i> . . . .	conductance, the reciprocal of resistance.
<i>B</i> . . . .	susceptance (when with suffix), the reciprocal of reactance.
<i>Y</i> . . . .	admittance, the reciprocal of impedance.
<i>g<sub>m</sub></i> . . . .	mutual conductance of a valve, $\frac{\partial I_a}{\partial E_g}$ .
<i>R<sub>a</sub></i> . . . .	internal or slope resistance of a valve, $\frac{\partial E_a}{\partial I_a}$ .
$\mu$ . . . .	amplification factor of a valve, $\frac{\partial E_a}{\partial E_g}$ .
$\mu$ . . . .	permeability (chapters 10 and 11).
$\Delta\mu$ . . . .	incremental permeability.
<i>R<sub>D</sub></i> . . . .	resonant impedance of a tuned circuit.
<i>Z<sub>T</sub></i> . . . .	transfer impedance of a pair of coupled circuits, $\frac{\text{output voltage}}{\text{input current}}$
<i>Q</i> . . . .	magnification of a coil or tuned circuit, $\frac{2\pi fL}{R}$ or $\frac{1}{2\pi fCR}$ .
<i>F</i> . . . .	frequency ratio, twice the off-tune frequency $\Delta f$ to the resonant or mid-frequency ( $f_r$ or $f_m$ ).
<i>ω</i> . . . .	radio frequency pulsance, $2\pi fc$ .
<i>p</i> . . . .	low or audio frequency pulsance, $2\pi f_m$ .
<i>k</i> . . . .	coupling coefficient, normally, $\frac{M}{\sqrt{L_p L_s}}$ .
<i>n</i> . . . .	ratio of secondary to primary turns in a transformer.
<i>N<sub>p</sub></i> . . . .	number of turns on primary of a transformer.
<i>N<sub>s</sub></i> . . . .	number of turns on secondary of a transformer.
<i>A</i> . . . .	amplification when with suffix (chapter 9).
<i>A</i> . . . .	area when without suffix (chapters 10 and 11).
<i>V</i> . . . .	volume (chapters 10 and 11).
$\Phi$ . . . .	total flux.

*Symbols*

$B$	. . .	flux density when without suffix (chapters 10 and 11).
$H$	. . .	magnetic field strength.
$H_p$	. . .	polarizing D.C. magnetic field strength.
A.C.	. . .	alternating current.
D.C.	. . .	direct current.
C.B.	. . .	cathode ray.
A.F.	. . .	audio frequency.
I.F.	. . .	intermediate frequency.
R.F.	. . .	radio frequency.
V.F.	. . .	vision frequency.
H.T.	. . .	high tension.
L.T.	. . .	low tension.
A.F.C.	. . .	automatic frequency correction.
A.G.C.	. . .	automatic gain control (sometimes A.V.C.).
R.M.S.	. . .	root mean square.

*Signs*

$\sqrt{\quad}$	. . .	square root.
$<$	. . .	less than.
$\ll$	. . .	much less than.
$>$	. . .	greater than.
$\gg$	. . .	much greater than.
$=$	. . .	equals.
$\approx$	. . .	approximately equals.
$\times$	. . .	multiplied by.
$ A $	. . .	modulus of $A$ .
$\sphericalangle$	. . .	angle between $0^\circ$ and $180^\circ$ .
$\supset$	. . .	angle between $180^\circ$ and $360^\circ$ .
%	. . .	percentage.
+db.	. . .	gain.
-db.	. . .	loss.
$\lambda$	. . .	wavelength.
$\eta$	. . .	efficiency.
$\tan^{-1} A$	. . .	angle whose tangent is $A$ .
$j$	. . .	$\sqrt{-1}$ , vector operator.
$\Delta$	. . .	small change of.
$\partial$	. . .	partial differential.

*Suffixes*

$a$	. . .	anode circuit.
$a1$	. . .	aerial and coupling circuit.
$b$	. . .	bias or battery.
$c$	. . .	carrier signal (exception $C_c$ , coupling capacitance, chapter 9).
$co$	. . .	cut-off.
$d$	. . .	desired signal.
$f$	. . .	fundamental (exception feedback circuit in Section 10.10).
$g$	. . .	grid circuit.
$h$	. . .	high (chapter 9), harmonic (chapter 10), local oscillator (chapter 13), hum (chapter 14).

*Suffixes*

<i>k</i>	. . . .	cathode circuit.
<i>l</i>	. . . .	low.
<i>m</i>	. . . .	middle
<i>mod</i>	. . . .	modulation
<i>n</i>	. . . .	noise.
<i>i</i>	. . . .	input.
<i>o</i>	. . . .	output.
<i>p</i>	. . . .	primary.
<i>r</i>	. . . .	resonance.
<i>s</i>	. . . .	secondary (chapters 9, 10 and 11), screen (chapters 9 and 16), stray (chapter 9).
<i>sc</i>	. . . .	speech coil.
<i>u</i>	. . . .	undesired.

*Units*

H	. . . .	henrys.
<i>m</i> H.	. . . .	millihenrys.
$\mu$ H	. . . .	microhenrys.
$\mu$ F	. . . .	microfarads.
$\mu\mu$ F.	. . . .	micro-microfarads.
<i>mA</i>	. . . .	milliamperes.
$\mu$ A	. . . .	microamperes.
<i>mV</i>	. . . .	millivolts.
$\mu$ V	. . . .	microvolts.
<i>mW</i>	. . . .	milliwatts.
$\Omega$	. . . .	ohms.
<i>M<math>\Omega</math></i>	. . . .	megohms.
<i>db.</i>	. . . .	decibel.
<i>c.p.s.</i>	. . . .	cycles per second.
<i>kc/s</i>	. . . .	kilocycles per second.
<i>Mc/s</i>	. . . .	megacycles per second.
$\mu$ (as prefix)	. . . .	micro.

## PART II

### CHAPTER 9

## AUDIO FREQUENCY AMPLIFIERS

**9.1. Introduction.** An audio-frequency voltage amplifier stage is generally required between the detector and output valve, especially when the latter has a low power-sensitivity,\* or when an amplified A.G.C. system is employed (in this instance the maximum carrier voltage applied to the detector valve is about 3 volts R.M.S.). An A.F. stage is also necessary if the receiver is used in conjunction with a gramophone pick-up. In certain types of receivers an A.F. amplifier is not included, the detector being fed directly to a high power-sensitivity pentode or tetrode valve requiring about 4 volts R.M.S. input for maximum power output. It is not usual to find more than one stage of A.F. amplification—except in receivers with push-pull output—partly because it adds almost nothing to the selectivity of a receiver and partly because high A.F. amplification tends to instability (motor boating) and increased hum output. The design of the A.F. voltage amplifier is somewhat different from that of the output amplifier stage since maximum voltage, and not power, is required at the output. Resistance-capacitance or transformer coupling is generally employed; choke-capacitance coupling is rarely used because it is more expensive, has a less satisfactory frequency response and only a slightly higher amplification than resistance-capacitance coupling. The particular features of the first two types of coupling are discussed in Sections 9.3 and 9.4.

**9.2. The Characteristics Required of an A.F. Amplifier.** The most important characteristic required of an amplifier is that it shall reproduce faithfully at its output the shape of the input wave without adding noise or hum voltages. This statement may be qualified in the case of an audio frequency amplifier to “shall reproduce at its output the component input frequencies (and no others) in the same amplitude proportions as exist for the input signal”. Undesirable hum voltages are generally associated with the valve heater and H.T. supply, and they can be reduced to negligible proportions by adopting special forms of heater (e.g., the

\* Power sensitivity is defined as the output power (milliwatts) per volt (R.M.S.) input.

spiral type) and electrode construction, and by careful smoothing of the H.T. supply. In special cases when the input signal is small and considerable amplification is needed, for example, in a condenser microphone amplifier, the H.T. supply may be stabilized by using a gas discharge valve across it, and the heater of the first valve may be supplied with smoothed rectified D.C. Thermal and shot noise voltages are generally of no consequence in the A.F. stages of a receiver because A.F. amplification is not sufficient to bring them into prominence.

Distortion of the output wave shape from an A.F. amplifier may be of four kinds: attenuation (variation of amplification for the individual frequency components of the input signal), harmonic or non linear (involving the production of frequencies harmonically related to the input frequency components), phase (a variation in the time delay of the individual frequency components of the signal from input to output terminals), and transient distortion. The latter is caused by damped oscillations following upon shock excitation of the amplifier by a steep-fronted pulse.

Attenuation distortion results from the unequal amplification of the frequency components of the input signal, i.e., for zero attenuation distortion the frequency response of the amplifier must be flat over the range it is desired to accept. A reasonably sharp cut-off with considerable attenuation is desirable outside the required range as this assists in removing interference, hum or noise voltages from the output. A range from 30 to 18,000 c.p.s. is generally considered necessary for the faithful reproduction of musical sounds—a much smaller range is needed for speech—and an amplifier should normally be designed to have a flat frequency response over this range. Attenuation distortion resulting in loss of low-frequency response causes reproduction to be unnaturally brilliant, whilst high-frequency attenuation produces a muffled tone with reduced intelligibility for speech. If high and low frequencies are attenuated, reproduction is intelligible but lacks naturalness. An exception to the rule calling for a flat-frequency response is provided by tone control, which allows adjustment of the high and low frequency components relative to the middle frequencies (1,000 to 3,000 c.p.s.). Tone control may be used to compensate for deficiencies in the frequency response of other parts of the receiver. For example, attenuation of the high frequency modulation sidebands in the R.F. and I.F. stages can be counteracted to a large extent by an increase in the high-frequency response of the A.F. amplifier. Alternatively, greater attenuation of the high frequencies in the A.F. amplifier may be used

as an aid to selectivity. Control of low-frequency response may be included to give a better frequency balance when interference requires severe attenuation of the high audio frequencies. Furthermore, the characteristics of the ear are such that a change in average sound level causes an apparent change in the balance of the frequency components, a reduction in volume leading to an apparently greater reduction in the low and high frequency components compared with the middle frequencies. Discrimination in favour of the high and

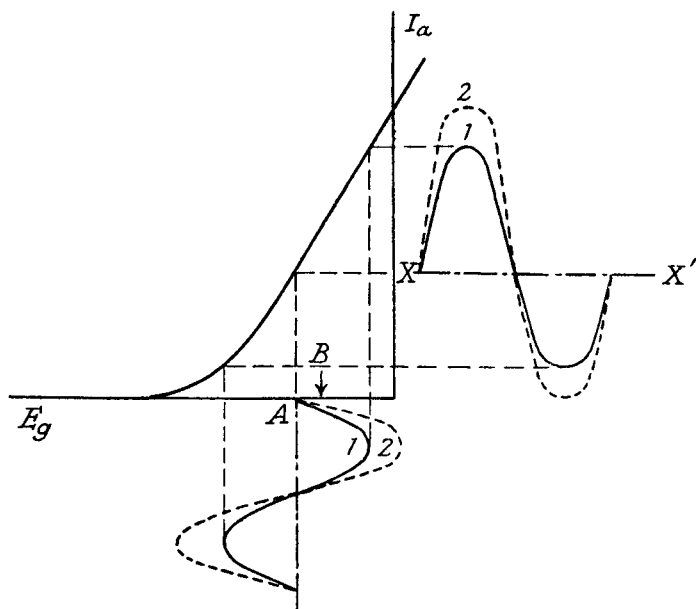


FIG. 9.1.—Distortion due to Curvature of the  $I_a E_g$  Characteristic and Grid Current.

low frequencies enables the balance to be retained as volume is reduced.

Amplitude or harmonic distortion is caused by variation of the instantaneous amplification over the input voltage cycle. It may be introduced by the valve, its associated circuits, or a combination of both. The valve produces amplitude distortion because of a non-linear  $I_a E_g$  relationship, or because grid current flattens the positive tip of the input voltage wave. The first causes flattening of the negative peak of anode current (see curve 1, Fig. 9.1), whilst the second causes the positive peak of the wave to be flattened (see curve 2, Fig. 9.1). Owing to curvature of the  $I_a E_g$  character-



istic as  $I_a$  approaches zero, the optimum working grid bias is always less than half the bias voltage needed to cut-off anode current; it is generally about 0.4 of this voltage. The positive peak of anode current may be flattened, as shown by curve 2, Fig. 9.1, even though the input voltage is insufficient to draw grid current, and this is due to the anode load resistance causing a turn-over, or top bending, of the  $I_a E_g$  characteristic. Triode valves seldom have this type of characteristic, but with tetrodes it is quite apt to occur, particularly if the load resistance is high. It is due to the load line entering the "knee" of the  $I_a E_a$  characteristic (see line  $AB'$  in Fig. 9.8). Amplitude distortion from a valve having a resistance anode load is caused usually by incorrect biasing and/or too large an input signal. Curve 1 (Fig. 9.1) shows the result of overbiasing, and distortion could be appreciably reduced by changing the bias point from  $A$  to  $B$ . Overloading by too large an input signal is illustrated by curve 2 (Fig. 9.1). It may be noted that both curves are symmetrical about a vertical line drawn through maximum or minimum amplitude. This is to be expected because the operating  $I_a E_g$  characteristic with a resistance anode load cannot exhibit a "hysteresis" loop, i.e., it must be the same for increasing input voltage (grid voltage becoming less negative) as for decreasing input voltage amplitude.

Amplitude distortion always produces frequencies additional to those present in the input, and Fourier analysis of the wave shape of curve 1 in Fig. 9.1 shows that it contains mainly even harmonics, the wave shape being asymmetrical about the datum line  $XX'$ ; curve 2, on the other hand, contains mainly odd harmonics, the wave shape being almost symmetrical about  $XX'$ . Figs. 9.2a and 9.2b show that the addition of a second and third harmonic frequency respectively to the fundamental results in wave shapes similar to those of curves 1 and 2. As a general rule the input voltage wave to an A.F. amplifier does not consist of a single sinusoidal frequency but of a number of such components, and amplitude distortion may cause intermodulation frequencies to appear in the output as well as harmonics of the original frequency components. These intermodulation products are sum and difference frequencies (the upper and lower sidebands) formed by combining the original frequency components or their harmonics. Thus for an input of two frequencies,  $f_1$  and  $f_2$ , the output may contain fundamental and harmonic frequencies of  $f_1$ ,  $mf_1$ ,  $f_2$  and  $nf_2$ , and also intermodulation frequencies of  $mf_1 \pm nf_2$ , and  $nf_2 \pm mf_1$ , where  $m$  and  $n$  are integers. Intermodulation tones generally have an inharmonic relationship to

the original frequencies, and in consequence tend to harsh and discordant reproduction.

A valve, which may not produce amplitude distortion of a given input signal with a resistance anode load, may, however, distort with a reactive anode load. A linear\* impedance of reactance and resistance is represented on the  $I_a E_a$  characteristics by a locus curve similar to a sheared ellipse, which may pass through the low  $I_a$  non-linear part of the characteristics (see Section 2.6, Part I, and Section 10.5) as shown by the section  $CD$  in Fig. 10.7a. The wave shape is distorted in the manner shown in Figs. 10.7a and 10.7b for an inductive and capacitive load respectively, the leading edge

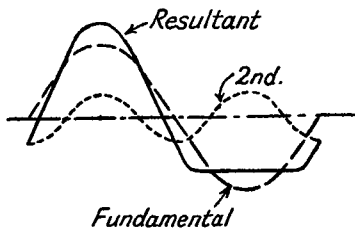


FIG. 9.2a.—Addition of Fundamental and Second Harmonic to produce a Wave Shape similar to Curve 1 in Fig. 9.1.

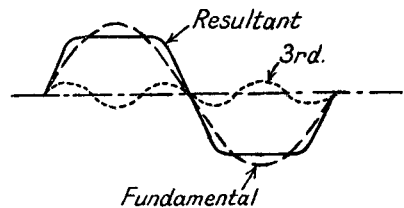


FIG. 9.2b.—Addition of Fundamental and Third Harmonic to produce a Wave Shape similar to Curve 2 in Fig. 9.1.

(increasing  $I_a$ ) rising more slowly than the trailing edge with an inductive load (Fig. 10.7a), and vice versa for a capacitive load (Fig. 10.7b). It should be noted that the wave shapes are asymmetric about a vertical line through maximum or minimum amplitude, i.e., the operating  $I_a E_a$  characteristic is no longer the same for increasing as for decreasing signal amplitude, but is rather similar to an iron  $B-H$  hysteresis loop as shown in Fig. 10.7b. The direction of progress round the loop is anticlockwise for an inductive anode load, maximum  $I_a$  (point  $F_1$ , Fig. 10.7b) occurring after maximum positive input voltage has been passed, whilst it is clockwise for a capacitive load, maximum  $I_a$  (point  $F_2$ , Fig. 10.7b) occurring before maximum positive input voltage.

Amplitude distortion may also be produced by circuits associated with the valve; for example, an iron-cored coil may act as a non-linear impedance, its inductance varying with the current through it because of a non-linear relationship between the magnetic flux

\* A linear impedance consists of an inductance, capacitance and/or resistance, the value of which is constant and independent of the amplitude or frequency of the voltage applied to it, or of the current passing through it.

and current. Distortion of a symmetrical input wave by non-linear action of an iron-cored inductance usually results in an asymmetrical output wave owing to the hysteresis loop of the  $B-H$  curve.

Phase distortion occurs in an amplifier when the frequency components of the input wave suffer differing time delays in passing through the amplifier. An example of the change in output wave shape caused by delaying the fundamental frequency component of Fig. 9.2*b* by  $60^\circ$  of its cycle, i.e.,  $\frac{60}{360f} = \frac{1}{6f}$  seconds with respect to

the third harmonic frequency, where  $f$  = frequency of the fundamental, is illustrated in Fig. 9.2*c*. Despite the difference in wave shape between the two figures, the ear is unable to detect any noticeable difference in sound characteristic. This applies also to frequencies not harmonically related, so that we can ignore phase distortion in A.F. amplification unless the time delay becomes much larger than is usually

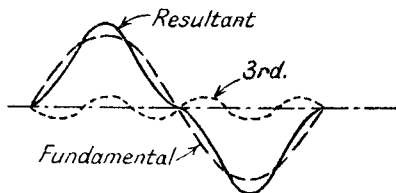


FIG. 9.2*c*. — The Effect of Phase Change on Wave Shape shown in Fig. 9.2*b*.

encountered in practice. Phase distortion is very important in television reception because there is a marked difference between the equivalent light contents of the output waves of Figs. 9.2*b* and 9.2*c*.

Transient distortion can occur in an amplifier if the latter contains a tuned circuit, or its equivalent, comparatively lightly damped, i.e., has a frequency response peaked over a narrow band. A steep-sided pulse shock-excites the tuned circuit, and a train of damped oscillations follows the leading edge of the pulse. The decay of these oscillations is determined by the degree of damping on the tuned circuit, which is measured by the height of the peak above the average frequency response level in the vicinity of the peak. Transient distortion can usually be ignored if the peak-to-average response is less than 1 db., provided a peak in one stage of an amplifier is not being cancelled by a dip in another. Large transient distortion produces blurring of the sound output.

### 9.3. Resistance-Capacitance Coupling Circuits.<sup>10</sup>

**9.3.1. Frequency Response and Amplification.** A typical resistance-capacitance coupled A.F. amplifier is shown in Fig. 9.3; triode valves are illustrated in the figure, but they may be replaced

by tetrodes, and the modifications needed to make the formulae applicable to tetrodes will be indicated as the analysis proceeds. The input voltage variations, developed in amplified form across  $R_o$ , are transferred to the next stage through the coupling capacitance  $C_c$ , which prevents the application of the D.C. component of

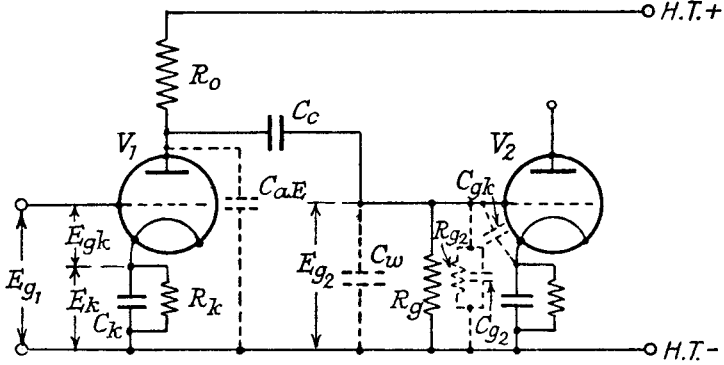


FIG. 9.3.—The Circuit for a Typical Resistance-Capacitance Coupled A.F. Amplifier.

anode voltage to the grid of the second valve  $V_2$ . The D.C. path from the grid of valve  $V_2$  to H.T. negative or a suitable bias voltage is completed by the grid leak resistance  $R_g$ . Grid bias for the

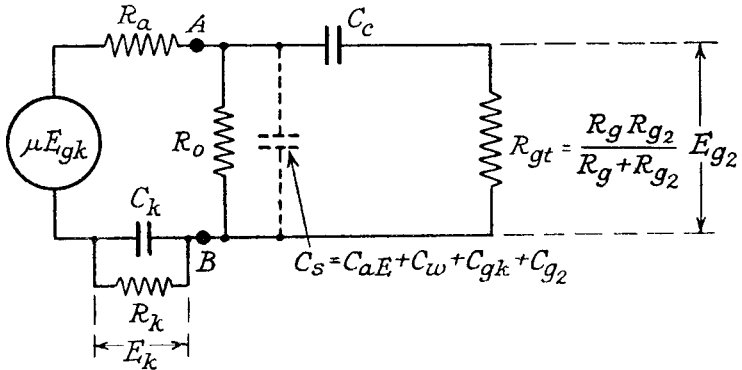


FIG. 9.4a.—A Simplified Diagram of a Resistance-Capacitance Coupled A.F. Amplifier.

stages may be derived from the anode current passing through a self-bias resistance ( $R_k$  between the cathode of  $V_1$  and H.T. negative) if the valves are indirectly heated. Directly heated valves (battery) generally require the bias to be inserted between the end of the grid leak,  $R_g$ , and H.T. negative or earth. A potential divider carrying the total anode current of all stages or a separate bias

battery may be provided. The self-bias resistance  $R_k$  must be paralleled by a capacitance  $C_k$  if reduced amplification by degenerative A.F. voltages across  $R_k$  is to be prevented.

A simplified diagram of the stage is shown in Fig. 9.4a; the valve is considered as a constant voltage generator of  $\mu E_{gk}$ — $\mu$  is the amplification factor of the valve  $V_1$ —and the output capacitance of  $V_1(C_{aE})$ , the input capacitance of  $V_2(C_{g2} + C_{gk})$ , and the wiring capacitance  $C_w$  are represented by  $C_s$  across  $R_0$ . This is permissible because  $C_c$  is, as a rule, much larger than  $C_s$ .  $C_{gk}$  is the grid-cathode interelectrode capacitance of  $V_2$ ;  $C_{g2}$  and  $R_{g2}$  are the parallel capacitance and resistance components reflected from the anode of  $V_2$  through its anode-grid capacitance (see Section 2.8.2, Part I). Overall amplification, given by the ratio of the output to input voltage,  $\frac{E_{g2}}{E_{g1}}$ , varies over the frequency range due to the reactance variations of  $C_c$  and  $C_s$ .

Taking first the separately biased amplifier ( $R_k = 0$ ), amplification is

$$A = \frac{E_{g2}}{E_{g1}} = \frac{\mu Z_{AB}}{R_a + Z_{AB}} \cdot \frac{R_{gt}}{R_{gt} + \frac{1}{j\omega C_c}}$$

where  $R_a$  = the slope resistance of the valve,  $V_1$ ,

$Z_{AB}$  = impedance across the points  $AB$  looking from the generator

$R_{gt}$  = the effective resistance of  $R_g$  and  $R_{g2}$  in parallel.

Generally for an A.F. amplifier stage  $R_{g2}$  is large compared with  $R_g$  and can be neglected; in the analysis which follows we shall assume that only  $R_g$  need be considered.

$$Z_{AB} = \frac{\frac{R_0}{j\omega C_s} \left( R_g + \frac{1}{j\omega C_c} \right)}{\frac{R_0}{j\omega C_s} + R_0 \left( R_g + \frac{1}{j\omega C_c} \right) + \frac{1}{j\omega C_s} \left( R_g + \frac{1}{j\omega C_c} \right)}$$

$$A = \frac{\mu R_0 R_g}{R_0 \left( R_g + \frac{1}{j\omega C_c} \right) + R_a \left( R_0 + j\omega C_s R_0 \left( R_g + \frac{1}{j\omega C_c} \right) + R_g + \frac{1}{j\omega C_c} \right)} \quad 9.1.$$

The effect of the variables, the reactances of  $C_c$  and  $C_s$ , on the frequency response of the amplifier is best examined by dividing the audio frequency range into three separate bands, of low, medium and high frequencies. In the medium frequency band, the series reactance of  $C_c$  is negligible compared with  $R_g$ , and the parallel

reactance of  $C_s$  is large compared with  $R_0$ ; the equivalent circuit is that of Fig. 9.4*b* and the amplification at the medium frequencies is therefore :

$$A_m = \frac{\mu R_0 R_g}{R_0 R_g + R_a (R_0 + R_g)} \quad . \quad . \quad . \quad 9.2a$$

$$= \frac{\mu R_0'}{R_a + R_0'} \quad . \quad . \quad . \quad . \quad 9.2b$$

where  $R_0' = \frac{R_0 R_g}{R_0 + R_g}$  = effective anode load resistance at the medium frequencies.

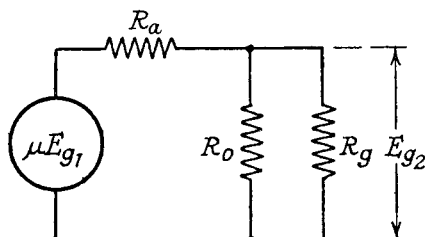


FIG. 9.4*b*.—The Equivalent Circuit of a Resistance-Capacitance Coupled A.F. Amplifier over the Medium Frequency Band.

In the low frequency band, the reactance of  $C_c$  increases and becomes comparable with  $R_g$ , whilst the reactance of  $C_s$  can still be

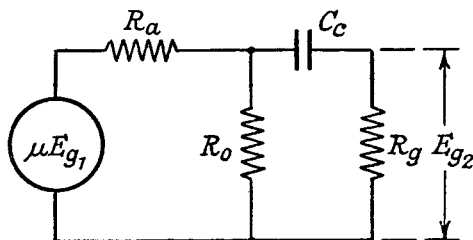


FIG. 9.4*c*.—The Equivalent Circuit of a Resistance-Capacitance Coupled A.F. Amplifier over the Low Frequency Band.

neglected. Fig. 9.4*c* is the equivalent diagram and expression 9.1 is amended to

$$A_l = \frac{\mu R_0 R_g}{R_0 \left( R_g + \frac{1}{j\omega C_c} \right) + R_a \left( R_0 + R_g + \frac{1}{j\omega C_c} \right)} \quad . \quad . \quad . \quad 9.3a$$

$$= \frac{\mu R_0 R_g}{(R_a + R_0) \left( R_g + \frac{1}{j\omega C_c} \right) + R_a R_0} \quad . \quad . \quad . \quad 9.3b$$

Combining 9.2a and 3b

$$\begin{aligned} \frac{A_t}{A_m} &= \frac{\frac{R_o R_a}{R_o + R_a} + R_g}{\frac{R_o R_a}{R_o + R_a} + R_g + \frac{1}{j\omega C_c}} \\ &= \frac{1}{1 - j \frac{X'}{R'}} \end{aligned} \quad \dots \quad 9.4a$$

where  $X' = \frac{1}{\omega C_c}$  and  $R' = \frac{R_o R_a}{R_o + R_a} + R_g$ .

Hence

$$\left| \frac{A_t}{A_m} \right| = \frac{1}{\sqrt{1 + \left( \frac{X'}{R'} \right)^2}} \quad \dots \quad 9.4b.$$

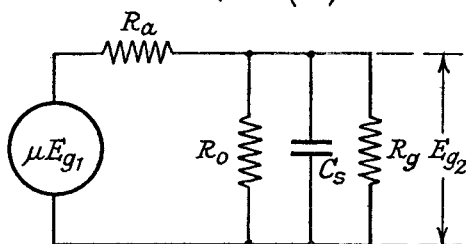


FIG. 9.4d.—The Equivalent Circuit for a Resistance-Capacitance Coupled A.F. Amplifier over the High Frequency Band.

For the high frequency band, the shunting effect of  $C_s$  is important, but the reactance of  $C_c$  is very small. The equivalent circuit is shown in Fig. 9.4d and expression 9.1 is modified to

$$\begin{aligned} A_h &= \frac{\mu R_o R_g}{R_o R_g + R_a (R_o + j\omega C_s R_o R_g + R_g)} \\ &= \frac{\mu \frac{R_o R_g}{R_o + R_g}}{\frac{R_o R_g}{R_o + R_g} + R_a + \frac{j\omega C_s R_o R_g R_a}{R_o + R_g}} \end{aligned} \quad \dots \quad 9.5.$$

Combining 9.2a and 5

$$\begin{aligned} \frac{A_h}{A_m} &= \frac{\frac{R_o R_g}{R_o + R_g} + R_a}{\frac{R_o R_g}{R_o + R_g} + R_a + \frac{j\omega C_s R_o R_g R_a}{R_o + R_g}} \\ &= \frac{1}{1 + j \frac{R''}{X''}} \end{aligned} \quad \dots \quad 9.6a$$

where  $R'' = \frac{R_o R_g R_a}{R_o R_g + R_a (R_o + R_g)}$  = resistance of  $R_o$ ,  $R_g$  and  $R_a$  in parallel.

$$X'' = \frac{1}{pC_s}$$

Thus 
$$\left| \frac{A_h}{A_m} \right| = \frac{1}{\sqrt{1 + \left( \frac{R''}{X''} \right)^2}} \quad \dots \quad 9.6b.$$

By denoting zero level (0 db.) as  $20 \log_{10} A_m$  we can express the reduction in amplification over the low and high frequency ranges as

$$\begin{aligned} -20 \log_{10} \left| \frac{A_m}{A_l} \right| &= -10 \log_{10} \left( 1 + \left( \frac{X'}{R'} \right)^2 \right) \text{ db.} \\ &= -10 \log_{10} \left( 1 + \frac{1}{x^2} \right) \text{ db.} \quad \dots \quad 9.4c \end{aligned}$$

and 
$$\begin{aligned} -20 \log_{10} \left| \frac{A_m}{A_h} \right| &= -10 \log_{10} \left( 1 + \left( \frac{R''}{X''} \right)^2 \right) \text{ db.} \\ &= -10 \log_{10} (1 + x^2) \text{ db.} \quad \dots \quad 9.6c. \end{aligned}$$

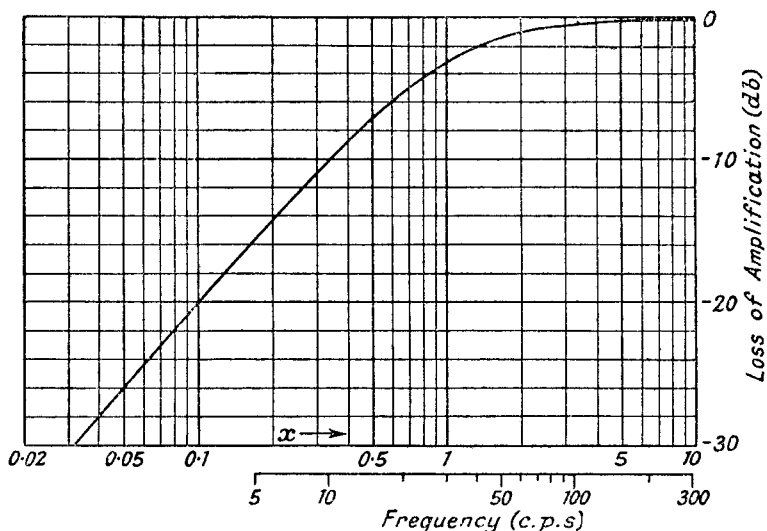


FIG. 9.5a.—Generalised Low Frequency Response of a Resistance-Capacitance Coupled A.F. Amplifier.

The negative sign in expressions 9.4c and 9.6c denote that it is a loss of amplification. From these two expressions we may plot two generalised amplification curves of frequency response (db.) against



$x\left(\frac{R'}{X'} \text{ and } \frac{R''}{X''}\right)$  to a logarithmic scale as in Figs. 9.5*a* and 9.5*b*.

Since these two ratios,  $\frac{R'}{X'}$  and  $\frac{R''}{X''}$ , are both directly proportional to frequency, we can find the frequency response of any amplifier by suitably positioning a logarithmic scale, marked in frequency, beneath the  $x$  scale in a similar manner to the method described in Sections 4.2.3 and 7.4 (Part I).

Taking as an example the following values for the constants of an amplifier

$$R_0 = 200,000 \Omega$$

$$R_a = 50,000 \Omega$$

$$R_g = 1 \text{ M}\Omega$$

$$C_c = 0.005 \mu\text{F}$$

$$C_s = 0.0005 \mu\text{F}$$

$$R' = R_g + \frac{R_a R_0}{R_a + R_0} = 1.04 \times 10^6 \Omega$$

$$R'' = \frac{R_a R_0 R_g}{R_0 R_g + R_a (R_0 + R_g)}$$

$$= 3.84 \times 10^4 \Omega.$$

For the low frequency response  $\frac{R'}{X'} = 1$  when  $R'2\pi f C_c = 1$

or  $f = 30.6 \text{ c.p.s.}$

The logarithmic frequency scale is therefore moved until 30.6 c.p.s. is located immediately beneath  $x = 1$  as shown in Fig. 9.5*a*, and the response at any frequency is read directly. Thus at 50 c.p.s. the response is  $-1.4 \text{ db.}$ , whilst at 100 and 25 c.p.s. it is  $-0.4$  and  $-3.95 \text{ db.}$  respectively.

For the high frequency response  $\frac{R''}{X''} = 1$ ,

$$\text{when } f = \frac{1}{2\pi C_s R''}$$

$$= 8,280 \text{ c.p.s.}$$

The frequency scale is moved until 8,280 c.p.s. is located immediately beneath  $x = 1$  (see Fig. 9.5*b*) and the response at any particular frequencies such as 5,000 and 10,000 c.p.s. is noted to be  $-1.35$  and  $-3.9 \text{ db.}$  respectively. The complete frequency response of this amplifier over the frequency range 30 to 18,000 c.p.s. is obtained by joining the two curves for the low and high frequency sections.

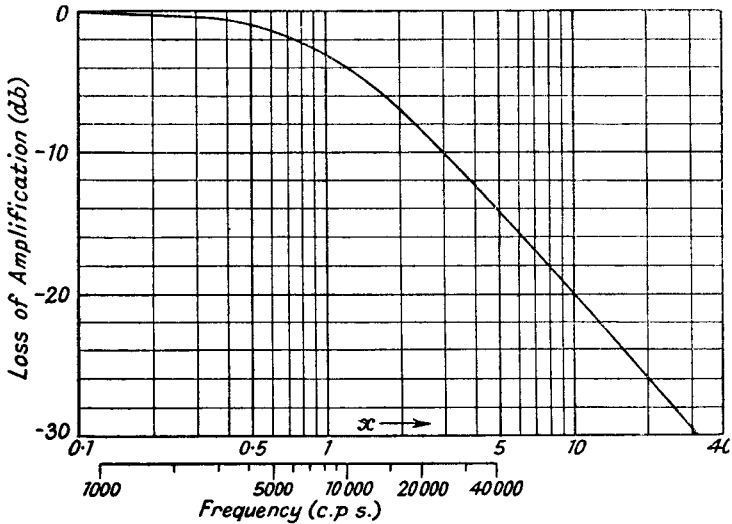


FIG. 9.5b.—Generalised High Frequency Response of a Resistance-Capacitance Coupled A.F. Amplifier.

The maximum overall amplification of the amplifier (in the middle range of frequencies) may be calculated from expression 9.2b, and it is conveniently expressed in terms of the amplification factor of the valve as

$$\frac{A_m}{\mu} = \frac{1}{1 + \frac{R_a}{R_o'}} \quad \dots \quad 9.2c.$$

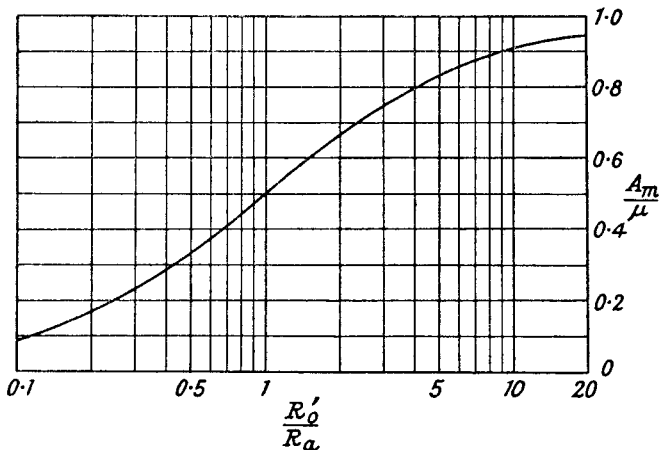


FIG. 9.6.—The Variation of Medium Frequency Amplification with Change of Anode Load Resistance.



The latter has an important bearing on high frequency response, because it increases the grid input capacitance by an amount equal to the grid-anode capacitance multiplied by  $(1+A)$ , where  $A$  is the amplification from the grid to the anode of the valve. For example, average values of  $C_{ga}$  and  $A$  for a triode valve are  $3 \mu\mu\text{F}$  and 50, respectively, giving a grid input capacitance, additional to the "cold" input capacitance of  $3 \times 51 = 153 \mu\mu\text{F}$ ; average values for a tetrode are  $0.01 \mu\mu\text{F}$  and 100, respectively, giving an additional input capacitance of  $0.01 \times 101 = 1.01 \mu\mu\text{F}$ . Hence the use of a tetrode contributes to an improved high frequency response from the stage preceding it, because it reduces the stray capacitance  $C_s$ . The chief disadvantages of a tetrode are greater

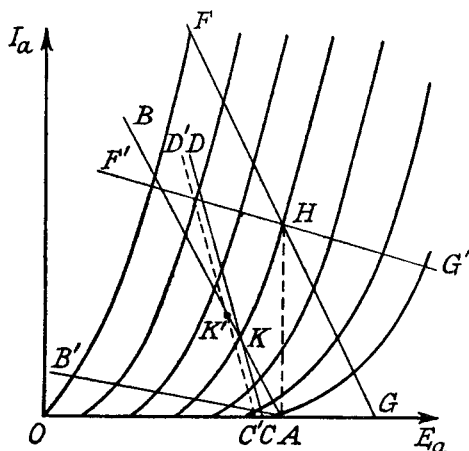


FIG. 9.7.—The Representation of Load Resistance on the  $I_a E_a$  Characteristics of a Triode Valve.

circuit complication (a screen resistance and capacitance are required) and the more objectionable type of distortion, consisting of higher order harmonics and intermodulation products (see Section 10.7).

The reason for the smaller distortion (of lower order harmonics) produced by the triode can be seen by referring to the  $I_a E_a$  characteristic curves in Fig. 9.7. The anode load resistance  $R_o$  is represented by the straight line  $AB$  starting from an anode voltage equal to the total H.T. voltage to the stage (if there is no decoupling resistance). The angle of  $AB$  to the  $E_a$  axis is determined by the value of  $R_o$ , a large value being represented by a line of lower slope such as  $AB'$ . Maximum harmonic distortion for a fixed large input voltage is obtained when  $R_o$  is small; the output voltage

wave shape is flattened at the high  $E_a$  end where the load line enters the cramped part of the  $I_a E_a$  characteristics and is peaked at the low  $E_a$  end. This type of wave is shown in Fig. 9.2a to contain mainly even harmonic (chiefly second) distortion. As  $R_o$  is increased, the top end (low  $E_a$ ) of  $AB$  leaves the region where the  $I_a E_a$  characteristics have opened out, and enters the lower current cramped region, where the intercepts with the constant grid voltage lines are smaller but more equal. Hence distortion progressively falls as  $R_o$  is increased, and at the same time output voltage amplitude tends to increase. The maximum value of  $R_o$  is fixed by the grid leak resistance of the succeeding valve (Section 9.3.3)

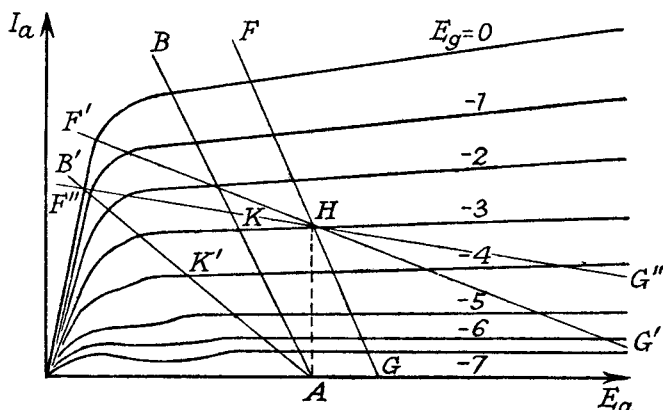


FIG. 9.8.—The Representation of Load Resistance on the  $I_a E_a$  Characteristics of a Tetrode Valve.

and also by high frequency considerations, because the larger  $R_o$  is made the greater is attenuation and phase distortion due to stray capacitance. As pointed out in the previous section the rate of increase of amplification for a constant value of  $\mu$  and  $R_a$  falls as  $R_o$  is increased above  $R_a$ , and there is seldom any advantage in making the ratio of  $\frac{R_o}{R_a}$  greater than 3 to 4.

The effect on harmonic distortion of varying  $R_o$  is different in the case of the tetrode valve. Referring to the tetrode  $I_a E_a$  characteristic curves of Fig. 9.8, we see that a low load resistance (line  $AB$ ) produces an output voltage wave which is flat at high  $E_a$  and peaked at low  $E_a$  values in a manner similar to that for low  $R_o$  with a triode valve. Hence distortion consists mainly of even harmonics. As  $R_o$  is increased the high  $E_a$  end of the output wave tends to become less flat and the low  $E_a$  end less peaked;

a value of  $R_0$  is eventually reached when the output wave has both ends flattened to almost the same degree. The resulting symmetrically shaped wave, as shown in Fig. 9.2*b*, contains chiefly odd higher harmonics, and intermodulation products are produced if more than one frequency is present at the input. A further increase in  $R_0$  flattens the low  $E_a$  part of the output wave, which now enters the very cramped "knee" of the characteristic, and opens out the opposite end. This results in the reappearance of even harmonics; odd harmonics are also increased in amplitude. Reduced harmonic distortion and increased amplification are realized for high values of  $R_0$  by increasing grid bias so as to bring the low  $E_a$  part of the output voltage away from the knee. For example, in Fig. 9.8, greater amplification with less distortion is obtained for  $R_0$  corre-

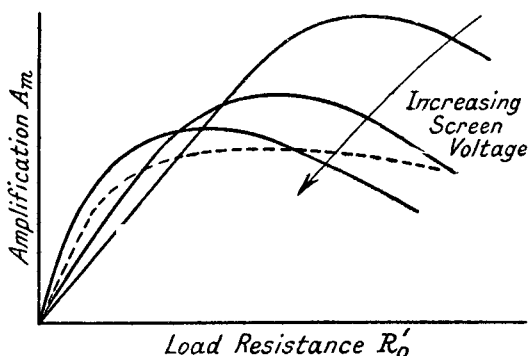


FIG. 9.9.—The Effect of Screen Voltage on the Amplification at Medium Frequencies of a Tetrode A.F. Amplifier with Resistance-Capacitance Coupling.

sponding to line  $AB'$  by increasing the bias from  $-3$  to  $-4$  volts (point  $K'$ ). Thus we see that, unlike the triode, the tetrode has for maximum amplification an optimum bias, which increases with increase of  $R_0$ . If the bias voltage is fixed, an optimum value of  $R_0$  is found for maximum amplification; this optimum value depends on screen voltage and it increases as the latter is decreased. Usually there is an optimum screen voltage for maximum possible amplification, and Fig. 9.9 gives curves of amplification against  $R_0$  for three values of screen voltage. For low values of  $R_0$ , expression 9.2*e* is applicable and maximum amplification is determined solely by  $g_m$ , the greater this is the greater is amplification, i.e., a high screen voltage is required. For high values of  $R_0$  maximum amplification is determined by  $g_m$  and  $R_a$ , increase of both increasing amplification (expression 9.2*d*). Increase of screen voltage generally causes  $R_a$  to

fall and it falls at a greater rate than  $g_m$  increases. Hence greatest amplification is obtained with low screen voltages.

The optimum value of grid bias is often greater than that of a triode of similar  $g_m$ , and maximum permissible output voltage is obtained without the positive peak of the input voltage approaching close to the bias voltage at which grid current starts, i.e., it is the knee of the  $I_a E_a$  characteristics which limits input voltage rather than grid current. With triodes of high  $\mu$ , optimum bias is the lowest consistent with zero grid current on peak signals, and the bias must be adjusted to be able to deal with the valve having the most negative start of grid current. This type of triode tends to show considerable variation of anode current cut-off from valve to valve, so that fairly large changes of amplification are likely to be experienced between valves.

Summarising, we may say that the triode is the better type of valve for audio frequency amplification because the harmonic distortion it produces can be made small and is, in any case, less objectionable than that from a tetrode. Attenuation distortion due to its greater input capacitance need not present a serious problem because the highest required frequency is 20,000 c.p.s.

### 9.3.3. The Grid Leak and its Effect on the Anode Load.

The grid leak resistance  $R_g$  in Fig. 9.3 is only in parallel with  $R_0$  as far as the A.C. load is concerned, so that if  $R_0'$  is very much less than  $R_0$  we must represent this condition by two lines on the  $I_a E_a$  characteristics as described in Section 2.6, Part I. This is shown in Fig. 9.7 by the two lines  $AB$  and  $CD$ , the former is the D.C. load line corresponding to  $R_0$ , whilst the latter is the A.C. load line corresponding to  $R_0' = \frac{R_0 R_g}{R_0 + R_g}$ . The point  $K$ , the intersection

between  $AB$  and  $CD$  for small A.C. grid voltages, is the intersection of the D.C. load line  $AB$  and the normal operating bias line. If, however, the A.C. grid voltage is large enough to take the anode current down to the curved part of the characteristics, the output wave is flattened, i.e., partially rectified, and the D.C. anode current is increased so that the A.C. operating line is centred at  $K'$  instead of at  $K$ . The chief effect of the difference between the A.C./D.C. load lines is that distortion is increased for large input signal voltages, and output voltage is decreased; it is important therefore to make the ratio A.C./D.C. load resistance as near unity as possible.

The maximum permissible value of  $R_g$  is determined by the succeeding valve. If it is a voltage amplifier, the safe limit is usually from 1 to 2 M $\Omega$ , whereas the limit may be as low as 0.1 M $\Omega$  for

a large power-output valve, if softness (Section 2.8.1, Part I) is to be avoided. A  $RC$  coupled amplifier stage connected to a large power-output valve cannot therefore be designed with a very high effective load resistance, for it is inadvisable to make the ratio of A.C./D.C. load ( $R_o'/R_o$ ) less than about 0.8.

**9.3.4. Self Bias for a  $RC$  Coupled Amplifier.** A valve with an indirectly heated cathode can be made to provide its own grid bias voltage by inserting a resistance ( $R_k$ ) between the cathode and H.T. negative line as in Fig. 9.3. The D.C. anode current component flowing through  $R_k$  produces a positive voltage between the cathode and H.T. negative, and since the grid leak is returned to H.T. negative it means that the grid is biased negatively with respect to the cathode. The cathode resistance  $R_k$  must be by-passed by a large capacitor  $C_k$  in order to prevent A.F. voltages being developed across  $R_k$  by the A.C. components of the anode current. A.C. voltages developed across this resistance are in opposition to the grid voltages producing them, and overall amplification may be seriously reduced. This can be seen by considering the applied grid voltage as increasing positively; this increases the anode current and the voltage across  $R_k$ , so that the net positive increase in grid-to-cathode voltage, the difference between the positive increase of the input voltage and the positive increase of cathode voltage, may therefore be quite small. The insertion of  $R_k$  without a by-pass capacitor is a form of current negative feedback (see Section 10.10.4).

The capacitor  $C_k$  clearly cannot be equally effective at all frequencies, and negative feedback occurs at the lower end of the frequency range due to an increase in its reactance. Its influence on the overall frequency response can be calculated as follows:

Neglecting the effect\* of  $C_c$  and  $C_s$ , the output voltage (see Fig. 9.4a)

$$E_{g2} = \frac{\mu E_{gk} R_o'}{R_a + R_o' + Z_k} \quad \dots \quad 9.7a$$

where  $E_{gk}$  = net A.F. voltage input from grid to cathode.

$$R_o' = \frac{R_o R_g}{R_o + R_g}$$

$Z_k$  = impedance of the self-bias circuit

but  $E_{gk} = E_{g1} - E_k$

\*  $C_s$  normally has little influence as its reactance is important only at frequencies where  $C_k$  has no effect. If  $C_c$  is small enough for its reactance to be greater than  $R_g$  over the frequency range affected by  $C_k$ ,  $R_o'$  in expression 9.7a should be replaced by  $R_o$ .



where  $E_{g1}$  = input voltage from grid to earth (Fig. 9.3)  
and  $E_k$  = voltage developed across  $Z_k$ .

$$\text{but } E_k = \frac{\mu E_{gk} Z_k}{R_a + R_o' + Z_k}$$

$$\therefore E_{gk} = \frac{E_{g1}(R_a + R_o' + Z_k)}{R_a + R_o' + Z_k(1 + \mu)}$$

Replacing this in 9.7a

$$E_{g2} = \frac{\mu E_{g1} R_o'}{R_a + R_o' + Z_k(1 + \mu)} \quad . \quad . \quad . \quad 9.7b.$$

$$\text{Amplification with feedback} = A_f = \frac{E_{g2}}{E_{g1}}$$

$$= \frac{\mu R_o'}{R_a + R_o' + Z_k(1 + \mu)}$$

$$\text{Normal amplification without feedback} = A_m = \frac{\mu R_o'}{R_a + R_o'}$$

The ratio loss of amplification due to feedback is therefore

$$\frac{A_m}{A_f} = \left( 1 + \frac{Z_k(1 + \mu)}{R_a + R_o'} \right) \quad . \quad . \quad . \quad 9.8a.$$

Replacing  $Z_k$  in 9.8a by  $\frac{R_k}{1 + jpC_k R_k}$ , we have

$$\frac{A_m}{A_f} = 1 + \frac{R_k(1 + \mu)}{(R_a + R_o')(1 + jpC_k R_k)}$$

$$= \frac{1 + \frac{R_k(1 + \mu)}{R_a + R_o'} + jpC_k R_k}{1 + jpC_k R_k}$$

$$\left| \frac{A_m}{A_f} \right| = \sqrt{\frac{\left( 1 + \frac{R_k(1 + \mu)}{R_a + R_o'} \right)^2 + (pC_k R_k)^2}{1 + (pC_k R_k)^2}} \quad . \quad . \quad . \quad 9.8b$$

The loss in amplification (db.) is  $-20 \log_{10} \left| \frac{A_m}{A_f} \right|$

$$= -10 \log_{10} \left[ \frac{B^2 + x^2}{1 + x^2} \right] \quad . \quad . \quad . \quad 9.8c$$

where  $x = pC_k R_k = \frac{R_k}{X_k}$

and  $B = 1 + \frac{R_k(1 + \mu)}{R_a + R_o'}$ .

Expression 9.8c is plotted in Fig. 9.10 against  $x$ , i.e.,  $\frac{R_k}{X_k}$ , to a

logarithmic scale for different values of  $B$ . As  $x$  increases, i.e.,  $C_k$  becomes more effective as a by-pass, the loss of amplification decreases to zero, but when it decreases, the loss tends to the value which would be realized with  $C_k = 0$ .

This value depends on  $B$  and is given from 9.8c as

$$\text{loss} = -20 \log_{10} B = -20 \log_{10} \left[ 1 + \frac{1+\mu}{R_a+R_0'} \cdot R_k \right] \quad 9.8d.$$

For a particular value of  $R_k$ , the loss is increased when  $\mu$  is increased, or  $R_a$  or  $R_0'$  decreased. Expression 9.8d for a pentode amplifier becomes  $20 \log_{10} (1+g_m R_k)$ , since  $\mu \gg 1$  and  $R_a \gg R_0'$ .

The curves in Fig. 9.10 are generalized curves, and the frequency response may be determined by suitably locating (as for Figs. 9.5a and 9.5b) a logarithmic frequency scale beneath the  $x$  scale. We shall illustrate this by the following example.

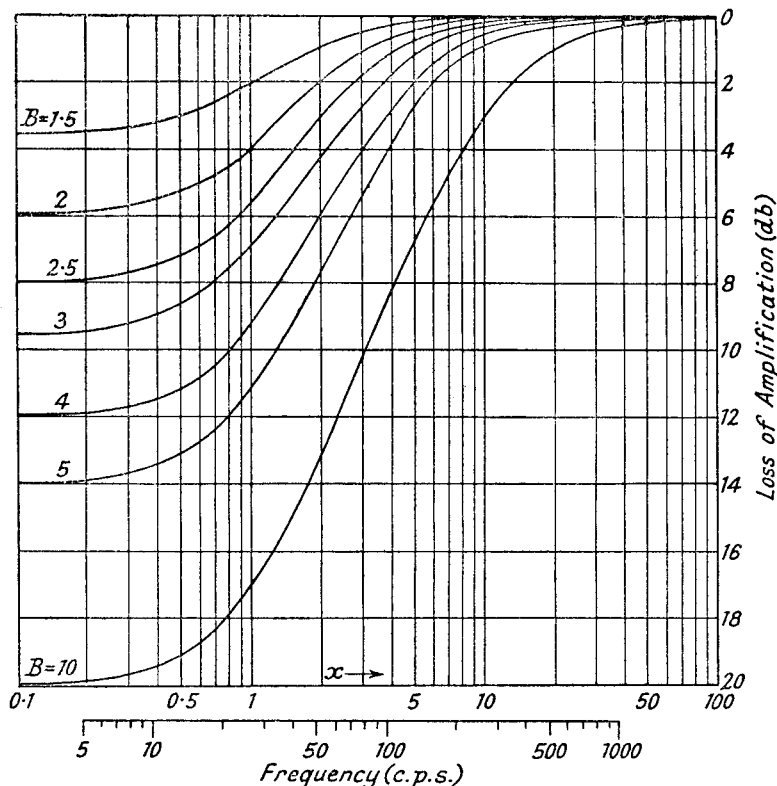


Fig. 9.10.—Generalised Curves for the Frequency Response of an A.F. Amplifier with Cathode Self Bias and Resistance-Capacitance Coupling.

$$R_0 = 200,000 \Omega, R_a = 50,000 \Omega, R_g = 1 \text{ M}\Omega, \mu = 100, \\ R_k = 3,000 \Omega, C_k = 2\mu\text{F}, R_o' = 166,666 \Omega.$$

$$\frac{\mu+1}{R_a+R_o'} = \frac{101}{216,666} = 4.65 \times 10^{-4}$$

$$B = 2.395.$$

$$\text{When } \frac{R_k}{X_k} = 1, f = \frac{10^6}{2\pi \times 2 \times 3,000} = 26.5 \text{ c.p.s.}$$

The logarithmic frequency scale is adjusted beneath the  $x$  scale as in Fig. 9.10, so that 26.5 c.p.s. locates with  $x = 1$ , and the frequency response due to self bias is then read by interpolating between the  $B = 2$  and  $B = 2.5$  curves. Thus at frequencies of 20 and 50 c.p.s. the loss is approximately  $-6.1$  and  $-3.0$  db. respectively.

The value of  $R_k$  required for any set of operating conditions is obtained by drawing the D.C. load line on the  $I_a E_a$  characteristic curves and estimating by inspection the bias voltage which gives maximum voltage output with minimum distortion. The locus of operation should be over that part of the load line which makes equal intercepts with lines of constant grid voltage difference; at the same time it must not be allowed to pass beyond the start of grid current. The ratio of the bias voltage, finally selected, to the anode current at the intersection of the load line with this bias voltage curve gives the required value of  $R_k$ . In many cases  $R_k$  will be a non-standard value and it is usual to select the nearest standard value. For a triode amplifier it is preferable to take the nearest lower standard value of  $R_k$ , since this reduces bias and takes the locus of operation further from the cramped low anode current region producing distortion. This does not necessarily apply to a pentode because cramping may occur at high as well as low anode current. The D.C. load line should be drawn for  $R_0 + R_k$ , but  $R_k$  is so much less than  $R_0$  that its effect may usually be neglected.

The total overall frequency response, including the effect of  $C_s$  and  $C_c$ , is obtained by adding the loss due to these two capacitances, as found from Figs. 9.5a and 9.5b, at the appropriate frequencies. Some error is introduced at the low frequencies due to the assumption in the above analysis that the reactance of  $C_c$  is small compared with  $R_g$ , but the effect will not usually be very serious and can be overcome by replacing  $R_o'$  by  $R_0$  in the above expressions.

**9.3.5. The Effect of the Screen Decoupling Circuit on the Frequency Response of a Tetrode Amplifier.** The screen

decoupling circuit of a tetrode amplifier has a capacitance to earth acting as a by-pass for audio frequencies. A voltage in this circuit (see Fig. 9.11), due to variations in screen current produced by the input grid voltage, tends to reduce the gain of the amplifier. Since the reactance of this capacitance increases with decrease of frequency, the effect is greatest at lowest frequencies, and is similar to that due to the rising reactance of the self-bias capacitor. For calculating the reduction in frequency response we shall take the fundamental equations for screen and anode currents, which are as follows :

$$\Delta I_a = g_m \Delta E_g + g_s \Delta E_s + g_a \Delta E_a \quad . \quad . \quad . \quad 9.9$$

$$\Delta I_s = G_m \Delta E_g + G_s \Delta E_s + G_a \Delta E_a \quad . \quad . \quad . \quad 9.10$$

where

$$g_m = \frac{\partial I_a}{\partial E_g}, \quad g_s = \frac{\partial I_a}{\partial E_s}, \quad g_a = \frac{\partial I_a}{\partial E_a} = \frac{1}{R_a},$$

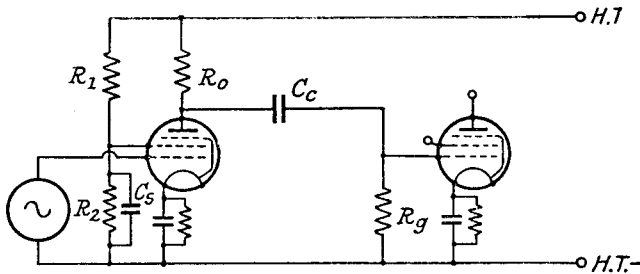


FIG. 9.11.—A Tetrode A.F. Amplifier with Resistance-Capacitance Coupling.

[Note : for  $C_s$  read  $C_s''$ .]

and  $G_m, G_s, G_a$ , are similar derivatives of  $I_s$  with respect to the voltages. The voltage changes  $\Delta E_a$  and  $\Delta E_s$  are those produced across the anode-cathode and screen-cathode circuit and, when they are caused by changes of  $I_a$  and  $I_s$ , are in such a direction as to oppose the current changes, i.e., increasing  $I_a$  and  $I_s$  causes a reduction in anode and screen voltage. Hence

$$\Delta E_a = - \Delta I_a Z_0 \quad . \quad . \quad . \quad 9.11.$$

$$\Delta E_s = - \Delta I_s Z_s' \quad . \quad . \quad . \quad 9.12$$

$Z_s'$  is the total impedance of the external screen circuit,  $\frac{R_s'}{1 + j\omega C_s'' R_s'}$ .

where  $R_s'$  = the equivalent A.C. resistance component in the screen circuit, which may be made up of a potential divider for D.C. voltages consisting of two resistances  $R_1$  and

$R_2$ . These two resistances, in series for D.C., are in parallel as far as A.C. is concerned.

$$= \frac{R_1 R_2}{R_1 + R_2}$$

$C_s''$  = the decoupling capacitance to earth in the screen circuit.

Combining 9.9, 9.10, 9.11 and 9.12.

$$\Delta I_a(1 + g_a Z_0) = g_m \Delta E_g - g_s \Delta I_s Z_s'$$

$$\Delta I_s(1 + G_s Z_s') = G_m \Delta E_g - G_a \Delta I_a Z_0$$

$$\Delta I_a(1 + g_a Z_0) = g_m \Delta E_g - \frac{g_s Z_s' (G_m \Delta E_g - G_a \Delta I_a Z_0)}{1 + G_s Z_s'}$$

$$\therefore \frac{\Delta I_a}{\Delta E_g} = \frac{g_m(1 + G_s Z_s') - g_s G_m Z_s'}{(1 + g_a Z_0)(1 + G_s Z_s') - g_s G_a Z_0 Z_s'}$$

$$\text{Amplification } A = \frac{\Delta I_a Z_0}{\Delta E_g} = \frac{Z_0 [g_m(1 + G_s Z_s') - g_s G_m Z_s']}{(1 + g_a Z_0)(1 + G_s Z_s') - g_s G_a Z_0 Z_s'} \quad 9.13.$$

When  $Z_s' = 0$

$$A_0 = \frac{g_m Z_0}{1 + g_a Z_0} = \frac{\mu Z_0}{R_a + Z_0}$$

$$\frac{A_0}{A} = \frac{1 + Z_s' \left( G_s - \frac{g_s G_a Z_0}{1 + g_a Z_0} \right)}{1 + Z_s' \left( G_s - \frac{g_s G_m}{g_m} \right)} = \frac{1 + j p C_s'' R_s' + R_s' \left( G_s - \frac{g_s G_a Z_0}{1 + g_a Z_0} \right)}{1 + j p C_s'' R_s' + R_s' \left( G_s - \frac{g_s G_m}{g_m} \right)} \quad 9.14a.$$

$$\text{If } Z_0 = R_0' = \frac{R_0 R_g}{R_0 + R_g}$$

$$\frac{A_0}{A} = \sqrt{\frac{B^2 + p^2 R_s'^2 C_s''^2}{D^2 + p^2 R_s'^2 C_s''^2}} \quad 9.14b$$

where

$$B = 1 + R_s' \left( G_s - \frac{g_s G_a R_0'}{1 + g_a R_0'} \right)$$

and

$$D = 1 + R_s' \left( G_s - \frac{g_s G_m}{g_m} \right).$$

But

$$\frac{G_m}{g_m} = \frac{\partial I_s}{\partial I_a} = \frac{G_s}{g_s} = \frac{G_a}{g_a}$$

$$\begin{aligned} \text{so that } B &= 1 + R_s' G_s \left( 1 - \frac{g_a R_0'}{1 + g_a R_0'} \right) \\ &= 1 + \frac{R_s' G_s}{1 + g_a R_0'} \end{aligned}$$

$$= 1 + \frac{\frac{R_s'}{R_{sg}}}{1 + \frac{R_0'}{R_a}} = 1 + \frac{R_s' R_a}{R_{sg}(R_a + R_0')}$$

and  $D = 1$

where  $R_{sg} = \frac{1}{G_s} = \frac{\Delta E_s}{\Delta I_s}$  = slope of the  $E_s I_s$  characteristic.

If  $R_0' \ll R_a$  then  $B = 1 + \frac{R_s'}{R_{sg}}$ .

$$\begin{aligned} \text{The loss of amplification is given by } & -20 \log_{10} \left| \frac{A_0}{A} \right| \\ & = -10 \log_{10} \left[ \frac{B^2 + p^2 C_s''^2 R_s'^2}{1 + p^2 C_s''^2 R_s'^2} \right] \quad . \quad . \quad . \quad 9.15a \\ & = -10 \log_{10} \left[ \frac{B^2 + x^2}{1 + x^2} \right] \quad . \quad . \quad . \quad . \quad 9.15b \end{aligned}$$

where  $x = p C_s'' R_s' = \frac{R_s'}{X_s'}$ .

This expression is identical in form to that of expression 9.8c and the generalized curves of Fig. 9.10 may be used as long as we note that  $x$  is  $\frac{R_s'}{X_s'}$  and  $B = 1 + \frac{R_s' R_a}{R_{sg}(R_a + R_0')}$ . The loss tends to become asymptotic to a value  $-10 \log_{10} B^2$  as the frequency is decreased and  $X_s'$  increased.

$$\text{Hence } \quad \text{max. loss (db.)} = -20 \log_{10} \left[ 1 + \frac{R_s' R_a}{R_{sg}(R_a + R_0')} \right] \quad . \quad 9.15c.$$

**9.3.6. The Effect of the Anode Decoupling Circuit on the Frequency Response of an A.F. Amplifier.** The reactance of the smoothing capacitance for the H.T. supply of a mains-operated receiver increases with decrease of frequency, and forms a common coupling impedance for the A.F. stages. (An 8- $\mu$ F capacitor has a reactance of 398  $\Omega$  at 50 c.p.s.) Voltages may be produced in this reactance by low-frequency current components from the output stage; other stages can likewise produce voltages, but their effect is much less important because current values are much smaller. These voltage components, if fed back to the grid of the output valve, or of a previous stage, via the preceding anode load connection to the H.T. supply, can either decrease or increase the overall A.F. response to the low frequencies. With RC coupling, the phase of the voltage is such as to cause low frequency degenera-

tion, if fed to the grid of the output valve, or regeneration if fed to the grid of the previous stage. For diode detection and one stage of A.F. amplification before the output valve (the A.F. amplifier grid circuit is not connected to the H.T. supply), the feedback is to the grid of the output valve only, and is degenerative. For two stages of A.F. amplification it is to the grid of the stage preceding the output valve as well, and the effect is predominantly regenerative. In extreme cases it may lead to low frequency oscillation (about 5 to 10 c.p.s.) known as "motorboating".\* Regenerative feedback can occur with one stage of RC coupled A.F. amplification if a cumulative-grid or anode-bend detector is employed, since the grid of the A.F. stage is then directly connected to the H.T. supply via the detector anode load resistance. For transformer-coupled A.F. stages

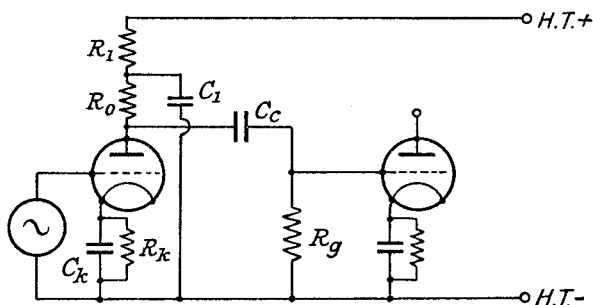


FIG. 9.12.—A Resistance-Capacitance Coupled A.F. Amplifier with an Anode Decoupling Circuit.

the phase of the feedback also depends on the sign of the mutual inductance coupling between the primary and secondary.

To reduce this form of feedback, a resistance-capacitance decoupling filter circuit is almost always included in the anode circuit of each A.F. amplifier as shown by  $R_1C_1$  in the diagram of Fig. 9.12. A similar circuit is also included in all R.F. stages, but resistance and capacitance values are then much smaller, about 1,000  $\Omega$  and 0.1  $\mu\text{F}$  as compared with 5,000  $\Omega$  and 2  $\mu\text{F}$  for A.F. decoupling.

The inclusion of the decoupling circuit  $R_1C_1$  affects the frequency response because it forms with  $R_0$  the anode load impedance of the valve. It tends to raise the amplification at low frequencies. For example, the amplification at medium frequencies, where the reactances of  $C_c$ ,  $C_k$  and  $C_1$ , can be neglected, is

\* The circuit acts as a multivibrator or relaxation oscillator.

$$A_m = \frac{\mu R_g}{R_a + R_g} \cdot \frac{R_0}{\frac{R_a R_g}{R_a + R_g} + R_0}$$

[Note that the alternative Thévenin development (see Appendix 3A) is more convenient and is used here.]

At low frequencies, assuming that the reactance of  $C_c$  is small and can be neglected,

$$A_l = \frac{\mu R_g}{R_a + R_g} \cdot \frac{R_0 + \frac{R_1}{1 + jpC_1 R_1}}{\frac{R_a R_g}{R_a + R_g} + R_0 + \frac{R_1}{1 + jpC_1 R_1}}$$

Replacing  $\frac{R_a R_g}{R_a + R_g} + R_0$  by  $R'$  we have

$$\frac{A_l}{A_m} = \frac{\frac{R_1}{R_0} + 1 + jpC_1 R_1}{\frac{R_1}{R'} + 1 + jpC_1 R_1} = \frac{\left(\frac{R'}{R_1 + R'}\right) \left(\frac{R_1}{R_0} + 1 + jpC_1 R_1\right)}{1 + \frac{jpC_1 R_1 R'}{R_1 + R'}}$$

$$\text{or} \quad \left| \frac{A_l}{A_m} \right| = \sqrt{\frac{\left(\frac{(R_1 + R_0)R'}{(R_1 + R')R_0}\right)^2 + \left(\frac{pC_1 R_1 R'}{R_1 + R'}\right)^2}{1 + \left(\frac{pC_1 R_1 R'}{R_1 + R'}\right)^2}} \quad \dots \quad 9.16a$$

$$= \sqrt{\frac{B^2 + x^2}{1 + x^2}} \quad \dots \quad 9.16b$$

where  $B = \frac{(R_1 + R_0)R'}{(R_1 + R')R_0}$

and  $x = \frac{R_1}{X_1} \cdot \frac{R'}{R_1 + R'} = \frac{pC_1 R_1 R'}{R_1 + R'}$ ,

i.e., low frequency increase in amplification is

$$+20 \log \left| \frac{A_l}{A_m} \right| = +10 \log \left( \frac{B^2 + x^2}{1 + x^2} \right) \text{ db.} \quad \dots \quad 9.16c.$$

Expression 9.16c is identical with 9.8c except for the sign, and the curves plotted in Fig. 9.10 can be used, but the vertical scale now represents a gain instead of a loss of amplification.

Since the decoupling circuit produces the opposite effect from that due to the self-bias capacitor, it is possible to choose values to cancel the loss of amplification due to the self-bias circuit. The conditions for exact compensation are that the values of  $x$  and the values of  $B$  for the two circuits should be equal. The former gives



$$C_k R_k = C_1 R_1 \frac{\frac{R_a R_g}{R_a + R_g} + R_0}{\frac{R_a R_g}{R_a + R_g} + R_0 + R_1} \quad . \quad . \quad . \quad 9.17a$$

and this fixes the position of the horizontal frequency scale.

The second condition is fulfilled by making

$$1 + \frac{R_k(1 + \mu)}{R_a + \frac{R_0 R_g}{R_0 + R_g}} = \frac{(R_1 + R_0) \left( \frac{R_a R_g}{R_a + R_g} + R_0 \right)}{\left( R_1 + R_0 + \frac{R_a R_g}{R_a + R_g} \right) R_0} \quad . \quad . \quad . \quad 9.17b$$

and this ensures that the maximum loss for the cathode circuit is exactly equal to the maximum gain of the anode circuit. Generally it will not be possible to satisfy expression 9.17b unless  $R_0$  is small

compared with  $R_a$  and  $R_1$ . This method of compensation has been employed in the video-frequency amplifiers of television receivers (Section 16.8.3). It may also be used in tone-control circuits when increased amplification is required at low audio frequencies.

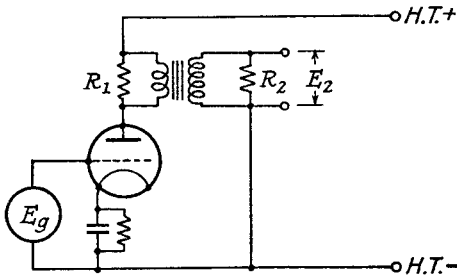


FIG. 9.13a.—A Transformer Coupled A.F. Amplifier.

### 9.4. The Transformer Coupled Amplifier.

Transformer coupling is shown in Fig. 9.13a. The resistances  $R_1$  and  $R_2$  may be included across the primary and secondary in order to improve the frequency response.  $R_1$  reduces the increase of amplification at the medium frequencies caused by the increasing reactance of the primary inductance, whilst  $R_2$  tends to flatten any peak in the high-frequency response due to resonance between the leakage inductance and stray capacitance across the secondary. The equivalent circuit of Fig. 9.13b indicates the separate impedances making up the transformer circuit, thus

$C_{aE}$  = anode-earth capacitance of the valve

$C_p$  = self-capacitance of primary of the transformer

$R_{hc}$  = resistance simulating the hysteresis and eddy current losses in the core

$R_p$  = A.C. resistance of the primary winding, for all practical purposes this is the D.C. resistance of the primary winding

$L_p$  = inductance of primary

$C_w$  = interwinding capacitance

$n$  = ratio of secondary to primary turns

$M$  = mutual inductance between primary and secondary =  $k\sqrt{L_p L_s}$

$k$  = coupling coefficient

$R_s$  = A.C. resistance of the secondary winding, approximately the  
D.C. resistance of the secondary winding

$L_s$  = inductance of secondary

$C_s$  = self-capacitance of secondary

$C_g$  = input capacitance of the next stage

$R_g$  = input resistance of the next stage.

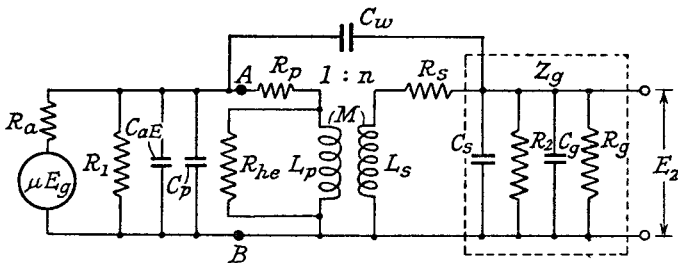


FIG. 9.13b.—The Equivalent Circuit for a Transformer Coupled A.F. Amplifier.

Generally  $C_{aE}$ ,  $C_p$ ,  $C_w$  and  $R_{he}$  have very small effects and will be neglected. For analysis it is convenient to transfer the secondary impedances to the primary side and include at the output a perfect

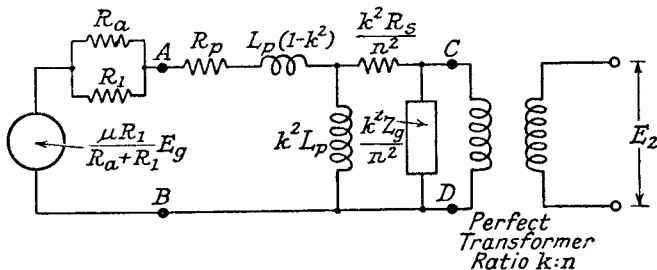


FIG. 9.13c.—A Simplified Diagram for a Transformer Coupled A.F. Amplifier.

transformer having a primary to secondary turns ratio of  $k$  to  $n$ . This is shown in Fig. 9.13c. That this circuit is equivalent to Fig. 9.13b can be proved by noting from Section 7.6 (Part I) that the impedance reflected from the secondary into the primary in

series with  $R_p$  and  $L_p$  is  $\frac{p^2 M^2}{R_s + jpL_s + Z_g}$ ; where  $Z_g$  is the impedance of  $C_s$ ,  $R_2$ ,  $R_g$  and  $C_g$  in parallel. Hence the total impedance across points  $AB$  in Fig. 9.13*b* is (neglecting  $C_{aE}$ ,  $C_p$ ,  $C_w$ , and  $R_{he}$ )

$$Z_{AB} = R_p + jpL_p + \frac{p^2 M^2}{R_s + jpL_s + Z_g} \quad . \quad . \quad . \quad 9.18.$$

The impedance across the same points  $AB$  in Fig. 9.13*c* is

$$\begin{aligned} Z_{AB} &= R_p + jpL_p(1 - k^2) + \frac{jpL_p k^2 \cdot \frac{(R_s + Z_g)k^2}{n^2}}{jpL_p k^2 + \frac{(R_s + Z_g)k^2}{n^2}} \\ &= R_p + jpL_p + \frac{p^2 L_p^2 k^2 n^2}{n^2 jpL_p + (R_s + Z_g)} \end{aligned}$$

but  $k = \frac{M}{\sqrt{L_p L_s}}$ , and  $n = \sqrt{\frac{L_s}{L_p}}$

$$\therefore Z_{AB} = R_p + jpL_p + \frac{p^2 M^2}{R_s + jpL_s + Z_g}$$

which is identical with 9.18.

From Section 7.3 (Part I) the secondary voltage developed across  $Z_g$  in Fig. 9.13*b* is (neglecting  $C_{aE}$ ,  $C_p$ ,  $C_w$  and  $R_{he}$ ),

$$E_2 = \frac{Z_3 Z_5 E}{Z_3(Z_4 + Z_5) + Z_2(Z_3 + Z_4 + Z_5)} = \frac{Z_3 Z_5 E}{(Z_2 + Z_3)(Z_3 + Z_4 + Z_5) - Z_3^2}$$

where  $E = E_{AB}$ ,  $Z_2 = R_p + jp(L_p - M)$ ,  $Z_3 = jpM$ ,

$Z_4 = R_s + jp(L_s - M)$ , and  $Z_5 = Z_g$ .

$$\therefore E_2 = \frac{jpM \cdot Z_g \cdot E_{AB}}{(R_p + jpL_p)(R_s + jpL_s + Z_g) + p^2 M^2} \quad . \quad . \quad . \quad 9.19a.$$

The secondary voltage, from Fig. 9.13*c*, is

$$\begin{aligned} E_2 &= \frac{n}{k} E_{CD} = \frac{n}{k} \cdot \frac{Z_g}{R_s + Z_g} \cdot \frac{jk^2 pL_p (R_s + Z_g) \frac{k^2}{n^2} E_{AB}}{\left[ jk^2 pL_p + (R_s + Z_g) \frac{k^2}{n^2} \right] Z_{AB}} \\ &= \frac{jknpL_p Z_g E_{AB}}{(jpL_s + R_s + Z_g) Z_{AB}} \quad . \quad . \quad . \quad 9.19b. \end{aligned}$$

Replacing  $Z_{AB}$  in the above by 9.18 and noting that  $knpL_p = pM$

$$E_2 = \frac{jpMZ_g E_{AB}}{(R_p + jpL_p)(R_s + Z_g + jpL_s) + p^2 M^2}.$$



Rewriting the above in terms of maximum possible amplification,  $\frac{n\mu R_1}{R_a + R_1}$ ,

$$\frac{A_m}{n\mu'} = \frac{1}{R_a' + \frac{R_s}{n^2} + 1 + \frac{R_{2t}}{n^2}} \quad . \quad . \quad . \quad 9.20b$$

where  $\mu' = \frac{\mu R_1}{R_a + R_1}$ , and  $R_a' = \frac{R_a R_1}{R_a + R_1} + R_p$ .

The similarity between expressions 9.20b and 9.2c can be noted and Fig. 9.6 is applicable when  $n\mu'$  replaces  $\mu$ . An important point is that maximum  $A_m$  is realized when  $R_1$  and  $\frac{R_{2t}}{n^2}$  are infinite. From the point of view of maximum amplification it is preferable to dispense with them. They also reduce the anode load impedance and therefore tend to increase distortion; their inclusion is only

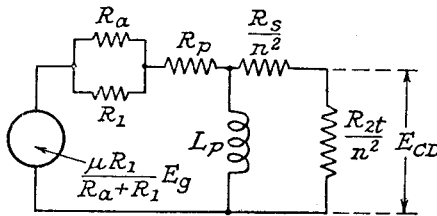


FIG. 9.14b.—The Transformer Coupled A.F. Amplifier at Low Frequencies.

justified for the purpose of improving low- and high-frequency response.

At low frequencies the reactance of the leakage inductance and secondary capacitance can be neglected, but  $L_p$  must be taken into account as its reactance is comparable with  $\frac{R_s + R_{2t}}{n^2}$ , with which it is in parallel. The equivalent circuit is that of Fig. 9.14b. Low-frequency amplification is

$$A_t = \frac{E_2}{E_g} = \frac{nE_{CD}}{E_g} = \frac{n\mu' \frac{R_{2t}}{n^2} j\omega L_p}{R_a' \left( j\omega L_p + \frac{R_s + R_{2t}}{n^2} \right) + j\omega L_p \left( \frac{R_s + R_{2t}}{n^2} \right)} \quad . \quad . \quad . \quad 9.21a$$



a  $RC$  coupling to the transformer, as described in Section 9.5, offers a solution to this difficulty.

The equivalent circuit for the high-frequency range is shown

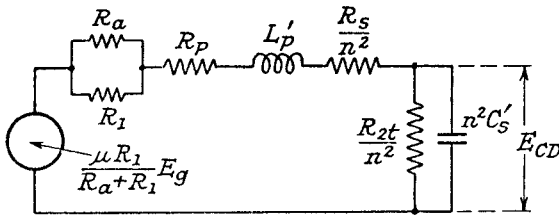


FIG. 9.14c.—The Transformer Coupled Amplifier at High Frequencies.

in Fig. 9.14c. The primary inductive reactance has little effect, but the leakage inductance and total stray capacitance  $C_s'$  across the secondary now have considerable influence. The amplification is

$$A_h = \frac{n\mu' \frac{R_{2t}}{n^2}}{1 + jpC_s' R_{2t}} \frac{\frac{R_{2t}}{n^2}}{R_a' + \frac{R_s}{n^2} + jpL_p' + \frac{R_{2t}}{n^2 + jpC_s' R_{2t}}}$$

where  $L_p' = L_p(1 - k^2)$

$$A_h = \frac{n\mu' \frac{R_{2t}}{n^2}}{\left( R_a' + \frac{R_s}{n^2} + jpL_p' \right) (1 + jpC_s' R_{2t}) + \frac{R_{2t}}{n^2}} \quad . \quad 9.23a.$$

$$1 + \frac{R_a' + \frac{R_s}{n^2}}{\frac{R_{2t}}{n^2}} - p^2 L_p' C_s' n^2 + jp \left( C_s' n^2 \left( R_a' + \frac{R_s}{n^2} \right) + \frac{L_p'}{\frac{R_{2t}}{n^2}} \right)$$

Let  $p_0 = \frac{1}{\sqrt{L_p' C_s' n^2}}$ , the resonant pulsance of  $L_p'$  and  $n^2 C_s'$  and

$$X_0 = p_0 L_p' = \frac{1}{p_0 C_s' n^2}$$

then

$$A_h = \frac{n\mu'}{1 + \frac{R_a' + \frac{R_s}{n^2}}{\frac{R_{2t}}{n^2}} - \left( \frac{p}{p_0} \right)^2 + jp \frac{p_0}{p_0} \left[ \frac{R_a' + \frac{R_s}{n^2}}{X_0} + \frac{X_0}{\frac{R_{2t}}{n^2}} \right]}$$

$$A_m \left( 1 + \frac{R_a' + \frac{R_s}{n^2}}{\frac{R_{2t}}{n^2}} \right) = \frac{R_a' + \frac{R_s}{n^2}}{1 + \frac{R_{2t}}{n^2} - \left(\frac{p}{p_0}\right)^2 + j\frac{p}{p_0} \left[ \frac{R_a' + \frac{R_s}{n^2}}{X_0} + \frac{X_0}{n^2} \right]} \quad 9.23b.$$

Owing to the series resonance of  $L_p'$  and  $C_s'$  there may be a gain or a loss at  $f_0$ , and it is preferable to express the response as

$$\text{Amplification} = 20 \log_{10} \left| \frac{A_h}{A_m} \right| = 10 \log_{10} \frac{\left( 1 + \frac{R_a' + \frac{R_s}{n^2}}{\frac{R_{2t}}{n^2}} \right)^2}{\left[ 1 + \frac{R_a' + \frac{R_s}{n^2}}{\frac{R_{2t}}{n^2}} - \left(\frac{f}{f_0}\right)^2 \right]^2 + \left[ \frac{f}{f_0} \left( \frac{R_a' + \frac{R_s}{n^2}}{X_0} + \frac{X_0}{n^2} \right) \right]^2} \quad 9.24.$$

When expression 9.24 has a positive sign an increase in amplification is obtained at high frequencies, whereas if it has a negative sign there is loss of amplification relative to the medium frequency amplification.

It is difficult to produce a series of generalized curves from expression 9.24 because there are three independent variables  $\frac{f}{f_0}$ ;

$\frac{R_a' + \frac{R_s}{n^2}}{X_0}$  and  $\frac{R_{2t}}{n^2}$ . The amplification (or loss) when  $f = f_0$  is, however, a valuable guide to the high frequency response, and Klipsch<sup>4</sup> has suggested a convenient method of graphing 9.24 when  $f = f_0$ .

He joins points of  $\frac{R_a' + \frac{R_s}{n^2}}{X_0}$  and  $\frac{R_{2t}}{n^2}$ , giving constant loss (-) and amplification (+), as illustrated by the full line curves in Fig. 9.15. For convenience, both parameters are plotted to a tangent scale,

e.g.,  $\frac{R_a' + \frac{R_s}{n^2}}{X_0} = 1 = \tan y$  gives  $y = 45^\circ$ , and  $\frac{R_a' + \frac{R_s}{n^2}}{X_0} = \infty$  gives



$y = 90^\circ$ . Hence the first point is half-way between 0 and  $\infty$ . It is important to note that  $f_0$  is not the frequency of maximum amplification, which is determined by the ratio of the two parameters,

$\frac{R_{2t}}{n^2}$  and always occurs at a frequency lower than  $f_0$ . The  $R_a' + \frac{R_s}{n^2}$  dotted-line curves in Fig. 9.15 join points of constant ratio  $\frac{R_{2t}}{n^2} / R_a' + \frac{R_s}{n^2}$ .

The latter also governs the general shape of the high-frequency response; a low ratio means that the frequency for maximum

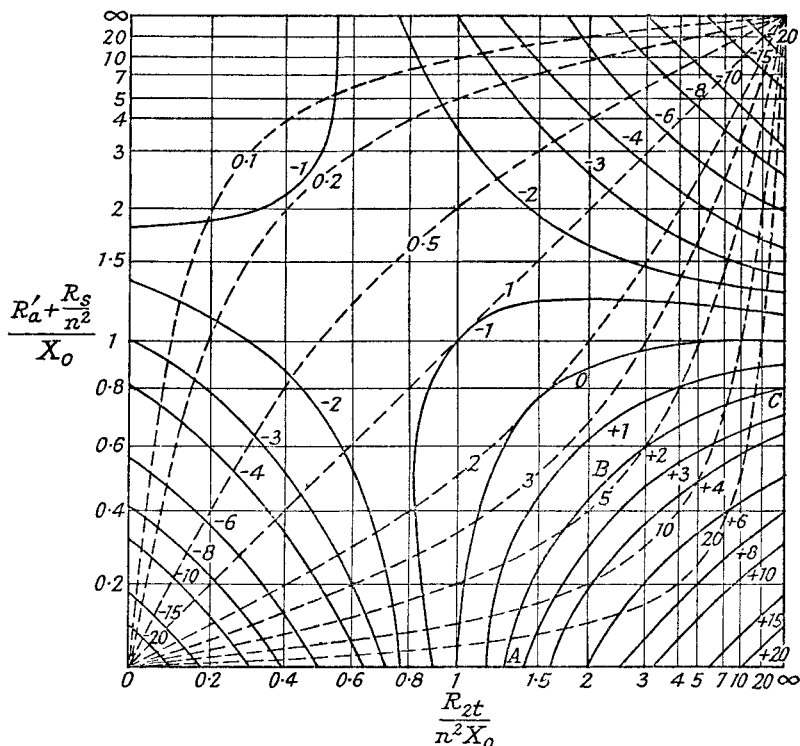


FIG. 9.15.—Loss or Gain in Frequency Response of a Transformer Coupled A.F. Amplifier at the Resonant Frequency of Leakage Inductance and Secondary Stray Capacitance.

Full Lines: Loss (-) or Gain (+) of Amplification (db.).

Dashed Lines: Constant Ratios of  $\frac{R_{2t}}{n^2} / R_a' + \frac{R_s}{n^2}$ .

amplification is close to  $f_0$ , maximum amplification is very little greater than amplification at  $f_0$ , and cut-off above  $f_0$  is not rapid; i.e., the response is generally flat. The converse is also true; a high

ratio of  $\frac{R_{2t}}{n^2}$  means a more peaked high frequency response with sharper cut-off. This is to be expected since  $R_a' + \frac{R_s}{n^2}$  is the series

resistance element in the series resonant circuit, while  $\frac{R_{2t}}{n^2}$  is a parallel resistance element.

To illustrate the use of the curves we shall find values of  $R_1$  and  $R_{2t}$  to give an amplification of +2 db. at  $f_0$  and a loss not exceeding -2 db. at 50 c.p.s., when the transformer and valve characteristics are as follows:

$$L_p = 100 \text{ H}, R_p = 500 \Omega, R_s = 5000 \Omega, n = 3, L_p' = 0.3 \text{ H}, \\ f_0 = 8 \text{ kc/s}, \mu = 30, R_a = 10,000 \Omega.$$

Low frequency response; since  $R_a' = R_p + \frac{R_a R_1}{R_a + R_1}$ ,  $R_a'$  cannot exceed the value for  $R_1 = \infty$ , i.e., 10,500  $\Omega$ . Hence  $R_t$  in expression 9.22b, which consists of  $R_a'$ , and  $\frac{R_s + R_{2t}}{n^2}$  in parallel, must be less than 10,500  $\Omega$ . Now  $X_l = 2\pi \times 50 \times 100 = 31,400 \Omega$ , and if we take the maximum possible value of  $R_t$ , we have  $\frac{X_l}{R_t} = \frac{31,400}{10,500} = 3$ . From Fig. 9.5a we find the loss for  $x = 3$  as -0.5 db., and this is the maximum possible. Hence, whatever value of  $R_t$  is fixed by high-frequency response, the loss at 50 c.p.s. will always be less than -0.5 db. High-frequency response; the

curve for +2 db. gain is ABC in Fig. 9.15 and any values of  $\frac{R_a' + \frac{R_s}{n^2}}{X_0}$

and  $\frac{R_{2t}}{n^2 X_0}$  lying on this curve satisfy the amplification requirement at  $f_0$ . Since the most level high-frequency response may be considered as desirable, we need to choose the lowest ratio value of

$\frac{R_{2t}}{n^2}$ . This, from Fig. 9.15, is seen to be about 4.6 and we will

$$R_a' + \frac{R_s}{n^2}$$

select 5. The latter intersects  $ABC$  at two points,  $\frac{R_{2t}}{n^2 X_0} = 3$  and

1.7 and  $\frac{R_a' + \frac{R_s}{n^2}}{X_0} = 0.6$  and 0.34. Both the ratios for  $\frac{R_a' + \frac{R_s}{n^2}}{X_0}$  are

possible since the maximum value of  $R_a' + \frac{R_s}{n^2}$  is  $10,500 + 555$

$= 11,055 \Omega$ ,  $X_0 = 2\pi \times 8,000 \times 0.3 = 15,080 \Omega$  and  $\frac{R_a' + \frac{R_s}{n^2}}{X_0}$  must

not therefore exceed 0.738. For maximum medium frequency amplification  $R_a'$  and  $\frac{R_{2t}}{n^2}$  require to be as high as possible. We will

therefore choose  $\frac{R_{2t}}{n^2 X_0} = 3$  and  $\frac{R_a' + \frac{R_s}{n^2}}{X_0} = 0.6$ . This gives

$$R_{2t} = 3n^2 X_0 = 27 \times 15,080 = 407,000 \Omega$$

$$R_a' + \frac{R_s}{n^2} = 0.6 X_0 = 9050 \Omega$$

$$R_a' = 8,495 \Omega = R_p + \frac{R_a R_1}{R_a + R_1}$$

$$\therefore R_1 = 39,800 \Omega.$$

Amplification at the medium frequencies is

$$A_m = \frac{n\mu R_1}{(R_a + R_1) \left( 1 + \frac{R_a' + \frac{R_s}{n^2}}{\frac{R_{2t}}{n^2}} \right)}$$

$$= 59.9.$$

Thus values for  $R_1$  and  $R_{2t}$  of 39,800  $\Omega$  and 0.407 M $\Omega$  satisfy the frequency response requirements with the particular valve and transformer constants given, and amplification at medium frequencies is 59.9.

**9.5. The RC Coupled Transformer Amplifier.** Considerable advantages are gained if the d.c. anode current component is by-passed from the transformer primary. Core material of high permeability may be used and the size of transformer for a given primary inductance reduced. This leads to a lower leakage inductance and secondary capacitance, with consequent improvement in

high-frequency response. A resistance or L.F. choke may be employed to carry the D.C. current component, the former is preferable on account of cost, saving of space and absence of iron, which may cause distortion or pick-up hum. Slightly less amplification is generally obtained from the resistance because of the lower D.C. anode voltage and consequently lower  $\mu$  and higher  $R_a$ .

In the typical circuit of Fig. 9.16, the transformer is shown with separated primary and secondary, but auto-transformer action with increased amplification can be obtained by connecting the earthed end of the secondary, point *B*, to the anode end of the primary, point *A*. The formulæ developed in Section 9.4 for high and medium frequency response are unaffected by the coupling capacitance  $C_c$ , since at these frequencies its reactance is negligible in comparison

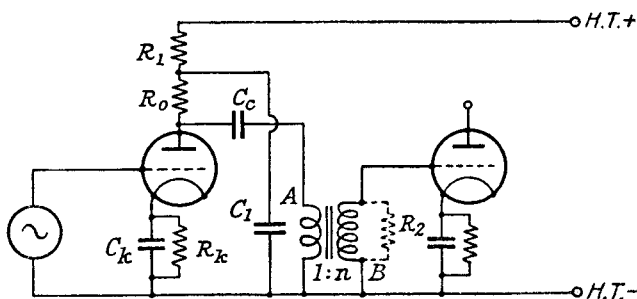


FIG. 9.16.—The RC Transformer Coupled A.F. Amplifier.

with other components. At low frequencies the reactance of  $C_c$  may become comparable with  $X_{L_p}$  and the amplification in expres-

sion 9.21b is modified by replacing  $R_a'$  by  $R_a' + \frac{1}{jpC_c}$  to

$$A_i = \frac{n\mu' \frac{R_{2t}}{n^2}}{\left[ R_a' + \frac{1}{jpC_c} + \frac{R_s + R_{2t}}{n^2} \right] \left[ 1 + \frac{\left( R_a' + \frac{1}{jpC_c} \right) \left( \frac{R_s + R_{2t}}{n^2} \right)}{\left( R_a' + \frac{1}{jpC_c} + \frac{R_s + R_{2t}}{n^2} \right) jpL_p} \right]} = \frac{n\mu' \frac{R_{2t}}{n^2}}{R_a' + \frac{R_s + R_{2t}}{n^2} - \frac{R_s + R_{2t}}{n^2} \left( \frac{p_0'}{p} \right)^2 - j \left[ \frac{X_0' p_0'}{p} + \frac{R_a' (R_s + R_{2t}) p_0'}{n^2 X_0' p} \right]}$$

where  $p_0' = \frac{1}{\sqrt{L_p C_c}}$  and  $X_0' = p_0' L_p = \frac{1}{p_0' C_c}$

$$\frac{A_l}{A_m} = \frac{R_a' + \frac{R_s + R_{2t}}{n^2}}{R_a' + \frac{R_s + R_{2t}}{n^2} - \frac{R_s + R_{2t}}{n^2} \left(\frac{p_0'}{p}\right)^2 - j \frac{p_0'}{p} \left[ X_0' + \frac{R_a' (R_s + R_{2t})}{n^2 X_0'} \right]}$$

The gain (+) or loss (-) in decibels relative to  $A_m$  is

$$20 \log_{10} \left| \frac{A_l}{A_m} \right|$$

$$= 10 \log_{10} \frac{\left[ 1 + \frac{n^2 R_a'}{R_s + R_{2t}} \right]^2}{\left[ 1 + \frac{n^2 R_a'}{R_s + R_{2t}} - \left(\frac{f_0'}{f}\right)^2 \right]^2 + \left[ \frac{f_0'}{f} \left( \frac{X_0' n^2}{R_s + R_{2t}} + \frac{R_a'}{X_0'} \right) \right]^2} \quad 9.25.$$

The above expression is seen to be similar in form to that of expression 9.24, and Fig. 9.15 may be used for calculating the loss or gain at the low frequency  $f_0'$  by considering the vertical axis as scaled in terms of  $\frac{R_a'}{X_0'}$ , and the horizontal in terms of  $\frac{R_s + R_{2t}}{n^2 X_0'}$ .

The values of  $R_0$  and  $R_2$  for a particular low- and high-frequency response at  $f_0'$  and  $f_0$  can be obtained as follows: Suppose both high- and low-frequency responses at  $f_0$  and  $f_0'$  are required to be +2 db. above the amplification at medium frequencies; curve  $ABC$

in Fig. 9.15 gives pairs of values of  $\frac{R_a' + \frac{R_s}{n^2}}{X_0'}$  and  $\frac{R_{2t}}{n^2 X_0'}$ , satisfying

the high-frequency response requirement. Pairs of values of  $\frac{R_a'}{X_0'}$

and  $\frac{R_s + R_{2t}}{n^2 X_0'}$  corresponding to the high-frequency response pairs are

calculated and plotted on a separate transparent sheet scaled according to a tangent law in the same manner as Fig. 9.15. This

curve now represents values of  $\frac{R_a'}{X_0'}$  and  $\frac{R_s + R_{2t}}{n^2 X_0'}$ , which satisfy the

high-frequency response condition of +2 db., and it is placed on top of Fig. 9.15. The point of intersection of the first curve on the

transparent sheet with the +2 db. curve  $ABC$  gives values of  $R_a'$

and  $\frac{R_s + R_{2t}}{n^2}$ , which satisfy both high- and low-frequency response

simultaneously. If the curve does not intersect  $ABC$  the chosen

values of response cannot be realized. A compromise is, however, usually possible giving responses within 1 db. of those required.

It should be noted that there is an upper limit to the value of  $R_0$  because it carries the D.C. anode current component, and it is generally inadvisable to exceed about  $3R_a$ .  $R_a' = \frac{R_a R_0}{R_a + R_0} + R_p$  must be made up bearing this limitation in mind.

## 9.6. Tone Control Circuits.

**9.6.1. Introduction.**<sup>1, 8</sup> Usually an A.F. amplifier is designed to have as little attenuation distortion as possible, but there are occasions when control of frequency response is desirable, and tone control circuits are then included to allow variation of amplification at the high and at the low frequencies as compared with the medium frequencies.

High-frequency attenuation is useful when interference, due either to an adjacent frequency transmission or to noise, is experienced. It is also advantageous for suppressing needle scratch from gramophone records. Noise interference may be caused by atmospherics or by electrical apparatus connected to the mains supply wiring. Reproduction is characterized by a mellow tone, which becomes muffled if attenuation is severe. High-frequency intensification is of service, when receiving a powerful local station, in compensating for loss of the high-frequency sidebands due to the selectivity of the R.F. and I.F. tuned circuits. An average broadcast receiver often attenuates severely modulation sideband frequencies exceeding 3 kc/s, and reproduction from the higher pitch instruments in an orchestral programme may lose its character or be absent from the output unless there is discrimination by the A.F. amplifier in favour of the high frequencies. Reproduction with marked high-frequency intensification is usually described as brilliant.

Low-frequency attenuation is often helpful in combating the tendency to muffled reproduction when severe high-frequency attenuation is necessary to eliminate interference. Low-frequency intensification relative to other frequencies leads to more balanced reproduction as volume is reduced. The characteristics of the average ear are such that a general reduction in the levels of all frequencies appears to reduce the output of lower frequencies (50 to 200 c.p.s.) to a much greater extent than the medium frequencies (1,000 to 3,000 c.p.s.). Thus for an output volume of about 6 dynes/sq. cm.<sup>6</sup> (intensity level of 90 db.) at each frequency (this corresponds to a very loud radio receiver output) balanced

reproduction is obtained and all frequencies appear of very nearly equal loudness, whereas for an output volume of 0.02 dynes/sq. cm. (intensity level 40 db.), frequencies below 100 c.p.s. are not heard, i.e., the output is below the threshold of audibility; at 1,000 c.p.s. the output appears to be 40 db. louder than at 100 c.p.s. For this same intensity level, viz., 40 db., there is a progressive decrease in loudness level as the frequency is increased above 2,000 c.p.s. Owing to limitations on needle movement, the low-frequency components in gramophone recordings are attenuated (about 15 db.) and low-frequency intensification in the A.F. amplifier can be used to compensate for this. It is also an aid in mitigating the effect of inadequate output transformer primary inductance and loudspeaker baffle area, but care must then be exercised to prevent overloading of the output stage.

For certain purposes it may be necessary to amplify or suppress a comparatively narrow band of audio frequencies; e.g., telegraphic communication generally calls for a very narrow pass range (about  $\pm 50$  c.p.s.) in the neighbourhood of 1,000 c.p.s. This band-pass characteristic is secured by the use of tuned circuits in the A.F. amplifier. Similar circuits arranged to perform the opposite function are occasionally employed to suppress heterodyne interference from an adjacent transmission, and needle scratch in gramophone reproduction.

**9.6.2. Types of Tone Control Circuits.**<sup>10</sup> Tone control circuits require the use of reactances in order to obtain variable frequency response, and almost always involve a reduction in the general level of amplification. A valve associated with these circuits should not, therefore, be primarily intended as an amplifier but should be considered as a tone controller, the desired A.F. amplification being obtained in other stages. Parallel or series resonant circuits, except for special purposes, are undesirable unless they are heavily damped. If in a parallel circuit of  $R$ ,  $L$  and  $C$ , the parallel resistance  $R$  is  $> \frac{1}{2}\sqrt{\frac{L}{C}}$ , damped oscillations may be set up by shock excitation from transients in the A.F. signal. In practice, owing to the series resistance of  $L$ , it is found that as long as  $R < \sqrt{\frac{L}{C}}$ , reproduction is not seriously impaired by "hangover" or "ringing". When tuned circuits are employed, the parallel resonant type is to be preferred to the series; the latter has a reduced impedance at resonance, thus tending to cause amplitude distortion in its associated triode valve anode circuit. A tetrode

valve has an optimum anode load impedance, and amplitude distortion increases for impedances greater or less than this value, so that series or parallel circuits produce much the same effect.

Tone control circuits depending on variation of anode load impedance, as distinct from the potential divider type, are less effective in the anode circuit of a triode than of a tetrode, because the former has a much lower slope resistance. In all types it is preferable to use capacitance rather than inductance elements. The inductance element is, as a rule, more costly, has a much higher resistance component, is liable to pick up hum and interference voltages, and has stray capacitance.

Control of tone may be in steps, by variation of the reactance element, or it may be continuously variable, the resistance element being adjustable. In some cases<sup>9</sup> the A.F. signal voltage may be passed to three separate amplifiers. One amplifies all frequencies equally, the second contains a low-pass filter which accepts only the low frequencies (below about 250 c.p.s.), and the third uses a high-pass filter to accept the high frequencies (above 2,000 c.p.s.). The outputs of the three amplifiers may be combined in a single loudspeaker, or may be fed to separate loudspeakers specially designed to cover the desired frequency range. Separate adjustment of a potentiometer in each amplifier enables almost any required tonal balance to be obtained.

Negative feedback, with frequency selective feedback circuits, can also be used to provide tone control. Thus, if there is maximum feedback in the range of medium frequencies, the result is equivalent to an intensification of the low and high frequencies.

**9.6.3. High-Frequency Attenuation.** Control of the higher audio frequencies is possible prior to the A.F. amplifier, and variable selectivity in the I.F. amplifier (see Section 7.7, Part I) can be used for high-frequency tone control as well as for discriminating against undesired signals. Reduced coupling between the I.F. tuned circuits causes high-frequency attenuation, and overcoupling, producing double-humped frequency response, causes high-frequency intensification.

In an A.F. amplifier high-frequency attenuation can be obtained by adding a capacitance in parallel with the anode load resistance. Its effect is identical with that of stray capacitance  $C_s$  in Fig. 9.4a. The loss of amplification for given values of  $R_a$ ,  $R_o$ ,  $R_g$  and  $C_1 + C_s$ , where  $C_1$  is the additional control capacitance, can be read from Fig. 9.5b as explained in Section 9.3.1. Variation of the high-frequency loss (in actual fact it is a variation in the maximum



amplification at the medium frequencies) is achieved by varying the load resistance  $R_0$ . Increase of  $R_0$  increases the high-frequency attenuation by increasing the amplification at the medium frequencies. A similar effect could be achieved by including a suitable inductance  $L_1$  between the anode of  $V_1$  and the junction of  $R_0$  and  $C_c$  in Fig. 9.3, or in series with  $C_c$  between the anode of  $V_1$  and the junction of  $R_g$  and the grid of  $V_2$ . Series resonance of  $C_c$  and  $L_1$  would be damped by the grid leak resistance,  $R_g$ . With the first connection, increase of  $R_0$  decreases the high-frequency attenuation, and with the second, tone control is achieved by variation of  $R_g$ , increase of  $R_g$  reducing the high-frequency loss. Stray capacitance across  $R_g$  may produce a series resonance peak in the frequency response at a high audio frequency; its effect is similar to that of leakage inductance and stray capacitance in the transformer coupled amplifier (Section 9.4). Other disadvantages of using inductance control are listed in 9.6.2.

**9.6.4. High-Frequency Intensification.** Increase of frequency response at the high audio frequencies can be obtained with either of the two circuits shown in Figs. 9.17a and 17b. Analysing Fig. 9.17a by means of Thévenin's Theorem, we have for the amplification at medium frequencies :

$$A_m = \frac{\mu R_g R_0}{(R_a + R_0) \left( R_g + \frac{R_a R_0}{R_a + R_0} \right)}$$

if the reactances of  $C_c$  and  $L_1$  are negligible. At the high frequencies

$$A_h = \frac{\mu(R_g + jpL_1)R_0}{(R_a + R_0) \left( R_g + jpL_1 + \frac{R_a R_0}{R_a + R_0} \right)} \quad . \quad . \quad . \quad 9.26.$$

Thus

$$\left| \frac{A_h}{A_m} \right| = \sqrt{\frac{1 + \left( \frac{X_1}{R_g} \right)^2}{1 + \left( \frac{X_1}{R} \right)^2}} \quad . \quad . \quad . \quad 9.27a$$

where  $R = R_g + \frac{R_a R_0}{R_a + R_0}$  and  $X_1 = pL_1$ .

The increase in amplification at the high frequencies expressed in decibels is therefore

$$+10 \log_{10} \frac{1 + \left( \frac{X_1}{R_g} \right)^2}{1 + \left( \frac{X_1}{R} \right)^2} = +10 \log \frac{1 + x^2}{1 + (Bx)^2} \quad . \quad . \quad . \quad 9.27b$$

where  $x = \frac{X_1}{R_g}$  and  $B = \frac{R_g}{R} = \frac{1}{1 + \frac{R_a R_0}{R_g(R_a + R_0)}}$ .

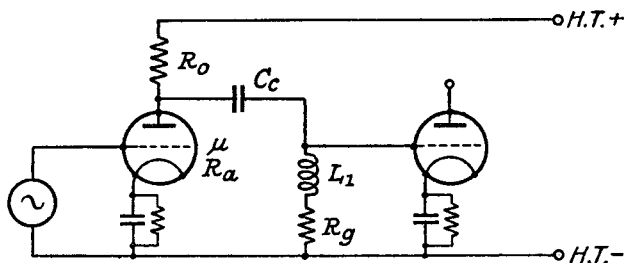


FIG. 9.17a.—A Circuit for Increasing High Frequency Response.

We may note that tone control, by varying  $R_g$ , is again obtained actually by reducing the amplification at the medium frequencies. Maximum amplification,  $A_{max.} = \frac{\mu R_0}{R_a + R_0}$ , is realized at the highest audio frequencies and is independent of  $B$ . Increased high-fre-

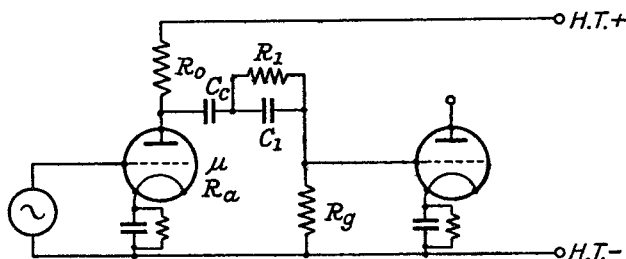


FIG. 9.17b.—A Circuit for Increasing High Frequency Response.

quency intensification is obtained by decreasing  $R_g$ . A series of curves of gain at high frequencies relative to the medium frequencies is plotted in Fig. 9.18 against  $x$ , i.e.,  $\frac{X_1}{R_g}$ , to a logarithmic scale for selected values of  $B$ . The horizontal  $x$  scale is converted to frequency by locating  $f_1 = \frac{R_g}{2\pi L_1}$  with  $x = 1$ , thus if  $R_a = 50,000 \Omega$ ,  $R_0 = 200,000 \Omega$ ,  $R_g = 40,000 \Omega$ ,  $L_1 = 3 \text{ H}$ , frequency response is read from the curve for  $B = 0.5$ , and  $f_1 = \frac{40,000}{6.28 \times 3} = 2,120 \text{ c.p.s.}$  is located with  $x = 1$ . Amplification at 5,000 and 10,000 c.p.s. is +4.5 and +5.5 db. respectively.

It may be observed in the above example that the A.C./D.C. load resistance ratio  $\frac{R_g}{R_g+R_0}$  is only  $\frac{1}{6}$ ; hence a large output voltage cannot be obtained from the tone control valve if distortion (see Section 9.3.3) is to be small.

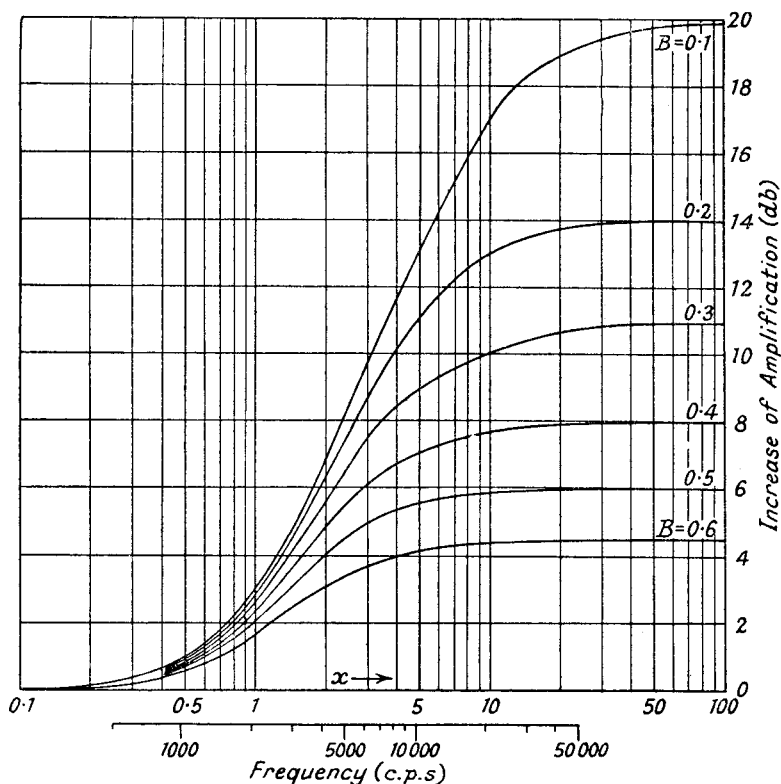


FIG. 9.18.—Generalised Curves of High Frequency Intensification Circuits.

For the circuit of Fig. 9.17b

$$A_m = \frac{\mu R_0 R_g}{(R_a + R_0) \left( \frac{R_a R_0}{R_a + R_0} + R_1 + R_g \right)}$$

and

$$A_h = \frac{\mu R_0 R_g}{(R_a + R_0) \left( \frac{R_a R_0}{R_a + R_0} + \frac{R_1}{1 + jpC_1 R_1} + R_g \right)}$$

$$\frac{A_h}{A_m} = \frac{1}{1 + j \frac{R}{R + R_1} p C_1 R_1}$$



ponent values, or vice versa, to be estimated rapidly. A circuit also producing low-frequency attenuation is shown in Fig. 9.19; variation of the resistance  $R_1$  controlling the frequency at which attenuation sets in. At medium frequencies, amplification is

$$A_m = \frac{\mu R_o}{R_a + R_o}$$

and at low frequencies, assuming that the reactance of  $C_o$  is so small that it can be neglected (the analysis becomes unduly complicated if this is not done)

$$A_l = \frac{\mu R_o}{R_a + R_o} \cdot \frac{j\omega L_1}{R_1 + \frac{R_a R_o}{R_a + R_o} + j\omega L_1} \quad . \quad . \quad . \quad 9.29$$

$$\left| \frac{A_m}{A_l} \right| = \sqrt{1 + \left( \frac{R}{X_1} \right)^2}$$

where  $R = R_1 + \frac{R_a R_o}{R_a + R_o}$

and low-frequency loss is

$$-20 \log_{10} \left| \frac{A_m}{A_l} \right| = -10 \log_{10} \left( 1 + \left( \frac{R}{X_1} \right)^2 \right) = -10 \log_{10} \left( 1 + \frac{1}{x^2} \right). \quad 9.30.$$

The above expression is identical with 9.4c, so that the curve in Fig. 9.5a gives the frequency response by locating  $f_1 = \frac{R}{2\pi L_1}$  c.p.s. with  $x = 1$ . There is a possibility of parallel resonance at a high audio frequency due to stray capacitance across  $L_1$ .

**9.6.6. Low-Frequency Intensification.** Increased amplification of the low frequencies relative to medium and high frequencies

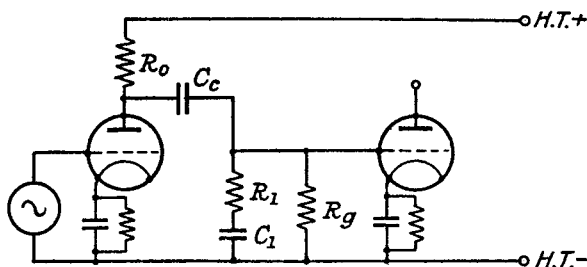


FIG. 9.20.—A Circuit for Increasing Low Frequency Response.

can be accomplished by the circuit shown in Fig. 9.20. At the medium frequencies

$$A_m = \frac{\mu R_o' R_1}{(R_a + R_o') \left( \frac{R_a R_o'}{R_a + R_o'} + R_1 \right)}$$

where

$$R_o' = \frac{R_o R_g}{R_o + R_g}$$

$$A_l = \frac{\mu R_o'}{R_a + R_o'} \cdot \frac{R_1 + \frac{1}{j\omega C_1}}{\frac{R_a R_o'}{R_a + R_o'} + R_1 + \frac{1}{j\omega C_1}} \quad . \quad . \quad . \quad 9.31.$$

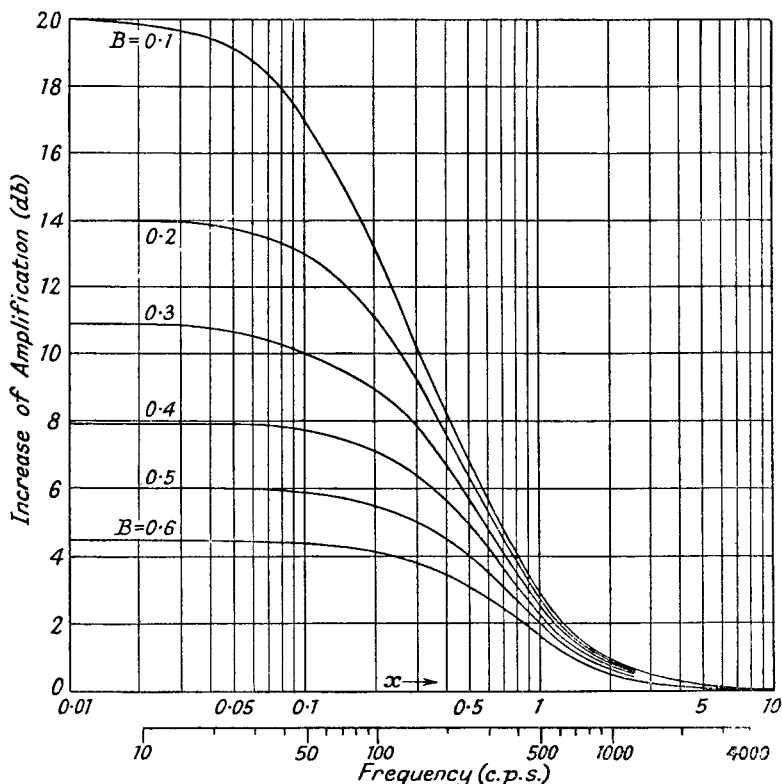


FIG. 9.21.—Generalized Curves for Low Frequency Intensification Circuits.

Increase in amplification at low frequencies is

$$+20 \log_{10} \left| \frac{A_l}{A_m} \right| = +10 \log_{10} \frac{1 + \frac{1}{x^2}}{1 + \left( \frac{B}{x} \right)^2} \quad . \quad . \quad . \quad 9.32$$

where  $x = pC_1R_1$ ,  $B = \frac{R_1}{R}$  and  $R = \frac{R_aR_0'}{R_a+R_0'} + R_1$ .

Curves are plotted in Fig. 9.21 of amplification in decibels against  $x$  for selected values of  $B$ , and the frequency response is read by locating  $f_1 = \frac{1}{2\pi C_1 R_1}$  with  $x = 1$ . Thus if  $R_a = 50,000 \Omega$ ,  $R_0 = 200,000 \Omega$ ,  $R_g = 1 \text{ M}\Omega$ ,  $R_1 = 40,000 \Omega$ , and  $C_1 = 0.008 \mu\text{F}$ ,  $f_1 = \frac{10^6}{6.28 \times 40,000 \times 0.008} = 497 \text{ c.p.s.}$  is registered with  $x = 1$  and frequency response is obtained from the curve for  $B = 0.5$  (the nearest curve to the actual value of  $B = 0.51$ ). Thus the increase in amplification at 50 and 100 c.p.s. is +5.8 and +5.5 db. respectively.

Yet another method of obtaining increased amplification at low frequencies is by a suitable choice of anode decoupling  $RC$  values as described in Section 9.3.6.

#### 9.6.7. Response confined to a Band of Audio Frequencies.

When a receiver is intended for telephonic communication, its audio frequency range can with advantage be confined to a band from 250 to 2,750 c.p.s. This comparatively narrow band contains almost all the frequency components necessary for good intelligibility, and at the same time tends to eliminate undesired frequencies due to hum, atmospherics, etc. As a rule a correctly terminated filter ( $R_0 = 600 \Omega$ ) is inserted in the A.F. amplifier; design procedure for this is beyond the scope of the book and reference should be made to Bibliography Nos. 13 and 14.

Frequency response limited to a very narrow band (about  $\pm 50$  c.p.s.) in the neighbourhood of 1,000 c.p.s. is quite often employed in communication receivers for telegraph operation. The narrow pass-band may be achieved by the use of a double-tuned iron-cored transformer with critical coupling between primary and secondary. The frequency response is similar to that for I.F. double-tuned coupled circuits, and the curves of Fig. 7.7 (Part I) can be used either to estimate the performance for given values of primary and secondary inductance, capacitance and  $Q$ , and the mutual inductance between the circuits, or to calculate component values for a given performance. An average value  $Q$  for iron-cored inductances is 5, but by special design, such as thinner iron laminations, it may be raised to 20. The factors influencing the  $Q$  of iron-cored coils have been examined in considerable detail by Arguimbau<sup>5, 11</sup>, who found that  $Q$  reaches a maximum value of

$$Q_{(max)} = \frac{1}{\delta} \sqrt{\frac{3\rho_i S A \alpha}{\rho_c t l}} \quad . \quad . \quad . \quad 9.33$$

at a particular frequency of

$$f_1 = \frac{10^9}{4\pi^2 \Delta\mu \delta} \sqrt{\frac{3\rho_c \rho_i t l}{S A \alpha}} \quad . \quad . \quad . \quad 9.34a$$

$$= \frac{3.10^9 \rho_i}{4\pi^2 \Delta\mu \delta^2 Q_{(max)}} \quad . \quad . \quad . \quad 9.34b$$

where  $\delta$  = thickness of laminations in cms.

$\rho_i$  = resistivity of lamination material in ohms per c.c.

$\rho_c$  = resistivity of copper winding in ohms per c.c.

$S = \frac{N\pi d^2}{4}$  = effective coil window area (total cross-sectional area of winding window in sq. cm.)

$d$  = diameter of wire.

$N$  = number of turns of copper.

$A$  = cross-sectional area of magnetic path in sq. cm.

$\alpha$  = stacking factor of iron (the ratio of effective area of core iron to inside area of coil tube, allowance is to be made for lamination insulation).

$t$  = average length of one turn of winding.

$l$  = mean length of magnetic flux path.

$\Delta\mu$  = incremental permeability of magnetic material.

In determining the above expressions it is assumed that the A.C. flux density is very small, i.e., hysteresis loss is small, that skin effect of the copper in the winding, leakage flux and eddy currents between laminations are negligible, and that resonance is remote. The following conclusions are reached by an examination of expressions 9.33, 9.34a and 9.34b :

- (1) Multiplication of overall dimensions by a factor “ $r$ ” increases

$$Q_{(max)} \text{ to } rQ_{(max)} \text{ and decrease } f_1 \text{ to } \frac{f_1}{r}.$$

- (2) Decrease of lamination thickness,  $\delta$ , increases  $Q_{(max)}$  (not quite in the same proportion as  $\delta$  is decreased, because the stacking factor,  $\alpha$ , is altered) and increases  $f_1$ .
- (3) When the winding area is not fully occupied ( $S$  is reduced),  $Q_{(max)}$  is decreased and  $f_1$  increased.
- (4) When the core is loosely stacked ( $\alpha$  reduced)  $Q_{(max)}$  is decreased and  $f_1$  increased.
- (5) Increase of core cross-sectional area increases  $Q_{(max)}$  and decreases  $f_1$ , but the change in  $A$  is offset by a similar



change in  $t$ . Doubling  $A$  only increases  $Q_{(max)}$  about 1.25 times.

- (6) Decrease of core material resistivity,  $\rho_i$ , decreases  $Q_{(max)}$  and  $f_1$ .
- (7) Increase of winding material resistivity,  $\rho_c$ , decreases  $Q_{(max)}$  and increases  $f_1$ .
- (8) Increase of air gap in a given design has no effect on  $Q_{(max)}$ , but decreases  $f_1$  if  $\Delta\mu$  is increased. If the core carries D.C. current,  $\Delta\mu$  may be increased by increase of air gap.

The value of  $Q$  obtained at a frequency,  $f$ , can be expressed in terms of  $Q_{(max)}$ ,  $f$  and  $f_1$  as follows :

$$Q = \frac{2 Q_{(max)}}{\frac{f}{f_1} + \frac{f_1}{f}} \quad \dots \quad 9.35$$

For a  $Q$  of 5, and  $f_r = 1,000$  c.p.s., frequency response for critical coupling is (see Fig. 7.7.) about 1 db. and 7 db. down at 100 and 200 c.p.s. respectively off-tune from 1,000 c.p.s., whilst for  $Q = 20$ ,  $f_r = 1,000$  c.p.s., the losses at the same frequencies are 18 and 30 db. respectively. When reduced overall amplification can be considered, greater selectivity is possible by using couplings less than critical. For example, at one-half critical coupling, the losses in the first case are increased to 4 and 11.5 db. respectively, but overall amplification is reduced by 2 db.

#### 9.6.8. Elimination of a Narrow Band of Frequencies.

The elimination of a narrow band of frequencies in the A.F. range is sometimes used for reducing needle scratch in the reproduction of gramophone records (the predominant frequency is about 11 kc/s), and also for reducing heterodyne whistle interference (about 9 kc/s) from an adjacent channel transmission. A possible circuit is shown in Fig. 9.22.

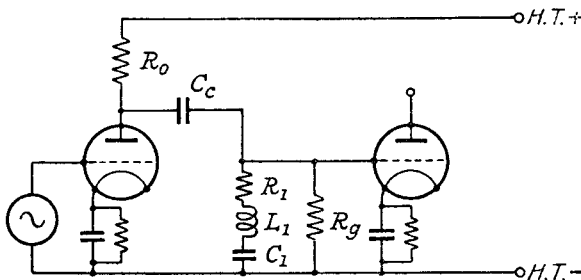


FIG. 9.22.—A Circuit for Eliminating a Narrow Band of Audio Frequencies.

The amplification at frequencies far removed from resonance is

$$A_n = \frac{\mu R_0'}{R_a + R_0'}$$

where

$$R_0' = \frac{R_0 R_g}{R_0 + R_g}$$

and at other frequencies

$$A = \frac{\mu R_0'}{R_a + R_0'} \cdot \frac{R_1 + j\left(pL_1 - \frac{1}{pC_1}\right)}{\frac{R_a R_0'}{R_a + R_0'} + R_1 + j\left(pL_1 - \frac{1}{pC_1}\right)}$$

At resonance, amplification is minimum and given by

$$A_r = \frac{\mu R_0'}{R_a + R_0'} \cdot \frac{R_1}{\frac{R_a R_0'}{R_a + R_0'} + R_1}$$

The ratio of  $A_n$  to amplification at any particular frequency is

$$\begin{aligned} \frac{A_n}{A} &= \frac{\frac{R_a R_0'}{R_a + R_0'} + R_1 + j\left(pL_1 - \frac{1}{pC_1}\right)}{R_1 + j\left(pL_1 - \frac{1}{pC_1}\right)} = \frac{\frac{R''}{R_1} + \frac{jp_r L_1}{R_1} \left(\frac{p}{p_r} - \frac{p_r}{p}\right)}{1 + \frac{jp_r L_1}{R_1} \left(\frac{p}{p_r} - \frac{p_r}{p}\right)} \\ &= \frac{B + jQ\left(x - \frac{1}{x}\right)}{1 + jQ\left(x - \frac{1}{x}\right)} \quad \dots \dots \dots \quad 9.33 \end{aligned}$$

where  $R'' = \frac{R_a R_0'}{R_a + R_0'} + R_1$ ,  $p_r = \frac{1}{\sqrt{L_1 C_1}}$ ;  $B = \frac{R''}{R_1}$ ,  $Q = \frac{p_r L_1}{R_1}$

and  $x = \frac{p}{p_r} = \frac{f}{f_r}$ .

The loss relative to  $A_n$  is

$$-20 \log \left| \frac{A_n}{A} \right| = -10 \log_{10} \frac{B^2 + Q^2 \left(x - \frac{1}{x}\right)^2}{1 + Q^2 \left(x - \frac{1}{x}\right)^2} \quad \dots \quad 9.34.$$

There are three possible variables,  $B$ ,  $Q$  and  $x$ , in 9.34, and a single series of generalized frequency response curves cannot be produced. Representative curves showing the effect of varying  $B$  for constant  $Q$ , and vice versa, are plotted in Fig. 9.23 against  $x$ . A similar

logarithmic frequency scale with  $f_r = \frac{1}{2\pi\sqrt{L_1C_1}}$  registered against  $x = 1$  enables frequency response for particular component values to be read. Thus if  $R_a = 50,000 \Omega$ ,  $R_o = 200,000 \Omega$ ,  $R_g = 1 \text{ M}\Omega$ ,  $R_1 = 10,000 \Omega$ ,  $Q = 10$  and  $f_r = 9 \text{ kc/s}$  the frequency scale is registered at 9 kc/s as shown and frequency response read from the curve  $Q = 10$ ,  $B = 5$  (this is nearest to the actual value of  $B = 4.85$ ), i.e., maximum loss at 9 kc/s is very nearly 14 db., whilst at 8 (or 10.1) kc/s and 7 (or 11.6) kc/s the loss is 7.2 and 3 db. respectively. The curves show quite clearly that  $Q$  controls the

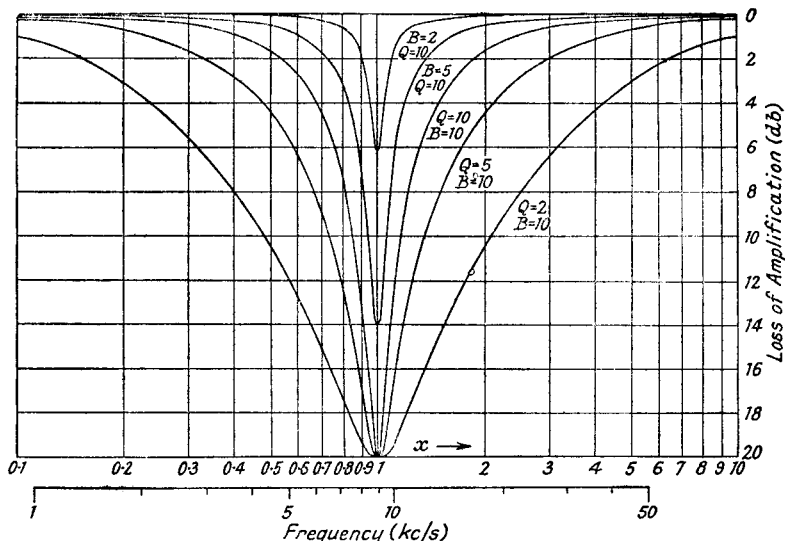


FIG. 9.23.—Generalized Curves for Narrow Band Elimination Circuit.

shape of the frequency response and  $B$  the maximum loss at the resonant frequency.

**9.6.9. Combined Volume and Tone Control.** Attempts have been made to overcome the lack of tonal balance as the loud-speaker average sound intensity is reduced (due to a greater apparent reduction in the low and high A.F. components) by linking the volume and tone control action. One of the simplest and earliest methods was by means of a parallel resonant circuit<sup>3</sup> (tuned to about 50 c.p.s.) or a series resonant circuit<sup>2</sup> (tuned to about 1,000 c.p.s.) connected to a fixed tapping point on the volume control potentiometer. As this point is approached by the slider of the potentiometer, low-frequency response is intensified (by the

parallel resonant circuit) or medium-frequency response is reduced (by the series resonant circuit). This method has the disadvantage that frequency response is not exactly related to the sound output as should be the case for correct tone-volume compensation. Combined volume and tone control can be realized by ganging the volume potentiometer and the resistance tone-control element. A separate tone control is, however, generally preferable since best tonal balance depends on site conditions (size and furnishing of room, signal-to-noise ratio, etc.), and is, to a large extent, a matter of personal taste.

#### BIBLIOGRAPHY

1. The Design of Tone Control Circuits. K. W. Jarvis, *Electronics*, Aug. 1930, p. 230.
2. Acoustically Compensated Volume Control. I. Wolff and J. I. Cornell, *Electronics*, Jan. 1933, p. 50.
3. Tone Compensation. M. G. Scroggie, *Wireless World*, Aug. 30th, 1935, p. 252.
4. Design of Audio Frequency Amplifier Circuits Using Transformers. P. W. Klipsch, *Proc. I.R.E.*, Feb. 1936, p. 219.
5. Losses in Audio Frequency Coils. L. B. Arguimbau, *General Radio Experimenter*, Nov. 1936, p. 1.
6. The Evolution of the Phon. D. B. Foster, *Wireless World*, July 9th, 1937, p. 32.
7. Flexible Tone Control. M. G. Scroggie, *Wireless World*, Sept. 10th, 1937, p. 263.
8. Tone Control. "Cathode Ray." *Wireless World*. Sept. 15th and 22nd, 1938, pp. 247 and 269.
9. New American Quality Receiver. L. G. Pacent and H. C. Likel, *Wireless World*, March 23rd, 1939, p. 271.
10. Tone Control Systems. W. T. Cocking, *Wireless World*, June 8th, 1939, p. 532.
11. How Good is an Iron-Cored Coil? P. K. McElroy and R. F. Fields, *General Radio Experimenter*, March 1942, p. 1.
12. *Radio Engineering*. F. E. Terman. McGraw Hill. Text-book.
13. *Transmission Circuits for Telephonic Communication*. K. S. Johnson. Van Nostrand. Text-book.
14. *Transmission Networks and Wave Filters*. T. E. Shea. Van Nostrand. Text-book.

## THE POWER OUTPUT STAGE

**10.1. Introduction.** The audio frequency output stage of a receiver differs from the other stages in that maximum power, as distinct from maximum voltage, is required from its anode circuit. This usually entails a definite relationship between the output load and the valve internal resistance, though the optimum load resistance is not determined only by maximum power but also by distortion considerations. Normally the optimum load is taken as that value of resistance which gives maximum output power for a total harmonic distortion of 5%.

Two types of valves are used, the triode and the beam tetrode or pentode, and each has its particular advantages. The output load may be supplied from a single valve, or a pair operating in push-pull, the particular features of the latter being (if matched valves, having identical  $I_a E_a$  characteristics are employed) cancellation of even harmonics, and zero D.C. polarization in the output transformer. Neither of these features is possessed by a pair of valves in parallel, and the only advantage of the parallel connection is that the equivalent generator internal resistance is halved. When a single valve supplies the output stage, it is usually biased to the centre of the straight part of its  $I_a E_g$  characteristic; this is not essential in push-pull stages, and in order to economize in current consumption both valves may be biased to the bend of their  $I_a E_g$  characteristic. Even harmonic distortion is produced in each valve but is cancelled by the push-pull connection. The first method is known as Class A operation and the second as Class B operation. There is also a third method, known as Class AB, which, together with the second method, is discussed in Section 10.8. Inverse or negative feedback from the output stage is employed to reduce amplitude and frequency distortion and to damp loudspeaker resonances, and details of the various forms of feedback circuits are given in Section 10.10.

**10.2. Conditions for Maximum Power Output.**<sup>48</sup> In order to calculate the load for maximum output power, some assumption of the form of the  $I_a E_a$  characteristics must be made. For convenience we shall consider a triode having a series of straight equally-spaced parallel lines, of slope  $\frac{\Delta I_a}{\Delta E_a}$  equal to the reciprocal of the valve

internal resistance  $R_a$ . The line  $OA$  in Fig. 10.1 is the boundary curve for  $E_g = 0$ , beyond which the valve may not operate unless the previous stage has been designed to supply the necessary power absorbed by grid current.

The analysis can also be applied to a tetrode, but the valve resistance  $R_a$  must then be taken as the value obtained from the boundary curve  $OA$ , and is not the normal valve slope resistance obtained with high anode voltage.

Five possible cases have to be considered, for all of which neither grid current nor distortion are permitted. The first has fixed A.C. input voltage to the grid, the second has fixed D.C. anode voltage and no limitations on D.C. anode current or A.C. input grid voltage. The third case is the same as the second except that the maximum D.C. power dissipation at the anode is fixed, i.e., maximum D.C. anode current, is fixed. The fourth has fixed D.C. power dissipation, but D.C. anode current and voltage can be varied so long as their product is constant. The fifth applies all the results to the practical form of triode  $I_a E_a$  characteristic, curved at low anode currents. This means that there is a minimum value of anode current, below which the valve must not be operated if distortion is to be small, and also that the straight part produced ( $MA$  in Fig. 10.2*b*) of the boundary line does not pass through the origin but a point corresponding to an anode voltage of  $\varepsilon$ .

CASE 1. *Grid current and distortion zero, fixed A.C. input voltage to the grid.*

The valve functions as a generator of constant voltage  $\mu E_g$ , having an internal resistance of  $R_a$ .

$$\text{A.C. power output } P_0 = \frac{(\mu E_g)^2 R_0}{(R_a + R_0)^2} \quad . \quad 10.1a$$

and is a maximum when  $\frac{dP_0}{dR_0} = 0$ ,

i.e., when  $R_0 = R_a$ .

This condition is illustrated on the  $I_a E_a$  characteristics of Fig. 10.1 by the load line  $B'D'$ , which can be located anywhere between  $OA$  and  $MN$  (the limiting grid voltage lines) so long as  $F'H' = H'B'$ . The best position is that shown,  $B'$  and  $M$  coinciding, since raising  $B'D'$  merely increases the D.C. power taken by the valve without increasing A.C. power output, which is the area of triangle  $H'F'Q$ .

Therefore  $P_0 = \frac{1}{2}(E_1' - E_2')I_1'$

But  $E_1' = \frac{3}{2}E_2'$  because  $R_0 = R_a$







exceeds  $\frac{P_D(max.)}{E_1}$ , the D.C. grid-bias voltage must be increased to reduce  $I_1$  to its maximum permissible value, and maximum power output is then obtained for  $R_0 > 2R_a$ . This condition is illustrated in Fig. 10.2a; the hyperbolic relationship between D.C. anode current and voltage for a fixed value of  $P_D(max.)$  is represented by the curve  $GHK$ .  $OA$  is the boundary line for zero grid current and  $BD$  is the load line drawn through the reference point  $H$  on the curve  $GHK$ . For zero distortion the change in anode current and voltage above  $H$  must equal the change below  $H$ . It is not an essential condition, however, that the full extent of the load line from  $B$  to  $F$  should be used, and the problem is one of determining whether maximum power output is obtained by an excursion over less than the length  $BF$ . If we ignore the limitations imposed by

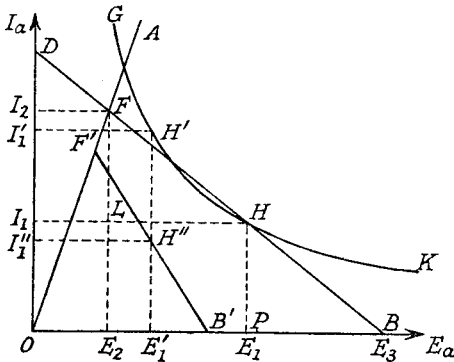


FIG. 10.2a.—Optimum Load Conditions for a Triode Valve of Fixed D.C. Power Dissipation.

the negative anode voltage swing (below  $H$ ), maximum power output is obviously obtained by using the full extent of  $HB$  and by making  $PB$  as large as possible. Power output, equal to  $\frac{1}{2}(E_3 - E_1)I_1$  is the area of the triangle  $HBP$ , and this is clearly a maximum when  $E_3$  is maximum. It must therefore be the negative anode voltage swing, which always determines the maximum power output. Power out-

put, equal to the area of triangle  $HFL$ , is zero when  $R_0$  is infinite ( $BD$  is horizontal) and when  $R_0 = 0$  ( $BD$  vertical); it is maximum when the slope of  $BD$  equals that of  $OA$ . It is equivalent to working with a fixed grid input A.C. voltage and is therefore case 1 over again. Two possible conditions, depending on the position of  $H$  relative to  $OA$  and the  $E_a$  axis, have to be considered. Suppose  $H$  is much closer to the  $E_a$  axis than to  $OA$ ; we find that as the point  $B$  on the load line, pivoted at  $H$ , is brought closer to  $E_1$ , the area of the triangle  $HBP$  is decreasing and that of triangle  $HFL$  increasing. Since  $H$  is assumed to be close to the  $E_a$  axis, the condition for maximum power output is that the areas of the triangles  $HBP$  and  $HFL$  are equal. When  $R_0 = R_a$  (giving maximum area of triangle  $HFL$ ) the area of triangle  $HFL$  is greater

than that of triangle  $HBP$ , and if distortion is to be avoided it entails reducing the negative anode voltage excursion from  $HF$  to a length equal to  $HB$ . This is clearly inefficient. For equal areas of the triangles, the maximum current  $I_2$  must be twice  $I_1$  and

$$E_2 = I_2 R_a = 2I_1 R_a.$$

$$\begin{aligned} \text{Power output } P_0 &= \frac{1}{2}(E_1 - E_2)I_1 \\ &= \frac{1}{2}(E_1 - 2I_1 R_a)I_1 \quad . \quad 10.3a. \end{aligned}$$

$$\begin{aligned} \text{Optimum load resistance } R_0 &= \frac{HL}{FL} = \frac{E_1 - E_2}{I_1} \\ &= \frac{E_1}{I_1} - 2R_a \\ &= R_{\text{D.C.}} - 2R_a \end{aligned}$$

where  $R_{\text{D.C.}}$  = D.C. resistance of the valve

$$\begin{aligned} \text{A.C. to D.C. conversion efficiency} &= \frac{\frac{1}{2}(E_1 - 2I_1 R_a)I_1}{E_1 I_1} \\ &= \frac{1}{2} \left( 1 - \frac{2R_a}{R_{\text{D.C.}}} \right) \quad . \quad 10.4. \end{aligned}$$

Maximum A.C./D.C. conversion efficiency approaches the same maximum value as for case 2, viz., 50% when  $R_{\text{D.C.}}$  is large compared with  $R_a$ . This is to be expected since a large value of  $R_{\text{D.C.}}$  implies a high value of  $E_1$  and low value of  $I_1$ ; both these effectively reduce  $E_2$ , as does a decrease in  $R_a$ .

The second condition, for which  $H$  is much closer to  $OA$  than to the  $E_a$  axis (see position  $H'$  in Fig. 10.2a), requires  $R_0$  to equal  $R_a$  for maximum power output, but the valve is then operating very inefficiently, only a small part of the load line between  $H'$  and  $B$  being used. The most efficient method of operation would be to reduce  $I_1'$  to  $I_1''$ , which gives  $H''F' = H''B'$  with a load line of  $R_0 = 2R_a$ .

The conclusion to be drawn from the analysis is that  $I_1$  should never exceed  $\frac{E_1}{4R_a}$  (this corresponds to an optimum load resistance of  $R_0 = 2R_a$ ), for increase of current above this value decreases power output and A.C./D.C. conversion efficiency. Optimum load resistance when  $I_1 > \frac{E_1}{3R_a}$  is  $R_0 = R_a$  but for  $I_1 < \frac{E_1}{3R_a}$  it is  $R_0 = \frac{E_1}{I_1} - 2R_a$ . Maximum power output is always realized for  $I_1 = \frac{E_1}{4R_a}$ , when optimum load resistance is  $R_0 = 2R_a$ .

CASE 4. *Zero grid current and distortion, fixed D.C. anode dissipation loss, no limitations on D.C. anode voltage.*

Expression 10.3a for power output may be written

$$P_o = \frac{1}{2}(E_1 I_1 - 2I_1^2 R_a) = \frac{1}{2}(P_D(max.) - 2I_1^2 R_a) \quad . \quad 10.3b.$$

Since  $P_D(max.)$  is a constant, it follows that maximum power output is obtained when  $I_1$  is as small as possible, i.e.,  $E_1$  is as large as possible. A.C. to D.C. conversion efficiency is a maximum at the same time. It must, however, be noted that increased efficiency in the anode circuit, brought about by increased D.C. anode voltage, entails a lower grid input voltage efficiency by requiring a steadily increasing input voltage. In most practical cases of Class A triode

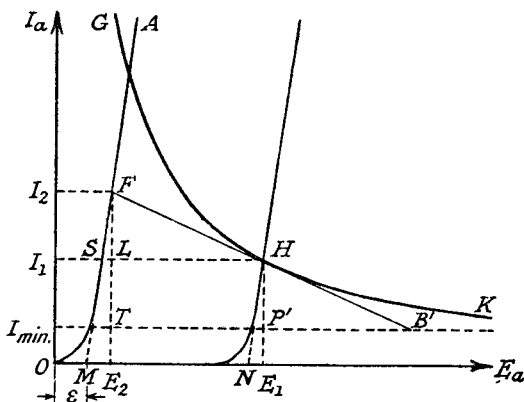


FIG. 10.2b.—Optimum Load Conditions for a Triode of Fixed D.C. Power Dissipation and Minimum Anode Current.

operation optimum overall input and output conditions are realized by making  $R_o = 2R_a$ .

As pointed out at the beginning of this section the analysis may be applied to a Class A tetrode valve provided it is remembered that  $R_a$  is the slope resistance of the boundary curve for small values of anode voltage. In almost all cases  $I_1 < \frac{E_1}{4R_a}$  and optimum load is

$$R_o = R_{D.C.} - 2R_a.$$

Often  $R_a$ , the slope resistance of the  $OA$  boundary line for small anode voltages (not exceeding 30 volts), is negligible in comparison with  $R_{D.C.}$  and

$$R_o = R_{D.C.}$$

gives a good approximation to the optimum load.

CASE 5. *Grid current and distortion zero, fixed D.C. anode dissipation loss, fixed minimum D.C. anode current, boundary line produced from its straight part passes through some positive value of  $E_a$ .*<sup>46</sup>

The practical form of  $I_a E_a$  characteristic is generally non-linear for low values of  $I_a$ , and this sets a limit on the minimum operative value of  $I_a$  if distortion is not to be excessive. For a triode valve the foot of the boundary characteristic ( $E_g = 0$ ) is often curved and the straight part (produced) cuts the  $E_a$  axis at some positive voltage. Fig. 10.2*b* illustrates the condition, the intersection of the boundary line  $OA$  (produced) cutting the  $E_a$  axis at  $+\varepsilon$  volts. The hyperbolic curve  $GHK$  is the fixed anode dissipation loss and it is cut eventually by the minimum anode current line drawn at  $I_a = I_{min.}$  Cases 1 and 2 are not affected by the new conditions, i.e., optimum load for fixed grid A.C. input voltage is  $R_a$ , and for fixed D.C. anode voltage and unlimited grid input voltage is  $2R_a$ , where  $R_a$  is the slope resistance of the line  $MA$ . Case 3 is, however, slightly modified; the triangles  $HFL$  and  $HP'B'$  must be equal, which means that

$$I_2 - I_1 = I_1 - I_{min.}$$

or

$$I_2 = 2I_1 - I_{min.}$$

$$\begin{aligned} \text{A.C. power output } P_0 &= \frac{1}{2}(E_1 - E_2)(I_1 - I_{min.}) \\ &= \frac{1}{2}[E_1 - (2I_1 - I_{min.})R_a - \varepsilon][I_1 - I_{min.}] \quad 10.5. \end{aligned}$$

$$\text{Optimum load resistance } R_0 = \frac{E_1 - E_2}{I_1 - I_{min.}} \quad 10.6a$$

$$\begin{aligned} &= \frac{E_1 - (2I_1 - I_{min.})R_a - \varepsilon}{I_1 - I_{min.}} \\ &= \frac{E_1}{I_1} \left( \frac{I_1}{I_1 - I_{min.}} \right) - R_a \left( 2 + \frac{I_{min.}}{I_1 - I_{min.}} \right) - \frac{\varepsilon I_{min.}}{I_{min.}(I_1 - I_{min.})} \\ &= R_{D.C.} - 2R_a + (R_{D.C.} - R_a - R_{min.}) \frac{I_{min.}}{I_1 - I_{min.}} \quad 10.6b \end{aligned}$$

where  $R_{D.C.}$  and  $R_{min.}$  are  $\frac{E_1}{I_1}$  and  $\frac{\varepsilon}{I_{min.}}$  respectively.

The above expression is the same as for case 3 when  $I_{min.}$  and  $\varepsilon$  are zero.

A.C. to D.C. power conversion efficiency

$$\begin{aligned} &= \frac{[E_1 - (2I_1 - I_{min.})R_a - \varepsilon][I_1 - I_{min.}]}{2E_1 I_1} \\ &= \frac{1}{2} \left( 1 - \frac{2R_a}{R_{D.C.}} + \frac{R_a I_{min.}}{R_{D.C.} I_1} - \frac{\varepsilon}{E_1} \right) \left( 1 - \frac{I_{min.}}{I_1} \right). \quad 10.7 \end{aligned}$$



### 10.3. The Characteristics Required of an Output Valve.

Certain characteristics are required of an output valve and the most important are :

(1) *High power sensitivity.* Power sensitivity is expressed as the R.M.S. output power (milliwatts) per input R.M.S. grid volt. The higher this value the lower is the grid voltage required for maximum power, so that less amplification is needed in preceding stages, and the possibility of distortion before the output valve is consequently reduced.

(2) *Low distortion.* Distortion should be low and confined mainly to the second harmonic. Higher harmonics indicate the probability of intermodulation products, which tend to produce rough and rasping reproduction.

(3) *High D.C. to A.C. conversion efficiency.* High efficiency, though desirable, is less necessary in A.C. mains than in battery operated receivers. It may be achieved by making the minimum anode voltage as low as possible, by using a high H.T. voltage and a Class B push-pull output stage.

(4) *High power output.* Power outputs of about 3,000 mW maximum are generally adequate for most living rooms, but much larger values are required for public address systems.

(5) *Low slope resistance.* This helps to damp out loudspeaker cone resonances. Most loudspeakers have several resonances, a major one occurring between 50 and 100 c.p.s., and they can be objectionable if not adequately damped.

A comparison can now be made between the two types of output valve, the triode, and the tetrode or pentode. The triode has a low power sensitivity; an average value for a D.C. power dissipation of 12 watts is about 150 mW per 1 volt R.M.S. grid input. The beam tetrode has a sensitivity of about 1,000 mW per volt for the same D.C. power. In a triode, distortion is largely confined to the second harmonic, and it falls as the load resistance increases. The beam tetrode has characteristics similar to the pentode and it therefore produces distortion containing a proportion of the higher harmonics. There is a load resistance value at which second harmonic is a minimum, but third harmonic steadily rises with increase of load resistance (see Fig. 10.10b). This is a disadvantage because the impedance of the loudspeaker speech-coil increases at the higher frequencies. This increase in load impedance<sup>8</sup> is often limited by a series combination of capacitance and resistance connected across the primary of the output transformer. The reactance of the capacitance falls as the frequency increases, and

the effect of the series resistance becomes more and more pronounced, thus tending to stabilize the output load. This also has the advantage of reducing the accentuation of the high frequencies. The accentuation is due to the rising impedance of the speech-coil in association with the high internal resistance of the tetrode, which tends to maintain a constant current through the speech-coil if no correcting circuit is applied.

Owing to the shape of its  $I_a E_a$  characteristics, the beam tetrode has a lower minimum anode voltage than the triode, and its maximum D.C. to A.C. conversion efficiency, in spite of the loss of power due to screen current, is therefore higher, about 35% as compared with 23% for the triode. For the same reason the tetrode produces a larger power output than a triode operating under similar H.T. conditions. The lower internal resistance of the triode is of considerable advantage in damping loudspeaker resonances.

Summarizing, the triode is preferable when high quality is essential, whilst the tetrode is better when high power sensitivity and efficiency are desirable.

**10.4. The Calculation of Power Output and Harmonic Distortion.**<sup>8, 9, 15, 17</sup> The power output and distortion produced by an output valve supplying a resistance load may be calculated from  $I_a E_a$  characteristic curves, taken at specified grid-bias voltages, generally equally spaced; the number of curves required is at least one more than the number of the harmonic, the amplitude of which is to be calculated. Thus, if distortion up to the fourth harmonic is to be calculated, curves are needed for five grid bias voltages. We shall take first the case of a triode having mainly second harmonic distortion. The normal grid bias for any given anode voltage is estimated from the  $I_a E_g$  characteristic curves; it should correspond approximately to the centre of the straight part of the characteristic, and generally is less than half (about 35 to 45% of) the cut-off grid bias voltage. Having determined the normal operating bias voltage ( $-E_{g1}$ ), the minimum negative grid voltage ( $-E_{g2}$ ) is fixed by start of grid current (in battery valves  $E_{g2}$  is slightly positive, but in mains valves it is negative, being about  $-0.5$  to  $-1$  volt). For a sinusoidal input voltage the maximum negative grid voltage  $-E_{g3}$  is equal to  $-(2E_{g1} - E_{g2})$ . The three  $I_a E_a$  characteristic curves for these grid bias voltages,  $-E_{g2}$ ,  $-E_{g1}$  and  $-E_{g3}$ , are the ones selected for calculating second harmonic distortion and power output, and they correspond to angular positions for a cosine\*

\* The cosine expression for input voltage is used in preference to the sine as was the case for Part I.

wave input voltage of  $0^\circ$ ,  $90^\circ$ ,  $180^\circ$ ,  $270^\circ$  and  $360^\circ$ . Fig. 10.3a shows the curves with a load line  $ZZ'$  drawn across them. Although

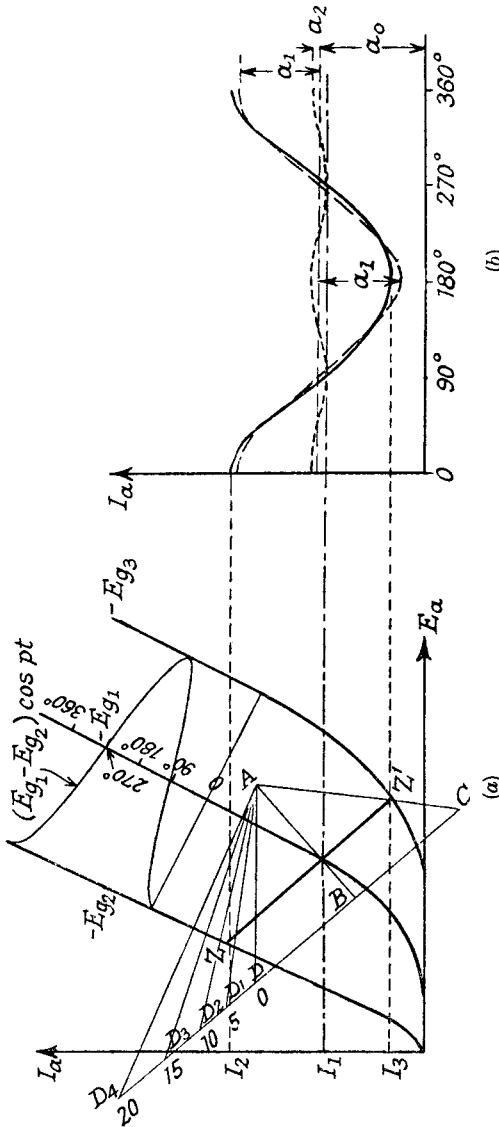


Fig. 10.3.—(a) Load Characteristic and Distortion with a Triode Valve.  
 (b) Time Relationships of the Fundamental and Harmonic Components of the Output Wave from (a).

the grid voltages are equally spaced, the separations between the curves are unequal, showing that the  $I_a E_g$  characteristic is non-linear and harmonic distortion is present. The shape of the output current



wave is shown to the right in Fig. 10.3*b*, and we will assume that it can be completely analysed into D.C., fundamental and second harmonic components; the expression for the output current is therefore

$$I_a = a_0 + a_1 \cos pt + a_2 \cos 2pt \quad . \quad . \quad . \quad 10.9$$

where  $a_0$  = D.C. component of current

$a_1$  = fundamental A.C. peak current

$a_2$  = second harmonic A.C. peak current

and  $p = 2\pi f$  = pulsance of the input frequency.

The three characteristic curves give three values of current  $I_2$ ,  $I_1$  and  $I_3$ , which satisfy expression 10.9, so that the values of  $a_0$ ,  $a_1$  and  $a_2$  in terms of these currents can be found as follows:

$$\text{At } -E_{g2}, pt = 0; I_a = I_2 = a_0 + a_1 + a_2. \quad . \quad . \quad . \quad 10.10.$$

$$\text{At } -E_{g1}, pt = 90^\circ; I_a = I_1 = a_0 - a_2. \quad . \quad . \quad . \quad 10.11$$

$$\text{and at } -E_{g3}, pt = 180^\circ; I_a = I_3 = a_0 - a_1 + a_2. \quad . \quad . \quad . \quad 10.12.$$

Subtracting 10.12 from 10.10 gives

$$a_1 = \frac{I_2 - I_3}{2} \quad . \quad . \quad . \quad . \quad 10.13.$$

Therefore Power output,

$$P_0 = \frac{a_1^2 R_0}{2} = \frac{(I_2 - I_3)^2 R_0}{8} \quad . \quad . \quad . \quad 10.14.$$

Adding 10.10 and 10.12

$$\begin{aligned} I_2 + I_3 &= 2(a_0 + a_2) \\ &= 2(I_1 + 2a_2). \end{aligned}$$

Therefore

$$a_2 = \frac{I_2 + I_3 - 2I_1}{4} \quad . \quad . \quad . \quad 10.15.$$

$$\text{Second Harmonic ratio} = \frac{a_2}{a_1} = \frac{I_2 + I_3 - 2I_1}{2(I_2 - I_3)} \quad . \quad . \quad . \quad 10.16.$$

A direct reading harmonic scale may be constructed<sup>20</sup> for placing over the  $I_a E_a$  curves so as to read percentage second harmonic directly. It is developed as follows:

If the Second Harmonic percentage =  $x$

$$\begin{aligned} \frac{x}{100} &= \frac{1}{2} \times \frac{(I_2 - I_1) - (I_1 - I_3)}{(I_2 - I_1) + (I_1 - I_3)} \\ &= \frac{1}{2} \cdot \frac{y-1}{y+1} \quad . \quad . \quad . \quad . \quad 10.17 \end{aligned}$$

where

$$y = \frac{I_2 - I_1}{I_1 - I_3}.$$



chosen to be equally spaced so that they correspond to angular positions of the cosine wave input voltage of  $0^\circ$ ,  $60^\circ$ ,  $90^\circ$ ,  $120^\circ$ ,  $180^\circ$ , etc. Three of the voltages are the same as for the second harmonic measurement, viz.,  $-E_{g2}$ ,  $-E_{g1}$ , and  $-E_{g3}$ , and the other two

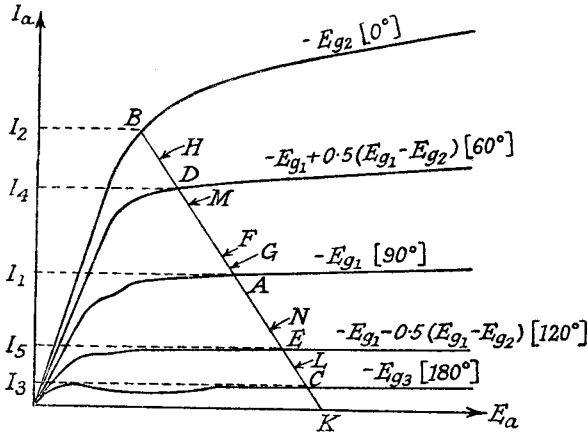


FIG. 10.5.—The Load Characteristic on the  $I_a E_a$  Curves of a Tetrode Valve.

voltages are  $-E_{g1} \pm 0.5(E_{g1} - E_{g2})$ . We will assume that the anode current expression is

$$I_a = a_0 + a_1 \cos pt + a_2 \cos 2pt + a_3 \cos 3pt + a_4 \cos 4pt \quad . \quad 10.19.$$

$$\text{At } -E_{g2}, pt = 0. \quad I_2 = a_0 + a_1 + a_2 + a_3 + a_4 \quad . \quad . \quad . \quad 10.20$$

$$-E_{g1} + 0.5(E_{g1} - E_{g2}), pt = 60^\circ.$$

$$I_4 = a_0 + 0.5a_1 - 0.5a_2 - a_3 - 0.5a_4 \quad . \quad 10.21.$$

$$-E_{g1}, pt = 90^\circ. \quad I_1 = a_0 - a_2 + a_4 \quad . \quad . \quad . \quad 10.22$$

$$-E_{g1} - 0.5(E_{g1} - E_{g2}), pt = 120^\circ.$$

$$I_5 = a_0 - 0.5a_1 - 0.5a_2 + a_3 - 0.5a_4 \quad . \quad 10.23$$

$$-E_{g3}, pt = 180^\circ. \quad I_3 = a_0 - a_1 + a_2 - a_3 + a_4 \quad . \quad . \quad 10.24.$$

Subtracting 10.24 from 10.20

$$I_2 - I_3 = 2(a_1 + a_3)$$

and 10.23 from 10.21

$$I_4 - I_5 = a_1 - 2a_3.$$

Solving the above for  $a_1$

$$a_1 = \frac{(I_2 - I_3) + (I_4 - I_5)}{3} \quad . \quad . \quad . \quad 10.25.$$

Therefore Power output,

$$P_o = \frac{1}{2} a_1^2 R_o = \frac{[(I_2 - I_3) + (I_4 - I_5)]^2 R_o}{18} \quad . \quad 10.26a.$$

Solving for  $a_3$

$$a_3 = \frac{(I_2 - I_3) - 2(I_4 - I_5)}{6} \quad . \quad . \quad . \quad 10.27.$$

$$\text{Third harmonic ratio} = \frac{a_3}{a_1} = \frac{(I_2 - I_3) - 2(I_4 - I_5)}{2[(I_2 - I_3) + (I_4 - I_5)]} \quad 10.28a.$$

Adding 10.24 to 10.20

$$\begin{aligned} I_2 + I_3 &= 2(a_0 + a_2 + a_4) \\ &= 2(I_1 + 2a_2). \end{aligned}$$

$$\text{Therefore} \quad a_2 = \frac{I_2 + I_3 - 2I_1}{4} \quad . \quad . \quad . \quad 10.29.$$

$$\text{Second harmonic ratio} = \frac{a_2}{a_1} = \frac{3}{4} \frac{I_2 + I_3 - 2I_1}{(I_2 - I_3) + (I_4 - I_5)} \quad . \quad 10.30.$$

Adding 10.21 and 10.23

$$\begin{aligned} I_4 + I_5 &= 2a_0 - a_2 - a_4 \\ I_2 + I_3 &= 2a_0 + 2a_2 + 2a_4. \end{aligned}$$

$$\text{Therefore} \quad I_2 + I_3 - I_4 - I_5 = 3a_2 + 3a_4.$$

Substituting 10.29 for  $a_2$  in the above

$$a_4 = \frac{1}{12}(I_2 + I_3 - 4I_4 - 4I_5 + 6I_1) \quad . \quad 10.31.$$

$$\text{Fourth harmonic ratio} = \frac{a_4}{a_1} = \frac{1}{4} \frac{(I_2 + I_3) - 4(I_4 + I_5) + 6I_1}{(I_2 - I_3) + (I_4 - I_5)} \quad . \quad 10.32.$$

Solving for  $a_0$  gives

$$a_0 = \frac{1}{6}(I_2 + I_3 + 2I_4 + 2I_5) \quad . \quad . \quad . \quad 10.33.$$

A direct reading third harmonic scale may be constructed in a similar way to the scale for second harmonic in the first example. Expression 10.27 may be written in terms of the percentage harmonic,  $x$ , and  $y$ , the ratio  $\frac{I_2 - I_3}{I_4 - I_5}$ ,

$$\frac{x}{100} = \frac{a_3}{a_1} = \frac{y - 2}{2(y + 1)} \quad . \quad . \quad . \quad 10.34a.$$

Rewriting 10.34a so as to give  $y$  in terms of  $x$

$$y = \frac{100 + x}{50 - x} \quad . \quad . \quad . \quad 10.34b.$$

The above expression is true when  $(I_2 - I_3) > 2(I_4 - I_5)$ , but for  $(I_2 - I_3) < 2(I_4 - I_5)$ ,  $a_3$  is negative and

$$y = \frac{100 - x}{50 + x} \quad . \quad . \quad . \quad 10.34c.$$

The values of  $y$  for different distortion percentages and the two conditions, (a)  $(I_2 - I_3) > 2(I_4 - I_5)$  and (b)  $(I_2 - I_3) < 2(I_4 - I_5)$  are as follows :

$x\%$	0	1	2	3	4	5	10	15	20
$y$	(a) 2	2.065	2.125	2.19	2.26	2.335	2.75	3.29	4
	(b) 2	1.942	1.885	1.83	1.777	1.728	1.5	1.308	1.142

For the direct reading scale, an isosceles triangle  $ABC$  is constructed as in Fig. 10.6. (The isosceles shape is merely for convenience and is not essential.) The base  $BC$  is bisected at  $E$ , which is joined to  $A$ . Lines  $AD$ , etc., are drawn from  $A$  to cut  $BC$  (condition  $b$ ) or  $BC$  produced (condition  $a$ ) such that  $BD/BC = y/2$ . The triangle  $ABC$  (on transparent paper) is placed over the  $I_aE_a$  curves with  $BC$  parallel to the load line,  $AB$  passing through

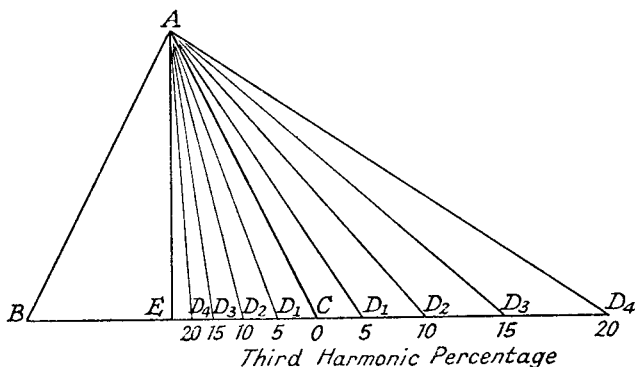


FIG. 10.6.—A Direct Reading Scale for Third Harmonic Percentage Distortion.

$I_4$  and  $AE$  through  $I_5$ . The triangle is now moved, maintaining  $BC$  parallel to, and at the same perpendicular distance from, the load line until  $AB$  passes through  $I_2$ . The distortion line  $AD$  passing through the intersection of  $I_3$  and the load line, i.e., point  $C$  in Fig. 10.5, gives the percentage distortion directly.

Second harmonic distortion may be measured using the direct reading scale with  $I_1$ ,  $I_2$  and  $I_3$  as indicated in the first example. This assumes that  $I_2 - I_3 \simeq 2(I_4 - I_5)$ , i.e., the third harmonic percentage is almost zero. The error introduced in the second harmonic percentage reading by this assumption is of the same percentage order as the third harmonic percentage. Thus the error introduced by 2% third harmonic is approximately 2% of the second harmonic percentage, i.e., a measurement of 5% second harmonic by the direct reading scale might be either 4.9% or 5.1%.

When the output wave shape is symmetrical about  $I_1$

$$\frac{I_2 + I_3}{2} = I_1 = \frac{I_4 + I_5}{2}$$

and there is no second and fourth harmonic.

The amplitudes of the individual current components in expression 10.19 can be determined by comparatively simple geometrical constructions.<sup>44</sup> The increase in d.c. component due to the application of the signal is, from 10.33,

$$\begin{aligned} a_0 - I_1 &= \frac{1}{3} \left[ \left( \frac{I_2 + I_3}{2} - I_1 \right) + 2 \left( \frac{I_4 + I_5}{2} - I_1 \right) \right] \\ &= \frac{1}{3}(FA + 2GA) \end{aligned}$$

where  $F$  bisects the line  $BC$  in Fig. 10.5 and  $G$  bisects  $DE$ . From 10.25

$$\begin{aligned} a_1 &= \frac{2}{3} \left[ \frac{I_2 + I_4}{2} - \frac{I_3 + I_5}{2} \right] \\ &= \frac{2}{3}(HK - LK) = \frac{2}{3}HL \end{aligned}$$

where  $H$  bisects  $BD$  and  $L$  bisects  $EC$ .

Expression 10.29 can be written

$$\begin{aligned} a_2 &= \frac{1}{2} \left[ \frac{I_2 + I_3}{2} - I_1 \right] \\ &= \frac{1}{2}(FK - AK) = \frac{1}{2}FA. \end{aligned}$$

The value of  $a_3$  can be expressed from 10.27 as

$$\begin{aligned} a_3 &= \frac{1}{3} \left[ \left( \frac{I_1 + I_2}{2} - I_4 \right) - \left( \frac{I_1 + I_3}{2} - I_5 \right) \right] \\ &= \frac{1}{3}(MD - NE), \end{aligned}$$

where  $M$  bisects  $BA$  and  $N$  bisects  $AC$ .

If  $M$  is a lower current point than  $D$ , as in Fig. 10.5,  $MD$  becomes  $-DM$  where  $DM$  is the distance from  $D$  to  $M$ .

From 10.31

$$\begin{aligned} a_4 &= \frac{1}{6} \left[ \left( \frac{I_2 + I_3}{2} - I_1 \right) - 4 \left( \frac{I_4 + I_5}{2} - I_1 \right) \right] \\ &= \frac{1}{6}(FA - 4GA). \end{aligned}$$

**10.5. Audio Frequency Distortion with a Complex Anode Load Impedance.** The analysis of Section 10.4 is developed on the assumption that the load impedance in the anode circuit of the output valve is resistive only, and this is generally true for the medium frequencies with transformer coupling. At low audio frequencies (50 to 150 c.p.s.) the inductance of the transformer primary may be comparable with the resistance load, whilst at high

frequencies (over 3,000 c.p.s.) stray capacitance and leakage inductance combine to produce a complex load. Furthermore, when the load on the output valve is the loudspeaker speech-coil, this forms a complex load, the resistive and reactive components of which vary with frequency. At low frequencies it is almost entirely resistive, but at high frequencies it is a mainly inductive impedance; there are rapid changes of impedance at frequencies in the neighbourhood of diaphragm resonances.<sup>1</sup> In spite of this, calculations and measurements assuming resistance loads are of value in determining the best practical operating conditions. Matching of the loudspeaker speech-coil to the output valve is performed by choosing an output transformer turns-ratio, which converts the modulus of the impedance of the speech coil at 400 c.p.s. to an impedance equal to the optimum load for the output valve. For example, suppose the optimum load is  $R_0$  and the speech-coil impedance at 400 c.p.s. is  $R_{sc} + jX_{sc}$ , then the primary/secondary turns-ratio is chosen as

$$\frac{N_p}{N_s} = \sqrt{\frac{R_0}{\sqrt{R_{sc}^2 + X_{sc}^2}}}$$

The representation of a complex load on the  $I_a E_a$  characteristics is (see Section 2.6, Part I) to be a closed curve similar in shape to a sheared ellipse, the inclination of the curve to the horizontal normally being fixed by the resistance component, and the width by the reactance component. When the reactance and resistance are in parallel, a large reactance leads to a narrow ellipse, but the reverse is true for a series circuit. The chief effect of a complex output load in the anode circuit of a valve having linear  $I_a E_a$  characteristics is to produce attenuation (frequency) distortion, causing a reduction in power output at low or high frequencies. The extent of the reduction depends on the relative value of the resistance and reactance and whether they are in parallel or series. Harmonic distortion is produced if the load curve enters the cramped low  $I_a$  region or if it cuts the  $E_a$  axis, i.e., if the valve is taken into the cut-off point of anode current.

With the practically realizable  $I_a E_a$  characteristics illustrated in Fig. 10.7a, it is important to note that harmonic distortion tends to be greater with a complex load than with a resistance load, for the locus curve passes through the more cramped low anode current region of the  $I_a E_a$  characteristics (see  $CD$  in Fig. 10.7a). A typical locus load line for an impedance consisting of resistance and reactance is shown in Fig. 10.7a. The direction of rotation round the locus curve depends on the type of reactance. If it is inductive

the direction is clockwise for input signal increasing in a positive direction, i.e., decreasing negative grid voltage, causes the anode current to rise according to the lower curve. The current wave shape tends to be asymmetric with respect to a vertical line through

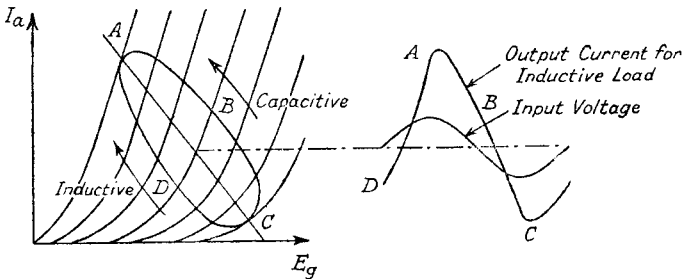


FIG. 10.7a.—A Reactive Locus Load Curve on the  $I_a E_g$  Characteristics with the Output Current for an Inductive Anode Load.

maximum amplitude, its leading edge being concave and trailing edge convex as shown in Fig. 10.7a. This is typical of the conditions obtaining with an output transformer at low audio frequencies. The direction round the locus curve is reversed for a capacitive load, increasing input signal causing anode current to rise according to the top curve. The operating  $I_a E_g$  characteristic has a shape similar to that of the locus curve on the  $I_a E_a$  characteristics as

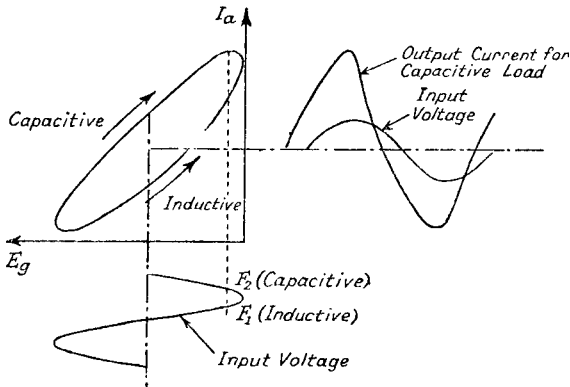


FIG. 10.7b.—A Reactive Locus Load Curve on the  $I_a E_g$  Characteristics with the Output Current for a Capacitive Anode Load.

illustrated in Fig. 10.7b. The lower curve represents the condition for increasing (positively) input voltage and the upper decreasing input voltage when the anode load is inductive; the reverse is true of a capacitive load. The current wave shape for the latter



is shown in Fig. 10.7*b*, and it is the reverse of that in Fig. 10.7*a*, its leading edge being convex and trailing edge concave. Maximum anode current does not occur at maximum instantaneous input voltage but later in the cycle (point  $F_1$ ) for an inductive load and earlier (point  $F_2$ ) for a capacitive load.

### 10.6. Measurement of Power Output and Distortion.

Measurement of power output and distortion is usually carried out at a fixed frequency, generally either the mains frequency or 400 c.p.s.

**10.6.1. Measurement with a Mains Frequency Voltage Source.** A schematic diagram of the apparatus is shown in

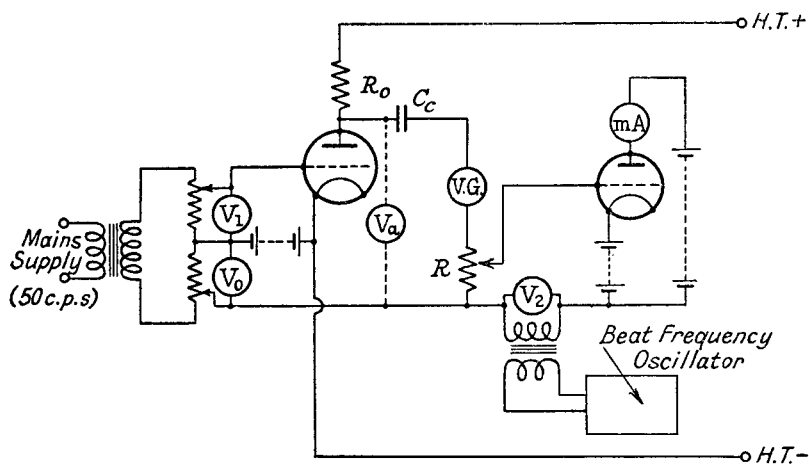


FIG. 10.8.—Measurement of Power Output at the Mains Frequency.

Fig. 10.8. Owing to the low frequency of the input signal the anode load is not by-passed by a choke, since it is difficult to make a choke with a high enough inductance. (100 H at 50 c.p.s. is only 31,416 ohms.) The resistance load is connected directly in the anode of the output valve, and constant D.C. anode voltage (the condition occurring when using a transformer) is maintained by increasing the H.T. voltage as the load resistance is increased. This is a serious disadvantage since very high H.T. voltages may be required; furthermore, push-pull measurements cannot be made. The fundamental 50 c.p.s. output anode voltage is measured by means of voltmeter  $V_0$ , connected across a back-balancing voltage obtained from the transformer supplying the input voltage  $V_1$ ; this back-balancing voltage is connected to the anode through a vibrating galvanometer (v.g.) and coupling capacitance  $C_c$ .

Between the galvanometer and the back balancing voltage is a high resistance ( $R$ ), across which are developed the harmonic distortion voltages. These voltages may be measured by a detector valve<sup>4</sup> or a dynamometer type milliammeter<sup>10</sup> acting as an harmonic analyser. In series with the grid circuit of this detector valve is a beat frequency oscillator, the frequency of which is adjusted close (within 1 c.p.s.) to that of the harmonic to be measured. The detector produces a beat, between the beat frequency oscillator output and the harmonic voltage, which causes the needle of a milliammeter (mA) in its anode circuit to oscillate at the difference frequency of approximately 1 c.p.s. The amplitude of this oscillation is a measure of the amplitude of the particular harmonic voltage. Each harmonic amplitude may be measured independently by suitably adjusting the frequency of the beat frequency oscillator, e.g., the fourth harmonic is measured by adjusting to approximately 201 or 199 c.p.s. The voltage output of the beat frequency oscillator, measured by  $V_2$ , must be maintained constant while the frequency is changed, and the detector may be calibrated initially against the fundamental mains frequency voltage with the oscillator frequency set at 49 or 51 c.p.s. For correct operation the input signal to the detector must not be excessive if the calibration is to hold, and for this reason it is essential that the fundamental component should be balanced out. A disadvantage of this type of harmonic analyser is the difficulty of reading an oscillating pointer, and the strain imposed on the operator.

### 10.6.2. Measurement with a 400 c.p.s. Voltage Source.

The great advantage of using 400 c.p.s. as the fundamental frequency is that a choke may be used to by-pass the D.C. current and, if a centre-tapped connection is employed, push-pull measurements may be made (see Fig. 10.9). A distortion factor meter or a harmonic analyser can be connected to the output to measure total harmonic distortion or to read the ratios (or percentages) of individual harmonics. It is important that the input impedance of the harmonic measuring equipment should be high and much greater than the highest load resistance (about 20,000 ohms) likely to be required. A high input impedance buffer amplifier may be necessary to ensure this. Alternatively a transformer connection may be used between the output valve and distortion measuring equipment, and this is the type of circuit shown in Fig. 10.9. An output voltmeter may be used to determine power output—its resistance must be taken into account as it forms part of the load resistance—or a variable (in steps) resistance output power meter

can be employed, combining the function of adjustable load resistance and power output meter.

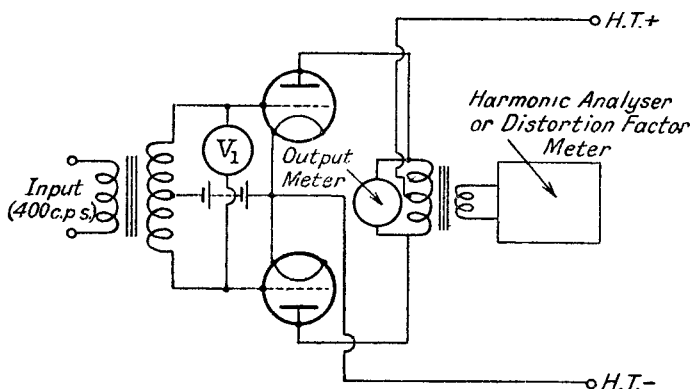


FIG. 10.9.—Measurement of Power Output at 400 c.p.s.

Representative curves of power output and distortion against load resistance are shown in Figs. 10.10a and 10.10b for a triode and tetrode valve. Referring to Figs. 9.7 and 9.8 showing characteristic  $I_a E_a$  curves for a triode and tetrode, respectively, we can see the reason for the particular shapes of the distortion curves. Since the output transformer primary carries the D.C. anode current,

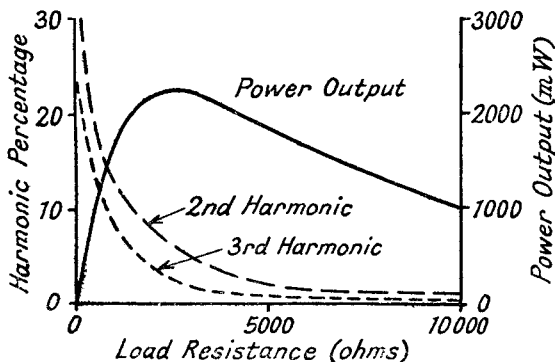


FIG. 10.10a.—Typical Power Output and Distortion Curves Against Load Resistance for a Triode Valve.

the D.C. anode voltage is practically the H.T. voltage. The load line  $FG$  is therefore pivoted at a point, such as  $H$  in Figs. 9.7 and 9.8, on the appropriate bias voltage line, immediately above an anode voltage equal to the H.T. voltage point  $A$ .

For the triode valve when the load resistance,  $R_o$ , is small, the

line  $FG$  in Fig. 9.7 approaches the vertical position, and its lower end projects into the cramped grid voltage—low anode current region. The output anode current wave shape tends to be flattened at its lower end, indicating chiefly second harmonic distortion. As  $R_o$  is increased the line  $FG$  becomes less vertical and its lower end is taken out of the cramped low  $I_a$  region (see  $F'G'$ ). Hence harmonic distortion decreases with increase of load resistance as shown in Fig. 10.10a.

The tetrode  $I_a E_a$  characteristics in Fig. 9.8 indicate that for low values of  $R_o$ , load line  $FG$ , the output current wave shape is cramped at the low current end, and second harmonic distortion is large. For an intermediate load resistance, line  $F'G'$ , high and low current

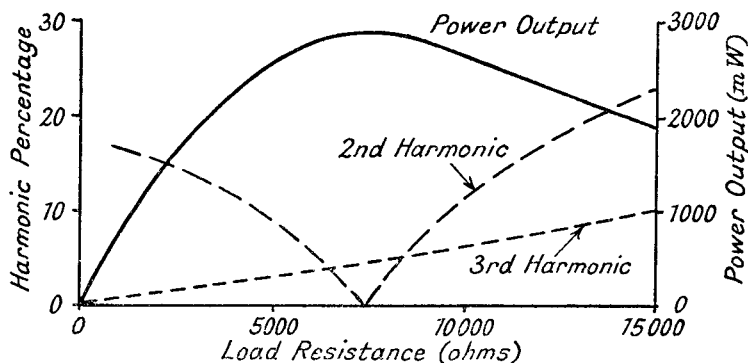


FIG. 10.10b.—Typical Power Output and Distortion Curves Against Load Resistance for a Tetrode or Pentode Valve.

ends of the line are cramped and distortion consists mainly of third harmonic, with second harmonic almost zero. This corresponds to a load resistance of 7,500 ohms on Fig. 10.10b, and usually to maximum power output. At high values of  $R_o$ , line  $F''G''$ , the high current end of the line is more, and the low current end is less, cramped. Second, as well as third, harmonic is now present.

**10.7. Non-Linear Harmonic and Intermodulation Distortion in Power Output Valves.** An absolute standard for permissible non-linear distortion is difficult to fix because of the number of different factors involved. The critical faculty of the listener and the overall frequency range of the receiver both play an important part; the tolerable distortion is reduced if direct comparison is possible between the undistorted and distorted sound. If the frequency range is reduced greater distortion can be permitted. Massa <sup>14</sup> gives the following as average values for distortion produc-

ing a detectable change of quality on speech. The effect of restricting the high-frequency range is indicated for three cut-off frequency limits. The lowest cut-off frequency (5,000 c.p.s.) gives a frequency range comparable to that of an average broadcast receiver.

Cut-Off Frequency.	DIRECT COMPARISON		NO COMPARISON.	
	Single Stage.	Push-Pull.	Single Stage.	Push-Pull.
14,000 c.p.s. .	5%	3%	10%	5%
8,000 „ .	5%	3%	10%	7%
5,000 „ .	12%	> 10%	17%	> 10%

More distortion is tolerable with the single stage having chiefly second harmonic than with the push-pull stage in which third harmonic distortion predominates, and greater distortion can be considered if the high-frequency range is reduced. The value of 5% total harmonic distortion, commonly used to specify the maximum power output condition, is open to criticism since the order of the predominant harmonic is so important in determining quality. The table shows that 3% of third harmonic is as objectionable as 5% of second. If, however, instead of total harmonic distortion the percentages of the individual harmonics are measured, a better estimate of distortion can be obtained. For comparison purposes the percentage of each harmonic is multiplied by the number of the harmonic, i.e., the distortion property of 5% second harmonic is represented by  $5 \times 2 = 10$ , and that of 3% third harmonic by  $3 \times 3 = 9$ . This is in accord with the results set out in the table above. Another method<sup>49</sup> is to insert in the distortion factor meter a network having an output voltage frequency response linearly proportional to frequency for a fixed amplitude of input signal. This is equivalent to multiplying the amplitude of each harmonic by its number.

Let us now consider why a given percentage of a higher order harmonic represents greater apparent distortion than the same percentage of a lower order harmonic. Relating harmonics to the musical scale we find that of the first ten all but the seventh and ninth are concordant with the fundamental. For most operational conditions the percentages of the discordant harmonics are very small—an exception is sometimes found in Class B operation—and it is not often possible to read the amplitudes of harmonics greater than the fifth. Hence it would appear that harmonic frequencies are not themselves generally responsible for harsh and discordant reproduction, and, for a single frequency input, whilst distortion causes a change in quality, reproduction is not necessarily rendered unpleasant. With the more usual input signal consisting of a series of frequencies, the property producing harmonic distortion can also

cause intermodulation between the frequency components; a low frequency,  $f_l$  may modulate a high-frequency component,  $f_h$ , to produce sidebands of  $f_h \pm f_l$ ,  $f_h \pm 2f_l$ , etc., which can be, and often are, discords with the input frequency components. The relationship between harmonic and intermodulation distortion can be shown by considering the following expression for anode current in terms of grid voltage:

$$I_a = a_0 + a_1 E_g + a_2 E_g^2 + a_3 E_g^3 \quad . \quad . \quad . \quad 10.35.$$

If  $E_g = \hat{E}_l \cos p_l t + \hat{E}_h \cos p_h t - E_b$

where  $\hat{E}_l \cos p_l t$  represents the low audio frequency

$\hat{E}_h \cos p_h t$  ,, ,, high ,, ,,

and  $-E_b$  ,, ,, grid bias voltage.

Replacing  $E_g$  in 10.35

$$\begin{aligned} * I_a &= a_0 + a_1 (\hat{E}_l \cos p_l t + \hat{E}_h \cos p_h t - E_b) \\ &\quad + a_2 (\hat{E}_l \cos p_l t + \hat{E}_h \cos p_h t - E_b)^2 \\ &\quad + a_3 (\hat{E}_l \cos p_l t + \hat{E}_h \cos p_h t - E_b)^3 \\ &= a_0 + a_1 (\hat{E}_l \cos p_l t + \hat{E}_h \cos p_h t - E_b) \\ &\quad + a_2 \left[ \frac{\hat{E}_l^2}{2} (1 + \cos 2p_l t) + \frac{\hat{E}_h^2}{2} (1 + \cos 2p_h t) + E_b^2 \right. \\ &\quad \quad \left. + \hat{E}_l \hat{E}_h [\cos (p_h + p_l)t + \cos (p_h - p_l)t] \right. \\ &\quad \quad \left. - 2\hat{E}_h E_b \cos p_h t - 2\hat{E}_l E_b \cos p_l t \right] \\ &\quad + a_3 \left[ \frac{\hat{E}_l^3}{4} (\cos 3p_l t + 3 \cos p_l t) + \frac{\hat{E}_h^3}{4} (\cos 3p_h t + 3 \cos p_h t) - E_b^3 \right. \\ &\quad \quad - \frac{3}{2} \hat{E}_l^2 E_b (1 + \cos 2p_l t) - \frac{3}{2} \hat{E}_h^2 E_b (1 + \cos 2p_h t) \\ &\quad \quad + 3\hat{E}_l E_b^2 \cos p_l t + 3\hat{E}_h E_b^2 \cos p_h t \\ &\quad \quad + \frac{3}{4} \hat{E}_l^2 \hat{E}_h (2 \cos p_h t + \cos (p_h + 2p_l)t + \cos (p_h - 2p_l)t) \\ &\quad \quad + \frac{3}{4} \hat{E}_l \hat{E}_h^2 (2 \cos p_l t + \cos (2p_h + p_l)t + \cos (2p_h - p_l)t) \\ &\quad \quad \left. - \frac{3}{2} \hat{E}_l \hat{E}_h E_b (\cos (p_h + p_l)t + \cos (p_h - p_l)t) \right] \quad . \quad . \quad 10.36. \end{aligned}$$

The modulation ratio of the first intermodulation sideband  $\frac{(p_h \pm p_l)}{2\pi}$  of the high audio frequency  $\frac{(p_h)}{2\pi}$  is

$$\begin{aligned} M_1 &= \frac{a_2 \hat{E}_l \hat{E}_h - \frac{3}{2} a_3 \hat{E}_l \hat{E}_h E_b}{a_1 \hat{E}_h - 2a_2 \hat{E}_h E_b + a_3 \left[ \frac{3\hat{E}_h^3}{4} + 3\hat{E}_h E_b^2 + \frac{3}{2} \hat{E}_h E_l^2 \right]} \\ &= \frac{\hat{E}_l (a_2 - \frac{3}{2} a_3 E_b)}{a_1 - 2a_2 E_b + a_3 \left[ \frac{3}{4} \hat{E}_h^2 + 3E_b^2 + \frac{3}{2} \hat{E}_l^2 \right]} \quad . \quad . \quad 10.37. \end{aligned}$$

$$* \cos^2 \theta = \frac{1 + \cos 2\theta}{2}; \quad \cos \theta + \cos \phi = \frac{\cos (\theta + \phi) + \cos (\theta - \phi)}{2}.$$

$$\cos^3 \theta = \frac{3 \cos \theta + \cos 3\theta}{4}.$$

The modulation ratio for the second sideband  $\frac{p_h \pm 2p_l}{2\pi}$  is

$$M_2 = \frac{\frac{3}{4}a_3\hat{E}_l^2}{a_1 - 2a_2E_b + a_3[\frac{3}{4}\hat{E}_h^2 + 3E_b^2 + \frac{3}{2}\hat{E}_l^2]} \quad . \quad . \quad 10.38.$$

If  $\hat{E}_h = 0$ , we have as the second harmonic  $\left(\frac{2p_l}{2\pi}\right)$  ratio of  $\frac{p_l}{2\pi}$

$$H_2 = \frac{\hat{E}_l\left[\frac{a_2}{2} - \frac{3}{2}a_3E_b\right]}{a_1 - 2a_2E_b + a_3[\frac{3}{4}\hat{E}_l^2 + 3E_b^2]} \quad . \quad . \quad 10.39$$

and for the third harmonic  $\left(\frac{3p_l}{2\pi}\right)$  ratio

$$H_3 = \frac{\frac{1}{4}a_3\hat{E}_l^2}{a_1 - 2a_2E_b + a_3[\frac{3}{4}\hat{E}_l^2 + 3E_b^2]} \quad . \quad . \quad 10.40.$$

If we neglect the second term  $-\frac{3}{2}a_3E_b$  in the numerators of 10.37, and 10.39, and terms containing  $\hat{E}_h$  and  $\hat{E}_l$  in the denominators of 10.37, 10.38, 10.39, and 10.40, we find that

$$M_1 = 2H_2$$

and

$$M_2 = 3H_3.$$

It is clear from the above expressions that the intermodulation terms responsible for unpleasant reproduction are proportional to the product of the individual harmonic of a single frequency input multiplied by the harmonic number. Hence "weighting" (as it is called) of the harmonics from a single frequency input is justified as a method of estimating apparent distortion. Higher power terms in the  $I_aE_g$  expression 10.35 introduce additional harmonic sidebands, and sidebands to harmonics of the high frequency. For example,  $a_4E_g^4$  added to 10.35, produces in the output the following additional intermodulation sidebands,

$$\frac{p_h \pm 3p_l}{2\pi}, \quad \frac{2p_h \pm 2p_l}{2\pi} \quad \text{and} \quad \frac{3p_h \pm p_l}{2\pi}.$$

An illustration of the way in which intermodulation <sup>24</sup> occurs is given in Fig. 10.11. The input signal consists of a large amplitude low audio frequency and a smaller amplitude high frequency. Typical operating  $I_aE_g$  characteristics for a triode (dotted extension) and tetrode (full line) are shown in the figure; the flattening of the tetrode  $I_a$  curve at low bias voltages is due to the load line projecting into the knee of the  $I_aE_a$  characteristics (see  $F'G'$  in Fig. 9.8). The wave shape of the high-frequency output current—the low frequency is omitted for the sake of clarity—shows that it is modu-

lated by the low frequency. For the tetrode the modulation envelope changes at the rate of  $2f_i$ , because amplification is reduced when the low-frequency input carries the grid voltage into the region  $BC$  and into the region of high negative voltage beyond  $A$ . With the triode, modulation in the region  $BC$  is absent; the modulation envelope has a fundamental frequency of  $f_i$ , i.e., there is no

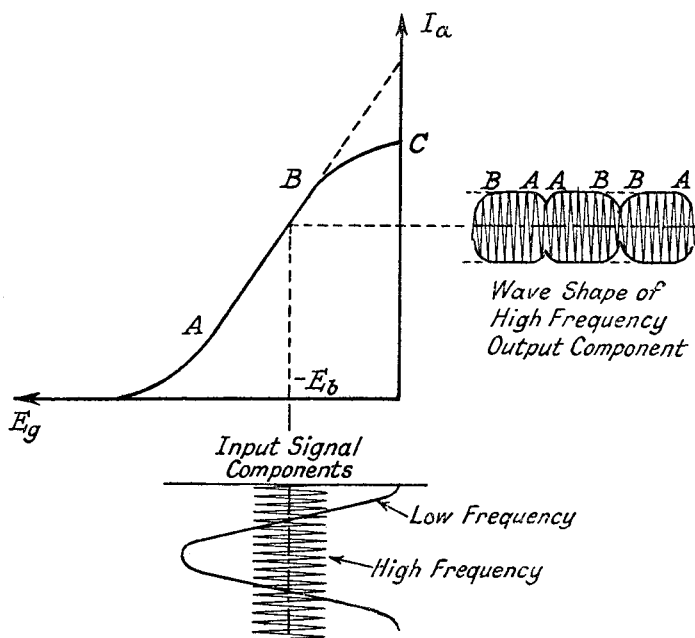


FIG. 10.11.—Intermodulation of a High Audio Frequency by a Low Audio Frequency.

dip in the envelope from  $B$  to  $B$ , and intermodulation distortion is much less.

Methods of estimating distortion by measuring intermodulation tones have been developed,<sup>35, 45</sup> though it is doubtful if the added complication of apparatus justifies their use in comparison with the single frequency method and harmonic ratios multiplied by their harmonic number. Harries, who appears to have been the first to suggest intermodulation distortion measurements, used two input frequencies of 70 c.p.s. and 1,000 c.p.s., having an amplitude ratio of 9 to 1. The amplitudes of the 1,000 c.p.s. frequency and its sidebands were measured with a harmonic analyser, the sidebands being expressed as a percentage of the 1,000 c.p.s. output. A triode was found to produce mainly first sideband voltages ( $1,000 \pm 70$  c.p.s.),



and all sideband amplitudes were generally small. A pentode valve showed a greater range of sidebands with the second ( $1,000 \pm 140$  c.p.s.) as the largest. The second harmonic frequency (2,000 c.p.s.) was overmodulated and had sidebands larger than itself. Under these conditions distortion was marked, and reproduction harsh. Harries finally suggests the following quality grades :

- (1) high quality : no sideband should represent more than 5% modulation where modulation percentage

$$= \frac{2 \times \text{sideband amplitude} \times 100}{\text{fundamental}} ;$$

- (2) good commercial quality : first and second sideband modulation percentages to be less than 30% and 5% respectively ;  
 (3) objectionable : this to be denoted by second sideband modulation percentage exceeding 5%.

“Undistorted” power output is to be defined as the power output given by a single frequency sine wave input of amplitude equal to the sum of the amplitudes of the two frequencies satisfying condition 2.

## 10.8. Push-Pull Operation.

**10.8.1. Introduction.**<sup>7</sup> Push-pull operation is obtained from a pair of valves by applying to the grid of one valve a voltage in phase opposition to that applied to the other (see Fig. 10.12). The anodes of these valves are joined to opposite ends of the primary of a transformer, the centre tap of which is connected to H.T. positive. The D.C. anode currents produce opposing voltages in the transformer primary, but the A.C. output currents, owing to the 180° phase shift between the grid voltages, are additive. Thus the total A.C. current in the primary is

$$\begin{aligned} I_{at} &= I_{a1} - (-I_{a2}) \\ &= I_{a1} + I_{a2}. \end{aligned}$$

Push-pull operation has four important advantages.

- (1) Even harmonic distortion produced in each output valve is partially (completely, if matched valves are employed) cancelled.
- (2) The D.C. current component in the output transformer is reduced considerably or cancelled. This means less attenuation (frequency) and non-linear (harmonic) distortion from, and more efficient operation of, the output transformer. A much smaller air gap is required so that



cancel in the output, leaving only the fundamental and odd harmonics with their intermodulation sidebands. If the two valves have slightly different  $I_a E_g$  characteristics, i.e., are not exactly matched, the proportion of even harmonic remaining depends on the amount of mismatching. If, for example, each valve normally produces 5% second harmonic and the mismatch in the values of  $a_2$  is 10%, the output contains 0.5% second harmonic.

Before considering the various types of push-pull operation we will consider the methods of obtaining the push-pull antiphase voltages for the grid circuits of the output valves.

**10.8.2. Methods of Producing the Push-Pull Grid Voltage.**<sup>21, 32</sup> A method of obtaining the push-pull grid voltage from

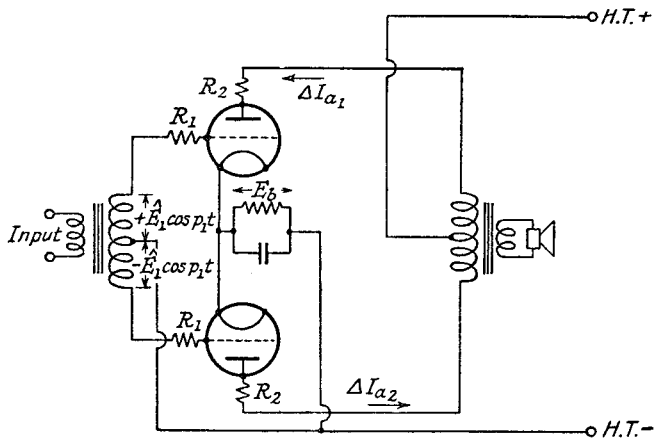


FIG. 10.12.—A Transformer Coupled Push-pull Output Stage.

a diode detector is described in Section 8.7, Part I. The disadvantage from which this suffers is that two ganged potentiometers are required for volume control, so that it is preferable to obtain the antiphase voltages from an A.F. stage after the detector volume control. One of the simplest methods is to use a transformer with centre-tapped secondary as in Fig. 10.12. Provided the transformer is designed to have a high primary inductance, low leakage inductance, and small and equal half secondary self-capacitances, and that the primary and half secondaries are electrically balanced with regard to the centre tap (this implies equal leakage inductances and interwinding capacitances from the primary to half secondaries), satisfactory performance over the A.F. range and the 180° phase shift between the two secondary voltages can be maintained.

A second method (Fig. 10.13), known as paraphase,<sup>3</sup> uses the

phase reversing property of a  $RC$  coupled A.F. amplifier. Part of the input voltage to one of the push-pull output valves  $V_3$  is taken to the valve  $V_2$ , the output of which is connected to the other push-pull valve,  $V_4$ . The proportion of voltage taken from the grid of  $V_3$  is equal to the inverse of the amplification from  $V_2$  to  $V_4$ , so that the input voltages to  $V_3$  and  $V_4$  are equal but  $180^\circ$  out-of-phase. Correct push-pull operation is achieved by adjustment of the potentiometer  $R_1$  to give minimum sound, with a suitable input frequency (400 or 1,000 c.p.s.), in telephones connected between the H.T. supply and the centre point of the primary of the output transformer. The disadvantages of the paraphase connection are :

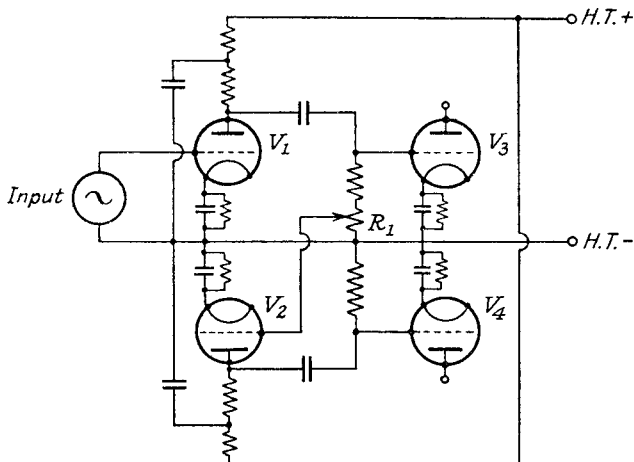


FIG. 10.13.—A Paraphase Push-pull Circuit.

(1) phase changes may occur between the input and output of  $V_2$  at high audio frequencies due to stray capacitance, so that the  $180^\circ$  phase relationship is not maintained, and (2) hum and noise voltages may be introduced and amplified by the extra valve  $V_2$ .

A third system employs a cathode as well as an anode load resistance in an amplifier, the voltage for one valve being derived from the cathode and that for the other from the anode circuit as in Fig. 10.14. The objection to this method is the high D.C. voltage between heater and cathode, the possibility of producing hum voltage from the heater circuit across the cathode load resistance  $R_k$ , and the comparatively large stray capacitance across the latter, which causes a reduction in gain at high frequencies. An alternative method of connection using negative feedback reduces the stray capacitance and also allows the input to the valve to be earthed.

The dotted lines in Fig. 10.14 show the change in the circuit. The grid leak connection does not affect the A.F. operation of the valve but merely ensures that the correct D.C. bias is applied. Connecting directly from grid to earth applies a large bias to the valve, causing it to operate over the curved portion of its  $I_a E_g$  characteristic. When negative feedback is employed, the output voltage to each push-pull stage is less than the input voltage to the phase-changing stage, but distortion is also very low. The preceding amplifier must therefore deliver a larger voltage than is required to operate the push-pull valves, and it is important to guard against distortion in this stage. Chokes<sup>40</sup> wound on the same core, so that D.C. currents neutralize each other, may replace the resistances  $R_0$  and

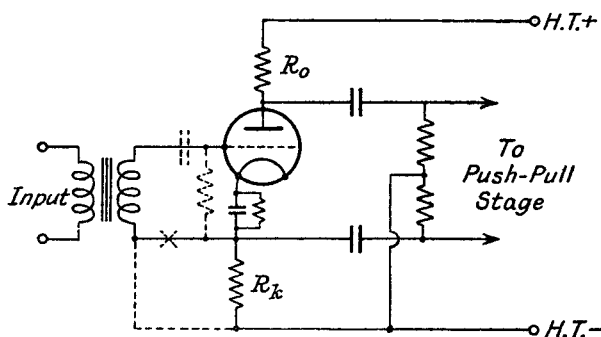


FIG. 10.14.—Push-pull Voltage Output by Means of Equal Anode and Cathode Load Resistances.

$R_k$  if the H.T. voltage is low. Tone control may be achieved by a capacitance shunting  $R_k$ ; this increases the output across  $R_0$  at high frequencies relative to that across  $R_k$ , so that the push-pull outputs at these frequencies are unequal. This is less important since the amplitude of high frequencies is usually small and their harmonics are approaching the inaudible range.

A small secondary winding on the output transformer has been employed to provide the input to the second valve of a push-pull stage. This cannot be entirely satisfactory since it tends to defeat the object of push-pull by applying distortion in the output of one of the push-pull valves to the grid of the second, and cancellation of even harmonics cannot be complete.

The possibility of using the antiphase relationship between screen and anode currents in a heptode<sup>37</sup> valve has been suggested, but great care has to be exercised if equal amplitudes of undistorted push-pull voltages are to be produced.

**10.8.3. Types of Push-Pull Stages.** Push-pull output stages may be divided into three groups, depending on the biasing point relative to the  $I_a E_g$  characteristic. In Class A operation both valves are biased to the centre of the straight part of their  $I_a E_g$  characteristics though, owing to the cancellation of even harmonics, the valves may be operated in push-pull beyond the straight part of their characteristics. This method is very satisfactory since distortion is low and anode current to both valves substantially constant; efficiency is, however, low (25% to 35%).

In Class B operation both valves are biased to the curved lower part of their  $I_a E_g$  characteristics, i.e., almost into cut-off, and each valve supplies approximately half the output wave shape. Its chief advantages are low current consumption with zero input voltage, and high efficiency (about 60%) for maximum input voltage. The D.C. anode current is initially small but increases with increase of input voltage, and there is considerable economy in H.T. consumption, a very desirable characteristic for the output stage of a battery receiver. For mains receivers H.T. economy is not so important and Class B operation is hardly ever employed. The varying current of a Class B stage would require a H.T. source having very good D.C. voltage regulation. If triodes are used in Class B push-pull, they are usually operated into the positive grid region in order to obtain high efficiency. A special amplifier stage, known as the driver, is needed to supply the power absorbed by the grid current taken on the peaks of input voltage, and the method of operation is generally known as Class B positive drive. With tetrodes the shape of the  $I_a E_g$  characteristic makes positive drive of no value, and the term quiescent push-pull is often applied to this mode of operation without grid current.

Class AB operation is sometimes employed in mains receivers with triode output valves to obtain high efficiency and power output. The valves are biased approximately half-way between Class A and Class B conditions and a driver stage is used to allow grid current to be taken. Anode current varies with signal voltage but to a much less extent than with Class B.

Push-pull stages are particularly liable to parasitic oscillation at ultra high frequencies since capacitance coupling between the grid of one valve and the anode of the other is in the correct phase to initiate oscillation. Short leads and resistances of 1,000 and 100 ohms in the grid and anode leads (see  $R_1$  and  $R_2$  in Fig. 10.12), as close to the valve pins as possible, help to prevent this.

**10.8.4. Class A Push-Pull.** The performance of a push-pull

output stage can be determined by constructing  $IE_a$  curves<sup>13</sup> from the  $I_aE_a$  characteristics of the individual valves. If the instantaneous anode currents in each valve are  $I_{a1}$  and  $I_{a2}$  and the coupling coefficient between the two half primaries is very nearly unity (a justifiable assumption for most iron-cored transformers), the effective composite current,  $I = I_{a1} - I_{a2}$ , can be considered as flowing through one of the half primaries. The composite  $IE_a$  curves are therefore obtained by subtracting appropriate pairs of  $I_aE_a$  curves of the two valves, so arranged that the grid voltage and anode voltage scales of one valve are in the reverse direction to

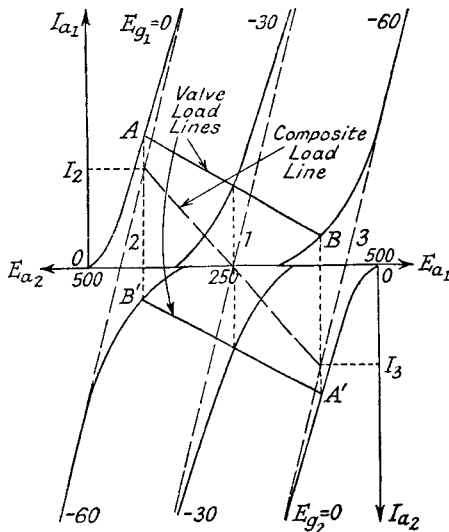


FIG. 10.15.—Composite Current-Anode Voltage Curves for a Class A Push-pull Amplifier.

those of the other. This essential condition of the push-pull connection is fulfilled by Fig. 10.15; the  $I_aE_a$  curves of the second valve, inverted and reversed with the  $E_{a2}$  scale running from right to left, are moved until the  $E_a$  points, corresponding to H.T. voltages of 250 on the normal and reversed scales register with each other. If the d.c. grid bias voltage on each valve is  $-30$  volts, the two  $I_aE_a$  curves for  $E_g = -30$  volts are added to form the dotted composite  $IE_a$  curve 1. The process is repeated for each appropriate pair of  $I_aE_a$  curves, thus the composite curve 2 is obtained by adding the curve for  $E_g = 0$  of the first valve to that for  $E_g = -60$  of the second. Composite curve 3 is plotted by a similar process. It is most important to remember that these composite curves refer to

one-half of the primary, and a load line drawn across them represents a load resistance across a half primary. Hence the equivalent load resistance across the whole primary, i.e., the anode-to-anode load on the valves, is four times this value. For example, an optimum load resistance for the composite curves of 2,000 ohms, requires an anode-to-anode load resistance of 8,000 ohms, and the secondary to total primary turns ratio is adjusted to give the equivalent of 8,000 ohms across the total primary winding. The composite load line passes through the H.T. voltage and a composite current point equal to the difference between the D.C. anode currents of the valves; if the latter are perfectly matched the composite current is zero as shown in Fig. 10.15. Power output and distortion may be calculated from the composite characteristics in the same manner as for a single stage. Thus, assuming even harmonics to be small in amplitude and third harmonics to be greatest, the power output is, from expression 10.26*a*,

$$P_o = \frac{[(I_2 + I_3) + (I_4 + I_5)]^2 R_o}{18} \quad . \quad . \quad 10.26b$$

where  $I_2$  is the intercept of the load line with the composite  $I E_a$  curve corresponding to  $E_g = 0$  on the first valve and measured on the  $I_{a1}$  scale and  $I_3$  is the counterpart of  $I_2$  measured on the  $I_{a2}$  scale. The negative sign before  $I_3$  and  $I_5$  in expression 10.26*a* becomes positive because  $I_3$  and  $I_5$  are numerical values of current. The currents  $I_4$  and  $I_5$ , measured on the  $I_{a1}$  and  $I_{a2}$  scales, respectively, are the load line intercepts with composite  $I E_a$  curves corresponding to  $E_g = -15$  and  $-45$  volts on the first valve. Third harmonic ratio is from 10.28*a*,

$$H_3 = \frac{(I_2 + I_3) - 2(I_4 + I_5)}{2((I_2 + I_3) + (I_4 + I_5))} \quad . \quad . \quad 10.28b.$$

Although the composite load line gives the equivalent half-primary load resistance, it is important to note that this is not the load resistance across each valve. The load line for each valve is obtained by projecting vertically (up or down) from the intersections of the composite load line and composite curves on to the corresponding  $I_a E_a$  curves for the single valve. Thus the valve load lines are represented by lines  $AB$  and  $A'B'$  in Fig. 10.15 and, since the valves are operating in Class A push-pull, each has a slope of nearly half that of the composite load line; i.e., it corresponds to twice the composite load resistance. If both valves have linear  $I_a E_a$  characteristics the composite curves are straight lines of twice the slope of the  $I_a E_a$  lines, and it may then be proved geometrically



that each equivalent valve load line has a slope of one-half that of the composite line. If the optimum load for a single valve stage is  $2R_a$  (the valve resistance), the optimum composite load is half this value, i.e.,  $R_a$ , so that the optimum anode-to-anode load becomes  $4R_a$ . The same conclusion is reached if we consider the push-pull stage as consisting of two valve generators connected in series. Their total internal resistance is  $2R_a$ , and by analogy with the single stage, the optimum load (from anode-to-anode) will be  $2 \times 2R_a = 4R_a$ . An important advantage of push-pull illustrated by the curves is that owing to the linearity of the composite characteristics, a complex load impedance giving an "elliptical" locus line as in Fig. 10.7a produces practically no harmonic distortion.

Owing to the predominance of odd harmonics when distortion occurs in push-pull stages, maximum "undistorted" power output should be assessed for a lower total harmonic percentage than a single valve, approximately in the ratio of 2 to 3 for triodes.

**10.8.5. Class B Push-Pull.**<sup>18, 25, 29, 31</sup> The performance of push-pull valves under Class B conditions may be shown by constructing composite  $IE_a$  curves in exactly the same way as for Class A, and these are shown in Fig. 10.16 for three grid bias voltages. Triode characteristics are used in the above illustration to preserve continuity with Fig. 10.15, but tetrode composite curves can be developed in like manner. The load line for each valve is obtained

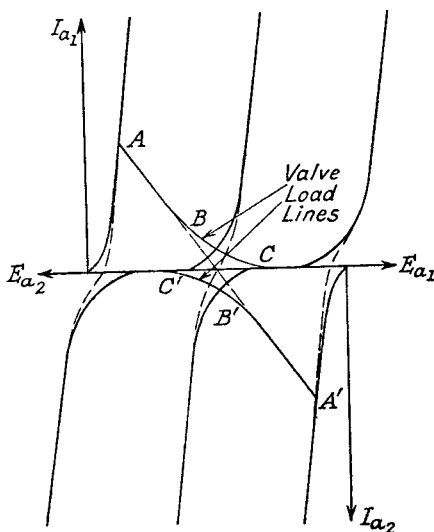


FIG. 10.16.—Composite Current-Anode Voltage Curves for a Class B Amplifier with High Grid Bias and Low Load Resistance.

by projection from the composite to the valve curves as described in the previous section. If the valves have linear  $I_a E_a$  characteristics and are biased to cut-off, each valve operates over half a cycle only, and the composite characteristics and load line are identical with the valve characteristics and load line. The anode-to-anode load resistance, which is four times the composite load resistance, is also four times the valve load resistance compared with twice for Class A. Since practical  $I_a E_a$  characteristics are always curved, the valves cannot be biased to cut-off and the valve load line only approaches the composite at the extremities of the grid voltage swing. Towards the centre, where both valves are operating, the valve load

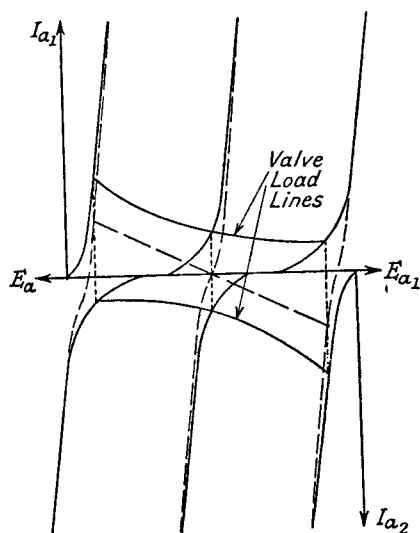


FIG. 10.17.—Composite Current-Anode Voltage Curves for a Class B Amplifier with Low Grid Bias and High Load Resistance.

resistance increases, eventually becoming infinite when the valve reaches cut-off. Hence the valve load line  $ABC$  is sharply curved as in Fig. 10.16. The degree of curvature is dependent on the grid bias voltage relative to the cut-off bias voltage and also upon the load resistance, a grid bias approaching cut-off bias and a low load resistance producing a more sharply curved load line (similar to  $ABC$  in Fig. 10.16), which rapidly approaches the composite load line. Conversely for a high load resistance and a bias voltage much less than cut-off bias, the valve load line is less sharply curved and has a slope of nearly twice that of the composite line; this is illustrated in Fig. 10.17.

It is much more difficult to obtain linear composite curves for Class B than for Class A operation, and generally there is a "kink" near zero current, the "kink" becoming more pronounced as the initial bias is increased. This "join-up" distortion,<sup>28</sup> as it is called, is greatest for small output voltages, and it places a limit on the maximum negative initial grid bias which can be employed.

The great advantage of Class B operation, apart from its low quiescent current consumption, is its high anode circuit efficiency. The theoretical maximum, assuming that each valve is biased to cut-off and that the anode voltage of each valve is taken to zero at the extremities of grid swing, is 78.5%. Each valve supplies half the wave shape so that the D.C. current is  $\hat{I}/\pi$  where  $\hat{I} \cos pt$  is the A.C. output current wave.

$$\text{Therefore D.C. power for two valves} = \frac{2E_1\hat{I}}{\pi}$$

where  $E_1 = \text{H.T. voltage}$ .

The A.C. output voltage wave is represented by  $E_1 \cos pt$ .

$$\text{Therefore A.C. power from two valves} = \frac{E_1\hat{I}}{2}$$

$$\text{A.C./D.C. efficiency} = \frac{\frac{E_1\hat{I}}{2}}{\frac{2E_1\hat{I}}{\pi}} = \frac{\pi}{4} = 78.5\%.$$

There is little essential difference between the two types of Class B operation, quiescent push-pull (Q.P.P.) and positive drive. With quiescent push-pull, tetrode valves are employed and the input voltage is restricted to the region where there is no grid current. Positive-drive Class B operation is applied to triodes to obtain a high anode circuit efficiency by reducing the minimum anode voltage (see Section 10.2), below that permitted by the bias line  $E_g = 0$ . Grid current is taken during the period while the input voltage swing makes the grid voltage positive. The amplifier (driver stage) before the Class B valves must supply power when grid current flows, and the points to be observed in its design are discussed in Section 10.8.6.

The chief features of a Q.P.P. stage are the centre-tapped high ratio step-up input transformer, and the output transformer. The former is necessary since each half of the secondary must supply a peak voltage very nearly equal to the cut-off bias (at the operating H.T. voltage) of the Q.P.P. valves. The self-capacitance of the secondary should be low to prevent peaked high-frequency response due to resonance with the leakage inductance. The output trans-

former also needs to have low leakage inductance and self-capacitance, because the resonant circuit so formed is capable of producing damped oscillations<sup>33</sup> under shock excitation from the half wave current impulses of each valve. Since each valve supplies half the output wave it is essential that the half-primary inductance and the leakage inductance between each half primary and secondary should be very nearly equal. Inequality causes the amplitudes of the two halves of the wave delivered to the output load to be unequal at low and high frequencies, thus producing distortion. Parasitic oscillation due to the push-pull connection is usually prevented by capacitors (0.002 to 0.005  $\mu$ F) connected across each half primary. High peak currents are taken during loud signals and the primary D.C. resistance must therefore be low. If high-frequency tone control is used, it should be included before the Q.P.P. output stage rather than across the output transformer. When the tone-control circuit is in parallel with the latter it tends to increase the peak output current during loud signals, and this may cause damage to the valves.

Triode valves in Class B positive drive may be designed to have high internal resistances and operate with zero grid bias, or to have low internal resistances and to operate with negative grid bias. Quiescent anode currents are approximately the same for both types of valves. The zero grid bias stage has the advantage of requiring no bias battery, but there is generally more "join up" distortion and heavier grid current damping of the driver stage. In addition, the optimum load resistance is high, and the output transformer primary inductance must consequently be large to prevent excessive attenuation (frequency) distortion at low frequencies. The second type has several advantages over the first, the grid bias of each valve can be adjusted to give reduced "join-up" distortion, a resistance can be included in parallel with the grid bias battery to reduce its voltage and keep it in step with the H.T. voltage as the H.T. battery becomes exhausted, driver stage damping is reduced, and the lower internal resistances of the valves assist in damping loudspeaker resonances. Class B positive drive is not now used to any large extent in receivers because quiescent push-pull gives results as satisfactory, without the complications of a driver stage. The design of the output transformer is similar to that for quiescent push-pull.

**10.8.6. The Driver Stage for Class B Positive Drive.** If the anode load resistance,  $R_0'$ , of a triode A.F. amplifier is steadily increased, overall amplification, at first proportional to  $R_0'$ , becomes

asymptotic to the amplification factor of the valve and is almost independent of changes of  $R_0$ . This occurs for values of  $R_0$  exceeding about  $4R_a$  (see Fig. 9.6). Owing to the fact that grid current is taken by each Class B valve, the equivalent load resistance in the driver valve anode circuit varies over its output voltage cycle from a very high to a low value, and unless this is controlled the output voltage wave shape is flattened at both ends of the cycle. If, however, the equivalent grid current load resistance is not allowed to fall below  $4R_a$ , the distortion produced in the output wave will not be serious. This result may be achieved by a suitable step-down interval transformer,<sup>26</sup> the step-down ratio being calculated from

$$\frac{\frac{1}{2}N_s}{N_p} = \sqrt{\frac{R_{g(mtn.)}}{4R_a(\text{driver valve})}}$$

where  $N_p$  = total primary turns,

$N_s$  = total secondary turns,

$R_{g(mtn.)}$  = minimum grid input resistance of the Class B stages

A higher step-down ratio would have the advantage of reducing the effect of variations of  $R_g$ , but this reduces the driver output voltage to the Class B valves, and the driver valve may then be overloaded before maximum output is obtained from the Class B stage.  $R_{g(mtn.)}$  is the slope resistance of the  $I_g E_g$  characteristic curve of the Class B valve at the maximum required positive value of grid voltage; a satisfactory approximation is given by the ratio of the positive bias voltage equal to the maximum positive voltage reached on the grid of the Class B valve to the D.C. grid current flowing at this bias voltage, i.e., it is the resistance corresponding to the chord to the  $I_g E_g$  characteristic curve instead of the tangent. A normal step-down ratio from primary to half secondary is 1 to  $\frac{3}{4}$ , or the ratio from primary to total secondary is 1 to 1.5. The transformer must have a high primary inductance, small leakage inductances between primary and both half secondaries—this is particularly important since the minimum grid input resistance may be as low as 20,000 ohms for battery-operated Class B positive drive—and the D.C. resistance of each half secondary must be low so as to reduce the D.C. voltage developed when grid current occurs.

An improved driver stage may be obtained by using a "cathode follower"<sup>12</sup> connection, i.e., the transformer is placed in the cathode circuit of the driver valve. This reduces the effective impedance of the valve to  $\frac{R_a}{1+\mu}$  (see Section 10.10.6), so that a step-up ratio may even be used. At the same time the effective amplification

of the valve is less than unity so that it acts simply as an impedance matching device.

**10.8.7. Class AB Positive Drive.** Class AB positive drive is sometimes used in a.c. mains-operated amplifiers to obtain the advantages of triode operation with high d.c. to a.c. conversion efficiency and high a.c. output. The triode valves are biased to a voltage approximately midway between the Class A and Class B positions. The zero-to-maximum signal d.c. current ratio is much less than that for Class B, about 2 to 1 as compared with 4 to 1, and "join-up" distortion is low. The changing anode current makes fixed grid bias (instead of cathode self-bias) and an inductance loaded h.t. supply (Section 11.2.6) essential.

## 10.9. The Output Transformer.

**10.9.1. The Design of an Output Transformer.** The basic principles, involved in output transformer design, are practically the same as for smoothing choke and mains transformer design, and we shall illustrate the method of procedure by the following example. Suppose the optimum load resistance referred to the primary side of the transformer is 6,000 ohms, the speech-coil impedance 5 ohms, and the primary d.c. current 40 mA. The required value of primary inductance is determined by the maximum permissible loss of response at a given low audio frequency, and we will assume this to be 2 db. at 50 c.p.s. From expression 9.22*b*, Section 9.4, 2 db. loss corresponds to a ratio of primary reactance to the total resistance of valve and load in parallel of very nearly 2 to 1. If the output valve is a tetrode the total parallel resistance can, for all practical purposes, be taken as the load resistance 6,000 ohms. Should the valve slope resistance be comparable with 6,000 ohms it merely improves the low-frequency response, making the loss less than 2 db. Hence the required value of primary inductance is

$$L_p = \frac{2 \times 6,000}{2\pi \times 50} = 38.2 \text{ H.}$$

For convenience let us take the same stampings as are used for the mains transformer design in Section 11.2.2, viz., Stalloy 32A. For one secondary and two primary sections, interleaved as shown in Fig. 10.18, insulation thicknesses of 0.075 ins. between winding and core, and winding and outside limb, and of 0.05 ins. between windings, and windings and sides, the total available winding area is  $(2.25 - 0.1)(1 - 0.25) = 1.612$  sq. ins. The most efficient use of the winding area is to divide it equally between secondary and

primary windings, so that the total area occupied by primary or secondary is 0.806 sq. ins. A suitable gauge of wire is 34 s.w.g.,

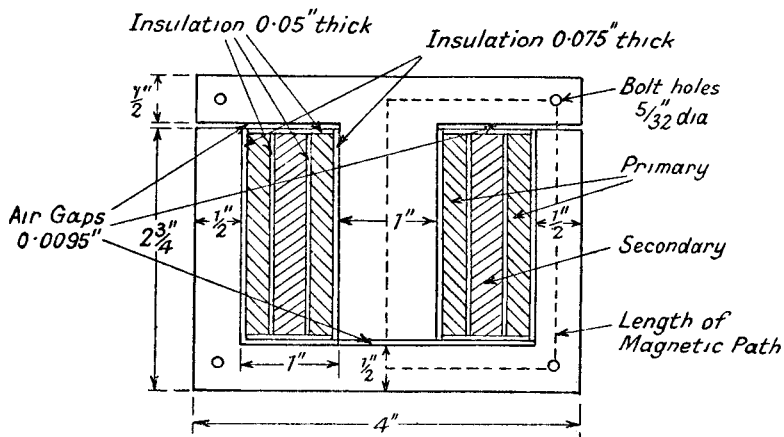


FIG. 10.18.—A Section Through a Typical Output Transformer.

which is rated to carry 66.5 mA, and if SSC is used, 8,730 turns can be accommodated per square inch (see Table 11.1).

The total primary turns in the available space =  $8,730 \times 0.806$   
 $= 7,040$

Length of the magnetic path (Fig. 10.18),  $l = 9$  ins.

Therefore turns per inch of magnetic path =  $\frac{7,040}{9} = 782$ .

D.C. ampere turns per inch of magnetic path =  $\frac{782 \times 40}{1,000} = 31.28$ .

In Fig. 11.17 we have two curves for the ratio of inductance, with and without D.C. polarizing, against D.C. polarizing ampere-turns per inch, curve 1 for a very small A.C. flux density and curve 2 for a R.M.S. flux density of 60 lines per square centimetre, and either can be chosen for design purposes. If the former is used a larger transformer is obtained and low-frequency response for all A.C. input voltages is better than required. Curve 2 is more often used, the flux density of 60 lines per square centimetre corresponding to an input voltage of 7% of the maximum in our particular example (the peak flux density for maximum input voltage is calculated at the end of the section to be 1,200 lines per square centimetre). Incremental permeability,  $\Delta\mu$ ,<sup>23, 27</sup> is shown in Fig. 10.20 to be proportional to peak A.C. flux density so that primary inductance for

voltages less than 7% of the maximum will tend to be less than that required, and conversely will be greater for larger voltages. The reduction in primary inductance is not generally sufficient to justify calculation on the basis of curve 1. From curve 2 the ratio of inductance with and without the D.C. polarizing current giving 31.28 D.C. ampere turns per inch is

$$\frac{L_{2(opt.)}}{L_1} = 0.273$$

and the optimum air gap ratio is

$$\frac{a_0}{l} = 0.0021.$$

Hence

$$L_1 = \frac{38.2}{0.273} = 140 \text{ H.}$$

Volume of iron required

$$\begin{aligned} &= \frac{L_1 \times 10^8}{1.255 \times 2.54 \times \Delta\mu \times (\text{turns per inch of magnetic path})^2} \\ &= \frac{140 \times 10^8}{1.255 \times 2.54 \times 900 \times (782)^2} \end{aligned}$$

$$\text{Volume of iron} = 8.0 \text{ cu. ins.}$$

Incremental permeability is 900 for a R.M.S. flux density of 60 lines per square centimetre.

The area of Stalloy 32A stamping allowing for  $\frac{5}{32}$ -in. diameter bolt holes is 8.4236 sq. ins. (Section 11.2.2).

Therefore thickness of core = 0.95 ins.

Let us take a thickness of 1 in., i.e., an overall thickness of 1.1 ins. (allowing for 10% insulation between laminations)

Number of laminations of 0.014 ins. thickness  $\simeq 79$ .

Total length of air gap = 0.0189 ins.

= 2 of 0.0095 ins. (the gap is divided between central and outside limbs).

It is of interest to compare with the above, the transformer design resulting from the use of curve 1.

$$\frac{L_{2(opt.)}}{L_1} = 0.465$$

and optimum air gap ratio

$$\frac{a_0}{l} = 0.00246.$$

Hence

$$L_1 = \frac{38.2}{0.465} = 82.1 \text{ H.}$$



Volume of iron required ( $\Delta\mu = 333$  for  $B$  very small)

$$= \frac{82.1 \times 10^8}{1.255 \times 2.54 \times 333 \times (782)^2}$$

$$= 12.65 \text{ cu. ins.}$$

Thickness of core = 1.5 ins.

$$= 1.65 \text{ ins., allowing 10\% insulation.}$$

Total length of air gap = 0.02215 ins.

$$= 2 \text{ of } 0.01107 \text{ ins. (the gap is divided between central and outside limbs).}$$

Greatly increased core thickness is needed if the required value of primary inductance is to be maintained at extremely low flux densities.

Details of windings.

(1) *Primary.*

Mean length of one turn = 8.2 ins.

$$\text{Total length of wire} = \frac{7,040 \times 8.2}{36} = 1,605 \text{ yards}$$

Total primary resistance =  $1.605 \times 361.2 = 580$  ohms

$$\text{D.C. voltage drop} = \frac{580 \times 40}{1,000} = 23.2 \text{ volts.}$$

(2) *Secondary.*

$$\text{Step-down turns ratio} = \sqrt{\frac{6,000}{5}} = 34.6$$

$$\text{Total turns in secondary} = \frac{7,040}{34.6} \approx 204$$

Available winding area = 0.806 sq. in.

$$\text{Therefore turns per square inch} = \frac{204}{0.806} = 253.$$

No. 18 s.w.g. ssc wire giving 400 turns per square inch is the nearest size.

$$\text{Total length of secondary wire} = \frac{204 \times 8.2}{36} = 46.5 \text{ yards.}$$

Total resistance of secondary =  $0.0465 \times 13.267 = 0.617$  ohms.

Neglecting iron losses, which are usually small compared with the copper resistance loss, the A.C. power efficiency for a 5-ohm secondary load resistance is

$$\eta = \frac{5}{5 + 0.617 + \frac{580}{(34.6)^2}} = \frac{5}{6.102} = 82\%.$$

This is a normal value for efficiency, though it could be made higher at the cost of a slight increase in step-down turns ratio by using No. 16 s.w.g. enamelled wire for the secondary winding. The area required by the 18 s.w.g. secondary is only 0.51 sq. in. (less than that available, 0.806 sq. in.), and from a practical viewpoint this has advantages since it allows insulation between windings to be increased, and ensures that the windings can be fitted into the winding window.

It will be noted that a section through the central core limb is almost square; this is considered to be the most economical shape of cross-section.

*Losses in the Iron Core.* Losses in the iron core of the transformer are a function of peak flux density  $\hat{B}$ , and, as  $\hat{B}$  is directly proportional to the applied voltage and inversely to the frequency, they are greatest at the lowest audio frequency. Taking the latter as 50 c.p.s., and the maximum applied R.M.S. voltage as 120 (this is a reasonable figure for a tetrode valve operating at a H.T. voltage of 250), we have for the flux

$$\Phi = \frac{E \times 10^8}{4.44fN_p}$$

where  $N_p$  = total primary turns

$$\begin{aligned} \therefore \hat{\Phi} &= \frac{120 \times 10^8}{4.44 \times 50 \times 7,040} \\ &= 7,680 \text{ lines.} \end{aligned}$$

$$\hat{B} = \frac{\hat{\Phi}}{A} = 7,680 \text{ lines per square inch.}$$

$$\simeq 1,200 \text{ lines per square centimetre.}$$

Actual volume of iron in core of 1 in. thickness = 8.4236 cu. ins.

Total weight of core = 8.4236  $\times$  0.28 lbs.

$$= 2.36 \text{ lbs.}$$

Milliwatts lost per lb. for  $\hat{B}$  of 1,200 lines per square centimetre = 12.

Therefore total milliwatts iron loss = 28.32

total output power milliwatts = 2,400.

The iron loss is therefore equivalent to a resistance of

$$6,000 \times \frac{2,400}{28.32} = 508,000 \Omega$$

in parallel with the primary inductance. Its effect on frequency response and general performance can justifiably be neglected.

The interleaved or sandwich type<sup>38</sup> of winding shown in

Fig. 10.18 has the merit of reduced leakage inductance compared with the non-interleaved type with a single primary winding. Interwinding capacitance is, however, usually slightly higher, though it can be reduced by bakelite separators. The self-capacitance of the windings can be reduced by sectionalizing instead of using a single continuous layer across the whole of the winding length. Reduced leakage inductance, winding and self-capacitance can be achieved by "pancake" coil construction with bakelite or bakelized paper spacers between the pancakes. For example, the above design could have employed three primary and two secondary interleaved pancake windings. The chief disadvantage of this type of winding is that it calls for a greater area of winding window and is not so robust; on the other hand, a defective winding is more easily replaced. The windings should be vacuum impregnated with a suitable varnish to prevent the ingress of moisture, and an iron case is required to give magnetic screening and some measure of electrical screening and mechanical protection. It is not usual to seal the transformer in a bituminous compound.

Push-pull transformer design follows the same lines except that the D.C. polarizing current can be assumed to be small. Since only matched valves give a total effective D.C. current of zero it is usual to design on the basis of 10 mA D.C. current.

**10.9.2. Output Transformer Attenuation (Frequency) Distortion.** The frequency response of an output transformer is calculated in the same manner as that of the intervalve transformer in Section 9.4. The A.F. band is divided into three ranges, and the response at low and high audio frequencies is determined relative to that at the medium frequencies. Thus the loss of response at the low frequencies is from expression 9.22*b*.

$$- 10 \log_{10} \left[ 1 + \left( \frac{R_l}{X_l} \right)^2 \right]$$

where  $X_l = pL_p$ , the reactance of the primary inductance,

$R_l =$  the resistance of  $R_a + R_p$  in parallel with  $\frac{R_s + R_{sc}}{n^2}$

$R_p =$  resistance of primary winding

$R_s =$  ,, ,, secondary winding

$R_{sc} =$  resistance equivalent of the speaker speech-coil

$n =$  secondary to primary turns ratio, which is generally much less than 1.

The resistance equivalent of the speech-coil is usually taken from the amplitude of the impedance  $(\sqrt{R_{sc}^2 + X_{sc}^2})$  at 400 c.p.s., so

that the calculated frequency response is simply a measure of transformer performance, and not that of the output stage in association with the loudspeaker. Most loudspeakers have a mechanical resonance at a low frequency near 100 c.p.s., and several resonances in the high-frequency range. At and around these resonant frequencies the speech-coil impedance varies appreciably.

At high audio frequencies leakage inductance plays an important part but, owing to the low impedance of the speech coil, secondary self-capacitance can often be neglected. Expression 9.24 is therefore modified to a loss at high frequencies relative to medium of

$$- 10 \log_{10} \left( 1 + \left( \frac{R_h}{X_h} \right)^2 \right)$$

$$\text{where } R_h = R_a + R_p + \frac{R_s + R_{sc}}{n^2}$$

$$X_h = pL_p'$$

$$L_p' = \text{leakage inductance.}$$

If the pass range of the output transformer is specified by those frequencies between which the maximum to minimum response is not greater than 3 db. (1.414 to 1), the lowest frequency is given by

$$X_i' = R_i'$$

$$\text{or } f_i' = \frac{(R_a + R_p) \left( \frac{R_s + R_{sc}}{n^2} \right)}{\left( R_a + R_p + \frac{R_s + R_{sc}}{n^2} \right) 2\pi L_p}$$

and the highest frequency by

$$X_h' = R_h'$$

$$\text{or } f_h' = \frac{R_a + R_p + \frac{R_s + R_{sc}}{n^2}}{2\pi L_p'}$$

$$\text{Ratio } \frac{\text{highest frequency}}{\text{lowest frequency}} = \frac{L_p(1+G^2)}{L_p'G} \quad . \quad . \quad 10.43$$

$$\text{where } G = \frac{R_s + R_{sc}}{n^2(R_a + R_p)}$$

Thus, for a given value of  $G$ , the pass-band of the output transformer is proportional to the ratio of primary to leakage inductance,<sup>30</sup> and it will therefore be clear that there is no advantage in increasing primary inductance (by, for example, increasing primary turns) if leakage inductance is proportionally increased. Push-pull, by

balancing out the D.C. polarizing current, does increase primary inductance without increasing leakage inductance. The use of a high inductance choke to carry the output valve D.C. current with capacitance coupling to the output transformer has the same effect. Primary inductance is dependent on the applied voltage, and it generally increases as the latter increases, because incremental permeability increases (see Fig. 10.20). Frequency response tends, therefore, to be best with high output voltages and it is usual to design for the required response at low output voltages. In the preceding section primary inductance is calculated on the assumption of an output voltage of 7% of the maximum.

**10.9.3. Output Transformer Amplitude (Harmonic) Distortion.**<sup>47</sup> A non-linear relationship between the flux density  $B$  and magnetizing force  $H$  is responsible for amplitude distortion in iron-cored transformers. When a generator of sinusoidal voltage is applied to an unloaded transformer, it may produce almost equal distortion of flux and magnetizing force, greater distortion of flux than magnetizing force, or vice versa. The final result actually depends on the relative magnitudes of the generator internal impedance and the non-linear impedance of the transformer. If the former is very large (e.g., for the tetrode valve) the current, and hence magnetizing force, in the transformer core is practically sinusoidal; flux and the unloaded secondary voltage are distorted in shape. On the other hand, a low generator impedance (e.g., for a triode valve) implies a voltage applied to, and flux in, the transformer of nearly sinusoidal shape, with a distorted magnetizing force (input current to the transformer primary). The unloaded secondary voltage is therefore almost sinusoidal. A point worth noting is that the transformer induced voltage, which opposes the applied voltage, is proportional to  $\frac{d\Phi}{dt}$ , where  $\Phi$  is the total flux in the iron core, so that each harmonic component in the flux wave is multiplied by its harmonic number in arriving at the harmonic voltage component. Hence the secondary output voltage wave shape has greater distortion than the flux wave shape.

The relative amplitudes of the harmonic currents produced in the transformer depend on the shape of the  $B$ - $H$  loop curve. This is symmetrical in the absence of a D.C. polarizing current, and distortion is confined mainly to odd harmonics with third predominating. An asymmetrical loop is obtained with a D.C. polarizing current, and both even and odd harmonics are present with second and third as the most important.





a known low resistance in series with the unloaded transformer, which should have the lowest possible primary winding resistance. Alternatively the known series resistance may be varied, and the ratio of the harmonic to fundamental voltages, measured across it, plotted against the sum of the known and primary winding D.C. resistance. The line so obtained can be produced to give the no-load current distortion ratio for zero known and primary winding resistance. The peak flux density can be calculated from the R.M.S. value of the fundamental voltage ( $E_f$ ) across the unloaded primary, by using the formula given in Section 11.2.2 (expression 11.2).

$$\hat{B} = \frac{E_f 10^8}{4.44 N_p A f} \text{ lines per square centimetre.}$$

where  $N_p$  = total primary turns

$A$  = area of iron core section in square centimetres.

$f$  = fundamental frequency.

Since  $\hat{B}$  is inversely proportional to  $f$ , it is clear that a given applied voltage produces maximum flux density, and hence maximum amplitude distortion, at the lowest audio frequency.

Expression 10.45c, as it stands, is applicable only to one particular design, and it would be preferable to convert it to a product of two factors, one dependent on the core material and peak flux density, and the other dependent on the shape and winding details of the transformer. This is possible because, in most practical cases,  $Z_f$  can be taken as the reactance of the primary inductance at the fundamental frequency. Taking the expression 11.19a, Section 11.2.9, for the primary inductance we have

$$Z_f = pL_p = \frac{2\pi f 1.255 N_p^2 A \Delta\mu}{10^8 l}$$

where  $\Delta\mu$  = incremental or A.C. permeability

$l$  = length of the magnetic path in centimetres (see Fig. 10.18) and  $N_p$  and  $A$  are as expressed above for  $\hat{B}$ .

Therefore 
$$Z_f = 7.88 \times 10^{-8} \Delta\mu \frac{N_p^2 A f}{l} \quad . \quad . \quad . \quad 10.47.$$

Replacing  $Z_f$  in the  $\frac{I_H}{I_f Z_f}$  part of 10.45c by 10.47 gives

$$\frac{I_H}{I_f Z_f} = \frac{I_H}{I_f} \frac{10^8}{7.88 \Delta\mu} \times \frac{l}{N_p^2 A f} \quad . \quad . \quad . \quad 10.48$$

and both the variables  $\frac{I_H}{I_f}$  and  $\Delta\mu$  in the first factor relate to the core material and peak flux density, whilst the second factor relates



to the particular design details of the transformer.  $\frac{I_H}{I_f}$  and  $\Delta\mu$  can be measured for different peak flux densities and D.C. polarizing field. The current distortion ratio generally increases with increase of peak flux density and D.C. polarizing field. If incremental permeability  $\Delta\mu$  is plotted against  $\hat{B}$  it is found to have a maximum at some value of peak flux density dependent on the core material and D.C. polarizing voltage. Generally  $\Delta\mu$  decreases for all flux densities as the D.C. polarizing voltage increases, but flux density for maximum  $\Delta\mu$  increases. Typical curves of current distortion and incremental permeability abstracted from the article<sup>47</sup> by Partridge (note

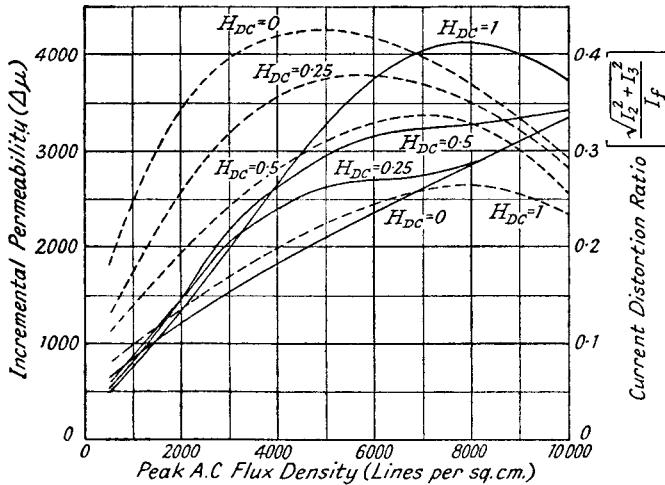


FIG. 10.20.—Incremental Permeability and Current Distortion Curves Against Peak A.C. Flux Density for Normal Stalloy Core.

Dotted Line : Incremental Permeability.  
Full Line : Current Distortion.

that his relative specific choke impedance  $Z_{sp} = 7.88\Delta\mu 10^{-8}$ ) are plotted in Fig. 10.20 against peak flux density for different values of D.C. polarizing field; the core material is Silcor 2 ( $3\frac{1}{2}\%$  silicon content) as used for the stalloy stamping of Section 10.9.1. The D.C. polarizing field is given in oersteds (gilberts per centimetre) and it is necessary to multiply by 2.02 to convert to D.C. ampere-turns per inch (see Section 11.2.9). The product  $\frac{I_H}{I_f} \frac{10^8}{7.88\Delta\mu}$  can be termed the distortion factor,  $D$ , of the core material, and it is plotted in Fig. 10.21 against peak flux density. The values are obtained from the curves in Fig. 10.20.

To illustrate the use of Fig. 10.21, let us consider the transformer designed in Section 10.9.1 and determine the transformer distortion occurring when operating under the full load conditions.

The peak flux density for a maximum applied R.M.S. voltage of 120 is 1,200 lines per square centimetre and the D.C. polarizing field is 31.28 ampere-turns per inch.

The curves in Fig. 10.21 are given for a maximum D.C. polarizing field of 2.02 ampere turns per inch, so we shall have to estimate a likely value for distortion coefficient. The correctness, or otherwise, of the estimate will not affect the general principles. For

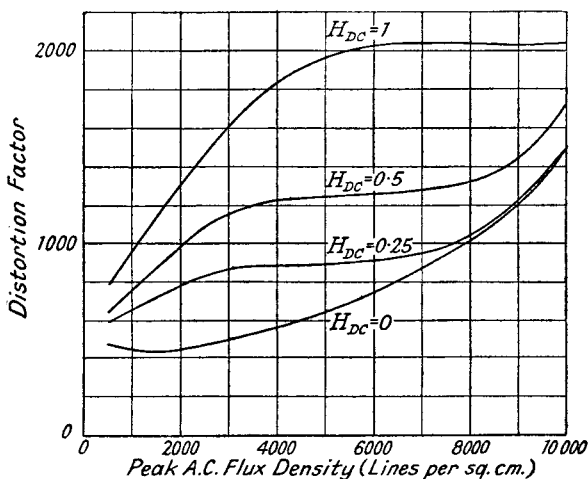


FIG. 10.21.—Distortion Factor-Peak A.C. Flux Density Curves for Normal Stalloy Core.

$H = 2.02$  ampere turns per inch the distortion coefficient at  $\hat{B} = 1,200$  lines per square centimetre is 1,050. The form of the current distortion curves suggests that an increase in D.C. field is unlikely to affect greatly the current distortion at  $\hat{B} = 1,200$  lines per square centimetre. The chief effect of an increase in  $H$  is to reduce incremental permeability, and a probable decrease of  $\Delta\mu$  of about 3 to 1 by changing  $H$  from 2 to 31.28 ampere turns per inch is suggested by the change in ratio of  $\frac{L_{2(opt.)}}{L_1}$  in Fig. 11.17. Let us therefore assume a distortion coefficient of 3,150. A probable value for valve (a tetrode) slope resistance is 30,000 ohms, thus for  $f = 50$  c.p.s.

$$R_o' = \frac{R_o(R_a + R_p)}{R_o + R_a + R_p} = \frac{6,000(30,580)}{36,580}$$

$$\simeq 5,000 \Omega$$

$$Z_f = pL_p = 12,000 \Omega.$$

By combining 10.45c and 10.48, voltage distortion

$$\frac{E_h}{E_f} = \frac{Dl}{N_p^2 A f} \cdot R_o' \left( 1 - \frac{R_o'}{4Z_f} \right)$$

$$= \frac{3,150 \times 9 \times 2.54}{(7,040)^2 \times (1 \times 2.54)^2 \times 50} \cdot 5,000 \left( 1 - \frac{5,000}{48,000} \right)$$

$$= 0.0201 = 2.01\%.$$

Note that  $l$  and  $A$  are in centimetres and square centimetres respectively.

Certain general conclusions can be drawn from the analysis.

(1) Harmonic distortion is a function of  $Z_f$ , and it can be decreased to very small proportions at any given frequency by increasing  $Z_f$ , i.e., by increasing  $\frac{N_p^2 A}{l}$ . However, for any given shape of transformer, leakage inductance and  $Z_f$  are directly proportional so that an increase in  $Z_f$  results in increased loss of high-frequency response. There is thus a limit to the improvement in harmonic distortion which can be achieved with any given transformer shape, and this limit is set by the tolerable loss at high frequencies.

(2) If attenuation (frequency), harmonic distortion and D.C. polarizing field are specified, the power-handling capacities of transformers of the same core material and geometrical proportions with given generator and load impedances are proportional to their volumes.

Specified attenuation (frequency) distortion implies that primary and leakage inductances are constant; the former decides the low-frequency response. Leakage inductance, which determines high-frequency response, is directly proportional to primary inductance for a given core material and geometrical proportions. Specified harmonic distortion for a constant D.C. polarizing field means that the peak A.C. flux density is constant, hence from expression 11.19a, Section 11.2.9.

$$L_p \propto \frac{N_p^2 A}{l}$$

and from expression 11.2, Section 11.2.2.

$$E_f \propto N_p A.$$

If the linear dimensions of the transformer are multiplied by  $k$ , and attenuation distortion is to be unchanged

$$L_p = L_{p1} \propto N_{p1}^2 \frac{k^2 A}{kl} \propto \frac{N_p^2 A}{l}$$

$$\therefore N_{p1} \propto \frac{N_p}{\sqrt{k}}$$

Using this in the expression for  $E_f$

$$E_{f1} \propto \frac{N_p}{\sqrt{k}} k^2 A \propto k^{\frac{3}{2}} E_f,$$

but power  $P_{f1} \propto E_{f1}^2 \propto k^3 P_f \propto$  volume of the transformer. When the D.C. current remains constant, increase in overall dimensions reduces the value of  $H_{D.C.}$  in the polarizing D.C. field, because

$$H_{D.C.} \propto \frac{N_p}{l} \propto \frac{1}{k^{\frac{3}{2}}},$$

and this allows a greater increase in power handling capacity to be obtained over that due to the increase in volume.

## 10.10. Negative Feedback.<sup>11, 16, 19</sup>

**10.10.1. Introduction.** Negative or inverse feedback is applied to A.F. amplifiers in order to change the frequency response and/or to reduce harmonic distortion, hum and noise produced in the amplifier itself. It is achieved by feeding back a proportion of the output to the input in such a way as to oppose the input voltage. The opposition voltage may be fed back through a resistive network or a circuit arranged to give phase and amplitude discrimination.

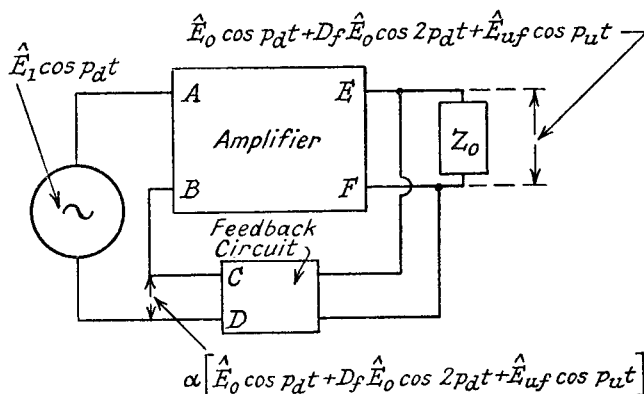


FIG. 10.22.—Schematic Diagram of Negative Feedback.

In both instances there is a possibility that at some frequency (usually outside the desired pass range of the amplifier) the phase shift may be such as to produce positive feedback, and special precautions are sometimes necessary, particularly when feedback occurs over a number of stages, to prevent self-oscillation. The usual method is to design the feedback circuit to attenuate severely frequencies outside the normal pass range of the amplifier.

Some of the properties of negative feedback can be demonstrated by considering the diagram in Fig. 10.22.

Let  $\hat{E}_1 \cos p_a t$  = input voltage

$\mu_0$  = overall amplification of the amplifier without feedback

$\mu_f$  = overall amplification of the amplifier with feedback.

$\hat{E}_0 \cos p_a t$  = fundamental component of the output voltage from the amplifier with feedback

$D_0$  = distortion ratio of the amplifier without feedback, the ratio of the amplitude of second harmonic (if this is the largest harmonic) to that of the fundamental in the output voltage

$D_f$  = distortion ratio of the amplifier with feedback

$\hat{E}_u \cos p_u t$  = undesired hum or noise voltage produced by the amplifier itself without feedback

$\hat{E}_{uf} \cos p_u t$  = undesired hum or noise voltage produced by the amplifier with feedback

$\alpha$  = feedback factor, i.e., the proportion of the output voltage applied to the input.

Voltage across  $CD$  due to feedback

$$= \alpha[\hat{E}_0 \cos p_a t + D_f \hat{E}_0 \cos 2p_a t + \hat{E}_{uf} \cos p_u t].$$

Voltage applied to the amplifier across terminals  $AB$

$$= \hat{E}_1 \cos p_a t - E_{CD}.$$

$$= (\hat{E}_1 - \alpha \hat{E}_0) \cos p_a t - \alpha D_f \hat{E}_0 \cos 2p_a t - \alpha \hat{E}_{uf} \cos p_u t.$$

Output voltage across  $EF$

$$= \mu_0[(\hat{E}_1 - \alpha \hat{E}_0) \cos p_a t - \alpha D_f \hat{E}_0 \cos 2p_a t - \alpha \hat{E}_{uf} \cos p_u t]$$

$$+ \mu_0 D_0 (\hat{E}_1 - \alpha \hat{E}_0) \cos 2p_a t + \hat{E}_u \cos p_u t$$

$$= \hat{E}_0 \cos p_a t + D_f \hat{E}_0 \cos 2p_a t + \hat{E}_{uf} \cos p_u t.$$

Equating fundamental components

$$\hat{E}_0 = \mu_0(\hat{E}_1 - \alpha \hat{E}_0)$$





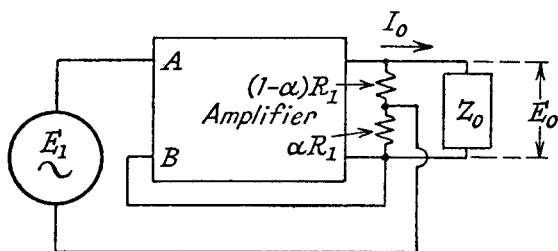


FIG. 10.23a.—Voltage Negative Feedback.

where  $\mu$  = amplification of the amplifier when  $Z_0 = \infty$   
and  $R_a$  = the slope resistance of the output valve

$$E_{AB} = E_1 - \alpha E_0.$$

Replacing the above for  $E_{AB}$  in 10.52.

$$\frac{E_0}{E_1} = \frac{\mu Z_0}{R_a + Z_0(1 + \mu\alpha)} = \frac{\frac{\mu}{1 + \mu\alpha} Z_0}{\frac{R_a}{1 + \mu\alpha} + Z_0} \quad \dots \quad 10.53.$$

By noting that  $\mu_0 = \frac{\mu Z_0}{R_a + Z_0}$ , expression 10.53 shows the expected reduction of overall amplification to  $\mu_f = \frac{\mu_0}{1 + \mu_0\alpha}$ , and at the same time the equivalent slope resistance of the output valve is decreased to  $\frac{R_a}{1 + \mu\alpha}$ . This reduction of generator resistance is particularly valuable when the load impedance is a loudspeaker speech coil, since it assists in damping cone resonances. One of the disadvantages of using a tetrode output valve, the accentuation of cone resonances, can be overcome by the application of voltage feedback, without losing the advantages of high A.C./D.C. power efficiency and (if feedback is not excessive) of high power sensitivity.

Some interesting effects result from the application of voltage feedback in special cases. For example, if  $R_a \ll Z_0$ , expression 10.53 becomes

$$\frac{E_0}{E_1} \approx \frac{\mu}{1 + \mu\alpha} \quad \dots \quad 10.54$$

i.e., output voltage is independent of  $Z_0$ . On the other hand if  $R_a \ll Z_0$ ,  $\mu\alpha \gg 1$  and  $\alpha = \frac{K}{Z_0}$ , output current instead of voltage is independent of  $Z_0$ .



$$I_0 = \frac{E_0}{Z_0} = \frac{\mu E_1}{\mu \alpha Z_0} = \frac{E_1}{K} \quad . \quad . \quad . \quad 10.55$$

**10.10.4. Current Feedback.** Current feedback is illustrated by the circuit in Fig. 10.23b, the feedback voltage being developed across the resistance  $R_f$  in series with the load impedance  $Z_0$ .

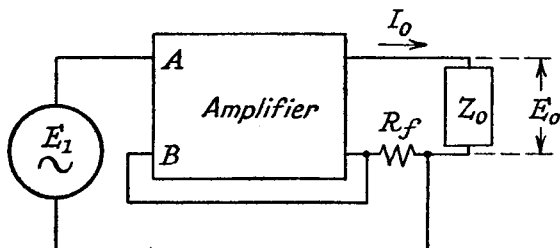


FIG. 10.23b.—Current Negative Feedback.

$$E_0 = \frac{\mu E_{AB} Z_0}{R_a + R_f + Z_0}$$

where  $R_a$  = slope resistance of the output valve

$$\begin{aligned} E_{AB} &= E_1 - I_0 R_f \\ &= E_1 - \frac{\mu E_{AB} R_f}{R_a + R_f + Z_0} \end{aligned}$$

Therefore

$$E_0 = \frac{\mu E_1 Z_0}{R_f(1 + \mu) + R_a + Z_0} \quad . \quad . \quad . \quad 10.56.$$

We see from the above expression that current feedback increases the equivalent slope resistance of the output valve by  $R_f(1 + \mu)$ , and the amplification factor with feedback is reduced only by reason of increased generator resistance.

Two special cases again arise ; if  $\mu$  is very large

$$E_0 = \frac{E_1 Z_0}{R_f}$$

and

$$I_0 = \frac{E_0}{Z_0} = \frac{E_1}{R_f} \quad . \quad . \quad . \quad 10.57.$$

When, in addition,

$$R_f = K Z_0$$

$$E_0 = I_0 Z_0 = \frac{E_1}{K} \quad . \quad . \quad . \quad 10.58.$$

In the first instance output current is independent of  $Z_0$ , and in the second output voltage is unaffected by  $Z_0$ .

Current feedback is not often employed in output stages, partly because of the increased equivalent generator resistance, which tends



(1) Constant output current and an equivalent generator impedance of  $Z_0$  by making  $\alpha = \frac{R_f}{Z_0}$  where  $R_f$  is constant. Neglecting  $R_a$  and  $Z_0$  in comparison with  $\mu R_f$  and  $\mu\alpha Z_0$  we have from equation 10.59.

$$E_0 = \frac{\mu Z_0 E_1}{\mu R_f + \mu\alpha Z_0} = \frac{E_1 Z_0}{R_f + \alpha Z_0} = \frac{E_1 Z_0}{2R_f}$$

$$\therefore I_0 = \frac{E_0}{Z_0} = \frac{E_1}{2R_f} = \text{constant}$$

and the equivalent generator impedance =  $\frac{R_f}{\alpha} = Z_0$ .

(2) Constant voltage and an equivalent generator impedance of  $Z_0$  by making  $R_f = \alpha Z_0$  where  $\alpha$  is constant.

$$E_0 = \frac{Z_0 E_1}{R_f + \alpha Z_0} = \frac{E_1}{2\alpha} = \text{constant}$$

and the equivalent generator impedance =  $\frac{R_f}{\alpha} = Z_0$ .

Other variations in the feedback circuit can be made to give constant equivalent generator impedance with constant voltage or current.

**10.10.6. Negative Feedback with a Cathode Follower Valve.**<sup>43</sup> A valve with its load resistance placed between the cathode and H.T. negative is a special case of negative feedback for which the feedback factor  $\alpha$  is 1. By analysis of the circuit in Fig. 10.24 we have

$$E_k = \frac{\mu E_g Z_k}{R_a + Z_k}$$

$$E_g = E_0 - E_k$$

$$E_k = \frac{\mu E_g Z_k}{R_a + (1 + \mu) Z_k}$$

$$= \frac{\mu}{1 + \mu} \frac{E_g Z_k}{\frac{R_a}{1 + \mu} + Z_k}$$

Therefore

The output voltage  $E_k$  is therefore less than the input, and the valve equivalent slope resistance is reduced to a very small value by the factor  $\frac{1}{1 + \mu}$ , and, if  $\mu \gg 1$ , it equals  $\frac{1}{g_m}$ . This type of negative feedback generator has two important advantages, low equivalent

generator internal resistance and low grid input admittance. The first means that it is particularly useful when constant output voltage is required across a variable load impedance. This property makes it a very satisfactory driver stage preceding Class B or Class AB

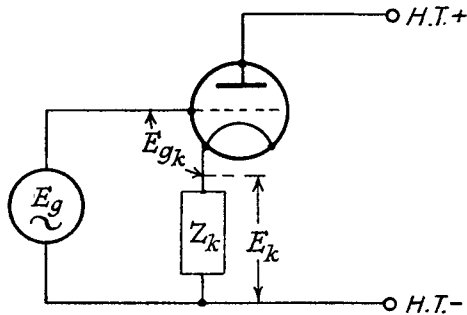


FIG. 10.24.—The Cathode Follower Circuit.

positive-drive output valves, the variable input impedance due to grid current causing practically no harmonic distortion of the output voltage. The valve may also be used as a D.C. voltage stabilizer; the D.C. voltage being taken between cathode and H.T. negative. Positive voltage between the grid and H.T. negative determines the D.C. output voltage, which is given by

$$E_{\text{D.C.}} = E_b + E_{c0}$$

where  $E_b$  = positive voltage applied to the grid

–  $E_{c0}$  = grid bias voltage required to cut off anode current for the given H.T. supply voltage.

Variations of the H.T. supply voltage are reduced by  $\frac{1}{1+\mu}$  at the cathode circuit. Good regulation is also obtained by reason of low generator internal resistance.

Low grid input admittance is of greatest value for radio frequency operation, and at ultra high frequencies this property has the effect of improving signal-to-noise ratio. Low input admittance is realized because the voltage between grid and cathode is so very much less than the input voltage; this necessarily implies a comparatively small current flowing in the interelectrode grid-cathode capacitance. Formulæ for the parallel resistance and capacitance of the input admittance components are developed in Section 2.8.3, Part I. Thus, from expression 2.21a, the equivalent parallel resistance is

$$R_g = \frac{(G_k + g_m)^2 + (B_{gk} + B_k)^2}{B_{gk}(G_k B_{gk} - g_m B_k)}$$

and, from expression 2.21*b*, the equivalent parallel capacitance is

$$C_g = \frac{C_{gk}[G_k(G_k + g_m) + B_k(B_{gk} + B_k)]}{(G_k + g_m)^2 + (B_k + B_{gk})^2}$$

where

$$B_{gk} = \omega C_{gk}$$

$C_{gk}$  = grid-cathode interelectrode capacitance

$g_m$  = mutual conductance of the valve

and  $G_k$  and  $B_k$  = conductance and susceptance of the cathode load admittance.

At audio frequencies  $B_k$  is often zero and  $B_{gk}$  can be neglected in the numerator, so that

$$R_g \simeq \frac{(G_k + g_m)^2}{G_k B_{gk}^2}$$

which is very large because  $B_{gk}$  is small, and

$$C_g \simeq C_{gk} \left( 1 - \frac{g_m}{G_k + g_m} \right) = C_{gk} \left( 1 - \frac{\mu R_k}{R_a + \mu R_k} \right).$$

Generally  $G_k$  is much less than  $g_m$  so that  $C_g$  approaches zero, i.e., the effective input capacitance is much reduced. It is clear, therefore, that grid input admittance will be low. The result of the cathode load resistance is actually a reversed Miller effect, the interelectrode capacitance being multiplied by 1 minus the approximate amplification of the stage. The negative sign is to be expected since a voltage across the cathode load resistance is 180° out-of-phase with a voltage across the same resistance placed in the anode circuit.

**10.10.7. Balanced Feedback.**<sup>42</sup> The chief disadvantage of negative feedback is that it reduces the overall amplification of any amplifier to which it is applied, and for the same output requires a larger input signal. This can be overcome if a combination of equal positive and negative feedback is employed, and this system is known as balanced feedback. It includes most of the advantages of negative feedback, viz., reduced interference voltages and distortion, and improved frequency response, without reducing the overall amplification (if the positive feedback is made equal to the negative).

Two controlling voltages are required; the negative feedback voltage is obtained from the output of the amplifier in the usual manner, but the positive feedback voltage is obtained either directly from the input voltage source or from the anode circuit of the first valve in the amplifier to which negative feedback is being applied.

The positive feedback voltage cannot be obtained from the amplifier output otherwise the negative feedback reduction of interference and distortion is cancelled as well as the input signal reduction.

The principle of balanced feedback is best shown by the following analysis.

Let  $E_{of}$  = fundamental output voltage with feedback

$D_f(E_{of})$  = distortion output voltage with feedback

$E_{uf}$  = undesired interference output voltage with feedback

$\alpha$  = negative feedback factor

$\beta$  = positive feedback factor

$\mu_0$  = overall amplification without feedback

$E_1$  = fundamental input voltage

$D_0$  = distortion coefficient without feedback

$E_u$  = undesired interference voltage without feedback.

The total input voltage to the amplifier is

$$E_1 + \beta E_1 - \alpha[E_{of} + D_f(E_{of}) + E_{uf}]$$

$$\begin{aligned} \therefore E_{of} + D_f(E_{of}) + E_{uf} &= \mu[E_1(1 + \beta) - \alpha(E_{of} + D_f(E_{of}) + E_{uf})] + E_u \\ &\quad + D_0(\mu E_1(1 + \beta) - \mu\alpha E_{of}) \\ &= \frac{\mu(1 + \beta)}{1 + \mu\alpha} E_1 + \frac{D_0(\mu E_1(1 + \beta) - \mu\alpha(E_{of}))}{1 + \mu\alpha} \\ &\quad + \frac{E_u}{1 + \mu\alpha} \quad . \quad . \quad . \quad . \quad 10.60. \end{aligned}$$

If  $\mu\alpha = \beta$ , i.e., the negative feedback voltage is equal to the positive

$$E_{of} + D_f(E_{of}) + E_{uf} = \mu E_1 + \frac{D_0(E_{of})}{1 + \mu\alpha} + \frac{E_u}{1 + \mu\alpha}.$$

The function of balanced feedback is seen to be that only distortion and interference voltages are fed back in the negative direction, the negative fundamental voltage being cancelled by the positive fundamental voltage. If an attempt were made to derive the positive fundamental voltage from the output it would be necessary to filter the distortion and interference voltages before application to the input circuit. Such a method would not be possible except for a single frequency input or a very narrow band of frequencies.

With balanced feedback the frequency response can be made independent of the amplifier response and dependent only on that of the input voltage source. Suppose the amplification of the amplifier is represented by  $\mu\phi(f)$  where  $\phi(f)$  indicates a function of frequency, and the positive feedback factor is  $\beta\phi'(f)$ , where  $\phi'(f)$  is

the frequency function for the input source. If the negative feedback circuit is independent of frequency,

$$\frac{E_{of}}{E_1} = \frac{\mu\phi(f)(1 + \beta\phi'(f))}{1 + \mu\alpha\phi(f)} \quad . \quad . \quad . \quad 10.61$$

if  $\mu\alpha \cdot \phi(f) \gg 1$ ,  $\beta\phi'(f) \gg 1$  and  $\mu\alpha = \beta$ .

$$\frac{E_{of}}{E_1} = \mu\phi'(f)$$

i.e., is dependent only on the frequency characteristic of the input voltage.

A possible circuit for obtaining balanced feedback is shown in Fig. 10.25. Positive voltage feedback is obtained via the resistances  $R_1$  and  $R_2$  from the anode of  $V_2$  to the grid of  $V_1$ .  $C_1$  acts as a coupling capacitance and has a high value. Negative voltage

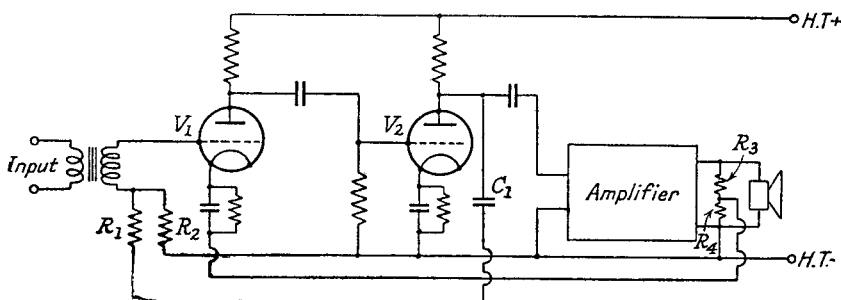


FIG. 10.25.—A Circuit for Obtaining Balanced Feedback.

feedback is obtained by connecting the cathode of  $V_1$  to earth through  $R_4$ , which forms with  $R_3$  a potential divider for the output voltage.

**10.10.8. Instability in Feedback Amplifiers.** From Section 9.3 we see that the gain of an amplifier over a frequency range must normally be represented by a complex number  $\frac{\mu_m}{1 \pm jx}$ , so that

unless the feedback factor is a conjugate  $\left(\frac{\alpha}{1 \pm jx}\right)$  of this, the feedback voltage phase relationship cannot be maintained at  $180^\circ$  to the input voltage for all frequencies. If it should happen at any frequency that the feedback phase-shift has been moved through  $360^\circ$ , positive feedback and, if  $\mu\alpha > 1$ , oscillation result, for expression 10.49 becomes

$$\frac{E_o}{E_1} = \frac{\mu}{1 - \mu\alpha} = \frac{\mu}{0} = \infty.$$

Let us examine the case of a  $RC$  coupled amplifier with a resistive feedback circuit. A single stage gives a gain  $\frac{\mu}{1 \pm jx}$  and the maximum possible phase shift through the amplifier is  $\pm 90^\circ$ . Such a stage cannot be unstable with negative feedback because the feedback voltage vector must lie between  $90^\circ$  and  $270^\circ$  with respect to the input voltage. A two-stage  $RC$  coupled amplifier gives an overall amplification of

$$\mu_t = \frac{\mu_1}{1 + jx_1} \cdot \frac{\mu_2}{1 + jx_2}.$$

The alternative negative sign is not included because it leads to the same conclusion as the positive.

$$\mu_t = \frac{\mu_1 \mu_2}{1 - x_1 x_2 + j(x_1 + x_2)}.$$

Owing to the term  $-x_1 x_2$ , the feedback voltage vector associated with  $\mu_t$  can be rotated beyond  $270^\circ$ , and tends, as  $x_1$  and  $x_2$  increase, to approach the in-phase position with the input voltage. It does not reach the  $360^\circ$  position until  $x_1 = x_2 = \infty$  when  $\mu_t$  is zero. Thus a two-stage  $RC$  amplifier with resistive feedback is theoretically stable. In practice phase changes in decoupling and feedback circuits occur, and oscillation is possible.

The gain for a three-stage amplifier is

$$\begin{aligned} \mu_t &= \frac{\mu_1 \mu_2 \mu_3}{(1 + jx_1)(1 + jx_2)(1 + jx_3)} \\ &= \frac{\mu_1 \mu_2 \mu_3}{1 - (x_1 x_2 + x_1 x_3 + x_2 x_3) + j(x_1 + x_2 + x_3 - x_1 x_2 x_3)}. \end{aligned}$$

The imaginary term disappears when

$$x_1 + x_2 + x_3 = x_1 x_2 x_3$$

and oscillation then occurs if

$$x_1 x_2 + x_1 x_3 + x_2 x_3 > 1.$$

By suitable proportioning of the stages, such as making  $x_1 = x_2$  and  $x_3$  as different as possible from  $x_1$  and  $x_2$ , the limiting feedback factor may be raised.

In transformer-coupled amplifiers leakage inductance and stray secondary capacitance produce resonance at some high frequency, and above this resonance the output voltage phase shift exceeds  $270^\circ$ . A single stage transformer coupling with resistive feedback is stable because the phase shift only reaches  $360^\circ$  when the amplification is too small to produce oscillation. Two stages of



transformer coupling, or one stage of  $RC$  and one stage of transformer coupling can, however, produce instability.

In a broadcast receiver we are mostly concerned only with one stage of amplification before the output stage, and the transformer of the latter is sufficiently damped by the load to reduce the phase-shift and amplification due to leakage inductance and stray capacitance resonance. If an intervalve transformer is used before the output stage, the tendency to instability may be checked by damping the secondary by a resistance. As the frequency of instability is often outside the pass range of the amplifier, self-oscillation can be prevented by inserting, in the amplifier or feedback circuit, a filter sharply attenuating undesired frequencies with little attenuation or phase shift in the desired frequency range.

**10.10.9. The Application of Negative Feedback to the Output Stage.** There is usually little advantage in applying negative feedback to a triode output stage, since a comparatively large input signal is needed without feedback and the slope resistance of the valve is in any case low. Furthermore, with feedback the increased input for a given power output tends to increase distortion in the preceding stage. The performance of a tetrode output stage can, however, be improved by voltage negative feedback, because distortion and generator impedance are reduced while still retaining the tetrode features of high efficiency and power output. Its power sensitivity is reduced, but since this is usually initially high, the extra input signal can often be obtained with little increase in distortion from the previous stage. Current feedback is practically never used in an output stage as it increases generator impedance and exaggerates loudspeaker resonances. Two methods of applying voltage feedback are shown in Figs. 10.26*a* and 10.26*b*. The first uses feedback into the grid circuit from the anode, the feedback ratio being  $\frac{R_2}{R_1 + R_2}$ . This method may not be used in a positive-

drive output stage taking grid current because of the resistance  $R_2$ . The capacitance  $C_1$ , which serves to isolate the d.c. anode voltage, may also be employed to reduce feedback at low frequencies, thus partially compensating for loss of low-frequency output due to the falling reactance of the output transformer primary. The earth capacitance of the input transformer secondary is in parallel with  $R_2$ , so that feedback at high frequencies is decreased. The feedback circuit cannot be connected directly to the grid of the output valve because coupling between anode and grid reduces its grid input resistance (Section 2.8.2, Part I), and so tends to increase distortion

in the preceding amplifier stage (Section 9.3.3). Fig. 10.26a cannot be used when the stage before the output valve has *RC* coupling because the grid leak from the grid to the junction of  $R_1$  and  $R_2$

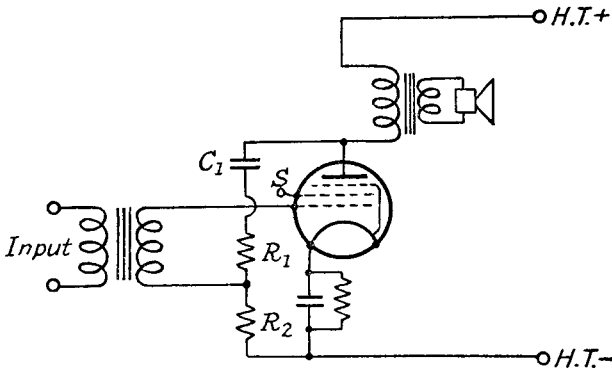


FIG. 10.26a.—Voltage Negative Feedback from the Output Transformer Primary to the Grid Circuit.

forms a potential divider, with the load and slope resistance of the previous valve, which reduces the proportion of feedback voltage across  $R_2$  effectively applied to the output valve grid.

The second circuit feeds back from the output transformer secondary to the cathode, and this helps to compensate for output

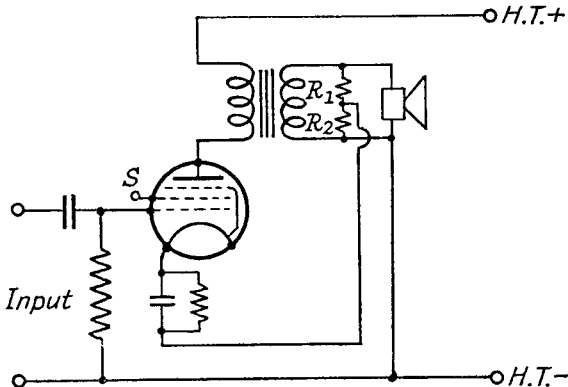


FIG. 10.26b.—Voltage Negative Feedback from the Output Transformer Secondary to the Cathode Circuit.

transformer harmonic distortion and the loss of low- and high-frequency response due to primary and leakage inductance. The resistance  $R_2$  produces some degree of undesired current feedback because it is included in the cathode circuit; this and the

secondary load impedance limit the maximum value of voltage feedback and make the circuit more satisfactory for feedback applied over two stages.

The circuit of Fig. 10.26a is suitable for application to a push-pull stage, but each half of the push-pull input transformer must have its own feedback circuit; the transformer must therefore have two separate secondary windings.

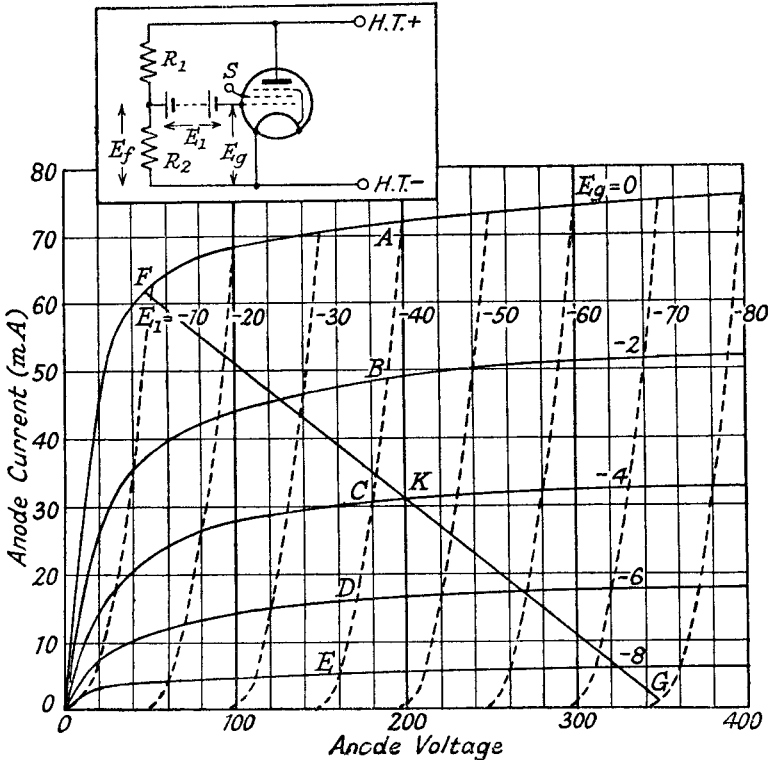


FIG. 10.27.—The Construction of Voltage Negative Feedback Curves for a Tetrode Valve.

Dotted Curves: Equivalent Negative Feedback Characteristics.

The performance of a tetrode output valve having voltage negative feedback may be examined by constructing special feedback curves on the  $I_a E_a$  characteristics. The circuit diagram for these curves is shown in Fig. 10.27, and in this same figure the feedback curves, shown dotted, are superimposed on the  $I_a E_a$  curves. The method of calculating the feedback curves from the  $I_a E_a$  curves is as follows. Suppose the total anode voltage is 200 and the feedback

ratio  $\alpha \left( \frac{R_2}{R_1 + R_2} \right)$  is 20%; the voltage ( $E_f$ ) across  $R_2$  is +40. Now the actual bias voltage ( $E_g$ ) applied between the grid and cathode is the sum of the grid to feedback point voltage ( $E_1$ ) and the feedback voltage ( $E_f$ ),

$$\text{i.e.,} \quad E_g = E_1 + E_f = E_1 + \alpha E_a \quad . \quad . \quad . \quad 10.62a$$

where  $\alpha$  = feedback ratio.

$$\text{If} \quad E_1 = -40, \quad E_g = -40 + 40 = 0 \text{ volts.}$$

Hence point *A* the intersection of the  $I_a E_a$  curve for  $E_g = 0$  with  $E_a = 200$  must give a point on the input feedback curve corresponding to  $E_1 = -40$ . When  $E_a = 190$  volts,  $E_f = +38$  and if  $E_1 = -40$ ,  $E_g = -2$ ; thus point *B*, the intersection of  $E_a = 190$  and the  $I_a E_a$  curve for  $E_g = -2$ , must be another point on the feedback curve for  $E_1 = -40$ . Points *C*, *D* and *E* for  $E_f = +36$ , +34 and +32 respectively are found by a similar process, which can be extended to produce feedback curves for other values of  $E_1$  as shown in the figure. For a different feedback ratio another set of curves must be constructed.

To illustrate the use of these curves we will assume that the optimum load (it is unaltered by feedback) is 5,000 ohms, the h.t. voltage = 200 volts, and normal operating bias is -4 volts. The load line is *FKG*. The feedback curve passing through *K* is  $E_1 = -44$ , and this is the datum curve. Maximum input voltage is determined by the peak input signal which just takes the load line excursion to *F*, the intersection of the load line and  $E_g = 0$ . The input voltage line through *F* is  $E_1 = -9$  so that the peak input voltage required is  $44 - 9 = 35$  volts.

It is important to note that the datum and boundary conditions (points *K* and *F*) are fixed by the  $I_a E_a$  curves and not by the feedback curves. Power output and distortion may be calculated from the intersection of the load line with the appropriate input voltage lines, and, if the procedure set out in Section 10.4 is followed, the current intercepts must be measured for  $E_1 = -9$ ;  $-26.5(-44 + 35 \times 0.5)$ ,  $-44$ ,  $-61.5$  and  $-79$  volts. The feedback curves make quite clear that distortion and equivalent generator impedance are considerably reduced. The generator impedance is decreased from an average of about 40,000 ohms to 700 ohms by this degree of feedback.

In designing an output stage for optimum performance, the highest feedback ratio is required, and the limit is set by the maximum output possible with low distortion from the previous

stage. If, for example, this must not exceed 20 volts peak, we can calculate the maximum permissible feedback ratio by using the modified form of expression 10.62a.

$$\Delta E_g = \Delta E_1 - \Delta E_f \quad . \quad . \quad . \quad 10.62b.$$

The negative sign before the change of feedback voltage,  $\Delta E_f$ , is necessary because feedback is negative and opposes the change of input voltage,  $\Delta E_1$ . Now  $\Delta E_f = \alpha \Delta E_a$ , so that  $\Delta E_g = \Delta E_1 - \alpha \Delta E_a$  and

$$\alpha = \frac{\Delta E_1 - \Delta E_g}{\Delta E_a} \quad . \quad . \quad . \quad 10.63.$$

Assuming the output valve to be operating for maximum power, the maximum change of anode voltage is

$$\begin{aligned} \Delta E_a &\simeq 150 \text{ volts (the horizontal distance between } K \text{ and } F) \\ \Delta E_1 &= 20. \end{aligned}$$

From inspection of Fig. 10.27,

$$\Delta E_g = 4 \text{ volts.}$$

Therefore

$$\begin{aligned} \alpha &= \frac{20 - 4}{150} \\ &= \frac{16}{150} = 10.66\%. \end{aligned}$$

Curves may be constructed for this value of  $\alpha$  as set out above and the performance of the output stage estimated.

**10.10.10. Two-Stage Feedback Circuits.**<sup>34, 36</sup> The application of negative feedback to a two-stage amplifier confers two advantages: (1) it raises the value of  $\mu_0$  in expression 10.49, so that for a fixed feedback ratio the output voltage approaches more closely to  $\frac{E_1}{\alpha}$  and overall frequency response is controlled to a large extent by the feedback circuit; (2) it reduces distortion and compensates for frequency response deficiencies in the stage preceding the output, and (3) it requires less feedback voltage than a single stage so that this voltage may be derived from the secondary of the output transformer.

In a two-stage amplifier it is only possible to indicate the general lines of a design since the particular form of feedback circuit has to be suited to amplifier and load characteristic. A representative circuit<sup>39</sup> is shown in Fig. 10.28. The chief points to note are that  $R_1$  and  $R_3$  are sufficiently large to prevent serious loss of power and that  $R_2$  is small enough to cause negligible current feedback

in the first valve. The inductance  $L_2$  is placed in parallel with  $R_2$  to reduce feedback at low frequencies (less than 100 c.p.s.), and compensate for the limited size of loudspeaker baffle, but sufficient feedback is allowed to reduce to some extent the resonance usually found between 50 and 100 c.p.s. Owing to the rise in speech-coil impedance as the frequency increases, it is advantageous to try to

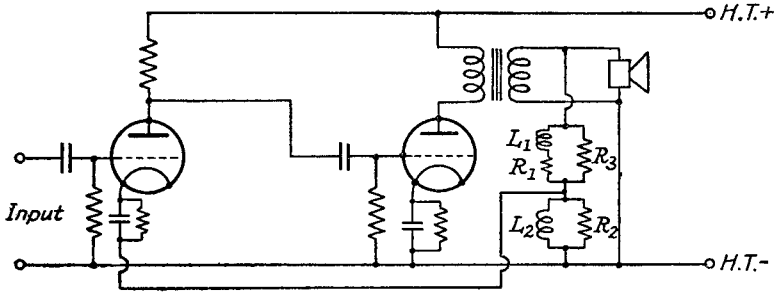


FIG. 10.28.—Negative Feedback in a Two-stage Amplifier.

maintain constant output current, and this is achieved by adjusting  $L_1R_1$  and  $R_3$  to satisfy expression 10.55 which requires  $\alpha$  to be  $\frac{K}{Z_0}$ . As an example, let us assume that the first valve has  $\mu = 30$  and  $R_a = 10,000$  ohms with a total anode load resistance  $\frac{(R_0R_g)}{R_0 + R_g}$  of 50,000 ohms; the second valve is a tetrode of  $g_m = 10$  mA/volt and an optimum output load resistance of 5,000 ohms, the speech-coil impedance is 5.5 ohms, and feedback reduces the overall amplification to  $\frac{1}{5}$  of its initial value.

Amplification of the first stage neglecting current feedback in  $R_2$

$$= \frac{\mu R_0'}{R_a + R_0'} = \frac{30 \times 50,000}{60,000} = 25.$$

Amplification of the second stage  $= g_m R_0' = \frac{10}{1,000} \times 5,000 = 50.$

Step-down ratio of output transformer

$$= \sqrt{\frac{5,000}{5.5}} \approx 30.$$

Overall voltage amplification to the secondary of the output transformer

$$= \frac{25 \times 50}{30} = 41.6.$$

$$\frac{1}{1 + \mu_0 \alpha} = \frac{1}{5}.$$

Therefore  $\mu_0\alpha = 4$  and  $\alpha = \frac{4}{\mu_0} = \frac{4}{41.6} = \frac{1}{10.4} = 9.6\%$ .

Assuming that  $L_1$  has not much effect at the medium frequencies,

$$\frac{R_2}{R_2 + \frac{R_1 R_3}{R_1 + R_3}} = \frac{1}{10.4}$$

A suitable value for  $\frac{R_1 R_3}{R_1 + R_3}$  is 200 ohms, for the loss of power is then negligible, and

$$R_2 = \frac{200}{9.4} = 21.3 \text{ ohms.}$$

Examining the effect of  $R_2$  in the cathode circuit of the first valve, we find that the voltage amplification of the first valve is

$$\begin{aligned} \text{Amplification} &= \frac{\mu R_0}{R_a + R_2(1 + \mu) + R_0} = \frac{30 \times 50,000}{10,000 + 660 + 50,000} \\ &= \frac{30 \times 5}{6.066} = 24.7, \end{aligned}$$

which shows that current feedback due to  $R_2$  can be neglected. The inductance of  $L_2$  must depend on the low-frequency compensation required and a probable value is that making the reactance at 100 c.p.s. equal to  $R_2$ , i.e.,

$$L_2 = \frac{21.3 \times 1,000}{6.28 \times 100} = 33.9 \text{ mH.}$$

The values of  $L_1$ ,  $R_1$  and  $R_3$  depend on the speech coil and should be adjusted to give an impedance at high frequencies proportional to the speech-coil impedance.

A similar circuit may be adopted with a push-pull stage. The feedback voltage must not be taken from either half primary of the output transformer, but from the secondary or a suitable third winding. The voltage across each half primary of the output transformer contains some of the distortion components produced by the valve, which are not cancelled because of the leakage inductance and resistance of the windings. These components do, however, cancel each other when the voltage is taken across the total primary and are therefore not present in the secondary. If these distortion components are fed back they tend to increase the overall distortion, and one advantage of feedback is lost.

If the first stage is transformer-coupled, a resistance may be required across the secondary to damp the resonance due to leakage inductance and stray capacitance, and to prevent excessive phase

shifts, which might lead to positive feedback and self-oscillation at some high frequency outside the normal audio frequency range.

## BIBLIOGRAPHY

1. An Apparatus for the Projection of Frequency Output Characteristics. C. G. Garton, and G. S. Lucas, *Wireless Engineer*, Feb. 1929, p. 62.
2. Output Characteristics of Thermionic Amplifiers. B. C. Brain, *Wireless Engineer*, March 1929, p. 119.
3. Push-Pull Amplification. F. Aughtie, *Wireless Engineer*, June 1929, p. 307.
4. A Thermionic Voltmeter Method for the Harmonic Analysis of Electrical Waves. C. G. Suits, *Proc. I.R.E.*, Jan. 1930, p. 178.
5. Effect of Output Load upon Frequency Distortion in Resistance Amplifiers. H. A. Thomas, *Wireless Engineer*, Jan. 1931, p. 11.
6. Percentage Harmonic Distortion. G. W. O. Howe, *Wireless Engineer*, July 1931, p. 347.
7. Push-Pull Problems. W. T. Cocking, *Wireless World*, 5th Aug. 1931, p. 128.
8. The Problem of Pentode Output Fidelity. L. Tulauskas, *Electronics*, Oct. 1931, p. 142.
9. Distortion in Valve Characteristics. G. S. C. Lucas, *Wireless Engineer*, Nov. 1931, p. 595. *Correspondence*, Dec. 1931, p. 660, Feb. 1932, p. 76.
10. A Simple Harmonic Analyzer. M. G. Nicholson and W. M. Perkins, *Proc. I.R.E.*, April 1932, p. 734.
11. Regeneration Theory. H. Nyquist, *Bell Technical Journal*, July 1932, p. 126.
12. Grid Current Compensation in Power Amplifiers. W. Baggally, *Wireless Engineer*, Feb. 1933, p. 65.
13. Graphical Determination of Performance of Push-Pull Audio Amplifiers. B. J. Thompson, *Proc. I.R.E.*, April 1933, p. 591.
14. Permissible Amplitude Distortion of Speech in an Audio Reproducing System. F. Massa, *Proc. I.R.E.*, May 1933, p. 682.
15. A Theory of Available Output and Optimum Operating Conditions for Triode Valves. M. V. Callendar, *Proc. I.R.E.*, July 1933, p. 909.
16. Distortion Cancellation in Audio Amplifiers. W. Baggally, *Wireless Engineer*, Aug. 1933, p. 413.
17. The Calculation of Harmonic Production in Thermionic Valves with Resistive Loads. D. C. Espley, *Proc. I.R.E.*, Oct. 1933, p. 1439.
18. High Quality Class B Amplification. K. A. Macfadyen, *Wireless World*, Dec. 15th, 1933, p. 454.
19. Stabilised Feedback Amplifiers. H. S. Black, *Electrical Engineering*, Jan. 1934, p. 114.
20. Direct Reading Harmonic Scales. D. C. Espley and L. I. Farren, *Wireless Engineer*, April 1934, p. 183.
21. Push-Pull Input Systems. W. T. Cocking, *Wireless World*, Sept. 21st, 1934, p. 245.
22. Measurement of Non-Linear Distortions. H. Faulhaber, *Elektrische Nachrichten Technik*, Oct. 1934, p. 351.
23. Incremental Permeability and Inductance. L. G. A. Sims, *Wireless Engineer*, Jan. (p. 8), Feb. (p. 65) 1935.



24. Intermodulation in Audio Frequency Amplifiers. A. C. Bartlett, *Wireless Engineer*, Feb. 1935, p. 70.
25. High Efficiency Push-Pull Output Stages. K. S. Macfadyen, *Wireless World*, 15th March 1935, p. 256.
26. Class B Transformers. N. Partridge, *Wireless World*, 22nd March 1935, p. 280.
27. Incremental Magnetization. L. G. A. Sims and D. L. Clay, *Wireless Engineer*, May (p. 238), June (p. 312) 1935.
28. Join-Up Distortion in Class B Amplifiers. F. R. W. Strafford, *Wireless Engineer*, Oct. 1935, p. 539.
29. Modifications of the Push-Pull Output Stage. K. S. Macfadyen, *Wireless Engineer*, Oct. and Dec. 1935, pp. 528 and 639.
30. Output Transformer Response. F. E. Terman and R. E. Ingobretsen, *Electronics*, Jan. 1936, p. 30.
31. Class B and Class AB Audio Amplifiers. G. Koehler, *Electronics*, Feb. 1936, p. 14.
32. Feeding Push-Pull Amplifiers. W. T. Cocking, *Wireless World*, Feb. 7th, 1936, p. 126.
33. Quasi Transients in Class B Audio Frequency Push-Pull Amplifiers. A. Pen-Tung Sah, *Proc. I.R.E.*, Nov. 1936, p. 1522.
34. Feedback Amplifier Design. F. E. Terman, *Electronics*, Jan. 1937, p. 12.
35. Amplitude Distortion. J. H. O. Harries, *Wireless Engineer*, Feb. 1937, p. 63.
36. Practical Feedback Amplifiers. J. R. Day and J. B. Russell, *Electronics*, April 1937, p. 16.
37. Phase Reversal in Push-Pull Amplifiers. C. C. Inglis, *Wireless World*, April 30th, 1937, p. 416.
38. Audio-Frequency Transformers. E. T. Wrathall, *Wireless Engineer*, June (p. 293), July (p. 363), Aug. (p. 414) 1937.
39. Inverse Feedback. B. D. H. Tellegen and V. C. Henriquez, *Wireless Engineer*, Aug. 1937, p. 409.
40. A New Push-Pull Feed Circuit. L. H. Cooper, *Wireless World*, Oct. 22nd, 1937, p. 411.
41. Some Properties of Negative Feedback Amplifiers. L. I. Farren, *Wireless Engineer*, Jan. 1938, p. 23.
42. Balanced Feedback Amplifiers. E. L. Ginzton, *Proc. I.R.E.*, Nov. 1938, p. 1367.
43. The Marconi-E.M.I. Television System. C. O. Browne, Part II, *Journal I.E.E.*, Dec. 1938, p. 767.
44. Distortion in Valves with Resistive Loads. A. Bloch, *Wireless Engineer*, Dec. 1939, p. 592.
45. Distortion Tests by the Intermodulation Method. J. K. Hilliard, *Proc. I.R.E.*, Dec. 1941, p. 614.
46. Optimum Conditions for Maximum Power in Class A Amplifiers. W. B. Nottingham, *Proc. I.R.E.*, Dec. 1941, p. 620.
47. Harmonic Distortion in Audio Frequency Transformers. N. Partridge, *Wireless Engineer*, Sept. (p. 394), Oct. (p. 451), Nov. (p. 503) 1942.
48. Optimum Conditions in Class A Amplifiers. G. W. O. Howe, *Wireless Engineer*, Feb. 1943, p. 53.
49. *Specification for Testing and Expressing Overall Performance of Radio Receivers*. Part II, Acoustic Tests, p. 15. Radio Manufacturers Association (England).

## CHAPTER 11

### POWER SUPPLIES

**11.1. Introduction.** The power supply circuits for the A.C., the A.C./D.C., the transportable (car) and the battery receiver have some common features, but also certain important differences. The power supply for the A.C. receiver consists of a mains transformer for the required heater and H.T. voltages, a rectifier and a smoothing filter for attenuating the rectified ripple voltage. In the A.C./D.C. receiver the mains transformer is omitted and the valve heaters are series-connected. The car receiver often uses the car battery for heater and H.T. supply, a vibrator (very occasionally a motor generator) acting as the converter for the H.T. supply. The battery receiver normally has an accumulator for L.T. and a dry battery for H.T. supply. The latter raises few problems; adequate decoupling is essential in each stage of the receiver, to prevent feedback coupling as the internal resistance of the battery rises during life. Only supply circuits for the first three types of receivers are reviewed in this chapter.

#### 11.2. A.C. Receiver Power Supply.

**11.2.1. Introduction.** A typical power supply circuit for an A.C. receiver is shown in Fig. 11.1. To suppress R.F. interference entering the receiver via the mains supply leads, an electrostatic

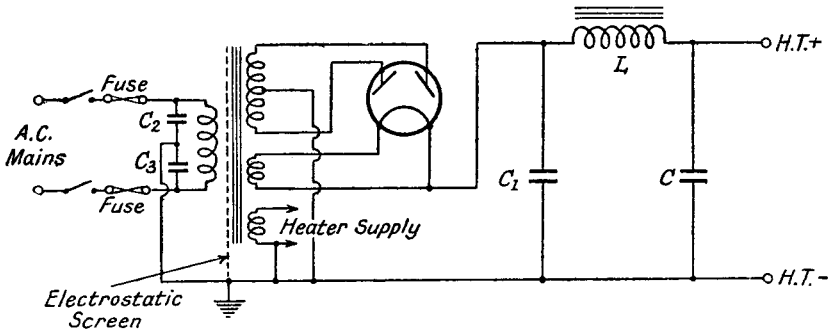


FIG. 11.1.—A Typical A.C. Receiver Power Supply Circuit.

screen is inserted between the primary and secondaries of the mains transformer, and two capacitances,  $C_2$  and  $C_3$  (about  $0.001 \mu\text{F}$ ) may be included from each mains lead to earth. The heater winding

may have a centre-tapped earth connection, but it is more common to earth one side of the winding. With indirectly-heated valves, hum and noise pick-up from the heaters can be almost entirely eliminated by connecting some point on the winding to earth. Directly-heated valves (normally only the output valves) must, however, be earthed at the centre tap in order to obtain electrostatic hum balance. An  $LC$  filter follows the reservoir capacitance  $C_1$ , and the full-wave rectifier. The filter choke has an air gap to prevent saturation of the iron core by the rectified current, and to maintain a high inductance value to the ripple voltage. The loud-speaker field coil is often employed as the filter choke. A small coil wound over the field winding is inserted in series with the speech coil to neutralize the effect on the latter of the A.C. ripple field.

**11.2.2. The Mains Transformer.**<sup>11</sup> The equivalent circuit for a mains transformer, having two secondary windings, shown in Fig. 11.2, gives a good indication of the features contributing to the production of a satisfactory component. The secondary winding resistances  $R_{s1}$  and  $R_{s2}$ , and the load resistances  $R_1$  and  $R_2$  are transferred to the primary side by dividing by the square of the ratios,  $n_1$  and  $n_2$ , of the secondary to primary turns. The primary winding resistance and inductance are  $R_p$  and  $L_p$  respectively, and the leakage inductance is  $L_p(1 - k^2)$  (Section 9.4), where  $k$  is the

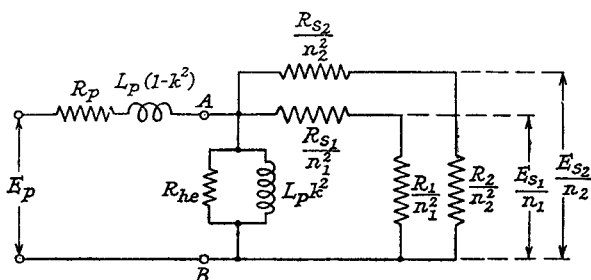


FIG. 11.2.—The Equivalent Circuit of a Mains Transformer.

coupling coefficient between primary and secondary. The leakage inductance is, in this case, considered to be the same for both secondary windings; the error involved in this assumption is not very large.  $R_{he}$  represents the hysteresis and eddy current loss in the iron core. The efficiency is governed by  $R_p$ ,  $R_{s1}$ ,  $R_{s2}$ ,  $R_{he}$  and  $k$ , and decrease of the first three and increase of the last two lead to a higher efficiency. For good regulation, low values of  $R_p$ ,  $R_{s1}$  and  $R_{s2}$ , and a high value of  $k$  are essential;  $R_{he}$  has little effect.

There are two alternatives for the winding positions; primary

and secondaries may be wound on top of each other, or they may be placed in separate sections side by side. In the first position the primary is usually nearest the centre limb of the core, and between it and the secondaries is the electrostatic screen, an open-circuited turn of copper foil or thin sheet. The H.T. and rectifier windings occupy the first two secondary positions respectively, and the L.T. heater winding is located in the outside position. For the second arrangement the primary winding is usually divided into two sections, each section being placed at the ends of the winding space. This reduces the leakage field (increases  $k$ ) between the primary and secondaries, which are separate windings placed between the half primaries. Adequate insulation must be provided between the layers. Joints in the wire should have no projections and should occur at the centre of the layer, because electrical stress between layers is least at this position. Electrical stress is increased at projections, and insulation breakdown at joints due to mechanical puncture or corona effects may occur. Sharp corners to winding bobbins are avoided since electrical and mechanical (heating and cooling) stresses are greatest at these points. The ingress of moisture is prevented, preferably by sealing the windings (by pitch compound impregnation).

The design of a mains transformer is best illustrated by an example. Suppose a transformer fulfilling the following requirements is to be designed :

Primary . . .	230-volt 50-c.p.s. mains supply.
Secondaries . . .	H.T. 300–0–300 volts 120 mA for full wave rectification, i.e., there is no D.C. polarizing current. The D.C. output for the above A.C. output would be about 280 volts, 90 mA. (See Section 11.2.5 for the method of calculating it.)
	L.T. 6.3 volts 2 amps.
	L.T. 6.3 volts 6 amps.

The fundamental equation for the induced voltage in any coil placed in a sinusoidal A.C. magnetic field is

$$E = 4.44 \hat{\Phi} f \times 10^{-8} \times N \text{ R.M.S. volts.} \quad 11.1$$

where  $\hat{\Phi}$  = peak value of the flux of the magnetic field.

= peak flux density ( $\hat{B}$ )  $\times$  area ( $A$ ) of a cross-section through which the field is threading.

$f$  = frequency in c.p.s.

$N$  = number of turns in the coil.

Rearranging 11.1.

$$\text{Turns per volt } \frac{N}{E} = \frac{10^8}{4.44 \hat{B} A f} \quad . \quad . \quad 11.2$$

where  $E$  has its R.M.S. value.

For Stalloy stampings a suitable value of  $\hat{B}$  is 10,000 lines per square centimetre (64,500 lines per square inch) and taking  $A$  as 1.5 sq. ins.

$$\text{turns per volt} = 4.65.$$

This permits the total primary turns to be calculated, but for estimating the secondary turns allowance must be made for the voltage drop in the primary and secondary winding resistance; i.e., the turns per volt for the secondary windings must be increased.

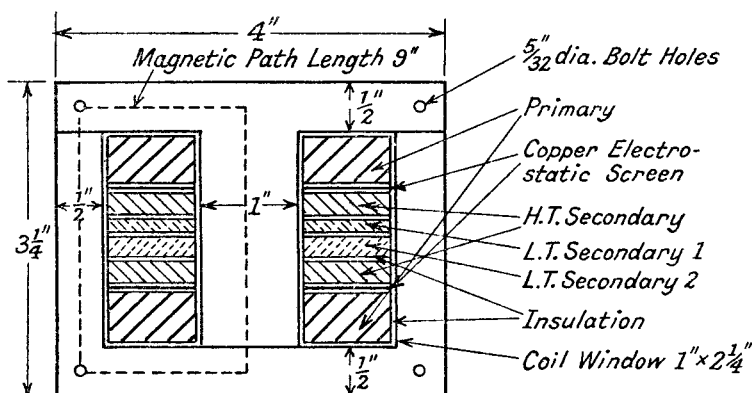


FIG. 11.3a.—A Section through a Typical Mains Transformer.

If we assume a power efficiency on full load of 85%, the voltage efficiency is approximately the square root of this, viz., 92%. For convenience the secondary turns per volt in subsequent calculations are taken as 5; this corresponds to a voltage efficiency of 92.5%.

The arrangement of the windings is shown in Fig. 11.3a, the primary winding being divided into two sections to reduce leakage inductance. The total number of turns for each winding and the number of sections are listed below.

Winding.	Total Turns.	Number of Sections.
Primary . . . . .	1,070	2
H.T. Secondary . . . . .	3,000	2
L.T. Secondary 1 . . . . .	31.5	1
L.T. Secondary 2 . . . . .	31.5	1

$$\begin{aligned} \text{Total output power from the transformer} &= 300 \times 0.12 + 6.3 \times 8 \\ &= 86.4 \text{ watts.} \end{aligned}$$

$$\text{Total input power for 85\% efficiency} = 101.6 \text{ watts.}$$

$$\text{Primary current} = \frac{101.6}{230} = 0.442 \text{ amps.}$$

Taking the permissible current density in all windings as 1,200 amps. per square inch, the required wire diameter can be calculated. The most suitable gauge of wire is then selected from Table 11.1 below, and the area taken by each winding estimated on the basis of double silk covering insulation for the primary and H.T. secondary, and enamel for the L.T. secondaries. The turns per square inch listed below<sup>21</sup> are calculated on the assumption that wires in consecutive layers are wound immediately above each other and not in the grooves between the wires of the layer below.

TABLE 11.1

S.W.G.	Wire Diameter (inches).	Resistance. Ohms per 1,000 yards.	Turns per Square Inch.				Enamel.
			SCC.	DCC.	SSC.	DSC.	
10	0.128	1.8657	54.1	49.6	58.3	57	—
12	0.104	2.8626	79.7	71.8	87.3	85	—
14	0.08	4.776	129	113	145	140	145
16	0.064	7.463	198	173	223	213	226
18	0.048	13.267	343	297	400	377	400
20	0.036	23.59	567	472	692	641	692
22	0.028	38.99	865	692	1,110	1,010	1,110
24	0.022	63.16	1,280	977	1,770	1,600	1,770
26	0.018	94.35	1,740	1,280	2,560	2,270	2,560
28	0.0148	139.55	2,310	1,630	3,650	3,160	3,760
30	0.0124	198.8	2,950	1,990	5,180	4,500	5,370
32	0.0108	262.1	4,010	2,550	6,610	5,650	6,890
34	0.0092	361.2	4,960	3,020	8,730	7,310	9,610
36	0.0076	529.2	7,430	4,110	12,100	10,300	13,500
38	0.006	849.1	10,000	5,100	17,800	14,700	20,400
40	0.0048	1,326.7	12,900	6,100	25,200	20,100	32,500

SCC = Single Cotton Covered. SSC = Single Silk Covered.

The details of each winding are therefore as follows :

Winding.	Required Wire Diameter (ins.) $I = 1,200 \text{ Amps. per sq. in.}$	Suitable S.W.G.	Winding Area (Sq. ins.).
Primary	0.02165	24	0.669
H.T. Secondary	0.00797	34	0.41
L.T. Secondary 1	0.0460	18	0.0788
L.T. Secondary 2	0.0797	14	0.217
Total =			<u>1.3748</u>

Note that the average current from each half-secondary is only 60 mA because it delivers 120 mA each half-cycle. The wire diameter is therefore calculated as for 60 mA.

The next step is to decide on the stamping for the core. The cross-section of the central limb must be 1.5 sq. ins. in order to satisfy expression 11.2, and a suitable width for the limb is 1 in. The area of the winding window must be able to accommodate the coils (1.3748 sq. ins.) and the insulation between them. Let us try Stalloy No. 32A, the dimensions of which are given in Fig. 11.3a, and assume that the insulation between the windings themselves, and the windings and core is 0.075 ins. thick, and that the insulation from the primary to electrostatic screen is 0.05 ins. The available winding area dimensions are

$$\begin{aligned}\text{Effective width} &= \text{total width} - \text{insulation} \\ &= 1 - (2 \times 0.075) = 0.85 \text{ ins.}\end{aligned}$$

$$\begin{aligned}\text{Effective height} &= \text{total height} - (\text{interwinding insulation} \\ &\quad + \text{winding to screen insulation} \\ &\quad + \text{electrostatic screens}) \\ &= 2.25 - (5 \times 0.075 + 2 \times 0.1 + 2 \times 0.01) \\ &= 1.655 \text{ ins.}\end{aligned}$$

$$\text{Therefore total winding area} = 1.408 \text{ sq. ins.}$$

There is a reasonable factor of safety upon that actually required, 1.3748 sq. ins.

The iron loss, copper loss and efficiency must now be checked.

#### (1) *Iron Losses.*

$$\begin{aligned}\text{Area of face of stamping} &= \text{total area} - \text{winding window area} \\ &\quad - \text{area for } \frac{5}{32} \text{ in. diameter bolts.} \\ &= 4 \times 3.25 - 2.25 \times 2 - \pi \left( \frac{5}{32} \right)^2 \\ &= 8.4236 \text{ sq. ins.}\end{aligned}$$

$$\text{Thickness of iron core} = 1.5 \text{ ins.}$$

$$\text{Total volume of iron} = 8.4236 \times 1.5 = 12.63 \text{ cu. ins.}$$

$$\begin{aligned}\text{Weight of iron (density 0.28 lbs. per cubic inch)} \\ &= 12.63 \times 0.28 = 3.54 \text{ lbs.}\end{aligned}$$

$$\begin{aligned}\text{Loss in standard Stalloy at } \hat{B} = 10,000 \text{ lines per square centimetre} \\ &= 0.65 \text{ watts per lb.}\end{aligned}$$

$$\text{Therefore loss in iron core} = 2.3 \text{ watts.}$$

Allowing 10% insulation between stampings, the total thickness of core = 1.65 ins.

$$\text{Number of laminations } 0.014 \text{ in. thick} = 118.$$

(2) *Winding Copper Loss.*

From Figs. 11.3a and 11.3b, the mean length of a winding turn is 9.3 ins. The total length of each winding, its resistance (obtained from Table 11.1) and power loss are tabulated below.

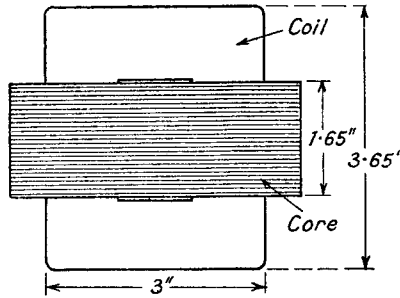


FIG. 11.3b.—A Plan View of the Mains Transformer of Fig. 11.3a.

Winding.	Total Turns.	Yards.	Ohms.	Current.	Power Loss.
Primary	1,070	276.5	17.7	0.442	3.42
H.T. Secondary	3,000	775	280	0.06	1.01
L.T. Secondary 1	31.5	8.14	0.1079	2	0.432
L.T. Secondary 2	31.5	8.14	0.0389	6	1.40

Total loss (iron + copper) =  $6.262 + 2.3 = 8.562$  watts.

$$\text{Efficiency} = \frac{86.4}{94.962} = 91\%.$$

This is slightly higher than the value assumed initially, but there is some increase in primary loss due to magnetizing current, which has not been considered in the above.

(3) *No-load and Full-load Operating Conditions.*

The no-load current of the transformer is determined mainly by the primary inductance, the formula for which is given in expression 11.19b, Section 11.2.9.

$$L = 1.255 \Delta\mu n^2 V 10^{-8}$$

where  $n$  = turns per centimetre of the magnetic path in the core.

$\Delta\mu$  = incremental a.c. permeability.

$V$  = volume of iron core in cubic centimetres.

From Fig. 10.20,  $\Delta\mu$  is 2,400 at  $\hat{B} = 10,000$  lines per square centimetre,  $H_{D.C.} = 0$ , but let us assume  $\Delta\mu$  is 2,000. The primary inductance is therefore

$$L_p = \frac{1.255 \times 2,000 \times 2.54 \times (1,070)^2 \times 12.63}{9^2 \times 10^8}$$

The factor 2.54 is included to convert turns per inch of magnetic



path and volume in cubic inches to turns per centimetre and cubic centimetres. The length of the magnetic path is 9 ins. (See Fig. 11.3a.)

Therefore  $L_p = 11.38 \text{ H}$

$$X_p = 2\pi f L_p = 3,570 \Omega.$$

The primary winding resistance has practically no effect on the no-load current which is

$$I_0 = \frac{230}{3,570} = 64.4 \text{ mA.}$$

By assuming a leakage inductance of 0.5% of  $L_p$  (a probable value), we can estimate the no-load and full-load voltages at the secondary terminals. On no load the primary winding resistance has practically no effect, so that all no-load secondary voltages are 0.5% lower than the values given from the turns ratio.

$$\text{H.T. half secondary open-circuit voltage} = \frac{230 \times 1,500 \times 0.995}{1,070} = 320$$

$$\begin{aligned} \text{L.T. secondary (1) and (2) open-circuit voltage} \\ = \frac{230 \times 31.5 \times 0.995}{1,070} = 6.72. \end{aligned}$$

To determine the full-load voltages it is necessary to estimate the secondary load resistances referred to the primary side. Thus, for the H.T. secondary, the total load resistance (including the winding resistance) for each half secondary is

$$\left[ 140 \text{ (winding)} + \frac{300}{0.06} \text{ (load)} \right] = 5,140 \text{ ohms,}$$

and the load resistance for both half secondaries referred to the primary side becomes  $2,570 \times \left( \frac{1,070}{1,500} \right)^2 = 1,310$  ohms. Similarly, the primary load resistances due to L.T. secondaries 1 and 2 are 3,770,  $\left[ \left( 0.1079 + \frac{6.3}{2} \right) \left( \frac{1,070}{31.5} \right)^2 \right]$  and 1,260 ohms. The total resistance load across the points  $AB$  in Fig. 11.2 is the resultant of 1,310, 3,770 and 1,260 in parallel, i.e., 549 ohms.

The equivalent impedance across the points  $AB$ , including the reactance of  $L_p k^2$ , ( $j$  3,552 ohms) is

$$\begin{aligned} R_{AB} + jX_{AB} &= \frac{549 \times (3,552)^2}{(549)^2 + (3,552)^2} + j \frac{3,552 \times (549)^2}{(549)^2 + (3,552)^2} \\ &= 537 + j 83. \end{aligned}$$

The induced voltage in the transformer primary, i.e., the voltage across  $AB$

$$\begin{aligned} &= E_p \sqrt{\frac{(R_{AB})^2 + (X_{AB})^2}{(R_{AB} + R_1)^2 + (X_{AB} + \omega L_p(1 - k^2))^2}} \\ &= 230 \sqrt{\frac{(537)^2 + (83)^2}{(554.5)^2 + (100.85)^2}} \\ &= 222 \text{ volts.} \end{aligned}$$

The voltage across each pair of secondary terminals is

$$E_{AB} \frac{N_s}{N_p} \cdot \frac{R_L}{R_W + R_L}$$

where  $N_s$  and  $N_p$  are the secondary and primary turns,  $R_L$  and  $R_W$  are the load and winding resistances of the secondary.

$$\text{H.T. half secondary voltage} = 222 \frac{1,500}{1,070} \frac{5,000}{5,140} = 302 \text{ volts.}$$

$$\text{L.T. secondary 1 voltage} = 222 \frac{31.5}{1,070} \frac{3.15}{3.2579} = 6.3 \text{ volts.}$$

$$\text{L.T. secondary 2 voltage} = 222 \frac{31.5}{1,070} \frac{1.05}{1.089} = 6.3 \text{ volts.}$$

It is interesting to note the effect of an increase in leakage inductance to 1% of  $L_p$ ;  $E_{AB}$  becomes 220 volts and the secondary voltages are reduced to 299 and 6.25 respectively. The need for keeping leakage inductance to the lowest possible value cannot be overstressed.

#### (4) *Transformer Temperature Rise on Full-load.*

For an air-cooled transformer an approximate value for the area required to dissipate 1 watt for a temperature rise of 1° C. in the iron is 30 sq. ins. and for the coils is 50 sq. ins.

The cooling area for the iron includes the top, sides, front and back faces, except that just underneath the coil, but does not include the bottom or central limb. The effective iron thickness of the core is 1.5 ins. Hence, from Figs. 11.3a and 11.3b.

$$\begin{aligned} \text{Total cooling area} &= (4 \times 1.5) + (3.25 \times 1.5)2 + (4 \times 0.5)2 \\ &\quad + (2.75 \times 0.5)4 = 25.25 \text{ sq. ins.} \end{aligned}$$

Watts lost in the iron core = 2.3

$$\text{Temperature rise of iron core} = \frac{30 \times 2.3}{25.25} = 2.73^\circ \text{ C.}$$

The cooling area for the coil includes all the area outside the iron core but excludes that at the bottom of the transformer.

$$\begin{aligned}\text{Cooling area of coil} &= (3 \times 1)^2 + (2.25 \times 1)^4 + (3 \times 2.25)^2 \\ &= 29.5 \text{ sq. ins.}\end{aligned}$$

$$\text{Watts lost in the coil} = 6.262$$

$$\text{Temperature rise of coil} = \frac{50}{29.5} \times 6.262 = 10.6^\circ \text{C.}$$

In actual practice some heat is transferred from the coil to the core so that the average temperature of the coil is likely to be slightly lower than that given, and that of the core slightly higher. The calculated temperature rises are, however, well within the permissible values.

In the above example we have assumed that there is no polarizing D.C. field since a full-wave rectifier is being used. If half-wave rectification is employed, there is a D.C. polarizing field in the core due to the rectified current flowing in the secondary winding. The chief effect of the D.C. polarizing field is to reduce the primary inductance, thereby increasing the magnetizing current and reducing efficiency. An air gap is desirable, and the design principles involved are as set out in Section 11.2.9, but modified by the fact that the A.C. flux density is large and in most cases greater than the D.C. polarizing flux density.

**11.2.3. The H.T. Rectifier.** There are four important types of rectifier circuits, the full-wave, half-wave, bridge and voltage-doubler. Examples of the last three are given in Figs. 11.4a, 11.4b and 11.4c. The full-wave rectifier, illustrated in Fig. 11.1, is the most common type of receiver rectifier, and among its outstanding features are cancellation of the fundamental mains frequency com-

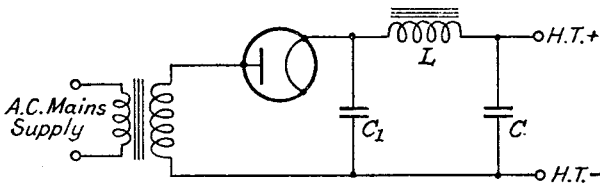


FIG. 11.4a.—A Half-wave Rectifier.

ponent in the rectified output, and cancellation of the D.C. current components through the mains transformer. This allows a smaller transformer core to be used and better voltage regulation to be obtained. On the other hand, a centre-tapped secondary winding is required, having a total A.C. peak voltage of approximately twice the D.C. output voltage. The half-wave rectifier has the merit of simplicity, reduced rectifier cost and only one secondary winding.

The secondary is half that of the full-wave rectifier secondary for the same D.C. output voltage. The D.C. output current is, however, only half that of the full-wave rectifier with similar secondary windings, and voltage regulation is worse. The simplified analysis of Section 11.2.5 shows that there should be little difference<sup>2</sup> between the R.M.S. to D.C. current ratios, but in practice it is generally found to be about 1.6 compared with 1.35 for full-wave operation. This, combined with the D.C. polarizing current in the secondary winding, tends to reduced transformer efficiency, whilst hum level of the D.C. output voltage is increased by the presence of a large mains fundamental frequency voltage component. The half-wave rectifier is most suitable for providing a high-voltage low-current D.C. output, such as that required for cathode-ray tube power supply circuits, but it is also used for A.C./D.C. operated receivers, which have no transformer connection to the mains supply.

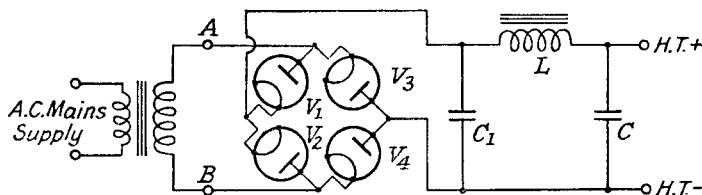


FIG. 11.4b.—A Bridge Rectifier.

Valves are practically never used in the bridge rectifier since four independent valve structures would be required, but the circuit is quite often employed with metal rectifiers. The bridge circuit, shown in Fig. 11.4b, is equivalent to a full-wave rectifier, but requires only a single secondary winding of half the A.C. voltage for the same D.C. output voltage as the full-wave circuit. The principle of operation is as follows. During the half-cycle when *A* is positive with respect to *B*, valves *V*<sub>1</sub> and *V*<sub>4</sub> are conducting, the current passing from the cathode of *V*<sub>1</sub>, through the reservoir capacitor *C*<sub>1</sub>, to the anode of *V*<sub>4</sub> and thence to *B*. For the opposite half wave, *B* is positive with respect to *A*, and valves *V*<sub>2</sub> and *V*<sub>3</sub> are conducting (*V*<sub>1</sub> and *V*<sub>4</sub> are inoperative), the current passing through *C*<sub>1</sub> in the same direction as when *V*<sub>1</sub> and *V*<sub>4</sub> conduct. Voltage regulation is practically the same as for the full-wave rectifier.

The voltage doubler rectifier of Fig. 11.4c requires two separate half-wave rectifiers, each charges its own reservoir capacitor (*C*<sub>1</sub> is that for *V*<sub>1</sub>) on alternate half-cycles. The two reservoir capacitors, *C*<sub>1</sub> and *C*<sub>2</sub>, are connected in series to give a D.C. output voltage of

approximately twice the secondary peak A.C. voltage. D.C. voltage regulation is usually not so good as that of the half-wave rectifier.

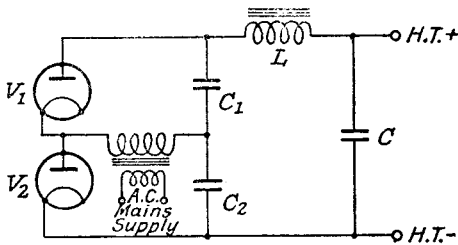


FIG. 11.4c.—A Voltage Doubler Rectifier.

The D.C. charging currents for capacitors,  $C_1$  and  $C_2$ , oppose in the secondary winding of the transformer, and the permeability of the core is unaffected by the rectifier action.

The most popular type of rectifier for receiver H.T. supply is the high vacuum diode valve. It is robust and can be made to have a high inverse negative voltage. The inverse voltage is the negative voltage which can be withstood without taking appreciable current in the reverse direction, from cathode to anode. For high rectification efficiency the conduction slope resistance should be low, and this is achieved by having a large emitting surface and minimum anode-to-cathode spacing. The former can be realized with little difficulty in a directly-heated valve by having a long filament, but there are limits to the size of the cathode in an indirectly-heated valve, and increased rectification efficiency is largely obtained by reducing the equivalent spacing between anode and cathode. A comparatively coarse mesh grid, connected to the anode, is inserted between anode and cathode to neutralize the electron space-charge at the cathode, and this effectively reduces the anode-cathode spacing without decreasing to any large extent the inverse voltage. With a very narrow anode-cathode spacing there is a possibility of some of the active cathode coating being deposited on the anode, the temperature of which may become sufficiently high, due to heat radiation from the cathode as well as electron bombardment, to cause "back" emission in the reverse direction, and so reduce rectification efficiency. The chief value of the indirectly-heated rectifier is that the H.T. supply is not applied until the valves in the receiver are conductive, and high initial D.C. voltages, imposing undue strain on capacitors or resistors, are avoided.

A possible alternative to the high vacuum diode is the mercury

vapour rectifier, which generally has a higher rectification efficiency. The voltage drop across the valve during conduction is constant at about 15 volts and independent of load current. Its disadvantages are that it tends to produce R.F. interference, is less robust, and, unless special precautions are taken, has a shorter life than the high vacuum diode. Inverse voltage is also limited, though this effect is of little importance in receiver H.T. supplies. The nature of the conduction characteristic is such that a very peaked current wave, rich in the higher harmonics, is produced in the reservoir capacitance, and these harmonics enter the R.F. range and may cause interference in the receiver. Bombardment of the cathode coating by positive ions of mercury vapour tends to reduce valve life; the velocity of these ions can become dangerously high if the A.C. anode voltage is switched on before the cathode is hot enough to emit a copious flow of electrons and so reduce the positive voltage between anode and cathode during conduction. Since practically all the mass of the gas atom is contained in the ion, its kinetic energy is considerable when its velocity is high, and the active material is stripped from the cathode.

The rectifier valve normally has a reservoir capacitance, which forms a capacitive load impedance. This increases rectification efficiency and attenuates A.C. fundamental and harmonic voltage components in the rectified output. An inductive load impedance may be used when high D.C. voltage regulation is desired, but rectification efficiency is then reduced. The mercury-filled diode valve is particularly suitable for use with an inductive load. A "pure" resistance load is never employed because it causes a low rectification efficiency—the D.C. output voltage is approximately  $\frac{1}{2}$  (half wave) or  $\frac{2}{3}$  (full wave) of that obtained with a capacitance load—and there is no attenuation of the A.C. voltage components in the rectified output. An examination of rectifier performance when supplying a resistance load is, however, helpful in understanding its operation with capacitive or inductive load.

**11.2.4. The H.T. Rectifier with Resistance Load.** When a H.T. rectifier has a resistance load, the unidirectional current pulses have half cosine wave shapes. For a half-wave rectifier these current pulses may be analysed into the Fourier Series \* given below

$$I_0 = \frac{2I}{\pi} \left[ \frac{1}{2} + \frac{\pi}{4} \cos pt + \frac{1}{3} \cos 2pt - \frac{1}{3.5} \cos 4pt + \frac{1}{5.7} \cos 6pt \dots \right]. \quad 11.3a$$

where  $I_0$  = current through the resistance load  $R$ .

\* See Appendix 2A, Part I.

and  $\hat{I} \cos pt =$  instantaneous current through the diode during the conduction period.

In a full-wave rectifier, the fundamental component is cancelled and the Fourier Series \* becomes

$$I_o = \frac{4\hat{I}}{\pi} \left[ \frac{1}{2} + \frac{1}{3} \cos 2pt - \frac{1}{3.5} \cos 4pt + \frac{1}{5.7} \cos 6pt \dots \right] \quad . \quad 11.3b.$$

The D.C. components for half- and full-wave operation are  $\frac{\hat{I}}{\pi}$  and  $\frac{2\hat{I}}{\pi}$  respectively. The voltage across the load resistance  $R$  is obtained by substituting  $E_o$  and  $\frac{\hat{E}_1 R}{R + R_d + R_t}$  for  $I_o$  and  $\hat{I}$  in the above expressions.  $R_d$  is the conduction resistance of the rectifier,  $R_t$  the sum of the winding resistance of the secondary and that reflected from the primary of the transformer supplying the rectifier, and  $\hat{E}_1 \cos pt$  is the secondary voltage. Generally,  $R \gg R_d + R_t$ , so that the D.C. output voltage,  $\frac{\hat{E}_1}{\pi}$  or  $\frac{2\hat{E}_1}{\pi}$ , is almost independent of load

resistance. The resistance loaded rectifier, therefore, has the advantage of good D.C. voltage regulation, but rectification efficiency is low (31.8% for the half-wave and 63.6% for the full-wave rectifier). To reduce A.C. voltages across the load resistance it is usual to insert an  $LC$  filter between the load resistance and rectifier. A single  $LC$  filter between rectifier and load resistance, as shown in Fig. 11.10, can, with suitable choice of  $L$ , give almost as good D.C. regulation as the resistance alone, and it is particularly useful for supplying a circuit requiring a variable current with little voltage variation, i.e., an output stage operating under Class B or Class AB conditions. The more common type of rectifier circuit includes a reservoir capacitance immediately following the rectifier. This raises rectification efficiency and D.C. output voltage, but decreases voltage regulation. We shall examine the capacitively loaded rectifier first.

**11.2.5. The H.T. Rectifier with Capacitive Load.** The action of the rectifier with a reservoir capacitance (Fig. 11.5) is similar to that of a diode detector having a capacitance shunted load resistance (Sections 8.2.5, 6, 7, and 13, Part I). The capacitance acts as a reservoir, storing energy when the A.C. voltage applied to the rectifier exceeds the voltage across the capacitance  $C_1$ . The stored energy is released through the load resistance  $R$  when the A.C. voltage falls below that across  $C_1$ , and the rectifier ceases to conduct. The gaps between successive half waves of A.C. voltage

\* See Appendix 2A, Part I.

are therefore filled as shown by the dotted curve  $E_c$  in Fig. 11.6. The diode starts to conduct at some angle such as  $-\alpha_1$ , and ceases at an angle corresponding to  $\alpha_2$ ,  $\alpha_1$  being numerically greater than

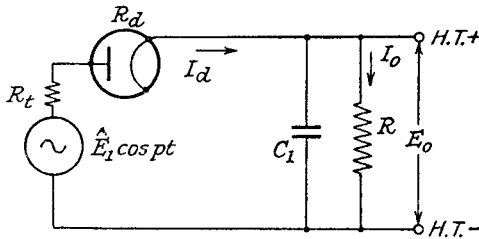


FIG. 11.5.—A Half-wave Rectifier with Capacitive Load.

$\alpha_2$ . The current pulse,  $I_d$ , through the diode, is shown under the second half wave.

The performance of the rectifier may be calculated by using the analyses developed in Sections 8.2.5 to 8.2.7, which assume that the voltage across the load resistance  $R$  is constant, and that diode conduction starts at  $-\phi$  and ends at  $+\phi$ . The error involved is not very large provided rectification efficiency is greater than 50%, i.e., the D.C. voltage exceeds half the peak A.C. voltage. The shape of the conduction current-anode voltage characteristic of the high vacuum diode rectifier is generally of the form shown in Fig. 11.7, the

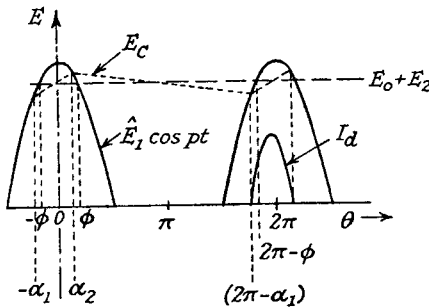


FIG. 11.6.—Voltage and Current Characteristics of a Half-wave Rectifier.

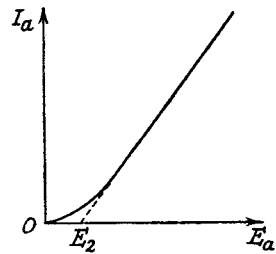


FIG. 11.7.—Conduction Current-Anode Voltage Characteristic of a Diode Rectifier.

straight part, produced, cutting the  $E_a$  axis at some positive voltage,  $E_2$ . If we neglect the initial curvature, and assume that the conduction characteristic is a straight line of slope resistance  $R_d$  passing through an anode voltage of  $+E_2$ , the expression for the rectified D.C. current through the load resistance  $R$  is, from Section 8.2.7,

$$I_0 = \frac{\hat{E}_1 K}{\pi(R_d + R_t)} \quad \dots \quad 11.4$$



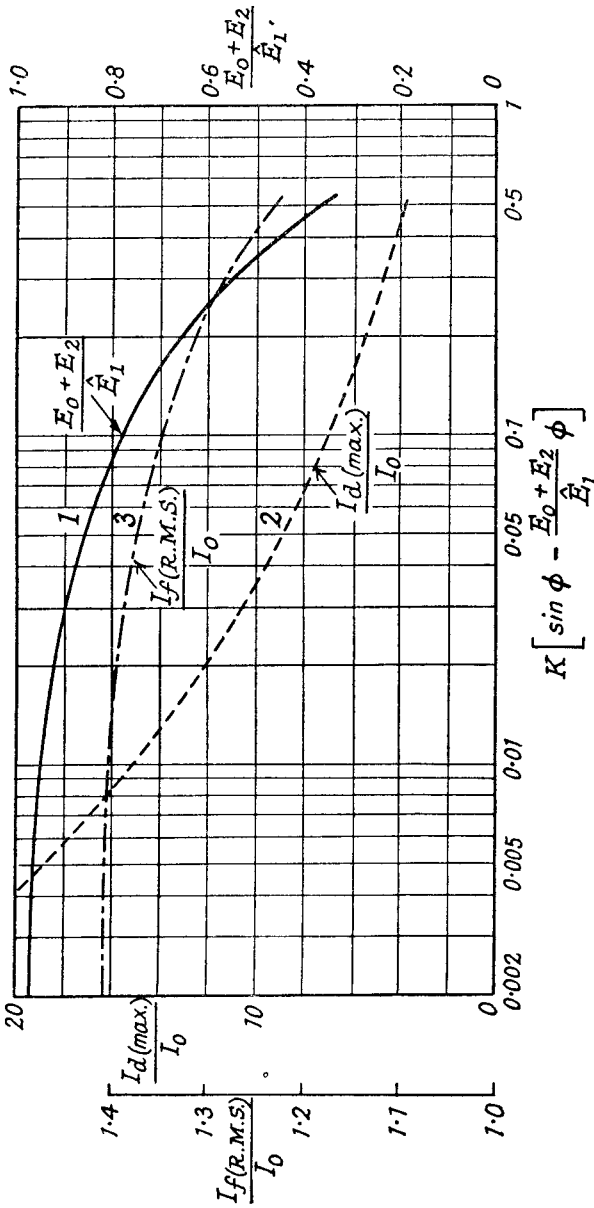


Fig. 11.8a.—Voltage and Current Relationships in a Diode Rectifier for Different Angles of Conduction.

where  $\hat{E}_1 \cos pt =$  A.C. voltage of the secondary on open circuit

$$K = \left[ \sin \phi - \left( \frac{E_0 + E_2}{\hat{E}_1} \right) \phi \right]$$

$E_0 =$  D.C. voltage across the load resistance  $R$ .

$$\phi = \cos^{-1} \left[ \frac{E_0 + E_2}{\hat{E}_1} \right]$$

and  $R_t =$  total winding resistance of secondary plus that reflected from primary.

The relationship between  $\frac{E_0 + E_2}{\hat{E}_1}$  and  $K$  is shown by the full line

curve 1 in Fig. 11.8a. To illustrate its application, the D.C. output voltage-current relationship will be calculated for a half-wave rectifier circuit having the following component values. The transformer secondary and reflected primary resistances are 300 and 100 ohms respectively (the R.M.S. voltage of the secondary is 300 volts). The half-wave rectifier has a conduction resistance of 200 ohms and begins conducting at the equivalent of +5 volts. The total resistance of the rectifier circuit (excluding the load) is 600 ohms, so that the D.C. load current is

$$I_0 = \frac{300 \times 1.414}{3.14 \times 600} K = 225K \text{ mA.}$$

Inserting selected values for  $I_0$  in the above gives the corresponding value of  $K$ , and reference to Fig. 11.8a enables the D.C. output voltage at the selected D.C. current to be calculated. The result is tabulated below.

$I_0$ (mA)	0	10	20	30	40	50	60
$K$	0	0.0444	0.0889	0.1333	0.1778	0.2223	0.2667
$\frac{E_0 + E_2}{\hat{E}_1}$	1	0.875	0.8	0.732	0.68	0.62	0.575
$E_0$ (volts)	419	366	334	306	283	258	239

In order to obtain these output voltages the reservoir capacitance is assumed to be large enough adequately to sustain the voltage across the load resistance during the non-conducting period of the rectifier. In Section 8.2.13, Part I, a curve (Fig. 8.13b) is developed for the minimum value of capacitance necessary to ensure this for different values of load and rectifier resistance. It is reproduced in

Fig. 11.9 as a curve of  $RC_1$  against  $\frac{R}{R_d + R_t}$ , where  $R = \frac{E_0}{I_0}$ . The vertical scale on the right is for half-wave rectification (ripple frequency 50 c.p.s.), and that on the left is for full-wave rectification (ripple frequency 100 c.p.s.). Thus for given values of  $R$ ,  $R_d$  and  $R_t$ , the minimum required value of  $C_1$  for full-wave rectification is half that for half-wave rectification. The values of  $C_1$  for the

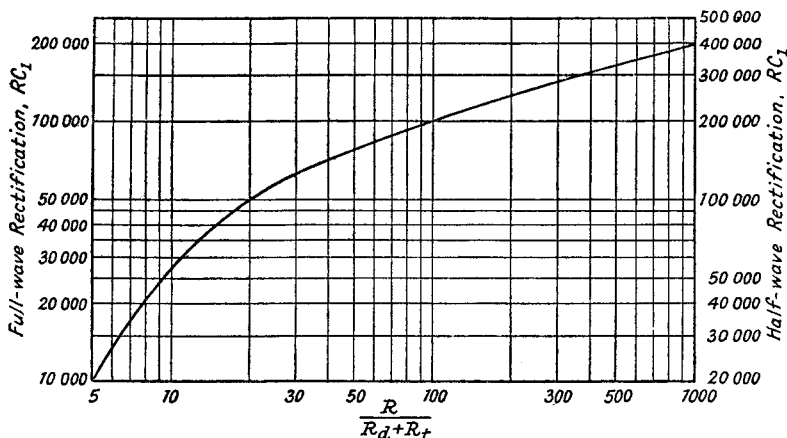


FIG. 11.9.—Optimum Capacitance Curves for a Full-wave and Half-wave Rectifier.

$R$  in ohms,  $C$  in  $\mu\text{F}$ .

selected values of  $I_0$  in the above example are tabulated below : a maximum is found at  $\frac{E_0 + E_2}{E_1} = 0.7$ , which corresponds to conduction starting at  $\phi = 45^\circ$ .

$I_0$ (mA)	10	20	30	40	50	60
$R$ (ohms)	36,600	16,700	10,200	7,075	5,160	3,983
$\frac{R}{R_d + R_t}$	61	27.8	17	11.8	8.6	6.64
$C_1$ ( $\mu\text{F}$ )	4.64	7.2	8.65	9.2	8.8	8.05

An average practical value for a half-wave rectifier capacitance is  $8 \mu\text{F}$ . For full-wave operation the minimum values of reservoir capacitance given above are halved for the same D.C. current ; the D.C. voltage across the load resistance is greater because the value of  $K$  for the same D.C. current is halved.

As a second illustration let us assume that the turns ratio, and

secondary voltage of a transformer, together with the reservoir capacitance, are to be found in order that a full-wave rectifier may deliver 50 mA at 400 volts. The supply is 230 volts, 50 c.p.s. and the rectifier conduction resistance is 200 ohms starting at +5 volts. Probable values of primary and secondary resistance are 20 and 300 ohms, respectively. As a first attempt let us try a primary to secondary turns ratio of 1 to 2. The total A.C. resistance in the rectifier circuit is

$$R_d + R_t = 200 + 300 + 2^2 \times 20 = 580 \text{ ohms.}$$

The D.C. current expression is twice that for half-wave working, i.e.,

$$I_0 = \frac{2\hat{E}_1 K}{\pi(R_d + R_t)}.$$

Therefore 
$$K = \frac{50 \times \pi \times 580}{1,000 \times 460 \times 1.414 \times 2} = 0.07$$

From Fig. 11.8a

$$\frac{E_0 + E_2}{\hat{E}_1} = 0.83$$

$$E_0 = 535 \text{ volts.}$$

This is too high ; a primary to secondary turns ratio of 1 to 1.6 gives

$$R_d + R_t = 551$$

$$K = 0.083$$

$$\frac{E_0 + E_2}{\hat{E}_1} = 0.81$$

and

$$E_0 = 416 \text{ volts.}$$

This is slightly higher than required, but a lower ratio would be inadvisable because no account has been taken of the voltage drop due to leakage inductance. This tends to reduce the voltage induced in the secondary, and would bring the D.C. voltage close to the required 400 volts. The load resistance  $R = \frac{E_0}{I_0} = 8,320 \Omega$ ,

and  $\frac{R}{R_d + R_t} = \frac{8,320}{551} = 15.1$  ; reference to Fig. 11.9 gives  $RC_1$  as 40,000, and the minimum required value of reservoir capacitance is therefore 4.8  $\mu\text{F}$ .

A characteristic of the rectifier with capacitive load is that the conduction current takes the form of pulses of large amplitude and short duration as shown in Fig. 11.6, and maximum current may be many times greater than the D.C. current. The reservoir capacitance, the rectifier conduction resistance and the transformer winding

resistance all influence the maximum rectification current. A large capacitance and low resistances lead to large maximum amplitudes of short duration. In some cases, when the mains supply to the rectifier has a very low resistance, it may be necessary to insert a resistance in series with the rectifier to limit the maximum conduction current and prevent damage to the valve. An example of this is afforded by the A.C./D.C. receiver, the half-wave rectifier for which often has a series resistance of about 50 ohms included to make up for the absence of the transformer winding resistances.

The maximum current, assuming conduction from  $-\phi$  to  $+\phi$  (Fig. 11.6) is given by

$$I_{d(max)} = \frac{\hat{E}_1(1 - \cos \phi)}{R_d + R} \quad . \quad . \quad . \quad 11.5a$$

and the ratio of maximum to D.C. current is

$$\frac{I_{d(max)}}{I_0} = \frac{\pi(1 - \cos \phi)}{K} = \frac{\pi(1 - \cos \phi)}{\sin \phi - \phi \cos \phi} \quad . \quad . \quad . \quad 11.5b.$$

This ratio is plotted against  $K$  as curve 2 in Fig. 11.8a, and it can be seen that even under normal operating conditions ( $K$  between 0.1 to 0.5), the maximum conduction current is about six times that of the D.C. output current. For convenience the ratio of  $I_{d(max)}$  to  $I_0$  is plotted against the ratio of  $(E_0 + E_2)$  to  $\hat{E}_1$  as curve 1 in Fig. 11.8b.

An estimate of the fundamental R.M.S. current supplied by the secondary winding of the transformer is required in order that the load from the rectifier can be determined for transformer design purposes. This can be obtained by calculating the fundamental peak current in the pulses shown in Fig. 11.6 and dividing by  $\sqrt{2}$ . Thus

$$\begin{aligned} \hat{I}_f &= \frac{2}{\pi} \int_0^\phi \frac{(\hat{E}_1 \cos pt - \hat{E}_1 \cos \phi)}{R_d + R_t} \cos pt \cdot d(pt) \\ \hat{I}_f &= \frac{2\hat{E}_1}{\pi(R_d + R_t)} \int_0^\phi \left[ \frac{1 + \cos 2pt}{2} - \cos \phi \cdot \cos pt \right] d(pt) \\ &= \frac{2\hat{E}_1}{\pi(R_d + R_t)} \left[ \frac{\phi}{2} + \frac{\sin 2\phi}{4} - \cos \phi \cdot \sin \phi \right] \\ &= \frac{\hat{E}_1}{\pi(R_d + R_t)} \left[ \phi - \frac{1}{2} \sin 2\phi \right] \quad . \quad . \quad . \quad 11.6a. \end{aligned}$$

The R.M.S. value of fundamental current

$$= I_f = \frac{\hat{E}_1}{\pi\sqrt{2}} \left( \frac{\phi - \frac{1}{2} \sin 2\phi}{(R_d + R_t)} \right).$$

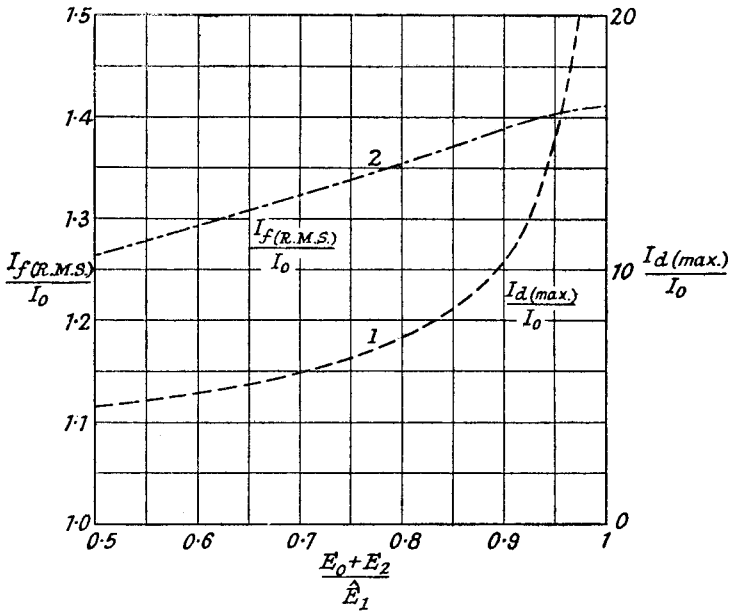


FIG. 11.8b.—R.M.S. and Conduction Current Ratios of a Diode Half-wave Rectifier in Terms of the D.C. Output Current.

The most useful method of expression for the above is in terms of the D.C. current  $I_o$ , hence using 11.4.

$$\begin{aligned} \frac{I_f}{I_o} &= \frac{\phi - \frac{1}{2} \sin 2\phi}{\sqrt{2K}} \\ &= \frac{0.707(\phi - \frac{1}{2} \sin 2\phi)}{(\sin \phi - \phi \cos \phi)} \end{aligned} \quad \dots \quad 11.6b.$$

This is plotted against  $K$  as curve 3 in Fig. 11.8a and against  $\frac{E_0 + E_2}{E_1}$  as curve 2 in Fig. 11.8b. The interesting point is that as  $K$  is decreased, or  $\frac{E_0 + E_2}{E_1}$  increased, the ratio of R.M.S. to D.C. current increases and approaches 1.414. On light loads the ratio is greatest, and as the load increases the ratio decreases.

The above calculation is based on half-wave operation, but the result is the same for full-wave working. For the same voltage ratio, i.e., a given value of  $\cos \phi$ , the D.C. and R.M.S. currents are doubled when full-wave rectification is employed, and their ratio is unaltered. An average value for the ratio of R.M.S. to mean current is about 1.35, and this is the figure used in estimating the

D.C. full load output from a rectifier connected to the transformer designed in Section 11.2.2.

**11.2.6. The H.T. Rectifier with Inductive Load.**<sup>7</sup> If a large inductance is inserted between the load resistance  $R$  and the rectifier, the D.C. performance is practically the same as that for a resistance load alone, viz., the D.C. voltage is much less than the peak A.C. applied voltage, but is practically independent of variations of  $R$ . The fall in D.C. voltage with increase of current is determined almost entirely by the resistance elements associated with the transformer, rectifier and added inductance. The chief advantage of the latter is that the A.C. current components in the load resistance are appreciably reduced, and all A.C. voltages across  $R$  are reduced by the factor  $\frac{R}{\sqrt{R^2+(pL)^2}}$  in comparison with their values before the inductance  $L$ . The reduction factor has more and more effect at the higher harmonic frequencies. The filter action of  $L$  can be

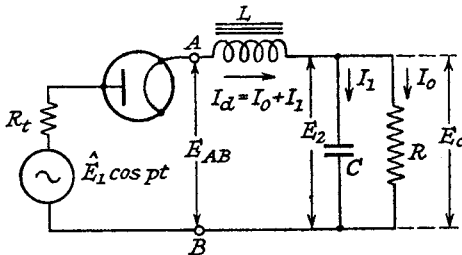


FIG. 11.10.—A Half-wave Rectifier with Inductive Load.

greatly increased by providing a by-pass capacitance  $C$  across the load resistance  $R$  as in Fig. 11.10, and D.C. performance is practically unaffected by the added capacitance unless the D.C. current falls below a certain value. For lower current values than the minimum, the D.C. current component is less than the A.C. current component; pulse charging of  $C$  results like that for the capacitively loaded rectifier, and, as the current is reduced, the D.C. voltage rises steeply to a value almost equal to the peak value of the A.C. voltage. Typical D.C. voltage-current curves (3 and 5) for the rectifier, with different values of inductance and a given value of by-pass capacitance  $C$  are shown in Fig. 11.11. Curve 3 is for a smaller inductance than curve 5. For comparison a curve (1) for the capacitively loaded rectifier is included to show the improved regulation obtained by the inductive load for currents above the critical minimum.

The action of this type of rectifier circuit can be quite simply analysed for D.C. currents exceeding the minimum value, if it is

assumed that the diode conduction resistance and transformer resistances are much less than the impedance of  $L$  and  $R$ . The wave shape of the voltage across the points  $AB$  in Fig. 11.10 is almost that of a half-cosine curve, so that the voltage applied to  $L$  and  $R$  is represented by

$$E_{AB} = \frac{2\hat{E}_1}{\pi} \left[ \frac{1}{2} + \frac{\pi}{4} \cos pt + \frac{1}{3} \cos 2pt \dots \text{etc.} \right] \quad . \quad 11.7$$

where  $\hat{E}_1 \cos pt =$  A.C. voltage applied to the rectifier.

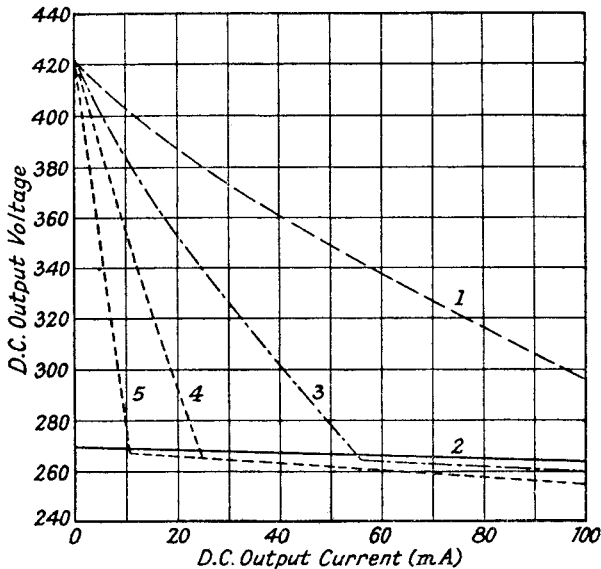


FIG. 11.11.—D.C. Output Voltage-Current Curves for a Half-wave Rectifier with Inductive Load.

Owing to the frequency discrimination of  $L$  the current  $I_d$  flowing from the rectifier has only two important components, a D.C. and fundamental A.C. The harmonic current amplitudes are inversely proportional to their harmonic number and directly proportional to the harmonic voltages, which themselves are much less than the fundamental voltage. The current  $I_d$  through the rectifier is therefore continuous, so long as its D.C. component exceeds the peak value of the A.C. current, i.e., the rectifier conducts during the whole of the cycle. This is an interesting case of the duality theorem<sup>22</sup> in networks, for it may be noted that the series combination of  $L$  and  $R$  is the dual of the parallel combination of  $C$  and  $R$  (the capacitively loaded rectifier). The voltage in the latter instance





$$\begin{aligned} \text{The ripple ratio } r &= \frac{E_2}{E_0} = \frac{\hat{E}_1 X_c}{2\sqrt{2}(X_L - X_C)} \cdot \frac{\pi}{\hat{E}_1} \\ &= \frac{\pi X_c}{2\sqrt{2}(X_L - X_c)}. \end{aligned}$$

Solving the above for  $LC$ ,

$$LC = \frac{\frac{\pi}{2r\sqrt{2}} + 1}{(2\pi f)^2} = \frac{1.11}{r} + 1 \quad . \quad . \quad 11.10a$$

where  $f$  = mains fundamental frequency.

The limiting condition for good D.C. voltage regulation is that the minimum D.C. current equals the A.C. peak current. Thus from 11.8a and 11.9b

$$I_{0(\min.)} = \frac{E_0}{R_{(\max.)}} = \frac{\sqrt{2}E_0}{X_L} \left( \frac{\pi}{2\sqrt{2}} - r \right)$$

and solving for  $L$  gives

$$\begin{aligned} L &= \frac{\left( \frac{\pi}{2\sqrt{2}} - r \right) 1.414 R_{(\max.)}}{2\pi f} \\ &= \frac{0.225 R_{(\max.)}(1.11 - r)}{f} \quad . \quad . \quad 11.11a. \end{aligned}$$

If full-wave rectification is employed the A.C. fundamental voltage across  $AB$  is zero; the second harmonic becomes the important voltage component,  $E_{AB\sim} = \frac{4\hat{E}_1}{3\pi\sqrt{2}}$  and expression 11.10a is modified to

$$LC = \frac{\left[ \frac{2}{3r\sqrt{2}} + 1 \right]}{(2\pi f)^2} = \frac{0.471}{r} + 1 \quad . \quad . \quad 11.10b$$

where  $f$  is still the mains fundamental frequency.

Similarly, expression 11.11a becomes

$$L = \frac{0.1125 R_{(\max.)}(0.471 - r)}{f} \quad . \quad . \quad 11.11b.$$

Comparing 11.11a with 11.11b, it is clear that half-wave rectification requires a larger value of inductance (approximately 4.7 times greater) than full-wave for the same value of  $R_{(\max.)}$  or  $I_{0(\min.)}$ .

As an example we shall calculate the values of  $L$  and  $C$  for a D.C. output voltage of 400 volts, a minimum D.C. current of 20 mA, and

a ripple voltage ratio of 1% from (1) half-wave and (2) full-wave rectification of a 50-c.p.s. supply.

$$R_{(max.)} = \frac{E_0}{I_{0(min.)}} = \frac{400 \times 1,000}{20} = 20,000 \text{ ohms.}$$

From 11.11a and 11.11b

$$L \text{ (half-wave)} = \frac{0.225 \times 20,000 (1.11 - 0.01)}{50} = 99 \text{ H}$$

$$L \text{ (full-wave)} = \frac{0.1125 \times 20,000 (0.471 - 0.01)}{50} = 20.8 \text{ H.}$$

Substituting in 11.10a and 11.10b

$$C \text{ (half-wave)} = \frac{112 \times 10^6}{39.5 \times 50^2 \times 99} = 11.5 \mu\text{F}$$

$$C \text{ (full-wave)} = \frac{48.1 \times 10^6}{158 \times 50^2 \times 20.8} = 5.82 \mu\text{F.}$$

Since the value of  $L$  determines the d.c. current minimum, above which good regulation is obtained, it cannot be reduced without increasing  $I_{0(min.)}$ . The effective impedance of  $L$  to the fundamental frequency may be increased ( $I_1$  and hence  $I_{0(min.)}$  are thus reduced) by tuning<sup>13</sup> with a suitable capacitance. The disadvantage of the method is that  $L$  is less effective as a filter for the harmonic currents of the ripple voltage. Yet another method of decreasing  $I_{0(min.)}$  is by means of a swinging choke. This is an iron-cored choke with an air-gap smaller than that required for maximum  $L$  at maximum d.c. current; its inductance is high for small d.c. currents and, though it falls for normal and maximum currents, it is high enough to provide satisfactory filtering. The dotted curves 4 and 5, Fig. 11.11, illustrate the effect of reducing air gap in a given iron-cored inductance, a smaller air gap being used for curve 5.

When the minimum d.c. load current taken by apparatus connected to the rectifier output is likely to fall below  $I_{0(min.)}$ , a resistance may be connected in parallel with the output to ensure that the output current is never less than  $I_{0(min.)}$ .

The inductive load is particularly suitable for use with gas-filled (mercury vapour) rectifier valves because of its low maximum conduction current to d.c. current ratio of about 2. Owing to the very low conduction resistance of these valves, very high peak currents are passed when the load is capacitive, and the emission property of the filament (or cathode) may be seriously damaged. The conduction angle ( $\phi$  in Fig. 11.6) may be as low as  $10^\circ$ , giving  $K = 0.00195$  and a maximum to d.c. current ratio of 24.5:1.

Besides providing good regulation, the inductive load also gives a better utilization factor (ratio of D.C. to A.C. power) to the transformer. The utilization factor is reduced by taking current pulses of large amplitude and short duration from the transformer.

It is possible that leakage inductance in the transformer supplying a capacitively loaded rectifier may act in a similar manner to  $L$ , but it is generally too small for the good regulation characteristic to be reached with normal load currents. The usual result of leakage inductance is to decrease the A.C. voltage applied to the rectifier and to make D.C. voltage regulation worse.

**11.2.7. Voltage Multiplier Rectifier Circuits.**<sup>19, 20</sup> It is possible to obtain a high D.C. voltage from a low voltage A.C. source by using voltage multiplier rectifier circuits. The voltage-doubler

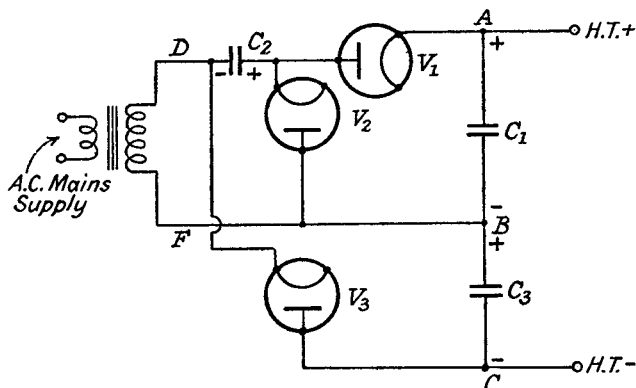


FIG. 11.12.—A Voltage Tripler Rectifier.

of Fig. 11.4c is an example of the multiplier circuit; two separate half-wave rectifiers, the D.C. output voltages of which are combined, are used with a mains supply voltage common to both. An alternative method of producing voltage doubling is shown by the two rectifiers  $V_1$  and  $V_2$  in the tripler circuit of Fig. 11.12. The double voltage is developed across the points  $AB$ . The circuit is like that of Fig. 11.4c, except that the positions of the mains input and  $C_1$  of Fig. 11.4c, are interchanged, and the  $C_1$  end of  $C_2$  in the same figure is connected to the junction of  $L$  and  $C_1$ . This changes the mode of operation since the two rectifiers no longer act independently of each other. When the point  $F$  is positive with respect to  $D$ , rectifier  $V_2$  conducts and charges  $C_2$  almost to the peak value of the A.C. voltage input, the polarity of  $C_2$  being as shown in Fig. 11.12. When  $F$  becomes negative with respect to  $D$ ,  $V_2$  ceases to conduct

and a positive voltage, equal to the sum of the D.C. voltage across  $C_2$  and the A.C. input, is applied to the anode of  $V_1$ . The latter conducts and charges  $C_1$  almost to twice the peak A.C. input voltage at  $DF$ . This circuit is less efficient than that of Fig. 11.4c and requires capacitance  $C_1$  to be rated for twice the voltage developed across it in Fig. 11.4c. D.C. voltage regulation is also lower.

The voltage-tripler rectifier consists of the doubler already described with an additional rectifier  $V_3$ , which acts independently of the other two. The voltage across its reservoir capacitance  $C_3$  is added to that across  $C_1$  to produce a total voltage equal to approximately three times the peak A.C. input voltage.

A voltage quadrupler rectifier is shown in Fig. 11.13, and it

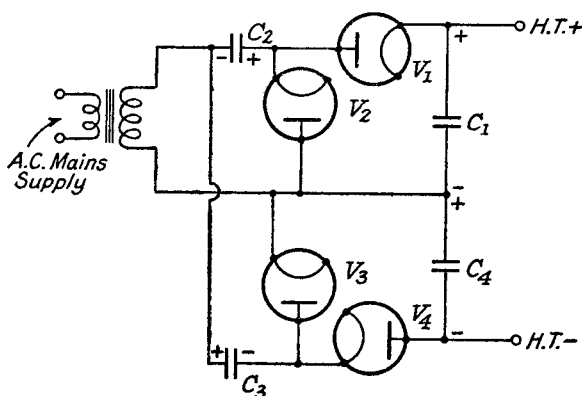


FIG. 11.13.— A Voltage Quadrupler Rectifier.

consists of two doubler circuits connected in series so that their D.C. output voltages add.

D.C. voltage regulation becomes worse as more multiplication is included; larger reservoir capacitances can help to counteract this, but are liable to cause damage to the valves because of high maximum conduction currents. Such circuits are, therefore, only suitable for supplying limited and constant D.C. currents.

**11.2.8. The Rectifier Ripple Filter.**<sup>8, 9, 14</sup> To reduce ripple voltages to the low level required for a receiver H.T. supply, an additional filter is needed between the D.C. load resistance  $R$  and reservoir capacitance. The most common type of filter consists of an iron-cored inductance  $L$  (often the loudspeaker field coil), in the H.T. positive lead from the rectifier, followed by a smoothing capacitance  $C$ . For some purposes (Section 12.5.4) the filter may be inserted in the negative lead<sup>6</sup>; care must then be taken to



150, 200 and 250 c.p.s. respectively. The loss for two similar filters is obtained by multiplying the loss scale by two.

As long as the product  $LC$  is constant and the conditions given above are fulfilled, viz.,  $p^2LC \gg 1$  and  $\gg \frac{pL}{R}$ , the actual values of  $L$  and  $C$  have little effect on filter characteristics, but for practical reasons it is better to use a large value of capacitance rather than a very large value of inductance. The latter is more difficult to make and has a higher D.C. resistance. Average values for  $L$  and  $C$  are 30 H and  $8 \mu\text{F}$  giving  $LC = 240$  and a loss of 27.5 db. at 50 c.p.s.

The iron-cored inductance must have an air gap to prevent saturation of the core by the D.C. current, and its design is detailed in the next section 11.2.9.

Special parallel and series circuits<sup>13</sup> tuned to the fundamental ripple frequency were at one time employed, but the use of electrolytic capacitances of comparatively high value has rendered these methods unnecessary. Furthermore, a tuned filter gives less discrimination against frequency components other than that to which it is tuned.

Resistance-capacitance smoothing filters may be used for low D.C. current outputs. The loss for this type is

$$-20 \log_{10} \sqrt{1 + (pCR_1)^2} \quad . \quad . \quad . \quad 11.15a$$

where  $R_1$  = filter resistance

$C$  = by-pass capacitance in parallel with the load resistance

$R$ , which is assumed to be much greater than  $\frac{1}{pC}$ .

Generally  $pCR_1 \gg 1$  and 11.15a becomes

$$\text{loss} = -20 \log_{10} pCR_1 \quad . \quad . \quad . \quad 11.15b.$$

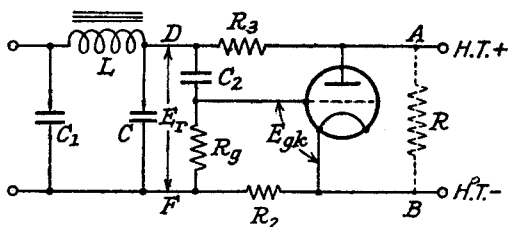


FIG. 11.15a.—Ripple Voltage Suppression by Means of a Valve.

An interesting method of neutralizing ripple voltage by means of a valve<sup>17</sup> is shown in Fig. 11.15a. The initial ripple voltage  $E_r$  across  $DF$  is applied to the valve grid through the large capacitance  $C_2$ , so that  $E_r$  effectively appears across the grid leak resistance

$R_g$ . The ripple voltage developed by the valve across  $AB$  is  $180^\circ$  out of phase with the grid voltage, i.e., with  $E_r$ . Some of the ripple voltage appearing across  $AB$  due to the potential divider action of  $R_3$  and  $R_a$  is cancelled by that in the valve, and  $E_{AB}$  has therefore a reduced ripple content. If the amplification of the valve is suitably adjusted and the initial ripple voltage is not large enough to cause distortion in the valve, complete cancellation is possible. The condition for ripple-free D.C. voltage across  $AB$  can be found from the equivalent circuit of Fig. 11.15*b*.

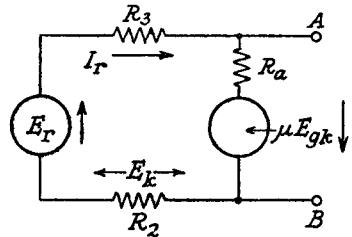


FIG. 11.15*b*. The Equivalent Circuit of Fig. 11.15*a*.

$$E_{AB} = \mu E_{gk} - I_r R_a = 0 \quad . \quad . \quad . \quad 11.16$$

where  $I_r$  is the ripple current in the circuit.

$$I_r = \frac{E_r + \mu E_{gk}}{R_2 + R_3 + R_a} \quad . \quad . \quad . \quad 11.17$$

because  $E_r$  and  $\mu E_{gk}$  are in phase with reference to the driving voltage for  $I_r$ .

Combining 11.16 and 11.17

$$\mu E_{gk} (R_2 + R_3) = E_r R_a$$

or 
$$R_2 + R_3 = \frac{1}{g_m} \frac{E_r}{E_{gk}} \quad . \quad . \quad . \quad 11.18a$$

is the condition for zero ripple volts across  $AB$ .

But

$$\begin{aligned} E_{gk} &= E_r - E_k \\ &= E_r - \frac{(E_r + \mu E_{gk}) R_2}{R_2 + R_3 + R_a} \end{aligned}$$

$$E_{gk} = \frac{E_r (R_3 + R_a)}{R_3 + (1 + \mu) R_2 + R_a} = \frac{E_r}{1 + \frac{(1 + \mu) R_2}{R_3 + R_a}}$$

Replacing  $E_{gk}$  in 11.18*a*

$$R_2 + R_3 = \frac{1 + \frac{(1 + \mu) R_2}{R_3 + R_a}}{g_m} \quad . \quad . \quad . \quad 11.18b.$$

To illustrate the action of the circuit, let the total D.C. load and valve current be 50 mA, and the valve constants be  $\mu = 30$ ,  $g_m = 3$  mA/volt,  $R_a = 10,000$  ohms at  $E_g = -2$  volts.  $E_a = 250$ .

$$R_2 = \frac{E_g}{I_o} = \frac{2 \times 1,000}{50} = 40 \text{ ohms.}$$



From 11.18*b*

$$R_3 + 40 = \frac{1 + \frac{31 \times 40}{R_3 + 10,000}}{3 \times 10^{-8}}$$

Solving the above for  $R_3$  gives

$$R_3 = 333 \text{ ohms.}$$

The total D.C. voltage drop between  $DF$  and  $AB$  is

$$I_0(R_2 + R_3) = 18.65 \text{ volts.}$$

One disadvantage of the method is that the A.C. impedance of the H.T. supply looking from the points  $AB$  is large, and adequate decoupling is necessary in all amplifier stages to prevent common impedance coupling and possible motorboating.

**11.2.9. The Filter Inductance with an Air Gap.**<sup>1</sup> The inductance of an iron-cored coil is given by

$$L = \frac{\Phi}{I} N^2 10^{-8} \text{ Henrys.}$$

where  $\Phi$  = total flux lines in the iron core

$I$  = current (in amps.) producing the flux

$N$  = total number of turns in coil

Now  $\Phi = B \times A$

where  $B$  = flux density, lines per square centimetre

$A$  = area of core cross-section in square centimetres

$B = \mu H$

where  $H$  = A.C. magnetizing force in oersteds

$\mu$  = permeability of the core when there is no air gap and no D.C. polarizing current.

$$H = \frac{4\pi NI}{10 l} = 1.255 \frac{NI}{l}$$

where  $l$  = the mean length (centimetres) of the magnetic path in the core.

The inductance to A.C. for no air gap and zero D.C. polarizing current is

$$L_1 = \frac{1.255\mu N^2 A 10^{-8}}{l} \text{ Henrys.} \quad . \quad . \quad 11.19a$$

or expressed in a more convenient form

$$\begin{aligned} L_1 &= 1.255\mu \frac{N^2}{l^2} A l 10^{-8} \\ &= 1.255 \mu n^2 V 10^{-8} \text{ Henrys} \quad . \quad . \quad 11.19b \end{aligned}$$

where  $n$  = coil turns per centimetre of the magnetic path in core  
 $V$  = volume of iron (cubic centimetres) in the core.

The term  $\mu$  in the above expression needs qualification, and it is generally defined as the incremental permeability,<sup>23</sup> being dependent in this particular case upon the core material and magnitude of the A.C. flux density in the core. In the more normal filter inductance having an air gap and carrying D.C. current it is also dependent on the length of air gap and on the D.C. current. As far as the A.C. flux density is concerned, incremental permeability, which is designated as  $\Delta\mu$  in succeeding expressions, is usually least for smallest A.C. flux densities (Fig. 10.20 shows curves of  $\Delta\mu$  against peak A.C. flux density), and in designing an inductance it is preferable to calculate for this value of  $\Delta\mu$ , which gives the minimum value of inductance. A polarizing D.C. current through the coil reduces appreciably the incremental permeability, and the effect is clearly shown in Table 11.2, which gives  $\Delta\mu$  for Stalloy<sup>3</sup> at different values of D.C. polarizing flux density and magnetizing force.

TABLE 11.2

D.C. Flux Density (B) (lines per square centimetre)	0	1,860	5,120	7,300	9,210	10,800	11,580
D.C. Magnetizing Force in iron ( $H_i$ ) (oersteds) . .	0	0.3	0.5	0.7	1	1.5	2
Incremental Permeability $\Delta\mu$ . .	333	328	278	233	180	125	100
$B$ . . .		12,300	12,960	13,280	13,580	13,900	14,180
$H_i$ . . .		3	5	7	10	15	20
$\Delta\mu$ . . .		75	57	48	42	40	38

The table shows that any method of reducing the D.C. magnetizing force for the iron increases incremental permeability and, if the A.C. magnetizing force for the iron remains unchanged, A.C. flux density and inductance. This can be partially achieved by including an air gap in the magnetic circuit; the total D.C. magnetizing force,  $H_t$ , is then divided between the iron and air gap such that  $H_t = \frac{H_i l + H_a a}{l + a}$ , where  $H_i$  and  $H_a$  ( $H_a$  is numerically equal to  $B$  because  $\mu = 1$  for air) are the magnetizing forces for the iron and air gap respectively, and  $l$  and  $a$  are the lengths of the magnetic path in the iron and air. As  $H_t$  is constant for a given D.C. current

and coil turns, increase of the air gap,  $a$ , must reduce  $H_i$  and, hence, increase  $\Delta\mu$ . However, the a.c. magnetizing force,  $\Delta H$ , for the iron is also reduced in accordance with the d.c. reduction, but it is decreased, at first, at a slower rate than  $\Delta\mu$  is increased. Thus a.c. flux density,  $\Delta B$ , and inductance,  $L_2$ , are increased. Eventually an air-gap width is reached at which the rate of decrease of  $\Delta H$  equals that of increase of  $\Delta\mu$ , and increase beyond this width reduces  $\Delta B$  and inductance. The air gap giving maximum  $\Delta B$  and inductance is known as the optimum air gap,  $a_0$ . The a.c. inductance  $L_{2(opt.)}$  for optimum air gap is always less than the a.c. inductance  $L_1$  for zero d.c. current and no gap. The ratio  $\frac{L_{2(opt.)}}{L_1}$  decreases

as the d.c. polarizing force is increased, and the air-gap ratio  $\frac{a_0}{l}$  increases. Beatty <sup>4</sup> has developed a graphical method of determining the inductance  $L_2$  for any air-gap ratio,  $\frac{a}{l}$ , and also the maximum

value of  $L_2$  ( $L_{2(opt.)}$ ) and optimum air-gap ratio  $\frac{a_0}{l}$ ; it is illustrated in Fig. 11.16. At the right-hand side is drawn the  $B$ - $H$  curve for Stalloy, the figures being taken from Table 11.2, whilst on the left-hand side from the same origin is drawn a curve of  $B$  against  $\frac{B}{\Delta\mu} - H_i$  derived from the  $B$ - $H$  curve and the values of  $\Delta\mu$  given

in the table above. For a given air-gap ratio  $\frac{a}{l}$  and d.c. polarizing force  $H_i$  oersteds (corresponding to  $OP$  in Fig. 11.16), a line is drawn from  $P$  to meet the  $BH$  curve at  $S'$ , such that the ratio  $\frac{S'U'}{PU'}$  of the sides of the right-angled triangle  $PS'U'$  ( $U'$  is vertically above  $P$ ) is equal to the air-gap ratio  $\frac{a}{l}$ , where  $S'U'$  is the numerical value of the d.c. polarizing force in oersteds and  $PU'$  is the numerical value of the flux density in lines per square centimetre. The horizontal line  $S'U'$  is produced to cut the left-hand curve 2 of Fig. 11.16 at the point  $R'$ , which is then joined to  $P$  by the straight line  $PL'$ . The area of the triangle  $OPQ'$  enclosed by the line  $PL'$  and the  $BH$  axes is equal to  $\frac{1}{2} \frac{L_2 I^2 10^7 4\pi}{V}$ , where  $L_2$  is in henrys,  $I$  is the d.c. current (amps.) and  $V$  is the volume of the iron core in cubic centimetres. Maximum area for triangle  $OPQ'$  (triangle  $OPQ$ , cross hatched in Fig. 11.16), which means maximum value

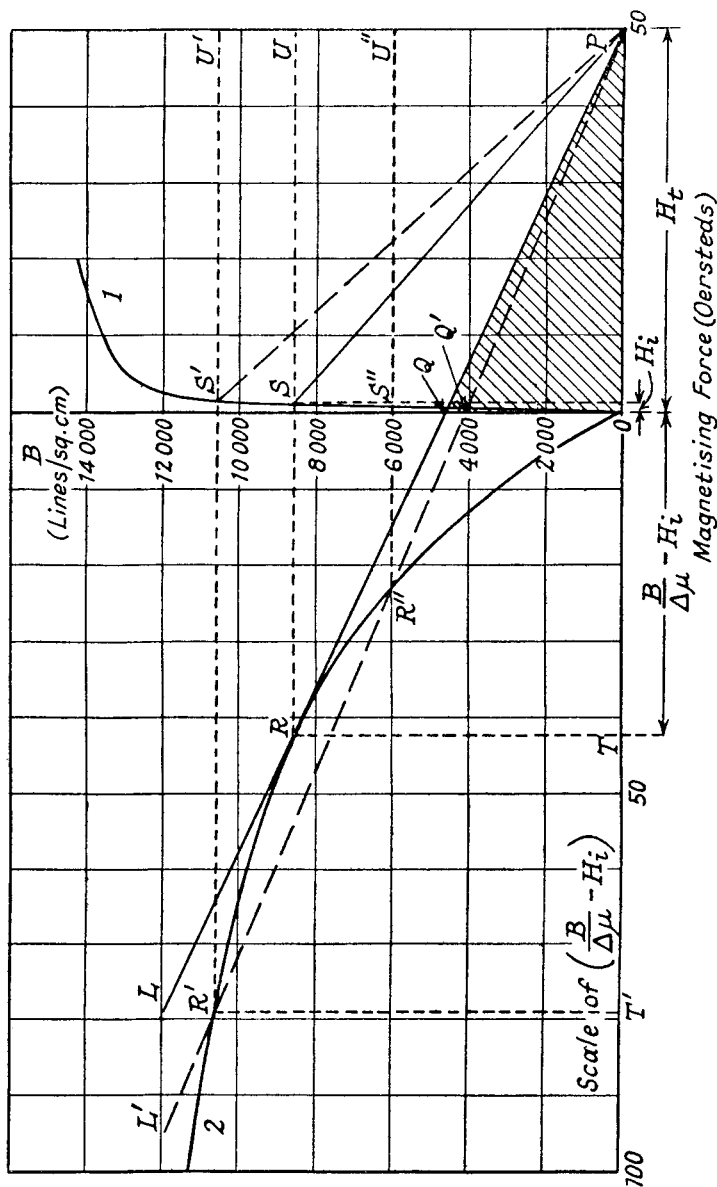


FIG. 11.16.—The Construction of  $B$ - $H$  Curves to give Optimum Inductance and Air Gap.

for  $L_2$ , is obtained when  $PL'$  is tangential to curve 2 as at point  $R$  in Fig. 11.16. A horizontal line from  $R$  intersecting curve 1 at  $S$  and the perpendicular from  $P$  at  $U$  gives the optimum air-gap ratio  $\frac{a_0}{l}$  as  $\frac{SU}{PU}$ . The proof that triangle  $OPQ'$  is equal to  $\frac{1}{2} \frac{L_2 I^2 10^7 4\pi}{V}$  is as follows:

The total magnetizing force = that for the iron + that for the air-gap

$$= H_i l + H_a a = H_i l + Ba.$$

In the succeeding analysis, the term  $H_a$  is dropped and  $B$  is substituted, but it must not be forgotten that the numerical value of  $B$  only is used, the actual units being in oersteds and not lines per square centimetre.

The total magnetizing force per centimetre of magnetic path

$$= \frac{H_i l + Ba}{l + a} = H_t.$$

Generally  $l \gg a$  and

$$H_t = H_i + \frac{Ba}{l} \quad \dots \quad 11.20.$$

Differentiating 11.20 with respect to  $B$ :

$$\frac{dH_t}{dB} = \frac{dH_i}{dB} + \frac{a}{l} = \frac{1}{\Delta\mu} + \frac{a}{l} \quad \dots \quad 11.21.$$

Combining 11.20 and 11.21 and eliminating  $\frac{a}{l}$

$$B \frac{dH_t}{dB} = \frac{B}{\Delta\mu} + H_t - H_i \quad \dots \quad 11.22.$$

$$\begin{aligned} \text{area of triangle } OPQ' &= \frac{1}{2} OP \cdot OQ' = \frac{1}{2} OP^2 \cdot \frac{OQ'}{OP} \\ &= \frac{1}{2} H_t^2 \frac{OQ'}{OP} \end{aligned}$$

$$\begin{aligned} \text{but} \quad \frac{OQ'}{OP} &= \frac{R'T'}{PT'} = \frac{B}{\frac{B}{\Delta\mu} - H_i + H_t} \\ &= \frac{dB}{dH_t} \quad (\text{see expression 11.22}) \end{aligned}$$

and the area of triangle  $OPQ'$

$$= \frac{1}{2} H_t^2 \frac{dB}{dH_t} \quad \dots \quad 11.23.$$

Now the inductance  $L_2$  to small A.C. currents is

$$\begin{aligned} L_2 &= \frac{d\Phi}{dI} N 10^{-8} \\ &= \frac{dB}{dI} N A 10^{-8} \\ &= \frac{dB}{dH_t} \frac{dH_t}{dI} N A 10^{-8} \quad . \quad . \quad . \quad 11.24. \end{aligned}$$

But 
$$H_t = \frac{4\pi NI}{10l}$$

where  $I$  = D.C. current in the coil.

Therefore 
$$\frac{dH_t}{dI} = \frac{H_t}{I}$$

and 
$$N = \frac{H_t l 10}{4\pi I}$$

Replacing  $\frac{dH_t}{dI}$  and  $N$  in 11.24 by the above expressions

$$\begin{aligned} L_2 &= \frac{dB}{dH_t} \frac{H_t}{I} \frac{H_t l 10 A}{4\pi I} 10^{-8} \\ &= \frac{dB}{dH_t} \frac{H_t^2}{I^2} V \frac{10^{-7}}{4\pi} \quad . \quad . \quad . \quad 11.25. \end{aligned}$$

Rearranging 11.25

$$\begin{aligned} \frac{1}{2} \frac{L_2 I^2 4\pi \times 10^7}{V} &= \frac{1}{2} \frac{dB}{dH_t} H_t^2 \\ &= \text{area of triangle } OPQ' \text{ (expression 11.23)} \quad . \quad 11.26. \end{aligned}$$

From 11.20

$$\frac{a}{l} = \frac{H_t - H_i}{B} = \frac{S'U'}{PU'} \quad . \quad . \quad . \quad 11.27.$$

For most practical purposes the gap ratio may be taken as  $\frac{H_t}{B}$ .

The ratio  $\frac{L_{2(opt)}}{L_1}$  and optimum gap ratio as determined from Fig. 11.16 is plotted against D.C. ampere turns per inch of the mean length of magnetic path as curves 1a and 1b in Fig. 11.17. The D.C. magnetizing force  $H_t$  is converted to D.C. ampere turns per inch (a more useful design parameter) by multiplying  $H_t$  oersteds by  $\frac{2.54}{1.255}$ , i.e., 2.02. Curves 1a and 1b are for a very small A.C. flux density, and for comparison similar curves 2a and 2b for a larger

flux density of R.M.S. value 60 lines per square centimetre are included on Fig. 11.17. These curves are often used for the design of an output transformer,<sup>21</sup> which normally has a higher average A.C. flux density than that produced by the ripple voltage in a filter inductance. The maximum inductance and optimum air-gap ratios are both decreased by having a larger A.C. flux density, though the actual value of  $L_{2(opt.)}$  at any given D.C. ampere turns is higher because  $L_1$  is so much higher. For example,  $\Delta\mu$  for zero D.C. current is 900 at  $\Delta B = 60$  lines per square centimetre (R.M.S. value), as compared with 333 at very small values of  $\Delta B$ , and

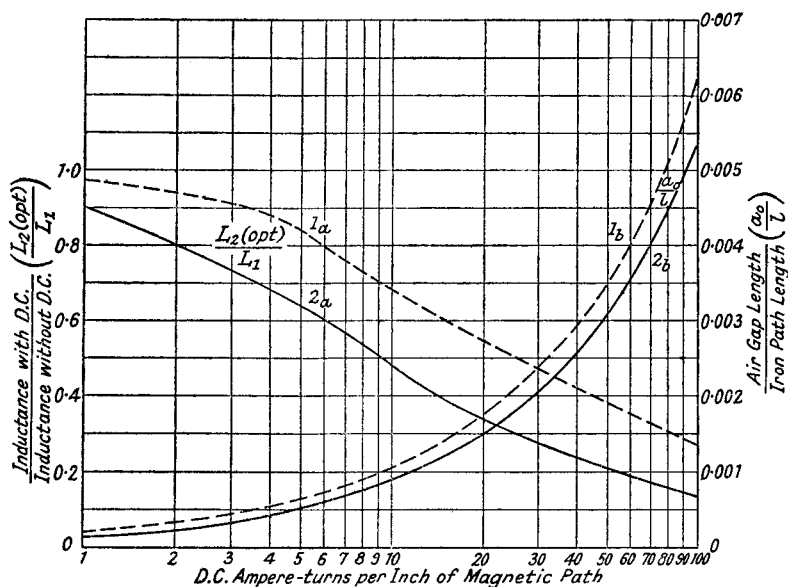


FIG. 11.17.—Optimum Inductance and Air Gap for Different D.C. Polarizations.

Curve 1: Low Flux Density.

Curve 2: R.M.S. Flux Density, 60 lines per sq. cm.

although the inductance ratio is (under worst conditions with large D.C. ampere-turns) halved for  $\Delta B = 60$  lines per square centimetre, the actual value of  $L_{2(opt.)}$  is approximately 1.35 times larger than when  $\Delta B$  is very small. This result is to be expected, for in Fig. 11.16 increase in  $\Delta\mu$  causes the rise of the left-hand curve 2 to become steeper; the line  $PL$  is therefore steeper and the area of the triangle  $OPQ$  is increased. At the same time the tangent point  $R$  is raised and  $PU$  increased, thus reducing the air-gap ratio  $a_0 \left[ \frac{SU}{PU} \right]$ .

This is a characteristic of iron-cored inductances up to an A.C. flux density of about 4,000 lines per square centimetre (R.M.S.) as shown by the incremental permeability curves in Fig. 10.20. Hence, as curves 1*a* and 1*b* are used in the design, the result represents the lowest possible value of A.C. inductance which will be obtained. If the A.C. flux density becomes very large (10,000 lines per square centimetre), lower values of inductance may then be obtained, but this is hardly likely to occur. A point worth noting is that there are always two air-gap ratios which will give a particular value of  $L_2$  less than the optimum value, for the line  $PL'$  cuts curve 2 at two points  $R'$  and  $R''$ . The second possible air-gap ratio is given by  $\frac{S''U''}{PU''}$  and is larger than the first  $\frac{S'U'}{PU'}$ .

Let us now use Fig. 11.17 to design a filter inductance having the following characteristics:  $L_{2(opt.)} = 20$  H for a D.C. current of 120 mA, the D.C. voltage drop is not to exceed 40 volts and Stalloy No. 32A stampings are to be used.

The dimensions of No. 32A Stalloy stampings are shown in Fig. 11.3*a*.

$$\text{Total winding area} = 2.25 \times 1 \text{ sq ins.}$$

and allowing for insulation thickness of 0.075 ins. all round the coil

$$\text{Available winding space} = (2.25 - 0.15) \times (1 - 0.15)$$

$$= 2.1 \times 0.85$$

$$= 1.785 \text{ sq. ins.}$$

Let us try scc. 30 s.w.g. wire for the coil. Table 11.1 gives 2,950 turns per square inch for this wire, so that

$$\begin{aligned} \text{Total turns in available space} &= 1.785 \times 2,950 \\ &= 5,260. \end{aligned}$$

$$\text{Mean length of magnetic path in core} = 9 \text{ ins.}$$

$$\text{Therefore turns per inch of magnetic path} = 585.$$

$$\text{D.C. ampere turns per inch} = 585 \times 0.12 = 70.2.$$

From curves 1*a* and 1*b*, Fig. 11.17.

$$\frac{L_{2(opt.)}}{L_1} = 0.33 \text{ and } \frac{a_0}{l} = 0.0046$$

$$L_1 = \frac{20}{0.33} = 60.6 \text{ H}$$

$$\text{and } a_0 = 9 \times 0.0046 = 0.0414 \text{ ins.}$$

The total air gap is divided between the core and side limbs, each of which has a gap of 0.0207 ins.



From 11.19*b*, after converting from centimetres to inches

$$L_1 = 1.255 \Delta \mu n^2 V \times 10^{-8} \times 2.54$$

where

$n$  = turns per inch of magnetic path

$V$  = volume of iron in cubic inches

$\Delta \mu$  = 333 from Table 11.2 (D.C. current zero).

Therefore

$$V = \frac{60.6 \times 10^8}{1.255 \times 333 \times (585)^2 \times 2.54}$$

$$= 16.63 \text{ cu ins.}$$

From Section 11.2.1

Area of No. 32A Stalloy = 8.4236 sq. ins.

Therefore required core thickness = 1.975

= 2.17 (allowing 10% for insulation).

Number of laminations 0.14 ins. thickness = 155.

Mean length of 1 turn of wire in coil = 10.34 ins.

Total length of wire = 1,514 yards.

Total resistance at 198.8 ohms per 1,000 yards = 301 ohms.

D.C. voltage drop =  $301 \times 0.12 = 36.1$  volts.

Summarizing the design, which fulfils the stated requirements; the inductance consists of 160 Stalloy 32A stampings, 5,260 turns of scc. 30 s.w.g. wire and 3 air gaps, each of length 0.0207 ins.

**11.2.10. Grid Bias Supplies.** The grid bias voltage for an indirectly-heated valve is generally derived from a resistance, paralleled by a capacitance, connected between its cathode and the H.T. negative lead. The cathode current flowing through this resistance produces the required grid bias voltage. The reactance of the capacitance must be low enough to by-pass A.C. anode current components, because these components develop A.C. voltages in the cathode circuit, which oppose the input voltage causing degenerative effects with attenuation (frequency) distortion (Section 9.3.4). A suitable value for the by-pass capacitance is  $0.1 \mu\text{F}$  for R.F., and from 25 to  $100 \mu\text{F}$  for A.F. amplifiers. Occasionally when an output valve, such as a triode, requiring a high grid bias voltage is employed, the bias voltage is obtained from a potential divider across the H.T. filter inductance, connected in the negative H.T. lead. The potential divider should have a resistance much greater than the inductive reactance of the filter inductance at 50 c.p.s., and an RC filter is necessary between the potential divider and output valve grid to filter the H.T. ripple voltage.

**11.3. The Power Supply for the A.C./D.C. Receiver.**

A typical power supply circuit for an A.C./D.C. receiver is shown in Fig. 11.18. It differs from that of the A.C. receiver in the direct connection to the A.C. mains supply, the series connection of the valve heaters, and the use of half-wave rectification. The direct mains connection necessitates an R.F. filter ( $L_2C_2$ ), for diverting from the receiver any R.F. interference conveyed by the mains leads, and also a capacitance earth connection ( $C_3$ ). The series heater connection calls for a certain valve order if hum voltages in the receiver output are to be minimum. The two valves which function by reason of non-linear  $I_aE_g$  characteristics (or their equivalent), the frequency changer and detector, must have the lowest A.C. voltage between heater and cathode. The frequency changer precedes the detector because it has the greater amplification following it. After

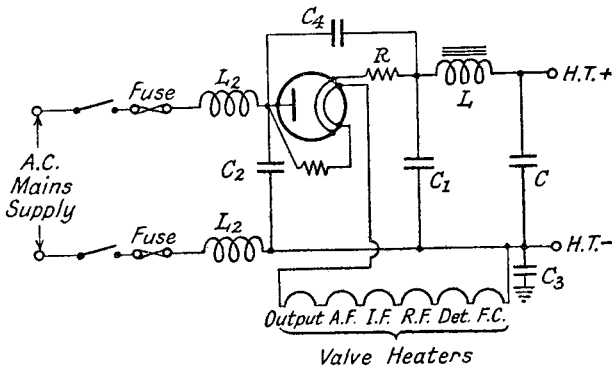


FIG. 11.18.—A Typical A.C./D.C. Power Supply Circuit.

the detector is placed the R.F. valve, and then the I.F. valve ; owing to the tuned anode circuits of these valves, hum voltages can be amplified only after modulating the signal voltage. Modulation hum is possible from the R.F. and I.F. amplifier because the variable mu. characteristic, needed for gain control purposes, necessarily involves a non-linear  $I_aE_g$  characteristic. It is greatest at a grid bias voltage (often about  $-10$  volts) corresponding to greatest change of curvature of the  $I_aE_g$  characteristic. Hum in the A.F. valve, following the I.F., is directly amplified, but it is less serious because there is less amplification after this stage. If a high power-sensitivity output valve is used, the A.F. amplifier may be omitted, the detector being directly coupled to the former. The rectifier valve, the last of the heaters to be connected, has to deliver as much (or more) D.C. current as the full-wave rectifier in the A.C. receiver, so that its conduction resistance must be low. This entails

a long cathode of large radius and small anode-to-cathode spacing. The anode-to-cathode gap is usually equivalently reduced by inserting a grid, connected to the anode, between these two electrodes, as described in Section 11.2.3. To prevent excessive peak conduction currents a limiting resistance  $R$  of about 50 ohms is normally included in series with the rectifier anode or cathode. If R.F. signal voltages are present in the rectifier circuit, due to insufficient decoupling or screening of the receiver R.F., I.F. or oscillator stages, or to pick-up from the mains leads, rectification may cause them to be modulated by hum voltages, which are then reproduced in the output of the receiver. This type of modulation hum can be eliminated by paralleling the rectifier with a small capacitance ( $C_4$ ) of about 0.001  $\mu\text{F}$ , which by-passes the R.F. voltages and prevents modulation occurring.

**11.4. Vibrator H.T. Supply.**<sup>5, 10, 15, 16</sup> L.T. supplies for a car receiver can satisfactorily be obtained from the car accumulator, and it is advantageous if the H.T. supply is derived from the same source. This can be achieved by means of a vibrator, which, by periodical interruption, can produce a comparatively high A.C. voltage pulse from a low voltage D.C. source. The A.C. voltage pulses are applied to a suitable transformer, which steps up the voltage prior to rectification. Alternatively, the primary of the transformer may be connected to the low voltage source via a pair of contacts on the vibrator reed, and its action is then independent of the current actuating the reed. The rectifying action is often performed by an extra contact on the reed. The frequency of vibration of the reed is comparatively low (between 50 and 100 c.p.s.), in order to prevent high transient voltages across the transformer and sparking at the contact points. A high frequency requires more energy for driving the reed, and makes it difficult to transfer sufficient energy to the transformer primary. The secondary, and often the primary, of the transformer is tuned to the reed frequency for single contact operation, or to twice that frequency for double contact excitation. This greatly improves transformer performance and efficiency, besides reducing sparking at the contacts.

A typical vibrator circuit is shown in Fig. 11.19. Double-wave excitation and rectification are achieved with contacts on both sides of the reed and a centre-tapped transformer primary and secondary. Double-wave excitation has the advantages of reduced ripple voltage, neutralization of the rectified D.C. current in the transformer secondary, and higher efficiency. The coil actuating the reed is independent of the transformer; this is a better arrangement than



input, 2 amps. for the L.T. supply, and 1.5 amps. for the loud-speaker field. Capacitances  $C_3$  and  $C_4$  are used to absorb low-frequency interference from the reed and have values of about  $1 \mu\text{F}$ ;  $C_v$  acts as an absorber across the vibrator coil when the contacts  $S_v$  open. Direct mechanical coupling between vibrator and receiver must be avoided, otherwise low-frequency interference may be experienced due to vibration of the valve electrodes or of the vanes of the oscillator tuning capacitance. Spring mounting of the vibrator element,<sup>12</sup> a double-walled container with a rubber seal and an air-tight inner container for the vibrator, have been used to reduce this type of interference. The R.F. interference filters for the vibrator input and output are usually contained in shielded com-

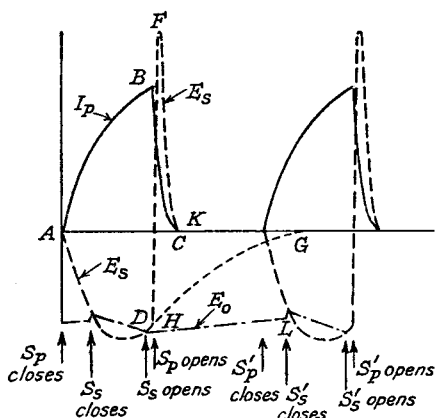


FIG. 11.20.—Primary Current and Secondary Voltage Wave Shapes for a Vibrator H.T. Supply.

partments, separate from the vibrator compartment but an integral part of the whole unit.

The operation of the vibrator is as follows. In the quiescent condition the reed  $R$  is held over by a spring, and contacts  $S_p$ ,  $S_s$  and  $S_v$  are all closed. A current  $I_p$  begins to flow in the half primary of the transformer as soon as the switch is closed, and it increases steadily in an exponential manner (see Fig. 11.20), becoming asymptotic to  $\frac{E}{R_p}$  amps., where  $E$  is the D.C. applied voltage and  $R_p$  is the half-primary resistance. A normal maximum value is about 4 amps. The shape of the secondary voltage  $E_s$  depends on the damping of the secondary circuit and, to a certain extent, on the characteristics of the transformer iron core. The shape generally obtained is of the form shown by the part  $AD$  of the

curve  $E_s$  in Fig. 11.20. The current in the vibrator coil ( $L_v$ ) rises in a similar manner to  $I_p$  and, eventually, the reed is attracted, opening contacts  $S_p$  and  $S_s$ . The primary current  $I_p$  collapses very rapidly by discharging through  $C_p$  as shown by the section  $BC$  in Fig. 11.20 (point  $B$  corresponds to the opening of  $S_p$ ). The sudden collapse of primary current induces a voltage in the secondary, and there is a very rapid reversal of secondary voltage from  $H$  to  $F$ . The shape of the curve from  $H$  through  $F$  to  $K$ , and the maximum value at  $F$  are determined by the rate of collapse of  $I_p$ , the secondary load, i.e., the D.C. output power supplied, and the value of the secondary capacitance  $C_s$ . A low D.C. output load resistance means heavier secondary damping, reduced rate of reversal of  $E_s$  and a lower maximum at  $F$ . Without collapse of  $I_p$ , the voltage  $E_s$  would decay exponentially as shown by the dotted curve  $HG$ . The D.C. reservoir capacitance  $C_1$  is connected to the half secondary when the contacts  $S_s$  are closed, and it is charged to a voltage,  $E_0$ , corresponding to  $D$  when  $S_s$  opens. It then discharges through the D.C. load until at  $L$  the second pair of contacts  $S_s'$  are closed and connect it to the other half secondary. The contacts  $S_s$  and  $S_s'$  are always arranged to close after, and to open before  $S_p$  and  $S_p'$ . The advantage of this is that the secondary voltage has had time to rise to a value approximately equal to that across the reservoir capacitance  $C_1$ ; the net voltage across  $S_s$  is therefore low and the reverse current (due to the discharge of  $C_1$ ) through the secondary is small. The importance of opening  $S_s$  before  $S_p$  is obvious from Fig. 11.20; the reverse secondary voltage from  $H$  to  $F$  would discharge  $C_1$  and produce severe sparking at the contacts.

The effect of incorrect choice of component values and contact operation can readily be understood from Fig. 11.20. If the primary capacitance  $C_p$  is too large, energy is diverted from the transformer primary, and the primary current rises slowly. This reacts on the secondary voltage reducing its rate of rise and maximum value. When  $C_p$  is too small the decay of primary current is rapid, producing high inverse secondary voltages. Too large a secondary capacitance  $C_s$  produces a slow rise of secondary voltage, reduced maximum value, and low D.C. efficiency, whilst too small a value causes a high inverse secondary voltage (point  $F$  in Fig. 11.20). A low resistance (not exceeding 50 ohms) is sometimes included in series with  $C_s$  to prevent damped oscillations occurring when  $S_s$  is opened. The D.C. load on the secondary plays an important rôle by affecting the rate of rise, and the maximum of the secondary voltage; any appreciable variation from the rated value causes sparking at the

contacts and a serious loss of efficiency. For example, an efficiency of 80% to 90% at a rated output of 200 volts 50 mA may fall to about 20% at 100 volts 10 mA. If reduced output is required from a vibrator it is preferable to reduce the applied battery voltage rather than to insert a resistance in series with the primary. A series resistance affects the rate of rise of primary current as well as the maximum value, and gives a lower efficiency than reduced battery voltage. Incorrect contact operation also reduces efficiency and increases sparking. If contacts  $S_p$  and  $S_s$  open too early the ripple voltage increases and D.C. regulation is worse, though there may be a slight increase in D.C. voltage. If  $S_s$  opens too soon the primary current is flowing without doing useful work, whilst if it opens after  $S_p$ , the inverse secondary voltage discharges  $C_1$  and causes sparking at the contacts. There is a tendency for the contact gap widths to increase during the life of the vibrator so that  $S_p$  and  $S_s$  close late and open early, and an initial efficiency of about 85% may fall to 70% after 1,000 hours' service because of contact wear. Increased reed amplitude, by increased current through the vibrator magnet coil, helps to offset this by keeping  $S_p$  and  $S_s$  closed for a longer time, and a variable resistance<sup>18</sup> may be included between the magnet coil and L.T. battery. The value of this resistance is decreased as the contact points wear. A possible alternative is a tapped magnet coil, though this is likely to be less satisfactory because the increase in current is partially cancelled by a decrease in the inductance of the magnet coil.

#### BIBLIOGRAPHY

1. The Design of Reactances and Transformers which carry Direct Current. C. R. Hanna, *Transactions Amer. I.E.E.*, p. 155, 1927.
2. The Design of Power Rectifier Circuits. D. McDonald, *Wireless Engineer*, Oct. 1931, p. 522. Correspondence, *ibid.*, M. V. Callendar, Jan. 1932, p. 24.
3. The Air Gap Transformer and Choke. F. W. Lanchester, *Journal I.E.E.*, Oct. 1933, p. 413.
4. The Alternating-Current Inductance of an Iron Cored Coil carrying Direct Current. R. T. Beatty, *Wireless Engineer*, Feb. 1934, p. 61.
5. Vibrator Power Supply from Dry Cells. W. Van B. Roberts, *Electronics*, July 1934, p. 214.
6. Note on a Cause of Residual Hum in Rectifier-Filter Systems. F. E. Terman and S. B. Pickles, *Proc. I.R.E.*, Aug. 1934, p. 1040.
7. Some Considerations in the Design of Hot Cathode Mercury Vapour Rectifier Circuits. C. R. Dunham, *Journal I.E.E.*, Sept. 1934, p. 278.
8. Analysis of Rectifier-Filter Circuits. M. B. Stout, *Electrical Engineering*, Sept. 1935, p. 977.

9. Power Supply Filter Curves. W. W. Waltz, *Electronics*, Dec. 1935, p. 29.
10. Vibrators. *Electronics*, Feb. 1936, p. 25.
11. Mains Transformer Design. H. B. Dent, *Wireless World*, June 18th, 1937, p. 593.
12. A Vibrator for the Connection of A.C. Receiving Sets to D.C. Mains. J. W. Alexander, *Philips Technical Review*, Nov. 1937, p. 346.
13. Solving a Rectifier Problem. R. Lee, *Electronics*, April 1938, p. 39.
14. Rectifier Filter Design. H. J. Scott, *Electronics*, June 1938, p. 28.
15. Vibrator Power Supplies. G. Hall, *Wireless World*, Dec. 22nd, 1938, p. 553.
16. Vibrators. W. H. Cazaly, *Wireless World*, June 29th, 1939, p. 594.
17. Valve Operated Smoothing Circuit. *Wireless World*, Nov. 1939, p. 28.
18. Vibratory H.T. Generators. *Wireless World*, March 1941, p. 90. Correspondence, *ibid.*, April 1941, p. 106.
19. Voltage Multiplying Rectifiers. W. T. Cocking, *Wireless World*, March 1942, p. 60.
20. The Half-Wave Voltage-Doubling Rectifier Circuit. D. L. Waidelich and C. H. Gleason, *Proc. I.R.E.*, December 1942, p. 535.
21. *Radio Data Charts*. R. T. Beatty, *Wireless World*, Messrs. Iliffe.
22. *Communication Networks*. E. A. Guillemin, Volume II, p. 246. Messrs. J. Wiley. Text-book.
23. British Standard Specification for Magnetic Materials for Use under Combined D.C. and A.C. Magnetisation. No. 933.



## AUTOMATIC GAIN CONTROL

**12.1. Introduction.**<sup>1, 7</sup> Automatic gain control, sometimes wrongly termed automatic volume control, denotes the process by which the amplification of a receiver is controlled by the output carrier voltage, so that only small changes of the latter result from large variations of input carrier voltage.

Its chief advantages are :

- (1) The increase in output voltage, which normally occurs when tuning from a weak to a strong station can be reduced to small proportions. For example, an 80-db. input change can be reduced to 10 db. output change.
- (2) The effects of fading can be minimized.

A satisfactory A.G.C. system must possess certain features. The control must be dependent on the output carrier voltage of the received signal, but be independent of the modulation envelope. Modulation envelope variation of A.G.C. bias leads to a reduction <sup>4</sup> in the output carrier modulation percentage. The A.G.C. should be inoperative until the aural volume is adequate. Variation in the gain of the receiver must not produce distortion, and the speed of control should be sufficient to follow normal fading. In superheterodyne receivers the control should not cause appreciable variation of oscillator frequency.

**12.2. Principle of Operation.** As early as 1923 <sup>6</sup> a form of A.G.C. was obtained by using triodes, biased from the detector valve, to shunt the aerial circuit. In this instance it was intended for limiting the noise produced by strong atmospherics. A later method <sup>2</sup> employed a mechanical control to reduce the capacitance between the aerial and receiver ; the moving coil of a milliammeter connected in the detector anode circuit actuated the moving vanes of the aerial capacitance.

The introduction of variable  $\mu$  R.F. valves marked a most important step in the history of A.G.C., for control of R.F. gain by grid bias, derived from the D.C. component of the detected carrier output voltage, became possible. Automatic control of A.F. stage gain has been used to improve A.G.C. action, but it is not very satisfactory because the variable  $\mu$  characteristic produces second

harmonic distortion (see Section 4.7.1, Part I). This distortion can be reduced by controlling two valves operating in push-pull, or a single multielectrode valve such as a hexode (Section 12.10.2). In the R.F. amplifier, the effect is not serious because the anode circuit rejects the second harmonic distortion of the carrier voltage and, if no higher harmonics are present, no distortion of the modulation envelope occurs. In Section 4.7, Part I, we see that modulation distortion can only be produced by terms higher than the second in the  $I_a E_g$  power series expression.

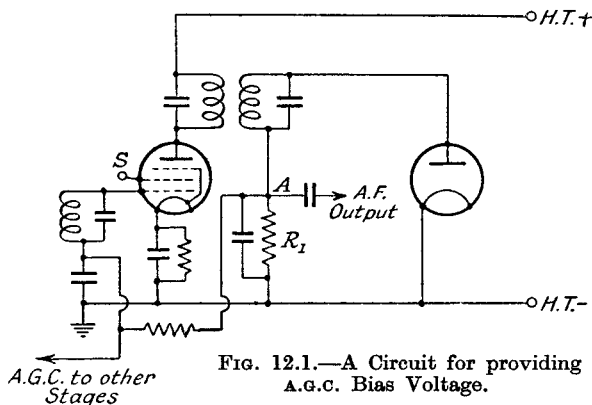
Absolutely level output voltage is not possible from an A.G.C. system controlling only stages before the detector, because the output carrier produces the bias variations for the controlled valves. The actual variation is dependent on the number, and the  $g_m E_g$  characteristics, of the controlled valves. It is least when there are several valves, each giving large changes of  $g_m$  for small changes of  $E_g$ . The maximum amplification of the receiver fixes a lower limit to the input signal voltage amenable to control, the upper limit being fixed by overloading of the detector or controlled valves. If the detector is a diode, the maximum input signal is limited only by distortion in the controlled valves, generally the last. Level or even falling output voltage for increasing input voltage is possible if the A.G.C. bias is used to control the gain of the A.F. amplifier stages. This method<sup>9, 13</sup> is, however, practically never used for the reasons stated above.

### 12.3. Methods of Obtaining the A.G.C. Bias Voltage.<sup>8, 17</sup>

The A.G.C. bias voltage is always produced by detection of the output carrier voltage, the D.C. component of which is arranged to increase the negative bias on the R.F. stages. Filters must be inserted to prevent application of the A.F. modulation components to the grids of the R.F. valves, and to decouple each R.F. stage from the others so that instability due to R.F. feedback may be prevented. The characteristics of this filter are discussed in Section 12.6. Methods of deriving the A.G.C. voltage are conveniently treated under two headings, non-amplified and amplified. With non-amplified A.G.C., the bias voltage, which is never greater than the output carrier voltage, may be obtained from the receiver detector or from a separate diode. A diode, additional to the receiver detector, is always required when the A.G.C. is only intended to come into operation above a given input signal voltage. With amplified A.G.C., the control bias voltage is considerably greater than the carrier voltage applied to the receiver detector.

### 12.4. Non-Amplified A.G.C.<sup>18, 32</sup>

**12.4.1. Unbiased Diode A.G.C.** The simplest form of A.G.C. bias circuit is shown in Fig. 12.1. The diode cathode is earthed, and the negative voltage, developed between *A* and earth when a carrier signal is received, is supplied through filters to the grid circuits of the R.F. valves. In this arrangement the last tuned circuit cannot be earthed, and it is therefore only applicable to a superheterodyne or preset-tuned R.F. receiver which has no tuning capacitor with an earthed rotor. When the tuned circuit must be earthed, the detector D.C. load resistance  $R_1$  may be connected in



parallel with the diode, at the cost of increased damping of the output circuit.

Calculation of the control<sup>17</sup> exercised by the unbiased diode is greatly facilitated by making the assumption that the cathode self-bias and screen voltages of the controlled valves are unaffected by A.G.C. action. There is generally a decrease of the first and increase of the second, but the effect causes only slight modifications to the A.G.C. curve. Let us first consider the case of a single controlled stage, the valve for which has the  $g_m E_g$  characteristic shown in Fig. 12.2; the detection characteristic of the diode is curve 1 in Fig. 12.3. The maximum A.G.C. bias must next be fixed; for calculation purposes the actual value is not important provided it is less than the bias voltage corresponding to zero anode current in the controlled stages. Let us assume a maximum A.G.C. bias of  $-40$  volts, making a total of  $-41.5$  volts with the cathode bias of  $-1.5$  volts. The next step involves conversion of the  $g_m E_g$  curve to a decibel ratio  $g_m E_g$  curve by plotting  $20 \log_{10} \frac{g_m}{g_m(E_g = -41.5)}$

for various values of  $E_g$  (see Fig. 12.4). Fig. 12.3 is similarly transformed to a decibel ratio curve of applied carrier voltage—total

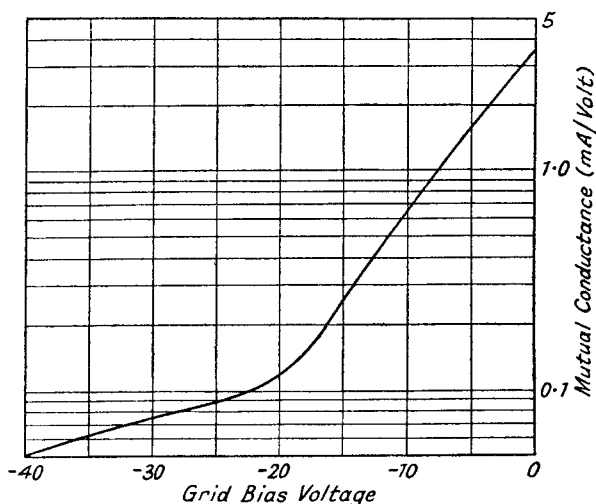


FIG. 12.2.—A Typical  $g_m E_g$  Curve of a Variable-Mu Valve.

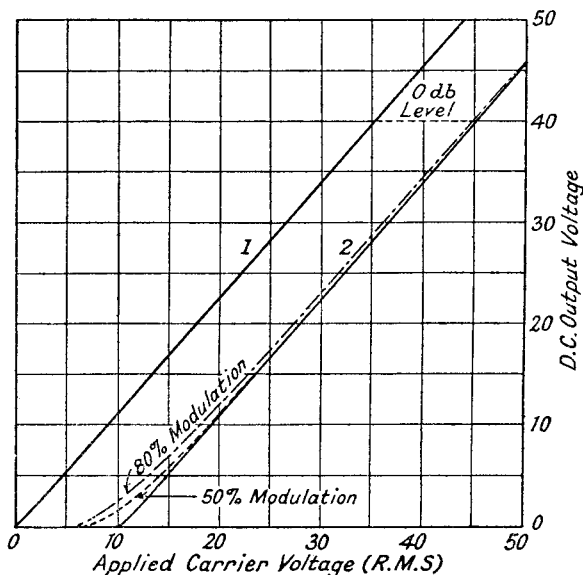


FIG. 12.3.—D.C. Output Voltage—R.M.S. Carrier Input Voltage Curves for Biased and Unbiased Diode Detector.

d.c. bias voltage as in Fig. 12.5 (curve 1). Any desired output carrier may be regarded as zero level (0 db.), but it is best to choose

the value giving the maximum required total bias, in our example — 41.5 volts, i.e., 40 volts A.G.C. bias. Thus 0 db. is equivalent to a R.M.S. carrier voltage of 35.6; this corresponds to 40 volts D.C.

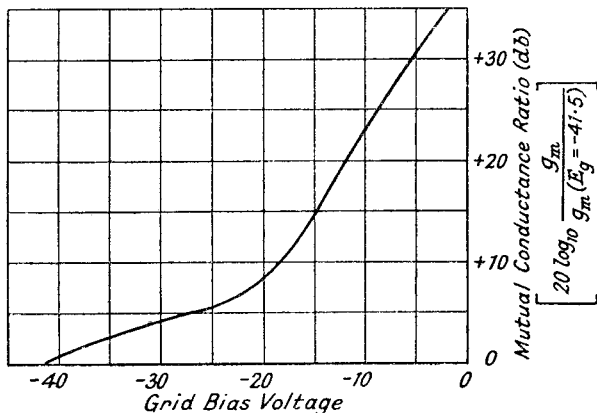


FIG. 12.4.—Decibel Ratio  $g_m E_g$  Curve of a Variable-Mu Valve.  
[Reference level 0 db.  $\equiv g_m$  at  $E_g = -41.5$  volts.]

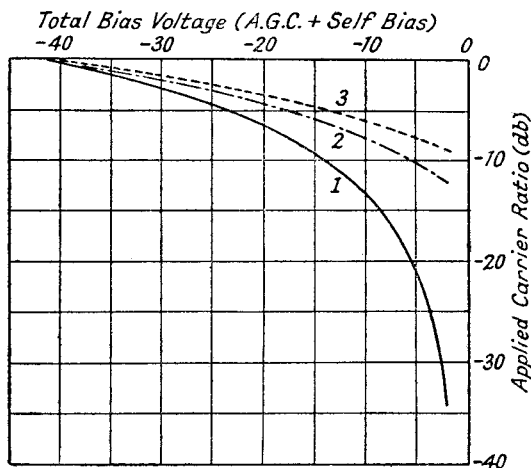


FIG. 12.5.—Decibel Ratio Applied Carrier Voltage—Total Bias Voltage Curves.  
[Reference level 0 db.  $\equiv$  carrier voltage at  $E_g = -41.5$ .]

- Curve 1: Unbiased Diode.
- Curve 2: Biased Diode,  $E_a = -10$  volts.
- Curve 3: Amplified d.c. Control.

output in Fig. 12.3. We can now combine Figs. 12.4 and 12.5 in the input-output decibel ratio curve 1 of Fig. 12.6. To illustrate the method let us find the input carrier level corresponding to — 10 db. output carrier. Fig. 12.5 shows that this corresponds to

a total bias of  $-14$  volts, or an A.G.C. bias of  $-12.5$  volts, and referring to Fig. 12.3, the R.M.S. output carrier for this A.G.C. bias is  $11.25$  volts. A total bias of  $-14$  volts results in an increase of mutual conductance ratio of  $16.5$  db. (Fig. 12.4) over that at  $-41.5$  volts total bias. Overall amplification has therefore been increased by  $16.5$  db. in reducing the output signal by  $10$  db. In the absence of A.G.C. action it would have been necessary to reduce the input carrier by  $10$  db. in order to achieve the same reduction of output carrier, but since overall amplification has been increased at the same time, it follows that the input carrier must be still further reduced by an amount equal to the increase in amplification. Thus for an output carrier of  $-10$  db. the input carrier must be

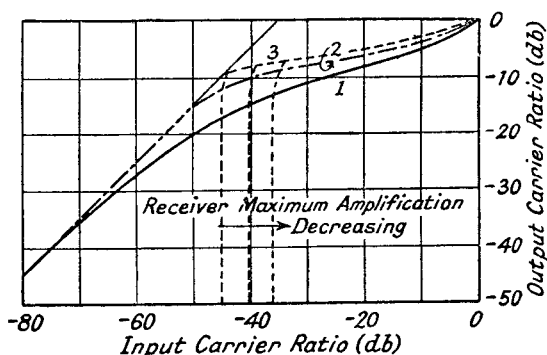


FIG. 12.6.—A.G.C. Characteristic of a Single Controlled Stage.

Curve 1: Unbiased Diode.  
 Curve 2: Biased Diode,  $E_a = -10$  volts.  
 Curve 3: Amplified d.c. Control.

$-(16.5 + 10) = -26.5$  db. below the level required to give an output carrier of  $0$  db. ( $35.6$  volts R.M.S.). One point on the input-output curve must therefore be  $-10$  db. output,  $-26.5$  db. input, and other points can be found by a similar method.

Curve 1, Fig. 12.6, shows that A.G.C. has a decreasing effect as the output falls to small values (less than  $1$  volt) and it becomes asymptotic to the  $45^\circ$  line corresponding to the non-A.G.C. condition. This is due partly to curvature of the diode characteristic, but it is mainly a result of  $g_m$  approaching a finite value as the A.G.C. bias falls to zero. To preserve constant control, the ratio change of  $g_m$  from  $-1$  to  $-0.1$  volt A.G.C. bias must be the same as from  $-0.1$  to  $-0.01$  volt, i.e.,  $g_m$  must rise to infinity as the A.G.C. bias is decreased. Over the useful range of curve 1 (Fig. 12.6) an input variation of  $50$  db. is reduced to an output variation of  $20$  db. At high output

voltages the control decreases owing to the reduced slope of the  $g_m E_g$  characteristic.

By controlling two similar R.F. stages the decibel input variation for a given output variation is doubled, and for  $n$  stages it is increased  $n$  times. If the R.F. stages have different  $g_m E_g$  characteristics, curves similar to Fig. 12.4 must be obtained for each stage. The separate curves are added together giving a composite curve, which then replaces Fig. 12.4 in the original calculations.

**12.4.2. Biased or Delayed Diode A.G.C.<sup>10</sup>** Unbiased A.G.C. is not ideal because it tends to reduce amplification for the smallest signal. It is preferable to delay the action until the output carrier voltage with average modulation (about 50%) gives a satisfactory aural output. This may be done by negatively biasing the anode of

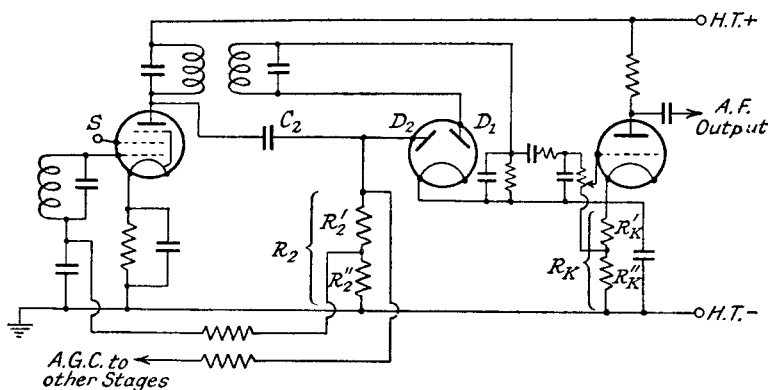


FIG. 12.7.—Biased or Delayed Diode A.G.C.

the diode producing the A.G.C. voltage, so that there is no detection until the applied signal exceeds a certain value. The receiver detector cannot be biased negatively without serious distortion accompanied by muting (no aural output below a certain carrier voltage), but a separately biased A.G.C. detector may be connected as in Fig. 12.7. In this diagram the cathode of the double diode is taken to the positive end of a split resistance  $R_k$ , inserted in the cathode circuit of the first A.F. amplifier valve. The voltage across this resistance is applied as negative bias to the anode of the A.G.C. diode  $D_2$  by returning its load resistance  $R_2$  to the earth line. The load resistance of the detector diode  $D_1$  is connected to the cathode of the double diode, and hence no bias is applied to it. Part of the voltage across  $R_k$  is also applied as bias to the first A.F. valve by returning its grid leak to the junction of  $R_k'$  and  $R_k''$ . A combined

double-diode triode valve may be used in place of the two separate double-diode and triode valves. The A.G.C. diode load resistance  $R_2$  may be tapped so that a portion only of the A.G.C. bias is applied to the last controlled stage, and the reason for this is explained later in this section.

In Fig. 12.7 the output voltage supplying the A.G.C. diode is obtained from the primary of the R.F. transformer. The primary is less selective than the secondary, and, as the receiver is detuned, the amplification rises less rapidly than is the case when the A.G.C. bias is obtained from the more selective secondary. This markedly reduces the tendency to screechy reproduction in tuning out of a station. The distorted reproduction is due to the unequal amplification of the modulation sidebands and an effective increase in modulation percentage of carrier voltage produced by the mistuned selectivity characteristic. It only becomes unpleasant when detuning causes a rapid increase in receiver amplification.

The performance of biased A.G.C. may be calculated in the manner indicated in 12.4.1. The delay voltage modifies the detector characteristic as shown by curve 2 in Fig. 12.3. The diode detects when the R.M.S. carrier voltage exceeds  $0.707 \times$  the bias or delay voltage. Taking a bias voltage on the A.G.C. diode of  $-15$  (this corresponds to a R.M.S. carrier of 10.6 volts for start of detection) we may redraw curve 2 of Fig. 12.3 as an output carrier voltage ratio-grid bias curve. This gives curve 2, Fig. 12.5, zero level (0 db.) being the R.M.S. carrier output (45.5 volts) giving an A.G.C. bias of  $-40$  or a total bias of  $-41.5$  volts. The input-output curve 2 of Fig. 12.6 is obtained by combining Fig. 12.4 and curve 2, Fig. 12.5. Thus for an A.G.C. bias of  $-18.5$ , i.e., a total bias of  $-20$ , curve 2, Fig. 12.5, gives a carrier voltage ratio of  $-4.5$  db. and Fig. 12.4, a mutual conductance ratio of 8.5 db. The input carrier ratio is therefore  $-(8.5+4.5) = -13$  db. and a point on curve 2, Fig. 12.6, is output carrier ratio  $-4.5$ , input carrier ratio  $-13$  db.; other points can be found by a similar process. The A.G.C. characteristic is noticeably flatter, and an even greater improvement can be obtained with a larger delaying bias. This must, however, be limited because the maximum required peak output carrier is approximately equal to the sum of the delay bias and maximum required bias voltage. Distortion in the R.F. amplifier supplying the carrier voltage to the A.G.C. diode results if the carrier output voltage is increased beyond a certain value. The critical value of output carrier and bias is obtained by superimposing the detection characteristic curves from Fig. 12.3 on the



signal handling capacity curves for the valve supplying the A.G.C. detector. Section 7.11, Part I, gives the method of determining this and a typical curve is shown in Fig. 12.8. The D.C. output voltage scale of Fig. 12.3 is taken to be the horizontal grid-bias voltage scale of Fig. 12.8 plus 1.5 volts (the assumed cathode self-bias on the valve); the same vertical scale is used for the R.M.S. carrier output voltage. The intersections of the detection curves for 0 and  $-15$  volts delay bias with the output carrier curve give limiting total bias voltages of  $-25$  and  $-22$ , respectively. If

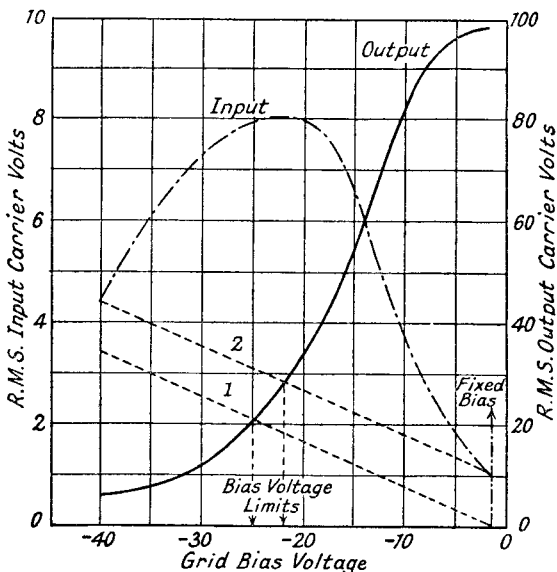


FIG. 12.8.—Output Voltage-Grid Bias Voltage Curve of the Last Controlled Valve illustrating A.G.C. Bias Voltage Limits.

only one stage is controlled, it means that the variation of input carrier, over which control is exercised, must be limited, and greater variations can only be accommodated by the inclusion of some form of manual control, such as a local-distant switch, to reduce the amplification before the controlled stage. When more than one stage is supplied with A.G.C. bias, all except that preceding the A.G.C. detector can be fully controlled. To the last stage a proportion only (generally  $\frac{1}{2}$  to  $\frac{1}{3}$ ) of the total A.G.C. bias is applied. The actual proportion depends on the maximum bias required by the other stages. For example, suppose for a delay bias of  $-15$  we need a maximum A.G.C. bias of  $-40$  volts; from Fig. 12.3 we note that with this delay bias 40 volts D.C. output requires a carrier

of 45.5 volts R.M.S., which can be obtained for a total bias voltage of  $-17$  (Fig. 12.8). The A.G.C. bias voltage is 1.5 volts less than the total, i.e., is  $-15.5$ , so that only  $\frac{15.5}{40}$  or 0.388 of the A.G.C. voltage can be applied to this stage.

An exception to the rule that all stages but the last should be fully controlled may occur with a frequency changer operating on the short-wave bands. Current variations in this valve tend to produce frequency drift (Section 5.8, Part I) of the receiver oscillator, and the effect is magnified as the operating signal frequency increases. A.G.C. may therefore be omitted to this valve.

Improved signal-to-noise ratio may also be obtained by only partial control of the R.F. amplifier stage, because generally maximum

value of  $\frac{g_m}{\sqrt{I_a}}$ , which is an important factor in determining signal-to-noise ratio (Section 4.9.3, Part I), is obtained at normal biases, and it decreases as the bias is increased. The best course would be to prevent A.G.C. being applied to this valve until a given input signal is reached, and afterwards to allow full A.G.C., but this is not so easily achieved as partial control.

**12.4.3. Distortion due to Biased Diode A.G.C.**<sup>27</sup> A negatively biased diode produces variable damping of the tuned circuit to which it is connected because, during the conduction period of the diode, an additional load is placed on the R.F. amplifier reducing its amplification. This effect may cause distortion of the modulation envelope. Figs. 12.9*a*, 12.9*b* and 12.9*c*, show what may happen for three different values of output carrier voltage. In Fig. 12.9*a*, the maximum modulation envelope amplitude is less than the delay bias voltage  $E_a$ . The A.G.C. diode is inoperative and there is no distortion. In Fig. 12.9*b*, the output carrier voltage is equal to the delay bias, and the top half of the positive modulation envelope is reduced in amplitude because of A.G.C. diode conduction current damping. Envelope as well as R.F. harmonic distortion is produced. The tuned transformer between A.G.C. diode and the A.F. detector rejects the R.F. harmonic distortion, leaving the original carrier with equal but distorted positive and negative envelopes. Detection of the modulated carrier results in an A.F. output containing harmonics of the original modulating frequency. In Fig. 12.9*c* the positive modulation envelope is completely damped, and it is identical in shape though reduced in size in comparison with the negative envelope. This represents R.F. harmonic distortion, which is rejected by the tuned transformer before the A.F. detector, leaving a modu-

lated carrier with equal undistorted positive and negative envelopes. The A.F. output from the detector is therefore undistorted. The A.G.C. diode only causes distortion of the detector output if the delay bias line cuts the positive modulation envelope; hence distortion is restricted to a range of carrier peak voltages from

$$\hat{E}_1 = \frac{E_d}{1+M} \text{ to } \hat{E}_3 = \frac{E_d}{1-M} \quad . \quad . \quad . \quad 12.1$$

with maximum distortion at  $\hat{E}_2 = E_d$ . The limits of the range are dependent on the modulation ratio  $M$ , being larger when the latter

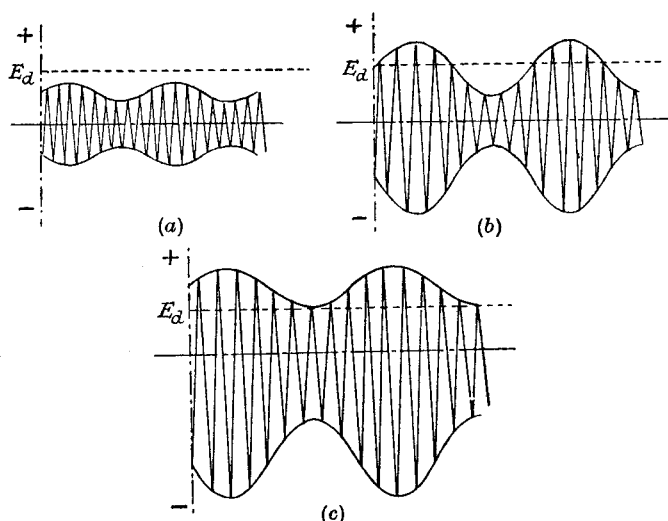


FIG. 12.9.—Various Stages of Input Voltage Damping due to Biased Diode A.G.C.

- (a) Modulation envelope less than bias voltage.  
 (b) Carrier peak voltage equal to bias voltage.  
 (c) Modulation envelope greater than bias voltage.

is larger. The carrier peak voltage  $\hat{E}_1$  gives the condition for the onset of distortion—the positive modulation envelope is just entering the A.G.C. diode conduction current region, and  $\hat{E}_3$  defines the end of distortion when the positive envelope is completely damped. These distortion limits are true only as long as the A.C. and D.C. load resistances of the diode are equal, and this is never so in practice because of the filter required between the A.G.C. diode and the grid circuits of the controlled valves. An A.C./D.C. load resistance ratio less than unity has no effect on  $\hat{E}_1$ , but  $\hat{E}_2$  and  $\hat{E}_3$  are increased to

$$\hat{E}_2 = \frac{E_d}{1 - \frac{M}{\pi} \frac{R_1}{R_2}} \text{ and } \hat{E}_3 = \frac{E_d}{1 - \frac{M(R_1 + R_2)}{R_2}} \quad . \quad . \quad . \quad 12.2$$

where  $R_1$  = the diode D.C. load resistance  
 and  $R_2$  = the input A.C. resistance of the filter looking from  $R_1$ .  
 The maximum value of distortion at  $\hat{E}_2$  is proportional to the ratio  
 of the dynamic or resonant impedance of the tuned circuit, across  
 which the A.G.C. diode is connected, to the equivalent damping  
 resistance of this same diode. The damping resistance is itself  
 proportional to the A.C. load resistance  $\frac{R_1 R_2}{R_1 + R_2}$ . Thus, for small  
 distortion, a low value of tuned circuit impedance and a large value  
 of A.C. load resistance are required. A reduction in the former  
 reduces the maximum output voltage which can be obtained from  
 the R.F. valve supplying the A.G.C. diode, so that it is desirable to  
 aim at the highest possible value of A.C. load resistance. This entails  
 a high value of  $R_1$  and  $R_2$ . The upper carrier limit  $\hat{E}_3$  is a minimum  
 when  $R_2$  is as large as possible.

Another effect, which should be noted, is that with biased A.G.C.  
 performance is no longer independent of the modulation envelope.  
 When the positive modulation envelope is cut by the delay bias  
 line, the envelope as well as the carrier is detected, and the D.C.  
 component is greater than it would be in the absence of modulation.  
 The effect of modulation on the detection characteristic is shown by  
 the dotted curves in Fig. 12.3, which merge into curve 2 when the  
 positive modulation envelope is completely damped. The initial  
 curvature of the detection characteristic due to envelope detection  
 affects the start of the A.G.C. output-input characteristic. Curve 2  
 in Fig. 12.6 begins at a smaller input voltage (less than - 50 db.),  
 is initially more curved, and finally merges into the curve for no  
 modulation envelope detection towards an input voltage correspond-  
 ing to 0 db. The range of carrier output voltage over which modula-  
 tion influences A.G.C. performance is the same as that over which  
 A.G.C. diode conduction current produces distortion.

#### 12.4.4. Biased A.G.C. using the Audio Frequency Detector.

A biased A.G.C. circuit, which uses the A.F. detector as the source of  
 control voltage and largely avoids the variable damping distortion  
 of the negatively biased diode, is shown in Fig. 12.10. The A.F.  
 detector cathode is connected to earth through a resistance  $R_3$ ,  
 producing a positive voltage between cathode and earth. The  
 A.F. detector load resistance  $R_1$  is returned to cathode in the usual  
 manner. A.G.C. bias is taken from the negative end  $A$  of  $R_1$  through  
 the filter formed by  $R_2$  and  $C_2$ . The positive delay voltage across  
 $R_3$  means that there can be no negative A.G.C. voltage across  $C_2$  until  
 the voltage across  $R_1$  exceeds that across  $R_3$ . To prevent the

application of positive bias (before A.G.C. comes into action) to the controlled valves, a second diode  $D_2$  is connected across  $C_2$ , and it acts as a short-circuit when the voltage across  $C_2$  is positive. It ceases to conduct when the voltage becomes negative, i.e., as soon as A.G.C. is functioning. It should be noted that distortion may be introduced into the A.F. output from  $D_1$  when  $D_2$  is conducting, for

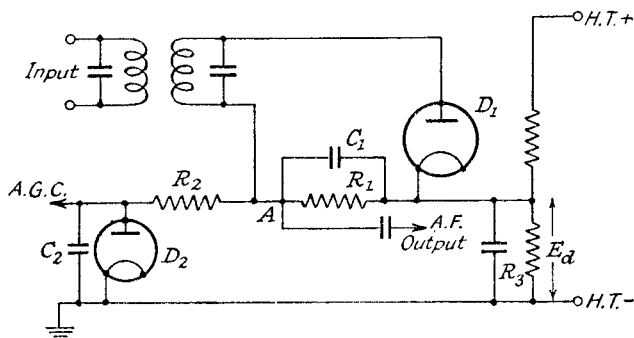


FIG. 12.10.—A Circuit for Reducing Distortion due to Biased Diode A.G.C.

[Westinghouse Brake and Signal Company, Patent No. 413,731.]

its conduction current passing through  $R_1$  applies a negative bias to the anode of  $D_1$ . The actual biasing voltage can be made small by using a large value for  $R_2$  and a small value for  $R_1$ . This form of distortion disappears when  $D_2$  ceases to conduct and A.G.C. bias is applied.

## 12.5. Amplified A.G.C. Systems.

**12.5.1. Introduction.** Distortion due to a delay bias and to overloading of the valve preceding the A.G.C. diode may largely be eliminated by amplifying the A.G.C. bias. The control action of the latter, measured by the slope of the input-output curve, is actually dependent only on the equivalent delay bias and the  $g_m E_g$  characteristics of the controlled valves. The improvement normally obtained from amplified A.G.C. is essentially due to an effective increase in the delay bias. For example, if in Section 12.4.1 an amplifier multiplying the A.G.C. bias by 10, is inserted between the D.C. output voltage from the A.G.C. detector and the controlled valves, the result is to change the reference level 0 db., for Fig. 12.5, e.g., the output carrier R.M.S. voltage for an A.G.C. bias of  $-40$  volts becomes approximately 3.56 instead of 35.6 volts. This has no influence on the shape of the input-output curve 1 of Fig. 12.6, and the only advantage gained is the reduced possibility of overloading the last controlled stage, which can be fully, instead of partially, controlled.

There are two important methods of obtaining amplified A.G.C. : (1) by R.F. amplification between the last controlled valve and the A.G.C. diode (it is assumed that the A.F. detector is connected to the output of the controlled valve and not to the output of the A.G.C. amplifier), and (2) by D.C. amplification between the A.G.C. bias voltage source and the controlled valves.

**12.5.2. R.F. Amplified A.G.C.** R.F. amplified A.G.C. in its simplest form consists of a fixed gain R.F. amplifier inserted between the A.G.C. diode and the R.F. valve supplying the A.F. detector. The amplifier should have an almost flat pass-band for frequencies within about  $\pm 20$  kc/s of the carrier frequency, as this reduces the tendency to sideband screech in the off-tune position as described in Section 12.4.2. The required pass-band may be obtained either by using an aperiodic anode circuit, or a double-tuned transformer with coupling greater than critical. When an aperiodic or low impedance circuit is employed, voltage doubling detectors can be used to increase the A.G.C. bias. Voltage doubling is not of much value with tuned circuits because it produces heavy damping, the damping resistance being reduced to half that for half-wave detection. The method of calculating the input-output curves is as described in Section 12.4 and, for the same delay bias voltages at the A.G.C. detector, the input-output curves are the same. The only difference is that the R.M.S. output carrier voltage corresponding to 0 db. is reduced in proportion to the increased amplification between A.G.C. detector and controlled R.F. stage. Owing to the A.G.C. amplification a larger delay bias may be applied to the A.G.C. detector without overloading the last controlled stage, and A.G.C. action can consequently be improved. The maximum delay bias depends on the maximum output carrier voltage which can be obtained from the A.G.C. amplifier. Referring to Fig. 12.8 we see that this may be as high as 100 volts, so that a delay bias of 50 volts is a possibility. Fig. 12.8 shows that there are limitations to the magnitude of input voltage which can be applied to the A.G.C. amplifier, but these can usually be overcome by supplying a proportion only of the output voltage from the last controlled stage to the A.G.C. amplifier. Anode circuit distortion can be tolerated in this amplifier as long as there is no feedback into the A.F. detector circuit, but grid circuit distortion, due to grid current, should not be permitted because it can produce variable damping distortion in a similar manner to the delay biased diode.

**12.5.3. A.G.C. Using a Combined R.F. and A.F. Amplifier.** A circuit producing R.F. amplified A.G.C. and requiring

no extra valves is shown in Fig. 12.11. The valve following the A.F. detector is used as a combined R.F. and A.F. amplifier.

The R.F. ripple voltage, produced across the detector load resistance  $R_1$ , is passed to the grid of the triode amplifier by means of the capacitance  $C_2$ . This capacitance ( $100 \mu\mu\text{F}$ ) allows wide variation of A.F. volume control without appreciably affecting the R.F. voltage applied to the amplifier. An R.F. choke  $L$  is inserted in the A.F. amplifier anode circuit, and the capacitance  $C_3$  transfers the R.F. output voltage to the diode. Detection of the A.F. anode voltages is avoided by making  $C_3$  small (about  $0.0001 \mu\text{F}$ ). A disadvantage of the method is the danger of overloading the amplifier and distorting the A.F. output voltage, the maximum value of which

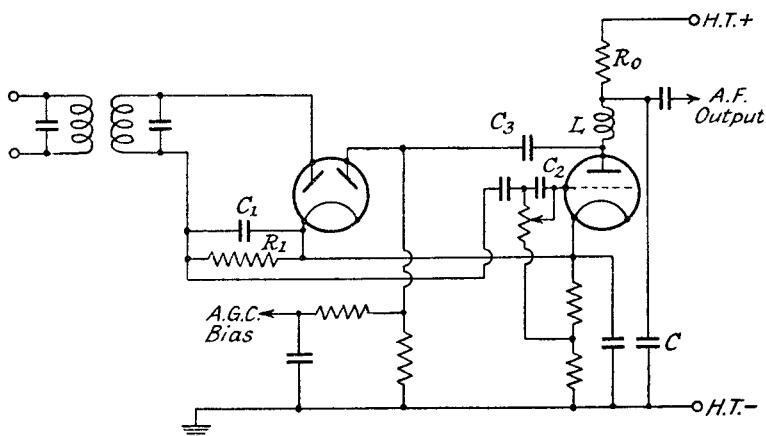


FIG. 12.11.—Amplified Biased or Delayed Diode A.G.C.

is reduced by the presence of the R.F. voltage. The A.F. amplification must be limited, and the load resistance,  $R_0$ , should not exceed the valve slope resistance.

It is possible to use the triode valve as a combined cumulative-grid detector and R.F. amplifier, but A.G.C. action may not then be so satisfactory since increasing carrier voltage biases the valve negatively and reduces its R.F. gain. This is to some extent offset if the delay bias voltage is obtained from a resistance through which the anode current from the cumulative grid detector is passing, because increasing carrier voltage decreases the anode current and delay bias voltage, and so tends to increase A.G.C. bias. The valve may also be used as an anode-bend detector and A.G.C. amplifier. This method of amplified A.G.C. has the usual disadvantages encountered when one valve is used for dual purposes, and much

more satisfactory operation is obtained by separating the functions of R.F. and A.F. amplification.

**12.5.4. D.C. Amplified A.G.C.<sup>11</sup>** D.C. amplification of the A.G.C. voltage may be achieved by the circuit shown in Fig. 12.12. A source of negative voltage is required, and it may be provided by the voltage drop across a resistance  $R_5$  (or the loudspeaker field coil) between the earth line and H.T. negative, or by a separate H.T. supply. The second method is generally more stable and free from hum. The A.G.C. voltage is derived from the cathode of the double-diode-triode valve through the diode  $D_2$ , and delay bias is obtained by adjusting the resistance  $R_4$  to give, in the absence of a carrier voltage, a positive bias on the cathode with respect to earth. A comparatively large capacitance  $C_4$  (about  $4 \mu\text{F}$ , paper, an electrolytic capacitor cannot be used because the cathode voltage changes from

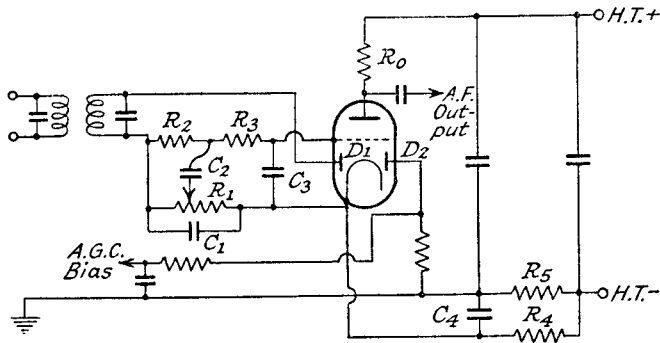


FIG. 12.12.—D.C. Amplified A.G.C.

positive to negative with respect to earth) is connected from the cathode end of  $R_4$  to earth in order to prevent A.F. voltages being developed in the cathode circuit. Any such voltages may be rectified by  $D_2$  to interfere with normal A.G.C. bias. The diode  $D_2$  prevents positive bias being applied to the controlled valves since it cannot conduct with a positive cathode. The triode portion is biased from the A.F. detector load resistance  $R_1$ , the voltage across which becomes increasingly negative as the applied carrier voltage increases. Consequently the triode-anode current decreases, and the voltage between its cathode and earth falls to zero from its initial positive value and finally becomes negative. Diode  $D_2$  then conducts, and a negative bias is applied to the controlled valves. The triode valve may be used as an A.F. as well as D.C. amplifier, the A.F. volume control being arranged as in Fig. 12.12 to leave the D.C. bias to the valve unchanged. The resistance  $R_2$  (about  $4R_1$ ) and capacitance



$C_2$  (about  $0.01 \mu\text{F}$ ) make this possible. It is undesirable that the R.F. ripple voltage should be passed to the triode grid, and  $R_3$  and  $C_3$  form an R.F. filter to prevent this. The A.F. output voltage from the triode is developed across  $R_0$ . It should be noted that the variable D.C. bias on the triode section may cause distortion of the A.F. output, because a large carrier voltage may take the operating bias voltage into the curved lower part of the triode  $I_a E_g$  characteristic.

The design procedure for this type of A.G.C. circuit is as follows. The negative voltage required across  $R_s$  must first be determined; this should be about twice the maximum desired A.G.C. bias, i.e.,

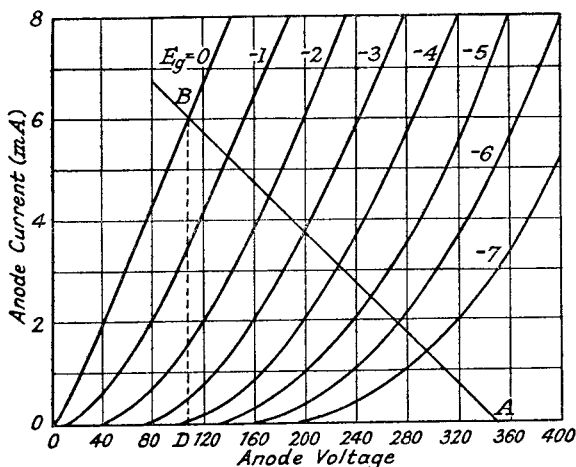


FIG. 12.13.— $I_a E_a$  Characteristics for D.C. Amplified A.G.C. using a Triode Valve.

about 100 volts. If the D.C. voltage applied to the other circuits in the receiver is 250, the total H.T. voltage required is 350 volts; the  $I_a E_a$  characteristics of the triode section are assumed to be those in Fig. 12.13, and the detection curve of  $D_1$  to be curve 1, Fig. 12.3. The triode slope resistance is approximately 20,000 ohms, so that a suitable value for  $R_0$  is 20,000 ohms (it must not be too high because it reduces the A.G.C. delay bias voltage and also the A.G.C. bias voltage to the controlled valves).  $R_4$  may be chosen to have the same value as  $R_0$ . The D.C. load line,  $AB$  in Fig. 12.13, having an inverse slope of 40,000 ohms, is drawn from  $E_a = 350$  volts (the total H.T. voltage). The D.C. voltage available across  $R_4$  is given by half the voltage difference between 350 and the intersection of  $AB$  with the particular grid bias voltage line being considered. Hence the relationship between the voltage across  $R_4$  and grid bias

can be obtained, and curve 1, Fig. 12.3, allows the conversion of grid bias (this is the D.C. output voltage of Fig. 12.3) to R.M.S. output carrier voltage. In Fig. 12.14 the cathode-to-earth voltage, i.e., the A.G.C. bias voltage when it is negative, is plotted against R.M.S. carrier voltage applied to  $D_1$ , and this is next converted to a decibel ratio output carrier voltage—total bias voltage curve, reference level 0 db. again corresponding to the R.M.S. carrier voltage giving an A.G.C. bias of  $-40$  volts, i.e.,  $3.95$  volts. This curve is shown in Fig. 12.5 as curve 3. Using the decibel  $g_m E_g$  characteristic of Fig. 12.4, we can now calculate the decibel ratio input-output curve 3 of Fig. 12.6, which gives the A.G.C. characteristic for a single

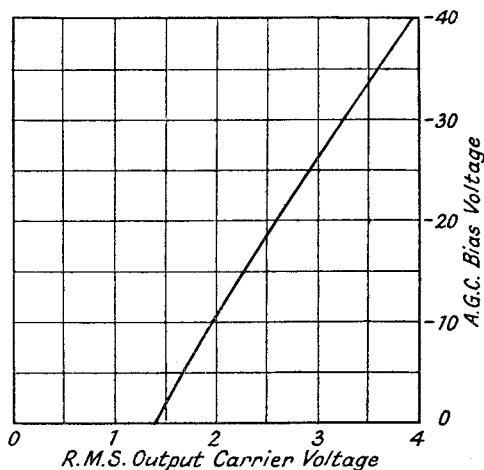


FIG. 12.14.—A.G.C. Voltage—R.M.S. Carrier Voltage for D.C. Amplified A.G.C.

controlled stage. Thus for an A.G.C. bias voltage of  $-8.5$  (output carrier =  $1.9$  from Fig. 12.14), the total bias voltage is  $-10$  volts and the output carrier is  $-6.4$  db. (Fig. 12.5, curve 3). A total bias of  $-10$  volts gives an increased amplification ratio of  $23$  db. (Fig. 12.4) so that the input voltage ratio is  $-(6.4 + 23) = -29.4$  db. One point on curve 3 of Fig. 12.6 is output carrier ratio  $-6.4$  db., input carrier ratio  $-29.4$  db. If more stages are biased, a composite  $g_m E_g$  curve must be obtained as discussed in Section 12.4.1. Curve 3 shows better control of output voltage than is obtained by the non-amplified systems, because of the increase in delay bias voltage, which is equal to the positive voltage between cathode and earth when the carrier voltage to  $D_1$  is zero. The delay voltage is therefore half the voltage difference  $AD$  (Fig. 12.13) minus  $100$  volts (the voltage across  $R_s$ ), which is  $21$  volts. The same curve can be

obtained from the non-amplified A.G.C. system with a delay bias of  $-21$  volts, but the output carrier voltage required to produce maximum A.G.C. bias cannot be realized without reduced control of the last R.F. stage.

**12.5.5. Anode-Bend Amplified A.G.C.**<sup>3, 25</sup> Another method of obtaining amplified A.G.C. is to use an anode-bend detector as shown in Fig. 12.15. The source of negative bias voltage may be a resistance between the earth and H.T. negative lead as for the D.C. amplified system, or a separate H.T. supply may be employed. In Fig. 12.15, two resistances,  $R_3$  and  $R_2$ , are connected between earth and H.T. negative to supply the negative bias. The voltage

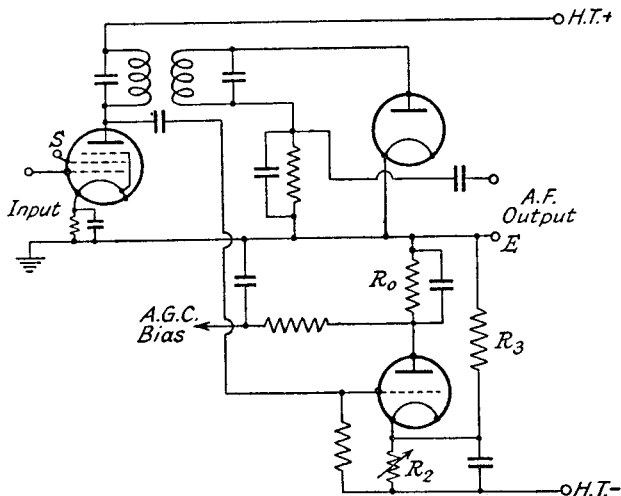


FIG. 12.15.—Anode Bend A.G.C.

drop across  $R_2$ , which can be varied, is used to bias the anode-bend A.G.C. detector. Variation of  $R_2$  changes the delay bias for A.G.C. operation, and the detector anode current is generally zero in the absence of a carrier voltage. The anode resistance  $R_0$  has a value of about 100,000 ohms. The parabolic detection characteristic of the anode-bend detector (see Fig. 8.19*b*, Part I) tends to give an improved A.G.C. characteristic, because A.G.C. bias increases at a greater rate than the carrier voltage.

**12.6. The Filter between the A.G.C. Detector and the Controlled Stages.** A filter must be inserted between the source of A.G.C. bias and the grid of the controlled valves in order—

- (1) to complete the circuit for R.F. voltages from the grid of the controlled valve to earth, and

- (2) to by-pass R.F. and A.F. voltages developed across the A.G.C. detector load resistance, and to permit only the D.C. component to reach the controlled stages.

Inadequate filtering may result in R.F. voltage feedback, causing instability and, in the superheterodyne receiver, interference whistles. If the A.F. voltages are not removed, the effective modulation ratio of the carrier applied to the A.F. detector is reduced, because the A.F. voltage feedback provides a variable A.G.C. bias. This bias operates on the input carrier envelope to reduce the output carrier envelope variation,<sup>5</sup> in the same way as the normal A.G.C. bias operates to reduce the much slower carrier variation due to fading.

The two objects mentioned above may be realized by employing a filter consisting of resistances and capacitances. The first condition merely requires a low R.F. impedance from the "earthed" end of the tuning impedance in the controlled valve grid circuit to the earth line. The second condition calls for the largest possible value of  $C$  and  $R$ . There is, however, one important condition which must be fulfilled by the filter, viz., its time constant must be low enough to allow the quick release or application of the A.G.C. bias when the input carrier varies. A time constant of  $CR = 0.1$  seconds is generally regarded as sufficiently fast to control normal fading variations. In any single stage  $RC$  filter the filtering action is dependent on the product of  $R$  and  $C$ , and a large value of  $R$  may be used with a small value of  $C$ , or vice versa. In Section 12.4.3 stress is laid upon the need for making the ratio of A.C. to D.C. load as near unity as possible, so that the highest value of  $R$  is required. The maximum value must, however, be limited if "softening" (Section 2.8.1, Part I) of the controlled valves is to be avoided, and generally the total D.C. resistance in the grid circuit must not be allowed to exceed  $2M\Omega$ . This limits  $R$  to 1 or  $1.5 M\Omega$  if the A.G.C. detector D.C. load resistance is  $0.5 M\Omega$ , and hence  $C$  may have a value of about  $0.1 \mu F$ .

There is always a difference between the charge and discharge time constants of the A.G.C. filter, the former being more rapid than the latter. During discharge the A.G.C. diode is non-conducting, and the resistance in the circuit is the sum of the filter and diode D.C. load resistances, whilst for charge the latter is effectively short-circuited by the conduction resistance of the diode. When more than one valve is controlled, separate filters may be necessary for each stage in order to prevent R.F. feedback between stages. Interaction between the filters modifies the time constant of each individual filter; this effect has been calculated,<sup>31</sup> and the time

constant of various types of coupled filters is estimated by the following procedure.

In Fig. 12.16*a* is given an example of the series type of filter applying the A.G.C. bias to three controlled stages. The resistance  $R$  is the A.G.C. detector load resistance; the R.F. coupling capacitance ( $C_2$  in Fig. 12.7) is virtually in parallel with  $R$ , but it is so small that it has practically no effect on the time constant and is therefore omitted. During the charging period, i.e., increasing carrier voltage,

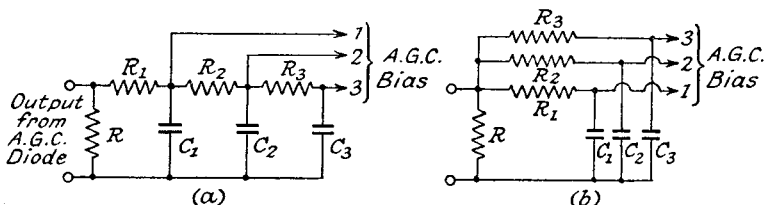


FIG. 12.16.—A.G.C. Filter Circuits.

(a) Series type.

(b) Parallel type.

the diode is conducting,  $R$  has no effect, and the maximum time constant, which occurs in A.G.C., line 3, is

$$T_c = R_1(C_1 + C_2 + C_3) + R_2(C_2 + C_3) + R_3C_3 \quad . \quad . \quad 12.3a.$$

During discharge the diode is non-conducting, and the total discharge current passes through  $R$ ; the time constant (line 3) for this condition is

$$T_d = C_3(R + R_1 + R_2 + R_3) + C_2(R + R_1 + R_2) + C_1(R + R_1) \quad . \quad . \quad 12.3b$$

which is greater than  $T_c$  by  $R(C_1 + C_2 + C_3)$ .

The alternative parallel type of filter shown in Fig. 12.16*b* is more common. The time constant for charge is that of the largest separate filter (e.g.,  $C_1R_1$  or  $C_2R_2$ , etc.), whilst for discharge it is

$$T_d = C_1(R_1 + R) + (C_2 + C_3)R \quad . \quad . \quad 12.4.$$

The discharge time constant is modified when the capacitances and resistances are very different in value, and this is fully discussed in the article<sup>31</sup> to which reference has already been made.

To determine the relative advantages of the two types of filters, let us assume that  $R = 0.5 \text{ M}\Omega$ , all the capacitances are  $0.1 \text{ }\mu\text{F}$ , the A.C./D.C. load resistance ratio is to be not less than 2:3, and all filter resistances are equal.

For the three stage series filter

$$\frac{R_{\text{A.C.}}}{R_{\text{D.C.}}} = \frac{2}{3} = \frac{R_1}{R_1 + 0.5}$$

or

$$R_1 = 1.0 \text{ M}\Omega.$$

The reactance of capacitance  $C_1$  at audio frequencies is considered to be negligible in comparison with  $R_1$ , so that the resistances  $R_2$  and  $R_3$  contribute nothing to the A.C. load resistance. Substituting numerical values in expressions 12.3a and 12.3b gives the charge time constant  $T_c$  as 0.6 seconds and the discharge  $T_d$  as 0.75 seconds.

Assuming that the same conditions hold for the parallel filter, i.e.,  $R_1 = R_2 = R_3$ ,  
 $C_1 = C_2 = C_3 = 0.1 \mu\text{F}$ ,  $R = 0.5 \text{ M}\Omega$  and A.C./D.C. load ratio =  $\frac{2}{3}$ ,

$$\text{we have} \quad \frac{R_{\text{A.C.}}}{R_{\text{D.C.}}} = \frac{2}{3} = \frac{\frac{R_1}{3}}{0.5 + \frac{R_1}{3}}$$

$$\text{or} \quad R_1 = 3 \text{ M}\Omega.$$

Hence  $T_c = 0.3$  seconds.

and  $T_d = 0.45$  seconds.

Thus we see that the parallel filter gives a lower time constant for charge and discharge than the series filter.

In both cases discussed above, the resistance in the grid return path of the controlled valves is  $3.5 \text{ M}\Omega$ , which is a higher figure than can be allowed; it would be necessary to reduce either the A.C./D.C. load resistance ratio or  $R$ , in order to reduce the grid D.C. resistance, and so prevent softness developing in the controlled valves.

For the D.C. amplified A.G.C. system (Fig. 12.12) two circuits separated by a valve contribute to the overall time constant, the value of which is very nearly given by the sum of the grid and cathode circuit time constants. Theoretically it is found<sup>35</sup> that the overall time constant is not exactly determined by the sum of the individual time constants, the error, which is not greater than 7%, being maximum when the individual time constants are equal. In the practical case an added complication is found due to the fact that  $\mu$  and  $R_a$  of the valve do not remain constant as the D.C. bias is varied, and a more correct expression for overall time constant is

$$T = KR_g C_g + \frac{R_k R_a'}{R_k + R_a'} C_k \quad . \quad . \quad . \quad 12.5$$

where  $K$  is a correction factor, a function of the grid bias, and is  $< 1$  for discharge and  $> 1$  for charge.

$R_g C_g$  is the time constant of the grid circuit.

$R_k$  is the cathode resistance across which the A.G.C. bias is developed ( $R_4$  in Fig. 12.12).

$R_a'$  is the sum of the valve slope resistance  $R_a$  and the anode circuit resistance  $R_o$ .

$C_k$  is the cathode-earth capacitance,  $C_4$  in Fig. 12.12.

**12.7. Dual A.G.C.<sup>33</sup>** When A.G.C. is applied to receivers having an R.F. stage before the frequency changer, certain conditions may arise to cause overloading of the latter. This is possible when a receiver is tuned to a weak station in the high field strength area of a local station, particularly if the two frequencies are not widely separated. The impedance of the signal tuning circuit in the anode of the R.F. valve at the undesired local station frequency may be sufficiently high to give amplification of this undesired signal, which can then produce interfering whistles (see Section 5.4) in the frequency changer. The undesired response is often large enough to cause serious interference with the A.F. output, but is not sufficient (owing to the selectivity of the I.F. circuits) to increase the A.G.C. bias to any great extent. By employing for the R.F. valve a separate A.G.C. bias obtained from an early, less selective, stage in the receiver, where the undesired signal is comparable with the desired, the A.G.C. bias is then controlled by both signals, and R.F. amplification is reduced as the undesired signal is increased. A diode detector produces the D.C. voltage component, and the A.G.C. source is usually a wide pass-band I.F. transformer (440 to 490 kc/s) in the anode of the frequency changer in series with the normal narrow band transformer to the first I.F. valve. The frequency response of the A.G.C. voltage source is therefore practically the same as that of the signal circuits, with the added advantage that the signal is amplified in the frequency changer. The wide pass-band transformer should have adequate cut-off at the oscillator frequency (615 kc/s) corresponding to the lowest required signal frequency (150 kc/s) otherwise the A.G.C. may be actuated by the oscillator voltage. A.G.C. bias, derived in the normal way from the last I.F. stage, is used to control I.F. and frequency changer stages, though the latter may be controlled from the R.F. amplifier bias. Such a scheme is known as dual A.G.C.

## **12.8. Inter-Channel Noise Suppression or Quiet A.G.C.<sup>4, 15, 22</sup>**

**12.8.1. Introduction.** A noticeable feature of receivers having A.G.C. is the increase in noise which occurs when tuning out a signal. This is due to the increase of amplification resulting from the decrease of input carrier voltage. It can be overcome to some extent by increasing the bias on the R.F. controlled valves to reduce their maximum amplification, but this is not a very satisfactory method as it limits the A.G.C. action at the same time. The ideal system is to silence the receiver for small input signals without affecting receiver performance for signals exceeding a given value, and this

may be realized by overbiasing the A.F. amplifier or negatively biasing the detector <sup>14</sup> by a voltage controlled by the input signal. Release of this biasing voltage is usually achieved by a valve controlled circuit. The use of a mechanical shorting device <sup>12</sup> is rare because the relay needed to operate it must be very sensitive and free from chatter.

**12.8.2. Biased Detector Quiet A.G.C.** Serious distortion occurs over a range of input signal voltages in a detector having negative bias, and it is therefore essential to obtain rapid and complete removal of the negative silencing voltage when the desired input voltage is reached. To operate successfully, the negatively

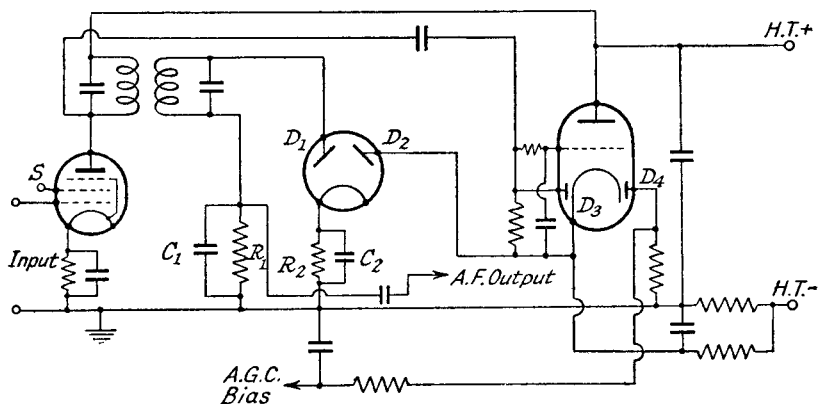


FIG. 12.17.—Quiet Delayed A.G.C. by Means of a Biased A.F. Detector Diode.

biased detector requires to be used with amplified A.G.C., and a suitable circuit is shown in Fig. 12.17.\* One diode ( $D_3$ ) of the double-diode triode acts as the A.G.C. detector, and the D.C. component from this is amplified by the triode section. The second diode ( $D_4$ ) prevents the application of positive bias to the controlled valves as described in Section 12.5.4. The A.F. detector is the diode ( $D_1$ ) of the double-diode valve; the other diode ( $D_2$ ) is connected to the cathode of the A.G.C. amplifier valve, and in the common cathode circuit of these two diodes is a resistance  $R_2$  paralleled by a capacitance  $C_2$ . As long as the cathode of the A.G.C. amplifier is positive with respect to earth, the diode  $D_2$  conducts and applies a negative bias to  $D_1$ . This bias disappears when the cathode becomes negative, i.e., when A.G.C. bias begins to function, and  $D_1$  detects normally. Part of the detected voltage

\* British Patent 498,842, Marconi's Wireless Telegraph Co. and K. R. Sturley.



is developed across  $R_2$ , but this loss need not be great, because  $R_2$  can be about  $\frac{1}{10} R_1$ . The value of  $C_2$  should be such as to make  $C_2 R_2 = C_1 R_1$ . Typical input-output curves are indicated as the dotted vertical lines in Fig. 12.6. The input voltage at which suppression is released may be controlled to a limited degree by varying the H.T. voltage of the triode D.C. amplifier, but it is preferably varied by reducing the maximum gain of the controlled valves. A similar method to the above, using a triple-diode triode, has also been developed.<sup>14</sup>

**12.8.3. Interchannel Noise Suppression by a Variable Capacitance across the A.F. Detector Load Resistance.** The A.F. output from a detector can be decreased by adding a large capacitance in parallel with the detector load resistance, and if it

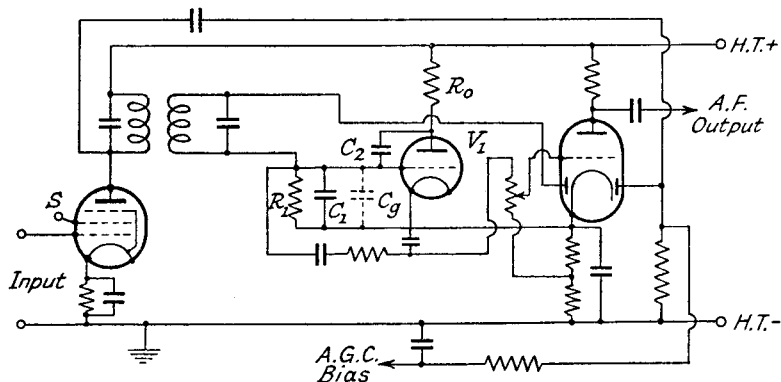


FIG. 12.18.—Quiet A.G.C. Using Miller Effect from a Triode across the A.F. Detector Load Resistance.

can be made to vary inversely as the carrier voltage, noise suppression can be achieved. This is possible by using the Miller effect, viz., the variation of grid input capacitance of a valve when its overall amplification is changed. A suitable circuit is illustrated in Fig. 12.18. The variable capacitance is provided by valve  $V_1$ , the anode-grid capacitance of which is increased by  $C_2$  in order to increase the variation of grid input capacitance  $C_g$ . The value of the latter is, from expression 2.13*b*, Part I,

$$C_g = C_{ga} \left( 1 + \frac{\mu R_0}{R_a + R_0} \right)$$

where  $C_{ga}$  = total anode-grid capacitance including  $C_2$ .

$R_0$  = anode external circuit resistance.

It should be noted that maximum  $C_g$  is obtained by making the

anode external impedance a resistance, any reactance element due to stray capacitance reduces  $C_g$ . As an example of the possible maximum value of  $C_g$ , let us consider the following component and valve parameter values,  $R_0 = 1 \text{ M}\Omega$ ,  $R_a = 10,000 \Omega$ ,  $C_{ga} = 0.001 \mu\text{F}$ ,  $\mu = 30$ ; a maximum value for  $C_g$  of  $0.0307 \mu\text{F}$  is obtained. By connecting the grid circuit of  $V_1$  across the D.C. load resistance  $R_1$  (Fig. 12.18) the valve is automatically biased by the detected carrier voltage D.C. component, which becomes increasingly negative as the carrier voltage is increased. For small carrier voltages, the negative bias is small,  $\mu$  is large,  $R_a$  small, and  $C_g$  is large. A.F. voltages across the load resistance  $R_1$  are therefore very much reduced and A.F. output is almost negligible. Increasing carrier voltage decreases  $C_g$ , until a bias voltage is reached which takes  $V_1$  to zero anode current and allows the detector circuit to function normally, giving full A.F. output. Since the shunt capacitance due to  $V_1$  has greater by-passing effect on the higher audio frequencies, a form of automatic tone control occurs. This has advantages for noise suppression, because the amplification of the receiver increases with decrease of carrier voltage, and interference voltages, having appreciable high audio frequency sideband components, normally become more noticeable. A disadvantage of the method is that distortion tends to occur if the A.F. voltage across  $R_1$  carries  $V_1$  over the anode current cut-off point or curved part of the  $I_a E_g$  characteristic of the valve; the grid input admittance then varies appreciably over the cycle of A.F. voltage.

**12.8.4. Noise Suppression by means of a Biased A.F. Amplifier.** Noise suppression may also be achieved by applying additional negative bias, controlled from the carrier voltage, to cut off the anode current of the first A.F. amplifier valve. This bias is either gradually reduced as the carrier voltage increases or is short-circuited at a particular value of the latter. In one method the negative voltage is developed across a resistance in the anode circuit of a valve biased from the A.F. detector or the A.G.C. diode. Increase of carrier voltage decreases the anode current of this valve to zero, so that the initial negative voltage between the H.T. positive for the biasing valve and its anode disappears. A disadvantage of the system is that the total H.T. voltage must be increased because the H.T. positive of the biasing valve is the H.T. negative of the A.F. amplifier.

An alternative method is to short the suppressing bias by a mechanical relay or a glow discharge tuning indicator,<sup>16</sup> fitted with an auxiliary anode. In the latter case the cathode and auxiliary

anode of the indicator are connected across the additional bias. When the glow column reaches the auxiliary anode, conduction occurs and the bias is shorted.

**12.9. Noise Limiters.**<sup>34</sup> A noise limiter differs from a noise-suppressing device in that it allows the normal A.F. signal to be accepted and seeks only to limit the unpleasant effects produced by atmospheric and similar disturbances. The simplest method is to use a biased diode in the A.F. or R.F. circuits. For normal signal amplitudes the diode is non-conducting, but a peaked signal of excessive amplitude (a typical noise pulse shape) applies a voltage exceeding the bias, and conduction current damps the circuit, so flattening the resultant A.F. output peak voltage. Two diodes, connected to conduct in opposite directions, are often used, one limiting excessive positive and the other excessive negative peaks. A circuit \* which avoids the necessity for fixed bias on the limiting

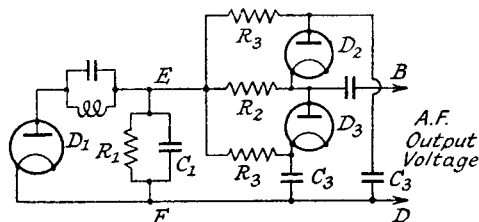


FIG. 12.19.—A Circuit for Limiting Interference on Noise Voltage Peaks.

diodes is shown in Fig. 12.19. The A.F. detector is  $D_1$ , and the noise limiting diodes,  $D_2$  and  $D_3$ , function to damp negative and positive peaks of noise respectively. Their biasing voltage is derived from detection of the A.F. output voltage across the detector load resistance,  $R_1$ . The damping of positive and negative half-cycles due to the load imposed by  $D_2$  and  $D_3$  is equal, so that the A.F. voltage across  $BD$  is undistorted. A short duration positive noise pulse of large amplitude, appreciably exceeding the bias due to detection of the desired A.F. voltage, causes diode  $D_3$  to take a large momentary current, which damps and flattens the output voltage noise peak across  $BD$  compared with the input voltage peak at  $EF$ . Diode  $D_2$  functions in the same manner for negative noise pulses. The resistances  $R_3$  ( $2\text{ M}\Omega$ ) and the common resistance  $R_2$  form the load resistances for  $D_2$  and  $D_3$ , and capacitances  $C_3$  ( $0.001\ \mu\text{F}$ ) act as the coupling to  $D_2$  and  $D_3$ . The resistance  $R_2$  ( $0.2\text{ M}\Omega$ ) is included

\* U.S. Patent Application, No. 391, 162. (1941) R. C. V. and V. A. Landon.

to form one arm of a potential divider, the other arm being the diodes  $D_2$  and  $D_3$ , and it aids in suppressing the noise peaks.

In another method of noise limiting<sup>19, 21</sup> the noise voltage peaks are amplified and detected separately from the desired signals; the D.C. component of the detected noise voltages is used to bias the I.F. amplifier before the A.F. detector and reduce considerably its amplification during interference peaks. The input voltage for the noise amplifier is derived from the input to the I.F. amplifier before the A.F. detector. The valve for the noise amplifier is of the non-variable-mu type and it is overbiased. The input-output voltage characteristic is parabolic, and normal modulated signals are not amplified to any great extent; the large amplitude noise peaks, however, produce appreciable output voltages, which are detected by a biased detector across the output circuit. Biasing is applied to this detector in order to ensure that there is no detection of normal modulated signals. The I.F. amplifier preceding the A.F. detector is of the heptode or hexode type, the negative bias from the noise detector being connected to the "oscillator" grid, and the desired modulated carrier to the control grid. The filter between the noise detector and hexode grid must have a low time-constant (not greater than about 0.01 seconds) in order to obtain a rapid increase and decrease of bias voltage. If the action is slow the noise suppression is ineffective at the beginning of the pulses, and also the normal signal may be rendered inaudible for some time after the noise pulse has passed. This low time-constant makes filtering difficult, and a push-pull noise detector is an advantage because of the lower I.F. ripple voltage.

## 12.10. Audio Frequency A.G.C.

**12.10.1. Introduction.** Automatic gain control may be applied to A.F. amplifiers to give decreasing or increasing gain as the A.F. signal is increased. Decreasing gain control is generally only applied in public address systems to prevent blasting, or to preserve a reasonably level output when amplifying speech. Increasing gain control, known as contrast expansion, may be used to counteract the compression in intensity level range that must be made at a transmitter to obtain efficient modulation operation without overloading. It can only be satisfactory if compression at the transmitter is performed automatically by apparatus, the characteristics of which can be reproduced in inverse form as expansion at the receiver. At present compression is performed manually by skilled operators, so that an expansion circuit giving

correct compensation is not possible. Expansion can, however, be used with advantage to compensate for volume contraction (which is usually performed electrically) in gramophone records.

Whilst contrast expansion often adds to the realism of an orchestral transmission, it is not suitable for all types of programme. For speech or song it is less satisfactory owing to the discontinuous nature of the signal.

**12.10.2. A.G.C. with Decreasing Amplification for Increasing A.F. Input.**<sup>29</sup> The basic principle is the same as that involved in the application of A.G.C. to R.F. amplifiers. The A.F. voltage is amplified, then detected, and the D.C. component from detection is used to control the amplification of one or more of the A.F. stages. Control of a single A.F. tetrode valve is not usually

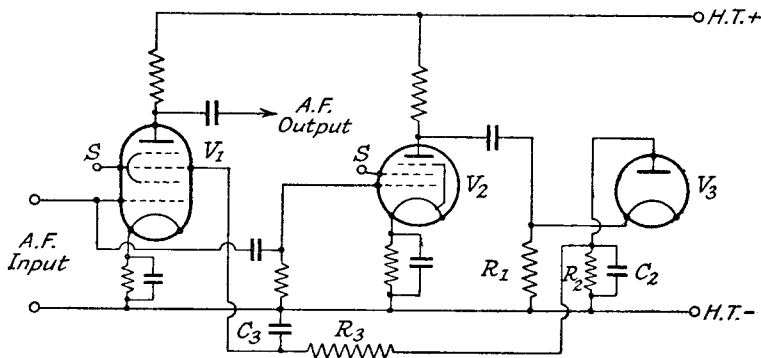


FIG. 12.20.—A.G.C. of an A.F. Signal Voltage.

satisfactory, because the curvature of its  $I_a E_g$  characteristic (this is essential in order to make  $g_m$  variable with grid-bias voltage) produces distortion of the A.F. voltage. This distortion results chiefly in even harmonic frequencies, and it may be almost entirely eliminated by using two valves in push-pull with the A.G.C. bias applied to the grid-earth return lead common to both valves. An alternative is to employ a pentode, heptode or hexode valve, and to apply the A.G.C. bias to the suppressor grid or the oscillator grid. If suppressor grid control<sup>30</sup> is used with a pentode valve, the latter usually has to be designed with a finer mesh suppressor grid than is normal, otherwise very large biases are required before any appreciable reduction in amplification can be achieved. A possible circuit using a hexode valve is shown in Fig. 12.20. The A.F. input voltage is applied to the signal grid of the hexode valve  $V_1$ , and also

to the grid of the buffer valve  $V_2$ , before the A.G.C. detector,  $V_3$ . The buffer valve is necessary to prevent distortion of the input A.F. wave shape by conduction current damping from  $V_3$ , but it also increases the effectiveness of the A.G.C. control. It should be noted that this circuit is not the same as that for amplified A.G.C. of R.F. stages, because the bias voltage is being used to control the gain of an amplifier after the point from which the operative voltage for A.G.C. is taken. In this case the effectiveness of control is dependent on the amplification of the buffer valve as well as upon the delay bias (if any). The A.G.C. detector D.C. load resistance is divided between two resistances,  $R_1$  and  $R_2$ , and the bias voltage is taken from  $R_2$ . Although the available bias voltage is reduced in the ratio  $\frac{R_2}{R_1 + R_2}$ , this method of divided load resistance has the advantage of making filtering of the A.F. voltages from the D.C. component easier. Only the ripple A.F. voltages appear across  $R_2$ , whilst across  $R_1$  is the full A.F. voltage as well as the ripple A.F. voltage. The time-constant of the A.G.C. filter circuit  $R_3C_3$  must not be so high as to cause overloading on the first syllables of words, nor low enough to cause serious mutilation of the A.F. output wave shape. A value of about 0.5 seconds is generally satisfactory. The degree of input-output control may be calculated by plotting input voltage change, expressed as a decibel ratio, against input voltage ratio increase plus the ratio reduction of  $g_m$  (due to the A.G.C. bias change) of  $V_1$ .

**12.10.3. A.G.C. providing Contrast Expansion.**<sup>26</sup> To make efficient use of a transmitter when broadcasting music, the normal intensity level variation (70 db.) of an orchestral programme must be compressed. The maximum possible modulation percentage is 100%, and the minimum, which is determined by the noise level, is about 1%, so that a maximum possible intensity variation of 40 db. only is permissible. Conditions at the receiver are usually such (owing to noise) as to limit the variation further to about 25 db. Although expansion to the original 70-db. range would not be desirable, and indeed would sound unnatural in a normal listening room, some degree of expansion is advantageous.

The circuit in Fig. 12.20 may be used for contrast expansion by reversing the anode-cathode connections to the A.G.C. diode  $V_3$ . This reverses the polarity of the A.G.C. bias to the hexode, so that increasing input voltage applies positive bias. An initial negative bias must be included in this circuit in order that the A.G.C. grid of the hexode may have a small negative bias even when the positive







Substituting 12.8 and 12.9 for  $I_1$  and  $I_2$  in the above, and noting that  $R_2$  is now  $R_2(max.)$

$$\text{loss (db.)} = -20 \log_{10} \frac{(R_1 + R_2(max.) + 2R_{sc})}{(R_2(max.) - R_1)} \quad .12.11b.$$

Equating 12.11a and 12.11b gives

$$R_1 R_2(max.) = R_{sc}^2.$$

Thus for  $R_{sc} = 2.5$  ohms, and loss at maximum power output from the valve of 3 db., we have,

$$\frac{R_1 + R_2(max.) + 2R_{sc}}{R_2(max.) - R_1} = \text{antilog}_{10} 0.15 = 1.413$$

and replacing  $R_2(max.)$  by  $\frac{R_{sc}^2}{R_1}$  gives after simplification

$$2.413R_1^2 + 5R_1 - 2.58 = 0$$

$$R_1 = 0.425 \Omega.$$

$$R_2(max.) = 14.7 \Omega.$$

#### BIBLIOGRAPHY

1. Automatic Gain Control. A. Dinsdale, *Wireless World*, Sept. 23rd (p. 290), and Sept. 30th (p. 327), 1932.
2. Automatic Volume Control. C. H. Smith, *World Radio*, Dec. 30th, 1932 (p. 1378), and Jan. 13th, 1933 (p. 53).
3. Practical Automatic Volume Control. W. T. Cocking, *Wireless World*, Jan. 6th (p. 2), and Jan. 13th (p. 29), 1933.
4. Automatic Volume Control. C. N. Smyth, *Wireless World*, Feb. 17th, 1933, p. 134.
5. The Influence of Fading Compensation on Contrast in Music. T. Sturm, *Funktechnische Monatshefte*, Feb. 1933, p. 139.
6. The History of A.V.C. *Wireless World*, March 31st, 1933, p. 236.
7. Automatic Gain Control of Radio Receivers. I. J. Cohen, *Post Office Electrical Engineers' Journal*, April 1933, p. 58.
8. Automatic Volume Control for Radio Receivers. C. B. Fisher, *Wireless Engineer*, May 1933, p. 248.
9. Corrected A.V.C. *Wireless World*, June 2nd, 1933, p. 386.
10. Delayed Diode A.V.C. W. T. Cocking, *Wireless World*, Sept. 8th, 1933, p. 208.
11. Delayed Amplified A.V.C. W. T. Cocking, *Wireless World*, Sept. 22nd, 1933, p. 244.
12. Q.A.V.C. F. L. Hossell, *Wireless World*, Jan. 19th, 1934, p. 43.
13. A.V.C. applied to A.F. Amplifier Tubes. J. R. Nelson, *Electronics*, Feb. 1934, p. 50.
14. Quiet, Amplified and Delayed A.V.C. with a Single Valve. *Wireless World*, April 27th, 1934, p. 296.
15. A.V.C. without Loss of Maximum Sensitivity. H. Pitsch, *Funktechnische Monatshefte*, May 1934, p. 182.

16. Methods of "Crack Killing". T. Sturm, *Funktechnische Monatshefte*, July 1934, p. 259.
17. The Design of A.V.C. Systems. W. T. Cocking, *Wireless Engineer*, Aug. (p. 406), Sept. (p. 476) and Oct. (p. 542), 1934.
18. The Determination of the Effectiveness of Antifading Devices. P. Mandel, *L'Onde Électrique*, Aug. 1935, p. 531.
19. A Noise Silencing I.F. Circuit for Superhet Receivers. J. J. Lamb, *Q.S.T.*, Feb. 1936, p. 11.
20. Light Bulb Volume Expander. *Electronics*, March 1936, p. 9.
21. Noise Elimination. *Wireless World*, March 27th, 1936, p. 314.
22. Delayed Detector Operation. J. H. Reyner, *Wireless World*, April 10th, 1936, p. 364.
23. Simplified Volume Expansion. W. N. Weeden, *Wireless World*, April 24th, 1936, p. 407.
24. Inexpensive Volume Expansion. R. H. Tanner and V. T. Dickins, *Wireless World*, May 22nd, 1936, p. 507.
25. Distortionless A.V.C. Systems. W. T. Cocking, *Wireless World*, June 12th, 1936, p. 574.
26. Contrast Amplification. W. N. Weeden, *Wireless World*, Dec. 18th, 1936, p. 636.
27. Distortion produced by Delayed Diode A.V.C. K. R. Sturley, *Wireless Engineer*, Jan. 1937, p. 15.
28. Contrast Expansion. G. Sayers, *Wireless World*, April 16th, 1937, p. 378.
29. A.V.C. in P.A. Equipment. *Wireless World*, Aug. 6th, 1937, p. 119.
30. Volume Expansion Problems. M. C. Pickard, *Wireless World*, Aug. 27th, 1937, p. 186.
31. Time Constants for A.V.C. Filter Circuits. K. R. Sturley, *Wireless Engineer*, Sept. 1938, p. 480.
32. A.V.C. Characteristics and Distortion. E. G. James and A. J. Biggs. *Wireless Engineer*, Sept. 1939, p. 435.
33. A.V.C. Developments. W. T. Cocking, *Wireless World*, Dec. 1939, p. 51.
34. Noise Suppression by Means of Amplitude Limiters. M. Wald, *Wireless Engineer*, Oct. 1940, p. 432.
35. D.C. Amplified A.V.C. Circuit Time Constants. K. R. Sturley and F. Duerden, *Wireless Engineer*, Sept. 1941, p. 353.

## CHAPTER 13

# PUSH-BUTTON, REMOTE AND AUTOMATIC TUNING CONTROL <sup>17</sup>

**13.1. Introduction.** Push-button tuning is incorporated in receivers so that predetermined stations may be tuned in immediately by pressing a switch.

By the extension, when practicable, of the push-button switching to a position at some distance from the receiver, remote control of tuning is possible. Special circuits have also been designed to give continuous tuning over a range of frequencies at a remote point. The A.G.C. action of a remotely-tuned receiver must be such as to reduce output volume changes due to input signal variations to small proportions, unless a remote volume control is used. The ideal remotely-tuned receiver should, of course, include remote control of all the functions normally operated by hand. Methods of achieving this are, however, discussed in their appropriate chapters, i.e., automatic variable selectivity in Section 7.10, Part I, and automatic gain control in Chapter 12.

The use of highly selective I.F. circuits in a superheterodyne receiver makes accurate tuning a necessity if correct reproduction, free from distortion, is to be obtained. An early method of ensuring correct manual tuning was to use a highly selective circuit, tuned to the I.F. carrier, to operate a muting device. The receiver was silenced until the I.F. carrier entered the narrow pass range of this circuit. This offered no solution to the problem of accurate tuning of push-button receivers. The method now adopted (known as automatic frequency correction) is to adjust automatically the oscillator frequency so as to set the I.F. carrier in the centre of the I.F. amplifier pass-band irrespective of the signal tuning. This means that the signal circuits may be mistuned, but the effect is much less serious than off-centring the I.F. carrier. A variable reactance, connected in parallel with the oscillator tuned circuit, is controlled by the degree of I.F. carrier tuning error and is varied in such a direction as to reduce the error.

## 13.2. Push-Button Tuning.

**13.2.1. Introduction.**<sup>7</sup> A broadcast receiver is usually operated on a few selected (often local) stations, and there are advantages

in being able to switch over almost instantaneously from one programme to another. This is possible with push-button tuning, which may be accomplished in either of two ways. In the first the tuning capacitor may be rotated mechanically by means of cams operated from push buttons, or electrically by a motor. The second switches in pretuned circuits. In both systems it is usual to silence the receiver whilst the change is being made from one station to another. Automatic frequency correction of the oscillator is almost an essential requirement if accurate tuning is to be achieved and maintained.

### 13.2.2. Mechanical Rotation of the Tuning Capacitor.<sup>13</sup>

There are a number of methods of mechanical tuning by push-button. One uses selecting levers connected to specially shaped cams equal in number to the stations required. Each cam is fixed to the rotor shaft of the capacitor. Pressure on the lever rotates the cam to the position corresponding to the desired station setting. The disadvantage of this system is that considerable pressure is required to operate the push-button, very careful mechanical design is necessary for reasonably accurate tuning, and wear of moving parts leads eventually to incorrect tuning.

Another mechanism employs spiral-shaped stator and rotor capacitor plates. Change of capacitance is obtained by moving the "rotor" in or out of mesh with the stator. The amount of mesh is determined by the travel of the push-button, the position of which is adjustable by means of a set screw. Each push-button can easily be set to any desired station in the wave range covered by the tuning capacitor variation, after the receiver has been installed.

A third method of rapid mechanical station selection is by an automatic telephone type dial fixed to the tuning capacitor shaft. A finger is inserted in the hole marked with the appropriate station and the dial is rotated until a stop is encountered. At this point the capacitor setting is correct for the desired station. Unlike the automatic telephone dial there is no return to the original position. The width of the finger-hole prevents the selection of stations close together in frequency though this difficulty may be overcome by staggering the holes. Another disadvantage is that the user cannot change to stations other than those already selected by the manufacturer.

### 13.2.3. Electrical Rotation of the Tuning Capacitor.<sup>10</sup>

Electrical rotation of the tuning capacitor is accomplished by a small reversible induction motor (24-volt) geared to the capacitor shaft. The motor is generally of the shaded pole type, with two field

windings, connected in series, and a metal disc (copper or brass) as a rotor. One of the two field windings is centre-tapped, only one half of the coil being in circuit at a time, and the centre tap is connected to one end of the other field winding. By changing the supply from one-half of the coil to the other, the direction of the motor is reversed. The motor may be arranged to reverse direction only at the ends of the capacitor shaft travel (the reversing switch is operated by a cam on the shaft), or the selector mechanism may be so connected that the capacitor is always turned towards the tuning point of the desired station, i.e., direct "homing" is used. The first method is less satisfactory because the capacitor is taken to the end of the scale and then reversed, when it is desired to accept a transmission "behind" the initial tuning setting. This entails loss of time in tuning and greater wear on moving parts.

In the first type each station has its own disc mounted on the capacitor shaft, and let into the disc is an insulating segment at a position corresponding to the correct station setting. One side of the push-button switch is connected to a brush rubbing on the disc circumference; the other side is joined to the motor, which itself is connected to a secondary of the mains supply transformer. The circuit is completed by the lead from transformer to disc. Closing of the push-button switch energizes the motor, which rotates until the insulating segment on the disc open-circuits the motor supply. The reversing switch is operated by a cam on the capacitor shaft when the latter reaches either end of its travel. A clutch disengages the motor drive immediately the supply is switched off. This is achieved by a spring-loaded armature, which in the rest position is out of line with the stator. Current induced in the armature pulls it into line with the stator, thus actuating the clutch. Contacts short-circuiting the loudspeaker speech-coil are also closed by the lateral movement of the armature.

Slight modification of the selector disc can give automatic reversal of the motor when the desired station setting is behind the starting position of the capacitor. The disc is divided into two equal sectors, one insulated from, and the other connected to, the tuning capacitor shaft as shown in Fig. 13.1. The insulated sector is connected via an insulated slip ring and sliding contact  $S_1$  to one end of the "forward" coil  $A$  of the driving motor. The other sector is connected through the sliding contact  $S_2$  on the capacitor shaft to the "reversing" coil  $B$  of the motor. The station selector contacts, two of which,  $SS1$  and  $SS2$ , are shown in Fig. 13.1, are joined to their appropriate push-button switches,  $B_1$ ,  $B_2$ , etc. They ( $SS1$ ,

etc.) are often mounted on a semicircular rail, coaxial with the disc, and their positions are adjustable in order that any desired transmissions can be selected. The selective operation is best illustrated by reference to Fig. 13.1. With push-button  $B_1$  closed, the supply is connected through  $SS1$ , the uninsulated sector, the tuning capacitor shaft and sliding contact  $S_2$  to the reversing field coil  $B$ . The motor rotates the capacitor shaft in an anti-clockwise direction until the insulation between the sectors breaks the supply circuit. The clutch from motor to the gear drive immediately dis-

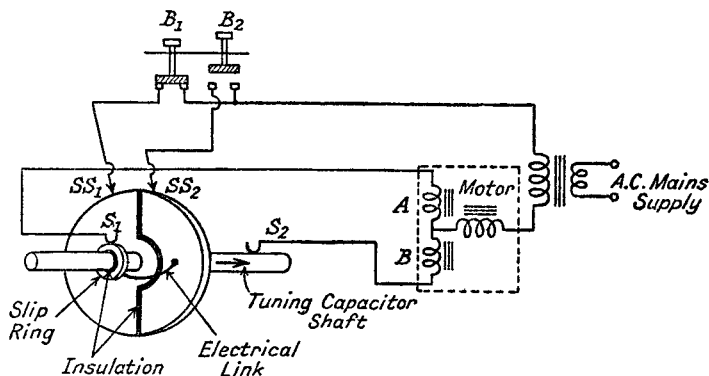


FIG. 13.1.—Reversible Motor Driven Tuning.

engages as described above, at the same time open-circuiting the loudspeaker speech-coil and allowing station 1 to be heard. Pressing  $B_2$  releases  $B_1$  and connects the supply through  $SS2$ , the insulated sector, slip-ring and sliding contact  $S_1$  to the forward coil  $A$  of the motor, which rotates the capacitor shaft in a clockwise direction until the insulation comes under  $SS2$ . The motor supply and speech-coil are open-circuited and station 2 is heard.

**13.2.4. Preset Tuned Circuits.** Push-button selection of desired transmissions may be achieved by switching capacitors in parallel with a given coil, or vice versa. The switched capacitor or inductor must be capable of being trimmed in order that receiver circuits can be either correctly tuned to the desired transmission or changed from their initial setting to any other within reasonable frequency range of the original. The trimming range (the variation from maximum to minimum capacitance or inductance) should not be too large otherwise tuning frequency adjustment becomes critical and susceptible to mechanical jarring and the effects of temperature. From this point of view a switched trimmed inductance is preferable

to a capacitance, its actual value varying less with temperature and humidity change than that of a trimmed capacitance.

With inductance switching a fixed capacitor of the silvered mica type is often used, because it can be made with a low negative capacitance-temperature coefficient, which helps to balance the positive inductance-temperature coefficient of the coil. Inductance trimming is generally realized by having a screwed central iron-dust core, with a slotted head to take a screwdriver. Alternatively the dust core may be attached to a metal screw, having a lock-nut; this has advantages because the threading on the iron-dust core is liable to wear, must be of coarser pitch and is less easy to lock than a metal threaded screw. A separate trimmed inductance is required for each push-button switch, but the same fixed tuning capacitance may be employed, e.g., in changing from the long- to medium-wave range, it is only necessary to switch the inductance. With switched capacitors it is generally necessary to change the fixed inductance when transferring from one range to another.

Of the two types of circuit involved in tuning the superheterodyne receiver, the oscillator is more critical than the signal-tuned circuit, and the highest possible stability is required of the tuning components of the former, unless automatic frequency correction is employed. Stability of component values, though desirable, is not so essential in the signal circuits, particularly in the case of short-wave operation.

There are three types of push-button switches meriting description. The simplest is the shorting bar, shown shaded in Fig. 13.2*a*;

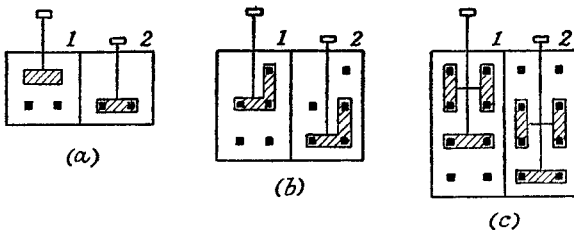


FIG. 13.2.—Examples of Push Button Switching.

- (a) Simple short-circuit strip. (b) L-shaped short-circuit strip.  
 (c) A more complicated three-section short-circuit strip.

in position 2 the switch is operative. It is suitable for selecting an inductance or capacitance and connecting it to its other tuning element, which must be permanently connected to the grid of the amplifying valve. The L-shaped shorting strip with three rows of contacts, as shown in Fig. 13.2*b*, has the following advantages:

(1) the extra contact in the top row can be used to short-circuit unwanted coils, the coil being connected between this contact and the right-hand one of the middle row immediately below it ; (2) the grid of the valve and the appropriate tuning capacitance need not be permanently connected, the former being connected to the bottom left-hand contact and the latter to the bottom right-hand contact. This is a particularly useful feature when one of the push-button switches is used to convert to manual tuning with the normal variable capacitor.

A more complicated four-row switch is illustrated in Fig. 13.2c. In the operating position 2, rows 1 and 2 are disconnected from each other, 2 and 3 are joined and row 4 is short-circuited. Such a switch could be used to open circuit a selected coil, connect it to its tuning capacitor and also select a reaction winding in an oscillator circuit.

### 13.3. Remote Control.

**13.3.1. Introduction.** Many methods of station selection at a point remote from the receiving apparatus have been developed. Rotation of the variable tuning capacitor by a magnetic relay or motor, a ratchet relay selecting preset components and operated by pulses sent via the mains supply wiring or direct from a portable oscillator, transfer of the R.F. and frequency changer stages to the remote point, magnetic tuning, and the use of tuned lines are some of the methods which have been successfully employed.

**13.3.2. Rotation of the Tuning Capacitor.** A very early method<sup>1</sup> of remote control used an iron-armature motor driving the tuning capacitor. The position of the armature was controlled by two field coils at right angles. Resistances across the end of the lines at the remote point controlled the current in each field coil, and the armature was rotated to the position of maximum magnetic field. The disadvantage was that only a small torque was available and friction had to be reduced to a low value. However, selection of any station in the wave band was possible.

The motor drive described in 13.2.3 is very suitable for remote control, since the push-button switches can easily be located at a distance from the receiver. Continuous tuning over the wave range is not, however, practicable.

**13.3.3. Pulse Control using Mains Supply Wiring.** Two methods of remote control by sending pulses to the receiver via the internal mains wiring have been developed. One uses D.C. pulses and the other R.F. pulses.



A simplified diagram of the circuit for D.C. control pulses<sup>16</sup> is shown in Fig. 13.3. The source of D.C. is a transformer  $T_1$ , developing a secondary voltage of about 8 volts, and a full wave rectifier producing about 1.5 amps. at 10 volts. The primary of  $T_1$  is connected in series with the D.C. circuit to act as a choke allowing the D.C. pulses to be passed without short-circuiting the mains supply. Closing switch  $S$  sends to the mains leads, a D.C. pulse which energizes a low voltage relay  $R$  (0.35 volts, 5 mA) at the receiver. The D.C. voltage across the relay is small because of the low resistance of the incoming mains supply network, which forms with the primary of  $T_1$  a potential divider for the D.C. voltage. A.C. must not be allowed to energize the relay, or chattering results. Cancellation of the A.C. voltage is obtained by connecting the relay between one terminal  $A$  of the primary and one terminal  $B$  of the secondary of a 1:1 transformer  $T_2$ . The A.C. voltages across

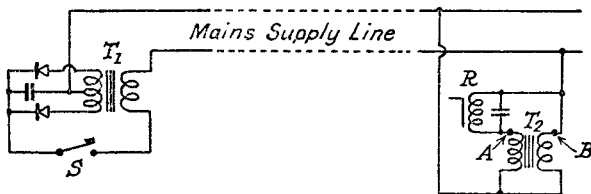


FIG. 13.3.—Remote Control by D.C. Pulses sent via the Mains Wiring.

primary and secondary are equal, so that the net A.C. voltage from  $A$  to  $B$  is zero and no A.C. load is applied to the transformer. The D.C. resistances of the primary and secondary are unequal so that a D.C. voltage is developed across the terminals  $AB$  during pulse excitation. The primary side  $A$ , which is in series with the relay, has a low resistance (about  $3.5 \Omega$ ), and the secondary side  $B$  has a high resistance ( $200 \Omega$ ). A large capacitance is connected across the relay as a precaution to by-pass any out-of-balance A.C. voltage. The relay itself has insufficient torque to drive a ratchet selector mechanism, and it is used to operate an intermediate relay from an auxiliary rectifier at the receiver. The number of pulses sent determines the station selected.

An interesting development<sup>11</sup> of remote control by transmission of modulated pulses of R.F. voltage along the mains leads is illustrated in Fig. 13.4. The R.F. oscillator heater and H.T. supplies are obtained by transformer from the mains supply, and no rectifier is used in the H.T. source. The result is that the oscillator output is modulated by half-sine waves of the mains frequency, oscillation

ceasing when the A.C. anode-to-cathode voltage begins its negative half-cycle. Apart from the elimination of a rectifier there are other important advantages conferred by using a half-sine modulated pulse, and these are discussed below. The modulated output is transmitted via the coupling coil  $L_1$  and capacitance  $C_1$  to the mains lead. The capacitance  $C_1$  (about  $0.001 \mu\text{F}$ ) has a low reactance to the radio frequency and a high reactance to the mains frequency, thus preventing a short-circuit of the mains supply by  $L_1$ . The R.F. voltage is accepted at the receiver via the capacitance  $C_2$ , of the same value as  $C_1$ , and coil  $L_2$ , and it operates one of two anode-bend detector valves,  $V_2$  and  $V_3$ , having in their anode circuits relays driving ratchet selector mechanisms. The H.T. supply to the detectors is derived from the mains without using a rectifier. This

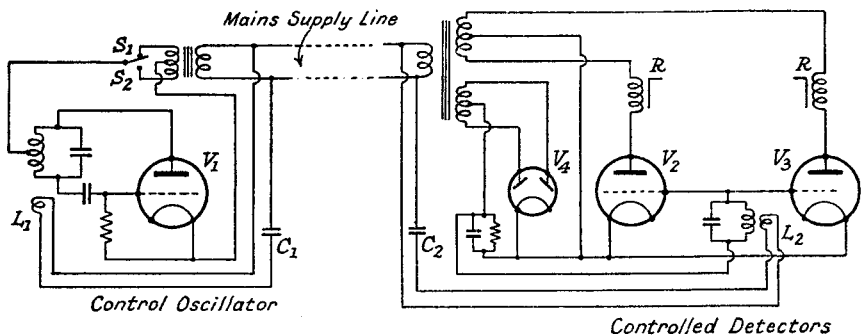


FIG. 13.4.—Remote Control by Pulses from a R.F. Oscillator.

method of detector and oscillator H.T. supply allows one oscillator to perform two functions, such as station selection and volume control, at the receiver. The relay in  $V_2$  anode circuit performs, for example, the first, and that in  $V_3$  anode circuit the second. Thus, with the oscillator switch in the  $S_1$  position, the positive H.T. cycle on the oscillator coincides with the positive H.T. cycle on the anode of  $V_2$ , and  $V_2$  is operative. Conversely with the switch in the  $S_2$  position, detector  $V_2$  is non-conducting when the oscillator functions and its relay is not energized. Detector  $V_3$ , with reversed H.T. supply, conducts during the same half-cycle as the oscillator, and its relay is, therefore, energized. The ratchet mechanism is operated each time switch  $S_1$  or  $S_2$  is closed. The pulse oscillator frequency is about 400 kc/s, and radiation beyond the house wiring is not usually serious. A R.F. filter may be inserted in the incoming mains leads as an additional protection. Loading of the mains

supply by other electrical apparatus, such as soldering irons and lamps, has little effect on the R.F. transmission characteristics of the leads. The oscillator has an output of about 100 watts and the resonant circuit at the detectors steps up the control voltage at the receiver from about 0.8 to 30 volts R.M.S. The rectifier valve  $V_4$  supplies D.C. grid bias for the anode-bend detectors.

A special cold cathode gas-filled valve is used for switching on the supply to the receiver, and no energy is consumed by the receiver until a suitable R.F. pulse is received from the control oscillator. The cold cathode valve is very suitable for use on a mains voltage of 110, but cannot be operated from 230 volts. It is similar in principle to the gas-filled discharge valve used for time-base operation with cathode ray tubes. The R.F. pulse from the oscillator starts conduction between auxiliary electrodes, and this initiates the main discharge which energizes the on-off relay. The H.T. for the discharge path is obtained from the mains, and ceases on negative half-cycles, so that the valve only functions as long as the R.F. pulse maintains the auxiliary discharge, i.e., switching off the oscillator also shuts down the receiver.

**13.3.4. R.F. Pulses from a Portable Oscillator.**<sup>14</sup> A small battery-operated oscillator is situated at the remote point, and R.F. pulses, produced by interruption of the filament supply to the oscillator, are transmitted direct to the receiver. A tuned circuit coupled to a detector at the receiver accepts the pulses, which operate a ratchet relay selecting the required coil or capacitor. An automatic telephone type dial is used to interrupt the portable oscillator, and the required station is selected in accordance with the number of pulses transmitted.

**13.3.5. Transfer of R.F. and Frequency Changer Stages to the Remote Point.**<sup>15</sup> The signal and frequency changer stages are connected to the rest of the receiver by a multi-core cable carrying the aerial, earth, I.F., A.G.C., manual volume control, H.T. and L.T. supplies, and on-off switch leads. Matching transformers are required at each end of the aerial and I.F. lines. The method has the advantage of allowing continuous tuning over the wave range, but the unit is comparatively bulky.

**13.3.6. Magnetic Remote Tuning.**<sup>6, 12</sup> The inductance of an iron-dust-cored coil may be varied by placing it in a strong D.C. magnetic field. An inductance variation of about 9 : 1 is achieved for a change of 1.5 to 5 watts in the D.C. power to the electromagnet. Inductance tuning is possible by controlling the D.C. polarizing field. The control resistances for each electromagnet coil are ganged and

placed at the remote control point. Continuous tuning over a wave band is possible.

**13.3.7. Tuned Lines.<sup>5</sup>** The reactance and standing wave properties of R.F. cables have been employed to give push-button and continuous tuning control. First circuit noise is usually of secondary importance in remote control since only stations of reasonable daylight strength are normally selected, and a low impedance cable is not therefore a serious disadvantage. Station selection on long and medium waves can be achieved at distances up to 100 feet from the receiver.

Signal and oscillator frequency preselection is shown in Fig. 13.5. The aerial is coupled through a R.F. cable to coil  $L_1$ , which is loosely

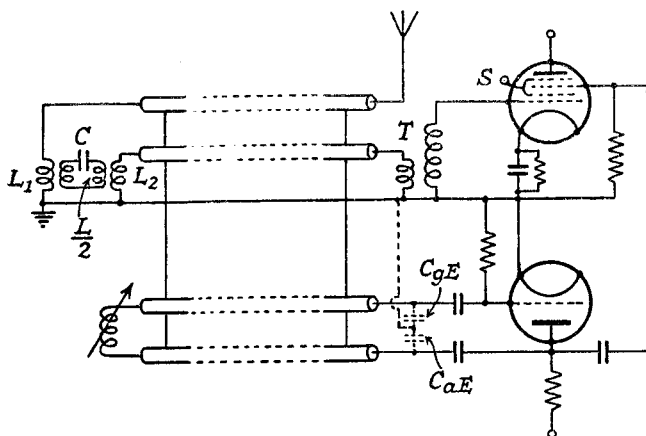


FIG. 13.5.—Remote Signal and Oscillator Tuning by means of Feeder Lines.

coupled to half the coil,  $\frac{1}{2}L$ , of the remote tuned circuit. The other half of  $L$  is loosely coupled to  $L_2$ , which connects to the screened cable. The receiver end of the screened cable is terminated in a wide frequency-acceptance-band transformer  $T$ , which steps up the voltage to the frequency changer grid. The tuning capacitance  $C$  has a series of preset values, which are switched in by push-buttons, and the tuning coil has a high  $Q$  value. The aerial-to-grid amplification is less than that of a single tuned circuit, but the selectivity is comparable. A Colpitts oscillator is shown, the cable acting as the splitting capacitance, but a back-coupled oscillator may also be used. For continuous tuning a high I.F. (about 2 Mc/s) is necessary, and the oscillator lead is used as a quarter-wave line. A small variable capacitor in series with an inductance at the remote end

controls the oscillator frequency, and it may be ganged with the capacitor tuning the signal circuits.

### 13.4. Automatic Frequency Correction.<sup>3</sup>

**13.4.1. Introduction.** Two effects, sideband "screech" and harmonic distortion, become very pronounced if the I.F. carrier frequency at the output of the frequency changer stage of a superheterodyne receiver is not correctly centred in the comparatively narrow pass-band of the I.F. amplifier. Sideband "screech" is characterized by high-pitched distorted reproduction, and it occurs when the I.F. signal carrier is detuned to the side of the I.F. selectivity curve. In this condition the equivalent of single sideband reception with over-accentuated high-frequency sideband components is obtained, because one set of sidebands is almost entirely eliminated, and the carrier and low-frequency sidebands are reduced by being outside the pass range. Harmonic distortion of the audio output is caused by the diode detector when one set of sidebands is removed. With normal pass-band widths ( $\pm 5$  kc/s) the maximum tolerable mistune is about  $\pm 1$  kc/s. Automatic correction of the oscillator frequency overcomes this difficulty by reducing the error produced by inaccurate tuning, or frequency drift of the oscillator due to temperature and other effects. For example, a signal-tuning error of 5 kc/s may be reduced to an I.F. carrier error of 50 c.p.s. by this method.

The two units of the automatic frequency corrector are a discriminator or error detector, and a control device. The former translates the error in the I.F. carrier into a voltage, the magnitude and sign of which is a function of the error. The latter, operated from the discriminator voltage, provides frequency correction of the oscillator tending to reset the I.F. carrier in the centre of the I.F. amplifier pass-band. The operation of the system can be represented by an overall characteristic giving the final intermediate frequency error with different signal frequency tuning settings, and this is described in Section 13.4.4. The shape of the overall control characteristic is mainly dependent upon the discriminator, but the action of the control device, especially if it has a non-linear characteristic, modifies the result.

**13.4.2. The Discriminator.** A typical discriminator voltage-frequency curve is shown as dashed curve *ABODE* in Fig. 13.6*a*. The accuracy of control is determined by the slope *BOD*, and the final frequency error after correction is least when *BOD* has the greatest slope. It should be noted that automatic frequency

correction is similar to A.G.C., i.e., control is only exercised when there is a change in frequency, and correction can very much reduce, but not eliminate (except in special cases), the error. Two important frequencies in A.F.C. are the "pull-in" and "throw-out" points. The former is the signal-tuning setting at which A.F.C. comes into operation when approaching the required station setting; it is governed by the outer portions *AB* and *DE* of the characteristic. The latter is the signal-tuning setting at which A.F.C. loses control when tuning away from a station; it is mainly determined by the

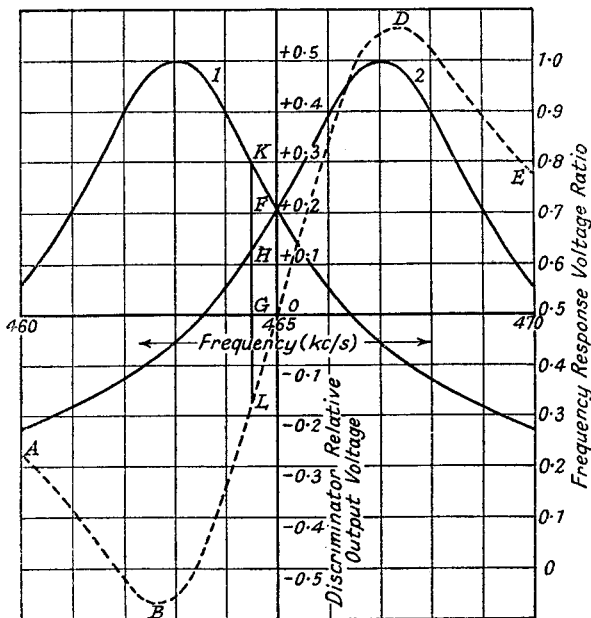


FIG. 13.6a.—Characteristic Curves for the Amplitude Discriminator.

distance of *B* and *D* from the horizontal axis. The "throw-out" signal-tuning setting is always greater than the "pull-in", and it may be several channels away from the correct setting, thus causing a number of stations to be skipped when tuning away from the station. For this reason during manual tuning it is usual to disconnect A.F.C. with a friction switch operated by rotation of the tuning capacitor. The actual values of the throw-out and pull-in frequencies can be calculated from the discriminator and control device curves as described in Section 13.4.4.

There are two types of discriminator, one known as the amplitude<sup>2</sup> and the other as the phase discriminator.<sup>4</sup> An example of

the first is shown in Fig. 13.7. Two circuits, one (No. 1) tuned to a frequency about 2 kc/s below, and the other (No. 2) to 2 kc/s above the correct I.F. carrier frequency, are transformer-coupled to the anode circuit of a valve, deriving its input voltage from a proportion of the output voltage of the last I.F. stage in the receiver. Provided stray coupling between 1 and 2 is small and the slope resistance of  $V_1$  is large compared with the maximum impedance across the primaries of 1 and 2, the frequency response of either circuit is unaffected by the other. The frequency response of each circuit relative to the response at the resonant frequency is shown by the curves 1 and 2 in Fig. 13.6a; these curves are obtained from the generalized selectivity curve of Fig. 4.3, Part I, as described below. They are identical in shape and displaced from each other by 4 kc/s. Diode detectors ( $D_1$  and  $D_2$  in Fig. 13.7) across these

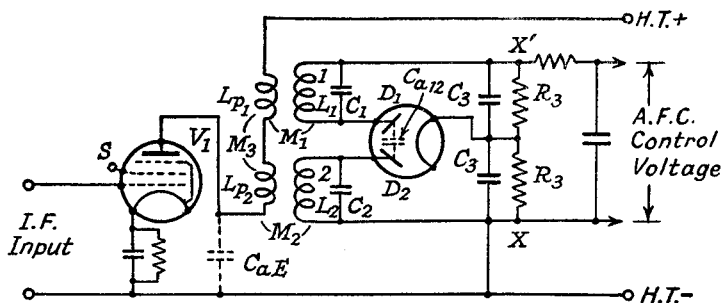


FIG. 13.7.—A Typical Amplitude Discriminator Circuit.

circuits, have their D.C. output voltages connected in series opposition. When there is no tuning error, the I.F. carrier voltages across 1 and 2 are equal (proportional to  $OF$  in Fig. 13.6a) and there is zero D.C. voltage across points  $XX'$  in Fig. 13.7. Mistuning to a lower I.F. carrier frequency (point  $G$  in Fig. 13.6a) increases to  $GK$  the proportional voltage applied to  $D_1$  and decreases to  $GH$  that applied to  $D_2$ . Hence the D.C. output voltage at  $XX'$  is negative and proportional to  $HK$ , i.e., to  $GL$ ; its actual value can be found by multiplying  $GL$  by the product of a constant  $K$  and the voltage detection efficiency of the diodes. The constant  $K$  is a function of the input unmodulated carrier peak voltage to, and  $g_m$  of, the valve  $V_1$  in Fig. 13.7, the ratio of mutual inductance to secondary tuning inductance, and the resonant or dynamic impedance of the secondary. Voltage detection efficiency,  $\eta_d$  in Chapter 8, Part I, is the ratio of the D.C. voltage across one of the load resistances,  $R_3$ , in Fig. 13.7 to the unmodulated carrier peak voltage output from 1 or 2. The

steepness of the slope  $BOD$  (Fig. 13.6a) is fixed by the  $Q$  of the circuits 1 and 2, the intermediate frequency mid-carrier value, and the frequency separation of points  $B$  and  $D$ , so long as the stray coupling between the circuits is small. For any particular frequency separation of the points  $B$  and  $D$ , there is a value of  $Q$  which gives maximum slope to  $BOD$  at  $O$ . Lower or higher values of  $Q$  give a smaller slope at  $O$  and also greater curvature to the line  $BOD$ .

Assuming that the  $Q$  values of circuits 1 and 2 are equal, the optimum  $Q$  can be calculated as follows: from Section 4.2.3, Part I, the selectivity of a single tuned circuit, i.e., its frequency response in terms of that at the resonant frequency, is shown to be equal to  $\frac{1}{\sqrt{1+Q^2F^2}}$ , where  $F = \frac{2\Delta f}{f_r}$ , and  $\Delta f$  is the frequency difference (or off-tune) between the particular frequency considered and the resonant frequency  $f_r$ . Thus

$$\text{Selectivity} = \frac{1}{\sqrt{1+Q^2F^2}} \quad . \quad . \quad . \quad 13.1$$

and the slope  $S$  of the selectivity curve at any off-tune frequency  $\Delta f$  is

$$\begin{aligned} S &= \frac{d(\text{Sel}^v)}{d\Delta f} = \frac{d(\text{Sel}^v)}{dF} \cdot \frac{2}{f_r} \\ &= \frac{-Q^2F}{(1+Q^2F^2)^{\frac{3}{2}}} \cdot \frac{2}{f_r} \\ &= \frac{-4Q^2\Delta f}{f_r^2(1+Q^2F^2)^{\frac{3}{2}}} \quad . \quad . \quad . \quad 13.2. \end{aligned}$$

The value of  $Q$  which gives maximum slope for a fixed value of  $\Delta f$  is found by differentiating 13.2 with respect to  $Q$  and equating to zero. This gives

$$2Q \left[ 1 + \left( \frac{Q^2\Delta f}{f_r} \right)^2 \right]^{\frac{3}{2}} - 3Q^3F^2 \left[ 1 + \left( \frac{Q^2\Delta f}{f_r} \right)^2 \right]^{\frac{1}{2}} = 0$$

$$\text{or} \quad Q = \frac{f_r}{\sqrt{2}\Delta f} = \frac{0.707f_r}{\Delta f} \quad . \quad . \quad . \quad 13.3a.$$

It is important to note that expression 13.3a does not give maximum possible slope with a given  $Q$ ; this is found by differentiating 13.2 with respect to  $\Delta f$  and equating to zero, when

$$\Delta f = \frac{f_r}{2\sqrt{2}Q} = \frac{0.3535f_r}{Q} \quad . \quad . \quad . \quad 13.3b.$$

Expression 13.3b gives a larger value of  $\Delta f$  than that used for



calculating  $Q$  in expression 13.3a, but, though it produces a more sensitive discriminator characteristic, it is less satisfactory because it tends to increase the “pull-in” and “throw-out” frequency separations from  $f_m$ .

Although the condition for maximum slope at  $O$  for a fixed value of  $\Delta f$  is provided by expression 13.3a, a larger value of  $Q$ , such as  $Q = \frac{f_r}{\Delta f}$  actually gives a better discriminator characteristic. The

slope at  $O$  is only slightly reduced compared with that for  $Q = \frac{0.707f_r}{Q\Delta f}$ , but the frequencies corresponding to the peaks  $B$  and  $D$  (Fig. 13.6a) are closer to  $\pm\Delta f$ , and the characteristic falls much more rapidly outside the peaks, which means less difference between the “throw-out” and “pull-in” frequencies. However, the value of  $Q$  calculated from expression 13.3a is often higher than can conveniently be achieved in practice, and a suitable compromise is

$$Q = \frac{f_r}{2\Delta f} = \frac{0.5f_r}{Q} \quad \dots \quad 13.3c.$$

Examples of the discriminator characteristic for  $Q = \frac{f_r}{\Delta f}$ ,  $\frac{f_r}{2\Delta f}$  and  $\frac{f_r}{4\Delta f}$  are shown by curves 1, 2 and 3 in Fig. 13.6b (only half the character-

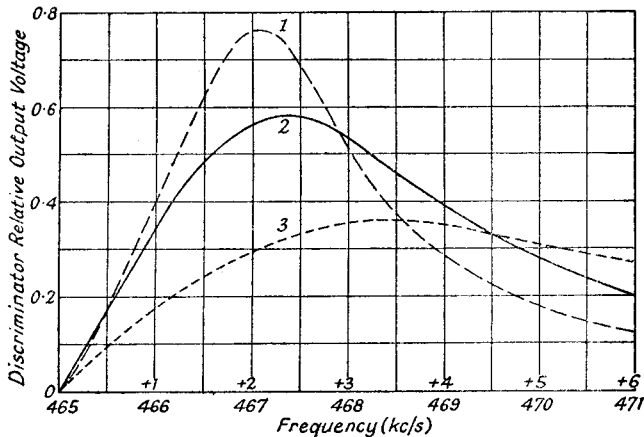


FIG. 13.6b.—Output Voltage Curves for an Amplitude Discriminator.

Curve 1.— $Q = \frac{f_r}{\Delta f}$ .      Curve 2.— $Q = \frac{f_r}{2\Delta f}$ .      Curve 3.— $Q = \frac{f_r}{4\Delta f}$ .

istic is illustrated, the other half on the negative side being identical in shape). The curves are derived from the single tuned circuit generalized selectivity curve of Fig. 4.3 (Part I) for  $f_r = 465$  kc/s,

$\Delta f = 2$  kc/s, as described later in this section. As  $Q$  is increased the frequency separation of peaks  $B$  and  $D$  is reduced and approaches  $2\Delta f$ , the peaks themselves increase in amplitude and the sections  $AB$  and  $DE$  fall away much more rapidly. Curve 1 ( $Q = \frac{f_r}{\Delta f}$ ) is similar to two  $S$  shapes joined at  $O$ ; the tail of the  $S$  at  $O$  is exaggerated in Fig. 13.6*b* in order to demonstrate the effect more clearly. Curve 2 ( $Q = \frac{f_r}{2\Delta f}$ ) is linear over most of the range  $BOD$  whilst curve 3 ( $Q = \frac{f_r}{4\Delta f}$ ) is appreciably curved from  $B$  to  $D$ , being similar to a single  $S$  shape. Frequencies of maximum response for curves 1, 2 and 3 are  $\pm 2.02$ ,  $\pm 2.4$  and  $\pm 3.5$  kc/s respectively. The "throw-out" and "pull-in" frequencies both tend to decrease as  $Q$  is increased, though the actual difference between the "throw-out" frequencies for curves 1 and 2 is dependent on the shape of the variable reactance characteristic (see Section 13.4.4) and may be quite small.

Substituting values of 465 and 2 kc/s for  $f_r$  and  $\Delta f$  gives  $Q$  values of 232.5, 116.25 and 58.125 kc/s for curves 1, 2 and 3. The first value is difficult to realize in practice, and in subsequent calculations we shall use expression 13.3*c* in determining  $Q$ . The discriminator characteristic is therefore that represented by curve 2, the resonant frequencies of circuits 1 and 2 (Fig. 13.7) are 463 and 467 kc/s and

$$Q_1 = \frac{463}{4} = 115.75.$$

$$Q_2 = \frac{467}{4} = 116.75.$$

For practical purposes we may take  $Q_1 = Q_2 = 116$ .

The two curves in Fig. 13.6*a* are obtained from Fig. 4.3, Part I, by taking  $Q$  as 116 and  $f_r$  as 465 kc/s, i.e., the off-tune frequency scale is positioned such that  $\Delta f = \frac{f_r}{2Q} = \frac{465}{232} \approx 2.0$  kc/s registers with  $QF = 1$ . The decibel scale of Fig. 4.3 is converted to a voltage ratio scale for plotting in Fig. 13.6*a*, curve 1 being plotted from a resonant frequency of 463 kc/s and curve 2 from a frequency of 467 kc/s. The error involved in fixing the position of the off-tune frequency scale for Fig. 4.3 by taking  $f_r$  as 465 instead of 463 and 467 kc/s is negligible.

Expression 13.2 gives the slope of the frequency response of one

of the tuned circuits, and it must be multiplied by 2 in order to obtain the slope at  $O$ . Hence maximum slope at  $O$  when  $\Delta f = 2$  kc/s is

$$S_{(max.)} = 2 \cdot \frac{4 \cdot (116)^2 \cdot 2}{(465)^2 (2)^{\frac{3}{2}}} = 0.352$$

= 0.352  $\eta_a K$  volts per kc/s off-tune per 1 volt peak input carrier.

If  $\Delta f$  is not fixed and a value larger than 2 kc/s can be tolerated, maximum slope for  $Q = 116$  is obtained when  $\Delta f = 2.828$  kc/s (expression 13.3b) and is

$$max. S_{max.} = 2 \cdot \frac{4 \cdot (116)^2 \cdot 2.828}{(465)^2 (1.5)^{\frac{3}{2}}} = 0.765.$$

In subsequent calculations we shall consider the condition that  $\Delta f$  is fixed and equal to 2 kc/s. On the assumption that  $R_a$  is much greater than the maximum primary impedance of circuit 1 or 2, the constant  $K$  is, from expression 4.30b, Section 4.4.2, Part I,

$$K = g_m \hat{E}_C R_D \frac{M}{L}$$

where  $g_m$  = mutual conductance of  $V_1$  in mA/volt

$\hat{E}_C$  = peak (unmodulated) carrier voltage applied to the grid of  $V_1$

$R_D$  = resonant or dynamic impedance of the secondary of 1 or 2.

$M$  = mutual inductance between primary and secondary

$L$  = inductance of the secondary.

Clearly greatest discriminator characteristic slope for a fixed  $g_m$  and  $\hat{E}_C$  requires  $R_D$  and  $\frac{M}{L}$  to be as large as possible. On the other

hand, too large a value of  $\frac{M}{L}$  and  $R_D$  produces a large primary impedance and causes the frequency response of one circuit to be affected by the other. Furthermore, stray capacitance coupling between the secondaries has a greater effect when  $R_D$  is increased.

Suitable values for  $R_D$  and  $\frac{M}{L}$  are 75,000 ohms and 0.3 respectively.

From Section 4.4.2, Part I, the maximum impedance across either primary (when the secondary is resonant) is  $R_D \frac{M^2}{L^2}$  (expression 4.29b),

i.e.,  $R_p = 75,000 \times 0.09 = 6,750$  ohms. This value is small compared with the probable minimum slope resistance of a tetrode

valve and the stray capacitance,  $C_{aE}$ , from anode to earth, so that we can safely assume that the series connection of the two primaries has little effect on the individual secondary frequency responses.

For the above selected values

$$\begin{aligned} K &= g_m \hat{E}_C \quad 75,000 \times 0.3 \\ &= 67.5 \hat{E}_C \end{aligned}$$

if  $g_m = 3 \text{ mA/volt.}$

Taking  $\hat{E}_C$  as 1 volt and  $\eta_d$  as 0.8, the maximum slope at  $O$  is

$$0.352 \times 0.8 \times 67.5 = 19.0 \text{ volts per kc/s off-tune per 1 volt peak input.}$$

The circuit constants for 1 and 2 may be calculated as follows :

*Circuit 1.*

$$Q_1 = 116, f_1 = 463 \text{ kc/s, } R_{D1} = 75,000 \text{ ohms}$$

$$\begin{aligned} L_1 &= \frac{R_{D1}}{\omega_1 Q_1} = \frac{75,000 \times 10^6}{6.28 \times 463 \times 10^3 \times 116} \\ &= 222 \mu\text{H} \end{aligned}$$

$$C_1 = 532 \mu\mu\text{F}$$

$$M_1 = 0.3L_1 = 66.6 \mu\text{H.}$$

A probable value for coupling coefficient,  $k_1 = \frac{M_1}{\sqrt{L_{p1}L_1}}$  between primary and secondary is 0.5, so that

$$L_{p1} = 80.5 \mu\text{H.}$$

If the detector load resistances  $R_s$  in Fig. 13.7 are 0.5 M $\Omega$ , the damping resistance due to diode conduction current is very nearly 0.25 M $\Omega$ . Hence the resonant impedance of the tuned secondary, in the absence of diode conduction current, must be

$$R_{D1}' = \frac{250,000 \times 75,000}{250,000 - 75,000} = 107,000 \text{ ohms}$$

and the  $Q$  of the coil is

$$Q_1' = \frac{R_{D1}'}{\omega_1 L_1} = \frac{107,000}{6.28 \times 463 \times 10^3 \times 222} = 165,$$

which is a practically realizable value.

*Circuit 2.*

Since the resonant frequency of circuit 2 is so close to that of 1, the circuit constants are almost equal, and the most practical

method is to use nominally identical circuits, and to off-tune the required 2 kc/s from 465 kc/s by trimming either the inductance or capacitance element.

The performance of the discriminator is adversely affected by stray coupling between the primaries or the secondaries of 1 and 2. These stray couplings cause the two peaks  $B$  and  $D$  to be unequal in distance from the frequency base line, and the line  $BOD$  tends to be curved in concave shape looking from  $A$ . Coupling is produced by the anode-earth capacitance  $C_{aE}$  of valve  $V_1$ , which allows a current to circulate in the two primaries, and also by the anode-to-anode capacitance  $C_{a12}$  of diodes  $D_1$  and  $D_2$ . The first effect is not very serious if the primary impedance is small and the primary to secondary coupling is loose. For example, the circuit constants selected above give a maximum primary impedance  $R_p$  of 6,750 ohms, so that the average stray anode-to-earth capacitance for  $V_1$  of

$$15 \mu\mu\text{F} \left( X_{aE} = \frac{10^{12}}{6.28 \times 465 \times 10^3 \times 15} = 22,800 \text{ ohms} \right) \text{ would}$$

have little influence on performance. The anode-to-anode capacitance  $C_{a12}$  of the diodes is much less (about  $1 \mu\mu\text{F}$ ), but the secondary impedances are much higher than the primary. Both effects may be reduced or even cancelled by including positive mutual inductance coupling  $M_3$  (see Section 3.4.2, Part I) between the circuits, a small coil in series with  $L_1$  being coupled to  $L_2$ , or vice versa. The direction of  $M_3$  is important, for if it is negative it adds to the stray capacitance coupling.

To economize in space the two circuits 1 and 2 may be wound at opposite ends of the same coil former, the stray mutual inductance being used to cancel the stray capacitance.

It is important to ensure that the resonant frequency of the two primaries with the stray capacitance  $C_{aE}$  is far removed from the I.F. or a low harmonic of the I.F., otherwise an asymmetrical discriminator characteristic with unequal positive and negative peak results. In the example quoted above the resonant frequency is 3.24 Mc/s with  $15 \mu\mu\text{F}$  stray capacitance.

The two primaries may be connected in parallel instead of in series, or the tuned circuits 1 and 2 may each be loosely coupled through small capacitances ( $5 \mu\mu\text{F}$ ) to the anode of the last I.F. amplifier valve in the receiver, but in both instances performance is less satisfactory and a symmetrical discriminator curve is difficult to obtain. The capacitively coupled circuits, even with small capacitance coupling, tend to modify the frequency response of the last I.F. transformer before the detector and to react one on the

other. The slope of the discriminator characteristic at  $O$  is also reduced.

An alternative method of connection using circuits 1 and 2 without transformer coupling is shown in Fig. 13.8. Its disadvantage is that the anode-earth capacitance of  $V_1$  has greater effect because  $R_{D1}$  and  $R_{D2}$  are much greater than  $R_{p1}$  and  $R_{p2}$ , but this stray

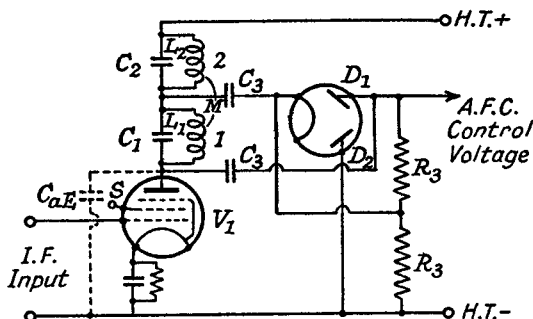


FIG. 13.8.—A Modified Form of the Amplitude Discriminator.

coupling may be cancelled by positive mutual inductance between the circuits satisfying

$$\frac{M}{\sqrt{L_1 L_2}} = \frac{C_{aE}}{\sqrt{C_1 C_2}}$$

The voltage applied to the discriminator circuits must not be allowed to vary over wide limits because this affects A.F.C. performance, increase of applied voltage improving control but also increasing the “throw-out” and “pull-in” signal frequency separations from the correct signal setting. This means that A.G.C. must be combined with A.F.C. if the latter is to be satisfactory.

Increased control accuracy (greater slope to  $BOD$ ) may be obtained by inserting between Nos. 1 and 2 and their respective diodes a circuit having a rejection frequency approximately equal to the correct I.F. carrier frequency  $f_m$ . The fall-away of the frequency response curves from each peak towards  $f_m$  is consequently made much steeper and the slope  $BOD$  increased. A suitable circuit<sup>17</sup> consists of two series inductance arms having positive mutual inductance between them, and a shunt capacitance arm connected to their junction point. The positive mutual inductance and shunt capacitance form a series rejection circuit at the frequency  $f_m$ .

A modification of the amplitude discriminator using only one tuned circuit is shown in Fig. 13.9a. Circuit  $L_1 C_1$  is tuned to a frequency about 2 kc/s above the correct I.F. value, so that for

frequencies below this value it presents an inductive reactance. Capacitance  $C_2$  across the diode  $D_2$  forms with the inductive reactance of  $L_1C_1$  a series circuit tuned to a frequency about 2 kc/s below the correct I.F. value. The R.F. choke  $L_2$  provides a D.C. return path for the conduction currents in diodes  $D_1$  and  $D_2$ .

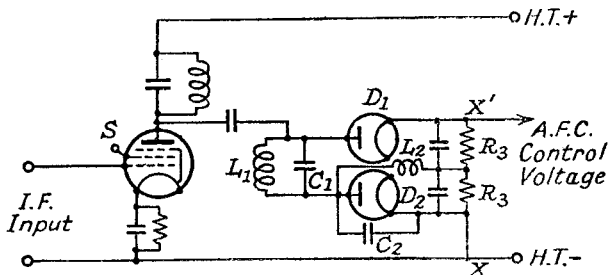


FIG. 13.9a.—An Amplitude Discriminator using a Single Tuned Circuit in Conjunction with a Capacitance.

The amplitude variation of the voltage applied to diode  $D_1$  (curve 1 in Fig. 13.9b) is a maximum at  $(f_m + 2)$  kc/s and a minimum at  $(f_m - 2)$  kc/s when the series circuit of  $L_1C_1$  and  $C_2$  is resonant. The amplitude variation of the voltage applied to  $D_2$  (curve 2 in Fig. 13.9b) is an image of that across  $D_1$ , being maximum at

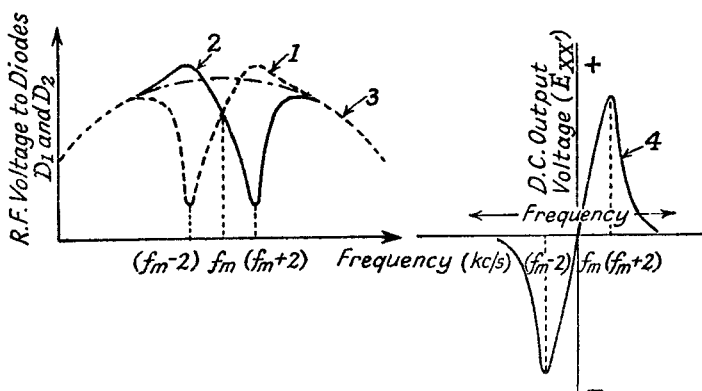


FIG. 13.9b.—Response Curves for the Single Tuned Circuit Amplitude Discriminator.

$(f_m - 2)$  kc/s and a minimum at  $(f_m + 2)$  kc/s when the circuit  $L_1C_1$  is resonant. The dashed curve 3 in Fig. 13.9b, symmetrical about  $f_m$ , is the frequency response of the source of I.F. The D.C. voltages across the load resistances  $R_3$  are in series opposition so that the total D.C. output voltage across points  $XX'$  varies with frequency as shown by curve 4 in Fig. 13.9b. Curve 4 can be moved above





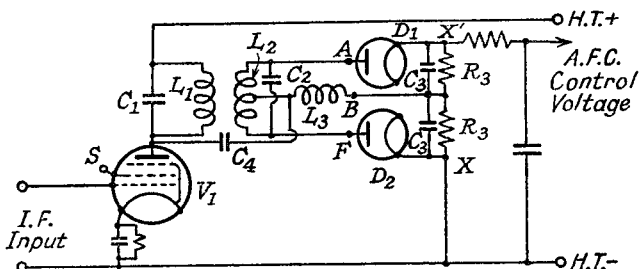


Fig. 13.10.—The Phase Discriminator.

centre tap and the centre point of the two diode load resistances  $R_3$ . Hence the carrier peak voltages applied to the diodes are

$$\hat{E}_{AB} = g_m \hat{E}_c R_{D1} \frac{1 + jQ_2 \left( F + \frac{k}{2} \sqrt{\frac{L_2}{L_1}} \right)}{(1 + jQ_1 F)(1 + jQ_2 F) + Q_1 Q_2 k^2} \quad 13.6a$$

and

$$\hat{E}_{FB} = g_m \hat{E}_c R_{D1} \frac{1 + jQ_2 \left( F - \frac{k}{2} \sqrt{\frac{L_2}{L_1}} \right)}{(1 + jQ_1 F)(1 + jQ_2 F) + Q_1 Q_2 k^2} \quad 13.6b$$

where  $\hat{E}_c$  = peak value (unmodulated) of the carrier voltage applied to the grid of  $V_1$ .

Converting 13.6a and 13.6b to voltage amplitudes  $|\hat{E}_{AB}|$  and  $|\hat{E}_{FB}|$  and plotting them against frequency produces curves somewhat similar to those for the amplitude discriminator shown in Fig. 13.6a, provided the coupling between primary and secondary is loose. The peaks are displaced from the correct I.F. carrier value  $f_m$  by almost equal off-tune frequencies. If the coupling coefficient is

increased to the critical value  $\left[ k = \sqrt{\frac{1}{2} \left[ \frac{1}{Q_1^2} + \frac{1}{Q_2^2} \right]} \right]$  (Section 7.3, Part I) and greater, the off-tune frequency peaks are displaced further from  $f_m$  and a second, much smaller peak appears on the opposite side of  $f_m$  to the main peak.

By subtracting  $|\hat{E}_{FB}|$  from  $|\hat{E}_{AB}|$  and multiplying by the voltage detection efficiency,  $\eta_d$ , of the diode detectors, the expression for the discriminator voltage-frequency characteristic is found to be

$$\eta_d [ |\hat{E}_{AB}| - |\hat{E}_{FB}| ] = g_m R_{D1} \hat{E}_c \eta_d \frac{\left[ 1 + Q_2^2 \left( F + \frac{k}{2} \sqrt{\frac{L_2}{L_1}} \right)^2 \right]^{\frac{1}{2}} - \left[ 1 + Q_2^2 \left( F - \frac{k}{2} \sqrt{\frac{L_2}{L_1}} \right)^2 \right]^{\frac{1}{2}}}{[[1 + Q_1 Q_2 (k^2 - F^2)]^2 + (Q_1 + Q_2)^2 F^2]^{\frac{1}{2}}} \quad 13.7.$$

The slope of the discriminator characteristic at the mid-frequency

$f_m$  is obtained by differentiating 13.7 with respect to  $\Delta f$  and equating  $F$  in the resulting expression to 0. Hence

$$S_{(F=0)} = \frac{d(\eta_d[|\hat{E}_{AB}| - |\hat{E}_{FB}|])}{dF} \cdot \frac{dF}{d(\Delta f)}$$

$$= \frac{2g_m R_{D1} \eta_d Q_2^2 \sqrt{\frac{L_2}{L}}}{f_m} \left[ \frac{k}{(1 + Q_1 Q_2 k^2) \left[ 1 + \frac{Q_2^2 k^2 L_2}{4L_1} \right]^{\frac{1}{2}}} \right] \quad 13.8$$

$S$  in 13.8 is in D.C. volts per kc/s off-tune per 1 volt grid peak input. The slope at  $F = 0$  can be varied by changing  $k$  and a maximum is found by differentiating the part of 13.8 inside the bracket with respect to  $k$  and equating the result to zero. Replacing  $Q_1 Q_2$  by  $a$  and  $\frac{Q_2^2 L_2}{4L_1}$  by  $b$

$$\frac{k}{(1 + Q_1 Q_2 k^2) \left[ 1 + \frac{Q_2^2 k^2 L_2}{4L_1} \right]^{\frac{1}{2}}} = \frac{k}{(1 + ak^2)(1 + bk^2)^{\frac{1}{2}}}$$

Differentiating with respect to  $k$  and equating to zero gives

$$1 - ak^2 - 2ab k^4 = 0$$

$$k^2 = + \frac{\sqrt{a^2 + 8ab} - a}{4ab}$$

$$\sqrt{Q_1 Q_2} k = \sqrt{\frac{+ \sqrt{Q_1^2 Q_2^2 + 2Q_1 Q_2^3 \frac{L_2}{L_1}} - Q_1 Q_2}{Q_2^2 \frac{L}{L_1}}} \quad 13.9.$$

The optimum values of  $\sqrt{Q_1 Q_2} k$  for different values of  $\frac{L_2}{L_1}$  and  $\frac{Q_2}{Q_1}$  are tabulated below.

TABLE 13.1

$\frac{L_2}{L_1}$	1	2	4	6	8	10	
$Q_1 = 0.5Q_2$	0.786	0.707	0.625	0.578	0.544	0.52	} $\sqrt{Q_1 Q_2} k$ .
$Q_1 = Q_2$	0.856	0.785	0.707	0.657	0.625	0.598	
$Q_1 = 2Q_2$	0.909	0.855	0.786	0.740	0.707	0.68	

The optimum value of  $\sqrt{Q_1 Q_2} k$  is always less than 1 and, for a given value of  $\frac{L_2}{L_1}$ , decreases as  $\frac{Q_2}{Q_1}$  decreases.

For discriminator design purposes it is necessary to determine the off-tune frequencies, which give maximum positive or negative

D.C. output voltage, corresponding to points *B* and *D* in Fig. 13.6*a*. These frequencies are found by differentiating expression 13.7 with respect to  $\Delta f$  and equating to zero. A complicated equation in  $\Delta f$  raised to the 5th power results, and a simpler solution of the problem is possible if it is assumed that the variation\* of the primary voltage  $\hat{E}_1$  over the frequency range between the two peaks *B* and *D* is negligible. The voltage vector diagram for the discriminator then becomes that of Fig. 13.11. The primary voltage is repre-

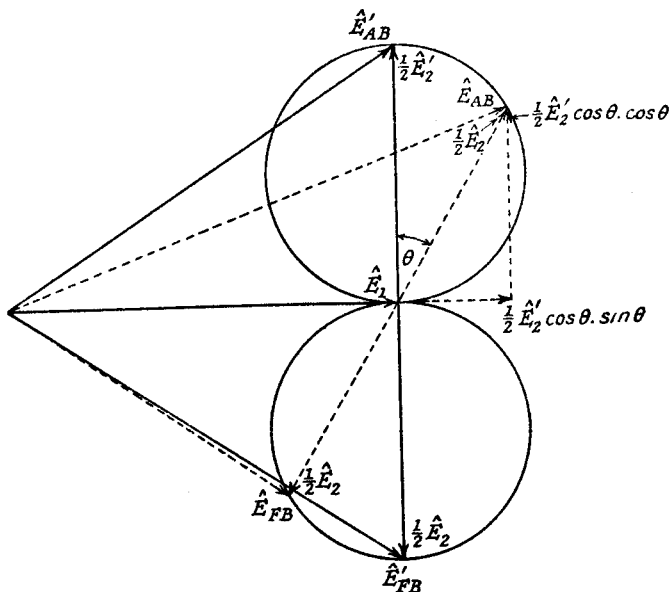


FIG. 13.11.—Vector Relationships of the Primary and Half Secondary Voltages in the Phase Discriminator.

sented by the horizontal vector  $\hat{E}_1$  of constant length, and the half-secondary voltages by vectors  $\pm \frac{1}{2} \hat{E}_2$ . The loci of the two half-secondary voltages are the two circles shown (the impedance of a parallel tuned circuit has a circle locus). The diameter of either circle is equal to the half-secondary voltage,  $\frac{1}{2} \hat{E}_2$ , at  $f_m (F = 0)$ , which in turn depends on the coupling coefficient  $k$  and  $Q_2$ . From expressions 13.4 and 13.5

$$\hat{E}_2'(F = 0) = -jQ_2k\sqrt{\frac{L_2}{L_1}} \cdot \hat{E}_1(F = 0) = -j\alpha \hat{E}_1(F = 0)$$

where  $\alpha = Q_2k\sqrt{\frac{L_2}{L_1}}$ .

\* The effect of the variation of  $E_1$  upon the discriminator characteristic is considered in Section 15.9.3.

Referring to Fig. 13.11

$$\hat{E}_{AB'} = \hat{E}_1 + \frac{\hat{E}_2'}{2} \sin \theta \cos \theta + j \frac{\hat{E}_2'}{2} \cos \theta \cos \theta$$

where  $\theta$  is the angle between the half-secondary voltage vector when  $F \neq 0$  and the vector  $\frac{\hat{E}_2'}{2}$  when  $F = 0$ , and

$$\begin{aligned} \tan \theta &= \frac{\text{secondary series reactance component}}{\text{secondary series resistance component}} \\ &= \frac{\omega L_2 - \frac{1}{\omega C_2}}{R_2} = Q_2 F \end{aligned}$$

$$\begin{aligned} \therefore |\hat{E}_{AB}| &= \hat{E}_1 \sqrt{\left(1 + \frac{\alpha \sin \theta \cos \theta}{2}\right)^2 + \left(\frac{\alpha \cos^2 \theta}{2}\right)^2} \\ &= \hat{E}_1 \sqrt{\left(1 + \frac{\alpha \sin 2\theta}{4}\right)^2 + \alpha^2 \left(\frac{1 + \cos 2\theta}{4}\right)^2} \\ &= \hat{E}_1 \sqrt{1 + \frac{\alpha^2}{8} + \frac{\alpha \sin 2\theta}{2} + \frac{\alpha^2 \cos 2\theta}{8}} \quad . \quad .13.10a. \end{aligned}$$

$$\text{Similarly } |\hat{E}_{FB}| = \hat{E}_1 \sqrt{1 + \frac{\alpha^2}{8} - \frac{\alpha \sin 2\theta}{2} + \frac{\alpha^2 \cos 2\theta}{8}} \quad . \quad .13.10b.$$

The maximum value of  $(|\hat{E}_{AB}| - |\hat{E}_{FB}|)$  is obtained by differentiating the difference between 13.10a and 13.10b with respect to  $\theta$  and equating to zero. Hence

$$\begin{aligned} &\left[1 + \frac{\alpha^2}{8} + \frac{\alpha \sin 2\theta}{2} + \frac{\alpha^2 \cos 2\theta}{8}\right]^{-\frac{1}{2}} \left(\alpha \cos 2\theta - \frac{\alpha^2 \sin 2\theta}{4}\right) \\ &- \left[1 + \frac{\alpha^2}{8} - \frac{\alpha \sin 2\theta}{2} + \frac{\alpha^2 \cos 2\theta}{8}\right]^{-\frac{1}{2}} \left(-\alpha \cos 2\theta - \frac{\alpha^2 \sin 2\theta}{4}\right) = 0. \end{aligned}$$

This finally reduces to

$$\cos^2 2\theta \left(1 + \frac{\alpha^2}{16}\right) + \cos 2\theta \left(1 + \frac{\alpha^2}{8}\right) + \frac{\alpha^2}{16} = 0$$

$$\text{or} \quad \cos 2\theta = \frac{-\alpha^2}{16 + \alpha^2} \quad \text{or} \quad -1.$$

The first root is the one required as it is a function of the coupling coefficient.

When the coupling coefficient is very small,  $\alpha$  is very small,  $\cos 2\theta$  is zero, and  $\theta$  is  $45^\circ$ , but as  $\alpha$  is increased  $\theta$  is increased above  $45^\circ$ . Thus the minimum value of  $\tan \theta$  is unity and this gives the



It is clear from expressions 13.11 and 13.12 that the diodes contribute very heavy damping to primary and secondary, particularly to the former. To obtain maximum slope of discriminator characteristic (expression 13.8 shows that  $R_{D1}$  and  $Q_2$  need to be large) and the required peak at 2 kc/s off-tune frequency, the detector load resistances must be made as high as possible. A maximum practical value for  $R_3$  is usually about 0.5 M $\Omega$ .

To illustrate the design features of the phase discriminator, let us take the following example :

$f_m = 465$  kc/s,  $R_3 = 0.5$  M $\Omega$ ,  $L_1 = 300$   $\mu$ H,  $Q_1' = Q_2' = 100$  where  $Q_1'$  and  $Q_2'$  are the normal undamped  $Q$  values for the primary and secondary circuits. For the amplifier valve preceding the discriminator primary  $R_a = 1$  M $\Omega$  and  $g_m = 2.5$  mA/volt. The damping resistances in parallel with the discriminator primary are 1 M $\Omega$  from the amplifier valve and 0.125 M $\Omega$  ( $\frac{1}{8}R_3$ ) from the discriminator detectors.

$$\text{Thus} \quad Q_1 = \frac{\omega L_1}{\frac{\omega L_1}{Q_1'} + \frac{(\omega L_1)^2}{R_a} + \frac{4(\omega L_1)^2}{R_3}}$$

$$\omega L_1 = \frac{6.28 \times 465 \times 10^3 \times 300}{10^6} = 875 \text{ ohms.}$$

$$\text{Therefore} \quad Q_1 = \frac{875}{8.75 + \frac{875^2}{10^6} + \frac{875^2}{0.125 \times 10^6}} = \frac{875}{15.638}$$

$$= 56.$$

We have seen from the previous analysis that  $Q_2$  determines the minimum value of the off-tune frequencies at which the peaks  $B$  and  $D$  (Fig. 13.6a) of the discriminator curve occur, and, if no conduction current damping of the secondary circuit is assumed, the off-tune frequency cannot be less than  $\Delta f_{(min.)} = \frac{f_m}{2Q_2'} = \pm 2.325$  kc/s. Since  $\Delta f_{(min.)}$  should not be large (the "throw-out" and "pull-in" frequencies are both increased with increase of  $\Delta f_{(min.)}$ ), it follows that  $Q_2$  should be as nearly equal to  $Q_2'$  as possible, i.e.,  $L_2$  must not be high in value. On the other hand,  $L_2$  must not have too low a value, because the factor  $\frac{L_2}{L_1}$  then reduces the slope of the discriminator characteristic (expression 13.8).

Let us take  $L_2 = L_1$ .

The diode conduction current damping across the secondary is  $0.5 \text{ M}\Omega$  ( $R_3$ ), so that the final  $Q$  of the secondary circuit is

$$Q_2 = \frac{\omega L_2}{\frac{\omega L_2}{Q_2'} + \frac{(\omega L_2)^2}{R_3}} = \frac{875}{8.75 + 1.535} \\ = 85.$$

Substituting  $0.658 Q_2$  for  $Q_1$ , and 1 for  $\frac{L_2}{L_1}$  in expression 13.9 gives

$\sqrt{Q_1 Q_2} k = 0.813$  for maximum slope at  $f_m$ , i.e.,  $k = 0.0118$ . The mutual inductance coupling between primary and secondary is  $M = k\sqrt{L_1 L_2} = 0.0118 \times 300 = 3.54 \mu\text{H}$ . The off-tune frequency corresponding to  $B$  and  $D$  in Fig. 13.6a is from Table 13.2

$$\left( Q_2 k \sqrt{\frac{L_2}{L_1}} \text{ very nearly equals } 1 \right) 1.0605 \times \Delta f_{(\text{min.})}$$

or 
$$\Delta f_{(B \text{ or } D)} = \pm 2.91 \text{ kc/s.}$$

The slope of the discriminator characteristic at  $f_m$  is from expression 13.8.

$$S_{(F-O)} = \frac{2 \times 2.5 \times 10^{-3} \times R_{D1} \times 0.8 \times (85)^2 \times 1}{465}$$

$$\left[ \frac{0.0118}{[1 + (0.813)^2] \left[ 1 + \frac{1}{4} \right]^{\frac{1}{2}}} \right]$$

where  $R_{D1} = \omega_m L_1 Q_1 = 875 \times 56 = 49,000 \Omega$

and  $\eta_d = 0.8$ .

Therefore  $S_{F-O} = 19.35$  volts per kc/s off-tune per 1 volt peak input carrier. Since the slope of the discriminator characteristic is dependent on the input carrier voltage at its amplifier valve, it is important, if A.F.C. is to hold its performance over wide variations of aerial input carrier voltage, that the receiver should have A.G.C. and that the discriminator voltage should be taken from the source supplying the A.G.C. detector.

The phase discriminator can itself be used as the A.F. detector at some sacrifice of quality by taking the A.F. output from one diode load resistance,  $R_3$ , and the A.G.C. diode may be supplied from the primary. Such a circuit is shown in Fig. 13.12. The R.F. choke  $L_s$  in Fig. 13.10 has been omitted, the centre tap on the secondary being connected to the centre point of the D.C. load resistances  $R_3$ , and the capacitances  $C_s$  being replaced by a single

capacitance  $C_3$  across both load resistances. There are disadvantages to this method of saving components; by using one of the discriminator diodes as A.F. detector, there is practically no gain in selectivity from the secondary circuit because the voltage applied to the detector is the sum of primary and secondary voltages. The overall amplification is, however, greater than if the A.F. detector were connected across the secondary only (the normal procedure). A further objection is that the frequency response for the applied voltage to diode  $D_2$ , providing the A.F. frequency output, has a maximum about 3 kc/s off-tune from  $f_m$ , and A.F. distortion tends to occur due to asymmetric sideband amplitudes. A better method giving much improved selectivity is to use a separate pick-up coil (coupled to the discriminator transformer) and tuned circuit for the

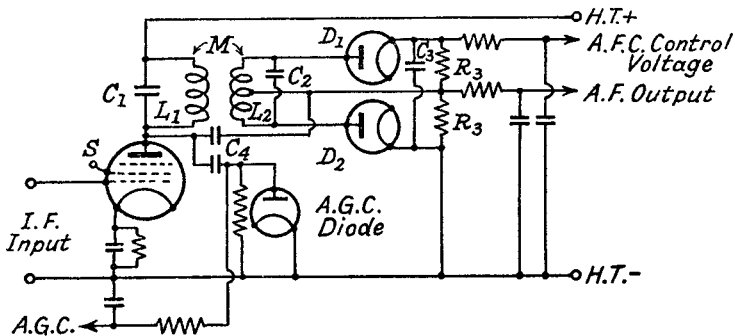


FIG. 13.12.—A Combined Phase Discriminator and A.F. Detector Circuit.

A.F. detector. The pick-up coil must be capacitively balanced to the discriminator secondary in order to prevent an asymmetric discriminator characteristic. This is achieved by disposing the pick-up coil symmetrically with respect to each half-secondary and by separating its output leads from the secondary leads. The third tuned circuit has an absorption effect, which decreases the slope of the discriminator characteristic and increases the frequency separation of the peaks  $B$  and  $D$  (Fig. 13.6a). Reduction of pick-up coil coupling reduces the effect, but at the same time decreases the A.F. output from the detector. The omission of the R.F. choke  $L_3$  and the substitution of  $R_3$  as the coupling impedance increases the damping on the primary, an additional damping resistance of  $\frac{1}{2}R_3$  being applied.

The capacitances to earth of each half-secondary should be equal, otherwise an asymmetric discriminator characteristic results;



a small trimmer capacitance may be included from the anode to cathode of one of the diodes in order to ensure this.

In adjusting the phase discriminator to give the required characteristic, the following points should be borne in mind :

(1) The mutual inductance coupling, when it is small, affects chiefly the amplitude and not the frequency separation of the peaks *B* and *D*. As it is increased, a point is reached after which the amplitudes of the peaks increase at a slower rate, but their frequency separation begins to be increased. Table 13.2 shows that variation of coupling coefficient has little effect on the off-tune frequency separation until  $Q_2 k \sqrt{\frac{L_2}{L_1}}$  exceeds 1.

(2) The primary tuning controls the symmetry of the discriminator characteristic about  $f_m$ ; a decrease in primary resonant frequency increases the off-tune frequency of the lower frequency peak *B* (moving it further from  $f_m$ ) and increases its amplitude. Conversely, increase of primary resonant frequency moves the upper frequency peak *D* further from  $f_m$  and increases its amplitude. The slope of *BOD* tends to become S-shaped.

(3) The secondary tuning has greatest effect on the central frequency (*O* in Fig. 13.6*a*), where the discriminator D.C. voltage passes through zero. If the secondary resonant frequency is decreased, the central frequency is reduced below  $f_m$ .

The procedure for obtaining the required discriminator characteristic is to disconnect  $C_4$  from the secondary centre tap and, with loose coupling between the primary and secondary, to tune both circuits for maximum voltage across one of the diode load resistances  $R_s$  when the frequency equals  $f_m$ .  $C_4$  is next joined to the centre tap of the secondary, and the primary retuned to give approximately equal positive and negative maximum voltages from the cathode of diode  $D_1$  in Fig. 13.10 to earth, i.e., across points *XX'*, when the input frequency is varied over the range  $f_m + 5$  kc/s to  $f_m - 5$  kc/s. The stray capacitance to earth from the secondary centre tap is often appreciable and retuning of the primary is essential. The secondary circuit is now trimmed to bring zero D.C. volts across the points *XX'* in Fig. 13.10 at  $f = f_m$ , and afterwards the primary tuning is again checked for equal positive and negative maxima. Finally, the mutual inductance coupling is increased until the off-tune frequencies at which the positive and negative maxima occur begin to move outwards from  $f_m$ . Finer adjustment necessitates taking the discriminator D.C. output voltage-frequency curve and is seldom necessary.

The discriminator D.C. output voltage is connected to the control device by a R.F. filter, consisting of a resistance and capacitance having a time-constant of about 0.1 seconds.

**13.4.3. The Variable Reactance Control Unit.** The discriminator D.C. output voltage, which is proportional to the I.F. carrier frequency error, must be translated into a correcting reactance across the oscillator-tuned circuit. This reactance, which can be capacitive or inductive, may actually be a variable capacitor or inductor, or it may be simulated by a valve.

One of the simplest forms of control is the motor-operated variable capacitor. The motor, similar to that already described in Section 13.2.3, is reversible; the A.C. currents in the forward and reverse coils are obtained from valves, the amplifications of which are controlled in opposite directions from the discriminator D.C. output voltage. When there is no error of the I.F. carrier, the currents exercise opposing effects on the rotor disc and the motor is stationary, but if the I.F. carrier is off-tune, the current in one coil increases and that in the other decreases, causing the motor to rotate and, through gears, drive the correcting capacitor. The motor continues to rotate until the currents in the coil are again equal. This method is unsuitable for broadcast reception on account of cost, but it has been used for large commercial receivers operating mostly on telegraph signals. Its outstanding advantages are: (1) the control is very sensitive and high tuning accuracy is easily secured, (2) the inertia in the control unit renders it less liable to lose control when the carrier signal is discontinuous as with keyed C.W. transmission, and (3) the device has a floating datum line, i.e., disappearance of the discriminator D.C. voltage output causes practically no change in oscillator frequency. Many variable reactance devices fail under similar conditions and sometimes transfer reception from the desired to an undesired transmission.

Another method of using a variable capacitor to control the oscillator frequency is by means of a milliammeter with a vane, interleaved between two fixed plates, in place of the pointer. The milliammeter coil is actuated by the anode current of a valve, biased from the discriminator voltage. Such a device is too fragile for most purposes and it suffers from the disadvantage that if the discriminator voltage fails the capacitor returns to its "zero" setting and changes the oscillator frequency. The latter may be within range of an adjacent transmission, which then tends to actuate the control and prevent tuning back to the desired transmission when it reappears.

A direct control device, which has the merit of extreme simplicity and reasonable sensitivity, is a capacitor, the value of which is varied by changing a D.C. polarizing voltage applied between the plates. One electrode of this polarized capacitor\* is a flat aluminium plate (about  $\frac{1}{32}$  in. thick) having a thin polished anodized surface. The other is a thin leaf of polished duralumin foil (0.001 in. thick) lying flat on the first electrode. Application of a D.C. polarizing voltage (its direction is unimportant, either surface can be positive) brings the foil into closer contact with the anodized surface and capacitance is increased. The polarizing voltage can be applied

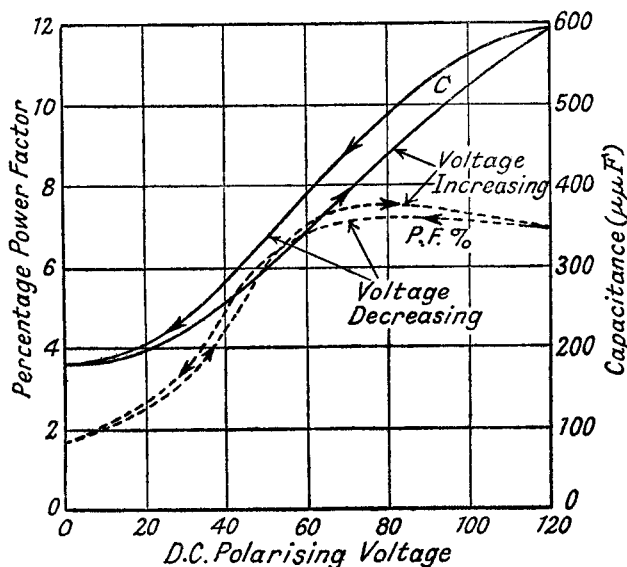


FIG. 13.13.—Curves of Capacitance—D.C. Voltage for the Polarized Capacitor with Increasing and Decreasing d.c. Voltage.

through a high resistance, 10 MΩ, so that circuit loss is negligible. A 3 to 1 change in capacitance is easily achieved by a polarizing voltage change of  $\pm 50$  volts about a mean of 70 volts. Typical curves of capacitance and percentage power factor

$$\left[ \frac{R}{\sqrt{R^2 + \left(\frac{1}{\omega C}\right)^2}} \right]$$

variation against polarizing voltage are shown in Fig. 13.13. The dimensions of the surfaces in contact for the capacitor whose

\* British Patent Nos. 522,476 and 522,564. Marconi's Wireless Telegraph Company. N. M. Rust, J. D. Brailsford, A. L. Oliver and J. F. Ramsay.



is by means of a valve. Many circuits have been devised, but the majority depend on the application of R.F. voltages between the anode and cathode, and between grid and cathode, having a phase difference of  $90^\circ$ . If the valve has a high slope resistance,  $R_a$ , e.g., it is a tetrode, pentode, hexode, etc., the R.F. anode current component is in phase with the applied grid voltage. Hence there is a  $90^\circ$  phase difference between the R.F. anode current component and the applied R.F. anode voltage, so that the valve functions as a reactance. The latter is inductive if the R.F. grid voltage lags behind the anode voltage, and is capacitive if the grid voltage leads upon the anode voltage. The magnitude of the reactance, which is inversely proportional to the R.F. anode current, decreases as the amplification of the valve is increased by decreasing the D.C. bias on the control grid or another electrode. Thus by connecting the anode and cathode of the valve across the oscillator-tuned circuit, and biasing it from the discriminator D.C. output voltage, the valve functions as a variable correcting reactance. Care must be taken to see that the bias is connected to give a change of reactance in the right direction. Let us suppose that the valve anode-cathode circuit appears as a capacitive reactance and the I.F. carrier frequency is higher than its correct value. Since the oscillator frequency is almost always greater than that of the signal, it follows that the former must be greater than its correct value, and it must be reduced by decreasing the valve capacitive reactance, i.e., by increasing the capacitance of the anode-cathode space. This is achieved by decreasing the negative bias on the valve; in other words, the discriminator D.C. output voltage must be connected to give a positive voltage when the I.F. carrier exceeds its correct frequency and a negative voltage when it falls below the correct frequency. This condition is fulfilled by the circuit shown in Fig. 13.7. If the anode-cathode circuit of the valve is equivalent to an inductive reactance, the discriminator voltage connections must be reversed in order to give a negative voltage when the I.F. carrier exceeds its correct frequency.

The properties required of a variable reactance valve are that it should affect oscillator frequency and not amplitude, that it should produce large changes of reactance over a restricted range of bias voltages, and, outside this desired range of bias voltages, the reactance should not vary appreciably. The advantage of this limited reactance characteristic is discussed in Section 13.4.4.

The basic reactance valve circuit is shown in Fig. 13.15. The valve is a hexode, the control grid being connected to the centre

point of the phase-shifting network  $Z_1$  and  $Z_2$ , and the oscillator grid to the discriminator D.C. output voltage. Considerable advantages are gained by using a hexode rather than a tetrode with the discriminator D.C. voltage applied to the control grid. The bias on the control grid can be set to its optimum value (often about  $-5$  volts), and variation of discriminator D.C. output voltage has little effect on the self-bias voltage derived from the cathode current of the valve. With the tetrode valve, change of control grid bias affects the self-bias voltage so as to reduce the reactance change for a given discriminator voltage change, and the initial bias must be much greater than optimum in order to allow the discriminator D.C. voltage to become positive without causing the control grid to take current. A pentode valve can be made to function in a manner similar to the hexode by applying the dis-

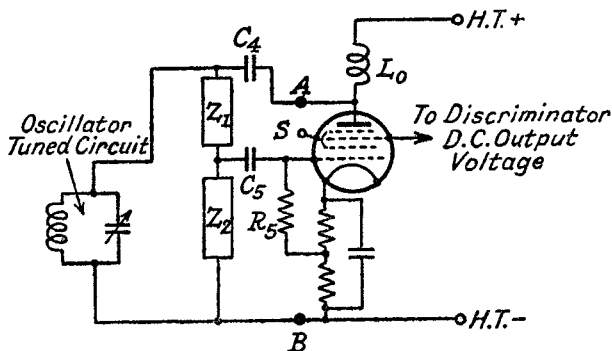


FIG. 13.15.—The Variable Reactance Valve Circuit.

criminator voltage to the suppressor grid, but a fine mesh suppressor grid is required if the control is to be sufficiently sensitive. The slope resistance of the valve is reduced (Section 2.5) by applying negative bias to the suppressor grid and its performance is not so satisfactory as that of a hexode. Impedances  $Z_1$  and  $Z_2$  act not only as a phase-shifting network but also as a potential divider for stepping-down the voltage applied to the grid from the oscillator-tuned circuit. A suitable peak value for the R.F. voltage at the grid of the reactance valve is about 4 volts. Capacitance-resistance coupling ( $C_5$  and  $R_5$ ) is shown from  $Z_2$  to the reactance valve grid in Fig. 13.15, but in certain cases this may be unnecessary. For example,  $C_5$  and  $R_5$  can be omitted if  $Z_1$  is a capacitance and  $Z_2$  a resistance. H.T. voltage for the reactance valve anode is obtained via the R.F. choke  $L_0$  and the R.F. voltage from the oscillator-tuned circuit is applied through the coupling capacitance  $C_4$ . If

the oscillator-tuned circuit is connected to a H.T. voltage source (e.g., a tuned anode oscillator), the anode of the reactance valve can be joined direct to the high R.F. potential end of the tuned circuit;  $C_4$  and  $L_0$  are then no longer required. If  $Z_1$  is a resistance  $R$ , and  $Z_2$  a capacitance  $C$ , and the valve has a high slope resistance, the admittance from anode to cathode (points  $AB$ ) is given by

$$Y_{AB} = \frac{I_a}{E_a} = \frac{g_m E_g}{E_a} \quad \dots \quad 13.13a$$

where  $g_m$  = mutual conductance of the variable reactance valve.

But 
$$E_g = \frac{E_a Z_2}{Z_1 + Z_2}$$

$$\therefore Y_{AB} = \frac{g_m Z_2}{Z_1 + Z_2} = g_m \frac{1}{1 + jR\omega C}$$

$$= \frac{g_m}{1 + (R\omega C)^2} - j \frac{g_m R\omega C}{1 + (R\omega C)^2} \quad \dots \quad 13.13b$$

which is equivalent to a resistance

$$R_{AB} = \frac{1 + (R\omega C)^2}{g_m}$$

in parallel with an inductance

$$L_{AB} = \frac{1 + (R\omega C)^2}{g_m R\omega^2 C}$$

Three other combinations of  $R$  and  $L$  or  $C$  are possible, and the resultant parallel resistance and reactance components of  $Y_{AB}$  are tabulated below. Approximate expressions for  $R_{AB}$  and  $X_{AB}$ , obtained by assuming that  $Z_2$  is small in comparison with  $Z_1$  (this is often true in practice because the R.F. voltage required at the grid of the reactance valve is generally much less than that across the oscillator-tuned circuit), are also given.

TABLE 13.3

$Z_1$	$R$	$C$	$R$	$L$
$Z_2$	$C$	$R$	$L$	$R$
$R_{AB}$	$\frac{1 + (R\omega C)^2}{g_m}$	$\frac{1 + (R\omega C)^2}{g_m (R\omega C)^2}$	$\frac{R^2 + \omega^2 L^2}{g_m \omega^2 L^2}$	$\frac{R^2 + \omega^2 L^2}{g_m R^2}$
$X_{AB}$	$L_{AB} = \frac{1 + (R\omega C)^2}{g_m R\omega^2 C}$	$C_{AB} = \frac{g_m RC}{1 + (R\omega C)^2}$	$C_{AB} = \frac{g_m RL}{R^2 + \omega^2 L^2}$	$L_{AB} = \frac{R^2 + \omega^2 L^2}{g_m R\omega^2 L}$
Approximate expressions $Z_2 \ll Z_1$				
$R_{AB}$	$\frac{(R\omega C)^2}{g_m}$	$\frac{1}{g_m (R\omega C)^2}$	$\frac{R^2}{g_m \omega^2 L^2}$	$\frac{\omega^2 L^2}{g_m R^2}$
$X_{AB}$	$L_{AB} = \frac{RC}{g_m}$	$C_{AB} = g_m RC$	$C_{AB} = \frac{g_m L}{R}$	$L_{AB} = \frac{L}{g_m R}$

From the above table it will be noted that the values of the resistance and reactance components of  $Y_{AB}$  are independent of  $R$  and  $L$ , or  $R$  and  $C$ , as long as  $\frac{L}{R}$  and  $RC$  remain constant. It is generally undesirable that the resistance and reactance of the phase-shifting network should be small because the latter is in parallel with the oscillator-tuned circuit. A low reactance makes ganging of the oscillator and signal circuits difficult, whilst a low resistance damps the tuned circuit and reduces oscillator amplitude. Hence  $C$  should be small and  $R$  large, or  $L$  and  $R$  both large. The components of  $Y_{AB}$ , when  $Z_1$  and  $Z_2$  are equal to  $R$  and  $C$  respectively, are similar in form to those when  $Z_1$  and  $Z_2$  are equal to  $L$  and  $R$  respectively. In like manner the components for a  $CR$  phase-shifting network are similar to those for a  $RL$  network. As a rule a resistance-capacitance phase shifting circuit is to be preferred to a resistance-inductance combination because a capacitance has negligible resistance component. The internal resistance component of the inductance prevents an exact  $90^\circ$  phase shift being realized, and stray capacitance across the inductance also introduces complications.

Some interesting conclusions may be drawn from the approximate expressions for  $R_{AB}$  and  $X_{AB}$ : the value of the resistance component is in every case inversely proportional to  $g_m$  so that an increase of discriminator D.C. output voltage in a positive direction tends to reduce oscillator amplitude. The change in amplitude can be made very small by a suitable choice of  $R$  and  $C$ , or  $R$  and  $L$ , and generally the effect may be ignored. In the  $RC$  and  $LR$  network,  $R_{AB}$  is directly proportional to the square of the frequency, and if A.F.C. is applied to a variable-tuned circuit, as distinct from a preset circuit,  $R_{AB}$  has greatest damping at the low-frequency end of the range. This is undesirable because the oscillator amplitude is usually a minimum at this end. With the  $CR$  and  $RL$  network the reverse is true, and the decrease in  $R_{AB}$  as frequency increases helps to stabilize oscillator amplitude (Section 6.4, Part I). Examination of the approximate equivalent inductance or capacitance due to the reactance valve shows that it is independent of frequency, and dependent only on  $g_m$  and the resistance and reactance components of the phase splitter. For preset oscillator tuning all of the reactance valve circuits are equally suitable, but for variable oscillator tuning the inductive variable reactance valve (the  $RC$  or  $LR$  network) is preferable, because it provides a more constant corrective effect over the frequency range than does the capacitive reactance valve.



This can be shown as follows: the oscillator frequency for the inductive reactance valve is given by

$$f_h = \frac{1}{2\pi \sqrt{\frac{L_h' L_{AB}}{L_h' + L_{AB}} \cdot C_h}} \quad . \quad . \quad . \quad 13.14$$

where  $L_h'$  and  $C_h$  are the oscillator main tuning components when the variable reactance valve is in circuit. Change of bias on the reactance valve alters  $L_{AB}$  to  $KL_{AB}$ , and the oscillator frequency to

$$f_h + \Delta f = \frac{1}{2\pi \sqrt{\frac{L_h' KL_{AB}}{L_h' + KL_{AB}} C_h}} \quad . \quad . \quad . \quad 13.15a$$

where  $K = \frac{g_{m0}}{g_m}$ , and  $g_{m0}$  is the mutual conductance for zero discriminator D.C. voltage.

Combining 13.14 and 13.15a

$$\begin{aligned} \frac{f_h + \Delta f}{f_h} &= 1 + \frac{\Delta f}{f_h} = \sqrt{\frac{L_h' L_{AB}}{L_h' + L_{AB}} \cdot \frac{L_h' + KL_{AB}}{L_h' KL_{AB}}} \\ &= \sqrt{1 + \frac{(1 - K)}{K} \cdot \frac{L_h'}{L_h' + L_{AB}}} \end{aligned}$$

If  $L_h$  is the oscillator-tuning inductance in the absence of the reactance valve

$$L_h = \frac{L_h' L_{AB}}{L_h' + L_{AB}}$$

or

$$\frac{L_h}{L_{AB}} = \frac{L_h'}{L_h' + L_{AB}}$$

Therefore

$$1 + \frac{\Delta f}{f_h} = \sqrt{1 + \frac{1 - K}{K} \cdot \frac{L_h}{L_{AB}}} \quad . \quad . \quad . \quad 13.15b$$

Now  $\frac{1 - K}{K} \cdot \frac{L_h}{L_{AB}}$  is generally very much less than 1, so that expression 13.15b may be written

$$1 + \frac{\Delta f}{f_h} \simeq 1 + \frac{1 - K}{2K} \cdot \frac{L_h}{L_{AB}}$$

or

$$\Delta f \simeq f_h \frac{1 - K}{2K} \cdot \frac{L_h}{L_{AB}} \quad . \quad . \quad . \quad 13.16a$$

$$\propto f_h \quad . \quad . \quad . \quad . \quad 13.16b$$

when  $\frac{1 - K}{2K} \frac{L_h}{L_{AB}}$  is a constant. Hence the degree of frequency

correction, exercised by the reactance valve is directly proportional to the oscillator mean frequency, i.e., A.F.C. gives least error for a given off-tune signal frequency setting at the high-frequency end of a range.

With the capacitive reactance valve the oscillator frequency is

$$f_h = \frac{1}{2\pi\sqrt{L_h(C_h' + C_{AB})}} \quad . \quad . \quad . \quad 13.17$$

where  $C_h'$  is the oscillator-tuning capacitance when the reactance valve is in circuit, and  $C_h$  is the tuning capacitance in the absence of the reactance valve, i.e., it equals  $C_h' + C_{AB}$ .

$$f_h + \Delta f = \frac{1}{2\pi\sqrt{L_h(C_h' + KC_{AB})}} \quad . \quad . \quad . \quad 13.18$$

where  $K = \frac{g_m}{g_{m0}}$ .

Combining 13.17, and 13.18.

$$1 + \frac{\Delta f}{f_h} = \sqrt{\frac{C_h' + C_{AB}}{C_h' + KC_{AB}}} = \frac{1}{\sqrt{1 + \frac{(K-1)C_{AB}}{C_h' + C_{AB}}}}$$

or 
$$\frac{\Delta f}{f_h} \simeq \frac{(1-K)C_{AB}}{2(C_h' + C_{AB})} \quad . \quad . \quad . \quad 13.19$$

because  $(1-K)\frac{C_{AB}}{C_h' + C_{AB}}$  is generally  $\ll 1$ .

Expression 13.19 may be rewritten.

$$\Delta f = f_h \frac{(1-K)C_{AB}}{2C_h} \quad . \quad . \quad . \quad 13.20$$

but 
$$f_h = \frac{1}{2\pi\sqrt{L_h C_h}}$$

or 
$$\frac{1}{C_h} = (2\pi)^2 f_h^2 L_h.$$

Therefore 
$$\Delta f \propto f_h^3.$$

This means that the degree of frequency correction is very much greater at the high-frequency end of a given range than at the low-frequency end. It is desirable to have smallest error at the low-frequency end because the signal circuits are more selective than at the high-frequency end, so that the capacitive reactance valve is much less satisfactory than the inductive reactance valve when oscillator tuning is by variable capacitance. When permeability

oscillator tuning is employed (the inductance is varied), the reverse is true, and the capacitive reactance valve is more suitable.

Let us take an example to illustrate these points, dealing first with a capacitive reactance valve applying A.F.C. to the medium wave band of a receiver. The signal frequency limits are 550 to 1,500 kc/s, the I.F. 465 kc/s and the oscillator limits 1,015 to 1,965 kc/s. The  $g_m E_{g3}$  characteristic of a typical hexode valve is shown in Fig. 13.16, for a bias of  $-5$  volts on the control grid,  $G_1$ . A bias voltage of  $-5$  means that the R.F. grid voltage should not exceed about 4 volts peak value if grid current is to be avoided. Taking  $Z_1 = R = 20,000$  ohms, a possible value for  $C$  is  $50 \mu\mu\text{F}$ , giving  $Z_2 = -j 3,140$  ohms at 1,015 kc/s and  $-j 1,624$  ohms at

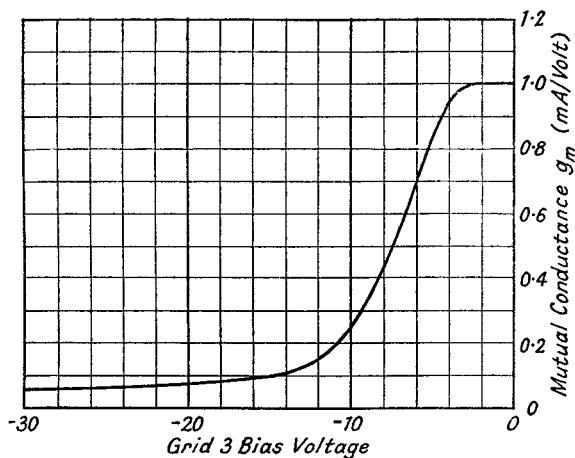


FIG. 13.16.—The Assumed  $g_m E_g$  Characteristic of the Variable Reactance Valve.

1,965 kc/s. The step-down voltage ratios from anode to grid are 0.155 and 0.0812 respectively, so that the oscillator-tuned circuit peak voltages should not exceed 25.8 and 49.3 respectively if the oscillator voltage at the grid of the reactance valve is not to exceed 4 volts. The voltages are greater than are likely to be met in a tuned-grid oscillator, but are less than might be obtained with a tuned-anode oscillator unless it is heavily damped. In the latter instance  $C$  should be increased to  $75 \mu\mu\text{F}$ , thus raising the anode maximum peak voltages to about 38.5 and 74 respectively.

The centre of the straight part of the  $g_m E_{g3}$  characteristic of Fig. 13.16, is at about  $-7$  volts, where  $g_{m0} = 0.56$  mA/volt, so let us take this as the initial setting of the reactance valve corresponding to zero discriminator D.C. output voltage. At the low-frequency

end of the medium wave range,  $f_h = 1,015$  kc/s, the parallel resistance component of the reactance valve is

$$\begin{aligned} R_{AB}(g_{m0} = 0.56) &= \frac{1 + (R\omega C)^2}{g_{m0}} = \frac{41.7}{0.56 \times 10^{-3}} \\ &= 74,500 \Omega \end{aligned}$$

and its minimum value at  $g_m = 1$  mA/volt is 41,700  $\Omega$

$$\begin{aligned} L_{AB}(g_{m0} = 0.56) &= \frac{1 + (R\omega C)^2}{g_{m0} R \omega^2 C} = \frac{41.7 \times 10^6}{0.56 \times 10^{-3} \times 4.07 \times 10^7} \mu\text{H.} \\ &= 1,832 \mu\text{H.} \end{aligned}$$

The frequency correction-discriminator D.C. voltage curve can be calculated by using expression 13.16a. Thus when  $g_m = 1$  mA/volt,  $E_{g3} = -2$  volts (from Fig. 13.16),  $K = \frac{0.56}{1} = 0.56$ . The oscillator-tuning inductance for the medium wave range is 77.4  $\mu\text{H}$  (see Section 6.12, Part I) so that

$$\begin{aligned} \Delta f &= f_h \left( \frac{1 - K}{2K} \right) \left( \frac{L_h}{L_{AB}} \right) = f_h \frac{0.44}{1.12} \frac{77.4}{1,832} \\ &= +0.0166 f_h \\ &= +16.8 \text{ kc/s for } f_h = 1,015 \text{ kc/s.} \end{aligned}$$

The frequency correction for other values of  $E_{g3}$  may be calculated in a similar manner, and the result is shown as the full line curve 1 of Fig. 13.17. The horizontal axis is scaled in  $E_{g3}$  bias volts as well as discriminator D.C. output voltage.

The effect of the phase-shifting network on the oscillator-tuned circuit must also be considered, and converting the series combination of 20,000 ohms and 50  $\mu\mu\text{F}$  into its equivalent parallel circuit we have for the parallel damping resistance

$$\begin{aligned} R_p &= \frac{1 + (R\omega C)^2}{R(\omega C)^2} = \frac{41.7}{2.035 \times 10^{-3}} = 20,450 \Omega \\ C_p &= \frac{C}{1 + (R\omega C)^2} = \frac{50}{41.7} = 1.2 \mu\mu\text{F.} \end{aligned}$$

The resistance damping effect is fairly considerable but, although it makes oscillation more difficult to sustain, it has the advantage of rendering variations of  $R_{AB}$  with change of discriminator bias of less importance. The added capacitance is seen to be negligible.

At the highest frequency in the oscillator tuning range,  $f_h = 1,965$  kc/s,

$$R_{AB}(g_{m0} = 0.56) = \frac{153.5}{0.56 \times 10^{-3}} = 274,000 \Omega$$

and its maximum value at  $g_m = 1$  mA/volt is  $153,500 \Omega$ . The value of  $R_{AB}$  given above is very nearly  $\left[ \frac{1,965}{1,015} \right]^2$  times that at  $f_h = 1,015$  kc/s, thus confirming the discussion on Table 13.3.

$$L_{AB}(g_{m0} = 0.56) = \frac{153.5 \times 10^6}{0.56 \times 10^{-3} \times 15.25 \times 10^7} = 1,795 \mu\text{H.}$$

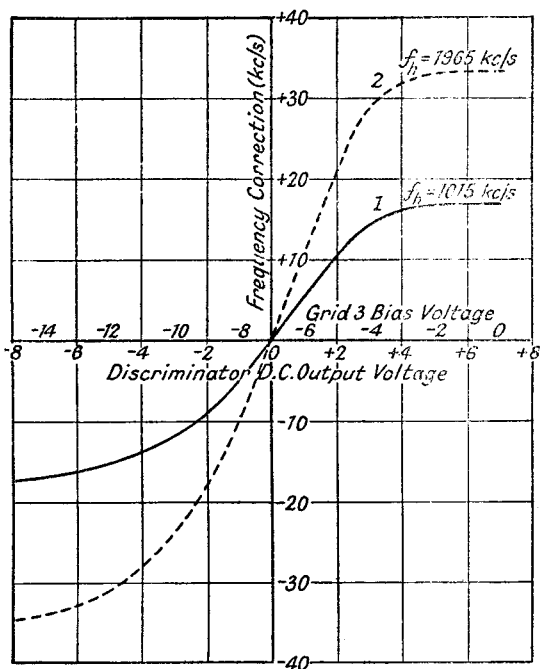


FIG. 13.17.—Frequency Correction—Discriminator Voltage Curves for the Inductive Reactance Valve.

Calculating the frequency correction from expression 13.16a we find that for  $g_m = 1$  mA/volt,  $E_{g3} = -2$  volts,

$$\begin{aligned} \Delta f &= +f_h \cdot \frac{0.44}{1.12} \cdot \frac{77.4}{1,785} \\ &= +0.0169 f_h \\ &= +33.2 \text{ kc/s, for } f_h = 1,965 \text{ kc/s.} \end{aligned}$$

The frequency correction is plotted as the dotted curve 2 in Fig. 13.17, against discriminator D.C. output voltage and  $E_{g3}$  bias.

The A.F.C. sensitivity measured by the slope of the curve at zero discriminator voltage is 10.3 kc/s per volt as compared with 5.2 kc/s per volt at  $f_h = 1,015$  kc/s, i.e., it is very nearly  $\frac{1,965}{1,015}$  times as sensitive, a result confirming expression 13.16*b*.

The equivalent parallel resistive and capacitive components of the phase-shifting network are

$$R_p = \frac{153.5}{7.625 \times 10^{-3}} = 20,100 \Omega$$

$$C_p = \frac{50}{153.5} = 0.326 \mu\mu\text{F}.$$

The damping resistance is very nearly the same as for  $f_h = 1,015$  kc/s, so that there is a tendency to stabilize oscillator amplitude. The capacitive component is again negligible.

Suitable values for the phase-shifting network over the long-wave range (signal frequencies from 150 to 400 kc/s) are  $R = 20,000 \Omega$ ,  $C = 100 \mu\mu\text{F}$ . The oscillator frequency range is from 615 to 865 kc/s and the oscillator inductance is about 370  $\mu\text{H}$ . Using these values, the results for the long-wave band are as follows :

Oscillator frequency . . . . .	615 kc/s	865 kc/s
Step-down ratio anode to grid . . . . .	0.1283	0.0915
$R_{AB}(g_{m0} = 0.56)$ . . . . .	108,600 $\Omega$	214,000 $\Omega$
$R_{AB}(g_m = 1)$ . . . . .	60,800 $\Omega$	119,500 $\Omega$
$L_{AB}(g_{m0} = 0.56)$ . . . . .	3,630 $\mu\text{H}$	3,600 $\mu\text{H}$
$\Delta f(g_m = 1)$ . . . . .	+ 24.6 kc/s	+ 35 kc/s
A.F.C. sensitivity (kc/s per volt) . . . . .	7.6	10.8
$R_p$ . . . . .	20,380 $\Omega$	20,200 $\Omega$
$C_p$ . . . . .	1.64 $\mu\mu\text{F}$	0.835 $\mu\mu\text{F}$

Over the short-wave range (signal frequencies from 6 to 15 Mc/s), suitable values for the phase-shifting network and  $L_h$  are 20,000  $\Omega$ , 5  $\mu\mu\text{F}$  and 1.5  $\mu\text{H}$  and the results are as tabulated below :

Oscillator frequency . . . . .	6,465 kc/s	15,465 kc/s
Step-down ratio anode to grid . . . . .	0.2395	0.1022
$R_{AB}(g_{m0} = 0.56)$ . . . . .	31,400 $\Omega$	170,500 $\Omega$
$R_{AB}(g_m = 1)$ . . . . .	17,550 $\Omega$	95,500 $\Omega$
$L_{AB}(g_{m0} = 0.56)$ . . . . .	190 $\mu\text{H}$	180.5 $\mu\text{H}$
$\Delta f(g_m = 1)$ . . . . .	+ 20 kc/s	+ 50.4 kc/s
A.F.C. Sensitivity (kc/s per volt) . . . . .	6.2	15.6
$R_p$ . . . . .	21,200 $\Omega$	20,250 $\Omega$
$C_p$ . . . . .	0.285 $\mu\mu\text{F}$	0.0523 $\mu\mu\text{F}$

It is clear from the above that satisfactory A.F.C. operation is less easy to achieve as the oscillator frequency increases. Stray capacitance across  $R$  becomes important and tends to prevent the 90° phase shift being obtained. It is therefore most necessary to

see that the leads from  $R$  and  $C$  to the reactance valve grid and anode are as short as possible. Interelectrode anode-grid capacitance is usually so small that it can be neglected, but allowance must be made for the grid-cathode interelectrode capacitance, which is a part of and may be comparable to the required value of  $C$ .

The less satisfactory performance of the capacitive reactance valve in correcting a capacitively tuned oscillator can be demonstrated by considering the medium-wave range. Suitable values for  $C$  and  $R$  are  $5 \mu\mu\text{F}$  and 5,000 ohms; a large value of  $R$  cannot be used because the grid-cathode capacitance of the valve is comparatively large (about  $3.5 \mu\mu\text{F}$ ), and if  $R$  is comparable with this

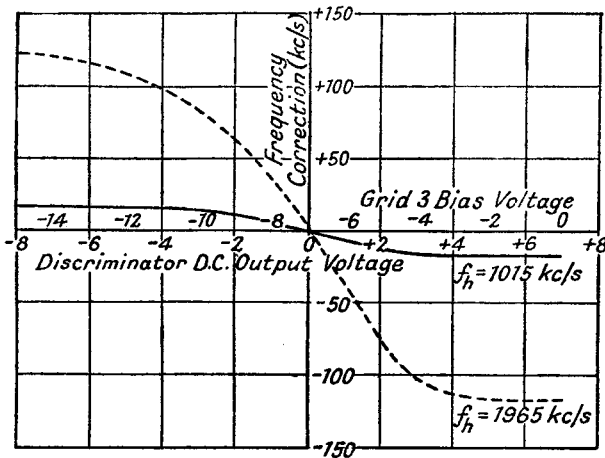


FIG. 13.18.—Frequency Correction—Discriminator Voltage Curves for the Capacitive Reactance Valve.

reactance the required  $90^\circ$  phase shift cannot be realized. The results at the extremes of the oscillator frequency range are tabulated below, and the frequency correction-discriminator voltage curve is shown in Fig. 13.18. The oscillator tuning capacitance at 1,015 and 1,965 kc/s is assumed to be 317 and  $84.8 \mu\mu\text{F}$  respectively, i.e.,  $L_h = 77.4 \mu\text{H}$ .

Oscillator frequency	. . . . .	1,015 kc/s	1,965 kc/s
Step-down ratio anode to grid	. . . . .	0.158	0.295
$R_{AB}(g_{m0} = 0.56)$	. . . . .	71,800 $\Omega$	20,550 $\Omega$
$R_{AB}(g_m = 1)$	. . . . .	40,200 $\Omega$	11,500 $\Omega$
$C_{AB}(g_{m0} = 0.56)$	. . . . .	13.63 $\mu\mu\text{F}$	12.75 $\mu\mu\text{F}$
$\Delta f(g_m = 1)$	. . . . .	- 17.15 kc/s	- 116.1 kc/s
A.F.C. sensitivity (kc/s per volt)	. . . . .	5.3	36.0
$R_p$	. . . . .	202,000 $\Omega$	57,900 $\Omega$
$C_p$	. . . . .	4.87 $\mu\mu\text{F}$	4.56 $\mu\mu\text{F}$





This result is very similar to that obtained for the inductive reactance valve with a  $RC$  phase-splitting network. The chief disadvantage of the method is that the addition of  $R$  in the oscillator-tuned circuit makes oscillation more difficult to sustain, and an oscillator valve having a high  $g_m$  is required.

The admittance of the capacitive arm of the oscillator-tuned circuit may be multiplied in the same manner by connecting the tuning capacitance in place of the inductance, but this is only possible with preset-tuned circuits which do not require the capacitance to be earthed.

Many other valve circuits are possible, and the variable reactance valve may, if desired, be applied via a separate coil coupled to the oscillator-tuned circuit. For satisfactory operation and high A.F.C. sensitivity, the control valve should have a high  $R_a$ , and a rapid and linear change of  $g_m$  with change of discriminator bias voltage.

**13.4.4. Estimation of A.F.C. Overall Performance.**<sup>8</sup> The operation of an A.F.C. circuit may be represented by an overall performance curve connecting signal tuning frequency setting with I.F. error. Such a curve is not satisfactory for design purposes since any change in the discriminator or variable reactance unit requires a different performance curve to be plotted. The overall characteristic is the result of two separate actions, and it is desirable to combine the characteristics of the discriminator and variable reactance unit in a way which preserves their separate identities. The method employed is illustrated in Fig. 13.19. The discriminator D.C. output voltage plotted against frequency error is represented by curve  $ABODE$ . The variable reactance characteristic  $FGH$  (frequency correction against control bias voltage), drawn on transparent paper, is rotated anti-clockwise through  $90^\circ$  so that its frequency correction axis is coincident with the frequency error axis of the discriminator and the two voltage axes are parallel. The reactance characteristic is moved over the discriminator curve for different tuning errors, always keeping the two frequency axes coincident. Thus the intersection of the voltage axis of the reactance unit with the frequency error axis, e.g., point  $M_1$ , gives the frequency error of the signal-tuned circuits, whilst a perpendicular from its intersection,  $N_1$ , with the discriminator characteristic on to the frequency axis gives the final I.F. tuning error  $OP_1$ . The proof of this is that the following equation is satisfied:

signal tuning error — frequency correction = final oscillator tuning error

$$OM_1 - M_1P_1 = OP_1.$$

By sliding the reactance unit characteristic over the discriminator curve (always maintaining the frequency axes coincident), the final oscillator (or I.F.) tuning error can be read directly for any value of signal tuning error. The "throw-out" and "pull-in" frequencies can also be found.

Five positions of signal frequency setting are illustrated on Fig. 13.19. In the first position the two curves intersect at the origin; the tuning setting is correct and no error exists. In position 1 the signal frequency setting error,  $OM_1$ , is corrected to an I.F. tuning error of  $OP_1$ . If the signal frequency error is progressively increased through  $M_2$ ,  $M_3$  to  $M_4$ , the final I.F. errors are  $OP_2$ ,  $OP_3$  to  $OP_4$ . At position 3 the reactance corrector curve just touches the discriminator characteristic, and a slight increase in

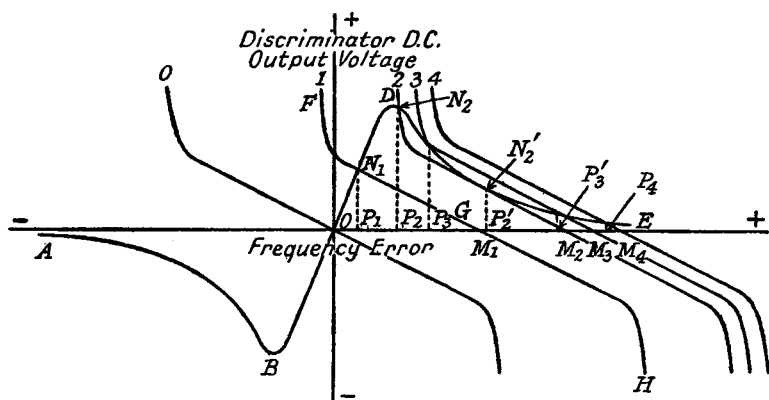


FIG. 13.19.—A Combined Form of Discriminator and Control Characteristic.

signal frequency error causes the I.F. error to jump from  $OP_3$  to  $OP_3'$ , i.e., A.F.C. has practically lost control.  $OM_3$  therefore gives the "throw-out" signal frequency. In position 4 the error is slightly less than the signal frequency error, but for all practical purposes the A.F.C. can be regarded as inoperative. Progressive decrease of signal frequency tuning error from  $OM_4$  towards  $O$  produces final I.F. errors of  $OP_3'$ ,  $OP_2'$  and  $OP_1$ . It should be noted that in position 3, the final I.F. error  $OP_3'$  is much greater when tuning towards  $O$  than away from  $O$ . At position 2, the reactance corrector curve is tangential to the discriminator curve at  $N_2'$ , and the slightest movement towards  $O$  causes the working point to jump from  $N_2'$  to  $N_2$ . A.F.C. now takes full control, the I.F. error falling from  $OP_2'$  to  $OP_2$ . The signal frequency error corresponding to  $OM_2$  gives the "pull-in" frequency setting. Between positions

2 and 3, there are three intersections of the reactance corrector and discriminator curves. The two extreme points give the operating points when tuning away from a signal (the I.F. error is less) and when tuning towards a signal (the I.F. error is greater), whilst the centre point represents an unstable position.

The reactance unit curve is shown in Fig. 13.19 as having a limited control characteristic, i.e., correction is confined to a range of discriminator voltages, and outside this range the reactance remains almost constant. Its chief advantage compared with the unlimited control characteristic is that it reduces the "throw-out" frequency and so reduces the transmission channel blotted out by A.F.C. action on either side of a strong signal. This is illustrated

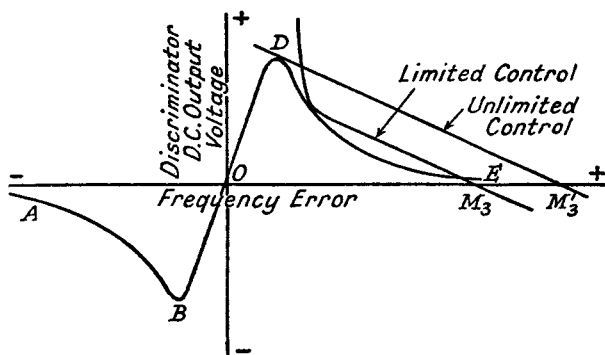


FIG. 13.20.—The Effect of Limited and Unlimited Control Characteristic on A.F.C.

in Fig. 13.20; the "throw-out" frequency, corresponding to  $OM_3'$ , for the unlimited control characteristic is greater than that,  $OM_3$ , for the limited characteristic. In other respects there is little difference between the two, and the "pull-in" frequency is the same for both.

#### BIBLIOGRAPHY

1. A New System for the Remote Control of Radio Broadcast Receivers. J. B. Sherman, *Proc. I.R.E.*, Jan. 1935, p. 47.
2. Automatic Frequency Control. C. Travis, *Proc. I.R.E.*, Oct. 1935, p. 1125.
3. A.F.C. Design Considerations. S. Y. White, *Electronics*, Sept. 1936, p. 28.
4. Automatic Tuning. D. E. Foster and S. W. Seeley. *Proc. I.R.E.*, March 1937, p. 289.
5. Remote Tuning Control. J. F. Ramsay, *Wireless World*, Sept. 3rd, 1937, p. 231.
6. Magnetic Tuning Devices. L. de Kramolin, *Wireless World*, Feb. 24th (p. 160) and March 3rd, 1938 (p. 186).
7. Push-Button Tuning Systems. *Wireless World*, March 10th, 1938, p. 206.

8. Automatic Frequency Correction. O. E. Keall and G. Millington, *Marconi Review*, April-June 1938, p. 1.
9. Theory of the Discriminator Circuit for Automatic Frequency Control. H. Roder, *Proc. I.R.E.*, May 1938, p. 590.
10. Automatic Tuning Systems. W. E. Felix, *Wireless World*, June 16th, 1938, p. 526.
11. Teledynamic Control by Selective Ionization with Application to Radio Receivers. S. W. Seeley, H. B. Deal, and C. N. Kimball, *Proc. I.R.E.*, July 1938, p. 813.
12. More about Magnetic Tuning. L. de Kramolin, *Wireless World*, July 7th, 1938, p. 5.
13. Olympia Show Review. *Wireless World*, Sept. 1st, 1938, p. 207.
14. Mystery Control. *Radio and Television*, Jan. 1939.
15. Remote Frequency Changer. E. Martin, *Wireless World*, March 16th, 1939, p. 249.
16. Remote Control. Cathode Ray, *Wireless World*, March 23rd, 1939, p. 266.
17. Broadcast Receivers. A. Review. N. M. Rust, O. E. Keall, J. F. Ramsay and K. R. Sturley, *Journal I.E.E.*, Part III, June 1941, p. 59.

## CHAPTER 14

# MEASUREMENT OF RECEIVER OVERALL PERFORMANCE

**14.1. Introduction.** The overall performance of a radio receiver requires to be measured not only to assess the relative merits of a particular design, but also to indicate its usefulness under any special operating conditions. In broadcast reception the exact location of a particular receiver is unlikely to be known so that the first viewpoint is the more important. The approximate site conditions may, however, be known to a designer of a communication receiver, and these may have considerable influence on the measurement tests required.

A series of tests has been standardized in America by the Institute of Radio Engineers<sup>1, 5</sup> and in England by the Radio Manufacturers Association<sup>2, 4</sup> as a guide for the designer of broadcast receivers. Their recommendations form the basis of the methods discussed in this chapter, and grateful acknowledgement is made for permission to use the specifications. The two series differ in certain respects, and where this occurs an attempt is made to assess the relative advantages of each method. Modifications or elaborations of any test are included—in their appropriate sections—after the standard specification. Electrical and acoustical tests are covered by the recommendations, which include measurements of sensitivity, selectivity, frequency response, automatic gain control, noise and hum. The electrical tests are treated first. The meanings of certain terms and a short description of the measuring apparatus are given before dealing with procedure.

## 14.2. Definitions.

**14.2.1. Standard Input Voltage.** This is the R.M.S. value\* of the input carrier in microvolts, or the ratio (in decibels) of the carrier referred to 1 microvolt as zero level (R.M.A.). A reference level of 1 volt is suggested by the I.R.E., but in most cases 0 db.  $\equiv$  1  $\mu$ V is to be preferred. The standard modulation frequency and percentage is 400 c.p.s. and 30% respectively. Terms

\* Wherever the term R.M.S. value of input carrier is employed it refers to the carrier voltage only, and excludes the sideband voltages; i.e., it is the R.M.S. value of the carrier voltage before it is modulated.

distant, mean, local and strong are applied (by the I.R.E.) to R.M.S. carrier voltages of 50, 5,000, 100,000  $\mu\text{V}$  and 2 volts respectively.

**14.2.2. Standard Output Power.** The I.R.E. suggest 50 mW and 500 mW as the standard outputs for receivers having maximum outputs less than and greater than 1,000 mW respectively. The R.M.A. recommend 50 mW for all receivers. There are advantages in the use of 500 mW for larger output receivers, because hum and noise may produce outputs comparable with 50 mW, particularly if the receiver is a superheterodyne with considerable I.F. amplification. The power is measured in a non-inductive resistance connected in place of the speaker speech-coil and having the same value as the modulus ( $\sqrt{R_{sc}^2 + X_{sc}^2}$ ) of the coil impedance at 400 c.p.s.

For communication receivers intended for phone operation or connection to a land line a suitable standard output power is 1 mW in a resistance equal to the impedance of the phones at 400 c.p.s., or equal to the characteristic impedance of the line (often 600 ohms).

**14.2.3. Sensitivity.** The sensitivity of an open aerial receiver is defined as the R.M.S. value of input carrier modulated 30% at 400 c.p.s. which, applied through an appropriate dummy aerial, gives the standard output power. Alternatively, sensitivity may be expressed in ratio form as decibels with reference to 1  $\mu\text{V}$  as zero level (R.M.A.). If other than standard output is used the actual power should be stated or the input carrier value corrected by

multiplying it by  $\sqrt{\frac{P_s}{P_a}}$  where  $P_a$  is the actual and  $P_s$  the standard power. This correction is only applicable when the characteristic of the A.F. detector is linear.

For a frame aerial receiver sensitivity is defined in microvolts per metre.

**14.2.4. Selectivity.** The selectivity of a receiver is defined as its capability of discriminating against undesired signals. It may be expressed in terms of the ratio of the sensitivity of the receiver when a standard modulated carrier is off-tuned a specified amount, to its sensitivity when the carrier is correctly tuned to the receiver signal tuning frequency. It may also be expressed in terms of the undesired modulated carrier level required to produce a given interference output.

**14.2.5. Fidelity or Frequency Response.** The fidelity (better termed frequency response) of a receiver is the degree to which it responds to different modulation frequencies. It is measured by

noting the variation in A.F. power output as the modulation frequency is varied from 30 to 15,000 c.p.s.

**14.2.6. Harmonic Distortion.** Audio frequency harmonic distortion is expressed as the percentage ratio of the R.M.S. value of the total harmonic voltages in the output to the R.M.S. value of the fundamental and harmonic voltages together. Usually the harmonic voltages are small enough not to affect the second reading to any great extent.

**14.2.7. Noise.** The noise produced in a receiver is the A.F. output power registered with an unmodulated input carrier voltage. Hum voltages must be excluded from mains receivers by suitable filters attenuating all frequencies below 300 c.p.s. When a receiver is used for c.w. reception, the definition may be modified to read the A.F. output power registered in the absence of an input carrier voltage.

**14.2.8. Hum.** Hum is measured in the same way as noise except that a low-pass filter is used for attenuating noise output. Both hum and noise outputs are best expressed as decibel ratios referred to the normal output power as zero level.

**14.2.9. Automatic Gain Control.** The performance of an A.G.C. device is measured by the change of output power produced by a given change of modulated input carrier.

**14.2.10. Standard Aerial.** An open single-wire aerial of 4 metres effective height is considered as the standard aerial for medium and long waves, and a non-inductive resistance of 400 ohms for short waves.

**14.3. The Apparatus required for the Overall Electrical Measurements.** The apparatus required for the overall electrical tests includes a standard signal generator, a dummy aerial for an open aerial receiver, a special shielded pick-up coil for frame aerial receivers, an output meter, a beat frequency oscillator and a distortion factor meter, or harmonic analyser.

**14.3.1. Standard Signal Generator.** This is a frequency calibrated R.F. oscillator capable of modulation to 90%. The output is taken from an attenuator calibrated in microvolts. The attenuator input, supplied from a pick-up coil connected direct to the oscillator or to a buffer valve, is monitored by a thermal instrument or a valve voltmeter. The thermal instrument may also be used as a percentage modulation indicator, for the R.M.S. value of modulated carrier current is

$$I_{c+m} = I_c \sqrt{\left(1 + \frac{M^2}{2}\right)}$$

where  $I_c$  is the R.M.S. value of unmodulated carrier. The initial modulation setting is made at 80% and lower modulation percentages are obtained from a calibrated potentiometer. When monitoring by valve voltmeter the latter is used to make direct comparison between the carrier and A.F. modulating voltage.

An internal 400 c.p.s. oscillator is incorporated, but external modulation can also be applied.

A slow-motion drive is required on the frequency control to allow selectivity measurements to be made.

The range of the attenuator is normally continuously variable from 1  $\mu$ V to 0.1 or 1 volt R.M.S., and it is an advantage if the attenuator scale is calibrated in decibel ratios (referred to 1  $\mu$ V as zero level) as well as microvolts. The output impedance of the attenuator should be low, and the oscillator frequency should not be affected by change of attenuator setting.

**14.3.2. Standard Dummy Aerial.** A standard dummy aerial is required between the signal generator and receiver to simulate an open aerial. The components are given in Fig. 14.1a and the

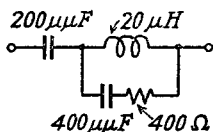


FIG. 14.1a.—Circuit Constants of a Standard Dummy Aerial for Long, Medium and Short Wave Bands.

impedance variation in Fig. 14.1b. The impedance approaches that of an open aerial of 4 metres effective height over the medium- and long-wave bands, whilst over the short-wave range it is equivalent to a resistance of 400 ohms. The impedance characteristic is affected by the signal generator attenuator output resistance, which should be much less than the series resistance or reactance component of the dummy aerial.

**14.3.3. The Shielded Pick-Up Coil for Frame Aerial Receivers.** A cylindrical shielded pick-up coil is necessary to provide magnetic coupling to frame aerial receivers. The following are the dimensions recommended by the R.M.A.: radius 5 cms., length 6 cms., turns 20 and approximate inductance 40  $\mu$ H. Electrostatic coupling is prevented by enclosing the coil in a wire cage. The shunt capacitive reactance of the coil and the leads to the signal generator attenuator must be large compared with the inductive reactance of the coil, and the latter should be much larger (at least 20 times) than the attenuator output resistance so that the output



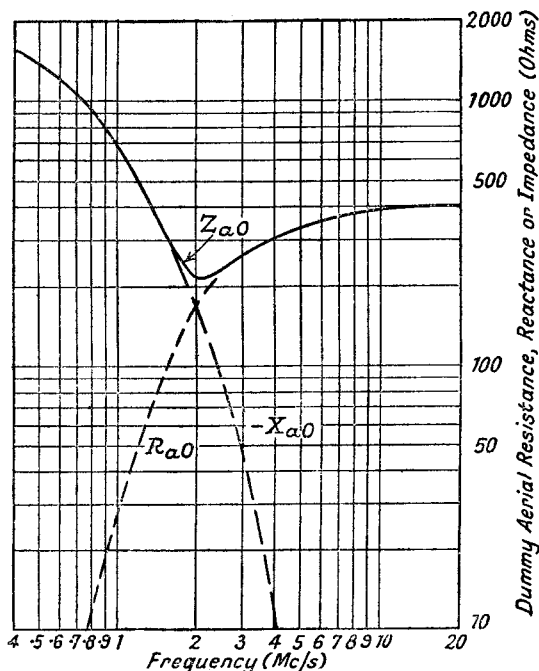


FIG. 14.1b.—Impedance Characteristics of a Standard Dummy Aerial.

voltage is unaffected by the coil connection. The coil and frame aerial are placed coaxially and the input to the receiver is

$$\frac{18,800 N r^2 E}{(r^2 + l^2)^{\frac{3}{2}} \omega L} \text{ microvolts/metre.} \quad . \quad . \quad 14.1a.$$

where  $E$  = attenuator R.M.S. carrier output in microvolts.

$N$  = number of coil turns.

$r$  = coil radius in centimetres.

$l$  = axial distance between the geometric centres of the coil and frame in centimetres.

$L$  = coil inductance in Henries.

This reduces to

$$\frac{4,670 E}{f} \text{ microvolts/metre} \quad . \quad . \quad 14.1b$$

for the above coil and the recommended distance  $l$  of 2 metres, where  $f$  is in c.p.s.

**14.3.4. Output Meter.** The output meter should be non-reactive and should present a constant resistance to frequencies from 30 to 10,000 c.p.s. If the resistance is variable in steps the meter

is usually scaled in milliwatts, but if it is fixed the reading is generally given in volts.

**14.3.5. Beat Frequency Oscillator.** A beat frequency oscillator is required to provide sufficient output to modulate the signal generator to 100%. Its total harmonic distortion at this output should not exceed 1%.

**14.3.6. Distortion Factor Meter.** The distortion factor meter consists of a filter for eliminating the fundamental, and a R.M.S. meter for measuring the harmonic voltages. A comparison method is employed, and a calibrated potentiometer across the input to the meter enables a proportion of the distorted input to be compared against the harmonic input. This potentiometer is scaled in percentage distortion. The distortion factor meter input impedance must be high enough not to affect the loading of the circuit to which it is connected. If this is not so, a buffer amplifier producing negligible harmonic distortion must be inserted before the meter.

**14.3.7. Harmonic Analyser.** A harmonic analyser is required for measuring the ratio of individual harmonics to the fundamental. Such apparatus generally uses the highly selective properties of a quartz crystal filter to separate each harmonic. The A.F. fundamental and harmonics are used to modulate a carrier frequency which is adjusted so as to bring the desired harmonic sideband into the very narrow pass-band of the crystal filter.

**14.4. Receiver Adjustments.** No special adjustments should be made to the receiver and the following recommendations are made by the R.M.A.

The receiver, in its own cabinet, is to be tested after it has been switched on for a half-hour. Mains receivers should be operated at the mean voltage of the particular transformer tapping point. Battery receivers are to have a resistance of ohmic value equal to the number of cells in the H.T. battery, inserted in the H.T. negative lead. This exaggerates any tendency to instability and is equivalent to a partially used battery. Tone, volume and selectivity controls are normally to be set for maximum 400 c.p.s. response. A "local-distant" switch, when fitted, is to be set to "distant" for sensitivity and selectivity tests.

## 14.5. Test Specifications.

**14.5.1. Sensitivity.** All sensitivity measurements on an open aerial receiver are to be made with the standard dummy aerial between the signal generator and receiver (see Fig. 14.2a). When the latter is intended to operate with a special aerial, the standard

is replaced by components giving an impedance characteristic similar to the special aerial. The R.F. input carrier modulated 30% at 400 c.p.s., is adjusted to give the standard output (1, 50 or 500 mW). If readings are not taken over each frequency range the suggested test frequencies are, long-wave range, 160, 200 and

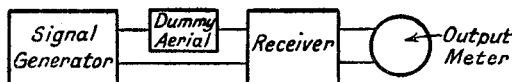


FIG. 14.2a.—Schematic Diagram of Apparatus for Measurement of Sensitivity.

300 kc/s, medium-wave range, 600, 1,000 and 1,400 kc/s, and short-wave ranges at the centre and ends of each range. The sensitivity may be plotted as a series of curves with a uniformly divided vertical decibel scale or logarithmically divided R.M.S. input carrier voltage scale against a linear or logarithmic frequency scale. The logarithmic frequency scale has the advantage that all the ranges can be accommodated on one graph as shown by the specimen full line curves in Fig. 14.2b.

For frame aerial receivers the shielded coil of 14.3.3, connected directly to the output of the signal generator, is placed coaxially with the frame at a distance of 2 metres (between geometric centres). Sensitivity is defined in microvolts per metre in accordance with the formula, 14.1b.

An additional test (I.R.E.) to show the sensitivity at maximum “undistorted” output (10% R.M.S. of A.F. total harmonic distortion) is

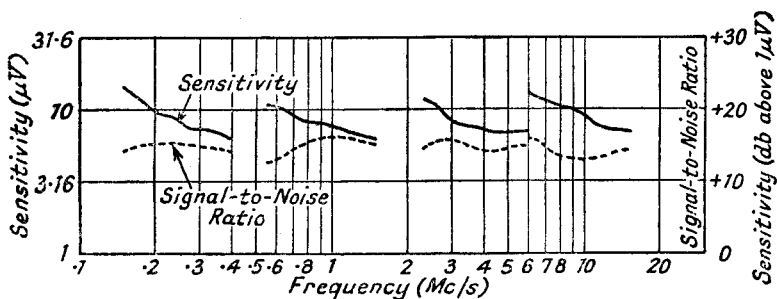


FIG. 14.2b.—Typical Sensitivity and Signal-to-Noise Ratio Curves for a Receiver.

useful, and it is carried out in the same manner as the normal test except that the input carrier is modulated 80%.

In the above tests no account is taken of noise level in determining the sensitivity, and it is clear that high sensitivity is quite valueless if the noise output is comparable with the standard 400 c.p.s. output.

Complete information on sensitivity therefore calls for a statement of signal-to-noise ratio, and the power output of noise at the sensitivity level of unmodulated carrier should be measured. The ratio, expressed in decibels, of standard modulated output to noise output, is included with the sensitivity curve for each range as shown by the dotted specimen curves in Fig. 14.2*b*.

A better estimate of sensitivity is obtained by associating it with a definite minimum signal-to-noise ratio. For example, sensitivity may be defined as the r.m.s. value of input carrier, which, modulated 30% at 400 c.p.s., gives standard output with a signal-to-noise ratio of not less than 15 db. This ratio is reasonably satisfactory for communication purposes, but a higher value is preferable for pleasurable reception. The procedure is to increase the modulated input carrier until standard power output is obtained, e.g., 50 mW; the modulation is then turned off and the noise power output measured. If this is less than 1.585 mW (this represents - 15 db. on 50 mW), the sensitivity is taken as the r.m.s. input carrier registered by the signal generator. On the other hand, if the noise power exceeds this, the volume control on the receiver is adjusted until the noise power is reduced to 1.585 mW. This reduces the modulated output from 50 mW, and it is returned to its original value by increasing the modulated carrier input. The modulation is again switched off and the noise power checked to see that it is still 1.585 mW; generally it is not changed to an appreciable extent by the increase in carrier voltage. The new carrier voltage giving the required signal-to-noise ratio with standard output is taken as the sensitivity of the receiver.

For receivers fitted with regeneration (reaction) control it is usual to take sensitivity with minimum and maximum reaction. The normal procedure is to increase the regeneration until oscillation begins. The control is then reduced until slight detuning of the receiver on either side of correct signal setting gives no sign of oscillation. The input carrier is then adjusted to give standard output. The values so obtained are liable to considerable variation, and to a large extent depend on the skill of the operator. A method giving more reliable results is to set the reaction control just to the oscillating point, and to detune the signal generator so that a difference frequency of approximately 400 c.p.s. is obtained. The unmodulated input carrier is then adjusted for standard output of the difference frequency, and this value is considered as the sensitivity. It generally gives a higher sensitivity value than that obtained by the first method.

**14.5.2. Selectivity.**<sup>7</sup> The large number of independent factors which affect selectivity make it extremely difficult to find an infallible measurement of the receiver discrimination against undesired signals. The chief interference effects are conveniently classified as follows :

(1) A heterodyne whistle, when the frequency difference between the desired and undesired carriers is equal to an audio frequency.

(2) Cross-modulation, the modulation frequencies of the undesired carrier are transferred to the desired carrier (see Section 4.7.3, Part I).

(3) A reduction in the desired audio output due to A.G.C. action and to demodulation at the detector (see Section 8.10, Part I) by the undesired carrier.

(4) "Monkey chatter" due to sidebands (or harmonic \* sidebands) of the undesired carrier, which fall in the pass range of the receiver and become sidebands to the desired carrier. The resultant A.F. output has an "inverted" frequency relationship to the undesired modulating frequency. For example, suppose a receiver having a pass range of  $\pm 15$  kc/s is tuned to a desired carrier of 1,000 kc/s in the presence of an undesired carrier of 1,020 kc/s modulated by 5, 8, and 13 kc/s. The lower sideband frequencies of the undesired signal are 1,015, 1,012 and 1,007 kc/s respectively, and these enter the pass range of the receiver to form sidebands for the desired carrier. Subsequent detection produces A.F. outputs of 15, 12, and 7 kc/s, i.e., the original low modulating frequency appears as a high audio frequency and the original high frequency as a low audio frequency, a process which is termed frequency inversion.

Distorted undesired output due to frequency inversion is the most serious form of interference, since the receiver cannot be made to discriminate against it without restricting the pass range to an undesirable extent. The effect is worse when the receiver is operating at a site close to a strong local station, and several frequency channels on either side of the local station tuning point may show serious interference. For example, suppose a local transmission of 1,000 kc/s frequency induces a voltage of 1 volt in the aerial of a receiver tuned to 1,023 kc/s. If it is modulated 50% (the voltage of each of the two sidebands is 0.25) at 5 kc/s and there is a fourth

\* The term harmonic sideband signifies a sideband produced from modulation of the carrier by a harmonic of the modulating frequencies, i.e., it is represented by  $f_c \pm n f_{mod}$ , where  $f_c$  and  $f_{mod}$  are the carrier and modulating frequencies, and  $n$  is a positive integer greater than 1.

harmonic sideband percentage of 0.1%, the amplitude of the upper frequency harmonic sideband (1,020 kc/s) is 500  $\mu$ V. A desired carrier of 1,023 kc/s and 100  $\mu$ V is overmodulated by the undesired harmonic sideband and the result is an A.F. output, which is a distorted reproduction of the frequency difference (3 kc/s) between the undesired harmonic sideband and the desired carrier. The only method of reducing this form of interference when the harmonic sidebands are produced by the transmitter is to reduce harmonic generation in the A.F. modulation amplifier stages and harmonic sideband production in the R.F. stages of the transmitter, and to include suitable filters attenuating severely modulating frequencies exceeding about 15 kc/s and radio frequencies outside the range  $f_c \pm 15$  kc/s, where  $f_c$  is carrier frequency.

The receiver itself can produce these harmonic sidebands due to distortion in the first R.F. stage (see Section 4.7.1, Part I), and high selectivity in the aerial-tuned circuits can appreciably reduce the interference effect by decreasing the undesired carrier and its sidebands. As a general rule, however, harmonic sideband production in the receiver is a second order effect, and is negligible in comparison with that produced by the transmitter. Under present conditions of transmission and reception little is to be gained in trying to develop a test to determine the interference due to the receiver itself from frequencies inside the pass-band. Measurements of heterodyne whistle, cross-modulation and demodulation, as far as interference outside the pass-band is concerned, are, however, useful.

There are two recognized methods of estimating selectivity, the first, using a single modulated R.F. carrier, indicates the discrimination of the receiver-tuned circuits against modulated off-tune carrier frequencies, and the graph obtained is really a tuning frequency response curve. The second method uses two signals, one (unmodulated) representing the desired and the other (modulated) the undesired. Adjustment of the modulated undesired is made until a certain A.F. output power level is reached.

We shall first consider the tuning frequency response method of selectivity measurement. The particular signal tuning frequencies at which these measurements are to be made are the same as those recommended for the sensitivity tests. In certain receivers, having high I.F. selectivity, measurements on the short-wave ranges may be unnecessary because the R.F. tuned circuits contribute very little to adjacent channel selectivity. The procedure is as follows: the receiver is tuned to one of the three selected frequencies in a given wave range, e.g., 1,000 kc/s, and readings are taken of the input

carrier voltage (modulated 30% at 400 c.p.s.) required to maintain a constant output power (usually the standard, 50 mW) as the frequency of the carrier is detuned on either side of 1,000 kc/s. The input carrier, preferably expressed in decibels as the ratio of the voltage at the off-tune to that at the correctly tuned position (1,000 kc/s), is plotted against a linear horizontal off-tune frequency scale. The off-tune frequency is carried to a point where the input carrier ratio is 80 db. or its actual value is 1 volt, and a specimen curve is shown in Fig. 14.3a. If the magnitude of the carrier voltage is plotted it should be to a logarithmic scale.

Selectivity may also be expressed in tabular form as the band

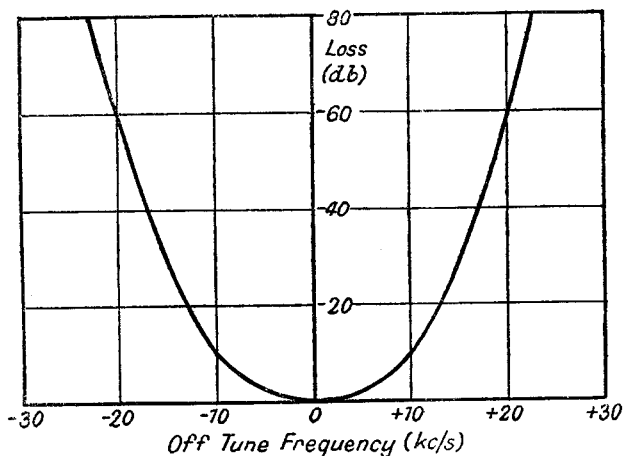


FIG. 14.3a.—An Example of a Tuning Response Curve.

width at certain specified input carrier ratios such as  $-6$ ,  $-20$  and  $-40$  db.

When the I.F. circuits are fitted with a variable selectivity control, its effect need only be tested at one signal frequency. Overall tests are normally carried out for minimum selectivity. Automatic (valve controlled) selectivity devices should be tested at different bias settings of the control valve or valves corresponding to maximum, half and minimum selectivity.

For receivers fitted with manual R.F. volume control, it is often desirable to check the selectivity curves at minimum and half-control settings, because bias changes affect the internal resistances of the amplifier valves and also feedback from the anode to grid due to the anode-grid capacitance. Both change the damping of the tuned circuit, and feedback also alters the tuning frequency (generally to

a lower frequency value). Receivers fitted with A.G.C., which cannot easily be disconnected, should be tested at a power output below that at which A.G.C. is operative. For broadcast receivers, 50 mW is likely to be satisfactory, but for communication receivers it should be limited to 1 mW. The effect of A.G.C. is to give a response wider than the true tuning frequency response.

This test yields results of value for assessing the performance of the tuned circuits, and it is a guide to the discrimination of the receiver against the first type of interference, viz., heterodyne whistle, but it provides incomplete information with regard to interference from undesired signals present at the grid of the first R.F. valve at the same time as the desired, i.e., cross-modulation and distortion in the first amplifier valve is ignored.

The second test (R.M.A.) is designed to include cross-modulation. The outputs from two signal generators, connected in series, are applied through a dummy aerial to the receiver. The two generators should be checked to ensure that the series connection has not affected their voltage calibration. Each in turn, with the other switched off, is set to the receiver tuning frequency, and the receiver output is noted for the same modulated signal generator voltage. The receiver output will be the same in both cases, if the series connection is satisfactory.

The selected test tuning frequencies are as for the first method. A low-pass filter is inserted in the receiver output to cut off all frequencies above 400 c.p.s. This is to prevent the beat frequency due to the desired and undesired carrier frequency separations from masking the cross-modulation effect. Correct tuning is first carried out with the undesired carrier off and the desired carrier modulated 30% at 400 c.p.s. and set for 1 millivolt R.M.S. The receiver volume control is adjusted to give one-quarter of the maximum rated output. The modulation of the desired carrier is switched off, and the undesired carrier modulated 30% at 400 c.p.s. is applied at different off-tune frequencies. Its voltage is adjusted to give an output power 40 db. below the original one-quarter maximum power. Thus an interference power of 0.1 mW is required from a receiver having maximum output of 4,000 mW. The undesired signal frequency is not normally adjusted closer than  $\pm 5$  kc/s to the desired frequency.

A specimen curve is shown as full line curve 1 of Fig. 14.3*b*. The interfering carrier is plotted to a vertical scale (logarithmic in  $\mu$ V or linear in decibels relative to 1  $\mu$ V) against off-tune frequency to a linear horizontal scale. Except for receivers having very poor



selectivity before the first R.F. amplifier valve, little difference is found to exist between the curves obtained by this and the first method. Since the second method is so much more complicated there is little value in using it in preference to the first. It is, however, useful in determining the selectivity of a receiver fitted with automatic selectivity or automatic frequency control. A similar test, known as the two-signal cross-talk interference test, is suggested by the I.R.E., but the interference power output is adjusted to 30 db. below standard output and three different levels of desired carrier, 50, 5,000 and 100,000  $\mu\text{V}$ , are used.

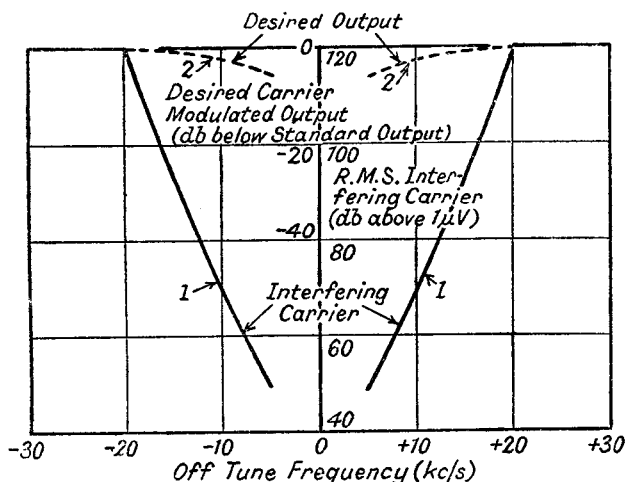


FIG. 14.3b.—A Selectivity Curve Obtained by the Two-signal Method.

This method of measuring selectivity gives no indication of the demodulating effect of the undesired carrier on the modulation of the desired at the detector, nor does it show the contribution of the undesired carrier to the A.G.C. voltage. The I.R.E. two-signal blocking interference test allows this effect to be measured, and is a further modification of the two-signal selectivity test. The modulation of the undesired signal is switched off after the correct interference power output has been obtained; the desired carrier is modulated at 30%, and the A.F. power output with the undesired carrier on is compared with its value when the undesired carrier is switched off. The reduction in desired output is plotted against off-tune frequency on the same graph as the two-signal selectivity curve (see dotted curve 2 in Fig. 14.3b).

Heterodyne whistle and "monkey-chatter" frequency-inverted

interference are not included in the above two-signal interference tests, but the latter can be modified to show this effect. The procedure is as follows: The two-signal generators are connected in series to the receiver through the dummy aerial and only the desired carrier is switched on. It is modulated 30% at 400 c.p.s. and its output set at a specified level (values are given later). If the A.F. output volume at this carrier level is greater than half the rated maximum output, the A.F. volume control is reduced to give this value. The desired modulation is now switched off and the undesired modulated carrier switched on and adjusted to a specified level. A 400 c.p.s. filter is not used, so that the interference power output includes heterodyne whistle and frequency-inverted components as well as cross-modulation. The interference power output is noted at different off-tune frequency settings of the undesired carrier and it is plotted in decibel ratio with reference to 1 mW as zero level. The minimum undesired-desired carrier spacing at which measurements are taken is that giving an interference power output equal to half the rated maximum. The test is carried out for the following carrier inputs—the suffix *D* denotes desired and *U* undesired carrier—50  $\mu\text{V}$  (*D*) and 50  $\mu\text{V}$  (*U*); 50  $\mu\text{V}$  (*D*) and 100,000  $\mu\text{V}$  or 1 volt (*U*); 5,000  $\mu\text{V}$  (*D*) and 5,000  $\mu\text{V}$  (*U*); 5,000  $\mu\text{V}$  (*D*) and 100,000  $\mu\text{V}$  or 1 volt (*U*). This simulates conditions for interference between two weak, a weak and powerful, two average, and an average and powerful signal. A typical result is shown by curve 1 in Fig. 14.3c; the curve is asymptotic to the inherent noise level of the receiver as the undesired carrier off-tune frequency separation from the desired is increased.

A 400 c.p.s. band-pass filter is next inserted between the output and output meter, and a test is carried out with the desired carrier modulated and the undesired unmodulated at the same input levels as those listed above. This measures the demodulating effect of the undesired and also the volume reduction of the desired modulation due to operation of the A.G.C. by the undesired carrier. Desired output is plotted against off-tune frequency as a decibel ratio with reference to 1 mW as zero level; curve 2 in Fig. 14.3c is a typical example.

The overall selectivity characteristic is expressed as the ratio of the desired to undesired output, and is obtained by plotting the difference between curves 1 and 2 in Fig. 14.3c. The result is indicated by curve 3 in Fig. 14.3c. This final curve gives a truer indication of interference discrimination than either single or normal two-carrier tests. For example, neither of the latter can indicate

the effect of a whistle filter in the A.F. stages, whereas the improvement in signal-to-interference ratio due to inclusion of the whistle filter is shown by the modified two-signal test as a dip in the interference output curve 1 at an off-tune frequency corresponding to the rejection frequency of the whistle filter and a rise in the signal-to-interference ratio curve 3. The whistle filter has no effect on the desired power output at 400 c.p.s., since it occurs after the detector where the demodulation is occurring.

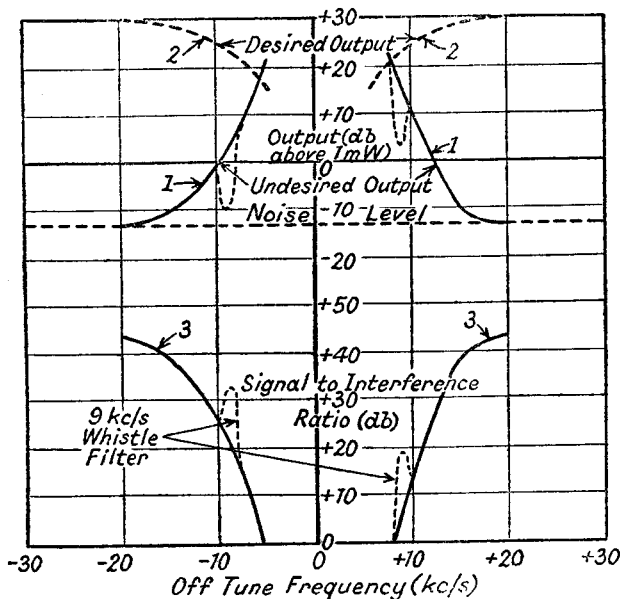


FIG. 14.3c.—A Modified Selectivity Test Curve.

**14.5.3. Electrical Frequency Response.** The electrical (as distinct from the acoustical) frequency response of a receiver is useful for assessing the attenuation of the higher-frequency modulation sidebands by the selectivity of the R.F. and I.F. tuned circuits, and the reduction of high or low audio frequencies due to tone control. The curve has only a general resemblance to the acoustical frequency response, which is chiefly determined by the audio radiation characteristics of the loudspeaker.

The test is performed at a carrier frequency of 1,000 kc/s, modulated 30%. The modulation frequency is varied from 30 to 10,000 c.p.s., and the power output variation noted. The carrier input is set at 5,000  $\mu\text{V}$ , and the volume control adjusted to give one-quarter of the rated maximum or 500 mW, whichever is the

greater, at a modulation frequency of 400 c.p.s. If the power output approaches the maximum at any modulation frequency (this might occur with tone control circuits), the output level at 400 c.p.s. must be reduced below the rated one-quarter maximum. The results are plotted in the form of a vertical logarithmic power output scale, or a linear power output decibel ratio scale (zero level being the output at 400 c.p.s.), against a logarithmic scale of modulation frequency. Curves (see the dotted extensions in Fig. 14.4) are taken for tone control and variable selectivity (if included) settings giving maximum and minimum low and high audio frequency response. If the setting of the volume control affects fidelity,

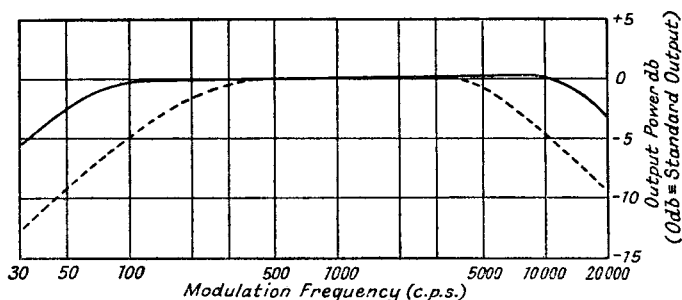


FIG. 14.4.—The Electrical Frequency Response of a Receiver.

curves should be taken at 400 c.p.s. power output levels differing by 10 db.

Electrical frequency response may be taken at carrier frequencies other than 1,000 kc/s, e.g., at the centre of the long-wave band, 200 kc/s; there is usually little to be gained by taking fidelity curves in the short-wave range because the selectivity of the signal-tuned circuits is relatively poor. Different input carrier levels should be tried if the receiver has automatic selectivity or tone control.

**14.5.4. Harmonic Distortion.** For this measurement care must be taken to ensure that the signal generator and audio frequency modulating source produce minimum sideband and audio frequency distortion. The tests can be conveniently subdivided to show the distortion introduced by the different stages in the receiver.

The A.F. stages may be checked by applying the audio frequency modulating source to the pick-up terminals or to the grid of the first A.F. amplifier valve. Readings of power output against distortion are obtained at, usually, three frequencies, 400, 1,500 and 3,000 c.p.s.



**14.5.6. Hum.** In measuring interference due to hum from the mains power supply, noise frequencies must be severely attenuated, and a low-pass filter, having a cut-off frequency of 300 c.p.s., is inserted between the output and the output meter. Hum may appear in the loudspeaker from the speaker field coil, the A.F. or the R.F. amplifier stages. Hum from the former is a result of using it as the smoothing coil. A "hum-bucking" coil (a few turns of thick wire wound on top of the field coil) in series with the speech-coil is employed for neutralizing purposes. In measuring hum injected into the speech-coil from the field coil, the voltage across, or current in the speech-coil is noted when the output valve anode is disconnected from the output transformer primary and connected direct to H.T. positive, and the primary shunted by a resistance equal to the output valve slope resistance. For A.F. and R.F. amplifier hum measurement the speech-coil is replaced by an output meter having a resistance equal to the modulus of the speech-coil at 400 c.p.s. Hum from the A.F. amplifier is due to direct amplification of hum voltages produced in the grid-cathode circuits by the heaters or is due to insufficient smoothing of the H.T. power supply. The R.F. circuits can only produce hum by modulation of the input carrier or of the oscillator in the frequency changer circuit. Since modulation is dependent on non-linear valve characteristics, the hum from the R.F. circuits usually reaches a maximum at some particular bias corresponding to maximum rate of change of the  $I_a E_g$  characteristic.

Hum due to the A.F. stages may be measured on the output meter with the A.F. volume control set to zero, but it is preferable to remove the last I.F. valve from its socket and to take the reading with the A.F. volume control at maximum. If the latter is at zero, hum in the grid-earth circuit of the first A.F. amplifier is not measured, and this may form an appreciable proportion of the interference.

Measurement of modulation hum is only necessary when it is comparable with hum from the post-detector stages, and it is made with an unmodulated 1,000 kc/s carrier. The receiver volume control is set at maximum and the output meter reading is observed as the carrier voltage is increased. If the output reaches a maximum at a particular carrier voltage (this is generally so if the receiver has A.G.C.), the power is noted and compared with the output registered when the 400 c.p.s. (30%) modulation is switched on. The hum filter is removed for the 400-c.p.s. reading and volume control adjustments are made if overloading of the A.F. amplifier is experienced, the hum power output being measured at the new volume

control setting. The hum modulation is expressed as a percentage modulation

$$M_h = 30 \sqrt{\frac{P_h}{P_0}} \% \quad . \quad . \quad . \quad 14.3$$

where  $P_h$  = hum power output

$P_0$  = 400-c.p.s. power output obtained for the same volume control setting as  $P_h$ .

**14.5.7. Automatic Gain Control.** The A.G.C. performance is normally measured at the mid-frequency of each waveband. The R.M.A. recommend that the input carrier modulated 30% at 400 c.p.s. should be set to 1 volt and the volume control adjusted to give one-quarter of the maximum rated output. The carrier input is reduced in suitable steps and the output noted. A curve is plotted of

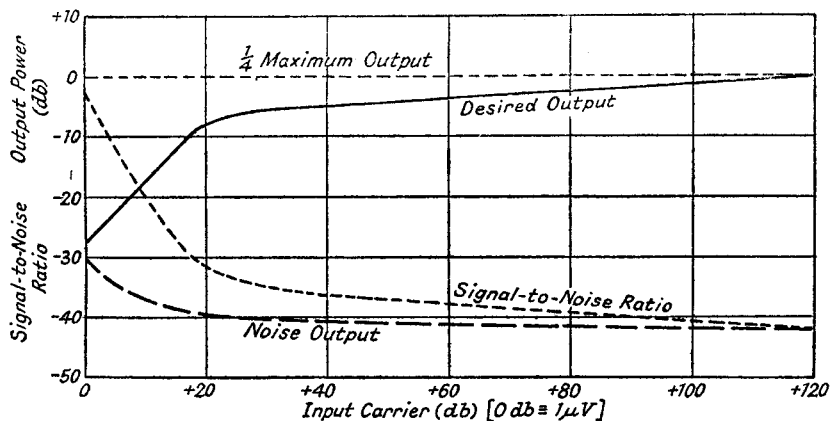


FIG. 14.5.—A.G.C. Characteristic Curves of a Receiver.

output power against input voltage to logarithmic scales, or of power and input carrier in decibel ratios to linear scales (Fig. 14.5), zero level being one-quarter of the rated maximum and 1  $\mu$ V respectively.

The I.R.E. test is very similar; the output power is adjusted to one-half the rated maximum when the carrier voltage is 1 volt. The output power ratio (0 db. =  $\frac{1}{2}$  maximum rated power) is plotted against a horizontal decibel scale of input carrier referred to a zero level of 1 volt. The suggested figure of merit is the input decibel reduction below 100,000  $\mu$ V necessary to produce a 10-db. change of output. For receivers operating on small signals the input decibel reduction may be taken from 5,000  $\mu$ V.

If an interchannel noise suppression circuit (Quiet A.G.C.) is

incorporated, the A.G.C. curve about the noise-suppression point should be taken for increasing as well as decreasing input carrier in order to show any backlash effect.

An alternative<sup>6</sup> method of measurement is to begin from minimum input carrier with the volume control set at maximum. The input is increased until the output reaches one-quarter of the maximum output. At this point the volume control is changed to reduce the output to one-tenth of its value. The input is again increased and the procedure repeated until 1 volt carrier is reached. The A.G.C. curve is made continuous by multiplying the second set of output readings by 10, the third by 100, and so on. The great advantage of this method is that it gives sensitivity directly and also indicates any need for changing the A.G.C. delay voltage. For example, suppose the maximum rated output is 3 watts, the A.G.C. delay — 15 volts, and the curve shows A.G.C. operation to commence at 10 watts output. This suggests that the delay voltage should be reduced to bring A.G.C. into operation at about 2,500 watts output, i.e., the delay voltage should be reduced to  $-15 \times \sqrt{\frac{2.5}{10}} = -7.5$ .

It is of considerable advantage to include with the A.G.C. characteristic a curve of noise power output against input carrier, the noise being measured for the unmodulated carrier. A suitable filter removing hum voltages is included between the A.F. output and the meter. Noise power output is plotted in decibel ratios (Fig. 14.5) with zero level the same as that for the A.G.C. curve. The signal-to-noise ratio for a given input carrier is found immediately by the difference between the A.G.C. and noise power levels.

**14.5.8. Frequency Changer Interference Effects.** The image signal, and harmonics of the oscillator, intermediate and undesired signal frequencies can interact in the frequency changer to produce interference with the desired signal. The first two are the most important and a measure of oscillator harmonic interference is usually an adequate guide to the smaller interference from intermediate and undesired signal harmonics.

The image signal sensitivity is found by varying the signal generator carrier frequency over a range covering a frequency of  $f_s + 2f_1$ , where  $f_s$  is the receiver tuning frequency and  $f_1$  is the intermediate frequency. The carrier is modulated 30% and its voltage is adjusted, when the frequency point of maximum audio output has been found, until standard power output is obtained. The result is plotted as  $20 \log_{10} \frac{\text{image signal sensitivity}}{\text{real signal sensitivity}}$  against real



signal frequency. Variation of the carrier frequency over a small range on either side of  $f_s + 2f_1$  is necessary because the receiver tuning-dial frequency setting cannot usually be read with sufficient accuracy.

For oscillator harmonic response the same procedure is followed. The signal generator frequency is varied over a small range, which includes an undesired signal frequency spaced from second and third harmonics of the oscillator by an amount equal to the intermediate frequency. Thus for an I.F. of 465 kc/s and a receiver tuning frequency of 1,000 kc/s, the oscillator frequency is 1,465, giving second and third harmonics of 2,930 and 4,395 kc/s. The signal generator is therefore set in turn to 2,465 and 3,930 kc/s, and the sensitivity measured. Curves are plotted of decibel ratio oscillator harmonic sensitivity to real-signal sensitivity against real-signal frequency.

**14.5.9. Oscillator Frequency Drift.** The oscillator for the frequency changer should be checked to determine the variation of frequency due to power supply changes, normal operating temperature variations and A.G.C. A detector having a grid circuit tuned to the oscillator frequency is loosely coupled to the oscillator (a wire connected to the detector grid lead placed near the oscillator valve or tuning capacitor is usually sufficient). In series with the detector grid circuit is the output from a frequency stabilized oscillator operating at a frequency separated from the receiver oscillator frequency by about 500 c.p.s. The audio note of 500 c.p.s. produced in the detector output is measured by a calibrated beat frequency oscillator. The receiver oscillator drift causes the detector output A.F. frequency to vary and the variation is noted on the beat frequency oscillator.

Frequency variation is measured for  $\pm 5\%$  mains supply variations, and readings are taken rapidly so as not to include temperature effects. The latter are noted by observing the variation of frequency over a given time period (about  $\frac{1}{2}$  hour) from switching on. A curve is plotted of frequency drift (vertical linear scale) against time (horizontal).

Automatic gain control causes frequency drift by varying the H.T. voltage and the frequency changer load on the oscillator (Section 6.6 and 6.8, Part I). A curve is suggested of frequency drift against microvolts input to a logarithmic scale or decibel ratio to a linear scale (zero level  $1 \mu\text{V}$ ). This and the first test should only be performed after the receiver has settled down to normal operating temperatures (about  $\frac{1}{2}$  hour after switching on). It is

not usual to take readings at other than the centre frequency of each wave range.

**14.5.10. Automatic Frequency Correction.** The performance of the automatic frequency corrector is checked by noting the off-tune frequencies at which the desired signal disappears and reappears. The signal generator input carrier is tuned away from the receiver tuning frequency, and the frequency at which the 400-c.p.s. output disappears is noted.

The carrier is then retuned towards the receiver frequency and the pull-in position noted. The A.F.C. is dependent on the amplitude of the input carrier, and it should be checked at the sensitivity input and also inputs of 5,000 and 100,000  $\mu\text{V}$ . The test should preferably be carried out at each end of a wave range.

**14.6. Acoustical Tests.** Acoustic measurements on a radio receiver are more difficult to perform than electrical tests. Recommendations have been made by the R.M.A. for the measurement and calculation of frequency response, acoustic sensitivity, output and hum. Two tests only are suggested by the I.R.E., one on frequency response similar to the R.M.A. specification and the other a qualitative examination of noise audibility. Some further definitions must be given and additional apparatus described before the tests are stated.

## 14.7. Definitions.

**14.7.1. Frequency Response.** The acoustic frequency response of a receiver is the relationship between the output intensity level, measured at a given position relative to the loudspeaker, and the output audio frequency.

**14.7.2. Intensity Level.** The intensity level of an audio frequency is the ratio in decibels of the measured output with reference to a sound pressure of  $2.04 \times 10^{-4}$  dynes/sq. cm. (i.e., a power of  $10^{-16}$  watts per square centimetre).

**14.7.3. Loudness Level.** The loudness level of an audio frequency note is the intensity level (expressed in phons) of a 1,000-c.p.s. note judged by the listener to be equal in loudness to the test frequency output. A direct measurement of loudness entails switching from the test to the 1,000-c.p.s. frequency. An examination by a number of observers<sup>3</sup> has produced an agreed average figure for loudness level for different frequencies and the relationship between loudness and intensity level for a 400-c.p.s. note is tabulated below.

Intensity Level (db.)	10	20	30	40	50	53	60	70	80	90	100
Loudness Level (phons)	0	11	22.5	35	47	50	58	69.5	80	91	99

**14.7.4. Overall Acoustic Sensitivity.** The overall acoustic sensitivity for an open aerial receiver is the input in microvolts needed to give a loudness level, at the measuring position, of 50 phons. The input carrier is modulated 30% at 400 c.p.s.

**14.7.5. Distortion Factor.** The distortion factor is defined as

$$\frac{1}{2} \sqrt{\frac{\sum_{n=2}^{\infty} n^2 E_n^2}{\sum_{n=1}^{\infty} E_n^2}} \quad . \quad . \quad . \quad 14.4$$

where  $E_n$  is the voltage across the speech-coil due to the  $n$ th harmonic. The arbitrary multiplication of  $E_n$  by  $n$  in the numerator is included since higher harmonics generally have greater interference capability (see Section 10.7). For example, 5% of third harmonic gives relatively greater interference than 5% of second harmonic.

**14.7.6. Total Harmonic Content.** The total harmonic content is

$$100 \sqrt{\frac{\sum_{n=2}^{\infty} E_n^2}{\sum_{n=1}^{\infty} E_n^2}} \% \quad . \quad . \quad . \quad 14.5.$$

**14.7.7. Free Space Conditions and their Approximation.**

Free space conditions of still air, absence of reflected waves and no distortion of the sound field by the microphone can be approached in the open air on a windless day at a considerable distance from the ground or any reflecting surface. They may also be simulated in a heavily damped room, the minimum internal volume of which should be 1,000 cubic feet.

**14.7.8. Hum.** Hum applies only to low-frequency mains interference due to inadequate filtering of D.C. voltage sources, vibration of mains transformers, and A.C. voltages induced from the heater supply. The result is expressed in phons.

**14.8. Additional Apparatus.** The apparatus required in addition to that listed in 14.3 is a pressure-operated microphone, calibrated in volts per dyne per square centimetre, an amplifier having a straight-line frequency response ( $\pm 0.5$  db.) from 30 to 10,000 c.p.s. for amplifying the microphone output, and distortion factor apparatus. The latter consists of an amplifier, having a flat frequency response from 30 to 10,000 c.p.s., a filter for attenuating

the fundamental, a circuit having a frequency response directly proportional to frequency, and a valve voltmeter. For measuring distortion factor, the filter and special frequency discriminating circuit are inserted and the R.M.S. output voltage noted. The filter and special circuit are next removed and a potentiometer calibrated in distortion factor is adjusted to give the same R.M.S. output voltage reading.

A diagram of the apparatus is shown in Fig. 14.6a, and details of the high-pass filter attenuating the fundamental are given in Fig. 14.6b. The frequency discriminating circuit consists of  $L_1$  and  $R_4$  connected to the anode of the first valve  $V_1$ . In the up position (1) of switch  $S_1$  a flat frequency response is obtained ( $R_4$  only is in circuit), whilst in the down position (2)  $L_1$  is inserted and the required rising fre-

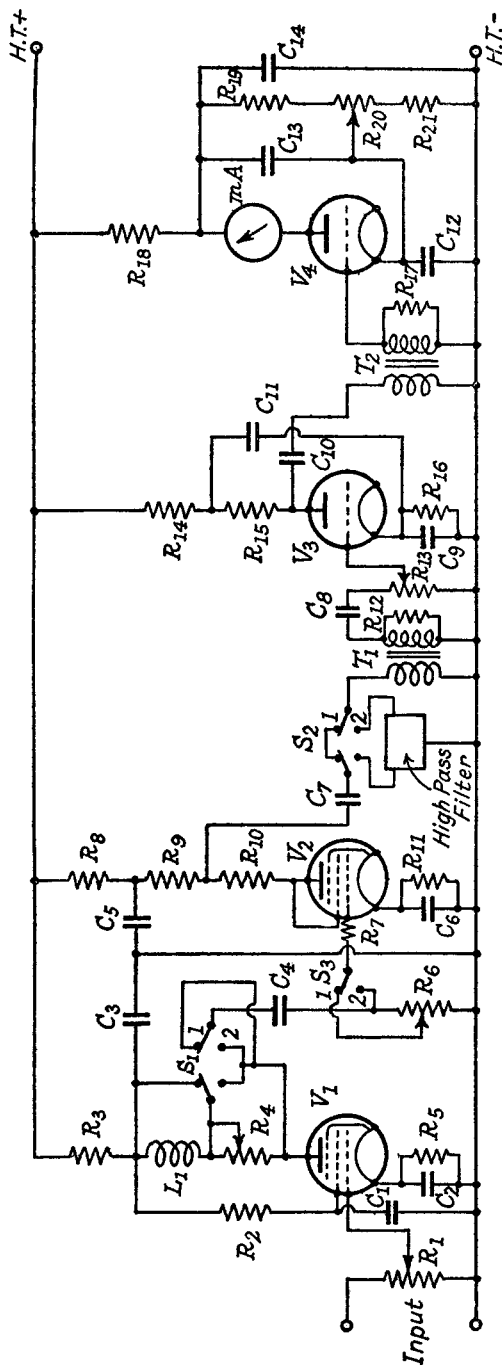


Fig. 14.6a.—Circuit Diagram of the Distortion Factor Test Apparatus for Acoustical Measurements.

quency characteristic is obtained, i.e., the amplitude of the output voltage from  $V_1$  for a fixed input voltage is directly proportional to frequency. Switch  $S_2$  in the up position (1) connects the output of the amplifier valve  $V_2$  direct to the transformer  $T_1$  in the grid circuit of another amplifier valve  $V_3$ . The latter is followed by the anode bend valve voltmeter  $V_4$ . With switch  $S_2$  in the down position (2), the high-pass filter is inserted between  $V_2$  and  $T_1$  and the fundamental 400-c.p.s. frequency is eliminated. Potentiometer  $R_1$  is an input control, selecting any desired proportion of the audio output voltage from the receiver. Potentiometer  $R_6$  measures and is directly calibrated in distortion factor.  $R_{13}$  is a preset gain control initially adjusted to give a satisfactory valve voltmeter reading. Switch  $S_3$  enables the total voltage across  $R_6$  or the voltage from the slider to earth to be measured.

The component values for Fig. 14.6a are :

Inductance  $L_1 = 0.1 H$ . Transformer  $T_1$ . 1 : 5 step-up ratio. Transformer  $T_2$ . 1 : 3.5 step-up ratio. Milliammeter 0 to 0.5 mA.

Resistances.		Capacitances.	
1.	0.1 M $\Omega$ (variable)	1.	8 $\mu$ F
2.	10,000 $\Omega$	2.	25 $\mu$ F
3.	2,500 $\Omega$	3.	8 $\mu$ F
4.	1,000 $\Omega$ (preset variable)	4.	0.1 $\mu$ F
5.	250 $\Omega$	5.	8 $\mu$ F
6.	0.1 M $\Omega$ (variable)	6.	50 $\mu$ F
7.	100 $\Omega$	7.	4 $\mu$ F
8.	1,000 $\Omega$	8.	0.1 $\mu$ F
9.	750 $\Omega$	9.	25 $\mu$ F
10.	2,500 $\Omega$	10.	1 $\mu$ F
11.	60 $\Omega$	11.	1 $\mu$ F
12.	25,000 $\Omega$	12.	25 $\mu$ F
13.	0.1 M $\Omega$ (preset variable)	13.	1 $\mu$ F
14.	5,000 $\Omega$	14.	8 $\mu$ F
15.	25,000 $\Omega$		
16.	320 $\Omega$		
17.	0.1 M $\Omega$		
18.	15,000 $\Omega$		
19.	20,000 $\Omega$		
20.	1,000 $\Omega$ (variable)		
21.	100 $\Omega$		

Valves.	
1.	MKT4
2.	KT41
3.	MH41
4.	MH41

The procedure for the initial calibration of  $R_6$  in terms of distortion factor is as follows. The filtered output voltage from a 400-c.p.s. oscillator is applied across  $R_1$ , and with switch  $S_2$  on position 1, the resistance  $R_4$  is adjusted until there is no change in the valve voltmeter reading when switch  $S_1$  is changed from position 2 to 1. This means that the amplification of  $V_1$  to the fundamental frequency is the same in position 2 as in position 1.

The filtered output from the 400 c.p.s. oscillator is used to modulate the signal generator and the output voltage from the receiver is applied across  $R_1$ . With switches  $S_1$ ,  $S_2$  and  $S_3$  in position 2,  $R_1$  is adjusted to give a convenient reading on the valve voltmeter; this measures the total distortion quality of the harmonics, i.e., the voltage represented by the numerator of expression 14.4.

Switches  $S_1$ ,  $S_2$  and  $S_3$  are now moved to position 1 and the slider of  $R_0$  is adjusted to give the same selected reading on the valve voltmeter; this is a measure of the voltage represented by the denominator of expression 14.4. The distortion factor is  $\frac{a}{2}$ , where  $a$  is the fraction of  $R_0$  needed to give the same voltmeter reading in position 1 as in position 2.

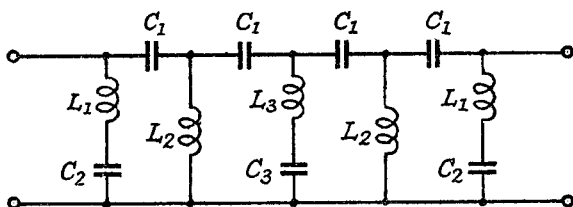


FIG. 14.6b.—The High Pass Filter for the Distortion Factor Apparatus.

Component values of the high-pass filter of Fig. 14.6b (used for removing the fundamental 400 c.p.s.) are as follows :

Inductance.	Capacitance.
1. 0.424 H	1. 0.249 $\mu$ F
2. 0.127 H	2. 0.373 $\mu$ F
3. 0.212 H	3. 0.746 $\mu$ F

Cut-off frequency, 500 c.p.s.

Maximum attenuation frequency, 400 c.p.s.

$R_0 = 800 \Omega$ .

Attenuation at and above 800 c.p.s. less than 1 db.

Attenuation at 400 c.p.s. 80 db. (minimum) for  $Q$  of coils = 50.

## 14.9. Acoustical Measurements.

**14.9.1. Frequency Response.** Measurements of frequency response are to be made in the free space approximate conditions. Calibrated records are used in the gramophone pick-up, and for the complete receiver a 1,000 kc/s carrier modulated at 30% and of R.M.S. value 20,000  $\mu$ V is applied through the dummy aerial. The tone and variable selectivity controls are set for maximum frequency

response. The input to a frame aerial receiver through the shielded coil is to be 20,000  $\mu\text{V}$  per metre. The receiver volume control is adjusted to give one-quarter of the maximum electrical power output to a load resistance corresponding to the speech-coil modulus at a frequency of 400 c.p.s.

The modulation frequency of the signal generator is varied from 30 to 10,000 c.p.s. and measurements of intensity level are made for two positions of the microphone :

- (1) On the axis of the speaker, with a distance of 3 feet between the planes of the microphone diaphragm and the loudspeaker grille or cabinet opening.
- (2) At a point in the horizontal plane at  $45^\circ$  to the axis of the loudspeaker ; the microphone and speaker separation is to be 3 feet and the microphone diaphragm is to be set perpendicular to the line joining microphone and speaker.

For all tests the centre of the loudspeaker is 3 feet from any boundary surface.

If recording apparatus is used to note the intensity level-frequency curve, all maxima and minima must be registered, and stopping the apparatus at one frequency must not change the intensity level reading by more than 2 db.

The axial and  $45^\circ$  responses are plotted on the same graph to a vertical linear decibel ratio scale and a logarithmic horizontal frequency scale. The reference level of 0 db. for the curves is the intensity level corresponding to the geometric mean of the pressures at 200 and 600 c.p.s., i.e., the intensity level is referred to  $\sqrt{P_{200} \cdot P_{600}}$  instead of 0.000204 dynes/sq. cms. For radio gramophone receiver tests the type of needle used must be stated.

**14.9.2. Acoustic Sensitivity.** The acoustic sensitivity is the modulated carrier required to give a loudness of 50 phons, or at 400 c.p.s. modulation an intensity level of 53 db. Its value may be calculated from the measurement made for the previous test (14.9.1). The intensity level at 400 c.p.s. is taken as the geometric mean of the pressures at 200 and 600 c.p.s. referred to a pressure of 0.000204 dynes per square centimetre.

Let  $In_w$  denote this geometric mean intensity level,  $S_E$  the electrical sensitivity giving 50 mW electrical output,  $S_A$  the acoustical sensitivity giving a 400 c.p.s. output intensity level corresponding to 53 db.,  $W$  the electrical power output at 400 c.p.s. for the frequency response test (of value about one-quarter of the maximum output).

If the electrical power output is directly proportional to the square of the input carrier

$$\frac{S_A}{S_E} = \sqrt{\frac{W_{53}}{50}}$$

where  $W_{53}$  is the electrical power output (mW) giving a 400-c.p.s. intensity level at the microphone of 53 db.

But 
$$In_W = 10 \log_{10} \frac{W}{W_0},$$

where  $W_0$  is the electrical power output (mW) giving zero intensity level at the microphone (a pressure of 0.000204 dynes/sq. cm.).

and 
$$53 = 10 \log_{10} \frac{W_{53}}{W_0}.$$

$$\frac{In_W - 53}{10} = \log_{10} \frac{W}{W_{53}}$$

$$\frac{W}{W_{53}} = 10^{\left(\frac{In_W - 53}{10}\right)}$$

or 
$$W_{53} = \frac{W}{10^{\left(\frac{In_W - 53}{10}\right)}}.$$

Replacing this in the first expression, the acoustical sensitivity is

$$S_A = S_E \sqrt{\frac{W}{50 \times 10^{(0.1 In_W - 5.3)}}} \quad . \quad . \quad . \quad 14.6.$$

**14.9.3. Hum.** For hum measurements, test-room disturbances and noise in the microphone amplifier are to be at least 5 phons below the lowest hum level. The microphone diaphragm is to be located on the speaker axis at a distance of 12 inches from the speaker grille. The mains supply voltage should contain approximately 3% of fifth harmonic. The fifth harmonic of the mains fundamental is chosen because it is found that this is the harmonic most frequently picked up by an unshielded grid lead. This requirement may be fulfilled by using a low-pass filter in the mains leads to suppress harmonics, the 3% of fifth harmonic being inserted from a valve generator, the output from which is connected across a series resistance in the filtered mains lead.

The overall frequency response characteristic of the microphone and amplifier is to be as follows to within  $\pm 2$  db.



Frequency.	Gain relative to 25 c.p.s.
25 c.p.s.	0
50 "	+ 12.5
100 "	+ 25
150 "	+ 31.5
200 "	+ 36
250 "	+ 40
300 "	+ 43.5
400 "	+ 48
500 "	+ 51.5
600 "	+ 52.5
700 "	+ 54
800 "	+ 55
Above 1,000 c.p.s.	Less than - 10

The above frequency characteristic may be realized by inserting a T-section equalizer at a suitable point in the straight-line frequency response amplifier mentioned in 14.8. The two series arms of the equalizer are capacitors of  $\frac{398}{R_0} \mu\text{F}$ , and the shunt arm consists of a resistance of  $0.117R_0$  ohms and inductance  $7.17R_0 \mu\text{H}$ , where  $R_0$  is the characteristic impedance of the equalizer. Frequencies above 800 c.p.s. must be attenuated by additional apparatus. The voltmeter at the output of the microphone amplifier is to measure R.M.S. values.

The hum loudness level is expressed as

$$L = 65 + 20 \log_{10} \frac{E}{pq} \text{ phons} \quad . \quad . \quad 14.7$$

where  $E$  = the R.M.S. output voltage from the microphone amplifier  
 $p$  = the ratio of the voltage across the output meter in the receiver to the voltage at the microphone at 400 c.p.s.  
 $q$  = the sensitivity of the microphone in volts per dyne per square centimetre at 400 c.p.s.

The hum level is quoted for (1) maximum output hum obtainable without the carrier but with any control setting, and (2) the maximum output for any carrier voltage up to 1 volt and any control setting.

**14.9.4. Acoustic Output and Distortion Factor.** For the acoustic output-distortion factor measurements, the input carrier (1,000 kc/s) modulated 60% at 400 c.p.s. is adjusted to 20,000  $\mu\text{V}$ .

Readings are taken of distortion factor for different settings of the A.F. volume control, and the result is plotted to a scale as

shown in Fig. 14.7. The intensity level  $In$  is calculated from the 400 c.p.s. electrical power output as follows :

$$In_{W_1} = In_W + 10 \log \frac{W_1}{W} \quad . \quad . \quad . \quad 14.8$$

where  $In_W$  is the intensity level defined in 14.9.2,

$W$  is the electrical power output defined in 14.9.2,

$W_1$  is the actual 400 c.p.s. electrical power output measured,

and  $In_{W_1}$  is the intensity level corresponding to an electrical power output of  $W_1$ .

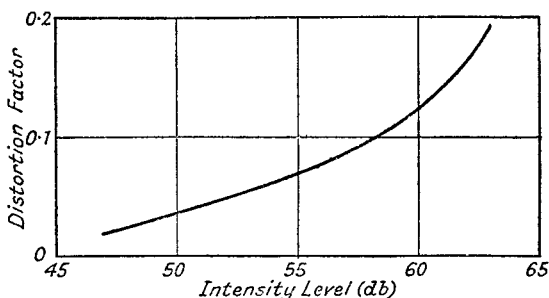


FIG. 14.7.—An Example of a Distortion Factor-Intensity Level Curve.

#### BIBLIOGRAPHY

1. *Year Book of the Institute of Radio Engineers*, 1931, p. 121.
2. Specification for Testing and Expressing Overall Performance of Radio Receivers. Part 1. Electrical Tests. Part 2. Acoustic Tests. Published by the Radio Manufacturers' Association (England). Dec. 1936.
3. The Evolution of the Phon. D. B. Foster, *Wireless World*, July 9th, 1937, p. 32.
4. Discussion on R.M.A. Specification. *Journal I.E.E.*, July 1937, p. 111.
5. *Standards on Radio Receivers*. The Institute of Radio Engineers. 1938.
6. The A.V.C. Characteristic. M. G. Scroggie, *Wireless World*, May 4th, 1939, p. 427.
7. Broadcast Receivers, A Review. N. M. Rust, O. E. Keall, J. F. Ramsay, K. R. Sturley, *J.I.E.E.*, Part III, June 1941, p. 59.

## CHAPTER 15

### FREQUENCY MODULATED RECEPTION <sup>19</sup>

**15.1. Introduction.** The difference between amplitude and frequency modulated transmissions has already been discussed in Chapter 1, Part I, where the corresponding vector and sideband representations are given. In frequency modulated transmission the amplitude of the carrier remains constant, variation of carrier frequency playing the same rôle as amplitude change in the amplitude modulated carrier. The magnitude of the frequency variation, or deviation, of the carrier is directly proportional to the intensity of the modulating signal. Thus, if the modulating signal voltage is doubled, the frequency deviation of the carrier is doubled. The rate at which the latter is varied is that of the modulating frequency. For example, if the intensity of the A.F. signal is such as to vary the carrier frequency by  $\pm 50$  kc/s, this variation occurs 1,000 times per second when the modulation frequency is 1,000 c.p.s. In the same manner as with amplitude modulation, the frequency modulated carrier can be resolved into a carrier, of fixed frequency equal to its unmodulated value, and sidebands spaced on either side of the carrier by frequency differences equal to the modulation frequency; unlike the amplitude modulated carrier, frequency modulation produces more than two sidebands for each modulation frequency. For a given modulating A.F. voltage, the frequency spectrum covered by the essential sidebands is practically independent of the modulating frequency, i.e., a low modulating frequency of given amplitude has a large number of sidebands closely spaced, and a high modulating frequency of the same amplitude has few sidebands widely spaced, covering approximately the same frequency range as the low modulating frequency sidebands. The amplitudes of the carrier and sideband components are a function of the modulating frequency and voltage, and each component passes through a series of zero amplitudes as the amplitude of the modulating voltage is increased from zero. The actual relationship between component amplitudes and modulating frequency and voltage is shown in expression 1.4, Part I, to be of Bessel function form in terms of the modulation index. The latter, which is the ratio of the frequency deviation of the carrier to the modulation frequency, is a function of the modulating voltage because frequency deviation is a result of, and is directly proportional to, the modulation ampli-

tude. The variation of the carrier ( $f_c$ ) and first ( $f_c \pm f_{mod.}$ ), second ( $f_c \pm 2f_{mod.}$ ) and third ( $f_c \pm 3f_{mod.}$ ) sideband component amplitudes are plotted against modulation index in Fig. 15.1. Taking the carrier component and a modulating frequency of 1,000 c.p.s., we see that the carrier component is zero at modulating voltages corresponding to the following carrier frequency deviations, 2,405, 5,520, 8,654, 11,792, 14,931, 18,071 c.p.s., etc. This feature<sup>8</sup> has been used to measure frequency deviation in a frequency modulated transmitter and to determine the range of modulating voltage over which there is a linear relationship between modulating voltage and carrier frequency deviation. The unmodulated carrier is tuned in on an

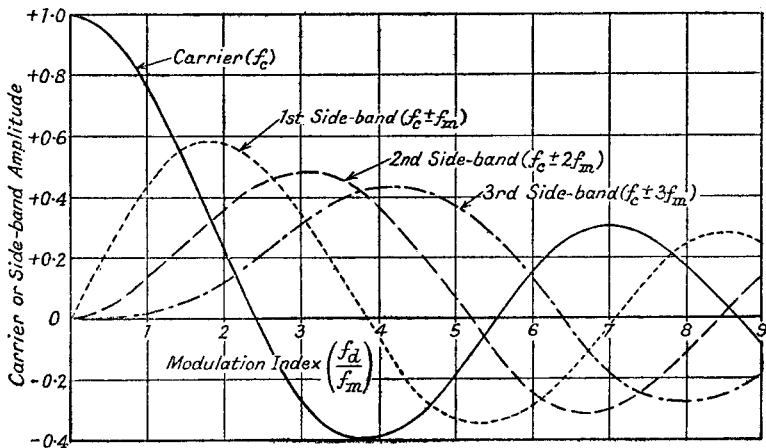


FIG. 15.1.—The Variation of Carrier and Sideband Amplitudes of a F.M. Transmission against Modulation Index  $\left[ \frac{f_d}{f_{mod.}} \right]$ .

[Note: For  $f_m$  read  $f_{mod.}$ ;  $f_a$  = carrier deviation frequency.]

amplitude modulation receiver having a heterodyne oscillator and a highly selective A.F. band-pass filter. The latter is tuned to some convenient audio frequency, such as 1,000 c.p.s., and has a sufficiently narrow pass range to prevent appreciable response from frequencies separated from the tuning frequency by an amount equal to, or greater than, the modulating frequency. Thus if  $f_{mod.} = 1,000$  c.p.s. the filter should attenuate severely frequencies above about 1,800 c.p.s. and below 200 c.p.s. The filter is terminated by an amplifier and any suitable indicator such as telephones or valve voltmeter. The carrier is now modulated and the modulating amplitude increased until the heterodyne whistle or voltage at the indicator falls to a minimum. This corresponds to a frequency

deviation of 2,405 c.p.s. when  $f_{mod.} = 1,000$  c.p.s. Other minima are found as the modulating voltage is increased and these correspond to 5,520, 8,654 c.p.s., etc., frequency deviations.

In a frequency modulated receiving system the semi-pass-band width of the receiver must never be less than the highest modulating frequency it is desired to accept, even though the frequency deviation of the carrier is less than the modulating frequency. For example, if the modulating frequency is 10,000 c.p.s. and its amplitude such as to give a carrier frequency deviation of 4,000 c.p.s., there are three pairs of sidebands up to  $(f_c \pm 3f_{mod.})$  kc/s, which have amplitudes exceeding 1% of the carrier component, and all these must be accepted by the receiver if correct reproduction is to be obtained, i.e., the receiver pass-band must be  $f_c \pm 30$  kc/s. As a general rule we may say that the receiver pass-band width is determined by the highest audio frequency modulating component, when the carrier frequency deviation is much less than the highest modulating frequency, whereas when the reverse is true the band width is determined by the frequency deviation.

There are certain advantages, notably in improved signal-to-noise ratio and reduced volume compression, to the use of frequency in place of amplitude modulation, and these are discussed more fully in the next section.

The receiver design is similar in principle to that of its amplitude modulated counterpart, except for the limiter and the converter for changing the frequency modulated carrier into an amplitude modulated carrier before detection. Some modifications may be necessary in receiving a high fidelity frequency-modulated transmission because the receiver pass-band may require to be about ten times the highest audio frequency (15 kc/s). With high fidelity A.M. transmission no increase in A.F. output is obtained by making the band-width greater than twice the highest audio frequency, and it possesses the serious disadvantage of increasing noise output.

**15.2. The Advantages and Disadvantages of Frequency Modulation.** Four important advantages can be gained by the use of frequency modulation instead of amplitude modulation, viz.,

- (1) greater signal-to-noise ratio
- (2) lower transmitter input power for a given A.F. output from the receiver
- (3) less amplitude compression of the A.F. modulating signal
- (4) larger service area, and smaller interference area between stations on adjacent carrier frequencies.

These advantages can only be realized under certain operating

conditions, chief of which is that reception must be confined to the direct ray <sup>3</sup> from the transmitter. Indirect ray communication, as in short-wave transmission over long distances, is subject to selective fading of the carrier and sidebands (see Section 3.2, Part I), and the audio frequency signal suffers severe distortion. This distortion is usually much worse with frequency than with amplitude modulation because of the large number of sidebands required to convey the correct character of the low-frequency components of the audio signal. Amplitude modulation is much less affected because there is only a pair of sidebands for each modulation frequency component. Hence this effect renders frequency modulation impracticable except on ultra-short waves. High fidelity frequency-modulated transmission with a large frequency deviation (up to  $\pm 75$  kc/s) also requires an ultra high frequency carrier.

To understand the reason for the greater signal-to-noise ratio obtained from a F.M. system it is necessary to examine the characteristics of noise, which may be caused by disturbances in, or external to, the receiver. Noise from external sources is mainly of the impulse type, and is due to atmospheric disturbances (these are not normally very serious at ultra high frequencies) or to interference from electrical machinery (the ignition system of a car, switching surges transmitted by the mains supply wiring, etc.). It often has high peak voltages and may be periodic, continuous or spasmodic. In a well-designed receiver, internal noise is due to random motion of the electrons in the conductors and the valves, the important sources being the aerial, the first tuned circuit and the first valve. Thermal (conductor) and shot (valve) noise—see Sections 4.9.2 and 4.9.3, Part I—have frequency components covering a very wide range and continually varying in amplitude. With an amplitude modulation receiver each noise voltage, in the absence of a carrier, can interact with other noise components within audible range of it to produce the characteristic A.F. hiss, and the wider the pass-band the worse is the noise. If a carrier is applied and is large enough to ensure linear detection, the noise voltages act as sidebands to the applied carrier and audible beats are now only produced between the carrier and noise, i.e., the carrier demodulates (see Section 8.10, Part I) the noise carriers and interaction between the noise components themselves is suppressed. Hence only those noise components within audio range of the carrier contribute to the noise output ; \*

\* It is this same principle which operates in the homodyne or reinforced carrier receiver to give increased selectivity when the amplitude of the incoming carrier is increased in the receiver.

in practice we more often find that the application of a carrier increases the noise output, and this may be due to noise on the carrier itself (from the transmitter) and to the fact that the noise voltages alone are not large enough to cause the linear detection point of the A.F. detector to be reached. However, it is still true that only those noise components within audio range of the carrier contribute to the output.

A special device, known as a limiter, is incorporated in a F.M. receiver to suppress amplitude changes of the carrier, so that noise cannot have the same effect as in an A.M. receiver. For the sake of clarity let us consider the action of a single noise frequency component,  $f_n$  kc/s, spaced an audio frequency ( $f_n - f_c$ ) kc/s from the carrier. By considering the carrier as a stationary vector,  $OA$ , the noise can be represented as a vector  $AB$  rotating round the carrier

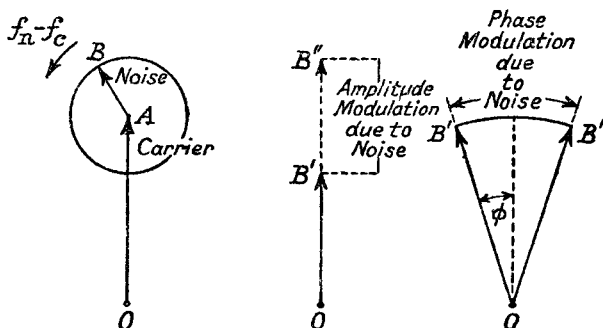


FIG. 15.2.—Amplitude and Phase Modulation of a Carrier Vector by a Single Noise Frequency.

at  $(f_n - f_c)$  kc/s as illustrated in Fig. 15.2. We see that there is both amplitude and phase change of the resultant carrier vector  $OB$ ; the former, which causes the noise output in the A.M. receiver, is suppressed by the limiter in the F.M. receiver, and the latter, which causes a frequency change of the carrier, produces the noise output in the F.M. receiver. A characteristic of phase modulation (see Section 1.4, Part I) is that carrier frequency deviation is directly proportional to the frequency of a constant amplitude modulating signal, so that noise sidebands near to the carrier give much less frequency deviation and consequently much less audio output from a F.M. receiver than those spaced farther from the carrier frequency. This "triangular" distribution of the effective noise sideband voltages reduces the R.M.S. noise voltage output for a maximum carrier frequency deviation of  $\pm 15$  kc/s to  $\frac{1}{1.73}$  of the noise output

from an A.M. receiver having the same maximum pass-band width of  $\pm 15$  kc/s. This means a signal-to-noise power ratio three times greater than for amplitude modulation, i.e., a gain of 4.75 db. in signal-to-noise ratio. In the case of impulse noise from car ignition systems, etc., Armstrong<sup>2</sup> estimates an improvement of 4 to 1 (6 db.) in signal-to-noise power ratio. It is not necessary to confine the frequency deviation of the carrier to  $\pm 15$  kc/s, and the signal output is proportionally increased by increasing frequency deviation in the ratio frequency deviation-to-maximum audio modulating voltage, e.g., if the carrier deviation is  $\pm 75$  kc/s and the maximum audio frequency  $\pm 15$  kc/s, the signal-to-noise voltage ratio is increased five times or 14 db. Taking the lower estimate for the "triangular" noise distribution, we have a total improvement in signal-to-noise power ratio of 75 to 1, or 18.75 db. The increase in receiver band width to accommodate the greater frequency deviation introduces extra noise sidebands, but if the carrier is large in comparison with the noise (at least twice the peak noise voltage) there is no increase in noise output because the phase modulation of the carrier by the additional noise sidebands is outside the audible range. When the peak carrier-to-noise ratio is less than unity, interaction occurs between the noise components, which phase modulate each other; in this case noise is increased and signal-to-noise ratio decreased by increasing the receiver pass-band. This causes a well-defined threshold area<sup>7</sup> to appear round a F.M. transmitter; outside this area better signal-to-noise ratio is obtained with reduced frequency deviation and a narrower receiver pass-band.<sup>1,2</sup> Inside this area the reverse is true.

Signal-to-noise ratio can be still further improved by the use of "pre-emphasis"—increased amplitude of the higher audio frequencies modulating the transmitter—at the transmitter followed by "de-emphasis" at the receiver. Pre-emphasis and de-emphasis can be applied to A.M. transmissions, but are less effective because all noise sideband voltages contribute equally to the noise output. An improvement in signal-to-noise power ratio of 5.4 to 1, 7.35 db.<sup>10</sup> is realized by pre-emphasis giving a total improvement of 405 to 1 or 26.1 db.

The second advantage of frequency modulation is that less power is required from the mains supply to the transmitter in order to produce a given audio power at the receiver output. In the power amplifier stage of an A.M. transmitter, the D.C. current must be sufficient to allow 100% modulation without serious distortion, i.e., it must be able to accommodate a carrier of twice the unmodulated



value. Since a F.M. carrier has constant amplitude it follows that, either the F.M. transmission gives twice as much effective power as the A.M. transmission for the same D.C. input power, or alternatively the same A.F. signal can be obtained at the output of the F.M. receiver by reducing the D.C. power at the transmitter by one-half. This represents a further increase in signal-to-noise power ratio of 2 to 1, giving a total improvement of 810 to 1 or 29.1 db. Successive stages of improvement are illustrated in Fig. 15.3.

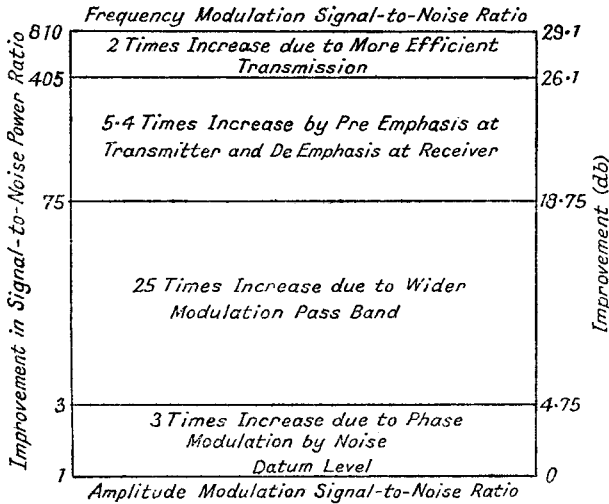


FIG. 15.3.—Successive Stages in Signal-to-Noise Ratio Improvement by the Use of Frequency Modulation.

Reduced compression of the audio signal in a F.M. transmitter really arises out of the increased signal-to-noise ratio. In an A.M. system maximum modulation percentage is limited by modulation envelope distortion to 90%, and a suitable minimum value is 5%, if low level sounds are not to be marred by noise; hence the maximum audio output voltage variation is 18 to 1, giving a power variation of 324 to 1 or 25 db. Clearly the maximum change of 70 db. between the loudest and softest orchestral passage would sound unnatural in a normal room and some compression is essential. The power ratio can, however, with advantage be raised another 20 db. to 45 db., and this is possible with F.M. because of its higher signal-to-noise ratio.

Apart from noise, a very important problem in radio communication is the separation of a desired programme from undesired programmes, and in an A.M. system this limits the closeness of

spacing between the carrier frequencies, and also the service area of a given transmitter. If the separation between the desired and an undesired carrier is equal to an audio frequency, an audible heterodyne note is produced at the receiver output, causing serious interference with the desired programme unless the desired carrier is at least ten times the undesired at the receiver aerial. This limits the service area of either transmitter, and between the two is a large area in which reception of one programme is marred by the other. Increased separation of the carrier frequencies can remove this interference outside the audio range, but the desired signal service area is still restricted by frequency inverted "monkey-chatter" due to fundamental or harmonic sideband overlap (see Section 14.5.2) from the undesired. Powerful A.M. transmitters need to be separated by at least 50 kc/s if the interference area between them is not to be large. A different state of affairs exists with two F.M. transmissions because the limiter in the receiver suppresses amplitude change. Interference, as in the case of noise, occurs due to phase modulation of the desired by the undesired carrier. This phase modulation produces an audio output of frequency equal to the carrier separation and of amplitude directly proportional to the separation frequency. Thus for small carrier separations interference is small; it is actually most noticeable at a carrier separation of 5 kc/s,<sup>10</sup> for though greater separations give greater equivalent modulation the resultant output becomes less audible. We therefore find that two F.M. transmissions can be operated with small carrier spacing and yet give quite a small interference area (where the desired to undesired carrier amplitude ratio is less than 2 to 1) between them. Interference is worst when both carriers are unmodulated. Although it is possible to operate with small carrier spacing it is usually considered better to adopt a spacing slightly beyond the audio range. Even so this does not call for modification of the statement that the interference area between two F.M. transmissions is very much smaller than the area between two A.M. transmissions of comparable performance.

**15.3. The Frequency Modulation Receiver.** The F.M. operating frequency ranges, which must be in the ultra short-wave band for the reasons given in Section 15.2, are likely to be from 40 to 50 Mc/s and from 100 to 120 Mc/s, so that the superheterodyne method of reception is essential to achieve sufficient overall amplification. A schematic diagram of a frequency modulation receiver is shown in Fig. 15.4, and we see that it only differs from that of the amplitude modulation receiver by the inclusion of the limiter and frequency-to-amplitude modulation converter stages. The dipole

aerial is connected to a R.F. stage followed by a frequency changer with a local oscillator. After the frequency changer is a series of intermediate frequency amplifier stages, the output of which supplies the limiter. Following the limiter is a converter for changing the

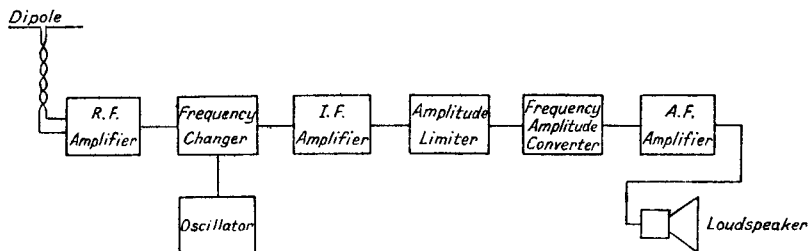


FIG. 15.4.—A Schematic Diagram of a F.M. Receiver.

frequency modulated carrier into an amplitude modulated one, which is then detected in the normal way. The detected output is amplified before it is applied to the loudspeaker.

The purpose for which the receiver is intended determines some of its design features ; if it is to be used for high fidelity broadcast transmission the pass-band is wide—about  $\pm 100$  kc/s—in order to accommodate the carrier frequency deviation, whereas for communication purposes a pass-band of about  $\pm 15$  kc/s only may be necessary. The latter type of receiver has approximately the same pass-band range as a high-fidelity A.M. receiver, and there is little difference between the design of the R.F., frequency changer and I.F. stages of the two types of receiver. On the other hand, the high-fidelity F.M. system operating with large carrier frequency deviations calls for greater damping of all tuned stages, a higher intermediate frequency and, in order to obtain the same amplification, a larger number of I.F. stages. Special methods<sup>15</sup> may be employed to compress carrier frequency deviation after the frequency changer, so as to reduce the required number of I.F. stages. The limiter stage is an essential part of the receiver because amplitude changes of the F.M. carrier, due to noise or transmission variations, are passed on through the frequency-to-amplitude converter to the detector, which is responsive to them. The conversion of the frequency into amplitude modulation is clearly necessary to regain the original character of the audio frequency modulating voltage, which is that of amplitude variation. The A.F. stages of the receiver are identical with those of the comparable A.M. receiver.

Starting from the aerial, we shall now turn to a more detailed examination of the separate stages, illustrating the various features

with special reference to a receiver for high-fidelity transmission, having a frequency deviation of  $\pm 75$  kc/s and preset signal-tuned circuits.

**15.4. The Aerial Input.** This consists of a plain or  $V$  dipole aerial dimensioned so as to act as a half-wave resonant aerial approximately at the centre of the range of F.M. transmissions it is desired to accept. Its overall length is about 5% less than one-half of the wavelength of its resonant frequency because, owing to end effects, the equivalent electrical length is always greater than the physical length. Normally a dipole aerial intended to cover a range of frequencies is adjusted to resonate at the geometric mean of the extreme frequencies, but in the case of F.M. transmission covering the range 40 to 50 Mc/s, having a small ratio change of frequency, the difference between the geometric mean 44.6 Mc/s and the arithmetic mean, 45 Mc/s, is negligible. Thus the overall length of a half-wave dipole suitable for the above frequency range is given by

$$l = \frac{0.95 \times v}{2f} \text{ cms.}$$

where  $v$  = velocity of the electro-magnetic wave  $\approx 3 \times 10^{10}$  cms./sec

$f$  = centre frequency of the range in c.p.s.

Therefore

$$l = \frac{0.95 \times 3 \times 10^{10}}{90 \times 10^6} = 316 \text{ cms.}$$

$$= 10.35 \text{ ft.}$$

If a reflector is used it is normally spaced about one-eighth to one-quarter of a wavelength away from the aerial, and it may be a half wavelength long or greater; a length greater (by about 10%) than a half wavelength helps to give a more constant response<sup>1,3</sup> over the frequency range. The split centre of the dipole is taken via a low impedance ( $Z_0 = 70$  to  $100 \Omega$ ) twin wire feeder to a centre-tapped coil coupled to the first tuned circuit of the receiver. The impedance variation of the dipole, and the transmission loss at the junction of dipole and feeder can be calculated by the methods set out in Sections 3.3.5 and 3.5.3, Part I. Motor-car ignition interference, a serious problem on ultra short waves, is mainly vertically polarized and best signal-to-noise ratio may be found with the dipole aerial horizontal.

**15.5. The R.F. Amplifier Stage.** The advantages of including a R.F. stage before the frequency changer are increased receiver sensitivity, signal-to-noise ratio, and selectivity against undesired I.F. responses due to interaction between undesired signals, or their

harmonics, and the oscillator, or its harmonics. The first two factors, which are interrelated, are most important. Owing to the use of a limiter stage a high degree of overall amplification (greater than for the corresponding A.M. receiver) is required, and as most of this must be obtained in the I.F. amplifier, instability is a real danger. Additional amplification at the signal frequency (it may be from 6 to 12 times with the high  $g_m$  (8 mA/volt) tetrode valve normally used for ultra-short wave amplification) is most desirable because it allows the I.F. amplification to be reduced for the same overall sensitivity. Highest sensitivity is obtained in the R.F. stage by employing optimum coupling between the feeder and first tuned circuit, a R.F. valve having a low input admittance and a high  $g_m$ , and an anode circuit having a high resonant impedance. These requirements may, however, conflict with those necessary for maximum signal-to-noise ratio and selectivity. The usual objection to optimum coupling, viz., that an appreciable reactive component is reflected into the first tuned circuit from the aerial, is much less serious at ultra high frequencies because of the feeder connection, which has a low, mainly resistive, and almost constant impedance over the tuning frequency range.

Two conflicting factors enter into the problem of obtaining greatest signal-to-noise ratio, and they arise because there are two sources of noise, the aerial-to-grid connection and the first R.F. valve itself. When valve noise predominates, greatest signal-to-noise ratio is realized by greatest possible signal voltage amplitude at the valve grid, i.e., by using optimum coupling (see Section 3.4.2, Part I) between the feeder and first tuned circuit. On the other hand, if aerial, feeder and first circuit noise is much larger than valve noise, maximum signal-to-noise ratio is realized by a coupling much greater than optimum. If it is assumed that the overall pass-band width of the receiver is independent of the selectivity of the first tuned circuit (this is certainly true of short and ultra short waves), maximum signal-to-noise ratio is obtained by dispensing with the first tuned circuit and coupling the aerial feeder direct to the grid of the first valve, at the same time neutralizing any reactive component in the aerial feeder connection by including an equal and opposite reactance. This procedure cannot, however, ordinarily be followed because of cross-modulation in the R.F. valve and the need to discriminate against signals which are not adjacent in frequency to the desired, but which might produce spurious I.F. responses in the frequency changer.

The signal-to-noise voltage ratio for optimum coupling between



$f = 45$  Mc/s, the conductance is  $224 \mu\text{mhos}$ , which is equivalent to an input parallel resistance of  $4,460 \Omega$ ; an average value for this type of valve is  $3,000 \Omega$ , including electron transit time. If the valve is connected across the whole of the tuned circuit, and optimum coupling is used to the aerial feeder, the maximum possible value of resonant impedance of the tuned circuit is  $\frac{3,000}{2}$  or  $1,500 \Omega$ .

Assuming a tuning capacitance of  $30 \mu\mu\text{F}$  (valve and stray wiring capacitances preclude a much lower value being used), the tuning inductance value at  $45$  Mc/s is  $0.416 \mu\text{H}$  and the maximum effective magnification of the tuned circuit is

$$Q = \frac{R_D}{\omega L} = \frac{1,500}{2\pi \times 45 \times 10^6 \times 0.416 \times 10^{-6}} \\ = 12.75.$$

The pass-band width, i.e., twice the off-tune frequency at which the response of the tuned circuit falls to  $0.707$  of its maximum value, is given by

$$2\Delta f = \frac{f_r}{Q} = \frac{45}{12.75} = 3.53 \text{ Mc/s.}$$

Such a circuit could therefore be used to accept transmissions covering a range approximately from  $43$  to  $47$  Mc/s when tuned to  $45$  Mc/s, and it is clear that signal tuning would confer little advantage over this range, which can accommodate twenty high-fidelity F.M. transmissions having frequency deviations not exceeding  $\pm 100$  kc/s. This wide pass-band range, together with the restricted range of ultra high frequency transmission, favours preset tuning of the R.F. stage to the centre of the desired range, discrimination against adjacent transmissions being achieved in the I.F. amplifier, and variable tuning by oscillator frequency adjustment. When signal circuit tuning is employed, selectivity can be improved, at the expense usually of sensitivity and signal-to-noise ratio, by tapping the valve grid into a portion only of the tuning coil. For example, if the grid of the valve is tapped halfway down the coil the equivalent parallel damping resistance across the whole tuning coil is increased to  $12,000 \Omega$  from the valve. This is reduced to  $6,000 \Omega$  by optimum coupling to the aerial feeder so that maximum possible  $Q$  is increased to  $51$  and the band width reduced to  $0.88$  Mc/s. Reduced aerial feeder coupling could be employed to raise  $Q$  still further, and it is interesting to note that in order to produce a pass-band of  $0.2$  Mc/s,  $Q$  would need to be raised to  $\frac{45}{0.2} = 225$ . As

a general rule an overall  $Q$  much higher than 50 would not be practicable in the first tuned circuit.

Adjustment of signal tuning may be by variation of capacitance or inductance. The disadvantage of variable capacitance tuning is that it increases the minimum tuning capacitance, reduces the already small value of tuning inductance, and also reduces the resonant impedance  $\left[ \frac{L}{CR} \right]$  of the tuned circuit. The latter is a more serious disadvantage in the anode circuit of the R.F. valve. Inductance tuning is usually accomplished by screwing a metal plunger in or out of the coil. The plunger, which acts as a short-circuited turn to reduce the inductance, must be of high-conductivity material (copper or brass) if it is not to reduce the  $Q$  of the coil to a very low value. This form of eddy current tuning has two disadvantages. Losses are introduced into the coil and the  $Q$  of the coil falls (rapidly at first) as the plunger or "slug" is inserted. The frequency range, which can be obtained, is limited due to the difficulty of designing a simple mechanical arrangement which will permit a high degree of coupling between coil and plunger. Stray wiring inductance, which has an effect similar to stray capacitance in the capacitively tuned circuit, also reduces the frequency range. A frequency range variation<sup>14</sup> of 1.5 to 1 is realizable practically, and the ratio change of  $Q$  over the same range of frequency is of the order of 0.4 to 1 for a copper plunger, and 0.3 to 1 for brass. Maximum  $Q$  is obtained at the low-frequency end of the range. The reduction in  $Q$  at the high-frequency end of the range is due to the reduction of effective inductance, the increase in the coil resistance and the resistance reflected into the coil from the plunger. Owing to this reduction in  $Q$  as tuning frequency increases, the resonant impedance is greatest at the low-frequency end of the range, and its variation over the range is generally greater than with capacitance tuning. Plotting tuning frequency against plunger position relative to the coil gives an S-shaped curve,<sup>14</sup> frequency change being less as the edge of the plunger is just entering the coil, being greatest when the edge is passing through the centre of the coil, and then reducing again as the edge of the plunger approaches the other end of the coil. Eccentricity of the plunger with respect to the coil appears to have very little effect on  $L$  and  $Q$ .

In the layout of the R.F. stage the usual precautions appropriate to ultra high frequency operation must be taken; leads should be as short as possible, all earth connections taken to the same point on the chassis, and there should be adequate decoupling, by mica



capacitors, of electrodes normally carrying only D.C. or A.C. supply voltages (screens, cathodes, heaters, etc.). A typical aerial and R.F. amplifier stage with preset signal tuning is illustrated in Fig. 15.5, which is drawn to emphasize the points enumerated above. Capacitors  $C_3$ ,  $C_4$ ,  $C_6$ ,  $C_7$  and  $C_8$  (mica 0.001  $\mu\text{F}$ ) are for by-passing radio frequencies to earth. The tuning capacitances in the grid and anode circuits are made up of the low value variable air capacitors  $C_2$  and  $C_5$  and the stray capacitances, consisting of the valve, wiring and coil self-capacitances, which are shown dotted as  $C_2'$  and  $C_5'$ . Alternatively the additional capacitors may be omitted and the inductance "trimmed" by using eddy current tuning with a plunger. The two capacitors  $C_1$  are inserted in each feeder line to neutralize the inductance of  $L_1$ , which would normally

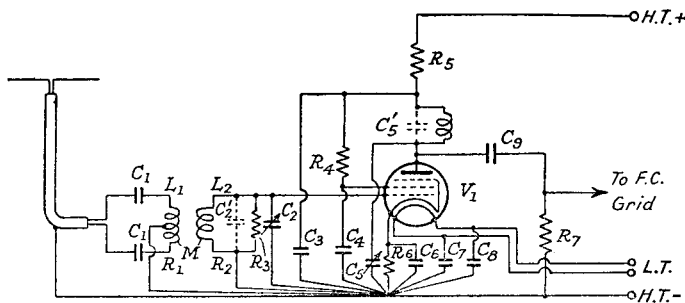


Fig. 15.5.—The Aerial and R.F. Amplifier Stage for a F.M. Receiver

[The coil in the anode of  $V_1$  is  $L_3$ .]

mean a reactive as well as resistive termination for the feeder. They are not essential if maximum possible sensitivity and signal-to-noise ratio (with optimum coupling) are not required. The series screen resistance  $R_4$  should be about 50,000  $\Omega$ , and if there is any tendency to parasitic oscillation a resistance of 50  $\Omega$  may be inserted between the screen pin and the junction of  $R_4$  and  $C_4$ . The anode decoupling resistance  $R_5$  is 1,000  $\Omega$ . A.G.C. bias can be applied to this stage, but is not desirable (and rarely necessary since the I.F. stages can provide the required control) because change of bias decreases grid input conductance and capacitance, so detuning the first tuned circuit and reducing its pass-band range. A self-bias resistance  $R_6$  of 150  $\Omega$  is suitable.

Assuming the R.F. stage to be preset tuned to 45 Mc/s with an overall pass-band of 4 Mc/s, the details of the aerial input circuit are as follows :

Radiation resistance of dipole aerial =  $80 \Omega$

Characteristic impedance of the aerial feeder =  $80 \Omega$

Total inductance of the centre-tapped primary coil  $L_1$  (any suitable value can be chosen. It should preferably be less than  $L_2$ , and, if  $C_1$  is not used, should be as small as possible consistent with obtaining the required value of  $M_1$  with  $L_2$ ) =  $0.28 \mu\text{H}$

Capacitance  $C_1$  ( $\frac{C_1}{2}$  tunes  $L_1$  to 45 Mc/s) =  $89 \mu\mu\text{F}$

Two capacitors of  $100 \mu\mu\text{F}$  would probably give satisfactory results.

Assumed total capacitance across secondary coil  $L_2$ , made up of  $15 \mu\mu\text{F}$  from valve interelectrode and electronic capacitance and  $15 \mu\mu\text{F}$  from wiring and coil self-capacitance =  $30 \mu\mu\text{F}$

Total inductance of secondary coil  $L_2$  =  $0.416 \mu\text{H}$

Assumed undamped  $Q$  of secondary circuit,  $Q_0$  = 150

Resonant impedance of the undamped secondary circuit =  $Q_0 \omega L_2 = 17,630 \Omega$

Grid input resistance,  $R_{g1}$ , of the R.F. valve at 45 Mc/s =  $3,000 \Omega$

Owing to the inclusion of  $C_1$  the aerial feeder-to-grid transformer has a tuned primary and secondary, and the  $Q$  of both these circuits influence the pass-band response. However, the  $Q$  of the primary (owing to the feeder connection) is so low that the pass-band is almost entirely determined by the  $Q$  of the secondary coil, and we need only consider the design of the grid-tuned circuit as far as pass-band characteristics are concerned. Hence, treating the aerial-grid transformer as a single tuned circuit and allowing a loss of  $-1.5$  db. at the extremes of the pass range, 43 and 47 Mc/s, we find from Fig. 4.3, Part I, that  $QF = 0.642$ , or the  $Q$  of the grid-tuned circuit is required to be  $Q_0'' = \frac{0.642f_m}{2\Delta f} = \frac{0.642 \times 45}{4} = 7.23$ .

This includes the damping due to the aerial feeder coupling, which is optimum and therefore halves the uncoupled  $Q$  value, so that the required  $Q$  in the absence of aerial feeder coupling is

$$Q_0' = 14.46$$



We can now check the assumption made above that the double-tuned feeder-to-tuned circuit transformer has a frequency response almost the same as that for a single-tuned circuit of half the  $Q$  of the secondary tuned circuit, i.e.,  $\frac{1}{2}Q_0'$ . From expression 7.2b, Part I, the modulus of the transfer impedance for two dissimilar circuits tuned to the same frequency is

$$|Z_T| = \frac{R_{D1}Q_2k\sqrt{\frac{L_2}{L_1}}}{\sqrt{[1+Q_1Q_2(k^2-F^2)]^2+(Q_1+Q_2)^2F^2}}$$

and the ratio frequency response is

$$\begin{aligned} \frac{|Z_T|_{F \neq 0}}{|Z_T|_{F=0}} &= \frac{1+Q_1Q_2k^2}{\sqrt{[1+Q_1Q_2(k^2-F^2)]^2+(Q_1+Q_2)^2F^2}} \\ &= \frac{2}{\sqrt{(2-Q_1Q_2F^2)^2+(Q_1+Q_2)^2F^2}} \quad \cdot \quad \cdot \quad 15.3a \end{aligned}$$

for optimum coupling when  $Q_1Q_2k^2 = 1$ .

Writing the above in terms of a decibel loss

$$\begin{aligned} \text{Loss (db.)} &= -20 \log_{10} \frac{|Z_T|_{F=0}}{|Z_T|_{F \neq 0}} \\ &= -10 \log_{10} \frac{(2-Q_1Q_2F^2)^2+(Q_1+Q_2)^2F^2}{4} \quad \cdot \quad \cdot \quad 15.3b. \end{aligned}$$

In the single tuned circuit we assumed a loss of  $-1.5$  db., which gives the expression

$$\frac{Q_0'}{2}F = 0.642.$$

or  $Q_0'F = Q_2F = 1.284$ .

$$Q_1 = \frac{\omega L_1}{R_{a1}} = \frac{6.28 \times 45 \times 0.28}{80} = 0.99.$$

Hence  $Q_1F = 0.088$ , and  $Q_1Q_2F^2 = 0.1131$ , so that

$$\begin{aligned} \text{loss (db.)} &= -10 \log_{10} \frac{(3.55+1.88)}{4} = -10 \log_{10} 1.358 \\ &= -1.32 \text{ db.} \end{aligned}$$

The actual frequency response is therefore slightly better than that obtained on the assumption that the feeder double-tuned transformer is equivalent to a single-tuned circuit of half the secondary circuit  $Q$  value. The difference is, however, so slight as to be almost insignificant. It is interesting to note that the generalized selectivity curves of Fig. 7.7, Part I, can be applied to double-tuned

coupled circuits of dissimilar characteristics<sup>17</sup> but tuned to the same frequency.

The formula for thermal noise R.M.S. voltage in the first tuned circuit is (expression 4.50, Part I)

$$E_n = 1.25 \times 10^{-10} \sqrt{R_D(f_1 - f_2)},$$

where  $R_D$  is the final resonant impedance of the secondary tuned circuit when damping from the feeder is taken into consideration, i.e., it equals  $\frac{1}{2}R'_D$ , and  $(f_1 - f_2)$  is the overall pass-band of the receiver.

$$\text{Thus} \quad R_D = \frac{R'_D}{2} = 850 \Omega,$$

and  $f_1 - f_2 = 200$  kc/s for high fidelity F.M. transmission of  $\pm 75$  kc/s frequency deviation. The noise in the R.F. valve is usually expressed in the form of a resistance, and when this is known it may be added to the resonant impedance of the tuned circuit in order to calculate the total effective noise voltage at the grid of the first valve. An average value for the type of valve used is  $1,500 \Omega$ , so that the total equivalent noise resistance is  $2,350 \Omega$  and the noise voltage at the grid is

$$\begin{aligned} E_n &= 1.25 \times 10^{-10} \sqrt{2,350 \times 200 \times 10^3} \\ &= 2.71 \mu V \\ &\equiv \frac{2.71}{T_R} \equiv 1.172 \mu V \end{aligned}$$

noise output at the feeder. If it is assumed that high fidelity transmission requires a signal-to-noise ratio not less than 20 db., the receiver fulfils this requirement for all carrier voltages exceeding  $11.72 \mu V$  at the feeder output. The decision not to exceed optimum coupling between feeder and first tuned circuit is seen to be justified because the valve noise resistance is greater than that of the circuit. Increased coupling reduces  $R_D$ , and hence the noise voltage at the grid of  $V_1$ , but the resulting reduction in transfer voltage ratio offsets this and increases the effective noise voltage at the output of the feeder, so reducing the overall signal-to-noise ratio. Since the reactance of  $L_1$  is neutralized by  $\frac{1}{2}C_1$ , no reactance component is reflected from the feeder into the tuned circuit, and tuning of the latter is unaffected by the coupling.

Should continuous capacitance tuning be required over the range 40 to 50 Mc/s (a ratio change of 1.25), a change of capacitance of 1.563 is needed. This can be achieved by a tuning capacitor of  $25 \mu\mu F$  maximum and  $5 \mu\mu F$  minimum value.

Alternatively, a larger capacitor may be used with a series padding capacitor inserted to reduce its range factor. The secondary inductance  $L_2$  must be reduced to  $0.287 \mu\text{H}$  so as to resonate at  $40 \text{ Mc/s}$  with  $55 \mu\mu\text{F}$  ( $C_2 + C_4(\text{max.})$ ). To make variable tuning of value, the damping across the tuned circuit from the valve must be reduced, and we shall assume that the valve is tapped across one-third of the coil. Optimum coupling between feeder and coil must still be retained in order to terminate the feeder in  $80 \Omega$ . The capacitors  $C_1$ , neutralizing the reactance of  $L_1$ , are omitted because it is not convenient to vary them in step with  $C_2$ , and unless this is done a large reactive component is reflected into the secondary circuit as the secondary tuning frequency is changed from the resonant frequency of the primary. The unneutralized reactance of  $L_1$  itself reflects a reactive component into the secondary, but it is shown later to be almost equivalent to a constant negative capacitance over the frequency range, and can be compensated by adding a capacitor in parallel with  $C_2$ .

For  $L_2 = 0.287 \mu\text{H}$ ,  $Q_0 = 150$ ,  $f = 45 \text{ Mc/s}$ , and the valve tapped across one-third of the coil, the equivalent valve damping resistance across the secondary tuned circuit ( $R_{p1} = 3,000 \Omega$ ) is  $27,000 \Omega$

$$\therefore Q_0' = \frac{Q_0 \cdot 27,000}{Q_0 \omega L_2 + 27,000} = 150 \cdot \frac{27,000}{39,190} = 103.3.$$

$$R_{D'} = Q_0' \omega L_2 = 103.3 \times 81.3 = 8,420 \Omega, \text{ and } R_2' = \frac{\omega L_2}{Q_0'} = 0.788 \Omega.$$

Assuming  $L_1 = 0.14 \mu\text{H}$ —it is deliberately reduced to improve feeder matching— $X_{a1} = 39.6 \Omega$ , and

$$Z_{a1} = \sqrt{R_{a1}^2 + X_{a1}^2} = \sqrt{80^2 + 39.6^2} = 89.2 \Omega.$$

The value of  $M_1$  for optimum coupling is

$$M_1 = \frac{Z_{a1}}{\omega} \sqrt{\frac{R_2'}{R_{a1}}} = \frac{89.2}{6.28 \times 45 \times 10^6} \sqrt{\frac{0.788}{80}} = 0.0313 \mu\text{H}.$$

The final  $Q_0''$  of the secondary circuit is halved by the feeder connection to  $51.65$  so that the pass-band width is

$$2\Delta f = \frac{45}{51.65} = 0.87 \text{ Mc/s}.$$

The pass-band is much larger than is required, but it must be remembered that this does not include the selectivity of the anode-tuned circuit of the r.f. amplifier, and the overall pass-band width would be about one-half this value, i.e.,  $0.435 \text{ Mc/s}$ .

The overall resonant impedance of the tuned circuit is

$$R_D'' = \omega L_2 Q_0'' = 81.3 \times 51.65 = 4,200 \Omega$$

and this is reduced to  $\frac{R_D''}{9}$  across the grid of  $V_1$ . Hence the total equivalent noise resistance in the grid circuit is 1,500 (valve) + 466 (circuit) = 1,966  $\Omega$  and the noise voltage is

$$\begin{aligned} E_n &= 1.25 \times 10^{-10} \sqrt{1,966 \times 200 \times 10^3} \\ &= 2.475 \mu\text{V}. \end{aligned}$$

The transfer voltage ratio from feeder to tuned circuit is

$$\begin{aligned} T_R &= \frac{1}{2} \sqrt{\frac{R_D''}{R_{a1}}} = \frac{1}{2} \sqrt{\frac{8,420}{80}} \\ &= 5.12. \end{aligned}$$

The transfer voltage ratio to the grid of  $V_1$  is one-third of this, viz., 1.706, so that the equivalent noise voltage at the output of the feeder is  $\frac{2.475}{1.706} = 1.45 \mu\text{V}$ ; hence there is some reduction in signal-to-noise ratio and also in sensitivity due to tapping down as compared with wide-band preset tuning at 45 Mc/s.

The reactive component reflected into the secondary from the unneutralized reactance of  $L_1$  is such as to increase the required value of tuning capacitance  $C_2$  (see expression 3.23b, Part I) to

$$C_2 = \frac{C_{20}}{1 - \frac{\omega^2 M_1^2 X_{a1}}{\omega L_2 |Z_{a1}|^2}}$$

where  $C_{20}$  = the initial tuning capacitance with no aerial feeder coupling.

The values of  $C_{20}$ ,  $\frac{\omega^2 M_1^2 X_{a1}}{\omega L_2 |Z_{a1}|^2}$ ,  $C_2$  and  $C_2 - C_{20}$  for 40, 45 and 50 Mc/s are tabulated below:

$f_r$	$C_{20}$	$\frac{\omega^2 M_1^2 X_{a1}}{\omega L_2  Z_{a1} ^2}$	$C_2$	$C_2 - C_{20}$
40 Mc/s	55 $\mu\mu\text{F}$	0.00397	55.22 $\mu\mu\text{F}$	0.22 $\mu\mu\text{F}$
45 "	43.5 "	0.00481	43.71 "	0.21 "
50 "	35.2 "	0.00566	35.4 "	0.21 "

The reflected reactive component is equivalent to an almost constant negative capacitance of 0.21  $\mu\mu\text{F}$  over the frequency range 40 to 50 Mc/s, and can therefore be neutralized by the addition of 0.21  $\mu\mu\text{F}$  across  $C_2$ .

The preset signal circuit between the R.F. and the frequency changer valves may be inserted in the anode of the former and connected by capacitance to the grid of the latter. This has the advantage of simplicity and, generally, highest stage gain from the grid of  $V_1$  to the grid of  $V_2$ , and it is quite satisfactory when preset tuning is employed. Its disadvantage, when continuously variable tuning is used, is that of high stray capacitance; the capacitances of both valves  $V_1$  and  $V_2$  are across the tuned circuit, and either transformer coupling must be used—this removes the anode-earth capacitance of  $V_1$  from the tuned circuit—or the minimum capacitance in the aerial tuned circuit must be increased, if signal circuit ganging is to be achieved. We shall assume, therefore, that the anode tuning capacitor of Fig. 15.5 is  $40 \mu\mu\text{F}$ , the extra  $10 \mu\mu\text{F}$  above that of  $C_2$  being due to the anode-earth capacitance of  $V_1$ ; hence  $L_3$  is  $0.312 \mu\text{H}$ . The resistance  $R_7$  is the grid leak for the frequency changer valve and also the damping resistance for widening the overall pass-band range to 4 Mc/s. The required final  $Q$  of the tuned circuit for a loss of  $-1.5$  db. over the range  $45 \pm 2$  Mc/s is the same as for the aerial circuit, i.e., 7.23. The coupling capacitance  $C_3$  ( $500 \mu\mu\text{F}$ ) is chosen to have negligible reactance in comparison with the resistance  $R_7$ , the value of which depends on the type of frequency changer used. A hexode frequency changer has a low positive grid input resistance component,  $R_{g2}$ , of the same order as that of the R.F. valve, whereas a heptode valve may present a high positive or even a negative resistance component (Section 5.8.3, Part I). For the purposes of calculation a hexode frequency changer of input resistance equal to  $3,000 \Omega$  is assumed. Taking the initial  $Q_0$  of the tuned circuit as 150, the total damping resistance to produce a final  $Q_0''$  of 7.23 is

$$R_T = \frac{\omega L_3 Q_0 Q_0''}{Q_0 - Q_0''} = \frac{88.2 \times 150 \times 7.23}{142.77} = 670 \Omega.$$

$$\therefore R_7 = \frac{R_{g2} \cdot R_T}{R_{g2} - R_T} = 862 \Omega.$$

The overall resonant impedance of the tuned circuit is  $\omega L_3 Q_0'' = 637 \Omega$ , which gives an amplification of 5.1 from the grid of  $V_1$  to the grid of  $V_2$  when the mutual conductance of  $V_1$  is 8 mA/volt.

**15.6. The Frequency Changer and Oscillator Stages.** The frequency changer and oscillator stages are considered as one unit because they are interdependent. A hexode, heptode, pentode, or diode frequency changer may be employed, but the former is most



popular, and a typical circuit diagram of a hexode valve with a separate triode oscillator is shown in Fig. 15.6. If a pentode valve is used as a frequency changer, the oscillator voltage is usually applied to the suppressor grid. Cathode<sup>9</sup> application has been tried, but is normally less satisfactory because the cathode-grid inter-electrode capacitance coupling between oscillator voltage source and signal circuit causes an appreciable oscillator voltage to appear in the signal circuit and also disturbs oscillator tuning.

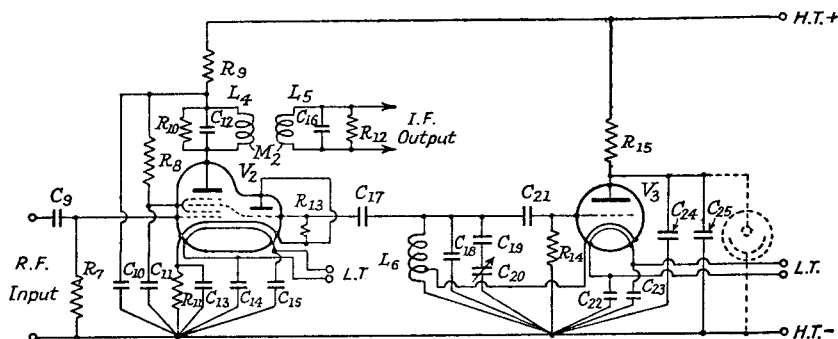


FIG. 15.6.—The Frequency Changer and Oscillator Stages of a F.M. Receiver.

The input to the frequency changer in Fig. 15.6 is the output across  $R_7$  in Fig. 15.5, and the resistance and capacitance numbers lead on from the latter figure. Capacitors  $C_{10}$ ,  $C_{11}$ ,  $C_{13}$ ,  $C_{14}$  and  $C_{15}$  ( $0.001 \mu\text{F}$  mica) by-pass radio frequencies to earth. Resistance  $R_8$  ( $25,000 \Omega$ ) is the voltage-dropping resistance for the screen,  $R_9$  ( $1,000 \Omega$ ) is a decoupling resistance and  $R_{11}$  ( $250 \Omega$ ) is the self-bias resistance. Coils  $L_4$ ,  $L_5$  and capacitors  $C_{12}$  and  $C_{16}$  are the tuning elements of the I.F. transformer, details of which are given in the next section, 15.7. The resistances  $R_{10}$  and  $R_{12}$  are damping resistances giving the required band width to the I.F. transformer.

The oscillator is a key point in the ultra high frequency super-heterodyne receiver, and a high degree of frequency stability is essential for a satisfactory receiver performance. Frequency error of the oscillator has an effect on frequency modulated reception different from that on amplitude modulation. In the latter case, unless the error is large, detuning results mainly in attenuation (frequency) distortion of the A.F. output with accentuated high-frequency A.F. components producing high-pitched shrill reproduction. With frequency modulated reception, oscillator error limits the maximum permissible frequency deviation of the I.F. carrier, because it off-centres the latter with respect to the frequency-

amplitude converter. Harmonic (amplitude) distortion of the audio output—flattening of the top or bottom half of the wave shape—therefore occurs at high modulation levels (large frequency deviation). The action of the limiter removes the amplitude modulation due to off-centring, and the attenuation distortion, noted with amplitude modulation, is absent. Rapid variation of the oscillator frequency due to hum or interference voltages has no effect in an A.M. receiver because the detector is not responsive to frequency variation but only to amplitude changes. In the F.M. receiver these rapid variations are serious since the frequency-amplitude converter changes them into amplitude variation, and undesired hum or noise interference audio outputs are obtained. We see, therefore, that oscillator long- and short-period frequency stability is of much greater importance in a F.M. system.

The causes of, and remedies for, variations of oscillator frequency are considered in detail in Sections 6.6, 6.7, 6.8 and 6.9, Part I, but for the sake of completeness a brief résumé is given in this chapter. Dealing with the long-period effects, slow drift of oscillator frequency is due mainly to temperature and humidity changes. The tuning inductance and capacitance tend to increase their values with increase of temperature, and heating of the valve changes the operating conditions with consequent change of oscillator frequency. It is generally more difficult to produce a variable capacitor with a low temperature coefficient than a variable inductance, so that inductance tuning is preferable. Inductance variations with temperature result from an increase in radius and length, the first increasing and the second decreasing inductance. Reduced variation is therefore possible by suitably proportioning the coefficients of radial and axial expansion (the radial expansion coefficient should be about half that of the axial). This can be achieved by winding the coil turns loosely on the coil former and fixing the ends firmly so that radial expansion is determined by the conductor, and axial by the coil former. An alternative is to reduce both axial and radial expansion by shrinking the coil on to a former having a low coefficient of expansion, e.g., ceramic material has a coefficient of about  $7 \times 10^{-6}$  as compared with  $17 \times 10^{-6}$  per degree centigrade for copper, so that the dimensional change of such a coil construction is only about one-third of that of the coil without the coil former.

Capacitance temperature changes are due to expansion and insulation dielectric variation. Expansion effects can be reduced by accurate centring of the rotor plates of a variable capacitor or by the use of silvered mica plates in fixed capacitors. Changes of

dielectric constants are reduced by using ceramic material. Certain types of capacitors can be constructed to give a negative temperature coefficient, i.e., capacitance falls as temperature rises, and they may be used to compensate for the positive temperature coefficient of the tuning inductance or main tuning capacitance. Compensation is, however, only complete at one particular setting of the main tuning capacitance, and the temperature of the corrector capacitor together with its rate of correction must follow that of the component it is intended to compensate. Hence it is essential to aim at the highest possible stability before applying correction.

Connecting leads should be short, securely fixed and not in tension. Preliminary cyclical heating is often an aid to frequency stability. Humidity effects are rendered less serious by the use of non-hygroscopic insulation material.

Valve temperature effects are due chiefly to interelectrode dimensional changes (a capacitance variation of the order of 0.02 to 0.04  $\mu\mu\text{F}$  is obtained from the initial to final operating temperature), and they can be reduced by employing loose coupling between active electrodes and the tuned circuit. In a capacitance-tuned oscillator, frequency changing with a harmonic of the oscillator reduces frequency drift from capacitance variations in inverse ratio to the harmonic employed, e.g., using the second harmonic of the oscillator as the active frequency tends to halve the capacitance-frequency drift. There are disadvantages with oscillator harmonic operation because signals separated by approximately the I.F. from the fundamental and other harmonics will produce spurious responses. Improved frequency stability may be realized by operating the oscillator at a frequency lower than the signal by an amount equal to the I.F., and this confers no disadvantages when the signal circuits have preset tuning. Supply voltage changes may cause slow or rapid changes of frequency. Heater voltage change is comparatively slow in action, affecting valve temperature, cathode emission and cathode heater resistance and capacitance. A palliative is loose coupling to the tuned circuit. Variation of H.T. supply controls frequency through its influence on the  $g_m$  and  $R_a$  of the oscillator valve, and it is largely responsible for interference frequency modulation troubles. Adequate decoupling and smoothing is an essential to stability, and feedback from the A.F. amplifier is lessened by using a push-pull output stage to the loudspeaker or even a separate H.T. supply.

The great difficulty with ultra high-frequency oscillators is to obtain sufficient amplitude of oscillation without squegging or

dead spots in the tuning range. A separate triode-valve oscillator should be used rather than the triode section incorporated in the frequency changer, because the former generally has a higher  $g_m$ , is more stable and maintains oscillation over a frequency range more satisfactorily. The modified Colpitts circuit (see Section 6.10, Part I)—the anode-cathode and grid-cathode interelectrode capacitances act as the capacitance splitter—is often favoured as it requires no separate reaction coil. Tuned-anode or tuned-grid oscillators are not so satisfactory, because it is not easy to obtain adequate coupling between tuned and reaction coils with a reasonable size of reaction coil. An alternative circuit is the electron-coupled oscillator, and this is the type shown in Fig. 15.6. It possesses three advantages: oscillation is not difficult to maintain over a range of frequencies, negative feedback due to the impedance of that part of the tuning coil between cathode and earth, assists amplitude and frequency stability, and one side of the tuning capacitance  $C_{20}$  is earthed. The inductance of the tuning coil  $L_6$  is  $0.416 \mu\text{H}$ , and the cathode tapping on this six-turn coil ( $\frac{1}{2}$ -in. diam. 16 s.w.g. at 10 turns per inch) occurs at approximately two turns up from the earthed end. The tuning capacitance is made up of the grid-earth capacitance of the triode section of  $V_2$  and  $V_3$  (about  $17 \mu\mu\text{F}$ ), wiring and coil self-capacitance (about  $5 \mu\mu\text{F}$ ), the fixed capacitor  $C_{18}$  ( $7 \mu\mu\text{F}$ ), and the series combination of  $C_{19}$  and  $C_{20}$ .  $C_{19}$  is a fixed capacitor of  $30 \mu\mu\text{F}$  restricting the effective range factor of  $C_{20}$ , a variable air dielectric capacitor with ceramic insulating supports and minimum and maximum values of 5 and  $20 \mu\mu\text{F}$  respectively. The oscillator frequency—in order to obtain greatest frequency stability—is selected to be lower than the signal frequency, and variation of  $C_{20}$  changes the oscillator frequency from 38.5 to 42.5 Mc/s (the I.F. = 4.5 Mc/s). The oscillator is coupled to the oscillation electrode of the frequency changer via the capacitance  $C_{17}$  and self-bias is provided by the resistance  $R_{13}$  ( $50,000 \Omega$ ). The value of  $C_{17}$  must not be made too large, otherwise the comparatively high input conductance of the oscillation grid of the frequency changer will appreciably reduce or even stop oscillation completely; about  $10 \mu\mu\text{F}$  often gives maximum voltage at the frequency changer electrode. The unused anode of the triode part of the triode hexode is returned to cathode. Constant H.T. supply to the oscillator anode is an essential requirement for frequency stability, and two decoupling capacitors are shown in Fig. 15.6 from the anode of  $V_3$  to earth.  $C_{24}$  ( $0.001 \mu\text{F}$  mica) by-passes radio frequencies and  $C_{25}$  ( $16 \mu\text{F}$  electrolytic) any audio or hum voltages in the H.T.

supply. Better H.T. regulation and smoothing can be obtained with a gas-filled device such as a neon tube in parallel with  $C_{24}$ ;  $C_{25}$  then becomes unnecessary.  $R_{15}$  must be reduced from 30,000  $\Omega$  to 10,000  $\Omega$  when the neon tube is included.

**15.7. The Intermediate Frequency Amplifier.** The actual value of the intermediate frequency for high fidelity F.M. transmissions ( $\pm 75$  kc/s frequency deviation) must be much higher than for high fidelity A.M. transmissions. The required pass-band (200 kc/s) limits the minimum I.F. to 2 Mc/s. A low value has the advantages of greater amplification and selectivity with stability, but the possibility of spurious responses from the frequency changer is greater. These responses (see Section 5.4, Part I) are, in order of importance :

1. The image frequency on the side of the oscillator frequency opposite to the real signal and separated from the latter by twice the intermediate frequency. When image response is only likely from undesired signals in the receiver tuning range, it can be avoided by making the I.F. half this range, e.g., for a receiver covering a range 40 to 50 Mc/s, an I.F. of 5 Mc/s or greater prevents image interference from transmissions in this band.

2. Oscillator harmonic response.

3. Signal harmonic response.

4. Signal and oscillator harmonic combinations.

5. I.F. harmonic response due to the desired signal being close in frequency to an I.F. harmonic.

6. Direct I.F. response, due to an undesired signal at the fundamental or submultiple of the I.F., the latter being converted to the I.F. by the non-linear action of the frequency changer.

7. Interaction between undesired signals separated by a frequency difference equal to the I.F.

8. Cross-modulation.

A high value of I.F. assists in reducing interference from 1, 2, 3, 4 and 7 by removing the interfering signal further from the desired, and allowing R.F. selectivity to be more effective. Interference from 5 and 6 is, however, increased, though that from 5 can generally be made very small by adequate I.F. decoupling of the limiter valve, the detector-A.F. amplifier connection and the A.G.C. line. It is not likely to be serious in this instance since the maximum probable value of I.F. is about 10 Mc/s and fourth harmonic feedback is needed to cause interference in the 40 to 50 Mc/s range. Cross-modulation is rarely a serious problem and Wheeler<sup>11</sup> states that it is negligible in F.M. reception. There are other methods of

reducing unwanted responses ; for example, the prevention of overloading of the frequency changer by applying A.G.C. to the R.F. stage, and increased R.F. selectivity decrease effects from 3 and 4, whilst the reduction of oscillator voltage to the lowest amplitude consistent with satisfactory frequency changing decreases responses from 2 and 4.

The limiter stage requires a certain minimum input voltage (about 2 volts) in order to remove amplitude variation, and overall I.F. amplification must be such as to bring the weakest probable signal up to the limiter input minimum. The intermediate frequency must therefore be fixed at a value which will give the required overall gain without instability or mutilation of the frequency response curve. A value between 4 and 5 Mc/s is a reasonable compromise and subsequent calculations are made on the basis of an I.F. of 4.5 Mc/s.

The problem to be solved in the design of the I.F. amplifier is to obtain highest overall amplification with a frequency response having a level pass-band, little affected by bias changes on the valves, and having rapid attenuation outside the pass range. The level pass-band is a more stringent condition than freedom from instability. Sources of feedback are coupling between input and output, common I.F. impedances in valve electrode leads normally carrying only D.C. or mains A.C. currents (anode H.T. supply, screen, grid bias, cathode and heaters) and grid-anode interelectrode capacitance. The first two can be reduced to negligible proportions by suitable shielding and decoupling. Decoupling capacitors should be connected to earth by the shortest possible leads, and when used to decouple tuned circuits should be included inside the screening cans enclosing the tuning elements. Common impedance coupling can largely be eliminated by connecting decoupling capacitors for each stage to a common earth point, as was done for the R.F. and frequency changer stages. Thus we come to the basic fact that the limit to maximum overall amplification is set by feedback through the anode-grid capacitance. This effect is discussed in detail in Section 7.8, Part I, where it is shown that feedback is negative when the anode circuit is capacitive, and positive when the anode circuit is inductive. The parallel-tuned circuit has a capacitive reactance at frequencies above resonance and an inductive reactance at frequencies below resonance, so that feedback from such an anode circuit is degenerative at the higher frequencies and regenerative at the lower frequencies. Its effect on overall frequency response is to produce a lop-sided curve with greater

amplification at frequencies below resonance. The degree of degeneration or regeneration is best expressed in the form of a positive or negative input resistance (see expression 7.23a, Part I)

$$R_g = \frac{(G_a + G_0)^2 + B_0^2}{g_m B_{ga} B_0} \quad . \quad . \quad . \quad 15.4a$$

where  $G_a = \frac{1}{R_a}$  = anode slope conductance

$G_0$  = conductance of external anode circuit

$B_0$  = susceptance of external anode circuit

$g_m$  = mutual conductance of valve

$B_{ga}$  = susceptance of anode-grid capacitance  
 $= \omega C_{ga}$ .

This resistance component has a minimum value and the condition for this is found by differentiating 15.4a with respect to  $B_0$  and equating to zero.  $B_0$  is treated as the variable because it changes rapidly in the region of resonance, from a high negative value below, through zero at resonance, to a high positive value above.  $G_0$  over the same range is practically constant and equal to the reciprocal of the resonant impedance, i.e.,  $\frac{1}{R_D}$  or  $\frac{1}{\omega_r L Q}$ . The condition for minimum  $R_g$  is found to be

$$B_0 = \pm(G_a + G_0)$$

and  $R_g(\text{min.}) = \frac{\pm 2(G_a + G_0)}{g_m B_{ga}} \quad . \quad . \quad . \quad 15.4b.$

In the particular case we are considering  $G_a \ll G_0$  and

$$R_g(\text{min.}) \simeq \frac{\pm 2G_0}{g_m B_{ga}} = \frac{\pm 2}{g_m B_{ga} R_D} \quad . \quad . \quad . \quad 15.4c.$$

If instead of a single-tuned circuit there is a double-tuned transformer in the anode circuit, calculation may be based on the assumption that coupling will be in the region of the critical value, and under these conditions one circuit reflects into the other a resistance equal to its initial resistance, i.e., the actual resonant impedance is half that of one tuned circuit alone and expression 15.4c becomes

$$R_g(\text{min.}) = \frac{\pm 4}{B_{ga} R_D g_m} \quad . \quad . \quad . \quad 15.4d.$$

If it is desired to obtain a more accurate value of  $R_g(\text{min.})$  reference should be made to Section 7.8, Part I, but expression 15.4d will be found to be satisfactory for all practical purposes.

In order that frequency response may be almost unaffected by

feedback, the minimum resistance component should be at least ten times the effective resonant impedance of the grid circuit, and this condition necessitates the use of a special buffer stage in the I.F. amplifier.

To obtain a flat frequency response over a given pass range it is necessary to combine single- and double-tuned over-coupled circuits, the peak of the single-tuned circuit falling in the trough of the two over-coupled circuits. Much the same effect can be obtained by the combination of a pair of over-coupled with a pair of under-coupled circuits of single-peaked response, and we shall use these principles in the design of the I.F. amplifier, the diagram of which is shown in Fig. 15.7. The frequency changer anode I.F. transformer of Fig. 15.6 is repeated in Fig. 15.7; in its anode circuit is a pair of critically coupled

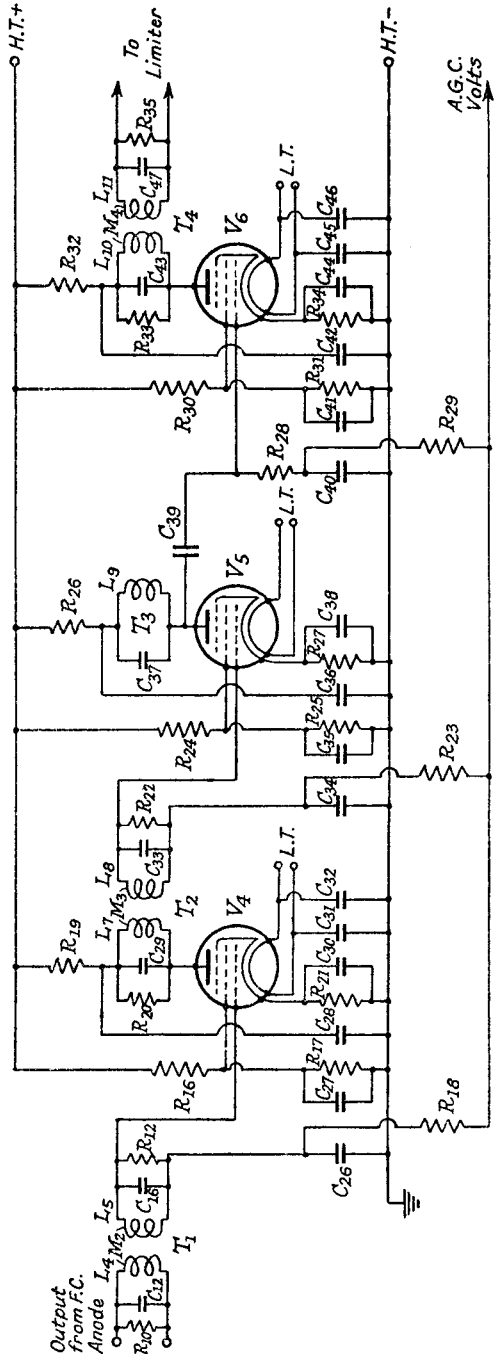


FIG. 15.7.—The I.F. Amplifier Stages of a F.M. Receiver.



supply. Better H.T. regulation and smoothing can be obtained with a gas-filled device such as a neon tube in parallel with  $C_{24}$ ;  $C_{25}$  then becomes unnecessary.  $R_{15}$  must be reduced from 30,000  $\Omega$  to 10,000  $\Omega$  when the neon tube is included.

**15.7. The Intermediate Frequency Amplifier.** The actual value of the intermediate frequency for high fidelity F.M. transmissions ( $\pm 75$  kc/s frequency deviation) must be much higher than for high fidelity A.M. transmissions. The required pass-band (200 kc/s) limits the minimum I.F. to 2 Mc/s. A low value has the advantages of greater amplification and selectivity with stability, but the possibility of spurious responses from the frequency changer is greater. These responses (see Section 5.4, Part I) are, in order of importance :

1. The image frequency on the side of the oscillator frequency opposite to the real signal and separated from the latter by twice the intermediate frequency. When image response is only likely from undesired signals in the receiver tuning range, it can be avoided by making the I.F. half this range, e.g., for a receiver covering a range 40 to 50 Mc/s, an I.F. of 5 Mc/s or greater prevents image interference from transmissions in this band.

2. Oscillator harmonic response.

3. Signal harmonic response.

4. Signal and oscillator harmonic combinations.

5. I.F. harmonic response due to the desired signal being close in frequency to an I.F. harmonic.

6. Direct I.F. response, due to an undesired signal at the fundamental or submultiple of the I.F., the latter being converted to the I.F. by the non-linear action of the frequency changer.

7. Interaction between undesired signals separated by a frequency difference equal to the I.F.

8. Cross-modulation.

A high value of I.F. assists in reducing interference from 1, 2, 3, 4 and 7 by removing the interfering signal further from the desired, and allowing R.F. selectivity to be more effective. Interference from 5 and 6 is, however, increased, though that from 5 can generally be made very small by adequate I.F. decoupling of the limiter valve, the detector-A.F. amplifier connection and the A.G.C. line. It is not likely to be serious in this instance since the maximum probable value of I.F. is about 10 Mc/s and fourth harmonic feedback is needed to cause interference in the 40 to 50 Mc/s range. Cross-modulation is rarely a serious problem and Wheeler<sup>11</sup> states that it is negligible in F.M. reception. There are other methods of

reducing unwanted responses ; for example, the prevention of overloading of the frequency changer by applying A.G.C. to the R.F. stage, and increased R.F. selectivity decrease effects from 3 and 4, whilst the reduction of oscillator voltage to the lowest amplitude consistent with satisfactory frequency changing decreases responses from 2 and 4.

The limiter stage requires a certain minimum input voltage (about 2 volts) in order to remove amplitude variation, and overall I.F. amplification must be such as to bring the weakest probable signal up to the limiter input minimum. The intermediate frequency must therefore be fixed at a value which will give the required overall gain without instability or mutilation of the frequency response curve. A value between 4 and 5 Mc/s is a reasonable compromise and subsequent calculations are made on the basis of an I.F. of 4.5 Mc/s.

The problem to be solved in the design of the I.F. amplifier is to obtain highest overall amplification with a frequency response having a level pass-band, little affected by bias changes on the valves, and having rapid attenuation outside the pass range. The level pass-band is a more stringent condition than freedom from instability. Sources of feedback are coupling between input and output, common I.F. impedances in valve electrode leads normally carrying only D.C. or mains A.C. currents (anode H.T. supply, screen, grid bias, cathode and heaters) and grid-anode interelectrode capacitance. The first two can be reduced to negligible proportions by suitable shielding and decoupling. Decoupling capacitors should be connected to earth by the shortest possible leads, and when used to decouple tuned circuits should be included inside the screening cans enclosing the tuning elements. Common impedance coupling can largely be eliminated by connecting decoupling capacitors for each stage to a common earth point, as was done for the R.F. and frequency changer stages. Thus we come to the basic fact that the limit to maximum overall amplification is set by feedback through the anode-grid capacitance. This effect is discussed in detail in Section 7.8, Part I, where it is shown that feedback is negative when the anode circuit is capacitive, and positive when the anode circuit is inductive. The parallel-tuned circuit has a capacitive reactance at frequencies above resonance and an inductive reactance at frequencies below resonance, so that feedback from such an anode circuit is degenerative at the higher frequencies and regenerative at the lower frequencies. Its effect on overall frequency response is to produce a lop-sided curve with greater

amplification at frequencies below resonance. The degree of degeneration or regeneration is best expressed in the form of a positive or negative input resistance (see expression 7.23a, Part I)

$$R_g = \frac{(G_a + G_0)^2 + B_0^2}{g_m B_{ga} B_0} \quad . \quad . \quad . \quad 15.4a$$

where  $G_a = \frac{1}{R_a}$  = anode slope conductance

$G_0$  = conductance of external anode circuit

$B_0$  = susceptance of external anode circuit

$g_m$  = mutual conductance of valve

$B_{ga}$  = susceptance of anode-grid capacitance  
=  $\omega C_{ga}$ .

This resistance component has a minimum value and the condition for this is found by differentiating 15.4a with respect to  $B_0$  and equating to zero.  $B_0$  is treated as the variable because it changes rapidly in the region of resonance, from a high negative value below, through zero at resonance, to a high positive value above.  $G_0$  over the same range is practically constant and equal to the reciprocal of the resonant impedance, i.e.,  $\frac{1}{R_D}$  or  $\frac{1}{\omega_r L Q}$ . The condition for minimum  $R_g$  is found to be

$$B_0 = \pm(G_a + G_0)$$

and 
$$R_g(\min.) = \frac{\pm 2(G_a + G_0)}{g_m B_{ga}} \quad . \quad . \quad . \quad 15.4b.$$

In the particular case we are considering  $G_a \ll G_0$  and

$$R_g(\min.) \simeq \frac{\pm 2G_0}{g_m B_{ga}} = \frac{\pm 2}{g_m B_{ga} R_D} \quad . \quad . \quad . \quad 15.4c.$$

If instead of a single-tuned circuit there is a double-tuned transformer in the anode circuit, calculation may be based on the assumption that coupling will be in the region of the critical value, and under these conditions one circuit reflects into the other a resistance equal to its initial resistance, i.e., the actual resonant impedance is half that of one tuned circuit alone and expression 15.4c becomes

$$R_g(\min.) = \frac{\pm 4}{B_{ga} R_D g_m} \quad . \quad . \quad . \quad 15.4d.$$

If it is desired to obtain a more accurate value of  $R_g(\min.)$  reference should be made to Section 7.8, Part I, but expression 15.4d will be found to be satisfactory for all practical purposes.

In order that frequency response may be almost unaffected by

feedback, the minimum resistance component should be at least ten times the effective resonant impedance of the grid circuit, and this condition necessitates the use of a special buffer stage in the I.F. amplifier.

To obtain a flat frequency response over a given pass range it is necessary to combine single- and double-tuned overcoupled circuits, the peak of the single-tuned circuit falling in the trough of the two overcoupled circuits. Much the same effect can be obtained by the combination of a pair of overcoupled with a pair of undercoupled circuits of single-peaked response, and we shall use these principles in the design of the I.F. amplifier, the diagram of which is shown in Fig. 15.7. The frequency changer anode I.F. transformer of Fig. 15.6 is repeated in Fig. 15.7; in its anode circuit is a pair of critically coupled

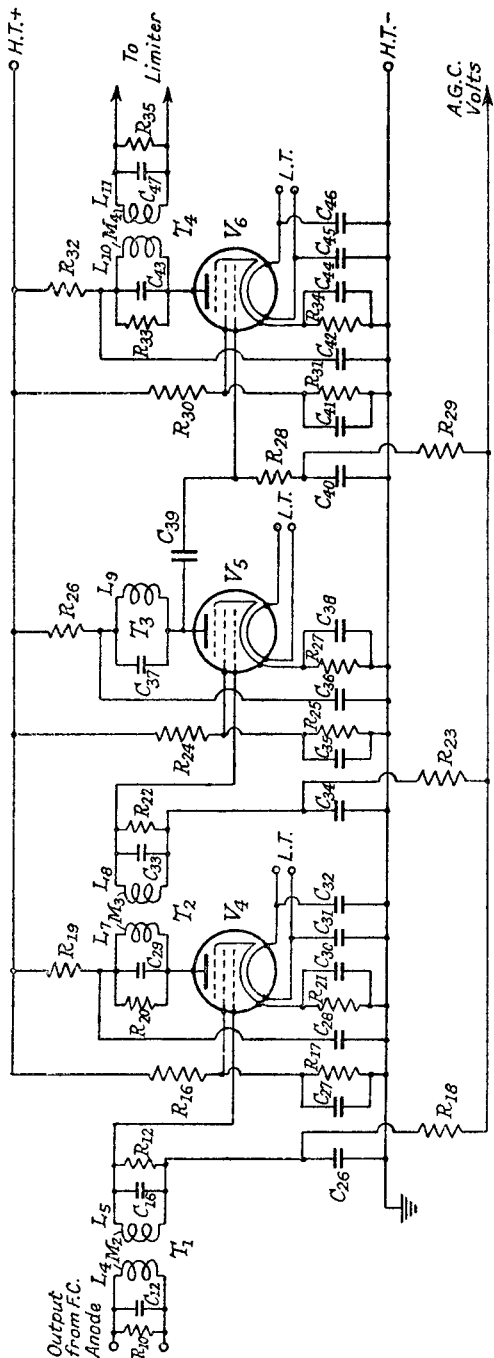


Fig. 15.7.—The I.F. Amplifier Stages of a F.M. Receiver.

tuned circuits. The first and third I.F. amplifier valves  $V_4$  and  $V_6$  each contain a pair of overcoupled circuits, and the second I.F. valve  $V_5$  has a single-tuned circuit. This stage is also acting as a buffer or isolator to reduce anode-grid capacitance feedback to a negligible value. By using the generalized curves of Figs. 4.3, and 7.7, Part I, for the frequency response of single- and double-tuned circuits (the primary of each transformer has constants identical with the secondary), and assuming that transformers  $T_2$  and  $T_4$  are identical, we find that an almost flat pass-band response is obtained by making  $T_2$  and  $T_4$  overcoupled circuits of constant  $Q_2k_2 = Q_4k_4 = 2$ ,  $T_1$  a pair of critically coupled circuits of  $Q_1k_1 = 1$ , and suitably choosing  $Q_3$  of the single-tuned circuit in the anode of  $V_5$ .  $k$  is the coupling coefficient, e.g.,  $\frac{M_2}{\sqrt{L_4L_5}} = \frac{M_2}{L_4}$  for  $T_1$ , and  $Q$  is the magnification of primary or secondary circuit when the other is not coupled to it. The overcoupled circuits  $T_2$  and  $T_4$  have maximum response at  $\frac{Q_2 2\Delta f}{f_r} = \pm 1.8$  (see the curve for  $Qk = 2$ , Fig. 7.7, Part I), where  $\Delta f$  is the frequency off-tune from  $f_r$ , the resonant or trough frequency, and the trough-to-peak ratio is  $-2$  db. By selecting  $Q_2$  to satisfy the above expression when  $\Delta f = \pm 100$  kc/s (the maximum required semi-band width), we have

$$Q_2 = \frac{1.8f_r}{2\Delta f} = \frac{1.8 \times 4.5}{0.2} = 40.5.$$

This fixes the position of the frequency scale on Fig. 7.7, and the combined frequency response of the two transformers is shown as the dotted curve 1 in Fig. 15.8. The single-peaked frequency response of transformer  $T_1$  and tuned circuit  $L_5C_3$ , have losses of 1 and 3 db. respectively at  $\frac{Q_2 2\Delta f}{f_r}$  and if  $Q$  is selected to make this expression unity when  $\Delta f = \pm 100$  kc/s, i.e.,

$$Q_1 = Q_3 = \frac{f_r}{2\Delta f} = 22.5$$

the loss in these two circuits at 100 kc/s exactly counterbalances the gain due to  $T_2$  and  $T_4$ . Curves 2 and 3 in Fig. 15.8 give the frequency responses for  $T_1$  and  $T_3$  respectively. There is not exact compensation at all frequencies in the pass-band, but the variation in the overall curve 4 does not exceed 0.7 db.

Having determined the  $Q$  values for all the circuits, we now have to select  $L$  and  $C$  values to give maximum overall amplification

and also a grid input resistance component for each valve not less than ten times the effective resonant impedance of its associated grid circuit. In designing the amplifier we shall assume that valves  $V_4$ ,  $V_5$  and  $V_6$  are identical and have the following constants:  $g_m = 2$  mA/volt,  $C_{ga} = 0.02 \mu\mu\text{F}$  and a slope resistance  $R_a$  much

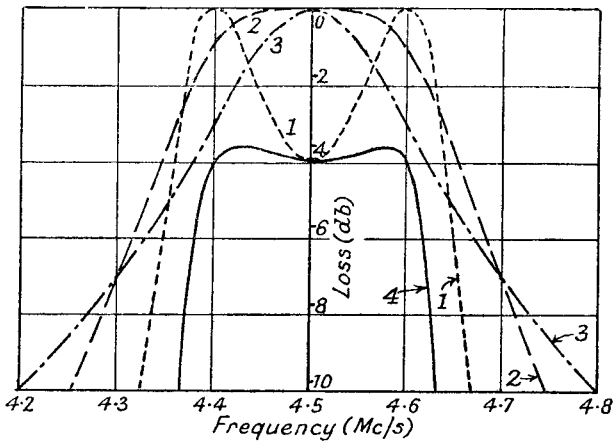


FIG. 15.8.—The Individual and Overall Frequency Responses of the I.F. Amplifier Stages of Fig. 15.7.

greater than the resonant impedance of any anode circuit. Maximum amplification in any stage is obtained by making the effective dynamic impedance  $R_D = Q\omega_r L = \frac{Q}{\omega_r C}$  as large as possible, i.e., the tuning capacitance  $C$  should be as small as possible. A suitable minimum value is  $50 \mu\mu\text{F}$  so that starting at the last I.F. amplifier with the overcoupled circuits, we have for  $f_r = 4.5$  Mc/s

$$\begin{aligned} C_{43} &= C_{47} = 50 \mu\mu\text{F} \\ L_{10} &= L_{11} = 25 \mu\text{H} \\ Q_4 &= 40.5 \\ Q_4 k_4 &= 2 \text{ or } k_4 = 0.0494 \\ M_4 &= k_4 L_{10} = 1.235 \mu\text{H}. \end{aligned}$$

The resonant impedance of either tuned circuit when not coupled to the other is

$$*R_{D4} = \frac{Q_4}{\omega_r C_{43}} = \frac{40.5 \times 10^{12}}{6.28 \times 4.5 \times 10^6 \times 50} = 28,700 \Omega$$

\*  $R_{D4}$  is the resonant impedance of either primary or secondary alone of the transformer  $T_4$ , i.e., the numeral suffix 4 denotes the transformer number in Fig. 15.7. Similarly,  $R_{D3}$  and  $R_{D2}$  apply to transformers  $T_3$  and  $T_2$ . The numeral suffix of  $Q$  also denotes the transformer number.

and maximum amplification at the peaks ( $f_r \pm 100$  kc/s) of the frequency response of curve 1 in Fig. 15.8 is (see the expression derived from 7.3f, Part I)

$$*A_6 = \frac{g_m R_{D4}}{2} = 28.7.$$

The damping resistances  $R_{33}$  and  $R_{35}$  for an initial coil  $Q_0$  of 150 are given by

$$R_{33} = \frac{\omega L_{10} Q_0 Q_4}{Q_0 - Q_4} = \frac{706 \times 150 \times 40.5}{150 - 40.5} = 39,200 \Omega.$$

and  $R_{35}$  has the same value if the succeeding limiter stage does not damp the circuit. In the next section a typical limiter stage is shown to have appreciable damping on the  $L_{11}C_{47}$  circuit and  $R_{35}$  has to have a higher value than  $R_{33}$ .

The minimum input resistance component at the grid of  $V_6$  is from expression 15.4d

$$R_{g6}(\text{min.}) = \frac{4}{g_m \omega C_{ga} R_{D4}} = \frac{4 \times 10^{12}}{2 \times 10^{-3} \times 6.28 \times 4.5 \times 10^6 \times 0.02 \times 28,700} \\ = 123,200 \Omega.$$

The resonant impedance of tuned circuit  $T_3$ , consisting of  $L_9$  and  $C_{37}$ , must not therefore exceed  $12,320 \Omega$  if the overall frequency response is not to be seriously affected by feedback. But  $Q_3 = 22.5$

$$\therefore C_{37} = \frac{Q_3}{\omega_r R_{D3}} = \frac{22.5 \times 10^{12}}{6.28 \times 4.5 \times 10^6 \times 12,320} \mu\mu\text{F} \\ = 64.5 \mu\mu\text{F}. \\ L_9 = 19.4 \mu\text{H}.$$

If  $Q_0 = 150$  and  $C_{39}$  ( $500 \mu\mu\text{F}$ ) has negligible reactance compared with  $R_{23}$ , then

$$R_{23} = \frac{\omega_r L_9 Q_0 Q_3}{Q_0 - Q_3} = \frac{549 \times 150 \times 22.5}{127.5} \\ = 14,550 \Omega.$$

Maximum amplification at  $f_r = 4.5$  Mc/s is, for the single-tuned circuit,

$$A_5 = g_m R_{D3} = 24.64.$$

\* The numeral suffix to Amplification  $A$  and minimum grid input resistance  $R_g(\text{min.})$  defines the number of the valve in Fig. 15.7, with which it is associated. Thus  $A_6$  is the amplification from the grid of  $V_6$  to its output across the secondary of  $T_4$ , and  $R_{g6}(\text{min.})$  is the minimum grid input resistance of valve  $V_6$ .

The minimum grid input resistance

$$R_{g5}(\text{min.}) = \frac{2}{g_m \omega C_{g5} R_{D3}} = 143,500 \Omega.$$

The effective resonant impedance of transformer  $T_2$ , which is identical with  $T_4$ , is  $\frac{R_{D2}}{2} = \frac{R_{D4}}{2} = 14,350 \Omega$ , and this fulfils the condition that it should be not greater than  $\frac{1}{10} R_{g5}$ . All the circuit constants for  $T_2$  are identical with those of  $T_4$ , i.e.,

$$C_{29} = C_{33} = 50 \mu\mu\text{F}$$

$$L_7 = L_8 = 25 \mu\text{H}$$

$$Q_2 = 40.5$$

$$M_3 = 1.235 \mu\text{H}$$

$$A_4 = 28.7 \text{ at the peaks } (f_r \pm 100) \text{ kc/s}$$

$$R_{g4}(\text{min.}) = 123,200 \Omega.$$

Transformer  $T_1$  must therefore have an effective resonant impedance not exceeding  $12,320 \Omega$ , i.e.,  $R_{D1} \nabla 24,640 \Omega$ . The maximum value of  $R_{D1}$  is, however, fixed because  $Q_1 = 22.5 \mu\mu\text{F}$  and  $C_{16}$  is not less than  $50 \mu\mu\text{F}$ .

$$\begin{aligned} \therefore R_{D1}(\text{max.}) &= \frac{Q_1}{\omega_r C_{16}} = \frac{22.5 \times 10^{12}}{6.28 \times 4.5 \times 10^6 \times 50} \\ &= 15,900 \Omega. \end{aligned}$$

This value cannot be exceeded without reducing  $C_{16}$ , but as it is less than the maximum permitted by feedback considerations it simply means that feedback has even less effect. The constants for  $T_1$  are therefore

$$C_{12} = C_{16} = 50 \mu\mu\text{F}$$

$$L_4 = L_5 = 25 \mu\text{H}$$

$$Q_1 = 22.5$$

$$Q_1 k_1 = 1 \text{ or } k_1 = 0.0445$$

$$M_2 = k_1 L_4 = 1.11 \mu\text{H}.$$

Maximum amplification at the peak of response ( $f_r$ ) for the frequency changer valve  $V_2$  is

$$A_2 = g_c \frac{R_{D1}}{2}$$

where  $g_c$  = conversion conductance of the frequency changer valve

$V_2$ . A probable value is  $0.3 \text{ mA/volt}$ .

$$\text{Hence } A_2 = 0.3 \times \frac{15.9}{2} = 2.385.$$

Feedback of I.F. voltage into the grid circuit of  $V_2$  through the



anode-grid capacitance can generally be neglected because the grid circuit is tuned to a much higher frequency.

The values of  $R_{10}$  and  $R_{12}$  are

$$\begin{aligned} R_{10} = R_{12} &= \frac{\omega_r L_4 Q_0 Q_1}{Q_0 - Q_1} = \frac{706 \times 150 \times 22.5}{127.5} \\ &= 18,700 \Omega. \end{aligned}$$

The overall amplification from the grid of  $V_2$  to the output of  $V_6$ , i.e., to the limiter, is

$$2.385 \times 28.7 \times 24.64 \times 28.7 \times 0.63 = 30,500.$$

The factor 0.63 is included because of the 4-db. peak-to-trough loss in  $V_4$  and  $V_6$ .

The total amplification from the grid of the R.F. valve  $V_1$  to the output of  $V_6$  is  $30,500 \times 5.1 = 155,500$ , and assuming a signal-to-noise ratio of 20 db., the minimum acceptable signal is  $27.1 \mu\text{V}$ , which produces an output voltage from  $V_6$  of  $27.1 \times 0.156 = 4.22$  volts. This is adequate for operating the limiter stage, the minimum required input voltage for which is usually about 2 volts.

Suitable values for the numbered resistances and capacitances in Fig. 15.7, which have not so far been specified, are tabulated below:

Capacitances.		Resistances.	
$C_{26} = 0.001 \mu\text{F}$	$C_{38} = 0.1 \mu\text{F}$	$R_{16} = 30,000 \Omega$	$R_{26} = 1,000 \Omega$
$C_{27} = 0.1 \mu\text{F}$	$C_{39} = 0.0005 \mu\text{F}$	$R_{17} = 20,000 \Omega$	$R_{27} = 300 \Omega$
$C_{28} = 0.1 \mu\text{F}$	$C_{40} = 0.001 \mu\text{F}$	$R_{18} = 0.1 \text{M}\Omega$	$R_{29} = 0.1 \text{M}\Omega$
$C_{30} = 0.1 \mu\text{F}$	$C_{41} = 0.1 \mu\text{F}$	$R_{19} = 1,000 \Omega$	$R_{30} = 30,000 \Omega$
$C_{31} = 0.01 \mu\text{F}$	$C_{42} = 0.1 \mu\text{F}$	$R_{21} = 300 \Omega$	$R_{31} = 20,000 \Omega$
$C_{32} = 0.01 \mu\text{F}$	$C_{44} = 0.1 \mu\text{F}$	$R_{23} = 0.1 \text{M}\Omega$	$R_{32} = 1,000 \Omega$
$C_{34} = 0.001 \mu\text{F}$	$C_{45} = 0.01 \mu\text{F}$	$R_{24} = 30,000 \Omega$	$R_{34} = 300 \Omega$
$C_{35} = 0.1 \mu\text{F}$	$C_{46} = 0.01 \mu\text{F}$	$R_{25} = 20,000 \Omega$	
$C_{36} = 0.1 \mu\text{F}$			

The A.G.C. capacitance-resistance filters ( $C_{26}R_{18}$ ,  $C_{34}R_{23}$  and  $C_{40}R_{29}$ ) have smaller values than their counterparts in the A.M. receiver because undesired amplitude change of the F.M. carrier, when fed back along the A.G.C. line, tends to cancel the amplitude variation of the carrier. It is a form of negative feedback. The A.G.C. voltage is often derived from the limiter stage grid circuit and the method of obtaining it is described in the next section.

## 15.8. The Amplitude Limiter.

**15.8.1. Introduction.** In order to take full advantage of F.M. transmissions, some circuit must be included in the receiver to reduce to negligible proportions any amplitude modulation of

the carrier due to noise or to variation in the overall frequency response of the pass-band. This is essential because the A.F. content of the F.M. signal is extracted by means of an amplitude detector, such as a diode, after its frequency variation has been converted to an amplitude modulation; an initial A.F. amplitude variation of the F.M. carrier is detected at the same time and produces an undesired audio output.

There are five possible types of amplitude limiter :

- (1) A saturated amplifier, having an amplification factor inversely proportional to the amplitude of the input signal.
- (2) A controlled local oscillator, locked by the frequency of the F.M. input but having an output voltage independent of the amplitude of the controlling signal. This type is discussed in Section 15.10.4 as it primarily acts as a frequency deviation reducer.
- (3) An integrating device, having an output voltage dependent upon the frequency of the input signal but independent of its amplitude. This form of limiter is also a frequency-to-amplitude converter and is described in Sections 15.9.4 and 15.9.5.
- (4) A negative feedback system which detects the amplitude modulation of the F.M. signal and uses it to supply A.G.C. bias to the I.F. valves to reduce envelope as well as carrier variations.
- (5) A neutralizing device which detects the amplitude modulation and supplies it in reversed phase to the F.M. audio output so as to cancel the initial undesired amplitude variation.

**15.8.2. The Saturated Amplifier Limiter.** The saturated amplifier is the most common form of limiter and will be considered first. A typical circuit is shown in Fig. 15.9. The carrier input is detected by the  $I_g E_g$  characteristic of the valve and automatic bias is produced across  $R_{3s}$ . A change in carrier amplitude causes a corresponding change in bias, i.e., increase of amplitude increases the negative bias across  $R_{3s}$ . Provided the overall amplification to the carrier fundamental frequency is inversely proportional to the grid bias, and the bias voltage is a faithful reproduction of the amplitude modulated envelope, there is no amplitude modulation at the output. This condition can be approached by operating the valve as a Class C amplifier with an  $I_a E_g$  curve having a low bias voltage cut-off ( $I_a = 0$ ) and a saturated characteristic for positive bias voltages. Hence the valve  $V_1$  has low screen and anode voltages (about 40 volts). The negative (low  $I_a$ ) half of the output current

wave shape is limited by the cut-off bias point, which is fixed by the screen voltage. The positive (high  $I_a$ ) half is limited by anode current saturation, which is determined by the anode voltage, and, to a less extent, by damping of the input voltage peak by grid current. A low anode voltage causes the load line to operate into the "knee" of the tetrode  $I_a E_a$  characteristics and a saturated  $I_a E_g$  curve is therefore produced. The resemblance of this type of limiter to the "leaky grid" detector may be noted; it is, in fact, this form of detector, working under saturated anode current conditions, with an anode circuit tuned to the carrier fundamental instead of an aperiodic circuit accepting audio frequencies. In the "leaky grid" detector the time constant of the self-bias circuit must allow the bias change to follow exactly the modu-

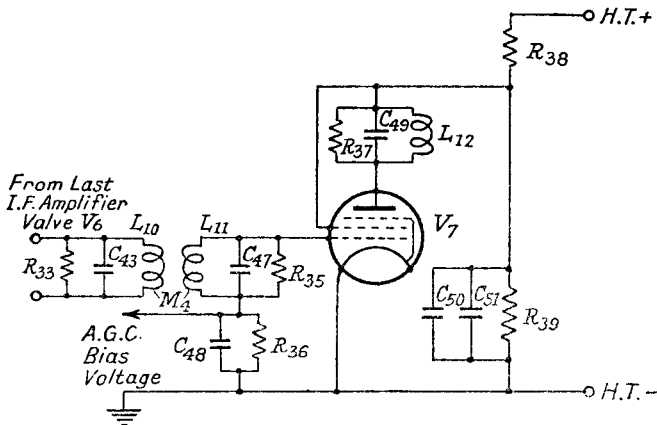


FIG. 15.9.—The Saturated Amplifier Limiter Stage.

lation envelope, and this also applies to the limiter. A suitable time constant is 10 to 20 microsecs. with  $R_{36} = 0.1 \text{ M}\Omega$  and  $C_{48} = 100 \mu\mu\text{F}$ . If the time constant is too large, the bias is not proportional to the amplitude modulation, and if it is too small, the bias change is reduced and amplification control compensation is inadequate. Typical limiter input-output curves are shown in Fig. 15.10; curve 1 represents optimum limiting conditions with a screen and anode voltage of approximately 40 volts; output voltage falls slightly as the input voltage is increased. If anode voltage is increased, output voltage increases (curve 2), but the general shape of the curve remains unchanged unless anode voltage is considerably increased, when output voltage often falls slightly after the first maximum and then rises as the input voltage is increased.

An increase in screen voltage (curve 3) moves the limiting point to a higher input voltage, roughly in proportion to the increase in  $E_s$ , and also tends to greater variation in output voltage.  $R_{3a}$  affects the rate of fall of output voltage with increase of input, a high value exaggerating the tendency to a decrease in output voltage (curve 4).

Variations in the frequency response over the pass range of tuned circuits following the limiter cause amplitude modulation of

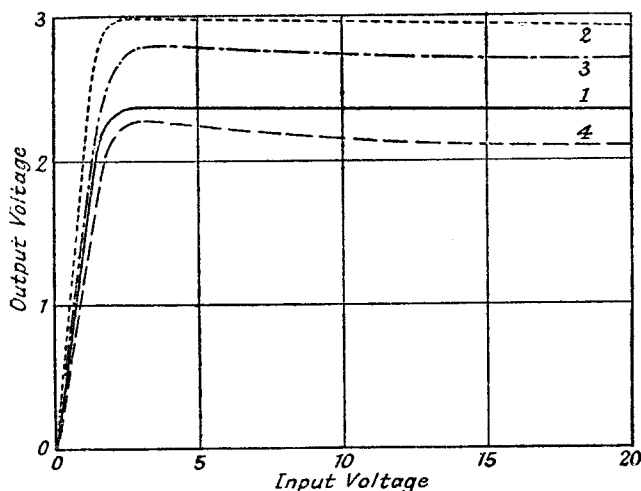


FIG. 15.10.—Input-Output Voltage Curves for the Saturated Amplifier Limiter.

- Curve 1.— $E_a = E_s \approx 40$  volts.  
 Curve 2.— $E_a > 40$  volts,  $E_s \approx 40$  volts.  
 Curve 3.— $E_a \approx 40$  volts,  $E_s > 40$  volts.  
 Curve 4.— $E_a = E_s \approx 40$  volts,  $R_{3a} = 1 M\Omega$ .

the F.M. signal, which results in harmonic distortion of the A.F. output when the frequency deviation of the signal is large. It is essential that these circuits should have least possible variation over their pass range, whilst offering appreciable attenuation to the harmonics of the F.M. signal produced by the limiting action. If the loss of response is symmetrical on either side of the tuning points, the A.F. distortion of the output consists mainly of odd harmonics (third, fifth, etc.). Variations in the frequency response of circuits preceding the limiter are compensated by its action. A suitable value for the  $Q$  of the anode circuit of the limiter is 4.5 if it is a single-tuned circuit or 14.2 if it consists of a pair of critically coupled tuned circuits. The single circuit gives a loss of approximately  $-0.15$  db. (representing 1.9% change of amplitude) at

$4.5 \pm 0.1$  Mc/s and a loss of  $-16.7$  db. (representing an amplitude reduction to 14.65%) at the I.F. second harmonic, 9 Mc/s. Owing to the large off-tune-to-resonant frequency ratio, the loss is calculated from expression 4.8c, Part I, using  $F = \left( \frac{\omega}{\omega_r} - \frac{\omega_r}{\omega} \right)$ . The corresponding values for a loss of  $-0.15$  db. at  $4.5 \pm 0.1$  Mc/s with a pair of critically coupled circuits is  $Q = 14.2$  and the loss at 9 Mc/s =  $-47.1$  db. (an amplitude reduction to 0.44%). The coupled circuits are clearly very much better than the single circuit. The frequency-amplitude converter, which follows the limiter, can, with advantage, constitute the anode load of the latter, but it may be preceded by a separate valve amplifier. Grid current, taken by the limiter valve  $V_7$ , has a damping effect on the tuned circuit  $L_{11}C_{47}$ , and it is equivalent approximately to a resistance of  $\frac{1}{2}R_{38}$  (see Section 8.2.5, Part I). Hence  $R_{38}$  must be such as to give a total resistance of 39,200  $\Omega$  when paralleled by 50,000  $\Omega$ , i.e.,

$$R_{38} = \frac{39,200 \times 50,000}{50,000 - 39,200} = 181,500 \Omega.$$

The required low value of 40 volts for screen and anode voltage is obtained from the 250 volts H.T. supply by means of the potential divider made up of  $R_{38}$  and  $R_{39}$ , 40,000 and 10,000  $\Omega$  respectively. The decoupling capacitors  $C_{50}$  and  $C_{51}$ , 0.1  $\mu\text{F}$  and 8  $\mu\text{F}$  (electrolytic) respectively, by-pass R.F. and A.F., the latter being produced by the limiter action.  $C_{50}$  is required in addition to  $C_{51}$  because the latter may not be non-inductive.

Since across  $R_{38}$  in Fig. 15.9 there is a negative voltage proportional to carrier amplitude, it forms a convenient source of A.G.C. voltage for the I.F. stages of the receiver. There are disadvantages as well as advantages to controlling the R.F. valve as well. The disadvantages are that bias changes on the latter alter its input admittance and affect appreciably the damping and tuning of the aerial circuit. On the other hand, reduced output from the R.F. valve helps to prevent overloading of the frequency changer with increase of input voltage, and so reduces the possibility of spurious responses.

**15.8.3. The Negative Feedback A.G.C. Limiter.** The negative feedback A.G.C. limiter \* principle could be applied to reinforce the action of the saturated amplifier limiter. It only involves modification of the A.G.C. filter, so as to allow the A.F. components

\* Patent. R. C. A., P. F. G. Holst and L. R. Kirkwood (U.S. Application No. 441,254).

across the load resistance  $R_{36}$  in the saturated amplifier grid circuit to be passed back to the controlled valves with practically no phase shift or attenuation up to frequencies of about 5 kc/s. Decoupling capacitors  $C_{26}$ ,  $C_{34}$  and  $C_{40}$  in Fig. 15.7 must be decreased to about 50  $\mu\text{F}$ , which means a maximum phase shift of  $9^\circ$  and attenuation of  $-0.1$  db. at 5 kc/s. Attenuation at 4.5 Mc/s is 43.0 db. Should any tendency to I.F. instability appear, the decoupling capacitor  $C_{26}$  should be increased first, as this has the greatest amplification after it. Any tendency to instability can often be prevented by placing  $C_{26}$  and  $R_{18}$  inside the screening can of their associated I.F. transformer. R.F. chokes may be used in place of the filter resistances to give more R.F. attenuation, but care must be exercised to see that they are properly shielded from hum, noise or R.F. pick-up. When this form of limiting is used alone, the A.G.C. voltage must be derived prior to the last I.F. stage, which is itself supplied with A.G.C. bias. If there is no controlled I.F. stage after the A.G.C. detector, amplitude limiting cannot be fully effective because the final output voltage supplies the A.G.C. bias, which must increase with increase of input voltage. Control of an I.F. amplifier following the A.G.C. detector enables a flat or falling output-input voltage characteristic to be obtained by suitably proportioning the A.G.C. bias applied to this stage.

**15.8.4. The A.F. Neutralizing Limiter.** The neutralizing limiter \* applies the audio output from the F.M. receiver detector to the grid of a frequency changer or modulator valve such as the hexode shown in Fig. 15.11. This output consists of the desired A.F. content of the F.M. signal, amplitude modulated by noise, interference, or the selectivity characteristic of the I.F. amplifier tuned circuits. The initial undesired amplitude variation of the F.M. signal is separately detected and applied to the other grid in reverse phase to that of the undesired amplitude modulation of the desired audio output. The amplitude of the undesired audio input to the hexode grid is adjusted to neutralize or demodulate the undesired A.M. of the desired audio input. The output of the hexode valve  $V_1$  now contains the desired audio output (free from undesired amplitude modulation) and also the undesired audio output. The latter is removed by applying the hexode output to the grid of one valve ( $V_2$ ) of a pair with push-pull input and parallel output circuits. To the other valve ( $V_3$ ) grid is applied a proportion of the undesired audio signal, which is just sufficient to cancel the undesired signal appearing in the parallel anode circuit from  $V_2$ .

\* Patent. R. C. A. and M. G. Crosby (British Application No. 360/43).

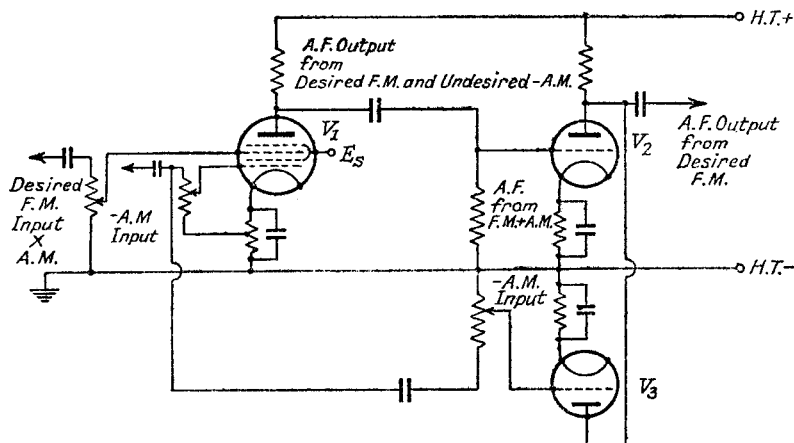


FIG. 15.11.—The A.F. Neutralizing Limiter.

## 15.9. The Frequency-Amplitude Converter.

**15.9.1. Introduction.** The chief difference between frequency and amplitude modulated reception lies in the method of making intelligible the A.F. signal conveyed in the modulation. There are two basic principles underlying methods of detecting frequency modulation, the more common system converts the frequency deviation into an amplitude change of carrier, and the resulting amplitude and frequency modulated signal is applied to an amplitude detector such as a diode. The latter is not responsive to the frequency variation and ignores it. The second method involves the use of an integrating device such as a valve charging or discharging a capacitor. The valve circuit may be of the super-regenerator, multivibrator or squegging oscillator type, and it is "triggered" by the I.F. input voltage. The duration (it must be much shorter than the period of the maximum I.F. frequency) and magnitude of the resulting pulse of current is determined solely by the valve and its associated circuit, i.e., it is practically independent of the amplitude of the "triggering" voltage. The number of pulses per second is, however, dependent on the intermediate frequency, and the mean current taken by the valve is therefore proportional to the I.F. The result at the output is an amplitude modulated signal, which is proportional to the original frequency modulation, and which can be detected by the normal methods.

We shall deal first with the frequency-amplitude converter type. The conversion must be accomplished in a linear manner, i.e., the

amplitude change is directly proportional to the frequency change, and it must be performed efficiently so that the resultant amplitude modulation is large. Many of the advantages of frequency modulation disappear if the frequency-amplitude conversion efficiency is low.

**15.9.2. The Amplitude Discriminator Converter.** One of the earliest methods<sup>1</sup> of frequency-to-amplitude conversion was to apply the F.M. signal to a circuit off-tuned from the carrier unmodulated value. For example, a parallel-tuned circuit, connected in the anode of a tetrode or pentode valve, produces an output voltage-frequency curve as shown in Fig. 15.12, when a constant-amplitude variable-frequency input voltage is applied. If this circuit is

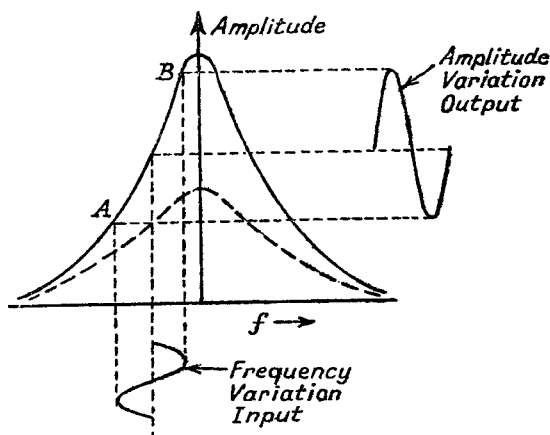


FIG. 15.12.—Frequency to Amplitude Conversion using the Selectivity Characteristics of a Parallel Tuned Circuit.

detuned (above or below) from the unmodulated carrier frequency, frequency modulation results in an output voltage of amplitude proportional to the frequency deviation of the carrier. It is, however, only linearly proportional if the carrier frequency deviation is confined to the approximately linear part *AB* of the curve, the centre of which occurs at a frequency, off-tune from the resonant frequency, of  $\Delta f = 0.375 \frac{f_r}{Q}$ . By applying the output voltage to an amplitude

detector, such as a diode, an A.F. signal, corresponding to the original signal modulating the carrier, is obtained. Although variation of frequency is occurring simultaneously with change of amplitude, only the latter is detected by the diode. Hence it is possible to receive and detect a F.M. transmission on an A.M. receiver provided the latter is off-tuned from the F.M. carrier unmodulated value. This method of detection is very inefficient, partly because it is



dependent on the slope of the output voltage-frequency curve, which for practical circuits is not very high, but mainly because the tuned circuit is operated in the detuned condition with consequent reduced overall amplification. Furthermore, full advantage cannot be taken of increased frequency deviation of the carrier, for the circuit must be damped (see the dotted curve in Fig. 15.12) to increase the linear part of the curve, and conversion efficiency is reduced.

A second method of frequency-amplitude conversion suppresses one set of sidebands. In Chapter I, Part I, a frequency modulated wave was shown to consist of a carrier vector (of frequency equal to the unmodulated value) and pairs of sidebands spaced  $\pm f_{mod.}$ ,  $\pm 2f_{mod.}$  etc., from the carrier, the odd numbered sideband pairs combining into a resultant vector at  $90^\circ$  to the carrier and the even pairs into

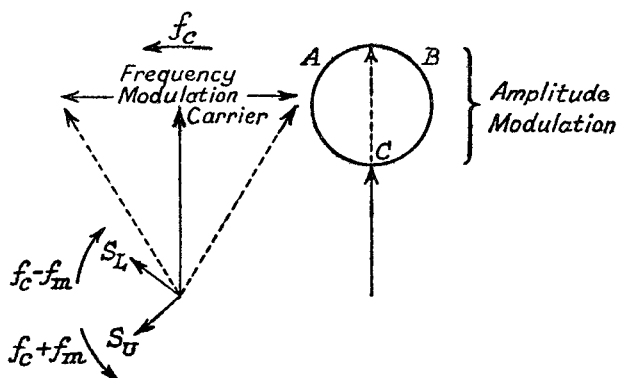


FIG. 15.13.—Frequency to Amplitude Conversion by Suppression of One of a Pair of Sidebands.

a resultant in line with the carrier. The addition of the first pair of sidebands ( $f_c \pm f_{mod.}$ ) to the carrier gives the frequency (and amplitude) modulated carrier of Fig. 15.13, and taking this as a basis we see that suppression of one of the sidebands results in the mainly amplitude modulated carrier vector, whose locus of operation is the circle  $ABC$ . The amplitude modulation is not directly proportional to the original modulation even when all sideband pairs are considered, and detection of the A.M. resultant by a diode produces a distorted A.F. output containing mostly second harmonic. The suppression of one-half of the sidebands is clearly inefficient since the transmitted energy in these is not being used. Both disadvantages may be overcome by applying the F.M. wave to two channels,<sup>4</sup> one having a filter suppressing the upper frequency sidebands and



and  $f_m$  = the mid frequency of the discriminator at which the d.c. output voltage is zero, i.e., it is the intermediate frequency.

Condition 15.5 is also that which gives maximum slope to the discriminator when  $\Delta f$  is fixed, and curve *ABODE* in Fig. 13.6a is therefore applicable to the frequency-amplitude converter. It is only necessary to change the frequency scale from 465 kc/s at 0 to 4.5 Mc/s, and 463 and 467 kc/s to 4.4 and 4.6 Mc/s to get the characteristic of a suitable frequency-amplitude converter for

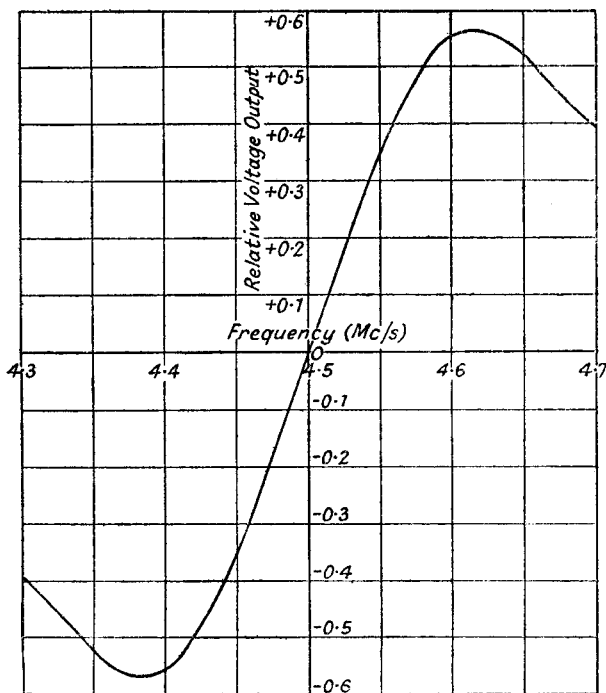


FIG. 15.15.—The Amplitude Discriminator Characteristic for Frequency-to-Amplitude Conversion.

$\Delta f = 100$  kc/s. This is done in Fig. 15.15. Calculation of the component values for the frequency-amplitude converter discriminator shown in Fig. 15.16 follows the lines set out in Section 13.4.2. The required average value of  $Q$  for the tuned circuits 1 and 2 is

$$Q = \frac{4.5}{0.2} = 22.5.$$

The maximum value of the resonant impedance of either circuit is limited by the anode-to-anode capacitance,  $C_{a12}$ , of the two diodes  $D_1$  and  $D_2$ , which forms a coupling between the two circuits.

Coupling is caused between the primaries by the anode-earth capacitance  $C_{aE}$  of the amplifier valve, and this sets a limit on the voltage transfer efficiency from primaries to secondaries. Assuming an anode-to-anode capacitance for the diodes of  $1 \mu\mu\text{F}$ , we have a coupling reactance between the circuits of  $35,400 \Omega$ , so that we cannot allow the resonant impedance of either tuned circuit to exceed about  $10,000 \Omega$ . In calculating the component values for

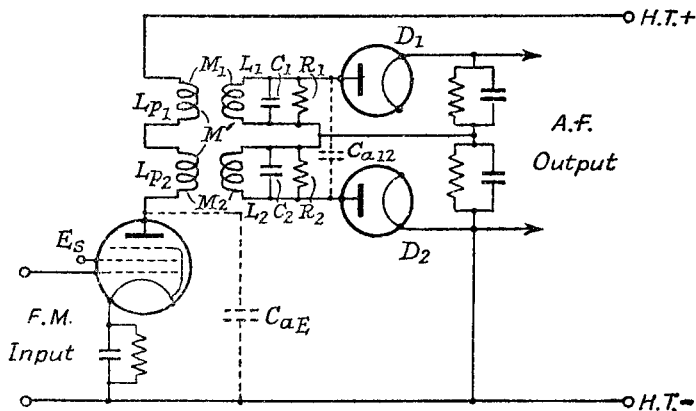


FIG. 15.16.—The Amplitude Discriminator as a Frequency-to-Amplitude Converter.

the circuits we shall take the mean frequency of  $4.5 \text{ Mc/s}$  and assume that the circuits are identical except for the values of  $C_1$  and  $C_2$ , which are adjustable for resonance at  $4.4$  and  $4.6 \text{ Mc/s}$ . Calculation of the damping resistances  $R_1$  and  $R_2$  is made on the assumption that the frequency is  $f_m$ . The error introduced is not very large and has little practical significance. Thus

$$L = L_1 = L_2 = \frac{R_D}{\omega_m Q} = \frac{10,000 \times 10^6}{6.28 \times 4.5 \times 10^6 \times 22.5} \\ = 15.7 \mu\text{H}.$$

$$C_1 = 83.2 \mu\mu\text{F} \quad (f_1 = 4.4 \text{ Mc/s})$$

$$C_2 = 76.0 \mu\mu\text{F} \quad (f_2 = 4.6 \text{ Mc/s}).$$

If the anode load resistances are  $0.1 \text{ M}\Omega$ , the damping due to conduction current is  $50,000 \Omega$ , so that the resonant impedance of the tuned circuit of initial  $Q = 150$  and excluding  $R_1$  is

$$R_D' = \frac{Q_0 \omega_m L \cdot 50,000}{Q_0 \omega_m L + 50,000} = \frac{66,500 \times 50,000}{116,500} = 28,600 \Omega.$$

$$\text{Hence } R_1 = \frac{28,600 \times 10,000}{18,600} = 15,350 \Omega.$$

The reactance of an anode-earth capacitance of  $15 \mu\mu\text{F}$  on the

primary side is  $2,360 \Omega$  at  $4.5 \text{ Mc/s}$ . The reflected resonant impedance across the primary is  $R_D \left(\frac{M}{L}\right)^2$ , and this must be much less than  $2,360 \Omega$ ; let us take a value of  $500 \Omega$ . Thus

$$\frac{M}{L} = \sqrt{0.05} = 0.2235$$

and

$$M = 3.51 \mu\text{H}.$$

A possible coupling coefficient  $k = \frac{M}{\sqrt{L_p L}} = 0.35$  is attainable, so that

$$L_p = 6.41 \mu\text{H}.$$

The resonant frequency of  $C_{aE}$  ( $15 \mu\mu\text{F}$ ) with the sum of the primary coil inductances,  $2L_p$ , is  $11.48 \text{ Mc/s}$ , which is sufficiently far away from the I.F. and the second and third harmonics of the I.F.

The slope of the frequency-amplitude conversion characteristic at the centre point  $O$  (Fig. 15.15) is given by twice expression 13.2 as

$$S(\text{max.}) = \frac{8 \cdot (22.5)^2 100}{(4.5 \times 10^3)^2 2^{\frac{3}{2}}} = 0.00707.$$

The slope of the characteristic  $O$  in volts per kc/s per 1 volt peak input is for  $g_m = 2 \text{ mA/volt}$  and  $\eta_a = 0.85$ .

$$\begin{aligned} S &= 0.00707 g_m R_D \frac{M}{L} \eta_a \\ &= 0.00707 \times 2 \times 10^{-3} \times 10^4 \times 0.2235 \times 0.85 \\ &= 0.0269 \text{ volts / kc/s off-tune / 1 volt peak input.} \end{aligned}$$

The stray capacitance coupling between the circuits can be neutralized by providing mutual inductance coupling between the coils. Cancellation is achieved by making

$$\frac{M'}{\sqrt{L_1 L_2}} = \frac{C_s}{\sqrt{C_1 C_2}}, \text{ i.e., } \frac{M'}{L} = \frac{C_s}{C_1},$$

where  $C_s$  is the total equivalent stray capacitance on the secondary side between the two tuned circuits. For cancellation  $M'$  should be in a positive direction (see Section 3.4.2, Part I); in a negative direction it adds to the coupling due to  $C_s$ .

**15.9.3. The Phase Discriminator Converter.**<sup>18</sup> Since the phase discriminator functions in a manner similar to the amplitude discriminator, converting a frequency into an amplitude change, it may be used as a frequency-to-amplitude converter in a F.M. receiver. The general behaviour of this discriminator has already been examined in Section 13.4.2, and the circuit diagram of Fig. 15.17 is very similar to that of Fig. 13.10. The valve feeding the dis-

criminator is assumed to be the limiter valve  $V_7$ . Resistances  $R_{37}$  and  $R_{40}$  are added across the primary and secondary of the phase discriminator in order to obtain the required pass-band width of  $\pm 100$  kc/s. The primary voltage is coupled to the centre-tap of the secondary through  $C_{52}$ , its voltage appearing across  $R_{41}$  and  $R_{42}$ , which are in parallel to the I.F. voltage. R.F. choke coupling ( $L_3$  in Fig. 13.10) is not used because the extra damping due to  $R_{41}$  and  $R_{42}$  being in parallel with the primary is still insufficient to give the band width, and an additional resistance  $R_{37}$  is required.

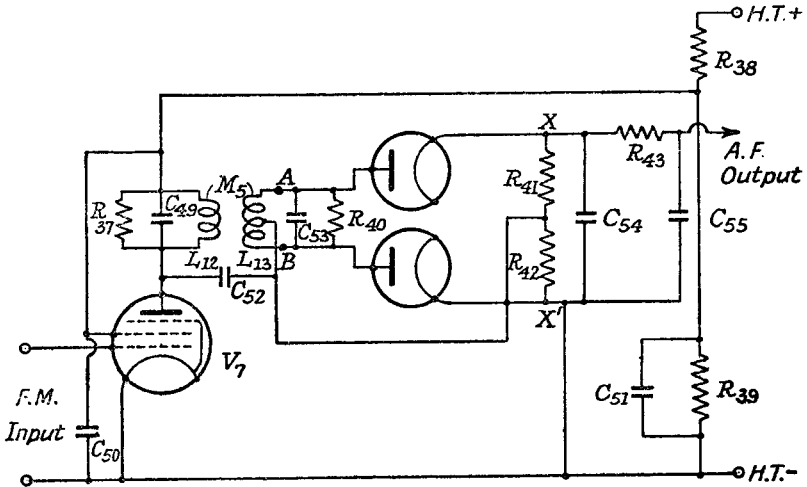


FIG. 15.17.—The Phase Discriminator as a Frequency-to-Amplitude Converter.

The characteristics required from the phase discriminator when it is to function as a converter are not exactly the same as those needed for A.F.C. purposes. Linearity of output voltage with change of frequency is all important, and maximum slope (the requirement for A.F.C.) must be sacrificed for this. To determine the shape of the characteristic and estimate the conditions for linearity of conversion over the desired pass-band range, we must turn to the fundamental equations for primary and secondary voltages set out in Section 13.4.2. These are, for the primary,

$$E_1 = g_m E_\sigma R_{D1} \frac{1 + jQ_2 F}{(1 + jQ_1 F)(1 + jQ_2 F) + Q_1 Q_2 k^2} \quad . \quad 15.6$$

and for the secondary

$$E_2 = g_m E_\sigma R_{D1} \frac{-jQ_2 k \sqrt{\frac{L_2}{L_1}}}{(1 + jQ_1 F)(1 + jQ_2 F) + Q_1 Q_2 k^2} \quad . \quad 15.7.$$

The total voltage applied to one diode is  $E_{AX} = E_1 - \frac{1}{2}E_2$  and to the other  $E_{BX'} = E_1 + \frac{1}{2}E_2$ , and the output voltage of the discriminator is the numerical difference between the amplitudes of  $E_{AX}$  and  $E_{BX'}$ , multiplied by the detection efficiency of the diodes, i.e.,

$$\begin{aligned} E_{XX'} &= \eta_d (|E_{AX}| - |E_{BX'}|) \\ &= \eta_d (|E_1 - \frac{1}{2}E_2| - |E_1 + \frac{1}{2}E_2|) . \end{aligned} \quad 15.8.$$

The secondary voltage can be rewritten in terms of  $E_1$  as

$$E_2 = E_1 \frac{-jQ_2k \sqrt{\frac{L_2}{L_1}}}{(1 + jQ_2F)} . \quad 15.9$$

so that

$$E_{AX} = E_1 \left[ 1 + \frac{jQ_2k \sqrt{\frac{L_2}{L_1}}}{2(1 + jQ_2F)} \right] = E_1 \left[ 1 + \frac{jQ_2k \sqrt{\frac{L_2}{L_1}}(1 - jQ_2F)}{2[1 + (Q_2F)^2]} \right]$$

$$\text{or} \quad \frac{E_{AX}}{E_1} = 1 + \frac{\alpha Q_2F}{2[1 + (Q_2F)^2]} - \frac{j\alpha}{2[1 + (Q_2F)^2]} \quad 15.10$$

where  $\alpha = \frac{E_2}{E_1} = Q_2k \sqrt{\frac{L_2}{L_1}}$  at  $F = 0$ , i.e., at the mid frequency  $f_m$ .

$$\therefore \frac{|E_{AX}|}{|E_1|} = \sqrt{\left[ 1 + \frac{\alpha Q_2F}{2[1 + (Q_2F)^2]} \right]^2 + \frac{\alpha^2}{4[1 + (Q_2F)^2]^2}} \quad 15.11a$$

$$\text{and} \quad \frac{|E_{BX'}|}{|E_1|} = \sqrt{\left[ 1 - \frac{\alpha Q_2F}{2[1 + (Q_2F)^2]} \right]^2 + \frac{\alpha^2}{4[1 + (Q_2F)^2]^2}} \quad 15.11b.$$

The vector relationship represented by expression 15.9 is shown in Fig. 13.11, and the variation in the length of  $\frac{|E_{AX}|}{|E_1|}$  can be measured from this figure for different values of  $Q_2F$  and selected values of  $\alpha$ , or alternatively it may be calculated from expres-

sion 15.11a.  $\frac{|E_{BX'}|}{|E_1|}$  can be found in a similar manner, and sub-

tracting it from  $\frac{|E_{AX}|}{|E_1|}$  gives the relative voltage output from the

discriminator if  $|E_1|$  has a constant amplitude. The relative voltage output is plotted in Fig. 15.18a over a range of  $Q_2F$  from 0 to +2 (the other half of the curve from  $Q_2F = 0$  to -2 is the same shape inverted) for  $\frac{E_2}{E_1} = 1, 2, 3, 4$  and 6. The most noticeable

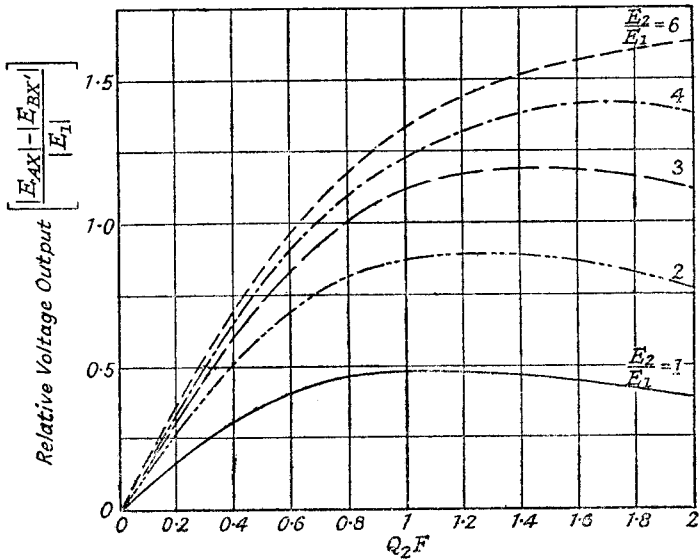


FIG. 15.18a.—The Variation of Phase Discriminator Output Voltage Against Frequency Off-tune from the Resonant Frequency. Primary Voltage is assumed constant.

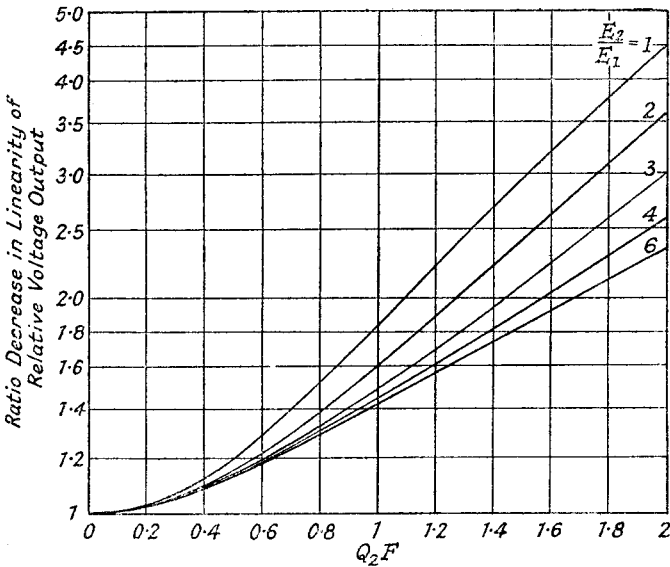


FIG. 15.18b.—Ratio Decrease of Linearity of Phase Discriminator Output Voltage against Off-tune Frequency. Primary Voltage assumed constant.



effect is that maximum output occurs at a large value of  $Q_2F$  as  $\frac{E_2}{E_1}$  is increased, and none of the curves is truly linear. A second set of curves is drawn in Fig. 15.18*b* to show the departure from linearity, which is expressed in the form of ten times the ratio of the relative voltage output at a particular  $Q_2F$  to the voltage output at  $Q_2F = 0.1$  multiplied by the particular value of  $Q_2F$  being considered. We see from Fig. 15.18*b* that the general tendency is for the curve to become more linear as  $\frac{E_2}{E_1}$  is increased, though there is not much difference between the curve for  $\frac{E_2}{E_1} = 4$  and that for  $\frac{E_2}{E_1} = 6$ .

The divergence of these curves from the required straight line characteristic can be offset if  $E_1$  can be made to increase with increase of  $Q_2F$ , and this is possible by a suitable choice of coupling between the secondary and primary. If we assume that  $Q_1 = Q_2$  a series of curves of the ratio increase of  $E_1$  upon its value at  $f_m (F = 0)$  can be plotted against  $QF$  for different values of the coupling factor  $Qk$ . The problem is greatly complicated if  $Q_1$  and  $Q_2$  are not equal, because a separate set of curves must be drawn for each value of  $Q_1$  and  $Q_2$ , and there is seldom any practical advantage to be gained by making them unequal. The ratio increase of  $E_1$  with increase of  $QF$  is, from expression 15.6,

$$\frac{|E_1|}{|E_1|_{F=0}} = \frac{[\sqrt{1+(QF)^2}][1+Q^2k^2]}{\sqrt{[1+Q^2(k^2-F^2)]^2+4Q^2F^2}} \quad . \quad 15.12$$

and it is plotted in Fig. 15.19 as a series of curves for selected values of  $Qk$ . To find the most suitable value of  $Qk$  for compensating the ratio decrease of Fig. 15.18*b*, the curves of Fig. 15.19 should be drawn on transparent paper and placed on top of those of Fig. 15.18*b*. Any two curves which then coincide will give the conditions for a linear characteristic over the range of  $QF$  for which they are coincident. Greatest range of  $QF$  over which a linear characteristic is obtained is from 0 to 1 with  $\frac{E_2}{E_1} = 2$  and  $Qk = 2$ . The resultant characteristic is linear up to  $QF = 0.8$  and falls away slightly at  $QF = 1$  where the output is about 2% low. A slightly lower value of  $Qk$  could be chosen with some reduction of the linear range of  $QF$ , and this has the advantage of giving a higher frequency-

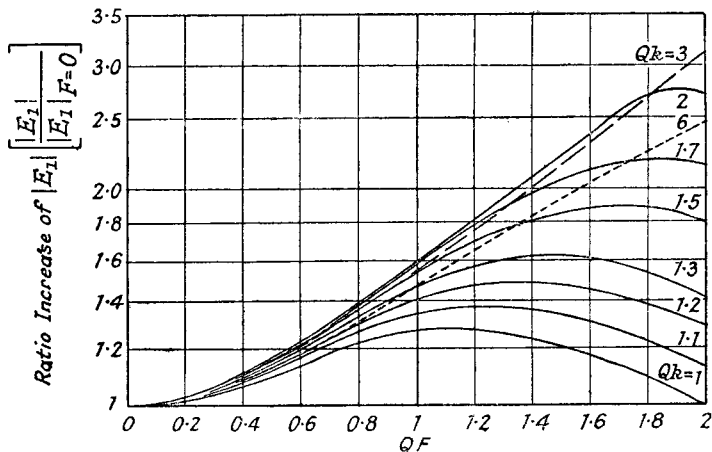


FIG. 15.19.—The Ratio Increase of Primary Voltage against Off-tune Frequency for the Phase Discriminator.

to-amplitude conversion efficiency. Thus for  $Qk = 1.5$ ,  $\frac{E_2}{E_1} = 2$ , the linear range of  $QF$  is reduced to approximately  $QF = 0$  to  $0.8$ , but conversion efficiency (expression 15.13) is increased in the ratio

$$\frac{1 + (Qk)^2}{1 + (Q_1 k_1)^2} = \frac{5}{3.25} = 1.535,$$

provided  $R_{D1}$  is unchanged. The relative voltage output- $QF$  characteristics for the two values of  $Qk$ ,  $1.5$  and  $2$ , are shown in Fig. 15.20. The peak of the characteristic for  $Qk = 1.5$  occurs at a much lower value of  $QF$  ( $1.5$ ) than that ( $1.9$ ) for  $Qk = 2$ , and this, coupled with its higher frequency-amplitude conversion efficiency, suggests the smaller value of  $Qk$  to be the better practical proposition, in spite of the reduced linear range of  $QF$ . It is interesting to note that  $Qk = 2$  gives the maximum possible correction over the useful range of  $QF$ , and a linear characteristic cannot be obtained for values of  $\frac{E_2}{E_1}$ , which correspond to curves on Fig. 15.18*b*, having a greater reduction than the correction produced by the curve for  $Qk = 2$  of Fig. 15.19. Thus a linear characteristic is unobtainable for values of  $\frac{E_2}{E_1} < 2$ . Correction is possible for higher values of  $\frac{E_2}{E_1}$  than  $2$ ; lower values of  $Qk$  are required and the linear range of  $QF$  is reduced, e.g.,  $\frac{E_2}{E_1} = 3$  requires  $Qk$  to be  $1.25$  and a linear range is obtained from  $QF = 0$  to  $0.85$ .

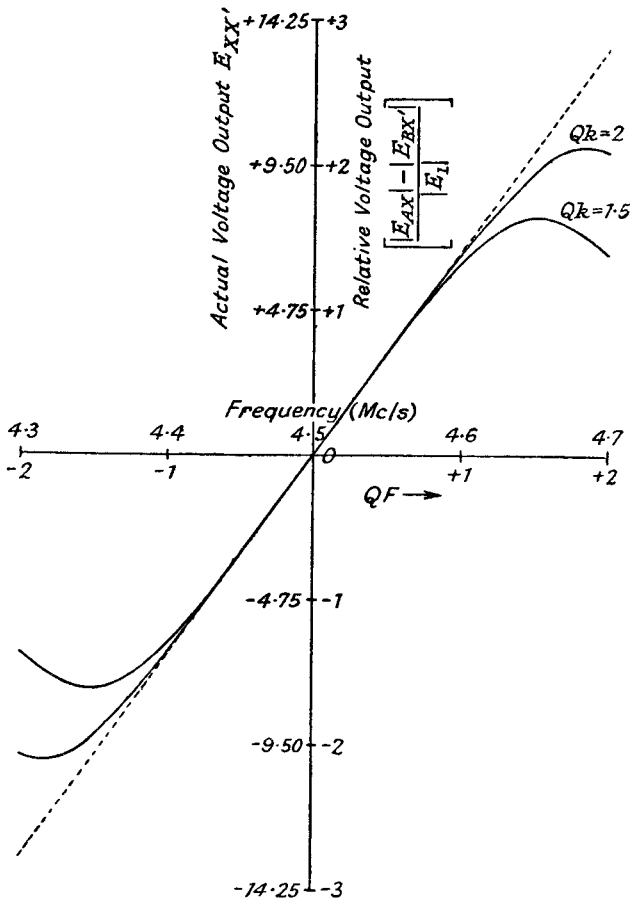


FIG. 15.20.—The Relative Voltage Output— $QF$  Characteristic of a Phase Discriminator for  $\frac{E_2}{E_1} = 2$  and  $Qk = 1.5$  and 2.

To illustrate design features the following constants are assumed :

$$f_m = 4.5 \text{ Mc/s, carrier frequency deviation} = \pm 75 \text{ kc/s,}$$

$$\frac{E_2}{E_1} = 2, Qk = 1.5,$$

hence

$$\frac{L_2}{L_1} = 1.77.$$

Taking  $QF = 1$  at  $\Delta f = 100 \text{ kc/s}$  allows the carrier frequency deviation of  $\pm 75 \text{ kc/s}$  to be accommodated on the linear part of the characteristic ; and this gives

$$Q = \frac{f_m}{2\Delta f} = \frac{4.5}{0.2} = 22.5$$

and

$$k = \frac{1.5}{Q} = 0.067.$$

In Section 13.4.2, expression 13.8 for the slope of the characteristic at  $O$  (Fig. 15.15), or the sensitivity of frequency-amplitude conversion at  $f_m(F = 0)$ , is

$$\begin{aligned} S_{(F=0)} &= 2g_m R_{D1} \eta_a E_{g1} \frac{Q_2^2 k \sqrt{\frac{L_2}{L_1}}}{f_m (1 + Q_1 Q_2 k^2) \left(1 + \frac{Q_2^2 k^2 L_2}{4L_1}\right)^{\frac{1}{2}}} \quad . \quad 15.13 \\ &= g_m R_{D1} \eta_a E_{g1} \frac{2 \times 22.5 \times 2}{4.5 \times 10^3 \times 3.25 \times \sqrt{2}} \\ &= 4.35 \times 10^{-3} g_m R_{D1} \eta_a E_{g1} \text{ volts per kc/s.} \end{aligned}$$

Maximum sensitivity is clearly obtained when  $R_{D1}$  is as large as possible, and this means the highest possible value of  $L_1$ , which in turn is limited by the maximum practicable value of  $L_2$ . The latter is determined by the minimum permissible value of secondary tuning capacitance, which we shall assume to be  $50 \mu\mu\text{F}$ . Thus referring to Fig. 15.17

$$C_{53} = 50 \mu\mu\text{F}, \quad L_{13} = 25 \mu\text{H}$$

$$L_{13} = \frac{L_{13}}{1.77} = 14.1 \mu\text{H} \text{ and } C_{49} = 88.5 \mu\mu\text{F}.$$

The higher value of primary capacitance,  $C_{49}$ , is an advantage because the stray capacitance, e.g., across  $R_{41}$  and  $R_{42}$ , is greater than across the secondary.

$$\begin{aligned} R_{D1} &= \omega_m L_{13} Q = 6.28 \times 4.5 \times 14.1 \times 22.5 \\ &= 9,000 \Omega. \end{aligned}$$

If  $g_m = 2 \text{ mA/volt}$  and  $\eta_a = 0.85$ , the sensitivity of frequency-amplitude conversion is

$$\begin{aligned} S_{(F=0)} &= 4.35 \times 10^{-3} \times 2 \times 10^{-3} \times 9,000 \times 0.85 \times 1 \\ &= 0.0665 \text{ volts per kc/s per 1 volt input at the grid of } V_7. \end{aligned}$$

The output voltage ( $E_{XX'}$ )-frequency characteristic of the discriminator is obtained by multiplying the vertical scale of Fig. 15.20 by 4.75, i.e., using the left-hand scale, and converting the  $QF$  scale to a frequency scale by noting that  $f = 4.5 \text{ Mc/s}$  at  $QF = 0$  and 4.4 and 4.6 Mc/s at  $QF = -1$  and  $+1$  respectively.

The damping resistances  $R_{37}$  and  $R_{40}$  in Fig. 15.17 have next to

be calculated. If the diode load resistances  $R_{41}$  and  $R_{42}$  are  $0.1 \text{ M}\Omega$ , the primary circuit is damped by these two in parallel ( $0.05 \text{ M}\Omega$ ) and also by the two diode conduction currents, which are equivalent to two  $0.05 \text{ M}\Omega$  in parallel, i.e.,  $0.025 \text{ M}\Omega$ . Hence the total damping resistance across the primary, apart from  $R_{37}$ , is equal to  $0.05 \text{ M}\Omega$  in parallel with  $0.025 \text{ M}\Omega$ , viz.,  $16,666 \Omega$ . If the initial  $Q_0$  of the coil is 150, the total damping resistance necessary to reduce this to 22.5 is

$$R_{tp} = \frac{\omega_m L_{12} Q_0 Q}{Q_0 - Q} = \frac{6.28 \times 4.5 \times 14.1 \times 150 \times 22.5}{127.5} \\ = 10,600 \Omega$$

$$\text{so that } R_{37} = \frac{16,666 \times 10,600}{6,066} = 29,200 \Omega.$$

For the secondary side

$$R_{ts} = \frac{\omega_m L_{13} Q_0 Q}{Q_0 - Q} = 18,800 \Omega$$

of which the damping resistance due to detection is that from the conduction resistances in series, i.e.,  $0.1 \text{ M}\Omega$ . Hence

$$R_{40} = \frac{100,000 \times 18,800}{81,200} = 23,100 \Omega.$$

The coupling capacitor  $C_{52}$  in Fig. 15.17 is  $100 \mu\mu\text{F}$ , the R.F. by-pass capacitor  $C_{54}$  is  $50 \mu\mu\text{F}$  and in the R.F. filter before the A.F. amplifier  $R_{43} = 0.2 \text{ M}\Omega$  and  $C_{55} = 100 \mu\mu\text{F}$ . The mutual inductance coupling  $M_s$  between  $L_{12}$  and  $L_{13}$  is  $k\sqrt{L_{12}L_{13}} = 1.255 \mu\text{H}$  ( $k = 0.067$ ).

Correct tuning and adjustment of the phase discriminator is best carried out in the manner described in Section 13.4.2. The primary and secondary, with  $C_{52}$  disconnected and coupling less than critical ( $Qk < 1$ ), are tuned for maximum voltage across either one of the diode load resistances,  $R_{41}$  and  $R_{42}$ , when the input frequency is  $4.5 \text{ Mc/s}$ .  $C_{52}$  is now connected and the primary re-tuned for equal positive and negative D.C. voltage peaks across the two load resistances (points  $XX'$  in Fig. 15.17) at approximately equal off-tune frequencies from  $4.5 \text{ Mc/s}$ . The secondary is next tuned to produce zero D.C. voltage across  $XX'$  at  $4.5 \text{ Mc/s}$ . Finally, the mutual inductance coupling  $M_s$  is increased until the equal positive and negative D.C. voltage peaks occur at  $4.65$  and  $4.35 \text{ Mc/s}$ . ( $QF = 1.5$  from Fig. 15.20.) The required linear characteristic should then be obtained.

The effect of primary and secondary mistuning on the discriminator characteristic has already been discussed in Section 13.4.2.

Variations of  $M_s$ , i.e.,  $Qk$ , cause the characteristic to pass through the phases illustrated by curves 1, 2 and 3 in Fig. 15.21. Curve 1 is obtained when  $M_s$  is too small, the linear range of  $QF$  is restricted and the peaks are close to off-tune frequencies corresponding to  $QF = 1$ . Curve 2 illustrates the case for the correct value of  $M_s$ , i.e.,  $Qk = 1.5$ , while curve 3 shows how linearity is lost by increasing  $M_s$  beyond its optimum value, a double S-shaped characteristic

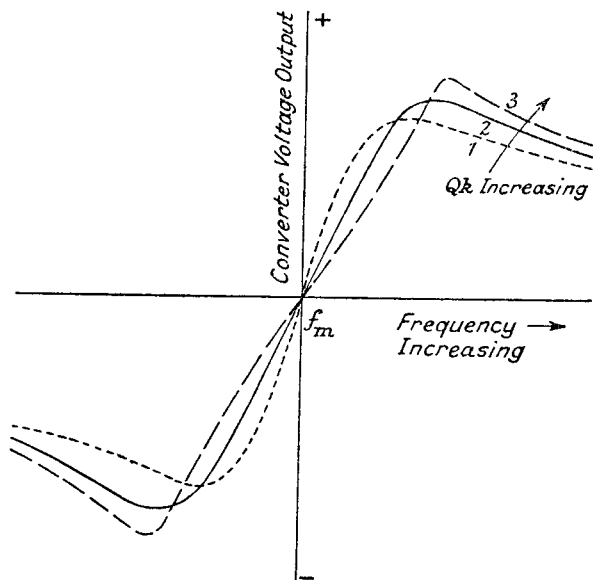


FIG. 15.21.—The Effect of increasing Mutual Inductance between Primary and Secondary of the Phase Discriminator.

- Curve 1:  $M$  too small.  
 Curve 2:  $M$  correct for maximum linearity.  
 Curve 3:  $M$  too large.

being obtained. As  $M_s$  is increased the positive and negative peaks continue to increase in amplitude.

**15.9.4. The Integrating Converter.** The integrating frequency-amplitude converter, which also acts as a limiter, may consist of a regenerative amplifier, a multivibrator, or a squegger oscillator, the operation of which is controlled or triggered by the intermediate frequency. All these circuits tend to produce short sharp pulses of current, the duration and amplitude of which are dependent on the circuit constants and are practically independent of the amplitude of the triggering voltage. The number of pulses produced are controlled by, and are directly proportional to, the frequency of the latter. The mean current value of these pulses is proportional

to the intermediate frequency so that the mean current amplitude varies in accordance with the frequency deviation of the I.F. carrier and reproduces the A.F. content of the latter.

An example of the regenerative\* type is shown in Fig. 15.22. Two pentode valves (hexodes may equally well be employed) are used in push-pull, and regeneration is applied to one grid from the anode of the opposite valve by means of the potential divider resistances  $R_2$  and  $R_3$ .  $C_1$  is a coupling capacitance of fairly high value ( $0.001 \mu\text{F}$ ) for isolating the D.C. voltage. Regeneration is critically adjusted so that the stage is very susceptible to small changes of voltage on the suppressor grids. A slight positive increase in voltage causes one valve to take a high value of anode

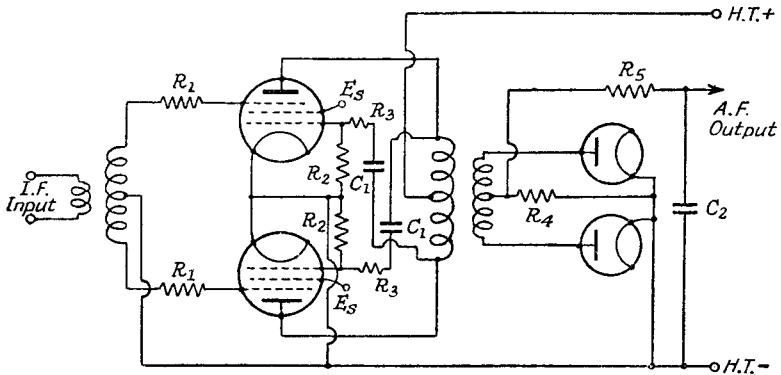


FIG. 15.22.—A Regenerator Type of Integrating Frequency-to-Amplitude Converter.

current and the other to take a small value. A large pulse of current therefore flows through the primary of the centre-tapped transformer connected to the anodes of the valves. The rate of rise and fall of anode current is very rapid and is determined solely by the regenerative circuit (the natural frequency of the primary inductance and stray capacitance is much higher than the highest intermediate frequency), so that the wave form (width and amplitude) of the current pulse is independent of the I.F. The number of pulses per second is, however, proportional to the I.F., occurring twice per cycle of the I.F. Provided the amplitude of the I.F. signal exceeds a certain minimum value, variation of amplitude has no effect, and the stage acts as an amplitude limiter. Resistances  $R_1$  in the input grid circuit help in attaining this condition by "squaring" the tops of the I.F. signal with the aid of grid current. A double-

\* Patent. R. C. A. and C. W. Hansell (British Application No. 8324/42).

diode full-wave detector is used across the secondary of the transformer in order to abstract the mean voltage variations from the A.C. voltage pulses appearing across the secondary. The mean variation of the pulse from each valve cannot be transferred through the transformer, but must be abstracted by subsequent detection. The detector must not be allowed to operate with a reservoir capacitance across its load resistance, as for an amplitude modulated signal, otherwise the capacitance fills in the gaps between the pulses (see Section 8.2.1, Part I) and there is no mean voltage variation. A resistance load is satisfactory without the reservoir capacitance as the half-wave voltage pulses appearing across it are of substantially the same shape as the section of the applied voltage wave which is producing them. Half-wave detection could be employed using the whole of the secondary as a voltage source, but it is no more efficient as regards A.F. output from a given I.F. deviation, and has the disadvantage of a large R.F. fundamental component (twice that for full-wave). This is different from the case of amplitude modulation for which half-wave detection normally gives an A.F. voltage output approximately twice that for full-wave.  $R_5$  and  $C_2$  form an R.F. filter between the load resistance  $R_4$  and the first A.F. valve.

The regenerator of Fig. 15.22 may be replaced by a multivibrator, or a squegger oscillator. The squegger or blocking oscillator, shown in Fig. 15.23, has very tight coupling between its regenerator

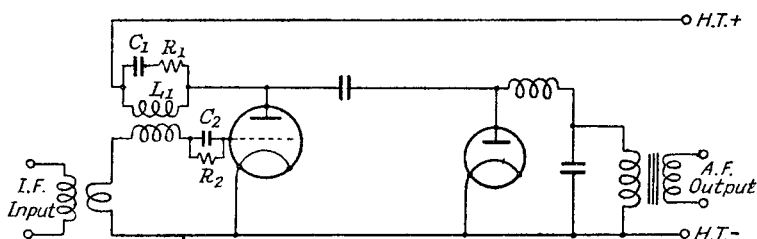


FIG. 15.23.—The Blocking Oscillator Integrator Converter.

oil and tuned circuit. Oscillation, when it occurs, is so violent that a very large pulse of grid current results and charges the capacitance  $C_2$  to a negative voltage many times greater than the cut-off bias voltage. Oscillation ceases and only recommences after  $C_2$  has discharged itself through  $R_2$  to a negative voltage sufficiently small to allow oscillations to begin again. If the tuned anode is sufficiently damped—this is the function of  $R_1$  in series with the tuning capacitance  $C_1$ —oscillations in the tuned circuit die away rapidly and there is only a single anode current pulse of short duration. The



actual period of the pulse is usually rather less than half a cycle of the normal oscillation frequency of  $L_1C_1$ , and is much less than the period of the maximum frequency of the triggering voltage. On the other hand, the time constant of the circuit  $R_2C_2$  must be greater than the period of the minimum I.F., so that the latter can trigger the valve satisfactorily. The amplitude and duration of the anode current pulse depends on the circuit constants, and above a certain value of triggering voltage is independent of the amplitude of the latter. The mean anode current taken by the oscillator is proportional to the number of pulses, which in turn is proportional to the intermediate frequency, and the A.F. content of the I.F. signal could be obtained across a resistance placed between the tuned circuit  $L_1C_1$  and H.T. positive. A capacitance of about 100  $\mu\mu\text{F}$  would be required across the resistance to by-pass radio frequencies. Alternatively the mean value can be abstracted from the pulses by means of the diode as shown in Fig. 15.23.

Another method of producing pulses of almost constant duration and amplitude, but of number proportional to the I.F., is by means of a hexode valve, to the control and oscillator grids of which antiphase ( $180^\circ$ ) voltages are applied. The bias on the grids is adjusted so that anode current flows when there is no I.F. signal, but is quickly cut off by a differential change of voltage on the grids. Hence a short pulse of anode current occurs every half-cycle of the I.F. as the instantaneous amplitude approaches and passes through zero. There is a change in pulse width with change in I.F. amplitude and this type is less satisfactory as an amplitude limiter.

**15.9.5. The Counter Type of F.M. Detector.** Detection of a F.M. signal can be accomplished by using the "counter" type of detector\* shown in Fig. 15.24. For the "counter" action to be satisfactory, the I.F. must have a comparatively low value, about 200 kc/s is usually chosen so that the lowest modulation frequency components (125 kc/s) are sufficiently far removed from the A.F. range of frequencies. This low I.F. necessitates double frequency changing in order to avoid image and undesired responses. The last I.F. amplifier following the limiter stage has a resistance,  $R_1$ , instead of a tuned circuit in its anode. It is biased by grid current and has low anode and screen voltages in order to "square" the top and bottom of the F.M. output signal. Capacitance  $C_1$ , initially charged by  $D_1$  to the maximum positive square top voltage, discharges to the minimum squared voltage through  $R_1$  and  $R_2$ , pro-

\* Patent. R. C. A. and W. Van B. Roberts (British Application No. 4019/42).

ducing across the latter a negative pulse, the duration of which is adjusted to be much less than the period of the maximum F.M. signal frequency. The number of these pulses and their mean value are proportional to the F.M. signal frequency and therefore to its modulation content. Hence a mean voltage variation proportional to the frequency deviation of the I.F. appears across diode  $D_2$  and is passed on to the A.F. amplifier.  $R_3$  forms with diode  $D_2$  a positive

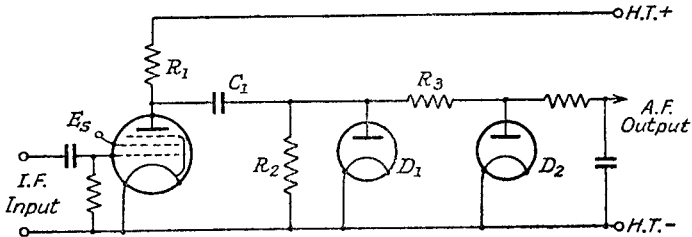


FIG. 15.24.—The Counter Type Frequency-to-Amplitude Converter.

pulse suppressor, which prevents the positive charging voltage pulse across  $D_1$  being passed on to the A.F. amplifier.

#### 15.9.6. The Hexode Frequency-to-Amplitude Converter.

The property of electron collection possessed by the signal grid of the hexode valve (see Section 5.8.2, Part I), as the frequency of the oscillator voltage is increased, has been suggested\* as a means of converting F.M. into an A.F. signal. The F.M. signal is applied to the oscillator grid, and a grid leak resistance ( $0.5\text{ M}\Omega$ ) and capacitance ( $50\ \mu\mu\text{F}$ ) are connected in parallel between control grid and cathode. A resistance anode load (R.F. is by-passed by a capacitance of about  $50\ \mu\mu\text{F}$ ) is used. It is found that under suitable conditions a linear variation of grid voltage of about 0.8 volts is obtained when the signal frequency is varied from 15 to 25 Mc/s. This grid voltage variation is amplified by the valve, and the resultant A.F. appearing across the anode circuit resistance is passed on to the A.F. amplifier. The chief disadvantage of the method is the high input signal frequency required and the low conversion efficiency.

### 15.10. Methods of Frequency Modulation Compression in the Receiver.

**15.10.1. Introduction.** The use of wide-band frequency modulation has certain disadvantages from the point of view of receiver design. It is not possible to use the same I.F. transformers for high fidelity amplitude modulation—the wide pass-band admits

\* Patent. R. C. A. and F. B. Stone (British Application No. 12097/42).

undesired noise components from outside the required pass range, and selectivity is inadequate—so that a receiver designed for dual operation must have two separate sets of I.F. transformer. If, however, the original frequency deviation of the F.M. signal could be compressed in the receiver from  $\pm 75$  kc/s to  $\pm 15$  kc/s, conversion to amplitude modulated reception would only involve a simple switching operation at the detector stage, the same transformers and I.F. amplifier circuits being used for both types of modulation. The phase discriminator stage is converted for A.M. detection by connecting the cathodes of the diodes together and taking the output for the A.F. amplifier from the centre point of the diode load resistances as shown in Fig. 15.25. The band width cannot be reduced below about  $\pm 15$  kc/s, otherwise both frequency and amplitude modulation suffer from attenuation distortion of the upper audio frequencies, and high fidelity is not possible. Advantages other than that of dual operation are gained by compressing the frequency-modulated deviation; the lower value of I.F. that is possible gives greater gain per stage and is more stable; the method of compression generally has a limiting action on any amplitude modulation so that a separate limiter stage (with, usually, loss of amplification) is not necessary. The reduction in modulation due to compression is largely offset by the increased sensitivity of the frequency-amplitude converter discriminator made possible by the reduced band width required.

There are various methods of compressing the frequency deviation. One uses a variable reactance valve, operated from the A.F. output signal from the receiver, to frequency-modulate the local oscillator and cause its frequency to follow the frequency deviations of the input signal. For example, suppose the input carrier is frequency modulated  $\pm 75$  kc/s, ranging from 45.075 to 44.925 Mc/s, the local oscillator frequency is frequency modulated to vary from 45.525 to 45.405 Mc/s (or 44.595 to 44.475) so that the resultant I.F. carrier is 465 kc/s, frequency modulated  $\pm 15$  kc/s. Another method uses a frequency divider to produce the I.F. carrier and at the same time reduce the frequency deviation. A third system employs an oscillator operating at a submultiple of the input signal and locked by it. The original frequency deviation is reduced in the ratio of the submultiple to the input frequency.

**15.10.2. Compression by Frequency Modulation of the Local Oscillator.**<sup>5, 6, 15</sup> A block schematic diagram of the apparatus is shown in Fig. 15.25. The variable reactance valve may be used to correct for slow as well as rapid changes of frequency by

applying to it D.C. bias as well as A.F. voltage from the output of the discriminator; the resistance  $R_2$  and capacitance  $C_2$  ( $0.1 \text{ M}\Omega$  and  $50 \mu\mu\text{F}$ ) in the diagram form a R.F. filter. This is an important point because harmonic distortion of the A.F. output tends to occur at high output levels if the frequency deviation is not centred correctly in the frequency-amplitude converter discriminator characteristic. Amplitude limiting results because the magnitude of the reactance variation of the reactance valve is dependent on the amplitude as well as the frequency of the input signal to the discriminator. Thus an initial amplitude variation of the input signal to the latter is applied to the reactance valve to frequency-modulate the local oscillator and produce an A.F. output at the discriminator

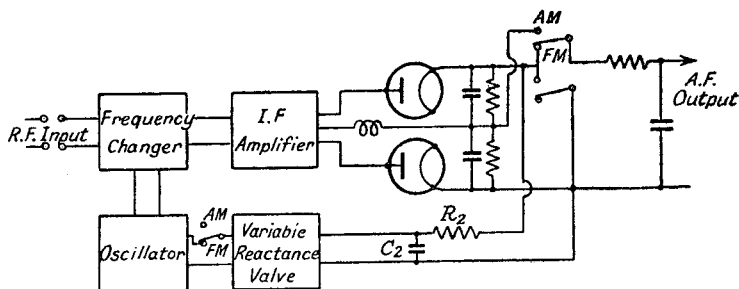


FIG. 15.25.—Frequency Deviation Compression by Frequency Modulation of the Receiver Oscillator.

$180^\circ$  out of phase with the A.F. output due to the initial amplitude modulation. The overall performance of the apparatus as regards signal-to-noise ratio is comparable with that of the wide-band amplifier with a saturated amplifier limiter. This type of compressor, which is an example of the negative feedback principle, possesses the advantage of reducing distortion, hum and interference produced in the I.F. amplifier.

For conversion to amplitude-modulated reception the switch is moved to position A.M. and the variable reactance valve is disconnected.

**15.10.3. The Frequency Divider Compressor.** The principle of frequency division\* can be applied in the F.M. receiver to compress the frequency deviation, and a circuit diagram is shown in Fig. 15.26. The input frequency,  $13 \text{ Mc/s}$ , modulated  $\pm 75 \text{ kc/s}$ , is obtained from an I.F. amplifier following the first frequency changer. This initial change of frequency is essential since a fair

\* Patent. R. C. A. and M. G. Crosby (U.S. Application No. 430,348).

degree of selectivity is necessary before the frequency divider stage, which has less adjacent channel selectivity than the normal frequency changer stage. The 13 Mc/s input is applied to two frequency changer valves. The first ( $V_1$ ) has an anode circuit tuned to the required I.F., e.g., 4.5 Mc/s, and its output is applied to the second I.F. amplifier and to the second frequency changer valve  $V_2$ . The anode circuit of  $V_2$  is tuned to the sum frequency of the two intermediate frequencies, i.e.,  $13 + 4.5 = 17.5$  Mc/s, and the output from this is connected to the other grid of the valve  $V_1$ , in which it reacts with the original 13 Mc/s to produce a difference frequency of

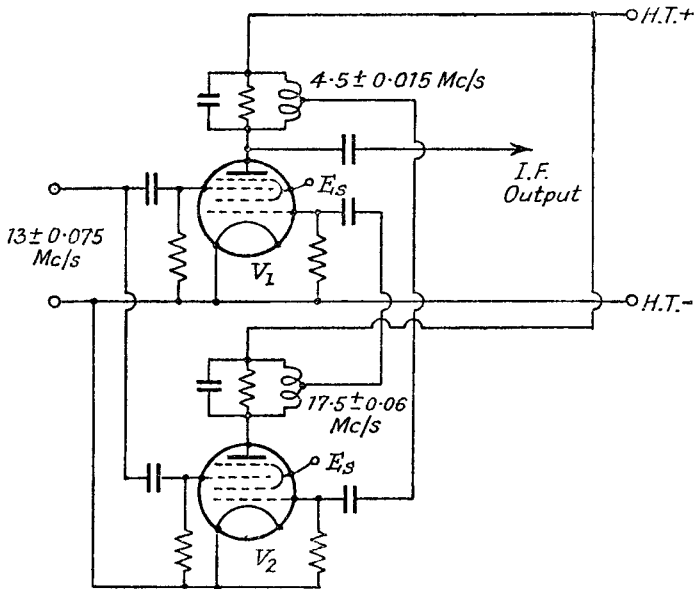


FIG. 15.26.—An Example of the Frequency Divider F.M. Compressor.

4.5 Mc/s. The extent of F.M. compression of the 4.5 Mc/s output depends on the relative selectivities of the 4.5 and 17.5 Mc/s tuned anode circuits. Equal selectivities divide the frequency deviation in equal proportions between the two frequencies, i.e.,  $4.5 \pm 0.0375$  and  $17.5 \pm 0.0375$  Mc/s, and the degree of compression is conveniently controlled by varying the selectivity of the 17.5 Mc/s circuit. Thus, if that of the latter is reduced to one-quarter of the 4.5 Mc/s circuit, the output frequency is 4.5 Mc/s modulated  $\pm 15$  kc/s. It is interesting to note that the 4.5 and 17.5 Mc/s frequencies are only generated when there is an input signal, and they disappear when it is zero. The reason for this is that the slightest shock

excitation of the 4.5 Mc/s and 17.5 Mc/s anode circuits, due to noise or switching on the 13 Mc/s signal, causes voltage components of these frequencies to appear in the circuits, and the process is self-sustaining as long as there is an input signal. The frequency divider stage has less adjacent channel selectivity than the normal frequency changer because the lower selectivity of the 17.5 Mc/s tuned circuit permits the sum frequency to be self-adjusting to a fairly wide range of input frequencies. Thus a 12 Mc/s input frequency shock-excites the 4.5 Mc/s circuit to produce a sum frequency in the anode circuit of  $V_2$  of 16.5 Mc/s so that the second I.F. amplifier offers no selectivity against this undesired frequency. This type of compressor also acts as a limiter and is capable of smoothing out wide variations of input signal amplitude.

**15.10.4. Frequency Compression by Submultiple Locked Oscillator.** A method of compressing frequency modulation by means of a locked oscillator operating at a submultiple\* of the I.F. has been developed, e.g., an I.F. of 4.5 Mc/s modulated  $\pm 75$  kc/s can be used to lock a submultiple oscillator of 0.9 Mc/s, the frequency modulation of which is reduced in the ratio of the fundamental frequency reduction of  $\frac{1}{5}$  to  $\pm 15$  kc/s. A circuit diagram of the

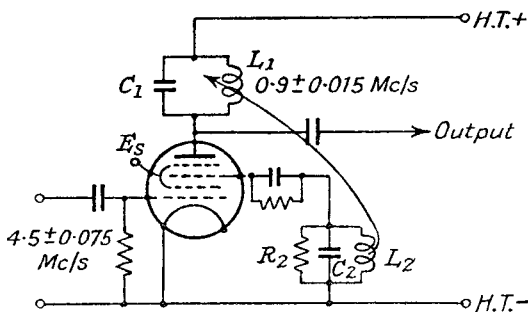


FIG. 15.27.—Compression of Frequency Deviation using a Submultiple Locked Oscillator.

apparatus is shown in Fig. 15.27. A frequency-changer type of valve is employed with the I.F. signal applied to the control grid, and the submultiple oscillation is generated by feedback from its tuned anode circuit to the oscillator grid. The regenerator circuit in the oscillator grid has a natural frequency greater than the submultiple frequency; its inductance is  $\frac{1}{5}$  or  $\frac{1}{8}$  of the anode inductance  $L_1$ , and its capacitance  $C_2$  is approximately three times that of the anode-tuning capacitance  $C_1$ .

\* Patent. R. C. A. and G. L. Beers (British Application No. 2310/43).

The locking range of the submultiple oscillator is governed by the  $\frac{L_1}{C_1}$  ratio and also by the damping of the anode circuits. A large  $\frac{L}{C}$  ratio and heavy damping tend to increase the locking range. By a suitable choice of coupling between  $L_1$  and  $L_2$ , and of supply voltages, the system can be made to function as a satisfactory limiter. Grid leak self-bias may be employed on the i.f. signal grid to aid limiting and provide A.G.C. voltage. The circuit is stated to possess particular advantages in reducing noise and adjacent channel interference because of its restricted locking range. Frequencies outside the selected range, which is limited to a little more than that required for the desired signal, are unable to lock and their effect is largely eliminated from the output.

#### BIBLIOGRAPHY

1. The Reception of Frequency Modulated Radio Signals. V. J. Andrews, *Proc. I.R.E.*, May 1932, p. 835.
2. A Method of Reducing Disturbances in Radio Signalling by a System of Frequency Modulation. E. H. Armstrong, *Proc. I.R.E.*, May 1936, p. 689.
3. Frequency Modulation Propagation Characteristics. M. G. Crosby, *Proc. I.R.E.*, June 1936, p. 898.
4. Communication by Phase Modulation. M. G. Crosby, *Proc. I.R.E.*, Feb. 1939, p. 126.
5. The Application of Negative Feedback to Frequency-Modulation Systems. J. G. Chaffee, *Proc. I.R.E.*, May 1939, p. 317.
6. Frequency Modulation. Theory of the Feedback Receiving Circuit. J. R. Carson, *Bell System Technical Journal*, July 1939, p. 395.
7. The Service Range of Frequency Modulation. M. G. Crosby, *R.C.A. Review*, Jan. 1940, p. 349.
8. A Method of Measuring Frequency Deviation. M. G. Crosby, *R.C.A. Review*, April 1940, p. 473.
9. Designing a Wide Range U.H.F. Receiver. F. W. Schor, *Q.S.T.*, Aug. 1940, p. 34.
10. N.B.C. Frequency-Modulation Field Test. R. F. Guy and R. M. Morris, *R.C.A. Review*, Oct. 1940, p. 190.
11. Two Signal Cross Modulation in a Frequency-Modulation Receiver. H. A. Wheeler, *Proc. I.R.E.*, Dec. 1940, p. 537.
12. Band Width and Readability in Frequency Modulation. M. G. Crosby, *R.C.A. Review*, Jan. 1941, p. 363.
13. The Design of Television Receiving Apparatus. B. J. Edwards, *Journal I.E.E.*, Part III, Sept. 1941, p. 191.
14. Eddy Current Tuning. C. C. Eaglesfield, *Wireless Engineer*, May 1942, p. 202.

15. Reduction of Band Width in F.M. Receivers. D. A. Bell, *Wireless Engineer*, Nov. 1942, p. 497.
16. Receiver Input Circuits. R. E. Burgess, *Wireless Engineer*, Feb. 1943, p. 66.
17. Coupled Circuit Filters. K. R. Sturley, *Wireless Engineer*, Sept. 1943, p. 426.
18. The Phase Discriminator. K. R. Sturley, *Wireless Engineer*, Feb. 1944, p. 72.
19. Frequency Modulation. K. R. Sturley, *Electronic Engineering Monograph*.



## TELEVISION RECEPTION

**16.1. Introduction.**<sup>18, 34, 35</sup> To obtain a clear idea of the problems involved in the reception of television signals and their conversion into an image of the original viewed object, a short description of the method of converting light, reflected from an object, into electrical impulses is necessary. Since the transmitter is, in effect, a single-channel system, it is quite incapable of conveying instantaneously the whole picture; to do so would require a large number of links each transmitting an electrical impulse proportional to the instantaneous light intensity from a small area of the object. The actual number of transmissions would depend on the detail required from the reproduced image, fine detail necessitating the selection of light from a very small area of the object and a very large number of transmitters. Owing to its property of persistence of vision, the eye is capable of seeing a composite image even when the light components are being interrupted, provided the rate of interruption exceeds about sixteen times per second. Hence a satisfactory picture can be obtained without each transmitter being in continuous operation, as long as the electrical pulses, proportional to the light from the particular area, are transmitted at least sixteen times per second. The brightness of reproduction would be reduced in proportion to the reduced time of transmission, and flicker would be evident, but the picture would be reproduced as a whole. Since continuous transmitter operation is not essential, it is clear that the separate transmitters could be replaced by a single transmitter successively modulated by the electrical impulses derived from the light areas originally associated with individual transmitters, and this is the principle involved in television. The loss of brightness due to successive transmission can be overcome by increased efficiency of the light to electrical impulse (and vice versa) conversion at transmitter and receiver, and flicker can be removed by increasing the rate of pick-up of light from a given area.

Conversion of the light to electrical impulses and successive pick-up are normally achieved by means of a special type of cathode-ray tube, known as the iconoscope, having a mosaic screen of photo-active material, which acts like a series of minute insulated photo-electric cells. The screen consists of a thin mica plate, on one side

of which is deposited the photo-active material, and on the other a conductive coating of colloidal graphite. The image of the object to be viewed is focused on to the screen, and the coating and photo-cell elements act as a series of capacitances, which are charged to voltages proportional partly to the brightness of the light falling on the cell element and partly to the time during which the cell is activated. These minute capacitors are discharged by the action of the cathode-ray beam, which is caused to scan the sensitive side of the mica plate in a series of almost horizontal lines one below the other. The beam is eventually returned to its starting-point and the whole image is repeatedly scanned. Discharge of the photo-electric capacitance elements causes a series of voltage pulses across a resistance connected between the mica conductive coating and a similar colloidal graphite coating round the inside of the neck of the tube. These voltage pulses are actually produced by secondary electrons, released by the cathode ray beam as it passes over the photo-electric elements and collected by the tube coating, which is at the same potential as the last anode. After suitable amplification the pulses are used to modulate the transmitter.

Interlaced scanning<sup>1</sup> is employed because it reduces flicker and gives better definition for a given pulse-frequency spectrum. Successive line scans are spaced a line width apart, so that half the image is scanned at a time, and the gaps between the lines of one vertical scan are filled in by the lines of the next vertical scan. It is achieved automatically in the iconoscope by using an odd number of lines per complete picture, alternate vertical scans starting half a line later. The number of vertical scans, or frames, is twice the number of complete pictures and, as far as flicker is concerned, it is equivalent to doubling the number of pictures transmitted. The number of frames per second must bear an integral or fractional relationship to the mains supply frequency, otherwise flicker is produced by small A.C. voltage components from the H.T. or heater supplies, which modulate the receiver light reproducer and cause alternate bands of light and shade to wander across the picture. Hence fifty frames are transmitted per second in England and sixty in America.

To achieve a high degree of definition the number of horizontal scanning lines must be large, and to remove flicker the number of complete pictures must not be less than 25 (50 frames).<sup>1</sup> This entails a large number of equivalent picture elements and, for sharp contrast, a high maximum modulating frequency. The limit of the latter is half the number of picture elements scanned per

second (a sine wave has a positive and negative half), which is determined by the number of horizontal lines per complete picture and the aspect ratio (width to height) of the latter. Taking the pre-war English standard of 405 lines per picture, 25 pictures per second, and an aspect of ratio of 5 to 4, the total number of elements in a vertical side is 405 and in a horizontal  $\frac{405 \times 5}{4} = 506$ , so that the maximum modulating frequency is

$$\frac{405 \times 506 \times 25}{2} = 2.56 \text{ Mc/s.}$$

An important feature of television transmission is therefore the large frequency spectrum occupied by the modulation sidebands. It is probable that development will be in the direction of even higher lines per picture, with consequent increase in sideband spectrum. In America a standard of 525 lines has already been adopted. Such a large modulation frequency spectrum can only be accommodated by using an ultra short-wave carrier frequency, such as 45 Mc/s or greater.

It is found in practice that the maximum modulating frequency, as calculated above, is actually higher<sup>12</sup> than is necessary because vertical resolution is less than horizontal and the number of active picture elements is less than the maximum. For example, it is possible that alternate vertical picture elements of black and white equal to one line width may be positioned such that half of each is scanned by a line. In this case the resultant pulse is equivalent to light halfway between black and white, and vertical definition is lost. It has been estimated<sup>34</sup> that only 65% of the total picture elements are fully effective, so that the maximum modulating frequency could be reduced from 2.56 to 1.66 Mc/s without impairing picture definition to any great extent.

In a television transmission channel, correct synthesis of the image at the receiver output is dependent on the light spot at the reproducer keeping step with the scanning spot at the transmitter, and some form of synchronizing signal must be incorporated in order to trigger the frame- and line-deflecting circuits at the correct time instants. The light signal must therefore be regularly interrupted to allow the transmission of a synchronizing signal at the end of each horizontal line and vertical frame scan. This is achieved by applying a synchronizing signal of opposite polarity to the light signal to modulate the carrier. The pre-war English<sup>15</sup> standard method of transmission is illustrated in Fig. 16.1. The

unmodulated carrier amplitude, corresponding to a black signal, is 30% of its maximum white amplitude, and modulation by the light signal always increases the mean carrier value. Hence average, as well as contrast brightness of picture is transmitted i.e., it contains the D.C. and A.C. components of the light signal. The synchronizing signals are transmitted by reducing carrier amplitude below its unmodulated or black value, and they have a rectangular shape. The line synchronizing pulse, which has a fundamental frequency of  $405 \times 25 = 10,125$  c.p.s., occupies 10% of the total line period, but the carrier level is maintained at black for a further 5% to allow 15% "flyback" time for the horizontal deflecting circuits. The light signal is therefore transmitted for 85% of the total line time. At the end of a vertical (frame) scan, the vision signals are suppressed for about 10 lines, and during part of this time the frame synchronizing pulse is transmitted. It consists of a series of rectangular pulses similar to the line pulses but four times as long, i.e., two are transmitted for every line period. During the  $\frac{1}{10}$ th line period interval between the pulses, the carrier is restored to its unmodulated black value. The number of frame pulses are usually eight, and for the rest of the 10-line suppression period the line-synchronizing signals are continued with carrier amplitude at 30% maximum for the intervening  $\frac{9}{10}$ ths line periods. The synchronizing signal for odd-numbered frames occurs in the middle of a line period and for

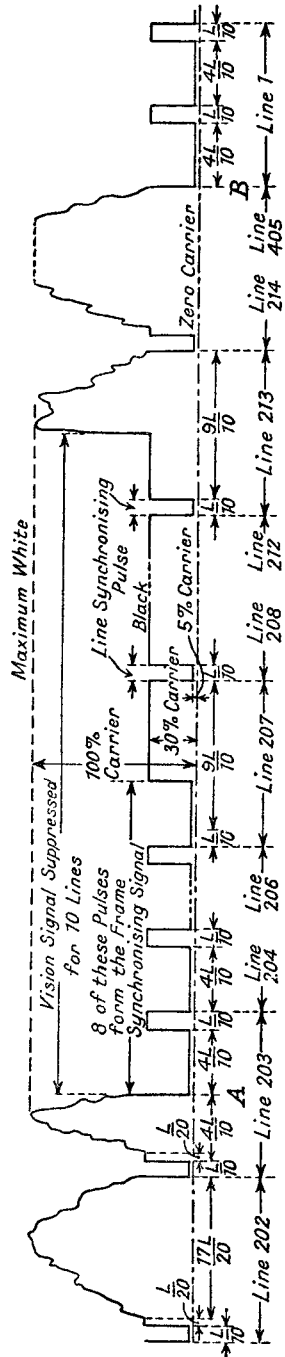


FIG. 16.1—The Waveform of the Vision Signal of the Pre-war English Transmission.

even-numbered frames at the end of a line period as shown by positions *A* and *B* in Fig. 16.1. The type of light modulation shown in this figure is known as positive modulation, and that for the synchronizing signal as negative modulation. The American system is the reverse of this, the picture modulation being negative with maximum brightness for minimum carrier, and the synchronizing modulation being positive. It is the mirror image of the English type of modulation envelope. The two systems also differ in two other respects; double sideband transmission with the associated audio\* programme at a frequency 3.5 Mc/s below the television carrier, and vertical polarization of the radiated television signal are used in England, whilst vestigial sideband (the upper with 750 kc/s of the lower) transmission with the audio carrier 4.5 Mc/s above the television carrier, and horizontal polarization are standardized in America. No fundamental modifications are, however, necessary to convert the receiver from one system to the other.

Having established the form of signal broadcast by a television transmitter, we are now able to consider the essential features of a receiver for reproducing correctly an image of the object being televised.

### 16.2. The Essential Features of a Television Receiver.

A block diagram showing the essential parts of a superheterodyne television receiver<sup>10, 13</sup> is given in Fig. 16.2. The dipole aerial, placed vertically if vertical polarization is used, or horizontally for horizontal polarization, has a length corresponding to half-wave resonance at approximately the centre of the frequency range covered by the vision channel. There is some attenuation of the audio signal, but little attenuation distortion because the audio sidebands cover such a small frequency range. Both signals are amplified together as far as the output of the frequency changer, the same local oscillator being used to provide the vision and audio intermediate frequencies. The anode of the frequency changer contains a special filter separating the two intermediate frequencies, but extra rejection of the audio I.F. may be required in the vision frequency I.F. amplifier in addition to the attenuation provided by the I.F. circuits. Single sideband vision reception is generally employed because a higher amplification per stage, and a more level frequency response can be obtained in the I.F. amplifier when the required band width is reduced. Proper reproduction of the

\* The prefix "audio" before "programme", "carrier" or "intermediate frequency" means the carrier or intermediate frequency which carries the audio frequency programme as sidebands.

vision signal can only be secured when the vision carrier is correctly tuned to the edge of the pass-band, and this is achieved by using the sound signal as a tuning indication. The I.F. amplifier for the audio signal usually has a pass-range about 100 kc/s wide (to allow for frequency drift of the oscillator), and correct tuning of the audio signal, within this pass-range, by variation of oscillator frequency, automatically involves correct tuning for the vision signal if the two I.F. channels are correctly aligned in the first place. The vision intermediate frequency must be carefully chosen to give an adequate pass-band without serious attenuation or phase distortion, and to avoid spurious responses, which produce chequerboard or wavy line patterns across the reproduced picture.

When only a single transmission is to be received, the amplifier before the vision frequency detector may be of the fixed tuned

R.F. type.<sup>6</sup> It has advantages over the superheterodyne that tuning is not dependent on a local oscillator, the frequency of which may drift appreciably during the first half-hour after switching on,

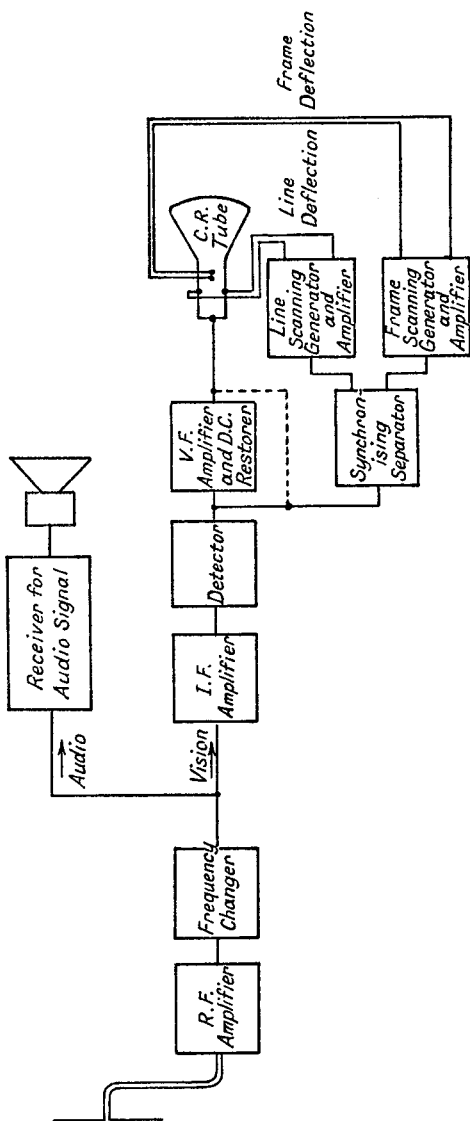


FIG. 16.2.—The Schematic Diagram of a Television Receiver.

that a flat pass-band can be more easily obtained at the higher frequency and that it does not produce spurious interfering frequencies. Its disadvantage is that more difficulty is experienced in removing the audio signal from the vision output, because the tuned circuits in the R.F. stages cannot normally provide sufficient attenuation unless the pass-band of the vision signal is severely restricted. With this type of receiver it is usual to divide the feeder line from the aerial into two channels, and to insert a filter in the vision channel to reject the audio transmission, and a vision frequency filter in the audio channel. Additional filters may be included in the vision R.F. amplifier so as to bring about an overall attenuation of the audio signal of 40 db. It will be noticed that by this system the audio and vision signals are separated at the aerial, and common amplification of the two is not employed. Sometimes the first stage in the vision R.F. amplifier is used to amplify both audio and vision, special narrow pass-band rejection circuits being inserted to provide sufficient overall attenuation of the audio signal in the remaining stages. Another possibility with double sideband transmission is to use single sideband reception, the sideband on the opposite side of the carrier to the audio signal being accepted; the chief difficulty with this method is that satisfactory operation depends on the R.F. circuits being, and remaining, correctly tuned.

The vision frequency detector is generally a diode, but a triode, functioning as an anode bend detector, may be used. The diode load resistance must be low, about  $5,000 \Omega$ , in order to prevent attenuation of the higher vision frequencies by the stray capacitance across it. The same is true of the anode load resistance of the vision frequency amplifier after the detector, and in this part of the apparatus special methods are adopted to neutralize the reactance of the stray capacitance. The V.F. amplifier is not usually a D.C. amplifier, and a diode or similar device is used to restore the D.C. component at the output.

The V.F. amplifier is connected to the voltage-light converter. The latter function is successfully performed by the cathode-ray tube, the beam of which is capable of intensity modulation by the application of a voltage to its grid (or gun electrode, as it is sometimes called). The grid voltage varies the density of the electrons in the beam and hence the brightness of the spot formed on the screen, a positive direction of voltage increasing brightness. The area, or focus, of the spot on the screen can be controlled by varying the D.C. current in a coil round the neck of the tube (magnetic

focusing)—a permanent magnet with a variable shunt may also be used—or by varying the voltage applied to an intermediate anode between the grid and final anode (electrostatic focusing). The diameter of the screen on which the image is formed is generally 9 or 12 inches; the useful picture area with the 12-inch diameter cathode-ray tube is 10 inches by 8 inches. The colour of the light depends on the screen material; the most popular colour is a bluish white obtained with a screen material of zinc sulphide or cadmium tungstate with zinc silicate.

A deflecting system is necessary to synthesize the light impulses into an intelligible picture, and arrangements must be made to deflect the beam horizontally and vertically in an identical manner to, and in step with, the scanning beam in the iconoscope. This can be achieved either by applying voltages of saw-tooth shape to deflecting plates mutually at right angles inside the C.R. tube, between the final anode and screen (electrostatic deflection), or by means of currents of saw-tooth shape in coils external to the C.R. tube (magnetic deflection). Magnetic deflection has the great advantage that it allows a much shorter tube to be used and a more compact receiver is therefore possible. The saw-tooth voltage or current generator consists usually of a resistance-capacitance charge circuit operating in conjunction with a triggering charge or discharge device, such as a blocking oscillator. The "free" frequency of the triggering action is set to a value slightly below the fundamental of the frame or line saw-tooth, and is pulled into step by means of the synchronizing pulses sent out by the transmitter. These pulses are separated from the vision signals by means of a special synchronizing separator stage, which usually incorporates a limiting action to prevent loss of synchronism due to noise or interference. A filter is employed to separate line pulses from the frame synchronizing pulse used to lock the frame-scanning generator.

The order of importance of the four types of distortion, harmonic, attenuation (frequency), phase and transient, in television reception is different from that for audio reception. Harmonic distortion has relatively little effect, but both attenuation and phase have a large influence on the picture. High-frequency cut-off attenuation distortion leads to a picture with blurred outlines giving the appearance of being out of focus, whilst high-frequency intensification in the video frequency amplifier, if carried too far (the increase should not exceed 1 db. above the average level), may result in transient distortion, i.e., damped oscillations producing a rippled effect following the trailing edge of a white or black vertical line. Low-



frequency cut-off in the v.f. amplifier causes uneven reproduction of large surfaces.

Phase distortion leads to a plastic relief type of image, a white or black vertical line being preceded by a black or white margin respectively, or, if it is excessive, multiple images may be formed. Phase distortion is zero if the time delay is constant for all the frequency components of the signal passing through the amplifier. This means that the phase angle shift between the output and input must be proportional to frequency. For example, suppose there is a constant time delay of 1 microsecond at all frequencies; this represents 1 cycle or  $2\pi$  radians at 1,000 kc/s,  $\frac{1}{2}$ -cycle or  $\pi$  radians at 500 kc/s,  $\frac{1}{10}$ -cycle or  $\frac{\pi}{5}$  radians at 100 kc/s, and so on.

Attenuation and phase distortion can occur in all stages of the receiver, but are generally greatest in the r.f. and i.f. stages, partly because there are more of them than of v.f. amplification. For a given pass-band width coupled or band-pass circuits can be designed to give less of both types of distortion than a single-tuned circuit.

We shall now examine the separate stages in the receiver, with particular reference to the English type of transmission, i.e., the vision signal is assumed to be double sideband transmission on a carrier of 45 Mc/s, with an audio programme on a carrier of 41.5 Mc/s. The required band width for adequate definition is assumed to be 78% of the maximum possible number of picture elements, i.e.,  $\pm 2.56 \times 0.78 = \pm 2$  Mc/s. Signal-to-noise ratio on full modulation (white) is to be not less than 30 db. for an input of 50  $\mu$ V at the aerial. The overall amplification of the receiver is to be capable of giving 25 volts swing, peak-to-peak, at the grid of the cathode-ray tube for a fully modulated input of 50  $\mu$ V at the aerial.

**16.3. The Aerial Circuit.**<sup>14</sup> Owing to the high modulation frequencies involved in television reception it is most important that reflected signals,<sup>9</sup> delayed in time with respect to the real signal, should be prevented from reaching the aerial input of the receiver at a strength comparable with the real signal. These delayed signals may be caused by reflections from large buildings, metal objects (aeroplane), changes in earth conductivity, or incorrectly terminated aerial feeder lines, particularly coaxial or parallel open wire lines, which have a much lower attenuation loss per unit length than twisted wire feeders. The latter have an attenuation loss of about 1 to 2 db. per wavelength as compared with 0.1 db. per wavelength for open wire lines and coaxial feeders. Particular

care must also be taken with parallel open wire lines to see that they are balanced with respect to earth for, unlike the coaxial cable with an earthed outer, they can pick up an appreciable signal voltage, which may be comparable with that picked up by the aerial itself. The signal voltages in each side of the parallel wires cancel at the receiver if the receiver input is centre-tapped to earth and the wires themselves are balanced to earth. The effect of the delayed signal depends largely on the time lag between it and the real signal; if the delay is large a "ghost" image, displaced from the real image, is produced, but, if it is small, blurring or a change in the light distribution of the image may result. For example, owing to a redistribution of the amplitude and phase of the side-bands of real and reflected signals, cancellation or intensification may change a vertical white line into black or vice versa. To gain some idea of the importance of the time delay effect, let us consider a receiver having a 12-inch diameter cathode-ray tube giving a picture area of 10 ins. by 8 ins. The speed at which the spot travels across the picture is  $405 \times 25 \times 10 \times 2.54 \div 0.85$  (lines per picture  $\times$  complete pictures per second  $\times$  length of line  $\div$  conversion factor allowing 15% flyback time) =  $3.02 \times 10^5$  cms./sec. The rate of-travel of the television signal in free space is  $3 \times 10^{10}$  cms./sec., i.e.,  $0.994 \times 10^5$  times faster than the C.R. tube spot. Hence, if there are two signal paths from the transmitter to the receiver, one 276 yards (252 metres) longer than the other, the longer path signal produces a second image displaced by  $\frac{1}{10}$ -in. from the real image on the C.R. tube screen. Normally the best position for the aerial is vertical for vertically polarized transmission, and horizontal, one end pointing towards the transmitter, for horizontally polarized transmission, but particular site conditions—congested areas with intervening high buildings—may call for special orientation in order to reduce reflected signal interference.

The most suitable type of aerial is the dipole or V dipole. The latter has the advantage (see Sections 3.3.5 and 3.5.3, Part I) over the former of having a lower characteristic impedance and hence less variation of terminal impedance over a given frequency range. This means less transition loss at the junction of aerial and feeder. The length of the dipole is not very critical and it is usual to select a value giving resonance at the centre of the frequency range, thus the length of a dipole to resonate at 45 Mc/s is

$$\frac{\lambda}{2.1} = \frac{3 \times 10^{10}}{45 \times 10^6 \times 2.1} = 318 \text{ cms.} = 10 \text{ ft. } 5 \text{ ins.}$$

The factor 2.1 instead of 2 is used because, owing to end effects, the electrical length of an aerial of brass, copper or aluminium is approximately 5% greater than its physical length. For steel-rod aerials the correction factor is about 2.2. A reflector may be used behind the aerial to increase the pick-up from the transmitter and reduce interference, such as that from motor-car ignition systems, from directions on the opposite side of the aerial to the transmitter. The reflector is usually spaced from  $\frac{1}{4}\lambda$  to  $\frac{3}{8}\lambda$  away from the aerial, and its length may be made greater than that of the latter so as to give a broad double-humped overall frequency response. The dimensions of one such type<sup>28</sup> are: a main aerial 10 ft. 1 in. long with a reflector 11 ft. 1 in. long, separated by a spacing of 4 ft. 4 ins.

The aerial-to-feeder connection is generally to the centre of the dipole, though the feeder may be connected to one end of the dipole by using a special  $\frac{1}{4}\lambda$  matching section,<sup>5</sup> made by two parallel wires  $\frac{1}{4}\lambda$  long, separated by  $1\frac{1}{2}$  to 2 ins. One of these wires forms an extension to the  $\frac{1}{2}\lambda$  dipole and the ends of both are joined to the twin wire feeder. For twin wire shielded feeder or low impedance (80  $\Omega$ ), the dipole is cut at the centre and each feeder wire goes to the end of one half-section. The distance between the two cut ends should be as small as possible compatible with satisfactory insulation; about 1 inch separation is generally adequate. Parallel wire feeders of high impedance (500  $\Omega$ ) can also be connected to the centre of the aerial, but in this case the latter is not cut into two half-sections. The feeder ends are fanned out in triangular manner from their normal separation of about 2 ins. to a separation of 26 ins. in a distance of 40 ins. ( $0.15\lambda$ ).<sup>30</sup> The mouth of the isosceles triangular shape of flare is connected to be symmetrically disposed about the centre of the dipole. Coaxial feeder may also be connected to the centre of a split dipole, the outer and inner conductors being joined to the near ends of the two half-sections. This is not the most efficient method, and a standing wave is produced on the outer conductor between the points where it joins the aerial and where it is earthed. A better system is to use a transformer with a balanced primary centre-tapped to earth, and a secondary, one end of which is connected to the inner and the other to the earthed outer. An electrostatic screen is desirable to prevent capacitive coupling from the primary to the secondary, causing unbalance of the primary.

The dipole aerial should be self-supporting, or alternatively stay wires must be broken up by insulators into lengths not equal to  $\frac{1}{2}\lambda$  or multiples of it. The feeder should be taken away at right

angles to a vertical dipole for a distance of about 20 ins. before turning it downwards. A shorter distance (but not less than 10 ins.<sup>25</sup>) may be used from aerial to the turn when necessary.

**16.4. The R.F. Amplifier.**<sup>23</sup> The design of the feeder-to-first tuned circuit connection of the receiver follows the lines set out in Section 15.5. The performance of the first R.F. valve has an influence on the design of the first tuned circuit. Maximum amplification requires the tuning capacitance of all tuned circuits to be as small as possible, so that valve grid input and anode output capacitances should be as small as possible. The input resistance of the valve at 45 Mc/s is less important than in the case of the frequency modulation receiver, because the pass-band width is very much greater and calls for heavy damping of the first tuned circuit. Mutual conductance must be as high as possible and, for minimum shot-noise resistance, total cathode current at minimum bias must be as small as possible. This means that alignment of grid and screen wires (this reduces screen current), and anode current cut-off at a comparatively low grid bias are required. The valve cannot, therefore, have a very good variable- $\mu$  characteristic and, although harmonic distortion is not so serious with a television as with an audio signal, control of amplification by grid bias variation is unlikely to be satisfactory. Another disadvantage of grid control of amplification is that it tends to vary the grid input resistance and capacitance of the valve; this effect can be reduced by the use of an unby-passed resistance in the cathode lead as discussed in Section 4.10.3, Part I. For design purposes we shall consider the R.F. valve to have characteristics similar (except for grid input resistance which is taken as  $8,000 \Omega$ ) to those of the valve in Section 15.5, viz.,  $g_m$  of 8 mA/volt, input and output capacitances of approximately 10 and  $8 \mu\mu\text{F}$ , and an equivalent shot-noise resistance of  $1,500 \Omega$ . Values as high as  $14,000 \Omega$ <sup>28</sup> for input resistance at 45 Mc/s can be obtained with special valve designs, but as long as it is greater than a certain value the chief advantage of a high resistance is that any variation from valve to valve, or due to control of amplification, has less effect when the majority of the damping is provided by a fixed resistance. A typical circuit showing the feeder to first tuned circuit coupling, and the R.F. amplifier valve is that of Fig. 16.3. The feeder is assumed to have a characteristic impedance of  $80 \Omega$ , optimum coupling is employed between the feeder coupling coil  $L_1$  and the secondary coil  $L_2$ , the inductive reactance of  $L_1$  is cancelled by the capacitive reactance of  $C_1$ , the tuning capacitance  $C_2$  (consisting only of valve, wiring

and coil self-capacitances) is assumed to be  $15 \mu\mu\text{F}$ . This low value of  $C_2$  can be realized by very careful layout. We must now decide the permissible attenuation loss at the maximum off-tune frequencies of  $\pm 2 \text{ Mc/s}$ . For a single-tuned circuit, phase and attenuation distortion are closely related and increase of the latter increases the former. It would therefore appear that the circuit should be designed to give minimum attenuation loss; the advantages of doing this are that a lower  $Q$  value is required so that the valve grid input resistance becomes of less consequence and the noise voltage at the grid of the first R.F. valve is reduced. On the other hand, transfer voltage ratio is decreased to a greater extent than the decrease of noise voltage and a larger signal output is required from the feeder to obtain the same signal-to-noise ratio. This feature

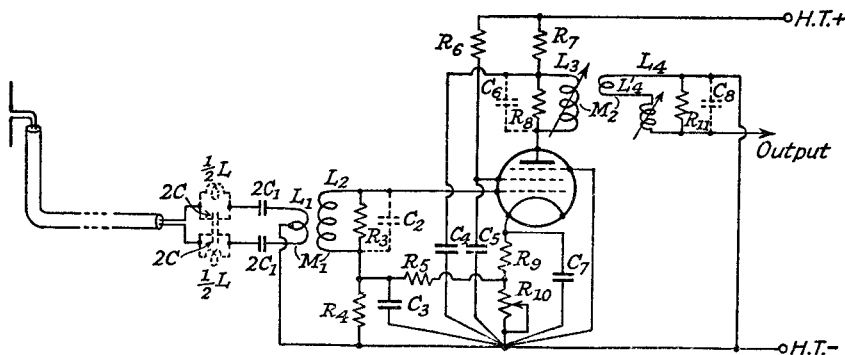


FIG. 16.3.—The Aerial and R.F. Amplifier Stage for a Television Receiver.

is illustrated later in the section. The reduction in transfer voltage ratio has practically no effect on the overall amplification of the receiver because the more constant frequency response over the pass-band range calls for less compensation in the tuned transformer stages, i.e., the coupling coefficient can be brought closer to its critical coupling value, the peak-to-trough ratio decreased and the gain of each transformer coupled stage therefore increased. The chief advantage of adopting a higher attenuation loss in the first tuned circuit (apart from greater overall sensitivity for a given signal-to-noise ratio) is that phase distortion in transformer stages giving a double-humped frequency response is in the opposite direction to that in the first tuned circuit, and it is reduced as the double-humped response is made more pronounced, i.e., coupling coefficient is increased, so that a closer approach to cancellation can be made. Usually about four transformer stages are employed and

there is therefore a tendency to obtain overcorrection of the phase distortion if the first tuned circuit has too small attenuation loss and phase distortion.

In order to estimate the effect of phase distortion, the phase angle shift and attenuation loss of a single-tuned circuit at different values of  $QF$ , i.e., different off-tune frequencies, are tabulated below. For zero phase distortion, the phase angle should be proportional to the off-tune frequency,  $\Delta f$ , i.e., to  $QF$ , and in the fourth row of Table 16.1, the difference between the required phase angle (proportional to  $\Delta f$ , and calculated by multiplying the phase angle at  $QF = 0.1$  by the ratio of the particular value of  $QF$  being considered to 0.1) and the actual phase angle is indicated.

TABLE 16.1

$QF$ . . . . .	+ 0.1	+ 0.2	+ 0.3	+ 0.4	+ 0.5
Attenuation Loss (db.) . . . . .	- 0.043	- 0.17	- 0.37	- 0.64	- 0.97
Phase Angle . . . . .	- 5° 43'	- 11° 19'	- 16° 42'	- 21° 48'	- 26° 34'
Phase Angle Error	0	+ 5'	+ 29'	+ 1° 7'	+ 2° 5'
$QF$ . . . . .	+ 0.6	+ 0.7	+ 0.8	+ 0.9	+ 1.0
Attenuation Loss (db.) . . . . .	- 1.335	- 1.73	- 2.15	- 2.58	- 3.01
Phase Angle . . . . .	- 30° 58'	- 34° 59'	- 38° 40'	- 41° 59'	- 45°
Phase Angle Error	+ 3° 25'	+ 5° 8'	+ 7° 10'	+ 9° 35'	+ 12° 18'

The time delay is greatest for the largest value of  $QF$ , and if  $QF = 1$  for  $\Delta f = 2$  Mc/s, the error in time delay is

$$\frac{12^\circ 18'}{360} \times \frac{1}{2 \times 10^6} \text{ seconds} = 0.0171 \mu \text{ secs.}$$

In Section 16.3 we showed that the spot on a typical C.R. tube for television signals travels at  $3.02 \times 10^5$  cms./sec., so that 0.0171  $\mu$  secs. corresponds to a displacement of 0.0516 mm., which will give negligible blurring of the picture. As far as the first tuned circuit is concerned we can allow an attenuation loss of - 3 db. at the maximum off-tune frequency of 2 Mc/s. A point to be watched is that compensation for this loss by doubled-humped response in subsequent stages does not introduce excessive overall phase distortion.

The final  $Q_2'$  of the secondary circuit including damping introduced by optimum coupling to the feeder of characteristic impedance 80  $\Omega$  is, for a loss of - 3 db. at  $\Delta f = \pm 2$  Mc/s, given by

$$Q_2' = \frac{f_m}{2\Delta f} = \frac{45}{4} = 11.25$$

or the  $Q$  of the secondary circuit when not coupled to  $L_1$  is

$$Q_2 = 2Q_2' = 22.5$$

and its resonant impedance is

$$R_{D2} = \frac{Q_2}{\omega_m C_2} = \frac{22.5 \times 10^6}{6.28 \times 45 \times 15} = 5,300 \Omega.$$

If the initial  $Q_0$  of the coil  $L_2$  is 150, the total damping resistance required across  $L_2$  is

$$R_{T2} = \frac{R_{D2} Q_0}{Q_0 - Q_2} = 6,240 \Omega.$$

The input resistance of the valve provides 8,000  $\Omega$  of this so that

$$R_3 = \frac{6,240 \times 8,000}{1,760} = 28,350 \Omega.$$

The transfer voltage ratio is (see expression 15.2)

$$T_R = \frac{1}{2} \sqrt{\frac{R_{D2}}{R_{a1}}} = \frac{1}{2} \sqrt{\frac{5,300}{80}} = 4.07$$

if the feeder characteristic impedance is 80  $\Omega$ .

For optimum coupling  $M_1 = \frac{\sqrt{R_{a1} R_2}}{\omega_m} = \frac{\sqrt{80 \times 10.45}}{6.28 \times 45} = 0.102 \mu\text{H}$

where  $R_2 = \frac{\omega_m L_2}{Q_2}$  = effective series resistance of the secondary circuit.

$$C_2 = 15 \mu\mu\text{F}, L_2 = \frac{1}{\omega_m^2 C_2} = 0.832 \mu\text{H}$$

$$L_1 = 0.416 \mu\text{H}, C_1 = 30 \mu\mu\text{F}$$

$$Q_1 = \frac{\omega_m L_1}{80} = 1.47.$$

Using expression 15.3*b* and noting that  $Q_2 F = 2$  and  $Q_1 F = 0.1305$ , we find that the actual loss at off-tune frequencies of  $\pm 2$  Mc/s is approximately  $-2.8$  db. If  $L_1$  is made equal  $L_2$ ,  $Q_1$  is doubled and the loss at  $\pm 2$  Mc/s is reduced to  $-2.6$  db.

The equivalent total noise resistance is the sum of the overall resonant impedance of the first tuned circuit, including damping from the feeder side, and the shot-noise resistance of the valve, i.e., it equals  $2,650 + 1,500 = 4,150 \Omega$ , so that the R.M.S. noise voltage at the grid of the first valve is

$$\begin{aligned} E_n &= 1.25 \times 10^{-10} \cdot \sqrt{4,150 \times 4 \times 10^6} \\ &= 16.1 \mu\text{V} \\ &= \frac{16.1}{4.07} \equiv 3.96 \mu\text{V} \text{ on the feeder side.} \end{aligned}$$

For satisfactory performance, signal-to-noise ratio should be of the order of 30 db., i.e., 31.6 to 1, so that the minimum acceptable signal output from the feeder is 125  $\mu\text{V}$ .

If the permissible loss at 45 Mc/s is reduced to  $-1$  db.,  $Q_2'F = 0.5$ ,  $Q_2' = 5.62$  for  $\Delta f = 2$  Mc/s,  $R_{D_2} = 2,650 \Omega$ , and

$$T_R = \frac{1}{2} \sqrt{\frac{2,650}{80}} = 2.88$$

$$E_n = 1.25 \times 10^{-10} \sqrt{(1,325 + 1,500) \times 4 \times 10^6}$$

$$= 13.3 \mu\text{V}$$

$$\equiv 4.62 \mu\text{V on the feeder side.}$$

Hence the minimum acceptable signal output from the feeder is 146  $\mu\text{V}$ . We see, therefore, that sensitivity (for a given signal-to-noise ratio) is approximately 20% better in the case of the  $-3$  db. attenuation loss than the  $-1$  db. loss.

Referring to Fig. 16.3, it will be seen that control of amplification is obtained mainly by suppressor grid bias variation, the variation of control grid bias being only approximately 3% of the suppressor grid change. The reason for this dual control is that it reduces the variation of grid input resistance and capacitance with change of amplification. The same result may be realized by the use of an unby-passed resistance in the cathode circuit (see Section 4.10.3) and by variation of screen voltage<sup>28</sup> to obtain amplification control. When screen voltage is varied cathode self-bias is not used, but fixed bias is obtained for the controlled valves from a resistance in the main H.T. supply lead. The values of the resistances in Fig. 16.3 are

$$R_4 = 100,000 \Omega, \quad R_5 = 3,000 \Omega, \quad R_6 = 50,000 \Omega,$$

$$R_9 = 150 \Omega, \quad R_{10} = 20,000 \text{ (max.) variable.}$$

The decoupling capacitors,  $C_3$ ,  $C_4$ ,  $C_5$ , and  $C_7$  are of mica and have values of 0.001  $\mu\text{F}$ .

Before considering details of the tuned transformer in the anode circuit of the valve in Fig. 16.3, it is advantageous to obtain generalized phase-angle error curves against  $QF$  for different values of  $Qk$  in order that overall phase distortion can be estimated.

In Section 7.3, Part I, the phase angle at the output of a tuned transformer with reference to the grid input voltage for any off-tune frequency is given by rationalizing expression 7.2a, i.e.,

$$\phi = \tan^{-1} \frac{(1 + Q_1 Q_2 (k^2 - F^2))}{-(Q_1 + Q_2)F} \quad . \quad . \quad 16.1$$



$\phi$  therefore varies from  $270^\circ$  to  $90^\circ$  as  $QF$  varies from 0 to  $+\infty$  ( $\Delta f$  changes from 0 to  $+\infty$ ).

As far as phase distortion is concerned, it is better to consider  $QF = 0$  as the reference point, and to call the phase angle at this value  $0^\circ$ . To do this expression 16.1 must be inverted and given a negative sign.

$$\phi' = \tan^{-1} - \frac{(Q_1 + Q_2)F}{1 + Q_1 Q_2 (k^2 - F^2)} \quad . \quad . \quad 16.2a.$$

The negative sign is necessary because expression 16.1 shows that the phase angle is reduced as  $QF$  increases positively.

If the primary and secondary circuits are identical

$$\phi' = \tan^{-1} \frac{-2QF}{1 + Q^2(k^2 - F^2)} \quad . \quad . \quad 16.2b.$$

The phase-angle error is calculated in the same way as that for the single-tuned circuit, viz., the correct phase angle is calculated by multiplying the phase angle at  $QF = 0.1$  by the ratio of the particular value of  $QF$  being considered to 0.1; the correct phase angle is subtracted from the actual phase angle to give the phase-angle error. A positive sign to the latter indicates that the required phase angle is negative and numerically less than the actual phase angle, i.e., it represents a time advance, or alternatively the time delay is less than it should be. Conversely, a negative sign means that the time delay is greater than it should be.

A series of phase-angle error curves is plotted in Fig. 16.4 against  $QF$  for different values of  $Qk$ . For reference purposes the error curve for a single-tuned circuit is also included, and is the dashed curve in the figure. An interesting point to note is that over the range from  $QF = 0$  to 1 the error is positive for couplings corresponding to  $Qk < 0.7$ . When  $Qk = 0.7$  the error is very small, and for  $Qk > 0.7$  the error becomes negative and reaches a maximum at about  $Qk = 1$ . For  $Qk > 1$ , the error decreases, slowly at first—there is little difference between  $Qk = 1$  and 1.5.

From these curves the overall phase error for any combination of single-tuned circuits and tuned transformers can be estimated.

For example, by combining a single-tuned circuit of  $Q = \frac{f_m}{2\Delta f}$  with two tuned transformers of the same  $Q$  as the tuned circuit and  $Qk = 1.5$ , phase distortion is almost zero over the range  $QF = 0$  to 1. The maximum phase-angle error is  $0^\circ 42'$  at  $QF = 0.6$ . Figs. 4.3 and 7.7, Part I, show that there is some attenuation distortion with

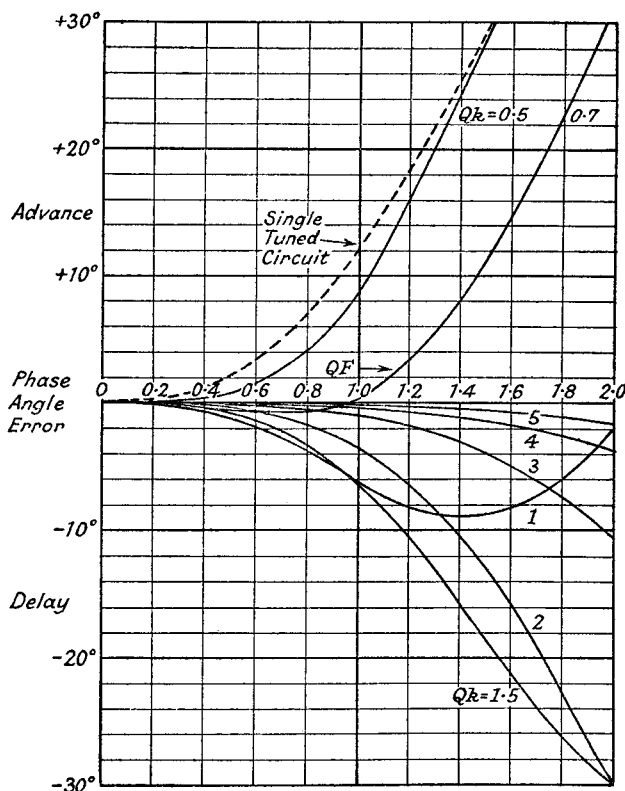


FIG. 16.4.—Phase Angle Error Curves of a Pair of Coupled Tuned Circuits for Different Values of Coupling.

this combination, the frequency response falling by 1 db. from  $QF = 0$  to 1.

**16.5. The Fixed Tuned R.F. Television Receiver.** Let us now consider the design of the R.F. stages of a fixed tuned R.F. receiver to provide a detector input peak voltage of 5 volts. The overall amplification to produce this from a feeder output signal of  $125 \mu\text{V}$  is 40,000, or 9,850 from the grid of the first valve ( $T_R$  for this feeder voltage = 4.07). A possible gain for each R.F. stage is 10, so that four stages are required. Examination of Fig. 16.4 suggests the use of four stages of coupling coefficient corresponding to  $Qk = 2$  and the same  $Q$  value as the first tuned circuit, if phase distortion is to be reduced to negligible proportions. On the other hand, this combination results in a lower overall amplification and a wider pass-band than is required (less discrimination is therefore obtained against the audio signal), and a better compromise is

obtained by using four stages of coupling coefficient corresponding to  $Qk = 1.5$  and the same  $Q$  value as the first tuned circuit. Overall phase distortion is increased, but is still small enough to be negligible, and the overall frequency response variation over the frequency range corresponding to  $QF = 0$  to 1 is not greater than 1 db. It actually rises from  $QF = 0$  to 1 by 1 db., and at  $QF = 1.5$  and 1.75 (this corresponds to the frequency of the audio carrier), there is a loss of  $-5$  and  $-8$  db. (add to the curve in Fig. 4.3, four times the curve for  $Qk = 1.5$  in Fig. 7.7, Part I), compared to the value at  $QF = 0$ . The overall loss of  $-8$  db. at the audio carrier frequency is quite inadequate and extra filtering is necessary to increase the loss at this off-tune frequency of  $-3.5$  Mc/s, i.e., the audio carrier frequency of 41.5 Mc/s, to about  $-40$  db. Methods of achieving this are discussed at the end of the section. The rise of 1 db. in the frequency response at the edges of the pass-band is an advantage because both detector and vision frequency amplifier stages tend to have reduced amplification at the higher modulating frequencies. The overall phase-angle error is obtained by adding four times the curve for  $Qk = 1.5$  in Fig. 16.4 to the dashed curve for the single-tuned circuit, and it is tabulated below from  $QF = 0$  to 1.

TABLE 16.2

$QF$ . . . . .	0	0.1	0.2	0.3	0.4	0.5
Overall Phase Angle						
Error . . . . .	0	0	$-1'$	$-9'$	$-30'$	$-1^\circ 3'$
$QF$ . . . . .	0.6	0.7		0.8	0.9	1.0
Overall Phase Angle						
Error . . . . .	$-2^\circ 4'$	$-3^\circ 38'$		$-4^\circ 56'$	$-9^\circ$	$-13^\circ 2'$

Time-delay error is maximum at  $QF = 1$ , i.e., an off-tune frequency of 2 Mc/s, and corresponds to a displacement of 0.0546 mm. for the same speed of spot as is assumed for the single-tuned circuit calculation given earlier. Hence phase distortion is negligible.

Details of the transformer in the anode circuit of the valve in Fig. 16.3 are therefore :

$$Qk = 1.5, Q = \frac{f_m}{2\Delta f} = \frac{45}{4} = 11.25 \text{ (this is the } Q \text{ of both primary}$$

and secondary circuits when not coupled together). No extra tuning capacitance is employed, it being made up of the valve, wiring and coil self-capacitances, viz., 15  $\mu\text{F}$ . Tuning is carried out by variation of the inductances either by means of an adjustable iron core or by eddy current (slug) tuning.  $L_4$  is divided into two

sections, one of which is directly coupled to  $L_3$  to provide the required coupling coefficient.

Thus

$$L_3 = L_4 = 0.832 \mu\text{H}$$

$$k = \frac{1.5}{Q} = 0.1333$$

$$M_2 = kL_3 = 0.111 \mu\text{H}.$$

Assuming a coupling coefficient of 0.3 between the section  $L_4'$  of the secondary and the primary  $L_3$ .

$$0.3 = \frac{M_2}{\sqrt{L_4' \times 0.832}} \quad \text{or} \quad L_4' = 0.165 \mu\text{H}.$$

The resonant impedances of primary and secondary circuits are

$$R_{D3} = R_{D4} = \frac{Q}{\omega_m C_6} = \frac{11.25 \times 10^6}{6.28 \times 45 \times 15} = 2,650 \Omega.$$

Amplification from the grid of  $V_1$  to the output terminals of the secondary  $= g_m \frac{R_{D3}}{2} \times 0.89 = 9.45$  when  $g_m = 8 \text{ mA/volt}$ . The factor 0.89 allows for the 1-db. fall from peak to trough. The required value of overall amplification is not reached in this design, and either an extra stage is needed or two of the overcoupled circuits must be replaced by two critically coupled stages.

If the initial  $Q_0$  of  $L_3$  and  $L_4$  is 150, the total additional damping resistance required across the primary and secondary is

$$\frac{R_{D3}Q_0}{Q_0 - Q_1} = \frac{2,650 \times 150}{138.75} = 2,870 \Omega. \quad \text{Hence } R_8 = 2,870 \Omega.$$

Across  $L_4$  the second R.F. valve already provides 8,000  $\Omega$  so that

$$R_{11} = \frac{2,870 \times 8,000}{5,130} = 4,460 \Omega.$$

Finally, we must make certain that feedback through the anode-grid interelectrode capacitance has negligible effect. From expression 15.4*d*, Section 15.7, the minimum value of grid input resistance due to anode-grid capacitance for a valve having a tuned transformer in its anode circuit is

$$\begin{aligned} R_g(\text{min.}) &= \frac{\pm 4}{g_m B_{ga} R_{D3}} \\ &= \frac{\pm 4 \times 10^6}{8.0 \times 10^{-3} \times 6.28 \times 45 \times 0.02 \times 2,650} \\ &= \pm 33,400 \Omega \end{aligned}$$

where

$$C_{ga} = 0.02 \mu\mu\text{F}.$$

Hence feedback through the anode-grid capacitance has negligible

effect on the grid circuit, the resonant impedance of which is only 2,650  $\Omega$ .

Thus a typical fixed tuned R.F. receiver consists of four stages of amplification with overcoupled ( $Qk = 1.5$ ) tuned transformers in the anode circuits in association with an input tuned circuit of the same  $Q$  value. All circuits are identical except for the last secondary circuit, the damping resistance for which is adjusted to suit the detector conduction damping resistance. Estimation of this resistance is left until Section 16.7, which deals specifically with detectors for television signals.

Earlier in this section it was shown that the overall attenuation at the audio signal carrier is only  $-8$  db., and a loss at this frequency of  $-40$  db. is required. The most convenient way of increasing the loss at this frequency is by the insertion of a parallel circuit, tuned to the audio carrier frequency, in the feeder line from the aerial to the first tuned circuit. If a coaxial feeder is employed only one tuned circuit is needed, but if a twin wire feeder is used, balance must be maintained by using a tuned circuit, of half the resonant impedance in each line. These circuits may be inserted at some convenient point in the feeder as shown by the dotted  $\frac{1}{2}L$  and  $2C$  circuits in Fig. 16.3. To obtain a loss of 40 db. the sum of the resonant impedances of both tuned circuits (at 41.5 Mc/s) must be 100 times the characteristic impedance of the feeder, i.e.,  $\omega LQ = 8,000$ , or if  $Q = 150$  (it should be as high as possible so as to reduce the loss at the vision carrier frequency, 45 Mc/s)  $L = 0.2045 \mu\text{H}$  and  $C = 71.8 \mu\mu\text{F}$ . The impedance of these circuits at 45 Mc/s is from expression 4.8b, Part I:

$$\frac{R_D}{1+jQF} = \frac{8,000}{1+j150 \times \frac{7}{41.5}} = \frac{8,000}{1+j25.3} \simeq -j316.$$

Hence there is a ratio loss at 45 Mc/s due to the introduction of the filter of

$$\frac{80}{\sqrt{80^2 + (316)^2}} = \frac{1}{4.08} \equiv -12.2 \text{ db.}$$

so that the net reduction of the audio carrier is  $8 + 40 - 12.2 = 35.8$  db.

The impedance of the tuned circuits at the maximum negative off-tune frequency of the vision signal, viz., 43 Mc/s is

$$\frac{8,000}{1+j150 \frac{3}{41.5}} = \frac{8,000}{1+j10.85} = -j735,$$

so that there is a ratio loss of  $\frac{80}{\sqrt{80^2 + 735^2}} \equiv -19.32$  db.

This means that the audio signal rejector has caused attenuation and phase distortion over the pass range, the frequency response falling by  $-7.12$  db. from 45 to 43 Mc/s. This fall may be partially offset by the fact that the generalized selectivity curves of Fig. 7.7 ignore a frequency factor which tends to give higher amplification of the sidebands lower in frequency than the carrier, and also by the fact that the sidebands higher in frequency than the carrier are attenuated to a decreasing extent by the filter as the off-tune frequency increases. Phase distortion can be checked by finding the phase angle shift due to the filter over the range 43 to 47 Mc/s. Phase-angle error is calculated by comparing the actual phase angle against the phase angle, which should have been obtained had the change been proportional to the change from 45 to 45.1 or 44.9 to 45 Mc/s. Selected values are given in the table below.

TABLE 16.3

$f$ (Mc/s)	43	44.9	45	45.1	47
$\Delta f$ , Mc/s (relative to 45 Mc/s)	-2	-0.1	0	+0.1	+2
Phase Angle	$-84^{\circ} 42'$	$-87^{\circ} 41'$	$-87^{\circ} 44\frac{1}{2}'$	$-87^{\circ} 48'$	$-88^{\circ} 34'$
Phase Angle Shift relative to 45 Mc/s	$+3^{\circ} 2\frac{1}{2}'$	$+3\frac{1}{2}'$	0	$-3\frac{1}{2}'$	$-49\frac{1}{2}'$
Phase Angle Error	$-1^{\circ} 52\frac{1}{2}'$	0	0	0	$+20\frac{1}{2}'$

It is clear from the above table that phase distortion due to the filter has negligible effect on the picture.

Another method of rejecting the audio signal, besides that of single sideband reception of the sidebands on the opposite side of the vision carrier to the audio carrier, is to use cathode feedback. A parallel circuit, tuned to the audio carrier, is included in the cathode lead of the first (or first two) R.F. valves as described in Section 7.9, Part I.

## 16.6. The Superheterodyne Television Receiver.

**16.6.1. Introduction.** The chief advantage of the superheterodyne over the tuned R.F. receiver is that it can more conveniently select any one of a number of different carrier frequency transmissions. This is more important in America where there are five television bands covering a range from 44 to 90 Mc/s. The disadvantages of the superheterodyne are poor signal-to-noise <sup>27</sup> ratio (particularly when no R.F. stage precedes the frequency changer), a tuning stability dependent on the frequency stability of a local oscillator, and the production of spurious frequencies,

which may be fed back to the input of the receiver to cause interference with the picture.

Signal-to-noise ratio in a superheterodyne having no R.F. amplifying stages is low because the frequency changer generally produces more noise and gives less amplification to the signal than a R.F. amplifier. The local oscillator, too, adds its own quota to the total noise. The special types of frequency changer, such as the hexode or heptode, take a much larger cathode current than a R.F. amplifier valve and their equivalent shot-noise resistance is consequently very high (of the order of  $0.25\text{ M}\Omega$ ). Hence they are not very suitable for use in receivers employing no R.F. stage. American practice, which often omits the R.F. stages, uses a pentode frequency changer with the local oscillator voltage applied to the grid-cathode circuit. This is the most efficient method of frequency changing for a given total cathode current, and the equivalent noise resistance can be reduced to quite a low value (about  $10,000\ \Omega$ ) when a high  $g_m$  pentode is used. A still lower equivalent noise resistance (about  $7,000\ \Omega$ ) can be obtained by using a triode valve as a frequency changer, but its conversion gain is low—it may be less than unity—so that higher amplification is needed from the I.F. stages to achieve a given sensitivity.

In the superheterodyne receiver it is normal to accept audio and vision signals up to the frequency changer output and to provide two separate I.F. channels. Frequency stability of the local oscillator is therefore more important from the point of view of the audio than of the vision signal, because the tuned circuits in the audio I.F. amplifier have much sharper selectivity. They may, however, be given a wider pass-band ( $\pm 50$  to  $\pm 100$  kc/s) than that ( $\pm 20$  kc/s) normally required for high fidelity amplitude modulated reception. There is usually a slight reduction in signal-to-noise ratio with the wider pass-band. Discrimination against the audio signal is carried out in the vision I.F. amplifier by means of special rejection circuits.

Full discussion of the types of interference frequencies produced by the frequency changer is found in Section 5.4, Part I, and Section 15.7. The chief cause of interference with the television signal is I.F. harmonic feedback into the signal circuits. These I.F. harmonics can be produced in the I.F. amplifier and are normally present across the detector load resistance in the form of a R.F. ripple. If these fall within the television signal pass-band and are fed back into the signal circuits, they may cause chequerboard patterns or alternate streaks of light and shade to appear across

the picture. The effect can be reduced to negligible proportions by careful shielding of components likely to produce I.F. harmonics, decoupling of all circuits (frequency changer, I.F. amplifier, detector to V.F. amplifier connection, and the V.F. amplifier) so as to prevent I.F. harmonics from entering the H.T. supply. Careful selection of the intermediate frequency and reduction of the I.F. amplifier pass-band by employing single sideband reception are also important.

Single sideband I.F. reception is almost a necessity in the superheterodyne, if adequate amplification and selectivity are to be obtained with a level frequency response over the pass-band range. This calls for careful tuning, otherwise there may be serious phase distortion producing a picture in relief, or attenuation distortion with loss of definition. Generally the best tuning position is with the carrier tuned outside the pass range to a point where amplification is one-half maximum. There can never be an abrupt cut-off outside the pass range, and double sideband reception of the lower modulation frequencies nearest the carrier occurs. Unless the carrier is detuned to about one-half amplitude, this double sideband reception results at the detector output in an accentuated low-frequency response with an apparent lack of definition. The English system of double sideband transmission allows selection of either sideband to be made; since the sound signal is lower in frequency than the vision, better discrimination against it can be realized in the vision I.F. amplifier by using the upper vision sideband. Vestigial sideband transmission (the upper vision sideband with 750 kc/s of the lower sideband) has been adopted in America and the vision I.F. carrier is tuned outside the level part of the I.F. pass range to one-half amplitude. The vision and audio I.F. amplifiers are lined up together so that when the audio signal is correctly tuned, the vision carrier is correctly located on the side of the I.F. response curve, i.e., the output from the audio receiver acts as a tuning indication. Vestigial sideband transmission is used in preference to single sideband because it is difficult to achieve a sharp cut-off of all sidebands below the carrier frequency without appreciable phase distortion of those above the carrier.

To demonstrate the design features of a superheterodyne receiver, we shall consider the American system of television transmissions, each in different, sometimes adjacent, frequency bands, because it leads to a more complex receiver than does the single English transmission. Each frequency band is 6 Mc/s wide, the vision carrier is 1.25 Mc/s from the lowest frequency of the 6 Mc/s pass-band, e.g., the carrier frequency for the band 44 to 50 Mc/s, is



45.25 Mc/s. Vestigial sideband transmission provides for 750 kc/s of the lower vision sideband and 4 Mc/s of the upper. The associated audio carrier is 4.5 Mc/s above the vision carrier, viz., 49.75 Mc/s for the band specified, and 0.25 Mc/s from the upper edge of the 6 Mc/s band. There are four other television bands, 50 to 56, 66 to 72, 78 to 84, and 84 to 90 Mc/s, and it will be seen that first and last pairs are adjacent. This means that filters must be included in the vision i.f. amplifier to discriminate not only against the associated audio carrier but also against the audio carrier of the adjacent lower frequency band, for this carrier is only 1.5 Mc/s below the vision carrier.

**16.6.2. The Frequency Changer Stage.** The design of a R.F. stage preceding the frequency changer of a superheterodyne receiver is identical with that of a R.F. stage in a tuned R.F. receiver, and no further discussion is needed. Whether or not the frequency changer is preceded by a R.F. stage (or stages) depends on the type of frequency changer. If it is a heptode or hexode, a R.F. stage is essential. On the other hand, if a pentode of high  $g_m$  is used with oscillator application to the grid-cathode circuit, the equivalent noise voltage is not so much greater than that of the tuned R.F. receiver in Section 16.4. In order to make comparison between the relative noise voltages at the grid of the first valve in the two types of receiver, we shall consider the same total pass-band width as in Section 16.4, viz., 4 Mc/s. If the R.F. valve cited in that section is used as a frequency changer, it will have a conversion conductance approximately equal to  $\frac{1}{4}g_m$ , i.e., 2 mA per volt; its shot-noise resistance as a frequency changer is therefore four times its resistance as an amplifier, i.e., 6,000  $\Omega$ . Allowing for an equivalent shot-noise resistance of 2,000  $\Omega$  for the oscillator valve, we have a total shot-noise resistance of 8,000  $\Omega$  for the valve as a frequency changer. If the feeder-first tuned circuit coupling is the same as that in Section 16.4 having a loss of 3 db., the noise voltage at the grid of the frequency changer is

$$\begin{aligned} E_n &= 1.25 \times 10^{-10} \sqrt{(8,000 + 2,650) \times 4 \times 10^6} \\ &= 25.8 \mu\text{V}, \end{aligned}$$

which is 1.6 times greater than that of the valve as a R.F. amplifier. This is not a large increase and it could be tolerated except for receivers operating at the edge of the service area of a transmitter. It should, however, be noted that as  $g_c$  is only  $\frac{1}{4}g_m$ , greater i.f. amplification is needed for the same overall gain as the tuned R.F. receiver. Since the pass-band width and minimum tuning

capacitance are the same for both types of receiver, the amplification of each I.F. stage cannot exceed that of a R.F. stage, so that an extra stage is needed in the superheterodyne receiver.

A heptode or hexode frequency changer has an equivalent shot-noise resistance of about  $0.25 \text{ M}\Omega$ , hence the noise voltage at the grid of this type of valve is

$$\begin{aligned} E_n &= 1.25 \times 10^{-10} \times \sqrt{(250,000 + 2,650) \times 4 \times 10^6} \\ &= 125.6 \mu\text{V}, \end{aligned}$$

which is 7.8 times greater than for the R.F. amplifier. The need for a R.F. amplifier in this case is obvious. Suppose we include the first R.F. stage of Section 16.5 before the frequency changer. The equivalent noise resistance in the frequency changer grid is  $251,325 \Omega$  (note that the resonant impedance of the secondary of the tuned transformer of Fig. 16.3 is  $\frac{R_{D^4}}{2} = 1,325 \Omega$ ), and

$$E_n = 1.25 \times 10^{-10} \sqrt{251,325 \times 4 \times 10^6} = 125.3 \mu\text{V}.$$

The additional equivalent noise voltage at the grid of the R.F. valve is this voltage divided by the gain (9.45) of the R.F. stage, i.e.,  $13.28 \mu\text{V}$ . The total equivalent noise voltage at the grid of the R.F. valve, including that due to R.F. valve and first tuned circuit, is

$$E_n = \sqrt{(16.1)^2 + (13.28)^2} = 20.85 \mu\text{V},$$

which is half-way between that of the R.F. valve used as an amplifier and that of the same valve used as a frequency changer. The use of two R.F. stages before the frequency changer reduces the equivalent frequency changer noise voltage at the grid of the first R.F. valve to 1.405, which makes practically no difference to the total noise voltage.

Another method of calculating the overall effect of noise in the frequency changer valve is to refer the total equivalent noise resistance in its grid circuit to the grid circuit of the R.F. valve by dividing the resistance by the square of the gain of the R.F. stage. The gain must be squared because noise resistance is proportional to the square of the noise voltage. Thus the equivalent frequency changer noise resistance at the grid of the R.F. valve is 2,810, giving a total resistance of  $4,150 + 2,810 = 6,960$  or

$$E_n = 1.25 \times 10^{-10} \sqrt{6,960 \times 4 \times 10^6} = 20.85 \mu\text{V}.$$

For two R.F. stages the frequency changer equivalent shot-noise resistance falls to  $31.6 \Omega$ .

Turning now to the design of the frequency changer stage,



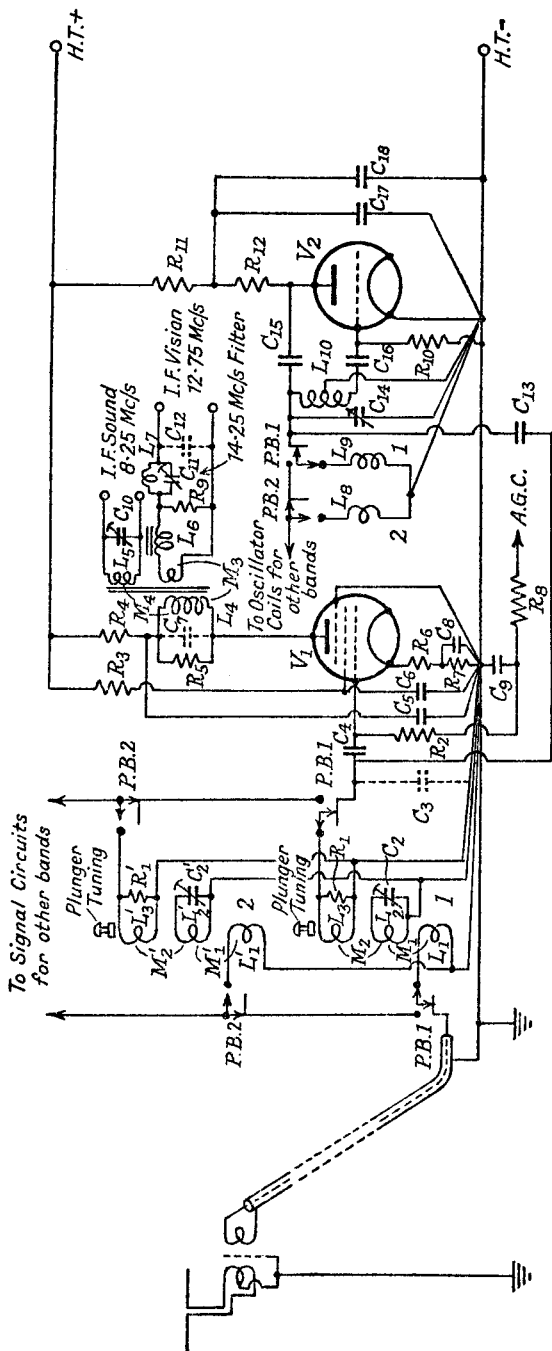


Fig. 16.5.—The Aerial and Frequency Changer Stages of a Superheterodyne Television Receiver.



$\omega L_2$ , must give a  $Q$  of 15.75 (neglecting losses in  $L_2$ ). Thus, when  $\omega L_1 \ll R_{a1}$ ,  $\omega L_2 / \omega^2 M_1^2 / R_{a1} = 15.75$  gives  $M_1 = 0.063 \mu\text{H}$ . In order to satisfy the condition that  $\omega L_1 \ll R_{a1}$ ,  $L_1$  should be as small as possible; it is fixed by the maximum possible coupling coefficient, which may be taken as 0.4. Thus

$$k = 0.4 = \frac{M_1}{\sqrt{L_1 L_2}}$$

or  
and

$$L_1 = 0.1085 \mu\text{H}$$

$$\omega L_1 = 30.7 \Omega.$$

The chief effect of  $L_1$  is to introduce a reactive as well as resistive component into the  $L_2 C_2$  circuit, but this may be compensated by retuning  $L_2 C_2$ . In the above example the circuit  $L_2 C_2$  is assumed to be tuned to 45 Mc/s in order to facilitate comparison with previous calculations based on the English transmission. For the American system the circuit is capacitance-tuned to the centre of each band, e.g., 47 Mc/s for the 44 to 50 Mc/s band. The grid coil  $L_3$  must be made as large as possible in order to obtain maximum transfer voltage ratio, and no tuning capacitance other than the wiring and valve capacitance, shown dotted as  $C_3$ , is used. Tuning of this circuit is accomplished by eddy current tuning of  $L_3$ . The plunger is inserted at the end of  $L_3$  opposite to  $L_2$ , so that variation of  $L_3$  has practically no effect on  $L_2$  or the mutual inductance coupling  $M_2$  between  $L_3$  and  $L_2$ . The coils  $L_1$ ,  $L_2$  and  $L_3$  are usually all wound on the same former,  $M_1$  being adjusted for optimum coupling between  $L_1$  and  $L_2$ , and  $M_2$  for the correct pass-band width of 4.5 Mc/s, which covers both vision and audio sidebands. The push-button switching is arranged so that all but the coils associated with the particular band are disconnected.

The grid input resistance of the frequency changer will be comparable with its resistance as an amplifier, and its value will determine the value of resistance  $R_1$  in parallel with  $L_3$ . It is quite common American practice to apply a.g.c. to the television receiver, and when the frequency-changer valve is controlled it is important that its input resistance and capacitance should not vary appreciably with change of bias, otherwise the grid circuit is off-tuned and its pass-band reduced as bias is increased. Accordingly an unby-passed resistance  $R_s$  (about  $50 \Omega$ ) is included in the cathode lead as described in Section 4.10.3. This resistance introduces negative feedback, and reduces the conversion gain of the frequency changer to about 65% of its value without the resistor. It increases input resistance, which means that  $R_1$  must be decreased, and changes

of input resistance therefore have less effect. Mutual inductance or capacitance coupling is employed between the oscillator and grid-tuned circuit to produce an oscillator peak voltage of 3 volts between grid and cathode of the frequency changer. The latter may have cathode self-bias as in Fig. 16.5, or when A.G.C. is not applied it may be biased by grid current. The extra damping due to grid conduction current is negligible compared with the input resistance of the valve if a comparatively high grid leak,  $R_2$  (0.5 M $\Omega$ ) is employed.

The values of the other components in the frequency changer section of Fig. 16.5 are

$$\begin{aligned} R_3 &= 50,000 \Omega, & R_4 &= 1,000 \Omega, & R_6 &= 50 \Omega, \\ & & R_7 &= 300 \Omega, & R_8 &= 0.5 \text{ M}\Omega. \\ C_2 &= 30 \mu\mu\text{F (max.)}, & C_4 &= 50 \mu\mu\text{F}, & C_5 &= 0.001 \mu\text{F}, \\ C_6 &= 0.001 \mu\text{F}, & C_8 &= 0.001 \mu\text{F}, & C_9 &= 0.01 \mu\text{F}. \end{aligned}$$

The heater leads are not shown in the diagram, but they are decoupled to earth by 0.001  $\mu\text{F}$  mica capacitors.

**16.6.3. The Oscillator.** A separator oscillator valve is almost an essential requirement for the high frequencies involved in television reception, because it is not possible to obtain a high enough  $g_m$  and low enough  $R_a$  for satisfactory operation from a triode and frequency changer combined in the same bulb. The types of oscillator circuit most often used are the Hartley or Colpitts, or modified forms of these. In most cases fine tuning is carried out by means of a small trimmer capacitance,  $C_{14}$  (2–5  $\mu\mu\text{F}$ ) in Fig. 16.5, across a part of the coil from anode or grid to earth. With the modified Hartley circuit of Fig. 15.6, the trimmer is placed across the whole coil.

Frequency stability is all important and care should be taken to carry out the principles laid down in Section 6.9, Part I, and Section 15.6. A negative temperature coefficient capacitor may finally be connected across a whole or part of the coil to compensate for the fall in frequency, which is associated with the normal increase in inductance and capacitance as the temperature rises. From the point of view of stability, oscillator frequency should be less than the signal frequency, but in American receivers it is generally greater than the signal frequency because this gives a lower I.F. for the sound signal. The disadvantage of the lower oscillator frequency is that the image frequency falls in a short wave range normally occupied by a large number of transmissions.

Change of range of oscillator frequency is usually accomplished

by switching coils in parallel with a part of the main tuning coil by push-button switches as shown in Fig. 16.5. Coupling to the frequency changer is by capacitance  $C_{13}$  (about 2 to 5  $\mu\mu\text{F}$ ) or by mutual inductance from the oscillator to signal circuit. This is possible because correct adjustment of oscillator amplitude can be made for each television band since the signal circuits are preset tuned. Typical values for the remaining components of the oscillator circuit are

$$R_{10} = 50,000 \Omega, \quad R_{11} = 5,000 \Omega, \quad R_{12} = 15,000 \Omega.$$

$$C_{15} = C_{16} = 20 \mu\mu\text{F}, \quad C_{17} = 0.001 \mu\text{F} \text{ (mica)}, \quad C_{18} = 2 \mu\text{F} \text{ (paper)}.$$

The capacitance  $C_{18}$  is intended to decouple the oscillator from any low-frequency components present in the H.T. source.

**16.6.4. The I.F. Amplifier.** The most serious form of interference in television superheterodyne reception is that from intermediate frequency harmonics, and not, as in sound broadcast reception on medium and short waves, that from oscillator harmonic and image signal responses. Provided the oscillator frequency is greater than the signal frequency, image signal response presents hardly any problem, though it may become more important as more use is made of the ultra high-frequency band. With the English system of audio signal lower than the vision, the lower oscillator frequency has the advantage of giving an audio I.F. lower than the vision I.F.

Referring to the English system of audio and vision carriers at 41.5 and 45 Mc/s, it is clear that an I.F. equal to the difference (or a multiple of this) between the two carriers, viz., 3.5, 7, 10.5, 14 Mc/s, etc., should be avoided. Since feedback of I.F. harmonics is the greatest source of interference, a submultiple frequency of the vision carrier, 22.5, 15, 11.25, 9 and 7.5 Mc/s, must not be employed for the vision I.F. carrier. The width of the vision sidebands, 2 Mc/s, precludes the use of a low I.F., and too high a value is unsatisfactory because it is then more difficult to discriminate against the associated audio signal, and also to I.F. harmonics, which happen to fall in the I.F. range. On the other hand, image signal response is reduced by a high I.F. From the point of view of overall amplification it does not matter what value of I.F. is chosen when the pass-band width and minimum tuning capacitance are fixed, because the resonant impedances of any tuned circuits are then independent of  $f_m$ , e.g.,

$$R_D = \frac{Q}{\omega C}$$



and for a fixed pass-band width  $QF = \text{constant}$ ,  $A$ ,

$$\text{hence} \quad Q = \frac{Af_m}{2\Delta f}$$

$$\text{Therefore} \quad R_D = \frac{Af_m}{2\pi f_m 2\Delta f C} = \frac{B}{\Delta f C} \propto \frac{1}{\Delta f C} = \text{constant}$$

when  $\Delta f$  and  $C$  are constant.

For a vision frequency band from 43 to 47 Mc/s, we find i.f. harmonic interference is possible over the following frequency ranges, 8.6 to 9.4, 10.75 to 11.75, 14.33 to 15.66, 21.5 to 23.5 Mc/s—we need not consider lower than the 5th submultiple—with clear reception from 9.4 to 10.75 (1.35), 11.75 to 14.33 (2.58), and 15.66 to 21.5 (4.83) Mc/s. Assuming single sideband i.f. reception (2 Mc/s total pass-band) with the upper sideband, a vision i.f. carrier of about 12 Mc/s is the lowest possible value; the i.f. audio carrier would be 8.5 Mc/s. Actually a lower i.f. (4.25 Mc/s with audio at 750 kc/s) has been successfully employed with narrowed sideband response. However, the general trend of television development is towards greater picture detail so that an i.f. of the order of 12 Mc/s is a better proposition. In America the vision i.f. carrier has been standardized at 12.75 Mc/s with 8.25 Mc/s for its associated audio carrier.

The circuits employed in the i.f. amplifier may consist of single-tuned circuits, having staggered resonant frequencies to cover the wide pass-band, coupled tuned circuits, or band-pass filters of the derived type with rejection frequencies for the associated audio programme and any other transmission likely to cause interference. The objection to single-tuned circuits with staggered resonant frequencies is that overall amplification is lower than for coupled circuits of the same pass-band width, and there is a danger of overloading the last stage in the amplifier unless the last tuned circuit has a flat frequency response over the pass range. Band-pass filters<sup>10</sup> generally require a low terminating impedance to give a practical value of capacitance element, and therefore stage gain tends to be low. Coupled tuned circuits<sup>29</sup> are the most popular type.

Coupled tuned circuits provide two possible methods of obtaining a flat overall frequency response; either each pair can be designed for a substantially flat response, or a combination of single- and double-peaked responses may be used. The former involves heavy damping and low  $Q$  values with consequent low amplification per stage; a combination of single- and double-peak responses is

therefore preferable because greater amplification can be realized. Overall phase distortion can also be reduced by suitably combining single- and double-peaked circuits, the distortion in single-peaked circuits often being in the opposite direction to that in double-peaked circuits. Excessive double-peaked response must be avoided, otherwise phase distortion (see Table 16.4) may become excessive ; for best compensation of attenuation distortion the value of  $QF$  at which the peak occurs should correspond to the edge of the pass-band, i.e.,  $\Delta f$  remains the same as the peak moves farther from the mid-frequency, and  $Q$  must be increased to satisfy the higher value of  $QF$ . Mutual inductance or capacitance coupling may be provided between the tuned circuits ; the advantages of capacitance coupling are that inductance tuning can be carried out without affecting the coupling, and adjustment of one side only of the response curve with respect to the mid-frequency is possible. However, mutual inductance coupling can be made almost independent of inductance tuning if the mutual inductance is obtained by coupling a part only of one coil to the other, and adjustment of one side only of the response curve is possible by variation of the resonant frequency of either circuit, i.e., by varying coil inductance. If the stray capacitances across primary and secondary coils can be controlled within as good a limit as the inductances, tuning may be dispensed with ; alternatively one circuit only may have variable tuning and be made to compensate for variations in the other one. If capacitance tuning is used in the latter case, it is better included on the secondary side because the input capacitance of a valve is generally higher than its output capacitance. The trimmer capacitance has a certain minimum value and the ratio increase in tuning capacitance is less, and therefore the ratio decrease in amplification less, by adding the trimmer to the higher initial capacitance circuit. Lower stage gain is, of course, inevitable with capacitance tuning.

To estimate the overall amplification required of the I.F. stages, let us imagine that the aerial circuit and frequency changer valve are as in Section 16.6.2, and that an output of 5 volts peak is required at the detector. The equivalent noise voltage at the grid of the frequency changer is  $25.8 \mu\text{V}$ , so that a signal-to-noise ratio of 30 db. fixes the minimum input signal at  $817 \mu\text{V}$ , and the total amplification required from the grid of the frequency changer to the detector is  $\frac{5 \times 10^6}{817} = 6,130$ . Allowing a frequency changer conversion gain  $\frac{1}{4}$  that of an I.F. stage and an I.F. stage gain of 13, we need three stages of I.F. amplification after the frequency changer,

and four pairs of I.F. coupled circuits. The pass-band of the R.F. tuned circuit before the frequency changer is wider than the I.F. pass-band (it has to include the audio signal as well), and we shall therefore neglect its effect on the overall frequency response in and around the I.F. pass range.

The design of the I.F. amplifier, which is detailed below, is considered with respect to the American form of multichannel vestigial sideband transmission, so that the vision I.F. carrier has to be tuned to a point on the side of the overall selectivity curve where the frequency response is one-half that of the average response over the pass-band. As 750 kc/s of the lower sideband is transmitted, it means that the flat pass-band response should begin about 500 kc/s above the vision I.F. carrier, the upper limit of the sidebands is 4 Mc/s, giving an effective overall pass-band of 3.5 Mc/s. Taking the band 50 to 56 Mc/s, for which the vision carrier is 51.25 Mc/s, the maximum upper sideband frequency, 55.25 Mc/s, and the associated audio carrier frequency, 55.75 Mc/s, an oscillator frequency of 64 Mc/s gives an I.F. vision carrier of 12.75 Mc/s, and a vision pass range from 12.25 to 8.75 Mc/s with a mid-frequency of 10.5 Mc/s. The associated audio carrier is 8.25 Mc/s and there is also the audio carrier (49.75 Mc/s) of the adjacent transmission producing an I.F. of 14.25 Mc/s. Special discrimination is needed against both these frequencies, and the filter circuits needed to suppress them may have considerable influence on the frequency response of the vision pass-band, particularly at the edges; the I.F. coupled circuits should therefore be designed in association with the filters. This, however, tends to mask some of the properties of the coupled circuits, and in this section we shall consider the performance of the latter only, leaving to the next section an examination of the I.F. amplifier with special filters, but noting that an overall response peaked at the edges of the pass-band will be an advantage in compensating for the attenuation caused by the filters.

When selecting the desired response of each pair of coupled circuits, we cannot afford to have single-peaked couplings less than critical because this entails loss of stage gain (maximum transfer

impedance for couplings less than critical equals  $\frac{R_{D1}Q_2k\sqrt{\frac{L_2}{L_1}}}{1+Q_1Q_2k^2}$ ).

However, the overall reduction of amplification is usually less than the stage gain reduction due to using under-coupled circuits, since

a level pass-band response calls for increased coupling in the double-peaked circuits and also a higher  $Q$  value, which therefore tends to give a higher trough stage gain at the mid-frequency,  $f_m$ . For the four pairs of coupled circuits, let us select three of  $Qk = 1.5$ , each having a peak-to-trough ratio of 0.7 db. with the peaks at  $QF = \pm 1.12$  (see Section 7.3, Part I), and one of  $Qk = 1$  with a fall of  $-1.8$  db. at  $QF = \pm 1.2$ . If  $Q$  is chosen to satisfy the values of  $QF$  quoted above at  $\Delta f = \pm 1.75$  (the total required pass-band is 3.5 Mc/s), there is a rise in the frequency response curve from the mid-frequency (10.5 Mc/s) to the edges of the pass-band. Maximum response of  $+0.9$  db. occurs at  $\Delta f = \pm 1.45$  Mc/s and at  $\Delta f = \pm 1.75$  Mc/s the response is  $+0.3$  db. with respect to, that at the mid-frequency. As stated above, this increase is an aid when the sound signal filters are incorporated. Component values for the coupled circuits are as follows: taking first the overcoupled circuits ( $Qk = 1.5$ ),  $QF = 1.12$  at  $\Delta f = 1.75$  Mc/s gives

$$Q = \frac{1.12f_m}{2\Delta f} = \frac{1.12 \times 10.5}{3.5} = 3.36.$$

For maximum stage gain the tuning capacitance must be a minimum and this may be taken as  $15 \mu\mu\text{F}$ . Referring to the typical I.F. amplifier circuit of Fig. 16.6 (valve  $V_4$  stage),  $C_{34} = C_{35} = 15 \mu\mu\text{F}$ ,  $L_{17} = L_{18} = 15.3 \mu\text{H}$ ,  $k = \frac{1.5}{Q} = 0.446$ ,  $M_6 = 0.446 \times 15.3 = 6.82 \mu\text{H}$  and

$$R_D = \frac{Q}{\omega C_{34}} = \frac{3.36 \times 10^6}{6.28 \times 10.5 \times 15} = 3,400 \Omega.$$

If the  $g_m$  of the I.F. valve is 8 mA/volt, the stage gain at the peaks of the frequency response is  $\frac{1}{2}g_m R_D = \frac{8 \times 3,400}{2 \times 10^3} = 13.6$ , or at 10.5 Mc/s is  $13.6 \times 0.923 = 12.55$  (the factor 0.923 takes into account the trough to peak ratio of  $-0.7$  db.). The damping resistances  $R_{25}$  and  $R_{28}$  are calculated, using the method applied for the R.F. amplifier in Section 16.5; the valve input resistances are much higher, approximately in proportion to the reciprocal of the square of the frequency ratio, i.e., about 100,000  $\Omega$ . If grid-bias control of the I.F. valve is employed some method of stabilizing grid input capacitance is necessary, and in Fig. 16.6 negative feedback stabilization with the unby-passed resistances  $R_{17}$  and  $R_{26}$  (about 50  $\Omega$ ) is shown. The values of the anode decoupling resistances ( $R_{16}$  and  $R_{24}$ ) are 1,000  $\Omega$ , the screen potential dividers,  $R_{14}R_{15}$  and  $R_{22}R_{23}$ , consist of 30,000 and 20,000  $\Omega$  resistances, the

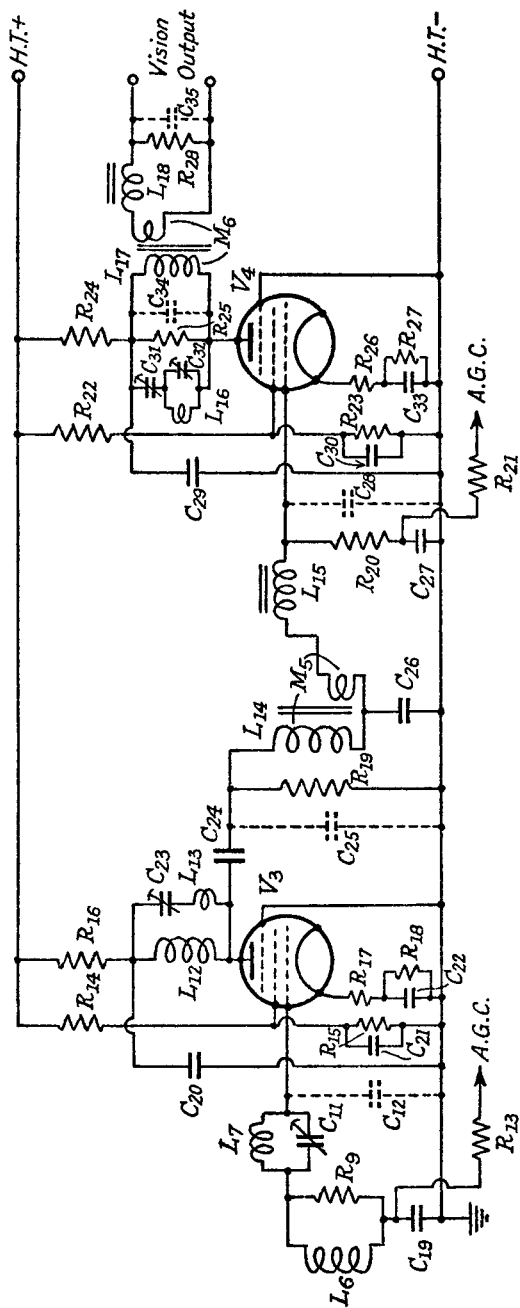


FIG. 16.6.—I.F. Amplifier Circuits of a Television Receiver with Audio Signal Rejector Circuits.

bias resistances  $R_{18}$  and  $R_{27}$  are  $150 \Omega$ , and decoupling capacitances  $C_{20}$ ,  $C_{21}$ ,  $C_{22}$ , etc., are  $0.01 \mu\text{F}$  (mica). The A.G.C. filter for the valve  $V_3$  stage is made up of  $C_{19}$  ( $0.1$  to  $0.5 \mu\text{F}$ ) and  $R_{13}$  ( $0.5 \text{ M}\Omega$ ).

For the critically coupled stage  $QF = 1.2$ ,  $Q = 3.6$ , and  $R_D = 3,640 \Omega$  ( $C_7$  and  $C_{12}$  in Fig. 16.5 are  $15 \mu\text{F}$ ), which gives a stage gain for the frequency changer of  $3.64$  if  $g_c = 2 \text{ mA/volt}$ . The total overall amplification is therefore  $7,200$  times, which more than satisfies the requirement originally postulated. This calculated gain ignores the reduction in amplification due to the negative feedback caused by resistances  $R_{17}$  and  $R_{28}$  in Fig. 16.6. Stage gain may be reduced to  $75\%$  of its normal value by the inclusion of these resistances, and when they are used an extra I.F. stage will be needed to reach the desired overall amplification of  $6,130$  times.

Since the gains of the I.F. amplifier stages are comparable with those of the tuned R.F. amplifier, and the mid-frequency is only one-quarter of the signal frequency, it follows that anode-grid interelectrode capacitance feedback, which was very small in the case of the R.F. amplifier, will be negligible in the I.F. amplifier.

Phase distortion can be checked in the manner described in Section 16.4. Since single sideband reception is being used the reference point is no longer the mid-frequency  $10.5 \text{ Mc/s}$ , but the vision carrier frequency  $12.75 \text{ Mc/s}$  and the curves in Fig. 16.4 are not applicable. The phase angles, derived from expression 16.2b, are tabulated on page 398 against  $QF$  for the two values of coupling  $Qk = 1$  and  $1.5$ . The modulation frequency corresponding to each  $QF$  value, and the phase angle error are also listed. The correct angle for zero distortion is calculated for the circuits of  $Qk = 1.5$  by subtracting from  $68^\circ 24'$  the phase angle difference between  $QF = +1.45$  and  $+1.4$  multiplied by  $20$  times the difference between the particular value of  $QF$  being considered and  $QF = 1.45$ . The latter value does not quite correspond to the vision I.F. carrier frequency ( $12.75 \text{ Mc/s}$ ), which gives  $QF = 1.44$ , but is sufficiently close for all practical purposes. Similarly, for the critically coupled circuit of  $Qk = 1$ ,  $QF = 1.55$  is taken as the reference point though  $QF = 1.545$  actually gives the vision carrier frequency.

The overall phase angle error is obtained by multiplying the error for  $Qk = 1.5$  by  $3$ , and adding to it the error for  $Qk = 1$ . Thus at modulation frequencies of  $3$  and  $4 \text{ Mc/s}$  the overall errors are  $-87^\circ$  ( $-106^\circ + 19^\circ$ ) and  $-104^\circ$  ( $-133^\circ + 29^\circ$ ), and these correspond to time delays of  $0.0805$  and  $0.0723 \mu \text{ secs}$ . respectively, which are satisfactory. Maximum time delay occurs at a modulation frequency at  $3 \text{ Mc/s}$ .

TABLE 16.4

$QF$ .	$f_{mod.}$ (Mc/s).	$\phi$ (actual).	Phase Angle Error.	$f_{mod.}$ (Mc/s).	$\phi$ (actual).	Phase Angle Error.
+ 1.55	0	- 97° 24'	—	—	—	—
+ 1.5	0.07	- 94° 46'	0	—	—	—
+ 1.45	—	—	—	0	- 68° 24'	—
+ 1.4	0.21	- 89° 11'	+ 0° 19'	0.06	- 65° 16'	0
+ 1.3	0.35	- 83° 12'	+ 1° 2'	0.22	- 59° 2'	- 0° 2'
+ 1.2	0.5	- 76° 52'	+ 2° 6'	0.375	- 52' 59'	- 0° 15'
+ 1.1	0.65	- 70° 15'	+ 3° 27'	0.53	- 47° 10'	- 0° 42'
+ 1.0	0.8	- 63° 26'	+ 5°	0.70	- 41° 38'	- 1° 26'
+ 0.8	1.1	- 49° 38'	+ 8° 16'	1.0	- 31° 29'	- 3° 49'
+ 0.6	1.375	- 36° 12'	+ 11° 10'	1.31	- 22° 33'	- 7° 25'
+ 0.4	1.73	- 23° 30'	+ 13° 20'	1.625	- 14° 31'	- 11° 55'
+ 0.2	1.96	- 11° 32'	+ 14° 46'	1.94	- 7° 6'	- 17° 2'
0	2.25	0	+ 15° 46'	2.25	0	- 22° 28'
- 0.2	2.54	+ 11° 32'	+ 16° 46'	2.56	+ 7° 6'	- 27° 54'
- 0.4	2.83	+ 23° 30'	+ 18° 12'	2.875	+ 14° 31'	- 33° 1'
- 0.6	3.125	+ 36° 12'	+ 20° 22'	3.19	+ 22° 33'	- 37° 31'
- 0.8	3.365	+ 49° 38'	+ 23° 16'	3.5	+ 31° 29'	- 41° 7'
- 1.0	3.71	+ 63° 26'	+ 26° 32'	3.81	+ 41° 38'	- 43° 30'
- 1.1	3.85	+ 70° 15'	+ 28° 5'	3.98	+ 47° 10'	- 44° 14'
- 1.2	4.0	+ 76° 52'	+ 29° 26'	4.125	+ 52° 59'	- 44° 41'
$Qk$	1	1	1	1.5	1.5	1.5

Expression 7.2c, Part I, enables the attenuation at the two audio carrier frequencies of 8.25 and 14.25 Mc/s to be calculated, and they are tabulated below. The reference point for 0 db. is taken as the value of  $|Z_T|$  at  $f_m$  and not the maximum value as is done in Section 7.4, Part I. Thus for three circuits of  $Qk = 1.5$  and one of  $Qk = 1$ , the following results are obtained.

TABLE 16.5

Audio Carrier Frequency (Mc/s).	$Af$ (Mc/s).	$QF$	$Qk$	Attenuation per stage (db.).	Total Attenuation (db.).
8.25	- 2.25	- 1.44	1.5	+ 0.4	- 2.66
		- 1.545	1.0	- 3.86	
14.25	+ 3.75	+ 2.4	1.5	- 4.44	- 24.12
		+ 2.58	1.0	- 10.8	- 24.12

A positive sign in the above represents a gain and a negative sign a loss. A point to be noted is that the vision carrier frequency loss

is the same as that at the lower audio carrier, viz.,  $-2.66$  db., and it is not sufficient to reduce the carrier to half amplitude ( $-6$  db.); however, the trap circuits for  $14.25$  Mc/s will introduce a loss at this frequency and the total loss at  $12.75$  Mc/s will be greater than that shown for  $8.75$  Mc/s in the table.

It is clear from the above that the attenuation at  $8.25$  and  $14.25$  Mc/s is insufficient, and we shall now consider the types of filter for rejecting these frequencies.

**16.6.5. Audio Signal I.F. Filter Circuits.**<sup>24</sup> Special care has to be exercised in the design of filter circuits required for suppressing undesired audio transmissions, otherwise the vision signal pass-band response may be seriously affected by the addition of the filter or trap circuit. It is better to employ a number of filters, each having equal attenuation at the rejection frequency rather than a single filter of the same total attenuation, because a series of filters produces a much sharper attenuation characteristic with less attenuation and phase distortion at the edges of the vision pass-band. To avoid cross-modulation the filters should be incorporated in the early stages of the I.F. amplifier.

The filter generally consists of a series or parallel circuit, tuned to the frequency it is desired to reject, and examples of some of the methods employed are shown in Figs. 16.5 and 16.6. In Fig. 16.5,  $L_5C_{10}$  is a resonant circuit coupled to the primary of the first pair of coupled circuits and acting as an absorber and also pick-up circuit for the associated audio signal.  $L_7C_{11}$  is a parallel resonant circuit which forms with the secondary tuning capacitance,  $C_{12}$ , a potential divider. A series resonant circuit,  $L_{13}C_{23}$  in Fig. 16.6 may be included in parallel with the primary or secondary to act as a shunt to the rejection frequency, and yet another type is the series parallel circuit,  $C_{31}$  and  $L_{16}C_{32}$ , of Fig. 16.6. The parallel section  $L_{16}C_{32}$  is tuned to the mid-frequency of the vision pass-band, and  $C_{31}$  is adjusted for resonance with the inductive reactance of  $L_{16}C_{32}$  at the lower audio carrier; it can only be used to reject frequencies lower than the vision frequencies, and if it is desired to reject higher frequencies  $C_{31}$  must be replaced by an inductance. Combined inductance and capacitance coupling may also be used to provide a rejection frequency; in Fig. 16.6  $M_5$  and  $C_{26}$  form a series resonant circuit, which reduces the coupling to zero at the resonant frequency. The sign of  $M$  must be positive (see Section 3.4.2, Part I).

Let us now examine in detail the absorber type of filter,  $L_5C_{10}$  in Fig. 16.5, assuming that it is coupled only to  $L_4$ , and therefore



has negligible effect on the  $L_6C_{12}$  circuit. This is not difficult to achieve in practice, particularly when  $L_6$  is split into a coupling and main section, with the latter separate from the former as shown in Fig. 16.5. The filtering action of the  $L_5C_{10}$  circuit is accomplished by virtue of the impedance it reflects into the  $L_4C_7$  circuit; this impedance has resistive and reactive components (see Section 7.6, Part I) of  $\frac{\omega^2 M_4^2}{R_5'^2 + X_5'^2} R_5'$  and  $-\frac{\omega^2 M_4^2 X_5'}{R_5'^2 + X_5'^2}$  respectively, where  $R_5'$  is the series resistance component of  $L_5$  and  $C_{10}$ , and  $X_5'$  is the series reactance component, i.e.,  $\omega L_5 - \frac{1}{\omega C_{10}}$ . It will be seen that the

reflected reactive component is negative (capacitive) when  $X_5'$  is inductive, a condition occurring when the applied frequency is greater than the resonant frequency of  $L_5C_{10}$ . The reverse is true when the frequency is less than the resonant frequency of  $L_5C_{10}$ .

This reflected impedance from  $L_5C_{10}$  modifies the transfer impedance formula of expression 7.2a, Part I, to

$$Z_T = \frac{-jR_{D1}Q_2k\sqrt{\frac{L_2}{L_1}}}{[1+A+j(Q_1F+B)][1+jQ_2F]+Q_1Q_2k^2} \quad . \quad 16.7a$$

where

$$A = \frac{\omega^2 M_4^2 R_5'}{(R_5'^2 + X_5'^2)R_1'}$$

and

$$B = -\frac{\omega^2 M_4^2 X_5'}{(R_5'^2 + X_5'^2)R_1'}$$

where  $R_1'$  is the equivalent series resistance of the primary of the transformer and is associated with  $Q_1$ .

Section 7.6, Part I, shows that the reflected impedance from  $L_5C_{10}$  effectively is in series with  $L_4$ , and the sign given to  $B$  in expression 16.7a is positive if the resonant frequency of  $L_5C_{10}$  is above the mid-frequency of the coupled circuits and negative if it is below. Assuming identical coupled circuits as for Section 16.6.4, expression 16.7a reduces to

$$Z_T = \frac{-jR_D Q k}{[1+A+j(QF+B)][1+jQF]+Q^2k^2}$$

$$|Z_T| = \frac{R_D Q k}{\sqrt{[1+Q^2(k^2-F^2)+A-BQF]^2+[2QF+AQF+B]^2}} \quad . \quad 16.7b.$$

It should be noted that  $L_5C_{10}$  has the same effect whether it is coupled to  $L_4$  or  $L_6$ , when these two circuits are identical.

The ratio loss introduced by filter at any frequency is therefore

$$\frac{|Z_T|_{+filter}}{|Z_T|} = \sqrt{\frac{[1+Q^2(k^2-F^2)]^2+[2QF]^2}{[1+Q^2(k^2-F^2)+A-BQF]^2+[2QF+AQF+B]^2}}$$

or  $\text{loss} = -20 \log_{10} \frac{|Z_T|}{|Z_T|_{+filter}} \text{ db.}$

$$= -10 \log_{10} \frac{[1+Q^2(k^2-F^2)+A-BQF]^2+[2QF+AQF+B]^2}{[1+Q^2(k^2-F^2)]^2+[2QF]^2} \quad 16.8.$$

If the coupled circuits  $L_4C_7$  and  $L_6C_{12}$  are the critically coupled pair of the previous section,  $Qk = 1$ , the value of  $QF$  corresponding to the frequency, 8.25 Mc/s, to which  $L_5C_{10}$  is tuned, is  $-1.545$ . Replacing  $Qk$  and  $QF$  in expression 16.8 by these numerical values and noting that  $B = 0$ , for  $X_5$  is zero when  $L_5C_{10}$  is resonant,

$$\begin{aligned} \text{Loss} &= -10 \log_{10} \frac{[-0.390+A_0]^2+[-(2+A_0)1.545]^2}{[-0.390]^2+[3.09]^2} \\ &= -10 \log_{10} \frac{9.712+8.78A_0+3.39A_0^2}{9.712} \\ &= -10 \log_{10} \frac{1,541.3}{9.712} \equiv -22 \text{ db.} \end{aligned}$$

if  $A_0 = 20 = \frac{\omega^2 M_4^2}{R_5' R_1'}$ .

This is a satisfactory value for the attenuation of a single filter circuit provided the effect on the vision pass-band is small. This can be checked as follows: at a frequency above the resonant frequency of  $L_5C_{10}$ , the series impedance of this circuit can be written  $Z_5 = R_5(1+jQ_5F')$ , where  $F' = \frac{2\Delta f'}{f_5}$ ,  $\Delta f'$  is the frequency

off-tune from the resonant frequency  $f_5$  of  $L_5C_{10}$  and  $Q_5 = \frac{\omega_5 L_5}{R_5'}$ ;

it is convenient to neglect the variation of  $\omega M_4$  over the frequency range considered—the error is not large and in any case the principle is applied in calculating  $Z_T$  and  $Z_5$ . Hence the value of  $A$  in expression 16.8 at frequencies above  $f_5$  is

$$A = \frac{A_0}{1+(Q_5F')^2}$$

and

$$B = -\frac{A_0 Q_5 F'}{1+(Q_5 F')^2} = -A Q_5 F'.$$

As an example, let us calculate the additional filter loss at the edge

of the vision pass-band, 8.75 Mc/s, for  $Q_s = 120$ ,  $f_s = 8.25$  Mc/s,

$$F' = \frac{+2 \times 0.5}{8.25} = +0.1212, \quad Q_s F' = +14.58, \quad A = \frac{20}{213} = 0.094,$$

$$B = A Q_s F' = -1.37, \quad QF = \frac{-1.545 \times 1.75}{2.25} = -1.2.$$

Loss

$$= -10 \log_{10} \frac{[0.56 + 0.094 - 1.37 \times 1.2]^2 + [-2.4 - 0.094 \times 1.2 - 1.37]^2}{6.064}$$

$$= -10 \log_{10} \frac{16}{6.064} \equiv -4.2 \text{ db.}$$

This procedure can be repeated for other frequencies and other values of  $Q_s$ . The additional attenuation at selected frequencies for two values of  $Q_s$ , 120 and 200 is tabulated below for the pair of overcoupled circuits ( $Qk = 1.5$ ) as well as the critically coupled circuits.  $A_0$  is constant at 20, so that the additional attenuation at the rejection frequency 8.25 Mc/s is practically constant at -22 db. A positive sign before the attenuation value indicates a gain and a negative a loss.

TABLE 16.6

$f$ (Mc/s).	Additional Attenuation (db.) due to Filter.				Coupled Circuits only.	Overall Response Coupled Circuits plus Filter.	
10.5	- 0.08	- 0.06	- 0.02	negligible	0	- 0.06	0
9.25	- 1.46	- 0.12	- 0.74	- 0.4	+ 0.52	+ 0.40	+ 0.48
8.75	- 4.2	- 1.93	- 2.52	- 0.8	+ 0.7	- 1.23	- 0.1
8.25	- 22	- 21.76	- 22	- 21.76	+ 0.4	- 21.36	- 21.36
$Qk$	1	1.5	1	1.5	1.5	1.5	1.5
$Q_s$	120	120	200	200		120	200

The need for the highest possible value for  $Q_s$  is plainly shown by the table, but an almost more important feature is the reduced attenuation at the edge of the vision pass-band brought about by using overcoupled circuits. The response of the overcoupled circuits of  $Qk = 1.5$  is set out in the sixth column, and in the seventh and eighth the overall frequency response of overcoupled circuits and filter is shown. An almost flat response is obtained for  $Q_s = 200$ , but the more likely practical value of  $Q_s$  is 120, and this produces a maximum variation of 1.63 db. over the range from 10.5 to 8.75 Mc/s. A slight reduction and better distribution of the

frequency response variation can be obtained by combining the frequency response of the absorber and coupled circuits with that of another pair of coupled circuits of  $Qk = 1.5$ ; the combined response ( $Q_s = 120$ ) then varies from  $+0.92$  db. at  $9.25$  to  $-0.53$  db. at  $8.75$  Mc/s. If a more level frequency response is desired over the pass-band the attenuation at the rejection frequency must be reduced; for example, if  $A_0$  is reduced to  $10$ , the following results are obtained with the overcoupled circuits:

TABLE 16.7

$Qk = 1.5$ ,  $QF = -1.12$  at  $\Delta f = -1.75$  Mc/s,  $f_m = 10.5$  Mc/s,  $A_0 = 10$ ,  
 $Q_s = 120$

$f$ (Mc/s).	Attenuation (db.).	Coupled Circuits plus Filter.
10.5	0	0
9.25	- 0.15	+ 0.37
8.75	- 0.68	+ 0.02
8.25	- 16.3	- 15.9

The advantage of using more filters (three would be required instead of two for an overall attenuation of not less than  $-40$  db.), to obtain a given attenuation is clearly shown.

Since the overcoupled circuits of  $Qk = 1.5$  produce a better pass-band frequency response than the critically coupled circuits, it is necessary to see if greater couplings might with advantage be employed. Thus the frequency response for a coupling of  $Qk = 2$  has a peak of  $+1.95$  db. at  $QF = \pm 1.732$  compared with the trough value at  $QF = 0$ , and letting this value of  $QF$  correspond to  $\Delta f = -1.75$  ( $f = 8.75$  Mc/s), the following results are obtained for  $A_0 = 20$ .

TABLE 16.8

$Qk = 2$ ,  $QF = -1.732$  at  $\Delta f = -1.75$  Mc/s,  $f_m = 10.5$  Mc/s,  $A_0 = 20$

$f$ (Mc/s).	Attenuation (db.).		Coupled Circuits only.	Overall Response Coupled Circuits plus Filter.	
	Very small	Very small			
10.5	Very small	Very small	0	0	0
9.25	+ 0.24	+ 0.25	+ 1.4	+ 1.64	+ 1.65
8.75	- 1.9	- 0.75	+ 1.95	- 0.05	+ 1.20
8.25	- 21.5	- 21.5	+ 1	- 20.5	- 20.5
$Q_s$	120	200		120	200

Comparing the above with Table 16.6, when  $Q_s = 120$ , there is little to choose between the two values of coupling as far as overall frequency response variation is concerned, but the smaller value ( $Qk = 1.5$ ) is preferable because it is possible in combination with another pair of coupled circuits to achieve a better frequency response distribution relative to 10.5 Mc/s. Overall frequency response for  $Q_s = 200$  is less satisfactory when  $Qk = 2$ .

A point which has to be considered is the frequency response variation for the half pass-band above 10.5 Mc/s. If filters are included to suppress the adjacent audio signal of 14.25 Mc/s, they can be made to correct the effect of the 8.25 Mc/s filter on the frequency response of the upper half pass-band. Alternatively, if no upper frequency filters are required, the mid-frequency of the pairs of coupled circuits not associated with the 8.25 Mc/s filters can be reduced in order to correct for the rise in response from the overcoupled circuits to which the filters are connected. If a 14.25 Mc/s absorber filter is required, expression 16.8 can be used for calculating its attenuation, because  $B$  and  $QF$  have the same sign—it is positive instead of negative—over the range 14.25 to 10.5 Mc/s, and the numerator is unaffected when the signs of both are changed. The attenuation at selected frequencies for  $Qk = 1.5$ ,  $Q_s = 120$  and 200,  $A_0 = 70$  is tabulated below:

TABLE 16.9

$Qk = 1.5$ ,  $QF = + 1.12$  at  $\Delta f = + 1.75$  Mc/s,  $f_m = 10.5$  Mc/s,  $A_0 = 70$

$f$ (Mc/s).	Attenuation (db.).		Coupled Circuits only.	Coupled Circuits plus Filter.	
10.5	- 0.51	- 0.2	0	- 0.51	- 0.2
11.75	- 1.25	- 0.34	+ 0.52	- 0.73	+ 0.18
12.25	- 3.3	- 1.5	+ 0.7	- 2.6	- 0.8
12.75	- 6.25	- 3.7	+ 0.4	- 5.85	- 3.3
14.25	- 30.7	- 30.7	- 4.4	- 35.1	- 35.1
$Q_s$	120	200		120	200

The combined frequency response of coupled circuit and filter causes a too rapid fall in frequency response when  $Q_s = 120$ —the overall response at the vision carrier frequency, 12.75 Mc/s, must not be more than 6 db. below the average response—and satisfactory performance could only be obtained at  $Q_s = 200$  if two filters are used. If more filters are possible, e.g., three, the value of  $A_0$  can be reduced to 30, which gives a maximum attenuation of - 18.0 db.

and a satisfactory frequency response for  $Q_s = 120$ , as shown in Table 16.10.

TABLE 16.10

$Qk = 1.5$ ,  $QF = + 1.12$  at  $\Delta f = + 1.75$  Mc/s,  $f_m = 10.5$  Mc/s,  $A_0 = 30$ ,  
 $Q_s = 120$

$f$ (Mc/s).	Attenuation (db.).	Coupled Circuits plus Filter.
10.5	- 0.1	- 0.1
11.75	- 0.18	+ 0.34
12.25	- 0.88	- 0.18
12.75	- 2.52	- 2.12
14.25	- 23.56	- 27.96

If we assume that three of the four pairs of coupled circuits in the I.F. amplifier have absorber filters with attenuation characteristics as set out in Tables 16.7 and 16.10, the overall frequency response of the three circuits is that given in the second column of Table 16.11. If the fourth pair of coupled circuits has a coupling corresponding to  $Qk = 1.355$ ,  $f_m = 10.75$  Mc/s,  $QF = 0.91$  at  $\Delta f = 2$  Mc/s, it has the attenuation characteristic shown in the third column. Overall I.F. frequency response of the four pairs is shown in the fourth column.

TABLE 16.11

$f$ (Mc/s).	Attenuation (db.).	Attenuation of Special Circuit.	Overall Attenuation.
8.25	- 47.7	+ 0.26	- 47.44
8.75	+ 0.06	+ 0.4	+ 0.46
9.25	+ 1.11	+ 0.3	+ 1.41
10.5	- 0.3	+ 0.05	+ 0.25
11.75	+ 1.02	+ 0.14	+ 1.16
12.25	- 0.54	+ 0.3	- 0.24
12.75	- 6.36	+ 0.4	- 5.96
14.25	- 83.88	- 1.05	- 84.93

The overall I.F. amplifier frequency response has a variation of about  $\pm 1$  db. over the pass range, with a response at the vision carrier frequency of almost exactly that required, viz., - 6 db. Attenuation is more than that specified at 8.25 Mc/s, and at 14.25 Mc/s.

To show the method of calculating the component values for

the absorber filters we shall assume that the primaries and secondaries of the three pairs of coupled circuits are identical, i.e., in Figs. 16.5 and 16.6,  $C_7 = C_{12} = C_{25} = C_{28} = C_{34} = C_{35} = 15 \mu\mu\text{F}$ , the inductances  $L_4, L_6$ , etc., are equal to  $15.3 \mu\text{H}$ ,  $Qk = 1.5$ ,  $QF = \pm 1.12$  at  $\Delta f = \pm 1.75 \text{ Mc/s}$ ,  $f_m = 10.5 \text{ Mc/s}$ ,  $Q = 3.36$ .

(a) 8.25 Mc/s Filter.

Let  $C_{10} = 15 \mu\mu\text{F}$ ,  $Q_5 = 120$ .

$$L_5 = \frac{10^{-6}}{(6.28 \times 8.25)^2 \times 15} = 24.8 \mu\text{H}.$$

$$R_5' = \frac{1}{Q_5 \omega_5 C_{10}} = \frac{10^6}{120 \times 6.28 \times 8.25 \times 15} = 10.7 \Omega.$$

$$* R_1' = \frac{1}{Q \omega_m C_7} = \frac{10^6}{3.36 \times 6.28 \times 10.5 \times 15} = 300 \Omega.$$

$$A_0 = 10 = \frac{\omega_5^2 M_4^2}{R_1' R_5'}.$$

$$M_4 = \frac{10^{-6} \sqrt{10 \times 10.7 \times 300}}{6.28 \times 8.25} = 3.46 \mu\text{H}.$$

$$k_4 = \frac{M_4}{\sqrt{L_4 L_5}} = \frac{3.46}{\sqrt{15.3 \times 24.8}} = 0.177.$$

(b) 14.25 Mc/s.

If  $C_{10} = 15 \mu\mu\text{F}$ ,  $L_5 = 8.35 \mu\text{H}$ ,  $Q_5 = 120$ ,  $R_5' = 6.2 \Omega$

$$A_0 = 30$$

$$M_4 = \frac{10^{-6} \sqrt{30 \times 6.2 \times 300}}{6.28 \times 14.25} = 2.63 \mu\text{H}.$$

$$k_4 = \frac{2.63}{\sqrt{15.3 \times 8.35}} = 0.233.$$

As described in Section 16.6.4, phase distortion can be derived from the phase angle,

$$\phi = \tan^{-1} \left[ - \frac{2QF + AQF + B}{1 + Q^2(k^2 - F^2) + A - BQF} \right].$$

The second type of filter is the parallel resonant circuit-capacitance potential divider formed by  $L_7 C_{11}$  and  $C_{12}$  in Fig. 16.6. Actually  $C_{12}$  is not the total tuning capacitance of the  $L_6 C_{12}$  circuit,

\* Note that  $R_1'$  is the equivalent series resistance of the  $L_4 C_7 R_5$  circuit in Fig. 16.5, and the value of  $Q$  used is that calculated in Section 16.6.4 for the overcoupled circuits of  $Qk = 1.5$ .

but is the wiring and valve input capacitance and so will have a value of about  $10 \mu\mu\text{F}$ . For rejection at  $14.25 \text{ Mc/s}$ , the resonant impedance  $R_{D7}$  of  $L_7C_{11}$  at this frequency must be approximately 10 times the reactance  $C_{12}$ , or

$$R_{D7} = 10 \frac{1}{\omega_7 C_{12}} = 10 \frac{10^6}{6.28 \times 14.25 \times 10} = 11,150 \Omega.$$

The impedance of the  $L_7C_{11}$  circuit at any frequency is  $\frac{R_{D7}}{1+jQ_7F}$  and it can be resolved into a resistance and reactive component of  $R_S = \frac{R_{D7}}{1+(Q_7F)^2}$  and  $X_S = \frac{-R_{D7}Q_7F}{1+(Q_7F)^2}$ , where  $Q_7$  is the  $Q$  of the circuit,  $F = \frac{\Delta f}{f_7}$  and  $\Delta f$  = frequency off-tune from the resonant frequency,  $f_7$  (in this case  $14.25 \text{ Mc/s}$ ). The attenuation due to

this type of filter is  $20 \log_{10} \frac{1}{\omega C_{12} \sqrt{R_S^2 + \left(X_S - \frac{1}{\omega C_{12}}\right)^2}}$ , and when

$Q_7$  is large it reduces to  $20 \log_{10} \frac{1}{X_S \omega C_{12} - 1}$  for all frequencies

except those close to series resonance of  $L_7C_{11}$  with  $C_{12}$ . Table 16.12 gives the attenuation at the selected frequencies for  $Q_7 = 120$  and 200.

TABLE 16.12

$$R_{D7} = 11,150 \Omega. \quad f_r = 14.25 \text{ Mc/s.}$$

$f \text{ (Mc/s)}$ .	$\frac{1}{\omega C_{12}}$	$X_S$	db.	$X_S$ .	db.
10.5	1,512	+ 176.5	+ 1.08	+ 106	+ 0.64
11.75	1,352	+ 265	+ 1.9	+ 159	+ 1.08
12.25	1,298	+ 331	+ 2.54	+ 199	+ 1.44
12.75	1,245	+ 442	+ 3.8	+ 265	+ 2.1
14.25	1,115	0	- 20.04	0	- 20.04
$Q_7$		120	120	200	200

The chief point of interest is that over the pass range there is a gain instead of loss; this is due to the fact that the  $L_7C_{11}$  circuit appears as an inductive reactance at frequencies below resonance, and eventually it forms with  $C_{12}$  a series resonant circuit. This series resonance occurs at about  $Q_7F = -9.5$ , and there is a peak in the



filter response at this frequency, 13.68 Mc/s for  $Q_7 = 120$ . Between 13.7 and 14.25 Mc/s the response falls away sharply to a maximum loss of  $-20.04$  db. The rise in response over the pass-band can be used to compensate for any fall in response due to the coupled circuits. The filter circuit is a part of the tuning of the secondary and it reduces the capacitive reactance of  $C_{12}$  over the pass-band range. This means that the factor  $(1+jQ_2F)$  in the denominator of the transfer impedance expression is increased to  $(1+j(Q_2F+x))$  and  $Z_T$  is therefore reduced, an effect which tends to offset the increase in frequency response due to the filter itself. Again, it can be observed that the filter has least influence on the pass range when  $Q_7$  is large. If this type of filter is used for rejecting 8.25 Mc/s,  $X_S$  is negative, the range 10.5 to 8.75 shows a fall in response, and there is no series resonance peak. The results for  $R_{D7} = 19,250 \Omega$ ,  $f_r = 8.25$  Mc/s,  $Q_7 = 120$  are :

TABLE 16.13

$f$ (Mc/s).	$\frac{1}{\omega C_{11}}$	$X_S$	db.
10.5	1,512	- 295	- 1.54
9.25	1,715	- 663	- 2.84
8.75	1,815	- 1,325	- 4.56
8.25	1,925	0	- 20.04

In this case the filter reduces the factor  $(1+jQ_2F)$  in the denominator of  $Z_T$  to  $(1+j(Q_2F-x))$  and thus tends to offset the fall in response due to the filter.

The values of  $L_7$  and  $C_{11}$  are calculated from  $R_{D7}$  and  $Q_7$ ; thus for 14.25 Mc/s

$$L_7 = \frac{R_{D7}}{\omega_7 Q_7} = \frac{11,150 \times 10^{-6}}{6.28 \times 14.25 \times 120} = 1.035 \mu\text{H}$$

$$C_{11} = 120 \mu\mu\text{F}$$

and for 8.25 Mc/s

$$L_7 = \frac{19,250 \times 10^{-6}}{6.28 \times 8.25 \times 120} = 3.09 \mu\text{H}$$

$$C_{11} = 120 \mu\mu\text{F}.$$

The series resonant circuit filter, exemplified by  $L_{13}C_{23}$  in Fig. 16.6, acts as a shunt in parallel with the primary impedance, and the attenuation it produces may be calculated from the ratio

of its impedance to the sum of its impedance and the primary impedance. The latter, from expression 7.7*d*, Part I, is

$$Z_p = \frac{R_{D1}(1+jQF)}{1+Q^2(k^2 - F^2) + 2jQF}$$

and taking the previous component values for the  $Qk = 1.5$  coupled circuits, the primary impedance at 8.25 Mc/s is

$$\begin{aligned} Z_p &= \frac{3,400(1 - 1.44j)(1.17 + 2.88j)}{(1.17)^2 + (2.88)^2} \\ &= \frac{3,400}{9.67}(5.32 + 1.193j) \\ &= 1,870 + 420j. \end{aligned}$$

For  $Q_{13} = 120$ ,  $C_{23} = 7.5 \mu\mu F$ ,  $L_{13} = 49.5 \mu H$ , the additional attenuation at 8.25 Mc/s is  $20 \log_{10} \frac{21.4}{\sqrt{(1,891.4)^2 + (420)^2}} = -39.12$  db.

for  $R'_{13} = \frac{\omega_{13} L_{13}}{Q_{13}} = 21.4 \Omega$ . At other frequencies the impedance of

the series circuit is  $R'_{13}(1+jQ_{13}F')$  where  $F' = \frac{2Af}{f_{13}}$ , so that at

10.5 Mc/s it is  $21.4(1+65.5j) \approx 1,400j$ . Hence there is a loss of  $20 \log_{10} \frac{1,400}{\sqrt{(3,400)^2 + (1,400)^2}} = -8.4$  db. at the centre of the pass

range. It is only possible to reduce this loss by increasing  $L_{13}$  because the impedance at 10.5 Mc/s is approximately equal to  $jR'_{13}Q_{13}F' = j\omega_{13}L_{13}F'$ . Such a large value of loss could hardly be tolerated and the series parallel filter  $L_{16}C_{32}$  and  $C_{31}$  in Fig. 16.6 is preferable. The parallel section is resonant at 10.5 Mc/s and has therefore an inductive reactance at 8.25 Mc/s. Series resonance is obtained by this inductive reactance in combination with  $C_{31}$ . Let us assume that the resonant impedance  $R_{D16}$  of  $L_{16}C_{32}$  at 10.5 Mc/s is 170,000  $\Omega$ —this involves a loss of  $-0.16$  db.—and that  $Q_{16}$  is 120; we therefore find that

$$L_{16} = \frac{170,000 \times 10^{-6}}{120 \times 6.28 \times 10^5} = 21.5 \mu H$$

and  $C_{32} = 10.7 \mu\mu F$ .

The reactance of this circuit at 8.25 Mc/s ( $Q_{16}F' = -51.4$ ) is

$$-j \frac{R_{D16}Q_{16}F'}{1+(Q_{16}F')^2} = +j3,310 \Omega.$$

and the capacitance value for  $C_{31}$  is

$$C_{31} = \frac{10^6}{6.28 \times 8.25 \times 3,310} = 5.84 \mu\mu F.$$

The series impedance of the filter at 8.25 Mc/s is the resistance component of the impedance of  $L_{16}C_{32}$ , i.e.,

$$\frac{R_{D16}}{1+(Q_{16}F')^2} = \frac{170,000}{2,640} = 64.5 \Omega$$

which causes an attenuation of

$$20 \log_{10} \frac{64.5}{|Z_p + 64.5|} = 20 \log_{10} \frac{64.5}{\sqrt{(1,934.5)^2 + (420)^2}} = -29.72 \text{ db.}$$

This type of filter is less satisfactory for suppressing frequencies above the vision pass-band because the reactance of  $L_{16}C_{32}$  is capacitive and series resonance can only be obtained at a higher frequency by replacing  $C_{31}$  by an inductance, the performance of which is considerably modified by its inherent self capacitance.

It is worth noting that the effect of the series or series-parallel filter circuit is the same whether it is connected across primary or secondary provided the latter are identical.

The rejection circuit formed by a resonant coupling between the primary and secondary is illustrated by  $M_5$  in combination with  $C_{26}$  in Fig. 16.6. The performance of the resonant coupling can

be calculated by replacing  $k$  in  $Z_T$  by  $\frac{\left(M_5 - \frac{1}{\omega^2 C_{26}}\right)}{\sqrt{L_{14} \cdot L_{15}}}$  and  $C_{26}$  is chosen to satisfy the expression

$$f = 14.25 \text{ or } 8.25 = \frac{1}{2\pi \sqrt{M_5 C_{26}}}$$

Appreciable values of attenuation can be obtained by this method because  $M_5$  has no resistance component and the resistance of the resonant coupling is determined only by the losses in  $C_{26}$ . On the other hand, the frequency response at the edges of the pass-band may be considerably affected.

Cathode feedback (Section 7.9, Part I) may also be used for suppression purposes, but to be fully effective the valve to which it is applied must not have grid-bias control.

**16.7. The Detector Stage.** The vision frequency detector stage is a modified form of the audio frequency detector, the modifications being rendered necessary by the much larger range of modulation frequencies (2 to 4 Mc/s as compared with 18 kc/s for audio signals). Both reservoir capacitance and load resistance must be small, otherwise the higher modulation frequencies are severely attenuated. Consequently detection efficiency is low; it is of the order of 50% for a single diode half-wave detector, provided that

the diode is designed to have a low anode-cathode capacitance and a low conduction resistance. The anode-cathode capacitance in conjunction with the low value of reservoir capacitance acts as a potential divider to reduce the effective R.F. voltage applied to the diode. A small value of anode-cathode capacitance calls for a large anode-cathode spacing, but this increases the diode conduction resistance, so that a compromise is necessary. Typical values for the anode-cathode capacitance and conduction resistance of a television diode detector are 1.5 to 2  $\mu\mu\text{F}$  and 1,000  $\Omega$  respectively. Both R.F. and superheterodyne receivers need special filters between the diode output and the vision frequency amplifier, though the need for filtering is less urgent in the R.F. than in the superheterodyne receiver, because feedback of I.F. harmonics into the signal circuits, which leads to serious interference with the picture, does not arise. Feedback of R.F. carrier is undesirable, but can only cause regeneration or degeneration, apart from harmonic distortion when large peak signals are applied to the V.F. amplifier. Regeneration can, of course, become serious if the receiver is brought near the point of oscillation (it may cause appreciable attenuation distortion), but such a situation rarely arises if normal precautions are taken.

Of the three types of diode detector circuit, the half-wave, the full-wave and voltage doubler, the former is the most popular on account of simplicity and, compared with the full-wave detector, less loss of amplification from input to output. The chief merit of the full-wave detector is that the vision carrier fundamental is cancelled, and only its harmonics have to be filtered from the output of the V.F. amplifier. The input voltage applied to each diode of the full-wave detector is halved by the centre tap, but detection efficiency ( $\eta_d$ ) is higher at about 70%. Thus the overall output-to-input voltage ratio is about 0.35 compared with 0.5 for the half-wave detector. Another disadvantage of the full-wave detector is that the centre-tapped output coil must be electrically balanced to earth, otherwise cancellation of the carrier fundamental is not realized. The voltage doubling type of detector is more useful when it is desired to operate the C.R. tube direct from the detector. For examples of this see Fig. 11.4c, and the alternative form provided by  $V_1$  and  $V_2$  in Fig. 11.12; the latter type is better than the former because there is less R.F. ripple across the reservoir capacitance  $C_1$ . Conduction current damping is twice that of the half-wave detector so that the equivalent damping resistance is approximately one-half the load resistance (see below).

An example of the half-wave detector is shown in Fig. 16.7. Damping of the tuned circuit feeding the detector is very much greater than in the case of the A.F. detector because of the low load resistance,  $5,000 \Omega$ , but this is not a serious disadvantage as the tuned circuit must be heavily damped to secure the wide pass-band. Since the detection efficiency is 50%, the conduction current damping resistance may be taken as equal to the load resistance (Section 8.2.5, Part I), and any additional damping resistance must be calculated with this in mind. The direction of the diode connections depends on the type of modulation and the number of v.F. amplifier stages. The circuit of Fig. 16.7 is suitable for detecting the English system of positive modulation with direct connection from detector to c.r. tube, or with an even number of v.F. stages between detector and c.r. tube. The same circuit can be used for the American system of negative modulation if an odd number of v.F. stages is employed ;

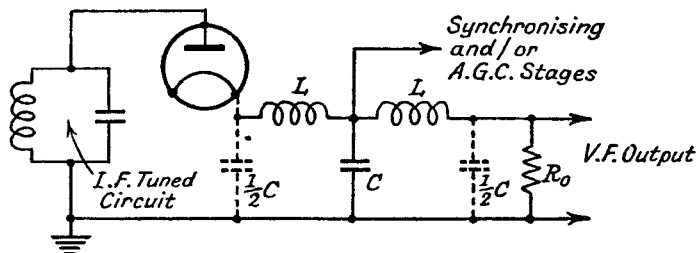


FIG. 16.7.—The Vision Signal Detector of a Television Receiver.

the anode-cathode connections of the diode must be reversed if direct connection or an even number of v.F. stages is desired between detector and c.r. tube. A two-stage low-pass filter is shown between the detector and its v.F. output, and the values of  $L$  and  $C$  may be calculated from the normal filter formulæ for constant  $k$  structures. Thus

$$L = \frac{R_0}{\pi f_c} \text{ and } C = \frac{1}{\pi f_c R_0}$$

where  $f_c$  = the cut-off frequency

and  $R_0$  = the characteristic and terminating resistance of the filter.

Generally the value of the reservoir capacitance, which is the capacitance  $\frac{1}{2}C$  of the shunt arm of the  $\pi$  section filter, shown in Fig. 16.7, is fixed by stray capacitance at not less than  $10 \mu\mu\text{F}$ , and this in turn limits the maximum value of  $R_0$  and  $f_c$ . From the point of view of detection efficiency  $R_0$  should be as large as possible ; small attenuation distortion over the pass-range calls for a high

value of  $f_c$ , though it must not be so high as to cause insufficient filtering of the I.F. A suitable compromise for 2 Mc/s pass-band is  $R_0 = 5,000 \Omega$  and  $f_c = 3.18$  Mc/s, i.e., approximately one and a half times the maximum vision frequency of 2 Mc/s, with  $C = 20 \mu\mu\text{F}$  and  $L = 500 \mu\text{H}$ . For the higher definition 4 Mc/s pass-band,  $R_0$  must be reduced to 3,000  $\Omega$ , thereby increasing  $f_c$  to 5.3 Mc/s with  $C = 20 \mu\mu\text{F}$  and  $L = 180 \mu\text{H}$ .

Attenuation and phase distortion for a low-pass filter have been examined in considerable detail elsewhere,<sup>31, 32</sup> and it is not proposed to do more than state the formulae involved and the probable performance of a suitable filter. The attenuation in decibels of a correctly terminated single section constant  $k$  low-pass filter

( $R_0 = \sqrt{\frac{L}{C}}$ ) is

$$\alpha = -20 \log_{10} \left\{ \frac{\sqrt{1 + \frac{Z_1}{4Z_2}} + \sqrt{\frac{Z_1}{4Z_2}}}{\sqrt{1 + \frac{Z_1}{4Z_2}} - \sqrt{\frac{Z_1}{4Z_2}}} \right\} \quad . \quad . \quad 16.9$$

$$= -20 \log_{10} \left[ \left( \sqrt{1 + \frac{Z_1}{4Z_2}} + \sqrt{\frac{Z_1}{4Z_2}} \right)^2 \right]$$

and the phase angle

$$\beta = \tan^{-1} \frac{j \text{ part of } \left( \sqrt{1 + \frac{Z_1}{4Z_2}} + \sqrt{\frac{Z_1}{4Z_2}} \right)^2}{\text{real part of above}} \quad . \quad . \quad 16.10$$

where  $Z_1 =$  impedance of a full series arm  $= \omega L$

and  $Z_2 =$  impedance of a full shunt arm  $= \frac{1}{\omega C}$ .

Thus if  $L$  contains no resistive component

$$\frac{Z_1}{4Z_2} = \frac{j\omega L}{4 \frac{1}{j\omega C}} = -\frac{\omega^2 LC}{4} = -\left(\frac{f}{f_c}\right)^2$$

for  $f_c = \frac{1}{\pi\sqrt{LC}}$ . On the other hand, if  $L$  has a resistive component  $R$ ,

$$\frac{Z_1}{4Z_2} = \frac{(R + j\omega L)j\omega C}{4} = -\frac{\omega^2 LC}{4} \left( \frac{R}{j\omega L} + 1 \right) = \left(\frac{f}{f_c}\right)^2 \left[ \frac{j}{Q} - 1 \right]$$

$$= \left(\frac{f}{f_c}\right)^2 \sqrt{\frac{1}{Q^2} + 1} \cdot \tan^{-1} \left( -\frac{1}{Q} \right) \quad . \quad . \quad . \quad 16.11.$$

To illustrate the use of the formulae 16.9 and 16.10, we shall take two cases :

$$(1) \frac{Z_1}{4Z_2} = 1/180^\circ = -1, \text{ and } (2) \frac{Z_1}{4Z_2} = 1.2/150^\circ = -1.04 + 0.6j.$$

(1)  $\frac{Z_1}{4Z_2} = 1/180^\circ$ . This corresponds to cut-off frequency and zero resistance in the  $L$  and  $C$  arms.

$$\left( \sqrt{1 + \frac{Z_1}{4Z_2}} + \sqrt{\frac{Z_1}{4Z_2}} \right)^2 = (\sqrt{-1})^2 = -1 = 1/\tan^{-1}(-1) = 1/180^\circ.$$

Therefore  $\alpha = 20 \log_{10} 1 = 0 \text{ db.}$   
 $\beta = \tan^{-1}(-1) = 180^\circ.$

(2)  $\frac{Z_1}{4Z_2} = 1.2/150^\circ = -1.04 + 0.6j$ . This corresponds to a frequency greater than cut-off with  $Q = \frac{\omega L}{R} = -\cot \phi = 1.732$

$$\begin{aligned} \left( \sqrt{1 + \frac{Z_1}{4Z_2}} + \sqrt{\frac{Z_1}{4Z_2}} \right)^2 &= (\sqrt{-0.04 + 0.6j} + \sqrt{-1.04 + 0.6j})^2 \\ &= -1.08 + 1.2j + 2\sqrt{-0.3184 - 0.648j}^* \\ &= -1.08 + 1.2j - 0.898 + 1.444j \\ &= 3.31/125^\circ 48' \end{aligned}$$

i.e.,  $\alpha = -10.4 \text{ db.}, \beta = 125^\circ 48'.$

Phase and attenuation distortion is affected by the  $Q$  of the coil  $L$  of the series arm, and  $Q$  is not easy to assess because it varies from a low value at the low-frequency end of the pass-band to a comparatively high value at the high-frequency end, e.g., 2 to 3 at 1 kc/s to 100 at 4 Mc/s. However, provided the maximum vision frequency does not exceed about  $0.75f_c$ , attenuation distortion is usually negligible for normal  $Q$  values. Suppose  $Q$  at 4 Mc/s = 100, and  $f_c = 5.3 \text{ Mc/s}$ , then

$$\begin{aligned} \frac{Z_1}{4Z_2} &= \left( \frac{f}{f_c} \right)^2 \sqrt{\frac{1}{Q^2} + 1} \left[ \tan^{-1} - \frac{1}{Q} \right] \\ &= \left( \frac{4}{5.3} \right)^2 \sqrt{1 + (0.01)^2} \left[ \tan^{-1} - 0.01 \right] \\ &= 0.57/179^\circ 25'. \end{aligned}$$

---

\* Note  $\sqrt{-0.3184 - 0.648j} = \sqrt{\sqrt{(0.3184)^2 + (0.648)^2}} \left[ \frac{1}{2} \tan^{-1} \frac{-0.648}{-0.3184} \right]$   
 $= 0.85/121^\circ 56'$   
 $= -0.449 + 0.722j$

The above value of  $\frac{Z_1}{4Z_2}$ , when replaced in expression 16.9, gives a loss of  $-0.2$  db. at 4 Mc/s, which is negligible.

At the vision I.F. carrier 12.75 Mc/s if  $Q$  is unchanged,

$$\frac{Z_1}{4Z_2} = \left(\frac{f}{f_c}\right)^2 / 179^\circ 25' = 5.8 / 179^\circ 25'$$

and the loss for this value of  $\frac{Z_1}{4Z_2}$  is found to be  $-26.6$  db.

For the two-section filter of Fig. 16.7, the loss at the vision I.F. carrier is twice this. There can be large variations in phase angle of  $\frac{Z_1}{4Z_2}$  with practically no effect on the attenuation in the cut-off region.

Greatest variation of frequency response over the pass-band is caused by reflection losses due to the mismatch between the filter input image impedance and the equivalent A.C. impedance of the diode, consisting of its slope resistance and anode-cathode inter-electrode capacitance in parallel. The diode slope resistance  $R_d'$  is generally about  $1,500 \Omega$ , and the anode-cathode capacitance of  $2 \mu\mu\text{F}$  has only a very small effect because its reactance ( $19,950 \Omega$  at 4 Mc/s) is very small compared with  $1,500 \Omega$ . The input image impedance  $Z'$  of the  $\pi$  section filter varies over the pass-band in accordance with the formula

$$Z' = \frac{R_0}{\sqrt{1 - \left(\frac{f}{f_c}\right)^2}} \quad . \quad . \quad . \quad 16.12$$

and the reflection loss due to mismatch is

$$\text{loss} = -20 \log_{10} \frac{1 + \frac{Z'}{R_d'}}{2 \sqrt{\frac{Z'}{R_d'}}} \text{db.} \quad . \quad . \quad . \quad 16.13$$

and it is tabulated on page 416 for  $R_d' = 1,500 \Omega$ ,  $R_0 = 3,000 \Omega$ , and  $f_c = 5.3$  Mc/s.

Reflection mismatch loss increases as the v.f. frequency increases because the input impedance of the  $\pi$  section increases. A T-section filter would have advantages in this respect because its input impedance falls over the pass-band from  $3,000 \Omega$  to zero at  $f = f_c$ . This will cause the loss to decrease with increase of frequency until  $Z'$  falls below  $R_d'$ , and the v.f. response will thus tend to increase. The T-section filter cannot, however, be used because



TABLE 16.14

$\frac{f}{f_c}$	0	0.1	0.2	0.3	0.4	0.5	0.6	0.7	0.8	0.9
$f(\text{Mc/s})$	0	0.53	1.06	1.59	2.12	2.65	3.18	3.71	4.24	4.77
$Z'(\text{ohms})$	3,000	3,020	3,060	3,145	3,275	3,465	3,750	4,200	5,000	6,880
Loss (db.)	-0.5	-0.51	-0.52	-0.58	-0.64	-0.74	-0.86	-1.08	-1.48	-2.32
Loss (db.) referred to $f = 0$	0	-0.01	-0.02	-0.08	-0.14	-0.24	-0.36	-0.58	-0.98	-1.82

the stray capacitance  $\frac{1}{2}C$  across the output of the diode and input of the filter cannot be eliminated. There is no phase shift due to the mismatch if the reactive component of the diode a.c. impedance is negligible, i.e., if the diode anode-cathode capacitive reactance is large compared with  $R_d'$ .

Phase distortion in the filter itself can be estimated by noting the departure of the phase angle (expression 16.10) from a linear relationship to frequency. It will be found to be greatest when there is no resistive component in the shunt and series arms of the filter, so that we shall gain an idea of the likely phase distortion by studying this condition, for which  $\frac{Z_1}{4Z_2} = \left(\frac{f}{f_c}\right)^2 \angle 180^\circ = -\left(\frac{f}{f_c}\right)^2$ , where  $\frac{f}{f_c} < 1$ . Hence

$$\begin{aligned} \left(\sqrt{1 + \frac{Z_1}{4Z_2}} + \sqrt{\frac{Z_1}{4Z_2}}\right)^2 &= \left(\sqrt{1 - \left(\frac{f}{f_c}\right)^2} + \sqrt{-\left(\frac{f}{f_c}\right)^2}\right)^2 \\ &= \left(\sqrt{1 - \left(\frac{f}{f_c}\right)^2} + j\frac{f}{f_c}\right)^2 \\ &= 1 - 2\left(\frac{f}{f_c}\right)^2 + j\frac{2f}{f_c}\sqrt{1 - \left(\frac{f}{f_c}\right)^2}. \end{aligned} \quad 16.14.$$

From which the phase angle

$$\beta = \tan^{-1} \frac{\frac{2f}{f_c} \sqrt{1 - \left(\frac{f}{f_c}\right)^2}}{1 - 2\left(\frac{f}{f_c}\right)^2}. \quad 16.15.$$

The phase angle and phase-angle error are given in Table 16.15 over the pass range of the filter for  $f_c = 5.3$  Mc/s. The correct phase angle is given by  $\beta = \tan^{-1} \frac{2f}{f_c}$  radians =  $57^\circ 18'$   $\tan^{-1} \frac{f}{f_c}$  degrees.

TABLE 16.15

$\frac{f}{f_c}$	0.1	0.2	0.3	0.4	0.5
$f$ (Mc/s).	0.53	1.06	1.59	2.12	2.65
Phase Angle	11° 26'	23° 2'	34° 53'	47° 9'	60°
Error	1'	+ 0° 8'	+ 0° 34'	+ 1° 19'	+ 2° 42'

$\frac{f}{f_c}$	0.6	0.7	0.8	0.9	1.0
$f$ (Mc/s).	3.18	3.71	4.24	4.77	5.3
Phase Angle	73° 46'	88° 51'	106° 14'	128° 19'	180°
Error	+ 5° 11'	+ 8° 38'	+ 14° 39'	+ 25° 17'	+ 65° 24'

The phase angle and phase-angle error is positive, so that there is a time delay amounting to approximately

$$\frac{12}{360 \times 4} = 0.00833 \mu \text{ secs. at } 4 \text{ Mc/s.}$$

This is very small compared with that caused by the I.F. amplifier.

In the example taken for high definition transmission, viz., maximum vision frequency 4 Mc/s,  $R_0 = 3,000 \Omega$ ,  $f_c = 5.3 \text{ Mc/s}$ , and a two-section filter, frequency response shows a loss of about  $2 \times (-0.8 \text{ (mismatch)} - 0.2 \text{ (filter, loss due to } Q \text{ of coil)})$ , i.e.,  $-2.0 \text{ db.}$  from low to high frequencies and time delay amounts to  $0.01666 \mu \text{ secs.}$  at the highest vision frequency.

The double value of shunt capacitance ( $20 \mu\mu\text{F}$ ) required at the junction of the two sections of the filter makes this a suitable point for connecting other circuits, such as the synchronizing and A.G.C. stage, which use the detector output as their source of voltage. Care must be exercised to keep the stray and self-capacitances of the filter inductances  $L$  to a minimum, because the parallel resonant circuit so formed, though increasing discrimination against a narrow band of frequencies, offers less attenuation to frequencies higher than this band. Alternatively the resonant frequency may be controlled and used to increase the effectiveness of the filter at the vision I.F. carrier fundamental (or second harmonic in the case of full-wave detection).

A.G.C. bias control, which may be derived from the detector output, is quite often employed in American receivers, but has not proved necessary with the single English transmission. The chief advantage of automatic gain control in television reception is for smoothing out variations in signal strength due to a swinging aerial

or lead-in (this is prevented by firm fixing), or to reflections from nearby moving objects, e.g., aeroplane flutter effect. It is also useful for stabilizing output when tuning from one transmission to another. The source of A.G.C. voltage must be the synchronizing pulse section of the carrier and not the vision signal section because the vision voltage varies between wide limits and depends on the average black or white content of the image. For the American system of negative modulation with synchronizing pulses applied at maximum carrier amplitude, A.G.C. voltage may be obtained by connecting a diode and its load resistance across the central capacitance  $C$  of the filter as shown in Fig. 16.8. The time constant of the load resistance  $R_1$  and reservoir capacitance  $C_1$  is sufficiently large to ensure that the A.G.C. diode acts as a peak voltage detector of the positive synchronizing pulses. The D.C. output voltage is positive

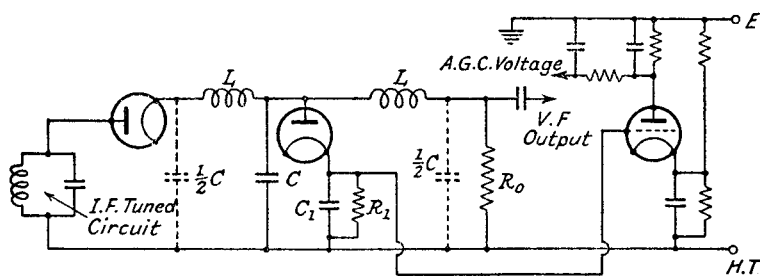


FIG. 16.8.—A Method of obtaining A.G.C. for the American Negative Modulation Transmission System.

[For H.T. read H.T. -]

and a phase-reversing valve must be used to change it to a negative voltage. The phase-reversing valve, which also acts as an amplifier, is connected between the earth line of the R.F. receiver and a source of negative voltage as shown in Fig. 16.8. If two stages of v.f. amplification are used the vision detector connections must be reversed for the American negative modulation, i.e., the cathode is connected to the R.F. voltage source and the anode to the vision detector filter. The synchronizing pulses are now negative and the A.G.C. diode connections must also be reversed. The D.C. voltage appearing across  $R_1$  has the correct polarity for applying direct to the R.F. valves. Much the same principle may be applied to obtain A.G.C. from the English positive modulation system.

It should be noted that the initial curvature of the vision detector characteristic reduces the synchronizing pulse of the English transmission and the white signal of the American. Vestigial and single sideband reception inevitably produce some harmonic distortion of

the vision frequency signal, but as explained previously, this type of distortion is much less important in television than in audio frequency reception.

Anode bend detection may be used in order to gain some amplification of the detected output voltage. Its chief disadvantage is its non-linear detection characteristic and restricted input signal handling capacity, though both effects can be mitigated by the use of negative feedback. Cathode self-bias cannot be employed because the average carrier level varies with the image brightness. A special compensating anode circuit is included to provide the required vision frequency response, and it is similar to those described in the next section.

## 16.8. Vision Frequency Amplification.<sup>2, 16</sup>

**16.8.1. Introduction.** Cathode ray tubes reproducing television images require a peak-to-peak signal voltage of about 25 volts for reproducing the full range of brightness from black to white. It is not normally possible to obtain this voltage direct from a detector stage without overloading the last R.F. or I.F. stage of the receiver, since the synchronizing pulses increase the required detected output voltage amplitude by another 43% (30% carrier represents black) to 35.75 volts peak-to-peak. Hence, allowing for a detection efficiency of 50%, the R.F. or I.F. voltage needs to be 71.5 volts. At least one stage of vision frequency amplification is needed between the detector and C.R. tube. The wide range of frequencies, from D.C. to 4 Mc/s, which are present in the vision frequency output from the detector, creates difficulties in the design of the v.f. amplifier. The D.C. component is essential for correct reproduction of the image as it provides the datum of average brightness, e.g., the average light content of the picture is reduced in passing from an outdoor to indoor scene, and this change can only be appreciated if the D.C. component is present at the grid of the C.R. tube reproducer. It would be possible to use a D.C. amplifier v.f. stage, but this generally leads to a more complicated power supply system, particularly if more than one stage of v.f. amplification is employed. Fortunately D.C. amplification is not essential because a diode connected across the output of the v.f. stage can be used to restore the D.C. component lost in the amplifier. Failure to restore this component also tends to make the flyback trace of the frame deflection visible across the image.

Increase of the reactances of the coupling and self-bias capacitances in the v.f. amplifier cause loss of low-frequency response and

phase distortion, which results in a brightness variation in a vertical direction when a white or black square is being transmitted. High-frequency attenuation due to stray and valve capacitances leads to a loss of horizontal detail. Phase distortion is not often a serious problem at the high-frequency end of the range and is usually negligible in comparison with that introduced in the R.F. and I.F. stages, because the number of reactances and therefore the total phase shift is small. Although minimum attenuation and phase distortion are not necessarily achieved at the same time, a flat high-frequency response generally results in small-phase distortion. At low frequencies phase distortion is more serious because a phase-angle error of  $1^\circ$  represents a time error of  $55.5 \mu$  secs. (16.78 cms. error on the C.R. tube screen) at 50 c.p.s., and it is preferable to aim at minimum phase rather than minimum attenuation distortion. A point always to be remembered when more than one v.f. stage is involved is that each stage should be compensated to give satisfactory phase and attenuation distortion independently of any other. It is most unwise to try and correct in one stage the deficiencies of several others.

There is another form of distortion to which v.f. amplifiers are susceptible, and that is transient distortion. It is caused by a transient pulse setting up damped oscillations in the  $LC$  circuit formed by the inductance used for compensating high-frequency loss, and the stray capacitance with which it is associated. It is a function of high-frequency response, and is liable to be produced when there is a peak exceeding 1 db. in the response curve. It causes a rippled effect on the picture immediately following a sharp transition from black to white, or vice versa. For this reason the ratio  $\frac{L}{CR^2}$  of the components used in a single stage v.f. amplifier should not exceed about 0.5. Since frequency response variations are additive it may be necessary to reduce the value of  $\frac{L}{CR^2}$  if more stages than one are used.

Tetrode or pentode valves (often of the power output type with normal operating anode current of 30 mA) are universally employed in the v.f. stages of a television receiver, partly because they give much greater amplification than triodes, but also because they have a low anode-grid interelectrode capacitance and therefore reflect a much smaller value of capacitance into their grid circuits. Harmonic distortion is relatively unimportant so that there is no advantage in using triodes.

We shall now consider the v.f. amplifier under three headings, viz., its performance at high frequencies, its performance at low frequencies, and the method of restoring the D.C. component to its output. It is convenient to start at the high-frequency end of the v.f. range because this determines overall performance by limiting the maximum value of resistance in the anode circuit, which in turn fixes maximum amplification.

**16.8.2. High-Frequency Performance.** Loss of high-frequency response in a v.f. amplifier is caused by wiring, valve input and output, and C.R. tube input capacitances, the values of which

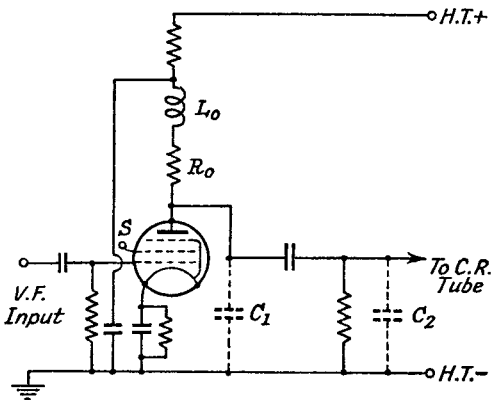


Fig. 16.9a.—A Typical v.f. Amplifier Circuit.

are about 5, 10, 10, and 15  $\mu\mu\text{F}$  respectively, making a total stray capacitance of 30  $\mu\mu\text{F}$  across the anode circuit of the last v.f. amplifier valve. At high frequencies the reactance of this capacitance falls to a low value, e.g., at 3.5 Mc/s it is 1,515  $\Omega$ , and this

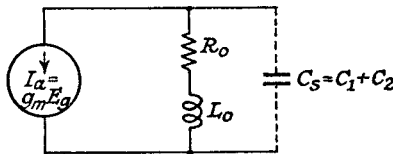


Fig. 16.9b.—The Equivalent Circuit for Fig. 16.9a.

limits the maximum value of the anode load resistance  $R_o$  to not more than 1,500  $\Omega$  if -3 db. loss is tolerable at this frequency. The circuit for this condition is that of Fig. 16.9a with  $L_o = 0$ ; its equivalent, assuming  $L_o = 0$  and  $R_a$  to be much greater than



frequency as 3.5 Mc/s, and permit a loss of - 1 db. at this frequency, we have  $f_0 = 7.0$  Mc/s (see Fig. 16.10a,  $\frac{f}{f_0} \approx 0.5$  for - 1 db. loss), so that  $R$  cannot exceed  $757 \Omega$ . If the  $g_m$  of the valve is 10 mA/volt, overall gain is 7.57, which is low. Phase-angle error at  $f = \frac{1}{2}f_0$  is from Fig. 16.10b ( $\frac{L_0}{C_s R_0^2} = 0$ )  $+2^\circ 5'$ , corresponding to a time advance of  $0.00166 \mu$  secs., which is negligible. The most serious disadvantage of the uncompensated circuit is therefore its low maximum amplification. It is possible to increase maximum amplification, without increasing attenuation or phase distortion, by neutralizing the stray capacitive reactance with an inductance  $L_0$  in series with  $R_0$  as shown in Fig. 16.9a. From expression 4.4, Part I, the load impedance is

$$Z_0 = \frac{R_0 + j\omega[L_0(1 - \omega^2 L_0 C_s) - C_s R_0^2]}{[1 - \omega^2 L_0 C_s]^2 + [\omega C_s R_0]^2} \quad . \quad . \quad 16.19a$$

$$= R_0 \left[ \frac{1 + \frac{j\omega L_0}{R_0} \left[ 1 - \omega^2 L_0 C_s - \frac{C_s R_0^2}{L_0} \right]}{[1 - \omega^2 L_0 C_s]^2 + [\omega C_s R_0]^2} \right].$$

If  $\omega_r = \frac{1}{\sqrt{L_0 C_s}}$ ,  $\frac{\omega L_0}{R_0} = \frac{f}{f_r} \frac{1}{R_0} \sqrt{L_0}$ , and  $\omega C_s R_0 = \frac{f}{f_r} R_0 \sqrt{\frac{C_s}{L_0}}$

$$\therefore Z_0 = R_0 \frac{1 + j \frac{f}{f_r} \alpha \left[ 1 - \left( \frac{f}{f_r} \right)^2 - \frac{1}{\alpha^2} \right]}{\left[ 1 - \left( \frac{f}{f_r} \right)^2 \right]^2 + \left[ \frac{f}{f_r} \cdot \frac{1}{\alpha} \right]^2} \quad . \quad . \quad 16.19b$$

where  $\alpha = \frac{1}{R_0} \sqrt{\frac{L_0}{C_s}} = \frac{f_0}{f_r}$ , for  $f_0 = \frac{1}{2\pi R_0 C_s}$ .

From the above, the attenuation at any frequency compared with the value at the lower middle frequencies is

$$20 \log_{10} \frac{|Z_0|}{R_0} = +10 \log_{10} \frac{1 + \left[ \frac{f}{f_r} \alpha \right]^2 \left[ 1 - \left( \frac{f}{f_r} \right)^2 - \frac{1}{\alpha^2} \right]^2}{\left[ \left[ 1 - \left( \frac{f}{f_r} \right)^2 \right]^2 + \left( \frac{f}{f_r} \cdot \frac{1}{\alpha} \right)^2 \right]^2}$$

$$= +10 \log_{10} \frac{1 + \left[ \frac{f}{f_0} \alpha^2 \right]^2 \left[ 1 - \left( \frac{f}{f_0} \alpha \right)^2 - \frac{1}{\alpha^2} \right]^2}{\left[ \left[ 1 - \left( \frac{f}{f_0} \alpha \right)^2 \right]^2 + \left[ \frac{f}{f_0} \right]^2 \right]^2} \quad . \quad . \quad 16.20a$$



$$\begin{aligned}\phi &= +\tan^{-1} \frac{f}{f_r} \alpha \left[ 1 - \left( \frac{f}{f_r} \right)^2 - \frac{1}{\alpha^2} \right] \\ &= +\tan^{-1} \frac{f}{f_0} \alpha^2 \left[ 1 - \left( \frac{f}{f_0} \alpha \right)^2 - \frac{1}{\alpha^2} \right] \quad . \quad . \quad . \quad 16.20b\end{aligned}$$

$$\begin{aligned}\text{and } \Delta\phi &= \tan^{-1} \frac{f}{f_r} \alpha \left[ 1 - \left( \frac{f}{f_r} \right)^2 - \frac{1}{\alpha^2} \right] - 57^\circ 18' \frac{f}{f_r} \alpha \left( 1 - \frac{1}{\alpha^2} \right) \\ &= \tan^{-1} \frac{f}{f_0} \alpha^2 \left[ 1 - \left( \frac{f}{f_0} \alpha \right)^2 - \frac{1}{\alpha^2} \right] - 57^\circ 18' \frac{f}{f_0} \alpha^2 \left( 1 - \frac{1}{\alpha^2} \right), \quad 16.20c.\end{aligned}$$

Attenuation and phase-angle error,  $\Delta\phi$ , are plotted in Figs. 16.10a and 16.10b against the ratio of actual frequency to  $f_0$ , for various values of  $\alpha^2 \left[ \frac{L_0}{C_s R_0^2} \right]$ , where  $f_0 = \frac{1}{2\pi R_0 C_s}$ . The frequency  $f_0$  is used

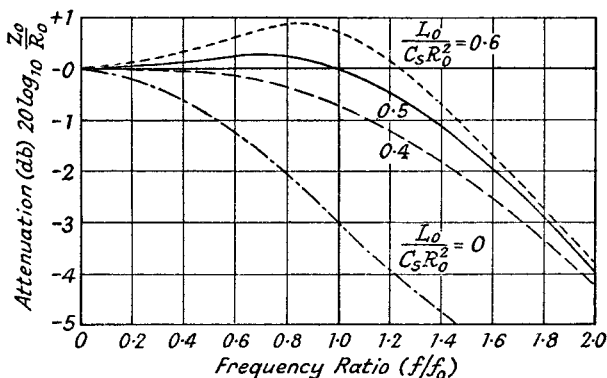


FIG. 16.10a.—The Attenuation Characteristics of an Inductance Compensated v.f. Amplifier.

as a parameter, rather than  $f_r$ , because it allows direct comparison with the uncompensated case, and also  $L_0$  is the essential variable.

It will be noted that for the values of  $\alpha$  chosen and  $\frac{f}{f_0} < 1.8$ , the actual phase angle is negative and greater than the required, hence phase-angle error is negative, indicating too much delay on each frequency vector. The most suitable value of  $\frac{L_0}{C_s R_0^2}$  as regards

frequency response is 0.5, but phase distortion is less for  $\frac{L_0}{C_s R_0^2} = 0.4$ .

Frequency response for  $\frac{L_0}{C_s R_0^2} = 0.5$  is almost level to  $\frac{f}{f_0} = 1$ , so

that 3.5 Mc/s may be considered as corresponding to  $\frac{f}{f_0} = 1$ . Hence

$$R_0 = \frac{1}{2\pi f_0 C_s} = \frac{10^{12}}{6.28 \times 3.5 \times 10^6 \times 30} = 1,515 \Omega$$

$$L_0 = 0.5 C_s R_0^2 = \frac{0.5 \times 30 \times (1,515)^2}{10^6 \times 10^6} = 34.5 \mu\text{H},$$

and the amplification of the compensated stage is double that of the uncompensated. Phase-angle error is  $-8^\circ 12'$ , and corresponds to a time delay of  $0.0065 \mu$  secs.; it is greater than that for the uncompensated circuit, but is still negligibly small. If a large

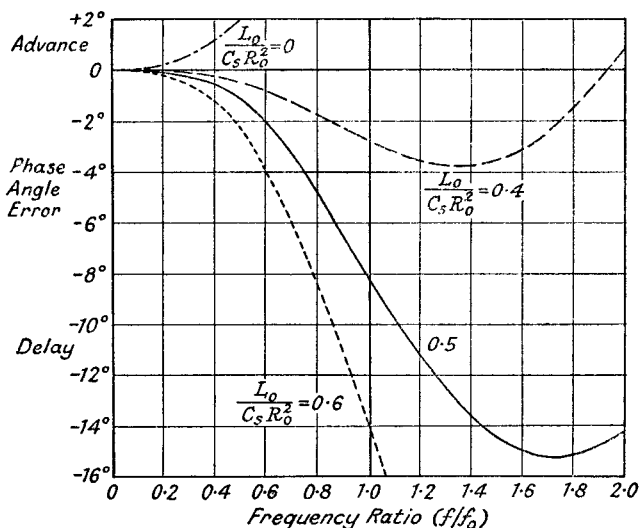


FIG. 16.106.—Phase Angle Error Curves for the Inductance Compensated v.f. Amplifier.

number of v.f. stages is required and phase-angle error, which is additive from stage to stage, must be reduced,  $\frac{L_0}{C_s R_0^2} = 0.4$  is more suitable. For satisfactory frequency response,  $\frac{f}{f_0} = 0.6$  should correspond to the highest vision frequency, and this reduces the maximum permissible value of  $R_0$  to  $910 \Omega$ ; overall amplification is reduced to 60% of the value at  $\frac{L_0}{C_s R_0^2} = 0.5$ . Values of  $\frac{L_0}{C_s R_0^2}$  greater than 0.5 are unlikely to be satisfactory as attenuation and phase distortion are increased. The rising frequency response characteristic tends also to introduce transient distortion.

Another type of compensated circuit is shown in Fig. 16.11; it is sometimes known as the series peaking circuit, the circuit of

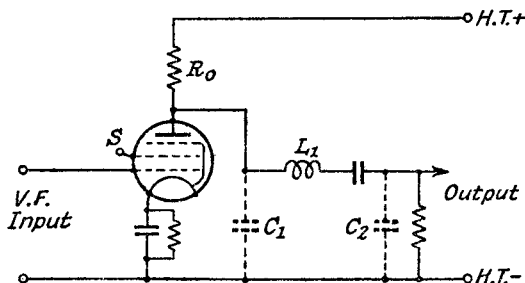


FIG. 16.11.—The Series Peaking Compensated v.f. Amplifier.

Fig. 16.9a being called the shunt peaking circuit. The circuit functions as a low-pass filter and the ratio of output-to-input voltage is

$$\frac{E_o}{E_g} = g_m \frac{R_o \frac{1}{j\omega C_1} \left( j\omega L_1 + \frac{1}{j\omega C_2} \right)}{j\omega L_1 + \frac{1}{j\omega C_1} + \frac{1}{j\omega C_2}} \cdot \frac{1}{j\omega C_2} \quad . \quad 16.21a.$$

$$= g_m \frac{R_o + \frac{1}{j\omega C_1} \left( j\omega L_1 + \frac{1}{j\omega C_2} \right)}{j\omega L_1 + \frac{1}{j\omega C_1} + \frac{1}{j\omega C_2}} \cdot \frac{1}{j\omega C_2} \quad . \quad 16.21b.$$

$$= g_m \frac{-R_o}{\omega^2 C_1 C_2} \frac{1}{R_o \left( j\omega L_1 + \frac{1}{j\omega C_1} + \frac{1}{j\omega C_2} \right) + \frac{1}{j\omega C_1} \left( j\omega L_1 + \frac{1}{j\omega C_2} \right)} \quad . \quad 16.21b.$$

Let  $R_o = \frac{1}{\omega_0 C_1 \sqrt{2m}}$  and  $L_1 = \frac{1}{2\omega_0^2 C_1}$ , where  $\frac{C_2}{C_1} = m$  and  $C_2 + C_1 = C_s$ .

Hence  $\frac{1}{C_1} = \omega_0 R_o \sqrt{2m}$ ,  $\frac{1}{C_2} = \omega_0 R_o \sqrt{\frac{2}{m}}$  and  $L_1 = \frac{R_o}{\omega_0} \sqrt{\frac{m}{2}}$ . Replacing  $L_1$ ,  $C_1$  and  $C_2$  in 16.21b by these expressions

$$\frac{E_o}{E_g} = g_m R_o \frac{\left( -\frac{2\omega_0^2}{\omega^2} \right)}{\left[ m - \frac{2\omega_0^2}{\omega^2} \right] + j \left[ \frac{\omega}{\omega_0} \sqrt{\frac{m}{2}} - \frac{\omega_0}{\omega} \left( \sqrt{2m} + \sqrt{\frac{2}{m}} \right) \right]} \quad . \quad 16.21c.$$

The most satisfactory overall performance is obtained for  $m = 2$ , when

$$\frac{E_o}{E_g} = g_m R_o \frac{\left[ -2 \frac{f_o^2}{f^2} \right] \left[ 2 \left( 1 - \frac{f_o^2}{f^2} \right) - j \left( \frac{f}{f_o} - 3 \frac{f_o}{f} \right) \right]}{\left[ 2 \left( 1 - \frac{f_o^2}{f^2} \right) \right]^2 + \left[ \frac{f}{f_o} - 3 \frac{f_o}{f} \right]^2} \quad 16.21d.$$

The attenuation characteristic is obtained by plotting

$$10 \log_{10} \frac{4 \frac{f_o^4}{f^4}}{\left[ 2 \left( 1 - \frac{f_o^2}{f^2} \right) \right]^2 + \left[ \frac{f}{f_o} - 3 \frac{f_o}{f} \right]^2} \quad 16.22$$

against  $\frac{f}{f_o}$  as in Fig. 16.12a (curve 1). Over the pass range up to  $f = f_o$  it is similar to the "shunt peaking" circuit for  $\frac{L_o}{C_s R_o^2} = 0.5$ ,

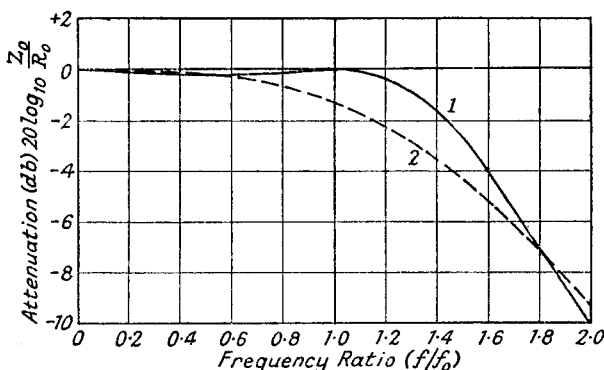


FIG. 16.12a.—Attenuation Characteristics of Compensated v.f. Amplifiers.

1. Series Peaking Circuit.
2. Combined Shunt and Series Peaking Circuit.

but at frequencies above  $f_o$  it has the advantage of more rapid attenuation. The phase angle

$$\phi = \tan^{-1} \frac{- \left( \frac{f}{f_o} - 3 \frac{f_o}{f} \right)}{2 \left( 1 - \frac{f_o^2}{f^2} \right)} \simeq -57^\circ 18' \frac{3f}{2f_o} \quad \text{when } f \ll f_o$$

and phase-angle error is

$$\Delta\phi = \tan^{-1} \frac{- \left( \frac{f}{f_o} - 3 \frac{f_o}{f} \right)}{2 \left( 1 - \frac{f_o^2}{f^2} \right)} + 57^\circ 18' \frac{3f}{2f_o} \quad 16.23$$

which is plotted against  $\frac{f}{f_0}$  in Fig. 16.12b (curve 1). Phase-angle error is very small over the pass range up to  $f = f_0$  and is much less

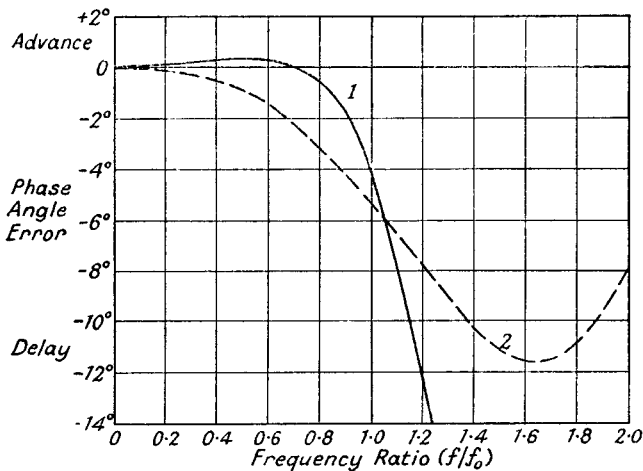


FIG. 16.12b.—Phase Angle Error Curves of Compensated v.f. Amplifiers.

1. Series Peaking Circuit.

2. Combined Shunt and Series Peaking Circuit.

than that of the previous case. If  $C_s$  and  $f_0$  have the same values as those for the shunt peaking circuit,  $R_0 = \frac{1}{2\omega_0 C_1} = \frac{3}{2\omega_0 C_s} = 2,270 \Omega$ ; hence amplification is 1.5 times as great as for the previous case.

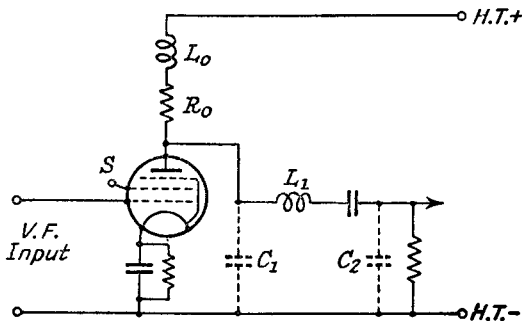


FIG. 16.13.—The Combined Shunt and Series Peaking Compensated v.f. Amplifier.

The net increase in amplification may not be as large as 1.5 because it may be necessary to add a trimmer capacitance to either  $C_1$  or

$C_2$  to obtain the required ratio of  $\frac{C_2}{C_1} = 2$ , and this increases  $C_s$  and so reduces amplification. Values of  $m < 2$  tend to give a more peaked frequency response, whilst values greater than 2 tend to cause a more rapid fall at high frequencies. The resistance component of  $L_1$  has little effect on performance provided it is not more than  $\frac{1}{20}\omega L_1$ .

Still greater amplification can be obtained by combining the shunt and series peaking circuits as in Fig. 16.13. The expression for the ratio of output-to-input voltage is found by replacing  $R_o$  by  $R_o + j\omega L_o$  in 16.21*b*, thus

$$\frac{E_o}{E_g} = g_m \frac{(R_o + j\omega L_o)}{\omega^2 C_1 C_2} \cdot \frac{1}{(R_o + j\omega L_o) \left( j\omega L_1 + \frac{1}{j\omega C_1} + \frac{1}{j\omega C_2} \right) + \frac{1}{j\omega C_1} \left( j\omega L_1 + \frac{1}{j\omega C_2} \right)} \quad .16.24a.$$

The following relationships between  $R_o$ ,  $L_o$ ,  $L_1$ ,  $C_1$  and  $C_2$  are suggested as providing a satisfactory frequency and phase characteristic.

$$R_o = \frac{1.8}{\omega_o C_s}, \quad C_s = C_1 + C_2, \quad C_1 = \frac{C_2}{m}, \quad m = 2,$$

$$\text{i.e.,} \quad C_1 = \frac{1}{1.66\omega_o R_o}; \quad C_2 = \frac{1}{0.833\omega_o R_o}.$$

$$L_o = 0.12C_s R_o^2 = \frac{0.216R_o}{\omega_o}$$

$$L_1 = 0.52C_s R_o^2 = \frac{0.937R_o}{\omega_o}.$$

Inserting these values in 16.24*a*, we get

$$\frac{E_o}{E_g} = \frac{g_m R_o 1.387 \frac{f_o^2}{f^2} \left( 1 + j0.216 \frac{f}{f_o} \right)}{1.387 \frac{f_o^2}{f^2} + 0.202 \frac{f^2}{f_o^2} - 2.099 + j \left( 2.5 \frac{f_o}{f} - 0.937 \frac{f}{f_o} \right)} \quad .16.24b.$$

The attenuation characteristic, curve 2 in Fig. 16.12*a*, is obtained by plotting

$$10 \log_{10} \frac{1.92 \frac{f_o^4}{f^4} \left( 1 + 0.0467 \frac{f^2}{f_o^2} \right)}{\left[ 1.387 \frac{f_o^2}{f^2} + 0.202 \frac{f^2}{f_o^2} - 2.099 \right]^2 + \left[ 2.5 \frac{f_o}{f} - 0.937 \frac{f}{f_o} \right]^2} \quad .16.25$$

against  $\frac{f}{f_0}$ ; the phase angle is

$$\phi = \tan^{-1} \frac{-2 \cdot 2 \frac{f_0}{f} + 0 \cdot 484 \frac{f}{f_0} + 0 \cdot 0437 \frac{f^3}{f_0^3}}{1 \cdot 387 \frac{f_0^2}{f^2} - 1 \cdot 559}$$

$$= 57^\circ 18' \times -1 \cdot 589 \frac{f}{f_0} \text{ when } f \ll f_0.$$

Phase-angle error is

$$\Delta\phi = \tan^{-1} \frac{-2 \cdot 2 \frac{f_0}{f} + 0 \cdot 484 \frac{f}{f_0} + 0 \cdot 0437 \frac{f^3}{f_0^3}}{1 \cdot 387 \frac{f_0^2}{f^2} - 1 \cdot 559} + 57^\circ 18' \times 1 \cdot 589 \frac{f}{f_0} \quad . \quad 16.26$$

and it is plotted in Fig. 16.12*b* as curve 2. For the particular component relationships chosen, neither attenuation nor phase characteristics are as good as those for the previous circuit.

Allowing a loss of  $-1$  db.,  $\frac{f}{f_0} = 0 \cdot 9$  for  $f = 3 \cdot 5$  Mc/s gives

$$R_0 = \frac{1 \cdot 8 \times 0 \cdot 9 \times 10^6}{6 \cdot 28 \times 3 \cdot 5 \times 30} = 2,455 \Omega.$$

Hence amplification is slightly higher for this combination of shunt and series peaking circuits.

There are many other possible forms of compensated circuit, including varieties of the constant  $k$  low-pass filter prototype and  $m$ -derived structures, and reference should be made to Bibliography 26.

The values of  $C_1$  and  $C_2$  can be measured by means of a circuit magnification or  $Q$  meter, or may be calculated by noting the frequency at which the amplification of the uncompensated amplifier falls to 0.707 of its maximum value, and by using the fact that

$$R_0 = \frac{1}{\omega C} \text{ at this frequency.}$$

Measurement of the amplification characteristic of a v.f. amplifier can be made, using the c.r. tube grid as a diode detector and noting the variation in amplifier input voltage necessary to preserve constant c.r. tube grid current. The phase shift characteristic can be noted by applying the input and output voltages of the amplifier to a horizontal and a vertical deflector plate of a c.r. tube. If the input and output voltages are adjusted to give equal amplitudes of deflection,  $0^\circ$ ,  $180^\circ$ ,  $360^\circ$ , etc., phase angles are denoted by a

straight line at  $45^\circ$  and  $135^\circ$ , and phase angles of  $90^\circ$ ,  $270^\circ$ , etc., by a circle. Alternatively, a calibrated phase-shifting network consisting of a resistance and capacitance can be included in the input or output lines so as to recover the  $0^\circ$  straight line condition.

**16.8.3. Low Frequency Performance.** Frequencies below 10 kc/s contribute very little to the horizontal detail of the picture but do affect vertical detail. Poor low-frequency performance affects background intensity causing it to vary from top to bottom of the picture, e.g., a transmitted all-white screen is reproduced as a screen gradually shading from white to grey from top to bottom, or vice versa. Phase distortion, which is caused by the increasing reactance of coupling and self-bias capacitors as the frequency is

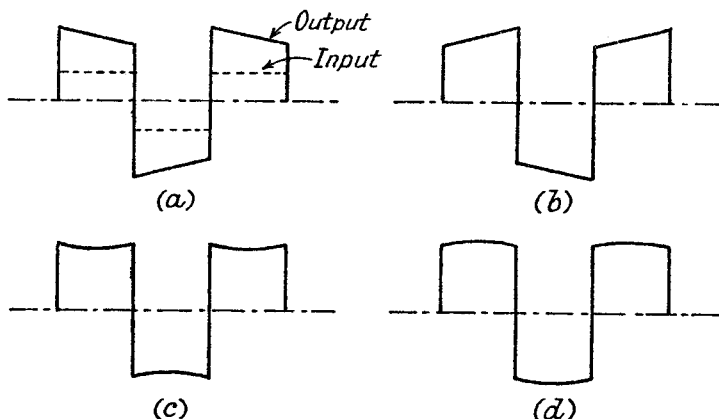


FIG. 16.14.—Examples of Phase and Attenuation Distortion of a Square Wave Input Signal.

decreased, is much more serious than attenuation distortion. A coupling capacitance of  $0.1 \mu\text{F}$  and resistance of  $0.5 \text{ M}\Omega$  in the grid circuit of a v.f. amplifier produce a frequency response at 50 c.p.s. of 99.82% of the maximum, but the phase shift is  $\tan^{-1} \frac{3.18}{50} = 3^\circ 38'$ , which is equivalent to a time advance of

$\frac{3^\circ 38' \times 10^6}{360 \times 50} = 201.5 \mu \text{ secs.}$  The effect of phase distortion is more

conveniently examined by applying an input voltage of square wave shape rather than a single-frequency voltage, and examples of types of distorted output wave shapes which may be obtained are shown in Figs. 16.14a, 16.14b, 16.14c and 16.14d. A square-shaped voltage wave applied to the coupling capacitance and resist-



ance in the grid circuit of a v.f. amplifier produces across the resistance the wave shape shown in Fig. 16.14*a*, the trailing ends of the upper and lower parts of the original square wave being tilted towards the centre line. The distorted section is part of an exponential curve  $E \varepsilon^{\frac{-t}{R_o C_c}}$ . If the wave has a fundamental frequency of 50 c.p.s. and  $C_c$  and  $R_o$  are  $0.1 \mu\text{F}$  and  $0.5 \text{ M}\Omega$ , the percentage fall in voltage from leading to trailing edge is  $(1 - \varepsilon^{\frac{-20}{100}}) 100\% = 18.2\%$  (note that  $t = \frac{1}{2 \times 50}$  secs.); for a fundamental frequency of 25 c.p.s., the percentage fall is 33%. This voltage fall can be reduced either by increasing  $C_c$  or  $R_o$ , or by including a compensating circuit in the anode of the v.f. amplifier. The maximum value of  $R_o$  is limited to about  $0.5 \text{ M}\Omega$  by considerations of valve life, so that only  $C_c$  can be increased. Making  $C_c = 0.5 \mu\text{F}$  reduces the fall to 3.92% at 50 c.p.s. and 7.69% at 25 c.p.s., which would generally be regarded as satisfactory. The increased bulk of  $C_c$  would tend to increase the input earth capacitance of the v.f. amplifier and so affect high-frequency response.

It is possible to produce a compensating tilt in the opposite direction by means of a decoupling capacitance ( $C_s$  in Fig. 16.15)

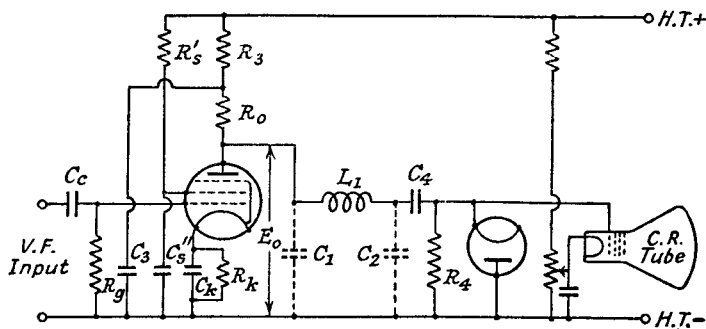


FIG. 16.15.—A Circuit for Improving the v.f. Amplifier Response to a Square Wave and for Restoring the D.C. Component of the Vision Signal.

in the anode circuit of the v.f. amplifier. A square wave of input voltage at the grid is caused by  $C_s$  in association with  $R_o$  to have the output voltage wave shape of Fig. 16.14*b*, and exact compensation of grid circuit distortion can be achieved by a suitable choice of  $C_s$ , provided  $R_s$  is much larger (about 10 times) than the reactance of  $C_s$  at the square wave fundamental frequency. Analysis of the circuit of Fig. 16.15 shows that amplification is

$$\frac{E_o}{E_g} = g_m \left( R_o + \frac{1}{j\omega C_s} \right) \left( \frac{R_g}{R_g + \frac{1}{j\omega C_c}} \right) \quad . \quad . \quad 16.27a$$

when  $R_s \gg \frac{1}{\omega C_s}$ , and  $R_s \gg R_o$

$$\begin{aligned} \frac{E_o}{E_g} &= g_m R_g \left( R_o + \frac{1}{j\omega C_s} \right) \frac{R_g - \frac{1}{j\omega C_c}}{R_g^2 + \left( \frac{1}{\omega C_c} \right)^2} \\ &= \frac{g_m R_g}{R_g^2 + \left( \frac{1}{\omega C_c} \right)^2} \left[ R_o R_g + \frac{1}{\omega^2 C_s C_c} - \frac{j}{\omega} \left( \frac{R_g}{C_s} - \frac{R_o}{C_c} \right) \right] \quad . \quad 16.27b. \end{aligned}$$

Phase distortion is, therefore, completely cancelled by making the time constant of the grid circuit equal to that of the anode circuit, i.e.,  $R_g C_c = R_o C_s$ , provided  $R_s$  can be neglected. The anode decoupling circuit is primarily a phase distortion compensator, and though it does tend to cancel attenuation distortion—it has a rising low-frequency response as frequency is decreased—it may not be sufficient to produce zero overall attenuation distortion. An example of the wave shape to be expected from a phase-corrected stage having a decreasing low-frequency response<sup>8</sup> is illustrated in Fig. 16.14c, and in Fig. 16.14d is shown the waveform resulting from a rising low-frequency response.

When  $R_s$  is comparable with the reactance of  $C_s$ —this occurs as the frequency approaches a very low value such as 5 c.p.s.—expression 16.27a is modified to

$$\begin{aligned} \frac{E_o}{E_g} &= g_m \left( R_o + \frac{R_s}{1 + j\omega C_s R_s} \right) \left( \frac{R_g}{R_g + \frac{1}{j\omega C_c}} \right) \\ &= g_m \left( \frac{R_o + R_s + j\omega C_s R_s R_o}{1 + j\omega C_s R_s} \right) \left( \frac{R_g}{R_g + \frac{1}{j\omega C_c}} \right) \\ &= g_m (R_o + R_s) \left( \frac{1 + \frac{j\omega C_s R_s R_o}{R_o + R_s}}{1 + j\omega C_s R_s} \right) \frac{R_g j\omega C_c}{(1 + j\omega C_c R_g)} \quad . \quad 16.27c. \end{aligned}$$

Exact phase compensation is no longer possible because rationalization of 16.27c produces a  $j$  term in the numerator of

$$j \left[ 1 + \frac{\omega^2 C_s R_s^2}{R_o + R_s} (C_s R_o - C_c R_g) \right]$$

and a real term of

$$p \left[ C_c R_g \left( 1 + \frac{p^2 C_3^2 R_3^2 R_0}{R_0 + R_3} \right) + C_3 R_3 \frac{R_3}{R_0 + R_3} \right].$$

Hence the phase angle can neither be made constant nor proportional to  $p$ , i.e., to frequency.

If  $\frac{C_3 R_3 R_0}{R_3 + R_0} = C_c R_g$ , expression 16.27c becomes

$$\frac{E_0}{E_g} = \frac{g_m R_0}{1 + \frac{1}{j p C_3 R_3}},$$

i.e., phase and attenuation distortion is a function of  $C_3$  and  $R_3$  and is independent of the grid circuit. There is, therefore, little advantage in using  $C_3$  and  $R_3$  for correcting grid circuit distortion unless the time constant of the decoupling capacitance and resistance can be made much greater than that of the grid circuit. Hence  $R_3$  should be given its highest possible value, and this is generally 5,000  $\Omega$  (a very high value cannot be considered because it reduces the D.C. anode voltage of the v.f. amplifier). If  $R_g = 0.5 \text{ M}\Omega$ ,  $C_c = 0.1 \text{ }\mu\text{F}$ ,  $R_0 = 2,500 \text{ }\Omega$  and  $R_3 = 5,000 \text{ }\Omega$

$$C_3 = \frac{R_g C_c (R_0 + R_3)}{R_0 R_3} = 30 \text{ }\mu\text{F}$$

$$C_3 R_3 = 0.15 \text{ secs.} = 3 C_c R_g.$$

Thus the use of the compensating decoupling circuit has reduced the frequency for a given loss and the phase shift to a third of its value for the uncompensated stage, i.e., a frequency of  $\frac{5.0}{3}$  or 16.66 c.p.s. now suffers a phase shift of  $3^\circ 38'$  and amplifier response at this same frequency is 99.82% of its maximum value.

The bias voltage for the v.f. amplifier may be derived from a fixed voltage source; it may be provided by the anode current passing through a cathode resistance, or by grid current produced by the input signal. Fixed bias voltage has the advantage that a simple filter circuit (for hum voltages) can be designed to produce very small phase and attenuation distortion of the signal, but it does not compensate for H.T. supply voltage changes; the grid resistance  $R_g$  must therefore be limited to a lower value than with cathode self-bias. Cathode self-bias causes phase and attenuation distortion at low frequencies unless the shunt capacitor  $C_k$  in Fig. 16.15 is made very large, e.g., 200 to 1,000  $\mu\text{F}$ . Low-frequency performance is improved by omitting  $C_k$ , but there is a large reduction in amplification, and high-frequency performance is affected

because stray capacitance across  $R_k$  tends to reduce the degeneration at high frequencies. Grid current biasing from the signal voltage has the advantage of retaining the D.C. component of the signal in the v.f. anode current, but there is a danger of taking too large an anode current when the signal ceases.

Phase and attenuation distortion from the cathode self-bias circuit can be compensated by a suitable choice of decoupling capacitance and resistance in the anode circuit. Since  $R_a \gg Z_0$

$$\frac{E_o}{E_g} = \frac{g_m Z_0}{1 + g_m Z_k}$$

where

$$Z_0 = R_0 + \frac{R_3}{1 + j\omega C_3 R_3}$$

and

$$Z_k = \frac{R_k}{1 + j\omega C_k R_k}$$

In order that the decoupling circuit may exactly compensate for the self-bias circuit

$$\frac{E_o}{E_g} = g_m R_0 = \frac{g_m Z_0}{1 + g_m Z_k}$$

i.e.,

$$(1 + g_m Z_k) = \frac{Z_0}{R_0}$$

or

$$1 + \frac{g_m R_k}{1 + j\omega C_k R_k} = 1 + \frac{R_3}{R_0(1 + j\omega C_3 R_3)}$$

Hence equating imaginary and real terms

$$C_k R_k = C_3 R_3$$

$$g_m R_k = \frac{R_3}{R_0}$$

or

$$g_m R_0 = \frac{R_3}{R_k} = \frac{C_k}{C_3} \quad . \quad . \quad . \quad 16.28.$$

Typical values for  $C_k$  and  $R_k$  are  $25 \mu\text{F}$  and  $150 \Omega$ , so that for  $g_m = 10 \text{ mA/volt}$  and  $R_0 = 2,500 \Omega$ ,  $C_3 = 1 \mu\text{F}$  and  $R_3 = 3,750 \Omega$ .

The following is the normal procedure for cathode circuit correction.  $C_k R_k$  and  $R_0$  are given their specified values,  $C_3$  is made about  $1 \mu\text{F}$  and  $R_3$  about  $5,000 \Omega$ . A 10 kc/s input voltage is applied and the amplification noted—at this frequency the reactances of  $C_k$  and  $C_3$  are negligibly small.  $C_k$  and  $C_3$  are next removed and  $R_3$  adjusted to give the same overall amplification as previously.

$R_3$  is then measured and  $C_3$  calculated from  $C_3 = \frac{C_k R_k}{R_3}$ .

The screen circuit, like the cathode circuit, can also produce

attenuation and phase distortion and it may be compensated by the anode decoupling circuit. Exact compensation is obtained by equating expressions for  $B$  and for  $x$  in Sections 9.3.5 and 6,

$$\text{thus} \quad \frac{R_3}{R_s'} = \frac{C_s''}{C_3} = \frac{R_0}{R_{SG}}$$

where  $R_s'$  = external resistance in the screen H.T. path

$C_s''$  = screen decoupling capacitance

$$R_{SG} = \text{slope resistance of the screen electrode} = \frac{\Delta E_s}{\Delta I_s}$$

It is clearly not possible to compensate for the grid, cathode and screen circuits in one stage, and it is usual when more than one stage is employed to use the decoupling circuit of one stage for grid circuit correction, one for cathode self-bias and one for screen circuit correction. Screen circuit components generally have less effect on attenuation and phase distortion than cathode self-bias components. When only one stage of v.f. amplification is employed, grid circuit correction may be used and the bias derived from a fixed voltage source, or the time constant of the grid circuit ( $R_g C_g$ ) may be made as large as possible and cathode self-bias distortion corrected in the anode circuit. Low-frequency performance will generally be found satisfactory if phase and attenuation is small down to a frequency of 25 c.p.s.

Motor boating is sometimes a problem, more particularly with a large number of v.f. stages, and great care must be taken to ensure that the power supply has a low impedance, i.e., large smoothing capacitors are needed. In extreme cases it may be necessary to reduce the grid coupling capacitors so as to attenuate very low frequencies.

**16.8.4. Restoration of the D.C. Component.** The need for restoring the D.C. component of the vision signal has been stressed in Section 16.8.1. If this component is absent, the vision output wave automatically centres itself so that "positive" and "negative" areas are equal, as shown beneath the beam current-grid voltage curve of the C.R. tube in Fig. 16.16. The bias position is  $A$  and the combined v.f. and synchronizing input signal automatically centres itself on the line  $AB$ . Thus position 1 corresponds to a maximum white line and position 2 to a black line. This means that the correct black position (line  $DF$ , the start of the synchronizing pulses) is variable in relation to the bias line  $AB$  and contrast is lost. The D.C. component can be restored if a variable positive bias just cancelling the difference in voltage,  $E_d$ , between

the correct black line  $HG$  and the vision signal black line  $DF$  is included in the grid circuit of the cathode ray tube. This can be accomplished by using a diode connected as shown in Fig. 16.15, to act as a peak voltage detector of the "negative" half of the vision a.c. wave, i.e., on the synchronizing pulse side. If the time constant of the coupling capacitance  $C_4$  and diode load resistance,  $R_4$ , which is also the coupling resistance to the c.r. tube, is made sufficiently large, the bias produced across  $R_4$  is nearly equal to the negative peak voltage,  $E_1$ , of the input wave. By suitable location of the bias point  $A$ ,  $DF$  can be made to coincide with  $GH$  as shown in position 3. The time constant must not, however, be so large that it makes the bias change sluggish to changes of picture background brightness. A time constant of 0.1 second is suitable; too low a value causes noticeable lack of contrast.

The action of the diode bias also tends to restore the downward tilt of a square wave input (Fig. 16.14a) due to phase and attenuation distortion in the v.f. amplifier, the direction of the variable diode bias being opposite to the wave tilt. In order to obtain this correction, the time constant  $C_4 R_4$  must be

not greater than that of circuit being corrected but must be much greater than the period of the line frequency.

It is possible to use the last v.f. amplifier as a D.C. restorer if the cathode ray tube grid can be directly connected to the amplifier anode, i.e., the cathode of the c.r. tube cannot be at vision receiver earth potential but must be connected to a potential divider across the receiver H.T. supply. The amplifier valve is operated as a cumulative-grid detector with zero standing bias, and D.C. restoration occurs by grid current detection. There are three serious objections to the method: if the receiver rectifier heats up more quickly than the v.f. amplifier, positive bias is applied to the c.r.

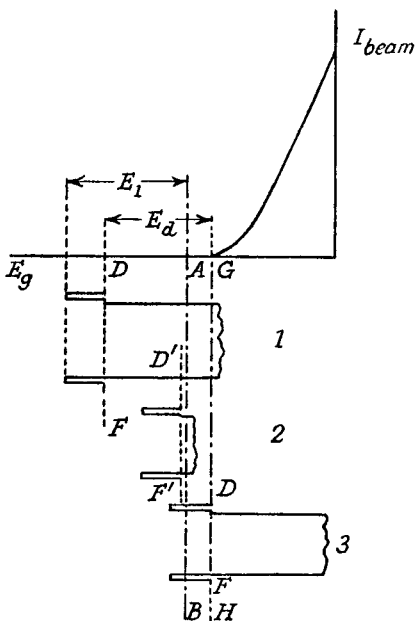


Fig. 16.16.—A Diagram Illustrating the Need for Restoring the D.C. Component of the Vision Signal.

tube grid, screen voltage tends to vary with changes of grid bias, and screen voltage must be reduced to prevent excessive anode dissipation in the absence of a signal, and this leads to a reduction in amplification.

With positive modulation transmission a biased diode limiter (see Section 12.9) may be incorporated to suppress "snowflake" interference on the picture. The diode is non-conductive for normal signals but peaked interference voltages cause it to conduct and apply a negative pulse to the c.r. tube grid, thus blacking out on interference. With negative modulation, peaks of interference automatically black-out the picture at the spot where they occur.

## 16.9. Synchronizing Pulse Separation.

**16.9.1. Introduction.** Two actions are involved in synchronizing pulse separation: the first, known as amplitude separation, divides the I.F. or V.F. signal into vision and pulse components and rejects the former; the second, known as frequency separation, divides the synchronizing voltage into frame and line pulses, which are then used to lock the frame and line scanning generators employed for deflecting the c.r. tube spot across the screen. Synchronism can be established with the scanning generator "free" frequency fast or slow, but slow running is preferable because stable locking is possible over a wider range of frequencies than if the generator frequency is fast. Correct polarity of synchronizing pulse is essential, and this depends on the type of scanning generator and the point at which the pulse is applied. If it is injected into the grid circuit of a slow-running generator, it must usually be in a positive direction, the start of the pulse, where it joins the vision component, being negative. With the American system of negative modulation and the v.f. detector connected as in Fig. 16.7, an even number of phase reversals must be included between the detector output and the scanning generator. The English system of positive modulation calls for an odd number of phase reversals between the detector output (Fig. 16.7) and the scanning generators, because the initial synchronizing pulse is in a negative direction.

For most satisfactory synchronization the free frequency of the scanning generator is set about half-way between the correct and "fall-out" frequency, so that the generator is held in synchronism when its free frequency varies in either direction. Variations of frequency are caused by supply voltage fluctuations, and hum or noise voltages injected into the scanning generator circuits. An adequately smoothed H.T. supply is most necessary, and if iron-cored

coils are used in the generator circuit they must be carefully screened from sources of A.C. mains magnetic field. Hum and noise voltages tend to affect interlacing, causing unequal spacing or weaving of interlacing lines. Limitation of pulse amplitude in a positive direction is advisable in order to reduce the effect of peaked noise pulses of large amplitude and short duration. The advantage of this limiting is particularly marked at the edge of the service area of a television transmission, and a steady picture can often be obtained from a signal one-fifth to one-tenth of that which is required to provide a steady picture when no limiter is employed. The voltages required for synchronizing depend on the type of scanning generator employed. The blocking or squegger oscillator requires from 5 to 15 volts, the multivibrator 0.5 to 2 volts, and about the same is needed for the gas-filled relay.

The line and frame pulses must be filtered from each other, and feedback between the two scanning generators must be prevented, otherwise the frame is liable to be triggered by the line, and interlacing is erratic.

**16.9.2. Amplitude Separation of the Vision and Synchronizing Components.**<sup>4,7</sup> Separation of the synchronizing pulses from the vision component of the television signal can be accomplished by using a detector type of valve, such as a diode, leaky grid or anode bend, and the principles involved are very similar to those of the amplitude limiter of the F.M. receiver. The input to the

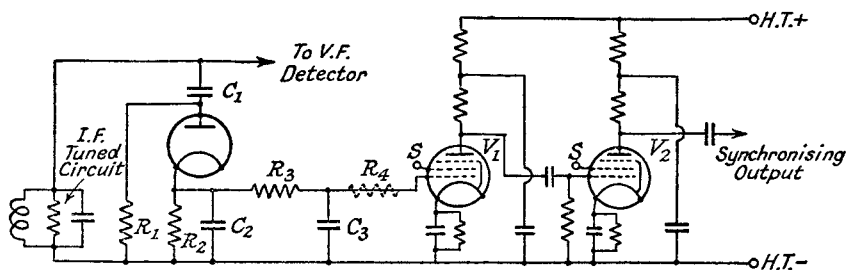


FIG. 16.17a.—Separation of the Synchronizing Signals from the Vision Signal for the American Type of Negative Modulation Transmission.

amplitude separator may be taken from the output of the last I.F. valve, the V.F. detector or a V.F. amplifier stage. An example of the diode separator operating from the I.F. output is shown in Fig. 16.17a, the circuit is only suitable for the American system in which the synchronizing pulses occur at maximum carrier. The time constant of the coupling capacitance  $C_1$  (0.05 to 0.1  $\mu\text{F}$ ) and



resistance  $R_1$  ( $0.5$  to  $1\text{ M}\Omega$ ) is large in order that the D.C. bias voltage across  $R_1$  shall remain almost constant at a value slightly higher than the start of the synchronizing pulse. The latter causes the diode to conduct and produce across  $R_2$  ( $3,000\ \Omega$  to  $5,000\ \Omega$ ) a voltage wave similar in shape to the synchronizing pulse. The by-pass capacitance  $C_2$  ( $100\ \mu\mu\text{F}$ ) is to assist in removing I.F. ripple and v.f. voltages from the output, and additional filtering is provided by  $R_3$  ( $2,000\ \Omega$ ) and  $C_3$  ( $100\ \mu\mu\text{F}$ ). The output voltage across  $C_3$  is directly connected to an amplifier valve biased almost to the anode current cut-off point, which is given a low negative value by using a low anode voltage<sup>3</sup> if the valve is a triode, or low screen voltage if a tetrode. A resistance  $R_4$  ( $0.1\text{ M}\Omega$ ) can be included in series with the grid of the amplifier valve to limit the pulse amplitude in a positive direction. The amplitude of the pulse and any interference, which is superimposed on it or breaks through the vision

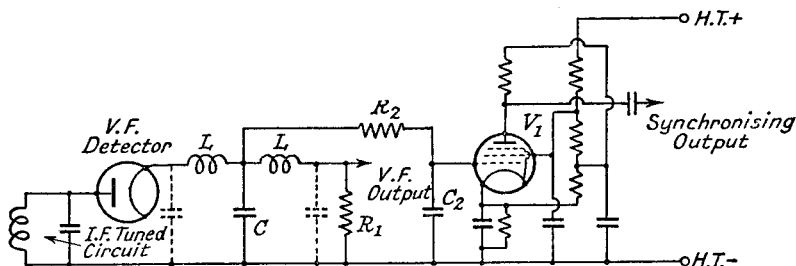


FIG. 16.17b.—An Anode Bend Type of Synchronizing Signal Separator for the English System of Positive Modulation

signal, cannot greatly exceed the cut-off bias voltage because grid current in association with  $R_4$  prevents the grid of the amplifier becoming appreciably positive. The synchronizing pulse is in a positive direction across  $R_2$  and an additional phase reversal is necessary after  $V_1$  to regain the positive direction. This is provided by including a second valve  $V_2$ . The latter can be omitted if the diode connections are reversed and the bias on  $V_1$  adjusted to a value sufficient to prevent grid current flowing. Pulse amplitude limitation is then brought about by anode current cut-off. Fig. 16.17b shows the anode bend type of separator. It may be supplied from the v.f. detector output if the English system of positive transmission is being received and the detector is connected to give a positive vision signal. The valve is biased into cut-off and the vision component is cut off by the action of the grid series resistance  $R_2$  ( $0.1\text{ M}\Omega$ ) and grid current. Screen voltage, which controls the

cut-off bias voltage, has a comparatively low value (30 to 40 volts), so that the pulse amplitude is limited, with consequent reduction in interference from noise. Not only is the vision component cut-off by the action of the grid circuit, but it may also be cut off by using a low anode voltage to produce a flat-topped  $I_a E_g$  characteristic at grid voltages near zero and in the positive bias region. A triode valve is not likely to be satisfactory in this type of separator because the vision component may be transferred from the grid to the anode circuit through the anode-grid capacitance. Phase reversal of the pulse direction occurs in valve  $V_1$ , which therefore gives a positive pulse output. The leaky grid amplitude separator, shown in Fig. 16.17c, will function with a v.f. input voltage provided the synchronizing pulses are positive. Low anode and screen

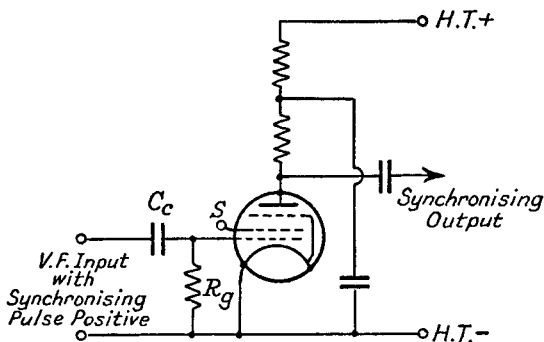


FIG. 16.17c.—The Leaky Grid Synchronizing Signal Separator.

voltages are employed to limit pulse amplitude and noise interference. The time constant of the grid circuit is sufficiently high (about 0.05 seconds) to prevent rapid changes of bias voltage due to the vision components. In order to obtain at the separator output a satisfactory synchronizing pulse shape independent of the vision signal, the input synchronizing amplitude should exceed a voltage equal to the cut-off bias of the valve. The latter may be operated from the i.f. output when the television signal has negative modulation. An additional phase reversing stage is necessary to convert the pulse output to a positive direction.

**16.9.3. Frequency Separation of the Frame and Line Pulses.** The frame and line synchronizing pulses must be separated from each other, and interaction between the scanning generators (particularly from line to frame) must be prevented, otherwise erratic interlacing occurs. Normal filter circuits do not provide

sufficient discrimination without severe mutilation of the pulse wave shape. Attenuation and phase distortion adversely affect the higher harmonic pulse components which control the slope of its leading edge. The latter should be as sharp as possible or synchronism becomes dependent on pulse amplitude and is liable to be affected by interference superimposed on the leading edge. The most satisfactory form of filter for selecting the line pulse has proved to be the differentiator type. This may consist either of a high resistance and an inductance, or a capacitance and a low resistance to which is applied a voltage of synchronizing pulse shape, the output voltage in the first case being that across the reactance and in the second that across the low resistance. The first is provided by a tetrode valve, which has an inductance in its anode circuit, and to the input of which is applied the rectangular synchronizing pulses. The tetrode, owing to its high slope resistance, produces an anode current wave identical in shape to the input voltage wave, and there appears across the inductance a voltage, the shape of which is a differential of the current wave  $\left(E_L = L \frac{dI_a}{dt}\right)$ . The actual voltage wave shape depends on the resistance component of the inductance, and if this is small it is a sharp pulse of much shorter duration than the rectangular synchronizing pulse, as shown in Fig. 16.18*a*. Increased resistance in the inductance causes a pulse of longer duration, slower rate of rise and smaller amplitude. There is a similar pulse in the opposite direction on the downstroke of the synchronizing pulse, but this has no effect on the scanning generator, being in the wrong direction for triggering it. For the second differentiator circuit the reactance of the capacitance at the fundamental frequency of the synchronizing pulse must be large compared with the output and generator resistance. Hence the valve supplying the voltage of synchronizing pulse shape must be a triode. The voltage appearing across the output resistance is a function of circulating current, which, if the total resistance is low, is a function of the differential of the applied voltage. These differentiator filters may also be considered from the angle of circuits having a frequency response proportional to frequency; the fundamental and lower harmonic components of the pulse have reduced amplification compared with the higher harmonics, thus tending to sharpen the leading edge of the pulse and reduce its duration. The inductance differentiator is more commonly used, and the line synchronizing output pulse may be obtained from a secondary coil connected to it. Phase reversal is then possible without an extra

valve stage. Line synchronizing is carried on during the frame synchronizing pulse in order that the first few visible lines at the beginning of a new frame may not be jumbled while the line scanning generator is being pulled into synchronism.

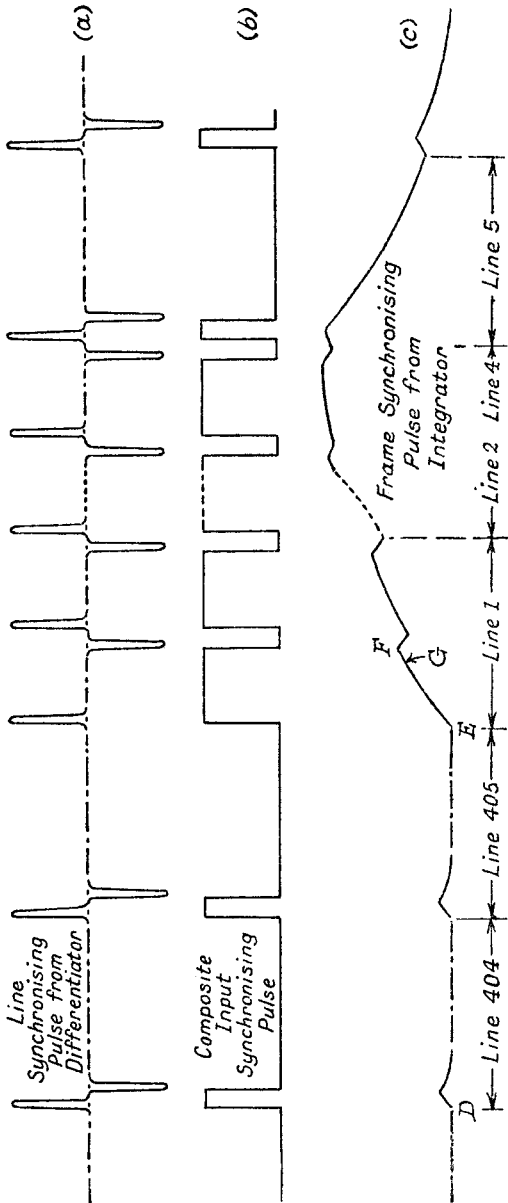


FIG. 16.18.—Illustration of the Method of Separating the Line from the Frame Pulse in the Synchronising Signal.

The frame synchronizing pulse is separated from the line by using an integrator circuit, consisting of a parallel combination of resistance and capacitance, to which is applied through a high resistance a voltage of synchronizing pulse shape. The frame output voltage is taken across the  $RC$  combination, and is an integral function  $\left(E_c = \int \frac{Idt}{C}\right)$  of the current through the capacitance. The frequency response of this circuit is the opposite of the differentiator, attenuation of the higher harmonic components of the pulse occurring. The voltage wave shape across the integrator circuit is shown beneath the synchronizing input wave shape in Fig. 16.18c. The line pulses produce a voltage across the integrator, but it is small because the line pulse duration is only 10% of the total line time and is insufficient to synchronize the frame scanning generator. The frame pulse of much longer duration (40% of the line time) produces a large voltage component as shown by the section  $EF$  in Fig. 16.18c. Synchronism should take place on the first up-stroke at about the point  $G$ .

A circuit diagram of a typical frequency separator is shown in Fig. 16.19. The inductance  $L_1$  forms the differentiator for the line

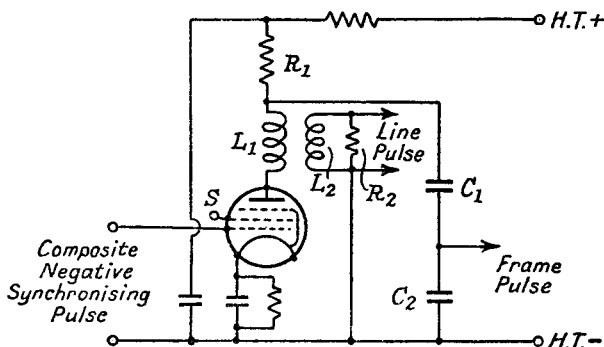


FIG. 16.19.—A Circuit for Separating the Line from the Frame Pulse in the Synchronizing Signal.

synchronizing pulses, which are taken from the secondary coil  $L_2$  to the line scanning generator. A comparatively low resistance  $R_2$  (3,000 to 5,000  $\Omega$ ) is connected across  $L_2$  to prevent damped oscillations occurring due to resonance of  $L_1$  or  $L_2$  with the stray capacitance. The frame integrator circuit is provided by  $R_1$  (10,000  $\Omega$ ) in parallel with  $C_1$  and  $C_2$  in series.  $C_1$  is about one-tenth of  $C_2$  (0.025  $\mu F$ ) and there is therefore a reduction in pulse amplitude. The chief advantage of this capacitance divider is that

$C_2$  can also be the grid blocking capacitor of a blocking oscillator acting as the frame scanning generator: a negative direction of synchronizing pulse is required at the input to the valve in order to give the required positive direction to the frame output pulse. The transformer connection between  $L_1$  and  $L_2$  allows phase reversal of the line synchronizing pulse, so that either a positive or negative input pulse could be used if only line synchronizing has to be considered.

Another form <sup>28</sup> of frequency separator is illustrated in Fig. 16.20. The valve, a pentode, is supplied from the output of a v.f. amplifier giving a negative vision signal and positive synchronizing pulse, and it operates as a leaky-grid detector to separate vision from synchronizing signals in the same manner as the circuit of Fig. 16.17c. The

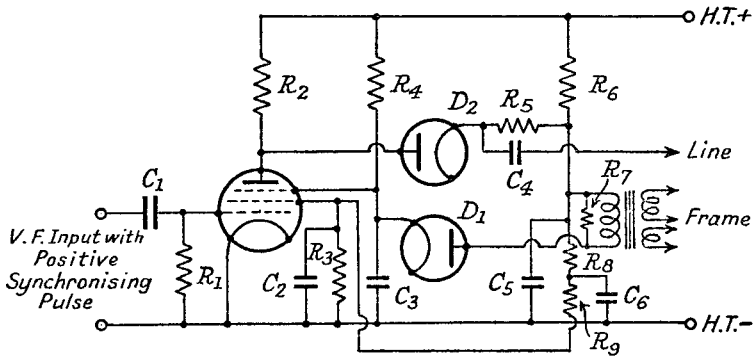


FIG. 16.20.—A Circuit for Separating the Line from the Frame Pulse in the Synchronizing Signal.

line and frame pulses at the output of the valve are therefore in a negative direction and they are taken from two separate electrodes, the anode and suppressor grid respectively; hence the possibility of interaction between line and frame scanning generators is almost negligible.

The suppressor grid external resistance  $R_4$  ( $0.25 \text{ M}\Omega$ ) is high, and this produces a saturated suppressor grid current-input grid voltage characteristic with a change from cut-off to the saturated current condition for  $0.75$  to  $1$  volts change of grid bias. Frame pulse amplitude is therefore limited in a positive as well as negative current direction. The resistance  $R_4$  and capacitance  $C_3$  ( $0.0003 \mu\text{F}$ ) form the integrator circuit, and the voltage pulses due to the line synchronizing (see section *DE* of the frame voltage integrated wave in Fig. 16.18c) are removed from the frame pulse by the biased diode

separator  $D_1$ , the anode of which is slightly negative with respect to the cathode in the intervals between frame synchronizing pulses. Phase reversal of the frame output signal is obtained by the transformer connection to the scanning generator coils. The line output pulse is not differentiated but appears in almost the original rectangular form across the anode load resistance  $R_2$ , which has a much lower value ( $5,000 \Omega$ ) than the suppressor grid resistance  $R_4$ , in order to prevent attenuation of the higher harmonic components. A diode  $D_2$ , connected in the opposite way to  $D_1$ , acts as an amplitude limiter. As the line pulse amplitude is increasing, the anode voltage is decreasing and the voltage on the anode of diode  $D_2$  eventually falls below that of the cathode, causing the diode current in the output resistance  $R_5$  ( $5,000 \Omega$ ) to become zero. Any increase in line amplitude produces no further change of voltage across  $R_5$ . The line synchronizing pulse is in a negative direction and the equivalent of a phase reversal is achieved by injecting it into the cathode instead of the grid circuit of the scanning generator. Component values for this type of amplitude separator are as follows :

Component	$C_1$	$C_2$	$C_3$	$C_4$	$C_5$	$C_6$
Value .	$0.001 \mu\text{F}$	$2 \mu\text{F}(\text{elec.})$	$0.0003 \mu\text{F}$	$0.1 \mu\text{F}$	$0.1 \mu\text{F}$	$2 \mu\text{F}(\text{elec.})$
Component	$R_1$	$R_2$	$R_3$	$R_4$	$R_5$	$R_6$
Value .	$5\text{M}\Omega$	$5,000 \Omega$	$15,000 \Omega$	$0.25 \text{M}\Omega$	$5,000 \Omega$	
Component	$R_6$	$R_7$	$R_8$	$R_9$		
Value .	$5,000 \Omega$	$10,000 \Omega$	$5,000 \Omega$	$70,000 \Omega$		

The H.T. voltage is between 300 and 350 volts.

## 16.10. The Scanning Generator.

**16.10.1. Introduction.** The voltage or current needed to produce the electric or magnetic field for deflecting the C.R. tube beam is usually obtained from an amplifier to which is applied a voltage from a scanning generator. The shape of the output voltage required from the latter depends on the method of deflection employed; if it is electrostatic, by voltages of saw-tooth shape applied to deflector plates mutually perpendicular inside the C.R. tube, a voltage of saw-tooth shape is required from the scanning generator. On the other hand, electromagnetic deflection, by a current of saw-tooth shape in coils mutually perpendicular outside the C.R. tube, requires from the scanning generator an output voltage of pulse form or a combination of pulse and saw-tooth shape (see Section 16.11.1). The most important features required of the scanning generator are: (1) the frequency and amplitude of its

output voltage should be stable (little affected by supply voltage and temperature changes) and yet susceptible to manual control, (2) synchronism should be easy to establish and (3) the output wave shape should conform to that required by the deflection amplifier (in the case of electro-static deflection the saw-tooth output voltage should be linear, i.e., its instantaneous amplitude should be proportional to time). The scanning generator normally consists of a resistance-capacitance charge circuit, across which the saw-tooth voltage is developed, and a device for periodically discharging or charging the capacitance. The pulse-shaped voltage may be obtained from the discharge current of the capacitance or from some part of the discharge oscillator circuit. The discharge device may be a gas-filled relay valve, a multivibrator (relaxation oscillator), or a blocking oscillator.

### 16.10.2. The Gas-Filled Relay Valve Scanning Generator.

The gas-filled relay valve is not now used to any great extent in television scanning generators because it is more erratic in performance—free running frequency and amplitude are affected by gas pressure, which is a function of temperature—has a shorter life and is more costly than the high vacuum valve multivibrator or blocking

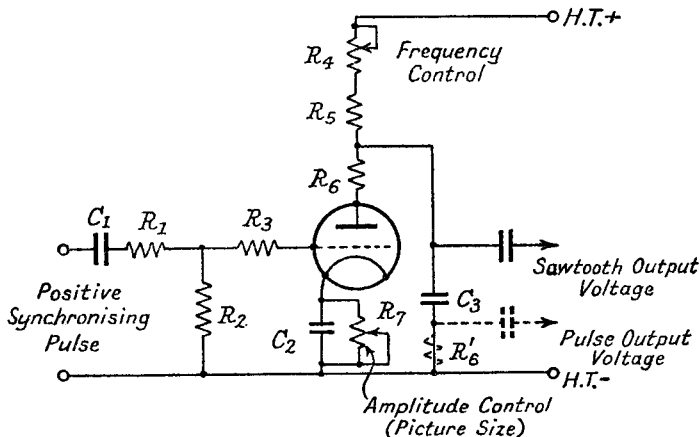


FIG. 16.21.—The Circuit for a Gas-Filled Valve Scanning Generator.

oscillator. Fig. 16.21 shows a circuit suitable for the gas-filled valve. The charge circuit consists of two resistances,  $R_4$  and  $R_5$ , 2 M $\Omega$  and 0.5 M $\Omega$  respectively, and the capacitance  $C_3$ .  $R_4$  is variable, providing means of controlling the rate of charge of  $C_3$ , and hence the frequency of the output voltage. The value of  $C_3$  is about 0.25  $\mu\text{F}$  and 0.0005  $\mu\text{F}$  respectively for the frame and line frequencies. The



voltage-time curve is exponential, but an almost linear saw-tooth shape can be obtained by having a discharge voltage of 10% or less of the H.T. voltage applied to the charge circuit. A characteristic of the gas-filled valve is that as soon as the gas is ionized it becomes practically a short circuit across  $C_3$ , and to prevent destruction of the cathode the maximum discharge current must be limited by including  $R_6$  in the discharge circuit. The anode voltage at which the gas ionizes—it is known as the striking voltage—depends on the grid bias voltage, and it is increased by increasing the negative bias. Once ionization has taken place the grid is surrounded by a sheath of positive ions (gas atoms with a deficiency of electrons), and it has no further control. The positive ions cause grid current to flow, and to prevent overheating of the grid  $R_3$  (20,000  $\Omega$ ) is inserted as a grid current limiter. The valve continues to take anode current until the anode voltage falls below the ionizing potential of the gas (approximately 15 volts for mercury vapour and argon), when current ceases. This voltage, known as the extinction voltage, should be as low as possible because it subtracts from the “linear” part of the exponential curve and reduces the maximum permissible saw-tooth amplitude. When conduction ceases, the grid loses its positive ion sheath and takes full control, preventing anode current until the striking voltage is once again reached. The ratio of the change in striking voltage to change of grid voltage producing it is known as the control ratio and is generally about 20. The anode current limiting resistance  $R_6$  has a value from 100 to 500  $\Omega$ ; it must not be increased unduly, otherwise the time of discharge (the flyback time) is prolonged and the output amplitude reduced by the voltage drop across  $R_6$ .  $R_6$  may be included between  $C_3$  and earth as shown dotted in Fig. 16.21, when a pulse voltage (developed across  $R_6'$ ) or a combination of pulse and saw-tooth voltage (developed across  $C_3$  and  $R_6'$ ) is required for the input to the deflection amplifier. Control of output voltage amplitude is achieved by variation of the cathode bias provided by  $R_7$  (5,000  $\Omega$  variable), which is paralleled by  $C_2$  (25  $\mu\text{F}$ ). Frequency is also varied, but  $R_7$  is primarily an amplitude control, increase of  $R_7$  increasing amplitude. The D.C. current component of the deflection amplifier can with advantage be diverted through  $R_7$  so as to give a more constant biasing action.  $R_1$  and  $R_2$  are adjusted to suit synchronizing input requirements. The larger  $R_1$  is made the less likelihood is there of feedback from one scanning generator to the other through the synchronizing separator stage.

**16.10.3. The Multivibrator Scanning Generator.** More stable operation is obtained from a high vacuum discharge device, and television scanning generators are almost entirely confined to the multivibrator or the blocking oscillator type of discharge unit. The chief advantage of the multivibrator is that, besides the valves, only resistance and capacitance elements are involved in the circuit. On the other hand, the output voltage wave shape is more easily controlled in the blocking oscillator, which does, however, require a more complicated and costly circuit because of the transformer oscillatory circuit. The absence of inductance (apart from that of the leads) gives the multivibrator low inertia and makes it susceptible to quite small synchronizing voltages (of the order of 0.1 volts). This confers disadvantages as well as advantages, and special care is needed in layout in order to prevent electrostatic pick-up of

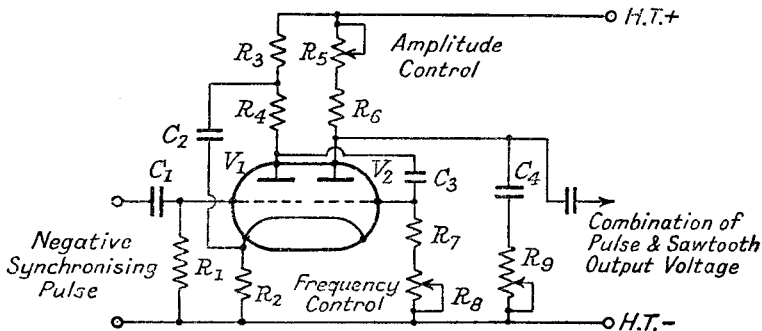


FIG. 16.22.—A Multivibrator Scanning Generator.

unwanted impulses and interaction between line and frame generators, both of which tend to cause loss of synchronism. The blocking oscillator requires about 5 volts for synchronizing and is less affected by undesired impulses. An example of the multivibrator scanning generator is given in Fig. 16.22. Two triode valves ( $V_1$  and  $V_2$ ) are used with a resistance in the common cathode circuit as the coupling unit. The second valve  $V_2$  acts as the discharge device across the capacitance  $C_4$  of the ( $R_5$  and  $R_6$ )  $C_4$  charge circuit. The action of the multivibrator is as follows: when the H.T. is initially applied to the circuit the anode voltage of  $V_1$  rises more rapidly than that of  $V_2$  because the time constant of the decoupling circuit  $R_3C_2$  is smaller than the time constant of the anode circuit of  $V_2$ . A bias voltage is established across  $R_2$ , and

this prevents the flow of anode current in  $V_2$  until the anode voltage reaches a certain value. As soon as  $V_2$  starts to take current, the bias voltage across  $R_2$  is increased and the anode current of  $V_1$  falls, thus causing its anode voltage to rise. A positive voltage pulse is therefore transmitted through  $C_3$  to the grid of  $V_2$ , and this further increases the current taken by  $V_2$ . The action is cumulative and leads to a rapid discharge of  $C_4$ . The valves return to the condition obtaining initially because the falling anode voltage on  $V_2$  reduces the rate of rise of anode current and eventually reverses it, causing the bias voltage across  $R_2$  to be reduced, the anode current of  $V_1$  to be increased, its anode voltage to be reduced and a negative voltage pulse to be applied to  $V_2$ . The action is again cumulative and  $V_2$  rapidly becomes non-conductive. Control of the multivibrator frequency within the limits required of a television scanning generator is achieved by varying the time constant of the grid circuit of  $V_2$  (resistance  $R_8$ ). Amplitude control is provided by varying the H.T. voltage applied to  $V_2$ , or the charging resistance  $R_5$ ; since discharge results from a decrease in the anode current of  $V_1$ , a negative synchronizing pulse is required at the grid of this valve. Typical values for the circuit constants of a multivibrator scanning generator for frame and line are :

Component . . .	$R_2$	$R_3$	$R_4$	$R_5$
Frame . . .	500 $\Omega$	50,000 $\Omega$	100,000 $\Omega$	2 M $\Omega$
Line . . .	500 $\Omega$	50,000 $\Omega$	50,000 $\Omega$	2 M $\Omega$
Component . . .	$R_6$	$R_7$	$R_8$	$R_9$
Frame . . .	0.5 M $\Omega$	0.5 M $\Omega$	1 M $\Omega$	5,000 $\Omega$
Line . . .	0.5 M $\Omega$	25,000 $\Omega$	50,000 $\Omega$	10,000 $\Omega$
Component . . .	$C_1$	$C_2$	$C_3$	$C_4$
Frame . . .	1 $\mu$ F	2 $\mu$ F	0.01 $\mu$ F	0.1 $\mu$ F
Line . . .	0.1 $\mu$ F	0.1 $\mu$ F	0.001 $\mu$ F	0.0005 $\mu$ F

A saw-tooth, pulse or combination of these voltages can be obtained at the output. When magnetic deflection is employed,  $R_9$  is generally made variable in order to allow adjustment of the deflecting current for the nearest approach to linearity of deflection. The decoupling capacitance  $C_2$  for the anode circuit of the first valve can be taken to H.T. negative, but the cathode connection <sup>11</sup> shown in Fig. 16.22 gives a more satisfactory performance because it prevents the anode current degenerative feedback caused when the A.C. component of the anode current of  $V_1$  is allowed to flow through  $R_2$ .

#### 16.10.4. The Blocking Oscillator Scanning Generator.

Any oscillator which derives its bias by grid current flowing in a resistance-capacitance combination, the time constant of which is much greater than the period of the normal oscillation, can be made to function as a blocking or squegger oscillator if very tight coupling is employed between the oscillator coils. The very large grid current pulse, caused by overcoupling, charges the grid bias capacitance to a negative voltage (with reference to the grid electrode) considerably greater than that required to cut off the anode current of the oscillator. Oscillation, therefore, ceases and cannot begin again until the capacitance has discharged through the grid leak resistance to a voltage low enough to permit anode current to flow. The cycle of operations, consisting of oscillation followed by a quiescent period, is then repeated. The length of time during which the valve anode current is cut off depends on the time constant of the grid self-biasing circuit and the degree of coupling, the greater either of these the longer is the quiescent period. When oscillation commences there may be one or a number of oscillation cycles, the actual number depending on the damping of the tuned circuit and its  $L/C$  ratio, a large  $L/C$  ratio and heavy damping tending to a single cycle of oscillation; damping must not be made too large, otherwise it may prevent the blocked condition being realized. Single pulse oscillation is desired in the blocking oscillator scanning generator and the highest possible  $L/C$  ratio is therefore required. Generally no tuning capacitance is employed other than that due to stray capacitance. The important advantages of this type of oscillator are that (1) the blocking frequency is relatively stable and only slightly affected by supply and temperature variations, (2) synchronism is easily maintained by a positive synchronizing voltage applied to the grid circuit, (3) pulse and saw-tooth voltages are generated and (4) the discharge or flyback time can be controlled by variation of the normal oscillation frequency of the tuned circuit.

An example of the blocking oscillator is shown in Fig. 16.23*a*, and the shapes of the voltage waves occurring across the different parts of the circuit are shown in Fig. 16.23*b*. The pentode valve in Fig. 16.23*a* performs two rôles: the control and screen grids act as the grid and anode of a blocking oscillator, and the anode-cathode circuit as the discharge device for the capacitance  $C_s$ , which is charged from the H.T. supply through the resistances  $R_3$  and  $R_4$ . The anode current is zero during the quiescent period of the oscillator and only flows when the positive oscillation pulse of the blocking

oscillator part renders the whole valve conductive. A saw-tooth voltage is developed across  $C_3$  or a combination of pulse and saw-tooth if  $R_5$  is included. The synchronizing input voltage is applied through a coupling coil  $L_3$  connected to the oscillator coils. Fig. 16.23*b* shows the impulse nature of the voltages  $E_{L_1}$  and  $E_{L_2}$  across the grid and screen coils respectively—these voltages are, of course,  $180^\circ$  out-of-phase with each other. A large value of tuning capacitance produces the lightly damped train of oscillations shown by the dotted  $E_{L_1}$  curve and may result in a second current pulse in the anode circuit, causing a second saw-tooth voltage as shown by dotted  $E_{C_3}$  curve in the figure. Linearity of saw-tooth voltage across  $C_3$  requires the H.T. voltage to be at least ten times the amplitude (peak-to-peak) of the saw-tooth output voltage. Changing the rate of charge of  $C_3$  by varying  $R_3$  controls the amplitude of the saw-tooth, frequency being governed entirely by the control

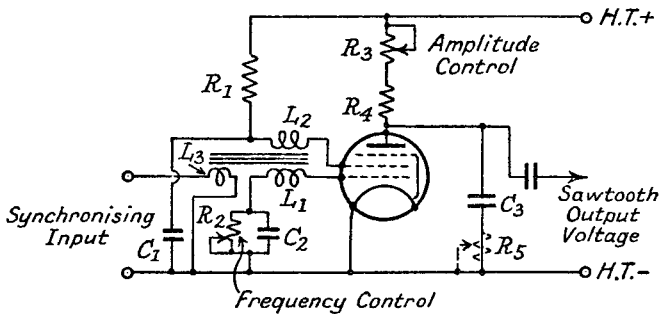


FIG. 16.23*a*.—A Blocking Oscillator Scanning Generator.

grid circuit time constant, i.e., by variation of  $R_2$ . It is seen from Fig. 16.23*b* that the exponential discharge curve of capacitance  $C_2$  approximates to the saw-tooth voltage shape, and if this shape of output voltage is required the pentode discharge section and the charge circuit can be omitted, the output voltage being taken across  $C_2$ . The voltage wave shape will not be linear as long as the discharge voltage for  $C_2$  is zero, but the resistance  $R_2$  can be returned to H.T. positive instead of to zero with consequent improvement in linearity. The effect of connecting  $R_2$  to a positive voltage  $E$  is illustrated by the dashed curve on Fig. 16.23*b*, it is equivalent to increasing the H.T. voltage on the anode charge circuit of a gas-filled valve generator.

Suitable component values for the circuit of Fig. 16.23*a* are :

Component	$R_1$	$R_2$	$R_3$	$R_4$
Frame . . .	20,000 $\Omega$	0.25 M $\Omega$ (var.)	2 M $\Omega$ (var.)	0.5 M $\Omega$
Line . . .	20,000 $\Omega$	0.25 M $\Omega$ (var.)	2 M $\Omega$ (var.)	0.5 M $\Omega$

Component	$R_5$	$C_1$	$C_2$	$C_3$
Frame . . .	5,000 $\Omega$	2 $\mu$ F	0.1 $\mu$ F	0.1 $\mu$ F
Line . . .	10,000 $\Omega$	0.1 $\mu$ F	0.0005 $\mu$ F	0.0005 $\mu$ F

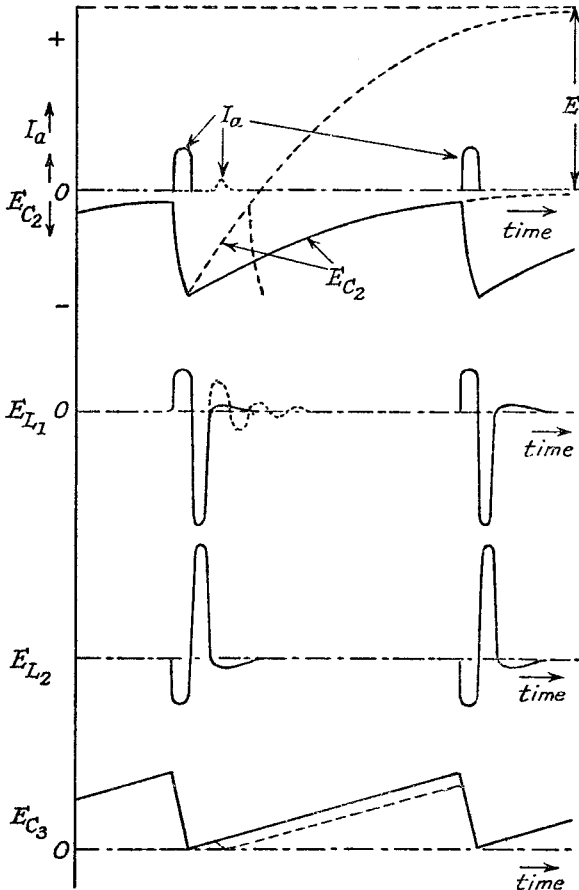


FIG. 16.23b.—Voltage and Current Waveforms in a Blocking Oscillator.

An alternative form <sup>28</sup> of blocking oscillator suitable as a line scanning generator producing a pulse output voltage is illustrated in Fig. 16.24. Synchronizing is effected by a negative pulse applied to the cathode circuit. The free frequency is controlled by variation

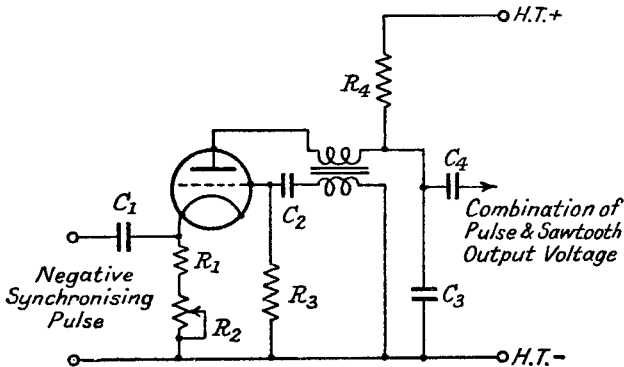


FIG. 16.24.—An Alternative Form of Blocking Oscillator Scanning Generator suitable for the Frame Scan.

of the resistance  $R_2$  in the cathode circuit. Component values are as follows :

$$R_1 = 1,000 \Omega, R_2 = 3,000 \Omega, R_3 = 0.15 \text{ M}\Omega, R_4 = 0.25 \text{ M}\Omega, C_1 = 0.1 \mu\text{F}, \\ C_2 = 0.0005 \mu\text{F}, C_3 = 0.002 \mu\text{F}, C_4 = 0.01 \mu\text{F}.$$

The resonant frequency of the inductance of the anode or grid coil, whichever is the larger, of the coupling transformer, and the stray capacitance determines the flyback time of the output voltage wave shape, and it should be not less than ten times the fundamental saw-tooth frequency. The frequency must not be made too high otherwise the discharging capability of the generator is reduced, because the maximum current taken by a high vacuum valve is very much less than that of a gas-filled valve. A resonant frequency of about 1,000 c.p.s. is suitable for the frame scanning generator, and an intervalve or output transformer of 1 to 2 turns ratio will usually fulfil this rôle satisfactorily. The line scanning generator requires a resonant frequency of 150 to 200 kc/s.

## 16.11. The Deflecting Circuits and Amplifiers.

**16.11.1. Introduction.** Deflection of the c.r. tube beam may be accomplished electrostatically or electromagnetically. Whilst both methods have their advantages and disadvantages, magnetic deflection is generally to be preferred. The chief point in favour of electrostatic deflection is that it deflects not only the electrons, but also the negative ions (atoms of residual gas to which electrons have attached themselves) contained in the c.r. tube beam. The negative ions have much greater mass than the electrons, and if they are allowed continuously to bombard a small area of the screen they destroy its luminosity. A magnetic deflecting field has much less influence on the ions than on the electrons, so that the ionic beam

tends to remain at the centre of the screen and cause an "ionic burn" or dark spot. The disadvantages of electrostatic deflection are that a long C.R. tube is required, comparatively high deflecting voltages (about 850 volts peak-to-peak on each plate) are needed, and there is distortion of the spot at the edges of the picture due to the non-uniform electric lens action between the deflector plates. A long C.R. tube means a more bulky cabinet and increased tube and cabinet cost. High deflecting voltages call for a high voltage H.T. supply with valves and capacitance components suitable for high voltage operation. Push-pull deflection is essential to prevent trapezium distortion. A further disadvantage of electrostatic deflection is that the coupling capacitances from the deflection amplifier to the plates must be capable of withstanding about 7,000 volts because the voltage between plates and earth is the same as from the C.R. tube anode to earth.

The advantages of magnetic deflection are reduced size of C.R. tube, beam distortion or defocusing during deflection is small, and the deflection amplifier can be operated from a low voltage supply (300 volts). The disadvantages of magnetic deflection are the negative ion burn, the higher deflecting power required, and the high induced voltage caused by the flyback of the line deflection current.

For electrostatic deflection a saw-tooth voltage must be applied to the deflector plates of the C.R. tube; electromagnetic deflection requires a saw-tooth current through the deflector coils. The actual shape of the input voltage to the magnetic deflection amplifier depends on the slope resistance of the amplifier valve. If it is a tetrode or pentode of high  $R_a$ , the input voltage shape should be saw-tooth because the current wave shape is independent of the external load. On the other hand, the input voltage shape to

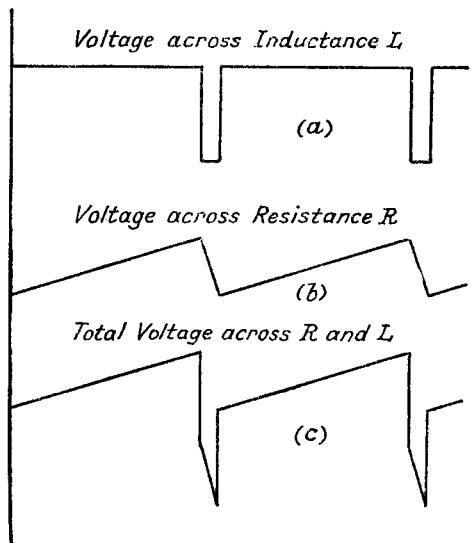


FIG. 16.25.—The Voltage Waveform required across a Coil to give a Saw-tooth Current Waveform through the Coil.



a triode of low  $R_a$  needs to be a combination of pulse and saw-tooth shape. The actual voltage required across the inductive part, as distinct from the whole coil, including the resistive component, is of rectangular pulse shape as shown in Fig. 16.25a. Integration of this shape  $\left(I = \frac{\int E}{L} dt\right)$  gives a saw-tooth current shape through the coil, and this saw-tooth current produces a saw-tooth voltage across the resistance component of the coil and the valve slope resistance (Figs. 16.25b). The input voltage shape must be equivalent to the sum of these two as shown by Fig. 16.25c, and it is obtained by adjusting a resistance in series with the charge capacitance as described in Section 16.10.

**16.11.2. Electrostatic Deflection.** The distance through which the beam of a C.R. tube is deflected by a voltage applied to a flat plate parallel to the beam is directly proportional to the length of the plate, its distance from the screen and the deflecting voltage; it is inversely proportional to the distance from the plate to the beam axis and to the voltage between the cathode and last anode of the C.R. tube.

Deflection of the C.R. tube beam by a saw-tooth voltage applied to one deflecting plate results in a variation of the mean potential difference between the last anode and the deflecting plate. This varies the speed of the electrons in the beam, causing them to travel faster when the deflecting voltage is increasing positively and to travel slower when the latter is decreasing negatively. When the electrons are travelling faster, they are under the influence of a deflecting field from a plate at right angles to the first plate for a shorter time, and the beam deflection due to the second plate voltage is therefore becoming less when the first plate voltage is rising positively. This results in trapezium distortion of the picture. It can be overcome by using push-pull deflection to both pairs of plates; the mean voltage between the plates and last anode is zero because a positive voltage on one is counterbalanced by a negative on the other.

An example of a push-pull deflection amplifier is shown in Fig. 16.26. For a satisfactory linear saw-tooth with rapid flyback, the amplifiers should have small attenuation and phase distortion up to at least the 10th harmonic of the saw-tooth fundamental frequency; this is adequate for a 10% flyback time, but there is slight distortion of the last 10% of the forward stroke. If the frequency range is extended to the 15th harmonic, the saw-tooth voltage is practically linear. Reversal of phase of the

input voltage for the second valve  $V_2$  is obtained from the output voltage of  $V_1$ , stepped down in the frame amplifier by the potential divider action of  $R_6$  and  $R_7$ . The ratio  $\frac{R_7}{R_6 + R_7}$  is approximately equal to the stage gain of  $V_1$ . A resistance potential divider is not satisfactory for the line deflection amplifier because the input capacitance of  $V_2$  (including the Miller effect of anode-grid capacitance) has a comparatively low reactance.  $R_6$  is therefore replaced by a variable capacitance, which forms a potential divider with the input capacitance of  $V_2$ .  $R_7$  is fixed and has a value much greater than the grid input reactance of  $V_2$ . Other possible methods of achieving phase reversal are discussed in Section 10.8.2.

In the frame deflecting amplifier  $C_3$  and  $C_5$  are often omitted, because unless they are made very large they cause attenuation

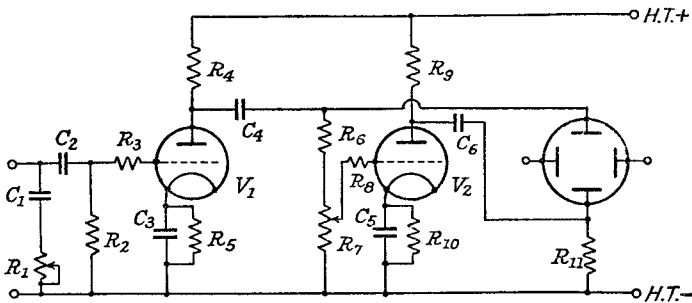


FIG. 16.26.—A Push-Pull Amplifier for Electrostatic Deflection of the Cathode Ray Beam.

and phase distortion of the lower frequency components of the saw-tooth. A larger anode load resistance is permissible in the frame than in the line amplifier since the reactance of stray capacitance is much greater at the frame frequencies, and this helps to reduce the loss of amplification due to the unby-passed cathode bias resistances  $R_5$  and  $R_{10}$ . If the valves  $V_1$  and  $V_2$  are accurately matched a common bias resistance can be employed and the degenerative cathode voltages then cancel each other. Some improvement in the wave shape (distorted by attenuation and phase shift of the higher frequency components due to stray capacitance) of the line deflecting voltage can be secured by applying a combination of saw-tooth and pulse input voltage. This is achieved by inserting the resistance  $R_1$  in series with the charge capacitance  $C_1$ . Typical component values for the frame and line amplifier are listed on page 458.

Component	$C_1$	$C_2$	$C_3$	$C_4$	$C_5$	$C_6$
Frame	0.5 $\mu\text{F}$	0.25 $\mu\text{F}$	0	0.1 $\mu\text{F}$	0	0.1 $\mu\text{F}$
Line	0.003 $\mu\text{F}$	0.01 $\mu\text{F}$	0.1 $\mu\text{F}$	0.002 $\mu\text{F}$	0.1 $\mu\text{F}$	0.002 $\mu\text{F}$

All capacitances except  $C_3$  and  $C_5$  should be 1,000-volt working.

Component	$R_1$	$R_2$	$R_3$	$R_4$	$R_5$	$R_6$
Frame	0	2 M $\Omega$	500 $\Omega$	0.2 M $\Omega$	10,000 $\Omega$	4 M $\Omega$
Line	400 $\Omega$	1 M $\Omega$	500 $\Omega$	0.1 M $\Omega$	5,000 $\Omega$	—

Component	$R_7$	$R_8$	$R_9$	$R_{10}$	$R_{11}$
Frame	1 M $\Omega$ (var.)	500 $\Omega$	0.2 M $\Omega$	10,000	5 M $\Omega$
Line	1 M $\Omega$ (fixed)	500 $\Omega$	0.1 M $\Omega$	5,000 $\Omega$	5 M $\Omega$

In the line deflecting amplifier  $R_6$  is replaced by a variable capacitance of 10  $\mu\mu\text{F}$ , and a resistance of 5 M $\Omega$  is included from the top deflecting plate to earth. The H.T. voltage required is 1,200 to 1,500 volts.

Step-up transformer coupling with a centre-tapped secondary may be used instead of push-pull r.c. coupling. The important point to observe is that the primary reactance of the frame transformer must be large compared with the valve slope resistance, in order that reactance variation with frequency shall have little effect. Leakage inductance and stray capacitance are the chief factors in the line deflection transformer, and primary to secondary coupling must be high and stray capacitance low.

**16.11.3. Electromagnetic Deflection.** Magnetic deflection of the C.R. tube beam is directly proportional to the length (in the beam axis direction) of the magnetic field, the distance from the coil to the screen and the flux density of the field; it is inversely proportional to the square root of the voltage between the cathode and last anode of the C.R. tube. Two pairs of coils are used at right angles to each other on the neck of the tube. The coils, of saddle shape, are surrounded by a magnetic yoke of *C* type laminations as shown in Fig. 16.27. The saddle shape of coil gives a field of maximum intensity with uniform distribution at right angles to the coil. A non-uniform field leads to "barrel" or "pincushion" distortion<sup>20</sup> of the picture with convex or concave edges. The electron travels in a direction perpendicular to the magnetic field, and either convex or concave field shape is obtained according to the way in which the magnetic lines of force are bent: step-down transformer coupling is employed from the valve to the coils as this prevents permanent deflection of the beam by the valve anode current, and also allows the inductance of the line deflecting coil to be smaller, with consequent reduction of the induced voltage on the flyback. It is easier to insulate the primary of a transformer

against high voltages than a deflecting coil. A low inductance deflecting coil of larger gauge wire is also stronger mechanically than a coil of many turns of fine wire. For maximum deflection the coil should be as long as possible, but it must not be made so long that the beam strikes the neck of the C.R. tube before reaching the full extent of its travel on the screen. Beam cut-off is overcome by reducing the coil length from the cathode end of the tube, if the other end of the coil is touching the flare. An average value for coil length is  $1\frac{3}{4}$  ins. The line and frame coils, mounted one above the other, are surrounded by a yoke of magnetic material which concentrates and makes the field more uniform. The yoke, which may be circular<sup>17</sup> or square in section, consists of laminations held in a frame (this is omitted in Fig. 16.27). An air gap of  $\frac{1}{8}$  in. to  $\frac{1}{4}$  in. is often included between the two halves of a C-type core.

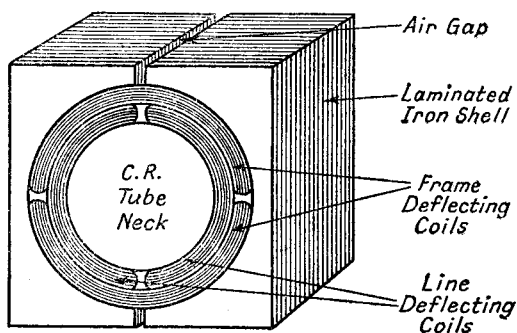


Fig. 16.27.—Coil Shape for Electromagnetic Deflection of the Cathode Ray Beam.

Each coil is wound on a special former<sup>22</sup> to give the saddle shape. Generally the separate layers are rectangular in shape and the turns decrease in size from the outside to the inside of the layer. The number of turns in each of the two line deflecting coils is of the order of 100 to 150 and in each of the frame coils 500 to 800. Adjacent ends of the line and frame deflecting coils are separated by about  $\frac{1}{4}$  in.

The deflection amplifier may have either a tetrode or a triode valve. The tetrode has the advantage of requiring a much smaller input voltage for a given output current change, but the triode gives less distortion; however, distortion from the tetrode can be reduced by applying negative feedback. A triode valve (or tetrode with screen and anode joined) is often used in the frame amplifier, and a tetrode in the line amplifier. A typical line deflection amplifier is shown in Fig. 16.28. A combination of saw-tooth and pulse input

voltage is required to produce a saw-tooth current through the deflecting coils. The valve is a high  $g_m$  tetrode having a normal D.C. dissipative power at the anode of 15 to 20 watts. A resistance  $R_2$  (1,000  $\Omega$ ) is included close to the grid pin of the valve to act as a suppressor of parasitic oscillations, to which high  $g_m$  valves are liable. The total H.T. voltage is about 320 volts, but the screen voltage is limited to a maximum of 250 volts by the resistance  $R_3$  (5,000  $\Omega$ ); the decoupling capacitance  $C_3$  is 0.1  $\mu\text{F}$ . Decoupling of the amplifier from the H.T. supply is provided by  $R_4$  (250  $\Omega$  variable) and  $R_5$  (500  $\Omega$ ) in series together with the capacitance  $C_2$  (16  $\mu\text{F}$ ). The variable resistance  $R_4$  varies the screen and anode voltage of the tetrode, and so controls the amplitude of the line deflecting current, i.e., it varies the width of the picture. The self-bias circuit consists of  $R_6$  (about 150  $\Omega$ ) and  $C_4$  (25  $\mu\text{F}$ ). The

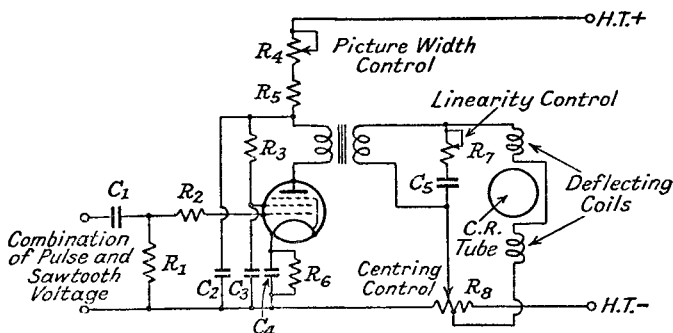


FIG. 16.28.—A Typical Line Deflection Amplifier for Electromagnetic Deflection of the Cathode Ray Beam.

output transformer has a step-down ratio of about 8 to 1, the primary inductance should be about ten times the reflected inductance due to the deflecting coils, in order that transformer volt-ampere efficiency may be high. Referred to the secondary side, this means that the ratio of secondary to deflecting coil inductance should be 10 to 1. Considerations of leakage inductance and winding capacitance (both are increased by using a large primary inductance, and cause loss of efficiency as well as distortion of the saw-tooth current) generally dictate a lower ratio, of the order of 5 to 1. Across the secondary is included a special circuit to limit the inverse voltage induced by the rapid change of current during the flyback period. The component values of this absorber circuit are  $R_7 = 5,000 \Omega$ ,  $C_5 = 0.005 \mu\text{F}$ . Part of  $R_7$  may be variable in order to assist linearization of the saw-tooth current as it approaches

the flyback point. Centring of the picture can be achieved by means of the centre-tapped potential divider  $R_8$  ( $20 \Omega$ ) in the main H.T. supply to the deflecting amplifier. It is not absolutely essential with magnetic focusing because the picture can be centred by movement of the focus coil.

The frame amplifier circuit may be similar to that shown in Fig. 16.28. Decoupling capacitances need to be much greater than those for the line amplifier, for example,  $C_2$  should be about  $32 \mu\text{F}$ ,  $C_3$   $16 \mu\text{F}$  and  $C_4$   $100 \mu\text{F}$ . The  $C_5R_7$  absorber circuit is no longer required since the rate of change of current on the flyback is much slower than for the line, and the inverse induced voltage is therefore very much less. To prevent excessive peak currents in the valve due to the reduced load reactance at the frame frequency, the frame deflecting coils have a higher inductance than the line (about fifty times as large) and a higher step-down ratio (12 to 1) is employed. A valve having a higher anode D.C. dissipative power is generally necessary to accommodate the higher peak currents due to the lower load reactance. A triode or tetrode with screen and anode joined together may be used, but this introduces only minor changes in circuit detail, e.g.,  $R_3$  and  $C_3$  are no longer required.

## 16.12. Power Supplies and Focusing of the C.R. Tube.<sup>33</sup>

**16.12.1. Introduction.**<sup>19</sup> The H.T. supply to the vision receiver, scanning generators and deflection amplifier can be obtained from the same power unit. The latter needs no special comment since it has a comparatively low output voltage (about 400 volts across the reservoir capacitance), and its design follows the lines set out in Chapter 11. The rectifier and smoothing choke must be capable of handling a current of 150 to 200 mA, and great care must be exercised to ensure adequate smoothing and decoupling, because scanning generator and deflection amplifier current changes are large. These are liable to interact upon each other and the vision amplifier if decoupling is insufficient; furthermore, hum voltages in the H.T. supply tend to cause erratic interlacing.

The C.R. tube requires a high-voltage H.T. supply (5,000 volts), but the load current is small, being little more than that taken by the potential divider providing the various auxiliary anode voltages. Consequently a resistance-capacitance filter can be employed for smoothing purposes. The number of auxiliary anodes (other than the last) is governed by the type of focusing; electrostatic focusing generally needs two, whilst none is required with magnetic focusing.

Electrostatic focusing has the advantage that temperature

changes have negligible effect and hardly any adjustment is entailed after the initial setting. On the other hand, it concentrates negative ions as well as electrons, causing ion burn unless electrostatic deflection is used. Extra decoupling capacitances and resistances are needed in the potential divider supplying the auxiliary anodes. Centring is only possible by means of a shift potential on the deflecting plates or a shift current through the deflecting coils.

Magnetic focusing has the advantage of giving a much higher beam current with less negative ion concentration than electrostatic focusing, and a much brighter picture results. Another advantage is that movement of the focus coil controls the centring of the picture and obviates the necessity for shift voltages or currents. Its chief disadvantages are that the focus coil takes power and that focus tends to drift from the cold to normal running condition due to a change in coil resistance.

**16.12.2. Electrostatic Focusing and the C.R. Tube Power Supply.** An example of the C.R. tube power supply for an electrostatically focused tube is shown in Fig. 16.29. The A.C. supply voltage is obtained from a 4,000-volt (R.M.S.) secondary winding, and half-wave rectification is used because it is very suitable for

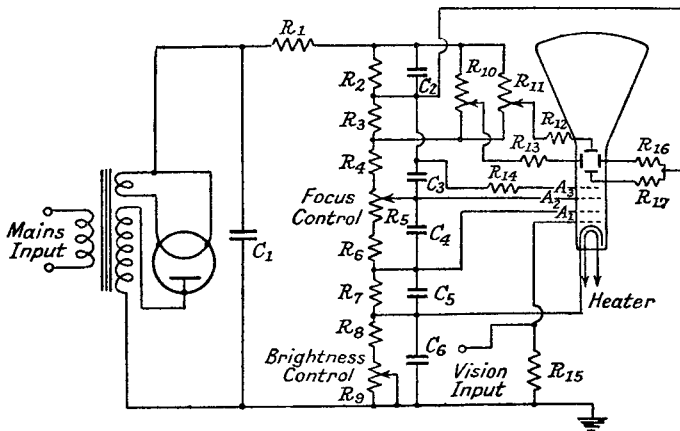


FIG. 16.29.—A Power Supply Circuit for a Cathode Ray Tube having Electrostatic Focusing and Deflection.

high voltage low current D.C. outputs. The anode of the rectifier is connected to one side of the secondary winding, and the cathode to the H.T. positive lead of the D.C. supply; hence the maximum voltage between the heater winding to earth is the peak A.C. voltage output of the high voltage secondary winding. If the cathode of

the rectifier is connected to the high-voltage winding, both heater winding and heater end of the high-voltage winding must be capable of withstanding nearly twice the peak A.C. voltage to earth, viz., 11,000 volts, because on the negative half-cycle the maximum voltage from heater winding to earth is the sum of the peak A.C. voltage across the high-voltage secondary and the D.C. voltage across the reservoir capacitance  $C_1$ . The C.R. tube has three anodes,  $A_1$ ,  $A_2$  and  $A_3$ , requiring approximately 400, 1,500 and 5,000 volts respectively to cathode.  $A_3$  is connected to the junction of  $R_2$  and  $R_3$ , across which are connected the shift potential dividers,  $R_{10}$  and  $R_{11}$ , for one of each pair of deflecting plates. The latter are connected to the push-pull deflection amplifier by capacitances, which must be capable of withstanding 7,000 volts. A resistance,  $R_{14}$  (0.1 M $\Omega$ ), is inserted between  $A_3$  and the supply to limit current in the event of a short circuit of  $A_3$  to earth.  $R_5$  controls the voltage applied to  $A_2$  and provides focus adjustment.  $R_9$  varies the cathode bias and so controls the average brightness of the picture. The vision input is applied between the C.R. tube grid and earth.

The values of the resistances and capacitances (the voltages in brackets indicate the required working values for the capacitances) in the potential divider for the anode voltages are listed below; the former are calculated on the assumption that the C.R. tube electrode currents are negligible.

Component	$R_1$	$R_2$	$R_3$	$R_4$	$R_5$	$R_6$	$R_7$	$R_8$
Value (M $\Omega$ )	0.5	0.5	0.5	2	0.5 (var.)	0.25	0.25	0.01

Component	$R_9$	$R_{10}$	$R_{11}$	$R_{12}$	$R_{13}$	$R_{14}$	$R_{16}$	$R_{17}$
Value (M $\Omega$ )	0.1 (var.)	0.5 (var.)	0.5 (var.)	5	5	0.1	5	5

Component	$C_1$	$C_2$	$C_3$	$C_4$	$C_5$	$C_6$
Value ( $\mu$ F)	0.1 (7,000)	1 (500)	1 (2,500)	1 (1,500)	1 (500)	4 (250)

When wiring the high voltage power supply, leads should be well spaced from each other and earth, and high voltage cable should be used for the output leads to  $A_2$ ,  $A_3$  and the deflector plates. It is advisable to include a safety switch attached to the back of the receiver so that  $C_1$  is automatically short-circuited when the back is removed for inspection purposes.

**16.12.3. Magnetic Focusing and the C.R. Tube Power Supply.**<sup>21</sup> The H.T. supply to the C.R. tube is greatly simplified by employing magnetic focusing. Only one anode (this may be provided by a graphite coating on the inside of the bulb) is required, or if two are used the first is at a low voltage (300 to 400 volts),



which can be obtained from the low voltage H.T. supply. A resistance shunt  $R_1$  is shown across the reservoir capacitance  $C_1$  in Fig. 16.30, as it provides cathode bias through  $R_2$  and  $R_3$  for the tube, and also discharges  $C_1$  after the receiver has been switched off.  $R_1$  has a value of about  $10\text{ M}\Omega$ ,  $R_2$ ,  $20,000\ \Omega$  and  $R_3$ ,  $0.25\text{ M}\Omega$ ,  $C_1$  is  $0.1\ \mu\text{F}$  (7,000-volt) and  $C_2$  is  $4\ \mu\text{F}$  (250-volt). A safety resistance  $R_4$  ( $0.1\text{ M}\Omega$ ) is inserted in series with the lead to the anode, which is formed by a conducting graphite coating inside the C.R. tube. Additional resistance-capacitance smoothing is not required, partly because the load current and the ripple voltage across  $C_1$  are so small, and partly because hum voltages on the last anode have much less effect than on intermediate anodes. If the shunt resistance  $R_1$  is not included, cathode bias can be derived from the low voltage H.T. supply. The vision input is applied across  $R_5$ .

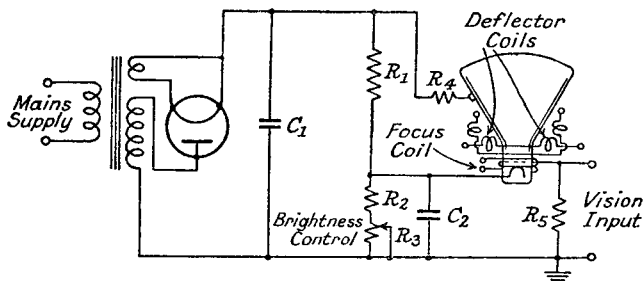


FIG. 16.30.—A Power Supply Circuit for a Cathode Ray Tube having Electromagnetic Focusing and Deflection.

Magnetic focusing may be provided by a permanent magnet with a variable shunt or by a coil wrapped round the tube so that its axis coincides with that of the beam. The former is seldom used because it is more costly and less easy to adjust. The focus coil may have a low resistance and be placed in series with the low voltage supply, or it may have a high resistance and be placed across it. The former is preferable because it is easier to construct, is more robust, and is less liable to current change from the cold to normal operating condition. The coil is connected in series with the H.T. supply to the scanning generators and deflection amplifiers; the current from the vision receiver should not be included because it varies when gain adjustments are made. It is shunted by a fixed and variable resistance in series, the latter providing focus control. A soft iron shell with an air gap normally encloses the coil so as to produce a uniform concentrated magnetic field; Fig. 16.31 is an example of the type of construction. The soft-iron shell, made in

two halves which slide over the coil as shown, has an external diameter of about 4 ins. and is about  $1\frac{1}{2}$  ins. deep. The air-gap is 1 cm. (approximately 0.4 in.) long and about 600 ampere-turns are required for focusing. Centring of the picture can be achieved by

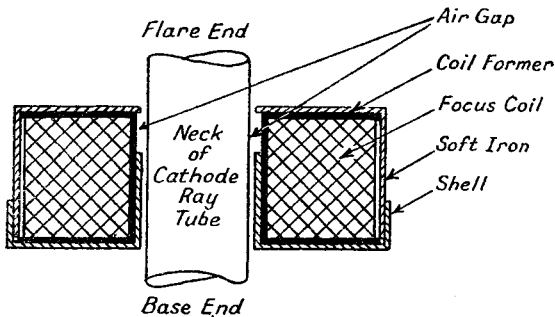


FIG. 16.31.—An Example of a Magnetic Focusing Coil.

altering the position of the coil, which may be mounted on gimbals and provided with adjusting and locking screws.

Magnetic fields from the mains transformer can affect C.R. tube and scanning generators, and the transformer must be located as far as possible from this part of the equipment, if necessary, being orientated so as to produce minimum field interference. For the same reason the flux density of the transformer core should not be allowed to exceed 50,000 lines per sq. in. Owing to the power supplied by the transformer and the rectifier units adequate ventilation is absolutely necessary. The actual voltage required of the high voltage secondary can be reduced by connecting its negative lead to the positive of the low voltage supply, cathode bias for the C.R. tube being obtained from the low voltage supply.

#### BIBLIOGRAPHY

1. A Study of Television Image Characteristics, Part II. E. W. Engstrom, *Proc. I.R.E.*, April 1935, p. 295.
2. Correction Circuits for Amplifiers. O. E. Keall, *Marconi Review*, May–June 1935, p. 15, Sept.–Oct. 1935, p. 9.
3. Synchronizing in Television. W. T. Cocking, *Wireless World*, Jan. 22nd, 1937, p. 74.
4. The Television Receiver. W. T. Cocking, *Wireless World*, May 14th, 1937, p. 475.
5. Television Aerials. H. B. Dent, *Wireless World*, May 28th, 1937, p. 506.
6. The Wireless World Television Receiver. W. T. Cocking, *Wireless World*, July 2nd, 1937, p. 2, to July 30th, 1937, p. 98.
7. Television Scanning and Synchronizing. P. D. Tyers, *Wireless World*, Aug. 6th, 1937, p. 115.

8. Some Notes on Video Amplifier Design. A. Preisman, *R.C.A. Review*, April 1938, p. 421.
9. Effect of the Receiving Antenna on Television Reception Fidelity. S. W. Seeley, *R.C.A. Review*, April 1938, p. 433.
10. Television Receivers. E. W. Engstrom and R. S. Holmes, *Electronics*, April 1938, p. 28, to Aug. 1938, p. 18.
11. Television Topics, *Wireless World*, April 21st, 1938, p. 354.
12. The Line Structure of Television Images. H. A. Wheeler and A. V. Loughren, *Proc. I.R.E.*, May 1938, p. 540.
13. Laboratory Television Receiver. D. Fink, *Electronics*, July 1938, p. 16, to Dec. 1938, p. 16.
14. Aerial Coupling Systems for Television. W. E. Benham, *Wireless Engineer*, Oct. 1938, p. 555.
15. The Marconi-E.M.I. Television System. Part I: The Transmitted Wave Form. A. D. Blumlein, *Journal I.E.E.*, Dec. 1938, p. 758.
16. Analysis and Design of Video Amplifiers. S. W. Seeley and C. N. Kimball, *R.C.A. Review*, Jan. 1939, p. 290.
17. Television Deflection Circuits. E. W. Engstrom and R. S. Holmes, *Electronics*, Jan. 1939, p. 19.
18. A Television Bibliography. *Electronics*, March 1939, p. 47.
19. Power for Television Receivers. E. W. Engstrom and R. S. Holmes, *Electronics*, April 1939, p. 22.
20. Line Deflectors. D. V. Ridgeway, *Wireless World*, June 15th, 1939, p. 550.
21. Magnetic Television Receiver. W. T. Cocking, *Wireless World*, June 29th, 1939, p. 602, to July 20th, 1939, p. 57.
22. Scanning Coil Construction. P. D. Tyres, *Wireless World*, Sept. 14th, p. 248, and Sept. 21st, 1939, p. 279.
23. Television Signal Frequency Circuit Considerations. G. Mountjoy, *R.C.A. Review*, Oct. 1939, p. 204.
24. Simplified Television I.F. Systems. G. Mountjoy, *R.C.A. Review*, Jan. 1940, p. 299.
25. Ultra-Short-Wave Aerial Systems. F. R. W. Strafford, *Wireless World*, April 1940, p. 224.
26. Video Output Systems. D. E. Foster and J. A. Rankin, *R.C.A. Review*, April 1941, p. 409.
27. Fluctuations in Space Charge Limited Currents at Moderately High Frequencies, Part V. W. A. Harris, *R.C.A. Review*, April 1941, p. 505.
28. The Design of Television Receiving Apparatus. B. J. Edwards, *Journal I.E.E.*, Part III, Sept. 1941, p. 191.
29. Coupling Circuits as Band-Pass Filters. E. K. Sandeman, *Wireless Engineer*, Sept., p. 361, Oct., p. 406, Nov., p. 450, Dec., p. 492, 1941.
30. Short Wave Dipole Aerials. N. Wells, *Wireless Engineer*, May 1943, p. 219.
31. *Transmission Circuits for Telephonic Communication*. K. S. Johnson. D. Van Nostrand. Text-book.
32. *Transmission Networks and Wave Filters*. T. E. Shea. D. Van Nostrand. Text-book.
33. *The Cathode Ray Tube*. G. Parr. Chapman & Hall. Text-book.
34. *Electron Optics in Television*. I. G. Maloff and D. W. Epstein. McGraw Hill. Text-book.
35. *Principles of Television Engineering*. D. Fink. McGraw Hill. Text-book.

## APPENDIX 3A\*

### THÉVENIN'S THEOREM

A MOST important and useful theorem in the analysis of circuits is that enunciated by Thévenin. It states that if an impedance is connected between any two points in a network consisting of linear impedances, the resulting (steady state) current through the impedance is the ratio of the open circuit voltage across the two points (before the impedance is connected) to the sum of the connecting impedance and the impedance of the network looking in from the two points. Taking the valve equivalent circuit of

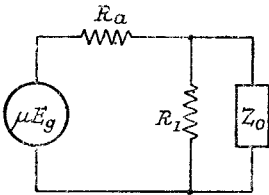


FIG. 3A.1.—A Valve Generator Circuit supplying a Resistance and Impedance in Parallel.

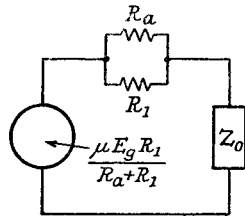


FIG. 3A.2.—The Thévenin Equivalent of Fig. 3A.1.

Fig. 3A.1, it means that the equivalent generator has a generated voltage of  $\frac{\mu E_g R_1}{R_a + R_1}$  and an internal impedance of  $R_a$  and  $R_1$  in parallel as shown in Fig. 3A.2.

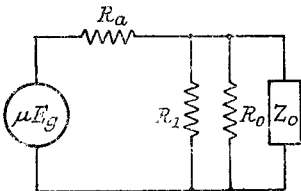


FIG. 3A.3.—A more Complicated Valve Generator Circuit.

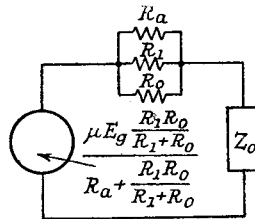


FIG. 3A.4.—The Thévenin Equivalent of FIG. 3A.3.

\* Appendix 1A and 2A appear in Part I.

The proof is as follows :

For Fig. 3A.1

$$E_0 = \frac{\mu E_g \frac{R_1 Z_0}{R_1 + Z_0}}{R_a + \frac{R_1 Z_0}{R_1 + Z_0}} = \frac{\mu E_g R_1 Z_0}{R_a (R_1 + Z_0) + R_1 Z_0}$$

and for Fig. 3A.2

$$E_0 = \frac{\frac{\mu E_g R_1}{R_a + R_1} Z_0}{\frac{R_a R_1}{R_a + R_1} + Z_0} = \frac{\mu E_g R_1 Z_0}{R_a R_1 + Z_0 (R_a + R_1)}$$

which is identical with the result obtained from direct analysis.

The same method may be used to show that the two circuits given in Figs. 3A.3 and 3A.4 produce the same result as far as the output voltage across, and current in,  $Z_0$  are concerned.

## INDEX

- A**, Class A amplification :  
introduction, 56  
push-pull stage, 84  
single valve stage, 57
- A.C./D.C. conversion efficiency of  
power output valves :  
fixed A.C. input voltage, 57  
fixed D.C. anode voltage and current, 59  
fixed D.C. anode voltage, no limitations on D.C. anode current or A.C. input voltage, 58  
fixed D.C. dissipation loss, minimum anode voltage and current, 63  
fixed D.C. dissipation loss, no limitation on D.C. anode voltage, 62
- A.C./D.C. receiver power supply, and heater connections, 172
- Acoustic frequency response, 285, 289
- Acoustic measurements on receivers :  
frequency response, 289  
hum, 291  
output and distortion factor, 292  
sensitivity, 290
- A.C. receiver power supply, 133
- Acoustic tests on receivers :  
distortion factor, 292  
free space conditions and its approximation, 286  
frequency response, 285, 289  
hum, 291  
intensity level, 285  
loudness level, 285  
overall sensitivity, 286, 290  
total harmonic content, 286
- Additional apparatus for acoustic tests on receiver, 286
- Adjustments to receiver for overall performance tests, 269
- Aerial circuit of—  
F.M. receiver :  
design of, 309  
noise in, 304  
television receiver:  
design of, 373  
dipole aerial and reflector for, 369  
noise in, 374  
reflections in, 369
- Aerial, dummy, *see* Standard
- Aerial, frame, pick-up coil for receiver tests, 267
- Aerial, standard, for receiver, 267
- Air gap inductance design :  
large A.C. flux density, 170  
small A.C. flux density, 170
- Amplification factor of a valve, 8
- Amplification at medium frequencies of A.F. amplifier, 8
- Amplification, loss of, due to—  
cathode self-bias circuit, 19  
coupling capacitance, 9  
stray capacitance, 10
- Amplitude compression and F.M., 300
- Amplitude discriminator for—  
A.F.C. control :  
conditions of maximum sensitivity, 227  
curves for, 225, 228  
design of, 231  
frequency-to-amplitude conversion :  
conditions for maximum linearity, 337, 344  
curves for, 338, 346  
design of, 339, 347
- Amplitude discriminator, types of :  
double tuned circuits, 226  
single tuned circuits, 234
- Amplitude limiter for F.M. receiver :  
A.M. neutralizing limiter, 333  
negative feedback limiter, 332  
saturated amplifier limiter, 329
- Analyser, harmonic, 269
- Anode decoupling circuit :  
compensation of cathode self-bias response by, 28  
frequency response due to, 27  
loss of amplification due to, 25
- Apparatus for receiver measurements of—  
acoustic performance, 286  
electrical performance, 266
- Attenuation distortion :  
calculation of, in output transformer, 102  
definition of, 2  
effect on audio frequency response, 2  
effect on television reception, 367
- Audio frequency amplifiers :  
characteristics required of, 1  
distortion in :  
amplitude, 3

- Audio frequency amplifiers—*contd.*  
 distortion in—*contd.*  
 attenuation, 2  
 intermodulation, 79  
 phase, 6  
 transient, 6  
*RC* coupled type :  
 high frequency response of, 13  
 low frequency response of, 11  
 medium frequency amplification of, 13  
*R.C.* transformer coupling, 38  
 transformer coupled type :  
 high frequency response of, 35  
 low frequency response of, 33  
 medium frequency amplification of, 33  
 Audio signal I.F. rejector circuits for television receiver :  
 attenuation characteristics of, 402  
 types of :  
 cathode feedback method, 410  
 parallel resonant absorber, 399  
 parallel resonant circuit—capacitance potential divider, 406  
 series-parallel resonant circuit, 409  
 series resonant circuit, 408  
 series resonant coupling, 410  
 vision pass-band, effect on, 402  
 Automatic frequency correction :  
 estimation of overall performance, 260  
 the error corrector or variable reactance device, 245  
 the frequency discriminator or error detector, 224  
 Automatic gain control :  
 applied to F.M. reception, 332  
 applied to television reception, 417  
 audio frequency :  
 with decreasing amplification, compression, 208  
 with increasing amplification, contrast expansion, 209  
 principle of operation, 180  
 radio frequency :  
 amplified :  
 anode bend amplified, 198  
 combined R.F. and A.F. amplified, 193  
 D.C. amplified, 195  
 R.F. amplified, 193  
 distortion due to, 189  
 Automatic gain control—*contd.*  
 radio frequency—*contd.*  
 filter for :  
 distortion due to, 191  
 parallel type, 200  
 series type, 200  
 time constant of, 201  
 methods of obtaining bias voltage, 181  
 non-amplified :  
 biased diode, 186  
 unbiased diode, 182  
 performance, calculation of, 184  
 Automatic selectivity, measurement of, 274  
 Automatic tuning control, *see* Automatic frequency correction
- B**, Class B, push-pull :  
 positive drive, 95  
 quiescent, 92  
 Balanced feedback :  
 advantages of, 120  
 methods of, 122  
 principles of, 121  
 Band elimination A.F. filter, 52  
 Band-pass tone control, 50  
 Beat frequency oscillator for receiver measurements, 269  
 Bessel coefficient amplitudes of F.M. carrier and sidebands, 295  
 Bias, self, for A.F. amplifier, 19  
 Blocking oscillator scanning generator for television, 450  
 Bridge H.T. rectifier, 143  
 Bridge negative feedback :  
 amplification with, 117  
 equivalent generator impedance for, 117
- C**apacitance coupling in A.F. amplifier, 6  
 Capacitance coupling, anode-grid in R.F. amplifier, 305  
 Capacitance stray, effect in—  
 A.F. amplifier, 11  
 R.F. amplifier, 315, 325  
 v.F. television amplifier, 421  
 Cathode follower stage :  
 amplification of, 118  
 characteristics of, 119  
 driver for Class B positive drive, 96  
 equivalent generator impedance of, 118

- Class A push-pull amplification, 84
- Class AB positive drive amplification, 97
- Class B—  
 positive drive, 95  
 quiescent push-pull, 94
- Colpitts oscillator for short waves, 319
- Complex anode load impedance and distortion, 73
- Composite anode current-anode voltage curves for—  
 Class A push-pull output stages, 90  
 Class B push-pull output stages, 92
- Compression of frequency deviation in F.M. receiver :  
 advantages of, 354  
 methods of,  
   F.M. of receiver oscillator, 354  
   frequency division, 355  
   submultiple locked oscillator, 357
- Contrast expansion, 209
- Control, automatic gain, *see* Automatic gain control
- Counter type F.M. detector, 352
- Cross-modulation in F.M. receiver, 320
- Current distortion in output transformer, curves for different D.C. polarizing voltages, 108
- Current negative feedback :  
 amplification of, 116  
 characteristics of, 116  
 equivalent generator impedance of, 116
- D**.c. component restoration in television reception, 436
- Decoupling circuit for A.F. amplifier in—  
 anode, 25  
 screen, 22
- De-emphasis in F.M. reception, 299
- Definition in television reception, 361
- Deflecting circuits of C.R. tube in television reception :  
 electromagnetic :  
   frame, 461  
   line, 460  
   output transformer for, 460  
   type of coil for, 459  
 electrostatic :  
   frame, 457  
   line, 457
- Deflecting circuits for C.R. tube in television reception—*contd.*  
 electrostatic—*contd.*  
   push-pull, 457
- Deflection methods for C.R. tube in television reception :  
 distortion, barrel and pincushion, 458  
 electromagnetic, 455  
 electrostatic :  
   distortion, trapezium in, 456  
   voltage wave shapes for, 456  
   voltage and current wave shapes for, 455
- Demodulation of carrier, 272, 276
- Detection in television reception :  
 efficiency of, 411  
 types of, 411
- Detector stage in television reception :  
 filter circuit for :  
   attenuation distortion in, 416  
   design of, 412  
   phase distortion in, 417  
   reflection losses in, 415  
 types of,  
   anode bend, 419  
   full wave, 411  
   half wave, 411  
   voltage doubler, 411
- Diode rectifier :  
 calculation of performance :  
   capacitive load, 146  
   inductive load, 154  
   resistance load, 145  
 conduction current characteristic, 147  
 high vacuum type, 144  
 inverse voltage of, 144  
 mercury vapour type, 145  
 rectification efficiency, 145
- Direct reading harmonic scales for—  
 second harmonic, 69  
 third harmonic, 72
- Discriminator for—  
 A.F.C. :  
   amplitude, 225  
   phase, 235  
 frequency to amplitude converter in F.M. reception :  
   amplitude, 337  
   phase, 340
- Distortion factor, 286
- Distortion factor meter, 286
- Distortion, join-up in Class B amplifiers, 94



- Distortion, measurement of individual harmonic amplitudes, 77, 269
- Distortion, measurements of, for receiver, 279
- Distortion in—
- audio frequency amplifiers :
    - attenuation, 2
    - harmonic, 3
    - phase, 6
    - transient, 6
  - direct reading scales for, 69, 72
  - intermodulation, 79
  - join-up distortion in Class B stages, 94
  - measurement of, 76
  - output transformer :
    - core material distortion factor, 108
    - current distortion ratio, 108
  - power output stages :
    - calculation of :
      - second harmonic, 68
      - third harmonic, 71
      - fourth harmonic, 71
  - push-pull stages, 84
  - television reception :
    - attenuation, 367
    - harmonic, 367
    - phase, 368
    - transient, 367, 420
- Divider compressor for F.M. reception, 355
- Doubler, voltage, rectifier, 144
- Double wave rectifier, *see* Full wave.
- Driver stage for Class B push-pull positive drive, 95
- Dummy aerial, *see* Standard aerial
- E**ddy current tuning, 307
- Electrical measurements on a receiver, 269
- Electromagnetic deflection of c.r. tube in television reception :
- distortion, barrel and pincushion, 458
  - frame amplifier, 461
  - line amplifier, 460
  - type of coils for, 459
  - voltage and current wave shape for, 455
- Electromagnetic focusing for television c.r. tube, 463
- Electron coupled oscillator, 319
- Electrostatic deflection of c.r. tube in television reception :
- distortion, trapezium, 456
  - frame amplifier, 457
  - line amplifier, 457
  - voltage wave shape for, 455
- Electrostatic focusing for television c.r. tube, 462
- Equivalent valve load impedance in push-pull stages, 91
- F**eedback :
- application to output stage, 124
  - curves for, 126
  - negative :
    - instability in negative feedback amplifiers, 122
    - reduction of distortion by, 113
    - reduction of gain by, 113
    - reduction of noise by, 113
    - two stage circuits, 128
    - types of :
      - balanced, 120
      - bridge, 117
      - current, 116
      - voltage, 114
- Fidelity of receiver, 265
- Filter A.G.C. :
- parallel, 200
  - series, 200
- Filter inductance with air gap, design of, 164
- Filter, rectifier ripple :
- attenuation characteristics for 50 c.p.s., 161
  - tuned type, 162
- Flicker in television, 361
- Focusing of c.r. tube in television receiver :
- electromagnetic :
    - advantages and disadvantages, 462
    - centring of picture by means of, 465
    - H.T. supply for, 464
    - method of producing, 464
  - electrostatic :
    - advantages and disadvantages, 461
    - H.T. supply for, 462
    - method of producing, 462
- Frame scanning generator for television reception, 447, 449, 453

- Free space conditions for receiver measurement, 286
- Frequency-amplitude conversion in F.M. reception :  
 amplitude discriminator, 335  
 counter detector, 352  
 hexode converter, 353  
 integrator, 349  
 phase discriminator, 340
- Frequency changer interference effects in—  
 F.M. reception, 320  
 television reception, 391
- Frequency changer stage in—  
 F.M. reception, 315  
 television reception :  
 design of aerial connection to, 386  
 input resistance of, 389  
 signal-to-noise ratio for, 385  
 types of frequency changer valve, 384
- Frequency correction, automatic :  
 estimation of overall performance, 260  
 measurement of, 285
- Frequency deviation measurement in F.M. transmission, 295
- F.M. compression in receiver by—  
 frequency division, 355  
 frequency modulation of local oscillator, 354  
 submultiple locked oscillator, 357
- F.M. detector, *see* Frequency-amplitude converter
- F.M. receiver, schematic diagram of, 302
- F.M. reception :  
 advantages and disadvantages, 296  
 aerial input for, 303  
 amplitude compression, 300  
 amplitude limiter for, 328  
 frequency-amplitude converter, 334  
 frequency changer for, 315  
 intermediate frequency amplification for, 320  
 R.F. amplification for, 303  
 service area, 301  
 signal-to-noise ratio, 300
- Frequency response of—  
 A.F. amplifier :  
 anode circuit, 6  
 anode decoupling circuit, 25  
 screen decoupling circuit, 22
- Frequency response of—*contd.*  
 A.F. self bias, 19  
 R.F. amplifier for—  
 F.M. reception, 311  
 television reception, 371
- Full wave H.T. rectifier, 133
- G**ain control, automatic :  
 amplified :  
 anode bend, 198  
 combined R.F. and A.F. amplified, 193  
 D.C. amplified, 195  
 R.F. amplified, 193  
 audio frequency :  
 with decreasing amplification, 208  
 with increasing amplification, 209  
 calculation of performance, 183  
 dual, 202  
 filter for, 198  
 methods of obtaining bias voltage, 181  
 non-amplified :  
 biased or delayed diode, 186  
 distortion due to biased diode, 189  
 unbiased diode, 182  
 principle of operation, 180  
 quiet or noise suppressed, 202  
 using A.F. detector, 191
- Gas-filled relay scanning generator for television, 447
- Generalised curves for—  
 A.F. amplifier :  
 high frequency response, 13  
 low frequency response, 11  
 self bias, 22  
 tone control, 46, 49, 54  
 frequency and phase response in television—  
 R.F. amplifier, 377  
 V.F. amplifier :  
 high frequency end of range :  
 combined shunt and series peaking circuit, 427, 428  
 series peaking circuit, 427, 428  
 shunt peaking circuit, 424, 425
- Grid bias supplies :  
 potential divider type, 172  
 self bias, 172

- Grid leak and its effect on the anode load of A.F. amplifier, 18
- H**alf wave rectifier :  
 efficiency of, 149  
 general performance of, 147  
 maximum conduction current—  
 D.C. current ratio, 153  
 R.M.S. fundamental current—D.C.  
 current ratio, 153
- Harmonic analyser, 77, 269
- Harmonic distortion in :  
 A.F. amplifiers, 3  
 television reception, 367
- Heater connections for A.C./D.C.  
 receiver, 173
- Heterodyne whistle interference sup-  
 pression, 52
- H**um :  
 loudness level, 292  
 measurements of, in receiver, 281,  
 291  
 modulation in—  
 frequency changer, 173  
 I.F. and R.F. valves, 173  
 oscillator, 317  
 rectifier of A.C./D.C. receiver, 174
- I**conoscope :  
 description of, 361  
 principles of, 361
- Image signal measurements, 283
- I**mpedance :  
 complex anode load, and distor-  
 tion, 73  
 equivalent valve load, in push-pull  
 stages, 91, 93  
 linear, 5  
 non-linear, 5
- Incremental permeability, 165
- Inductance tuning, 307
- Inductance with air gap, design of,  
 164
- Input transformer for Class B positive  
 drive, 96
- Input voltage, standard, for receiver,  
 264
- Integrating F.M. detector :  
 hexode, 352  
 multivibrator, 349  
 regenerator, 350  
 squegger, 351
- Interchannel noise suppression :  
 biased A.F. amplifier, 205  
 biased detector, 203  
 variable capacitance across detec-  
 tor load resistance, 204
- Interlaced scanning in television  
 reception, 361
- Intermediate frequency amplifier  
 for—  
 F.M. receiver :  
 choice of frequency, 320  
 design of, 323  
 instability in, 322  
 overall amplification of, 328  
 television receiver :  
 audio signal filter circuits, 399  
 choice of frequency, 391  
 coupling types, 392  
 design of, 395  
 overall amplification of, 397  
 phase distortion in, 397
- Intermodulation in—  
 A.F. amplifiers, 4  
 power output stages,  
 effect of, 82  
 measurement of, 83
- Inverted A.F. output, 272
- J**oin-up distortion in Class B  
 amplifiers, 94
- K**, constant  $K$  filters in television  
 amplifiers, 412
- L**imiter :  
 amplitude, in F.M. receiver,  
 298, 328  
 noise, 206
- Line scanning generator in television  
 reception, 448, 450, 453
- Loudness level, 285
- Loudspeaker field coil as H.T. power  
 supply filter, 134
- Loudspeaker speech coil impedance,  
 74
- Low frequency attenuation tone  
 control, 47
- Low frequency intensification tone  
 control, 48
- Low frequency response in—  
 A.F. amplifiers, 9  
 V.F. amplifiers for television, 431

- M**ains transformer :  
 design of, 135  
 effect of leakage inductance, 140  
 electrical stress in, 135  
 equivalent circuit for, 134  
 losses in, 138  
 no-load and full-load conditions, 139  
 temperature rise on full-load, 141  
 winding distribution, 136
- Maximum amplification of—**  
 tetrode A.F. amplifier, 14  
 triode A.F. amplifier, 13  
 v.f. stage in television, 423, 425, 430
- Measurement of receiver overall performance,** 264
- Modulation envelope distortion due to A.G.C.,** 180, 189
- Modulation hum,** 173, 281
- Modulation index,** 295
- Monkey chatter distortion,** 272
- Motor-boating in A.F. amplifiers,** 25
- Multivibrator scanning generator for television reception,** 449
- N**eedle scratch filter, 52  
 Negative feedback :  
 application to output stage, 124  
 application to two stages, 128  
 due to self bias, 19  
 instability in, 122  
 properties of, 113  
 reduction of distortion by, 113  
 reduction of noise by, 113  
 types of :  
 balanced, 120  
 bridge, 117  
 current, 116  
 voltage, 114
- Noise in F.M. reception :**  
 impulse, 299  
 phase modulation by, 298  
 thermal and shot, 297
- Noise limiters,** 206
- Noise measurements on a receiver,** 280
- Noise suppression, interchannel, see Interchannel noise suppression**
- Noise, thermal and shot, calculation of, for—**  
 aerial, 312  
 frequency changer, 384  
 R.F. amplifier, 374
- O**scillator frequency drift measurements, 284
- Oscillator frequency variations—**  
 due to heater voltage, 318  
 due to temperature, 317  
 due to valve, 318  
 reduction of, 317  
 types of, 317
- Oscillator harmonic responses, measurements of,** 284
- Oscillator stage of—**  
 F.M. receiver :  
 design of, 319  
 stability of, 317  
 undesirable modulation of, 317  
 television receiver :  
 design of, 391  
 stability of, 390  
 types of circuit for, 390
- Output meter,** 268
- Output power, standard, for receiver measurements,** 265
- P**araphase push-pull, 87  
 Parasitic oscillation in Class B stages, 95
- Pass-band width for F.M. reception,** 302
- Permeability, incremental,** 165
- Phase discriminator for—**  
 A.F.C. :  
 adjustment of, 244  
 design of, 241  
 optimum conditions for, 237  
 vector diagram for, 238  
 frequency-to-amplitude conversion in F.M. reception :  
 adjustment of, 348  
 characteristic curves for, 346  
 design of, 347  
 effect of mutual inductance, 349  
 effect of primary and secondary mistuning, 348
- Phase distortion in :**  
 A.F. amplification, 6  
 television reception :  
 general effect of, 368  
 in detector stage, 417  
 in I.F. amplifier, 397  
 in R.F. amplifier, 373  
 in v.f. amplifier, 425, 427, 430
- Phon, unit of loudness,** 285
- Positive drive, Class B,** 95

- Power handling capacity of output transformer, 111
- Power output :  
 calculation of, 66  
 conditions for maximum, 56  
 measurement of, at—  
 mains frequency, 76  
 400 c.p.s., 77
- Power output, maximum, grid current and distortion zero :  
 fixed A.C. input voltage, 57  
 fixed D.C. anode voltage and current, 59  
 fixed D.C. anode voltage, no limitations on D.C. anode current or A.C. input voltage, 58  
 fixed D.C. dissipation loss, fixed minimum anode voltage and current, 63  
 fixed D.C. dissipation loss, no limitations on D.C. anode voltage, 62
- Power output stages, 56
- Power sensitivity, 65
- Power supply for—  
 A.C./D.C. receiver, 172  
 A.C. receiver, 133  
 television C.R. tube, 461
- Power supply from vibrator, 174
- Pre-emphasis in F.M. transmission, 299
- Pull-in frequency in A.F.C., 225
- Push-button tuning by—  
 electrical rotation of tuning capacitor, 215  
 mechanical rotation of tuning capacitor, 215  
 preset tuned circuits, 217
- Push-pull input voltage, methods of obtaining, 86
- Push-pull operation :  
 advantages of, 84  
 driver stage for Class B positive drive, 95  
 methods of producing, 86  
 types of :  
 Class A, 89  
 Class AB positive drive, 97  
 Class B :  
 positive drive, 94  
 quiescent, 95
- Push-pull output transformer design, 102
- Push-pull stages :  
 cancellation of even harmonic distortion, 85
- Push-pull stages—*contd.*  
 cancellation of hum and interference from H.T. supply, 85  
 composite curves for, 90, 92, 93  
 distortion in, 85  
 equivalent load impedance for, 91
- Q**uadrupler voltage rectifier, 159
- Quality :  
 good commercial, 84  
 high, 84  
 objectionable, 84
- Quality and—  
 harmonic distortion, 80  
 restriction of frequency response, 79
- Quiescent push-pull, 94
- R**C coupled A.F. amplifier, 6
- RC transformer coupled A.F. amplifier, 38
- Reactance control for A.F.C..  
 limited characteristic, 262  
 types of :  
 motor operated, 245  
 polarized capacitor, 246  
 polarized inductor, 247  
 valve, 248  
 unlimited characteristic, 262
- Reactance valve for A.F.C. :  
 performance of, over—  
 long wave range, 257  
 medium wave range, 254  
 short wave range, 257  
 types of :  
 capacitive, 253  
 inductive, 253
- Receiver overall performance, measurements of :  
 acoustical :  
 distortion factor, 286  
 free space conditions, 286  
 frequency response, 285  
 hum, 291  
 intensity level, 285  
 loudness level, 285  
 overall sensitivity, 286  
 total harmonic content, 286  
 electrical :  
 adjustments for, 269  
 A.F.C. characteristics, 285  
 A.G.C. characteristic, 282  
 distortion, 279  
 fidelity or frequency response, 278

- Receiver overall performance, measurements of—*contd.*  
 electrical—*contd.*  
 frequency changer interference effects, 283  
 hum, 281  
 noise, 280  
 oscillator frequency drift, 284  
 oscillator harmonic response, 284  
 selectivity, 272  
 sensitivity, 269  
 standard input voltage, 264  
 standard output power, 265
- Rectifier diode :  
 calculation of performance with—  
 capacitive load, 146  
 inductive load, 154  
 resistive load, 145  
 conduction current—anode voltage characteristic, 147  
 inverse voltage of, 144  
 rectification efficiency, 145  
 types of :  
 high vacuum, 144  
 mercury vapour, 145
- Rectifier H.T. supply :  
 load conditions :  
 capacitive, 146  
 inductive, 154  
 resistive, 145  
 types of :  
 bridge, 143  
 full wave, 133  
 half wave, 142  
 voltage doubler, 144  
 voltage tripler, 159  
 voltage quadrupler, 160
- Rectifier ripple filter :  
 attenuation—*LC* characteristic for 50 c.p.s., 161  
 tuned type, 162
- Reflected signals in television reception, 369
- Regeneration in A.F. amplifiers, 26
- Remote tuning :  
 magnetic, 222  
 pulse control using mains supply wiring, 219  
 R.F. pulses from portable oscillator, 222  
 rotation of tuning capacitor, 219  
 transfer of R.F. and frequency changer stages to remote point, 222  
 tuned lines, 223
- Reservoir capacitance, in H.T. supply, 150
- Resistance, optimum load, of—  
 push-pull stage, 91  
 single valve stage, 57
- R.F. amplifier for—  
 F.M. receiver, 303  
 television receiver :  
 attenuation distortion in, 374  
 audio signal rejection circuits for 380  
 design of, 374  
 feedback in, 379  
 phase angle error curves for, 377  
 phase distortion in, 373  
 signal-to-noise ratio for, 374  
 time delay in, 373
- Ripple filter, rectifier, *see* Rectifier ripple filter
- Ripple neutralization, 162
- S**canning generators in television receivers :  
 special features of, 446  
 types of :  
 blocking oscillator, 450  
 gas-filled relay, 447  
 multivibrator, 449
- Screen decoupling circuit :  
 frequency response of, 24  
 loss of amplification due to, 25
- Selectivity of receiver, measurement of, 272
- Self bias for A.F. amplifier :  
 calculation of attenuation distortion, 21  
 compensation by anode decoupling circuit, 28  
 generalised frequency response curves for, 22  
 loss of amplification due to, 21  
 negative feedback due to, 19
- Sensitivity of receiver, measurement of, 269
- Series peaking circuit in V.F. amplifier of television receiver :  
 amplification of, 428  
 attenuation distortion, 427  
 phase distortion, 427
- Service area of F.M. signal, 301
- Shielded pick-up coil for frame aerial receiver measurements, 267
- Shock excitation in tone control circuits, 42

- Shunt peaking circuit in v.p. amplifier of television receiver :  
 amplification of, 425  
 attenuation distortion, 424  
 phase distortion, 425
- Sideband amplitudes in F.M. signal, 295
- Sideband screech, 187
- Signal generator, standard, 266
- Signal-to-noise ratio in—  
 F.M. reception, 312  
 television reception, 374, 384
- Slope resistance of valve, 8, 23
- Standard—  
 dummy aerial, 267  
 input voltage, 264  
 modulation frequency, 265  
 modulation percentage, 265  
 output power, 265  
 signal generator, 266
- Submultiple locked oscillator for F.M. compression, 357
- Superheterodyne television receiver :  
 choice of I.F., 391  
 I.F., harmonic response and, 391  
 signal-to-noise ratio of, 384  
 vestigial sideband reception with, 384
- Synchronizing signal separation in television reception :  
 amplitude separation from vision signal, 439  
 frequency separation of frame and line pulses :  
 frame selector integrator circuits, 444  
 line selector differentiator circuits, 442
- Synchronizing signals in television :  
 frame, 363  
 line, 363
- T**elevision receiver :  
 deflecting system, 454  
 distortion in :  
 attenuation, 367  
 harmonic, 367  
 phase, 368  
 transient, 367  
 electrical impulse to light converter, 366  
 essential features of, 364  
 power supplies and focusing, 461  
 scanning generators for, 446
- Television receiver—*contd.*  
 stages of :  
 aerial, 368  
 detector, 410  
 frequency changer, 384  
 I.F. amplifier, 391  
 oscillator, 390  
 R.F. amplifier, 371  
 v.F. amplifier, 419  
 synchronizing pulse separation :  
 frame from line, 441  
 vision from synchronizing, 439  
 types of :  
 superheterodyne, 381  
 tuned R.F., 377
- Television reception :  
 active picture elements, 362  
 conversion of light to electrical impulse, 360  
 definition in, 361  
 double sideband transmission, 364  
 frequency spectrum occupied, 362  
 scanning in, 361  
 successive transmission, 360  
 synchronizing signals for, 362  
 vestigial sideband transmission, 364
- Tetrode A.F. amplifier :  
 comparison with triode, 14  
 effect of grid leak on performance, 18  
 maximum amplification of, 14
- Thévenin's theorem, 467
- Threshold area in F.M. reception, 299
- Throw-out frequency in A.F.C., 225
- Time constants of A.V.C. filter circuits, 200
- Tone control circuits :  
 shock excitation in, 42  
 types of :  
 combined volume and tone control, 54  
 high frequency attenuation, 43  
 high frequency intensification, 44  
 low frequency attenuation, 47  
 low frequency intensification, 48  
 narrow band-pass filter, 50  
 narrow band rejector filter, 52
- Transfer voltage ratio, aerial to first R.F. valve, in F.M. receiver, 310
- Transformer :  
 input for Class B positive drive, 94  
 mains :  
 design of, 135  
 effect of leakage inductance, 140

- Transformer—*contd.*  
 mains—*contd.*  
 electrical stress in, 135  
 equivalent circuit for, 134  
 iron and copper losses, 138  
 no-load and full-load conditions, 139  
 temperature rise on full-load, 141  
 winding distribution, 136  
 output :  
 current distortion factor in, 106  
 design of, 97  
 distortion :  
 attenuation, 102  
 harmonic, 104  
 effect of D.C. polarizing current in, 108  
 for Class B operation, 95  
 leakage inductance of, 102  
 power handling capacity, 111  
 push-pull, 104  
 types of winding for, 102
- Transformer coupled A.F. amplifier :  
 high frequency response of, 35  
 leakage inductance in, 31  
 low frequency response of, 33  
 medium frequency amplification, 32  
 resonance in, 28  
 secondary distributed capacitance, 29
- Transient distortion in—  
 A.F. amplifiers, 6  
 television reception, 367
- Trebler, voltage, rectifier, 159
- Triangular noise distribution in F.M. reception, 298
- Triode A.F. amplifier :  
 comparison with tetrode, 14  
 effect of grid leak on performance, 18  
 maximum amplification of, 13
- Tuning :  
 automatic control of, 224  
 push-button, 214  
 remote, 219
- Two signal—  
 cross-talk interference test, 276  
 selectivity test, 275
- Variable reactance control for A.F.C. :  
 limited characteristic, 262
- Variable reactance control for A.F.C.—*contd.*  
 motor operated capacitor, 245  
 polarized capacitor, 246  
 polarized inductor, 247  
 unlimited characteristic, 262  
 valve, 248
- Variable reactance valve :  
 performance of, over—  
 long wave range, 257  
 medium wave range, 254  
 short wave range, 257  
 types of :  
 capacitive, 253  
 inductive, 252
- Vibrator H.T. supply :  
 action of, 176  
 efficiency of, 178  
 suppression of interference from, 175  
 types of, 174
- Vision frequency amplification in television :  
 effect of attenuation and phase distortion in, 367, 420  
 high frequency performance :  
 characteristic of, 419  
 compensation for stray capacitance :  
 combination of series and shunt peaking circuits, 428  
 series peaking circuit, 426  
 shunt peaking circuit, 421  
 distortion in :  
 attenuation, 420  
 phase, 420  
 measurement of amplification and phase shift, 430  
 low frequency performance :  
 compensation for attenuation and phase delay due to—  
 cathode self-bias circuit, 435  
 grid leak and coupling, 432  
 screen circuit, 436  
 distortion in :  
 attenuation, 420  
 phase, 420  
 motor boating, 436  
 output voltage required, 419  
 restoration of D.C. component by—  
 diode, 437  
 grid current in last valve, 437  
 transient distortion in, 420  
 types of valves for, 420
- Voltage doubler rectifier, 144



- Voltage negative feedback,  
  amplification with, 115  
  equivalent generator impedance,  
    115
- Voltage quadrupler rectifier, 160
- Voltage tripler rectifier, 159
- Volume, combined volume and tone  
  control, 54
- Volume compression, 207
- Volume expansion, 207

THE END